Université de Montréal
Faculté de médecine
Département de microbiologie, infectiologie et immunologie

Molecular Characterization of Th17 Lymphocytes and Monocyte-Derived Dendritic Cells in the Context of HIV-1 Infection

Présenté par:
Vanessa Sue WACLECHE

Sous la direction scientifique de la Dre Petronela Ancuta

Laboratoire Chimiokines et VIH-1

Le centre de recherche du CHUM

Thèse présentée à la Faculté des études supérieures de l'Université de Montréal en vue de l'obtention du diplôme de doctorat en microbiologie et immunologie

Montréal, le 7 Décembre 2015

SOMMAIRE

Le virus de l'immunodéficience humaine de type 1 (VIH-1) altère les fonctions du système immunitaire pour promouvoir sa persistance. Les composantes de l'immunité ciblées par le VIH-1 incluent les lymphocytes Th17 et les cellules dendritiques dérivées des monocytes (CDDMs). Deux sous-populations de lymphocytes Th17, nommées Th17 et Th1Th17, ont précédemment été décrites avec des propriétés transcriptionnelles et des spécificités antigéniques distinctes. Les cellules Th17 et Th1Th17 sont hautement permissives à l'infection par le VIH et leur fréquence est diminuée chez les sujets chroniquement infectés sous trithérapie antirétrovirale. Toutefois, seulement une fraction des lymphocytes Th17 est infectée par le VIH, indiquant l'existence de Th17 résistants à la réplication virale. Également, il est connu que l'infection à VIH induit une altération de la fréquence des monocytes reflétée par l'expansion de la population monocytaire exprimant le récepteur Fcγ de type III/CD16. Les monocytes sont des précurseurs de cellules dendritiques et une altération de ratio entre les monocytes $CD16^+$ et $CD16^-$ pourrait avoir des conséquences délétères sur la qualité des réponses immunitaires. Le rôle fonctionnel des CDDM exprimant ou non CD16 dans le contexte de la pathogénèse à VIH-1 demeure inconnu. Ce projet de thèse est divisé en 2 parties: ***1)*** l'étude de l'hétérogénéité des cellules Th17 et ***2)*** la caractérisation approfondie des CDDM $CD16^+$ et $CD16^-$ dans le contexte d'homéostasie et de la pathogénèse de l'infection à VIH. Dans la première partie, nous avons fonctionnellement caractérisé deux nouvelles sous-populations de lymphocytes Th17 avec une expression différentielle des récepteurs de chimiokines CXCR3 et CCR4 : nommés $CCR6^+$DN et $CCR6^+$DP, exprimant toutes les deux CCR6, marqueur de lymphocytes Th17. Nous avons démontré que les cellules $CCR6^+$DN et $CCR6^+$DP partagent des caractéristiques biologiques communes avec les cellules Th17 et Th1Th17 incluant la permissivité au VIH. Nos résultats indiquent que les cellules $CCR6^+$DN représentent un stade précoce de différentiation des lymphocytes Th17 et expriment des marqueurs de cellules T folliculaires. De plus, comparativement aux sous-populations Th17, Th1Th17 et $CCR6^+$DP, la fréquence et le compte des $CCR6^+$DN sont préservés au sein des sujets chroniquement infectés sous thérapie antirétrovirale. Nous proposons un modèle dans lequel les cellules $CCR6^+$DN représentent des lymphocytes Th17 résistantes à l'effet cytopatique du virus qui contribuent à la persistance virale par leur capacité de porter un virus compétent en matière de réplication. Dans la deuxième partie, nos résultats révèlent que les CDDMs $CD16^+$ et $CD16^-$ représentent deux populations uniques avec des propriétés transcriptionelles et fonctionnelles

distinctes. Les CDDMs $CD16^-$ détiennent un potentiel immunogène supérieur tandis que les CDDMs $CD16^+$ ont une meilleure capacité de transmettre le virus aux cellules T $CD4^+$ au repos. Également, nous confirmons l'effet néfaste du VIH sur les fonctions immunologiques des cellules DC à stimuler la prolifération et la polarisation des cellules Th17 spécifiques à *C. albicans* et à *S. aureus*. En conclusion, les résultats inclus dans cette thèse fournissent une compréhension détaillée sur l'hétérogénéité présente au sein des lymphocytes Th17 et des CDDMs et révèlent de nouveaux déterminants moléculaires de l'immunité exploités par le VIH au profit de sa persistance.

Mots-clés : VIH-1, Th17, Th1Th17, CCR6, cellules T-CD4, mémoires, profil transcriptionel, monocytes, cellules dendritiques, CD16

ABSTRACT

The ultimate aim of immunity is to restrict the emergence of exogenous pathogens while providing immune tolerance to self-antigens. The human immunodeficiency virus type 1 (HIV-1) disrupts the functions of the immune system to promote its own dissemination and persistence. The components of the host immunity targeted by HIV-1 include the Th17 lineage and the monocytes. The Th17 lineage was previously reported to include two different populations referred to as the Th17 and Th1Th17 cells exhibiting different transcriptional profiles and antigenic specificities. Both Th17 and Th1Th17 cells are permissive to HIV and their frequency is reduced in the blood and gut mucosa of chronically HIV-infected subjects. Nevertheless, HIV-1 infects only a fraction of the Th17 pool, suggesting the existence of Th17 cells resistant to HIV. In addition, it well documented that HIV-1 infection alters the pool of peripheral blood monocytes and induces the expansion of a monocytic population expressing the Fcγ receptor III/CD16. Monocytes are precursors for dendritic cells (DCs) and an altered CD16+/CD16- monocyte ratio may have deleterious consequences on the quality of immune responses. The functional features of $CD16^+$ *versus* CD16- monocyte-derived DCs (MDDCs) in the context of HIV infection remain to be elucidated. This thesis is divided in two parts: ***1)*** the study of Th17 cell heterogeneity and ***2)*** the in depth characterization of $CD16^+$ and $CD16^-$ monocytes-derived DCs (MDDCs) at homeostasis and during HIV-1 infection. In the first part, we have identified and functionally characterized two new previously uncharacterized subsets of $CCR6^+$ T-cells with differential expression of CXCR3 and CCR4, double negative $CCR4^-CXCR3^-$ ($CCR6^+$DN) and double positive $CCR4^+CXCR3^+$ ($CCR6^+$DP) subsets. We demonstrated $CCR6^+$DN and $CCR6^+$DP share cytokine production, antigenic specificity, lineage plasticity and HIV permissiveness with the previously characterized Th17 ($CCR6^+CCR4^+CXCR3^-$) and Th1Th17 ($CCR6^+CCR4^-CXCR3^+$) subsets. Among these four Th17 subsets, $CCR6^+$DN cells were found to represent an early stage of Th17 differentiation and expressed features of T follicular helper T-cells. Moreover, in contrast to Th17, Th1Th17 and $CCR6^+$DP subsets, the frequency and counts of $CCR6^+$DN cells was preserved in chronically HIV-infected subjects under antiretroviral treatments compared to uninfected controls. Our results suggest that $CCR6^+$DN represent long-lived Th17 cells contributing to HIV persistence by carrying replication-competent virus. In the second part, our results reveal that $CD16^+$ and $CD16^-$ MDDCs represent two distinct populations with unique transcriptional programs and immunological functions. $CD16^-$ MDDCs displayed a superior immunogenic potential, whereas

$CD16^+$ MDDCs exhibited a higher capacity to induce HIV replication in resting $CD4^+$ T-cells. Also, we confirmed the negative effect of HIV on DCs immunogenic function involving the stimulation of T-cell proliferation and Th17 polarization in response to pathogens such as C. albicans and S. aureus. Overall, in this thesis we provide a better understanding on Th17 and MDDC heterogeneity and reveal new molecular determinants of pathogenicity in immune cells that are exploited by HIV-1 to insure its persistence in the infected host.

Keywords: HIV-1, Th17, Th1Th17, CCR6, human CD4+ T-cells, memory, transcriptional profiling, monocytes, dendritic cells, CD16

TABLE OF CONTENTS

LIST OF FIGURES

ABBREVIATION LIST

Abs, antibodies

ADCC, Antibody-Dependent Cell-Mediated Cytotoxicity

AGs, Aicardi-Goutières syndrome

AhR, Aryl Hydrocarbon Receptor

APC, Antigen-Presenting Cells

AIDS, Acquired Immune Deficiency Syndrome

APOBEC3G, Apolipoprotein B editing catalytic polypeptide-like 3G

ART, Antiretroviral Therapy

ATP, Adenosine Triphosphate

AZT, Zidovudine

BATF, Basic Leucine Zipper Transcription Factor ATF-like

BBB, Blood-Brain Barrier

BCA, Breast Cancer-Associated Gene 2

BDCA, blood dendritic cell antigen

bNABs, Broadly Neutralizing Abs

BRD4, Bromodomain Containing 4

BSA, Bovine Serum Albumin

BSF-1, B-Cell Stimulatory Factor-1

BST-2, Bone Marrow Stromal Cell Antigen 2

CD, Cluster of Differentiation

CDK, Cyclin-Dependent Protein Kinase

cDNA, complementary DNA

CCL#, Chemokine (C-C motif) Ligand #

CCR#, Chemokine (C-C motif) Receptor #

C/EBPs, CCAAT/Enhancer-Binding Proteins Transcription Factors

CFSE, Carboxyfluorescein Succinimidyl Ester

CI on ART, Chronically Infected HIV Individuals on ART

CLA, Cutaneous Lymphocyte Associated Antigen

CLEC, C-type Lectin Domain Family

CMV, Cytomegalovirus

CPZ, Chimpazee

CTLA-4, Cytotoxic T-Lymphocyte Antigen 4

CXCL, Chemokine (C-X-C motif) Ligand

CXCR, Chemokine (C-X-C motif) Receptor

CypA, Cyclophilin A

DC, Dendritic Cells

DNA, Deoxyribonucleic acid

dNTP, Deoxynucleoside triphosphate

dU, Deoxyuridine

DTH, Delayed-Type Hypersensitivity

EAE, Experimental Autoimmune Encephalomyelitis

EGR2, Early Growth Response Gene

ELF4, E74-like factor 4

env , Envelop

ETS-1, E-Twenty Six 1

FACS, Fluorescence-Activated Cell Sorting

FBS, Fetal Bovine Serum

FDA, Food and Drug Administration

FOXO3a, Forkhead Box O3

FOXP3, Forkhead Box P3

GFI-1, Growth Factor Independent 1

GFRA2, Glial Cell Line-Derived Neurotrophic Factor Family Receptor-α2

GFP, Green Fluorescent Protein

GM-CSF, Granulocyte-Macrophage Colony-Stimulating Factor

gp, glycoprotein

gag, Group-Specific Antigen

GR-1, Granulocyte 1

HAART, Highly Activated Anti-Retroviral Therapy

HAD, HIV-Associated Dementia

HAND, HIV-Associated Neurocognitive Disorders

HDACi , Histone Deacetylase Inhibitors

HDF, HIV-Dependency Factors

HIFα, Hypoxia-Inducible Factor Alpha

HIES, Hyper IgE Syndrome

HIV, Human Immunodeficiency Virus

HLA, Human Leukocyte Antigen

HPV, Human Papilloma Virus

HSV, Herpes Simplex Virus

hs-CRP, High-Sensitivity C-Reactive Protein

HVTN , HIV-1 vaccine trials network

IBD, Inflammatory Bowel Disease

ICAM-1 Intercellular Cell Adhesion Molecule-1

ID3, Inhibitor of DNA-binding 3

IDO1, Indoleamine 2,3-dioxygenase 1

i.e., id est (latin)

IFN, interferon

Ig, Immunoglobulin

IKKα, Iinhibitor of nuclear factor-κB kinase-α

IκBζ, IkappaB-zeta

IL, Interleukin

IRF4, interferon regulatory factor 4

iTreg, inducible Treg

LAG-3, Lymphocyte-Activation Gene 3

LAV, Lymphadenopathy Associated Virus

LDLR, Low Density Lipoprotein Receptor

LEDGF, Lens Epithelium-Derived Growth Factor

LEF1, Lymphoid enhancer-binding factor-1

LFA-1, Leukocyte Function-Associated Molecule-1

LMNA, Lamin A/C

LPS, Lipopolysaccharide

LTR, Long Terminal Repeat

Ly-6C, Lymphocyte Antigen 6C

M, Main

MACS, Magnetic Associated Cell Sorting

M-CSF, Monocyte/Macrophage Growth Factor

mDC, myeloid DC

MDDC, Monocyte-Derived DC

MDR-1, Multi-Drug Resistance Type-1

MHC, Major Histocompatibility Complex

MIP, Macrophage Inflammatory Protein

mIR, micro-RNA

MOG, Myelin Oligodendrocyte Glycoprotein

mRNA, messenger RNA

MS, Multiple Sclerosis

mTOR, Mammalian Target of Rapamycin

M-tropic, Macrophage

N, New

Nef, Negative Factor

Neg, Negative

NF-κB, Nuclear Factor Kappa Beta

NIAID, National Institute of Allergy and Infectious Diseases

NIH, National Institutes of Health

NK, Natural Killer

NKT, Natural Killer –T-cell

NNRTI, Non- Nucleoside Reverse Transcriptase Inhibitor

NO, Nitric Oxide

NRTI, Nucleoside Reverse Transcriptase Inhibitor

nTh17, natural Th17

nTreg, natural Treg

O, Outlier

p24, protein 24

P, Putative

PBMC, Peripheral Blood Mononucleated Cells

PBS, Phosphate-Buffered Saline

PCR, Polymerase Chain Reaction

PD-1, Programmed Death 1

pDC, Plasmacytoid DC

PGE2, Prostaglandin E2

PHAC, Public Health Agency of Canada

PIC, Pre-integration Complex

PKC, Protein Kinase C

PLZ, Promyelocytic Leukemia Zinc Finger

PMA, «Phorbol Myristate Acetate»

pol, Polymerase

PPARγ, Peroxisome Proliferator-Activated Receptor Gamma

PrEP, pre-exposure prophylaxis

PIAS3, Protein Inhibitor of Activated STAT3

PSGL, P-Selectin Glycoprotein Ligand-1

PTEFB, Positive Transcription Elongation Factor B

RA, Rheumatoid Arthritis

RANBP2, RAN Binding Protein 2

RANTES, Regulated upon Activation Normal T-cell Expressed and Secreted

R4, CCR4

R5, CCR5

R6, CCR6

Rev, Regulator of Expression of Virion

RNA, Ribonucleic Acid

RPMI, Roswell Park Memorial Institute

RORγt, Retinoic Acid Related Orphan Receptor gamma t

ROS, Reactive Oxygen Species

RUNX1, Runt-Related Transcription Factor 1

sCD14, Soluble CD14

SAMHD1, Sterile alpha motif domain- and HD domain-containing protein 1

SCARB1, Scavenger Receptor Class B type-1

SEB, Staphylococcal Enterotoxin B

SHIV, HIV-SIV Hybrid Virus

siRNA, Small Interfering RNA

SIV, Simian Immunodeficiency Virus

SLAN, 6-sulfo LacNAc

SLE, Systemic Lupus Erythematosus

SM, Sooty Mangabey

STAB1, Stabilin-1

STAT, Signal Transducer and Activator of Transcription

SOCS3, Suppressor of Cytokine Signaling-3

SOX5, SRY-related high-mobility-group-box 5

Tat, Trans-Activator of Transcription

Tbet, T-box transcription factor expressed in T cell

TCF-1, T-Cell Factor 1

$T_{CM,}$ Central Memory T-cells

TCR, T-Cell Receptor

$T_{EM,}$ T effector memory

TEM, Tie2-Expressing Monocyte

Tfh, Follicular Helper T-cells

TGF, Transforming Growth Factor Beta 1

Th, T Helper

TLR, Toll-like-receptor

TM, Transitional Memory

TNF, Tumor Necrosis Factor

TNPO3, Transportin 3

T_R1, T Regulatory Type 1

Treg, Regulatory T-cell

TRIM5, Tripartite Motif 5

tRNA, Transfer RNA

T_{SCM}, Stem Memory T cells

T-tropic, T-cell Tropic

T_{TM}, Transitional Memory T-Cells

$T_{TE,}$ Terminally effector T-Cells

TWIST1, Twist Family bHLH Transcription Factor 1

USA, United State of America

Vif, Viral Infectivity Factor

Vpr, Viral Protein R

Vps, Vacuolar Protein Sorting

Vpu, Viral Protein U

Vpx, Viral Protein X

YPD, Yeast Peptone Dextrose

X3, CXCR3

X4, CXCR4

α, alpha

β, bêta

ºC, degré Celsius

δ, delta

γ, gamma

μ, micro

θ, Thêta

%, percent

ACKNOWLEDGMENTS

I want to first thank God for the inspiration, passion and courage I was blessed with during the past 6 years. This has been an interesting journey that I will never forget as it irreversibly shaped my life. I have grown into a stronger person that is more eager to discover diverse facet of life.

I want to thank my supervisor and mentor, Dr. Petronela Ancuta, for her guidance, her passion as a scientist and her confidence in me. It has been a privilege to be your first graduate student. Even in dark periods, you never ceased to believe in me. Thank you for the time invested on teaching me how to be a scientist and guiding me in becoming a stronger and more mature person. I will always be grateful for the opportunity you gave me as a master and a Ph.D. student, allowing me to develop my scientific creativity. Despite the end of this chapter of my life, you will always remain my mentor, the one I will seek advice when needed.

In addition to Dr. Petronela Ancuta, I want to thank the members of my jury: Dr. Nathalie Arbour, Dr. Rupert Kaul and Dr. Cheolho Cheong for their time spent in reviewing my thesis. It has been an honor for me to have you as members of my Ph.D. defense committee.

Special thanks to the present and past members of Dr. Ancuta's lab, especially Dr. Patricia Monteiro and Dr. Marie-Claude Gaudreau who generated preliminary results that represented the prelude of my thesis. I would like to thank all of the colleagues and co-authors that helped me in generating results included in three manuscripts.

Special thanks to my colleagues of the CRCHUM from other labs for their scientific advise and for their time spent conversing with me. The list is long and I prefer not including names out of fear of forgetting one.

I want to thank my close friends, especially Maria Dimitropoulos, for being there for me when I needed the most. I don't think I would have made it through without your support.

Lastly, I want to thank my entire family, especially my grandmother and mother for whom I have the upmost respect and admiration. You have been supporting and encouraging me ever since I shared with you my ambition to become a scientist. You have been my rock and anchor during this adventure. Thank you for believing in me. I love you.

CAPTATIO BENEVOLENTIAE

Since the establishment HIV pandemics, a total of 39 millions of individuals have died from AIDS, the final clinical stage of HIV-infection associated with the failure of the immune system to control HIV and other opportunistic pathogens. Considerable achievements were made in recent decades in the field of HIV research, resulting in the discovery of conventional antiretroviral therapy that increased the life expectancy of HIV-infected individuals. Nevertheless, the antiretroviral therapy does not cure HIV nor does it restore the function of the immune system. Furthermore, HIV-infected individuals under treatment experience co-morbidities including cardiovascular disease and cognitive impairment. Therefore, the search and development for a cure aimed at the HIV eradication is the current goal in the field of HIV research. One of the main priorities in the field is to determine the mechanisms that contribute to the establishment and maintenance of latent infection. Here, this thesis focuses on two components of the immune system that HIV targets: the Th17 lineage and the myeloid dendritic cells. The purpose of this thesis is to provide a further understanding on the biology of the adaptive and innate immunes system and on the mechanisms by which HIV modulates host defense to promote its dissemination and persistence. Our discoveries will orient novel therapeutic strategies for the development of an HIV cure.

CHAPTER 1: INTRODUCTION

1.1 HIV INFECTION

1.1.1 HIV GENERALITIES

The human immunodeficiency virus type 1 (HIV) (Figure 1) belongs to the retroviridae family, member of the genus lentivirus (1). HIV causes acquired immune deficiency syndrome (AIDS), a disease associated to active viral replication, diminished T CD4 counts (<200 cells/µl), and susceptibility to multiple opportunistic infections. HIV was isolated the first time in 1983 from a lymph node biopsy of a patient suffering from lymphadenopathy by the group of Dr. Luc Montagnier and so was referred to as Lymphadenopathy Associated Virus (LAV) (2). In 1986, the retrovirus was formally named HIV by the International Committee on Taxonomy of Viruses (3). According to the World Health Organization (WHO), 35 million people lived with HIV at the end of 2013, and 2.1 million new cases of infection were reported the same year (4). In Canada, the Public Health Agency of Canada (PHAC) estimated that 71,300 people were infected with HIV or were living with AIDS at the end of 2011 (5). The HIV-1 infection is most widespread in African countries. This virus is the most pathogenic and infectious of all lentiviruses. Two types of HIV exist: HIV type 1 (HIV-1) and HIV type 2 (HIV-2). HIV-2 is genetically similar to the simian immunodeficiency virus (SIV) that infects its natural hosts, the sooty mangabey (SIV_{SM}), while HIV-1 is similar to the SIV infecting the non-human primate, the chimpanzee (SIV_{cpz}); both HIV-1 and SIV_{cpz} cause AIDS (6, 7). Worldwide, HIV-1 is the most pathogenic and predominant type of this virus. In addition, HIV-1 is easily transmitted and is mainly responsible for the AIDS pandemic. This virus is classified into four groups: M (main), O (Outlier), N (New), and P (Putative) (8, 9). The M group is the most preponderant worldwide and is divided into nine sub-types (A, B, C, D, F, G, H, J, K). Sub-type B is the most prevalent in North America. The other sub-types are observed in infected individuals from African countries. The N and O groups are rare and found in infected individuals from central Africa. Recently in 2009, a study identified a new type of HIV in a woman from Cameroon and was designated as group P (10).

In the past 30 years, the HIV research field has been marked with successes and disappointments. Discoveries regarding the biology, transmission, and pathogenesis have led to a better understanding of virus interaction with the host cell and targets for the development of antiviral drugs. Currently, with the findings of efficient antiviral treatments, HIV is not considered a lethal but manageable infection that has little effect on life expectancy. Nevertheless, HIV eradication is

not achieved with current antiretroviral therapies and a life-long treatment is a heavy burden for both the patient and the healthcare system.

1.1.2. HIV STRUCTURE

Retroviruses are positive-sense RNA viruses (80 to 120 nm diameter) that are generated from budding of infected cells (11). All retroviruses commonly encode for the enzyme reverse transcriptase, which is responsible for the generation of complementary DNA (cDNA), from an RNA template. HIV-1 particles are surrounded by a nucleocapsid and an external envelope constituted of phospholipid bilayer derived from the host cell membrane and viral glycoproteins gp120 and gp41. The gp41/gp120 complex forms a trimeric structure at the cell surface. The viral core encloses the matrix composed of viral protein p17. The matrix itself encloses the nucleocapsid constituted of viral protein p24 where two copies of positive-sense single-stranded RNA are located together with three virion-associated enzymes, reverse transcriptase, integrase and protease.

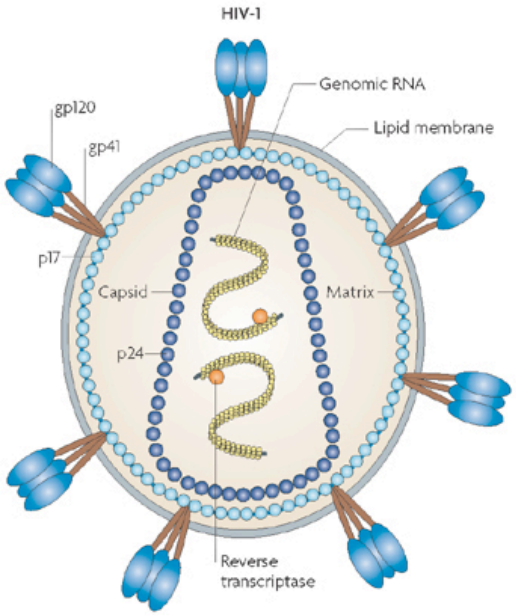

Figure 1: HIV-1 Structure. Shown are various components of the HIV-1 virions including the envelope proteins gp120 and gp41, the capsid protein p24, the two copies of single stranded RNA and the two molecules of the reverse transcriptase enzyme. Figure reproduced with the permission of Macmillan Publisher Limited: Nature Reviews in Immunology (12) author copyrights 2008.

1.1.3 HIV-1 GENOME

The HIV-1 genome (Figure 2) is of 9.2kb length and is encoded for structural, as well as accessory genes (13). The structural genes are Gag (group-specific antigen), Pol (polymerase) and Env (envelop). The accessory genes are Trans-Activator of transcription (Tat), Regulator of expression of virion (Rev), Negative factor (Nef), Viral Infectivity Factor (Vif), Viral Protein R (Vpr), and Viral protein U (Vpu). The proviral DNA, or cDNA, that is integrated in the host genome, includes an U3-R-U5 identical sequence referred to as Long Terminal Repeat (LTR) at the 5' and 3' extremities. These sequences allow the viral DNA to integrate into the host genome.

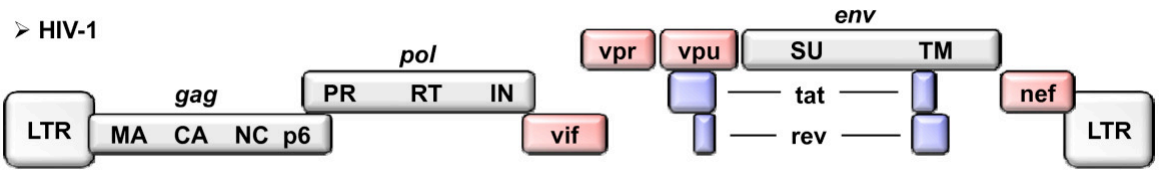

Figure 2: HIV-1 Genome. This figure illustrates the structural and accessory genes that compose the HIV genome. Figure reproduced with the permission of Retrovirology (14), author copyrights 2010.

The structural proteins Gag, Pol and Env code for the nucleocapsid, viral enzymes and surface proteins, respectively (11, 13). The *gag* gene is originally transcribed into a Gag-Pol precursor of 55 kDa, which will be cleaved into the matrix protein p17 and the nucleocapsid protein p24. The *pol* gene encodes for the viral enzymes protease, integrase, RNase H, and reverse transcriptase. The protease is responsible for the cleavage of polyproteins into functional proteins. The integrase forms the pre-integration complex (PIC) and mediates the integration of the viral DNA into the host genome. All viral enzymes are generated following the cleavage of the Gag-Pol poly-protein. This later precursor is translated after a ribosomal frame shift signal allowing for not only Gag but also Pol expression. The *env* gene is translated into a gp160 poly-protein precursor before getting cleaved into gp120 and gp41 *via* host cell proteases such as Furin (15, 16).

The accessory proteins are non-structural proteins that are very important for viral replication. Vif has a role in viral assembly and maturation (17). Vpr is involved in the induction of cell apoptosis, the disruption of cell-cycle regulation, the nuclear transport of the viral pre-integration complex as well as in the suppression of immune activation (18). Vpr was also reported to facilitate reverse

transcription and to transactivate the viral LTRs. Tat is a regulatory protein that activates viral transcription (19, 20). Rev is another regulating protein and is essential for the transport, stabilization, and translation of messenger RNA (mRNA) from the nucleus to the cell cytoplasm (21, 22). Nef is the most immunogenic accessory protein as it is involved in enhancing viral infectivity and cell apoptosis (23). Vpu is exclusively specific to HIV-1 and has a role in CD4 degradation and release of viral particles from the surface membrane of infected cells (24).

1.1.4 HIV TARGET CELLS

The HIV-1 targets the cells of the immune system, mainly $CD4^+$ T lymphocytes but also macrophages, monocytes, and dendritic cells (DCs) (25, 26). All these leukocytes express at their surface the transmembrane glycoprotein CD4which is used by HIV as the main receptor for entry (27). $CD4^+$ T-cells have important roles in orchestrating adaptive immune responses against various pathogens, including viruses. Macrophages, monocytes and DCs are antigen-presenting cells (APCs) and act as bridges between the innate and adaptive immune system (28). Originally, the HIV-1 tropism was characterized based on the type of infected cells. The M-tropic strains referred to viruses infecting macrophages, whereas the T-tropic strains referred to viruses infecting T-cells (29). In 1996, the chemokine receptors CCR5 and CXCR4 were identified as major co-receptors for HIV entry (30-36). This discovery led to the current classification of viral strains based on the type of co-receptor used for entry. Viruses using CCR5 as a co-receptor are now termed R5 strains, whereas viruses using CXCR4 are termed X4 strains (37). This classification is more suitable as it is now well established that the R5 and X4 strains can infect both T and macrophages.

1.1.5 HIV-1 REPLICATION CYCLE

The HIV-1 replication cycle involves two main phases: early and late (38) (Figure 3). Each step within these two phases has been further studied to identify antiviral targets for therapies that focus on stopping the viral replication cycle. The early phase includes the steps from viral entry into target cells until integration into the human genome. The late phase involves all steps from post-integration including transcription and translation of viral protein, assembly, and budding.

First, the virus interacts with the target cells *via* the binding of the viral glycoprotein gp120 to the CD4 receptor located on the cell membrane (38, 39). This interaction induces a conformational change in gp120 allowing the glycoprotein to bind to chemokine receptors, CCR5 or CXCR4. The later step is followed by a second conformational change of the gp120, which allows the release and implantation of gp41 into the cell membrane. The fusion between the viral and the cellular membrane occurs and allows entry of the virus to its target cell. The nucleocapsid penetrates into the cytoplasm and is degraded, releasing the two copies of single-stranded RNA and associated viral enzymes known as the reverse transcription complex that includes reverse transcriptase, integrase, protease, and accessory proteins. Reverse transcription then ensues and the RNA is retro-transcribed into double stranded DNA. The initiation of this step requires the host transfer RNA (tRNA), which serves as primers. Upon viral cDNA synthesis, the PIC is formed, involving the integrase, Vpr and cellular proteins such as LEDGEF (40). The viral double-stranded DNA is transported from the cytoplasm into the nucleus where integration into the host genome occurs *via* the integrase activity. The period from integration to viral transcription is undetermined. The integrated viral DNA likely stays in a latent form for years until reception of a signal initiating transcription. Spliced mRNA are produced and exported from the nucleus to the cytoplasm where translation takes place. The first proteins to be synthesized are Nef, Tat and Rev. The unspliced mRNAs, including sequences coding for precursors Gag, Gag-Pol and Env, are later transcribed, and their export is dependent on Rev expression. The gp160 precursor is translated followed by the translation of poly-proteins Gag and Gag-Pol. Once the translation step is completed, viral assembly ensues. Viral proteins associate with viral genome to form virions. The enveloped proteins are inserted into host cell membrane. Viral particles are then ready for budding. Maturation is still underway after budding with the cleavage of precursors into functional proteins, which is performed by viral protease.

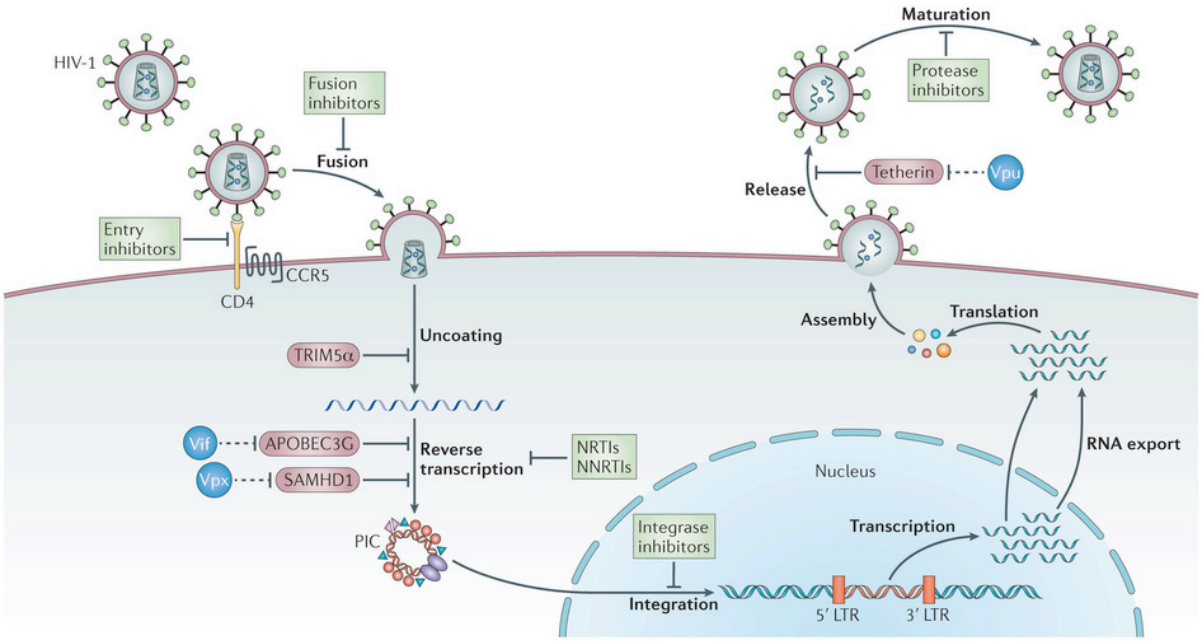

Figure 3: The regulation of the HIV-1 replication cycle by host factors and antiviral drugs. Shown are the multiple steps of the HIV replication cycle that are interrupted by host restriction factors and also steps targeted by current antiretroviral therapeutic strategies. Reproduced with the permission of Macmillan Publisher Limited: Nature Reviews in Immunology (41), author copyrights 2013

1.1.6 HIV-1 PATHOGENESIS

HIV-1 infection causes massive depletion of $CD4^+$ T-cell, leading to an impaired immune system incapable of mounting appropriate adaptive responses against HIV-1 and various opportunistic pathogens (42). Infection with HIV-1 is divided in three phases: acute, asymptomatic, and AIDS (42, 43) (Figure 4). The infection starts with a symptomatic acute phase that may last a few weeks and is characterized by active viral replication, establishment of viral reservoirs, and important depletion of $CD4^+$ T-cells in the peripheral blood as well as the intestinal mucosal tissues. At the end of the acute phase, the viral replication temporarily decreases as the specific immune response mediated by the cytotoxic $CD8^+$ T-cells and B cells are developed, allowing a partial restoration of peripheral $CD4^+$ T-cell counts. The asymptomatic phase, also referred to as the chronic phase, is associated to persistent viral replication, chronic immune activation, and progressive depletion of $CD4^+$ T-cells. The AIDS phase is declared when the $CD4^+$ T-cell count is equal or lower than 200 cells/µl. This phase is associated with an increase in the viral load as well as the occurrence of

opportunistic infections and cancers. All these three phases are clinically distinct as detailed below.

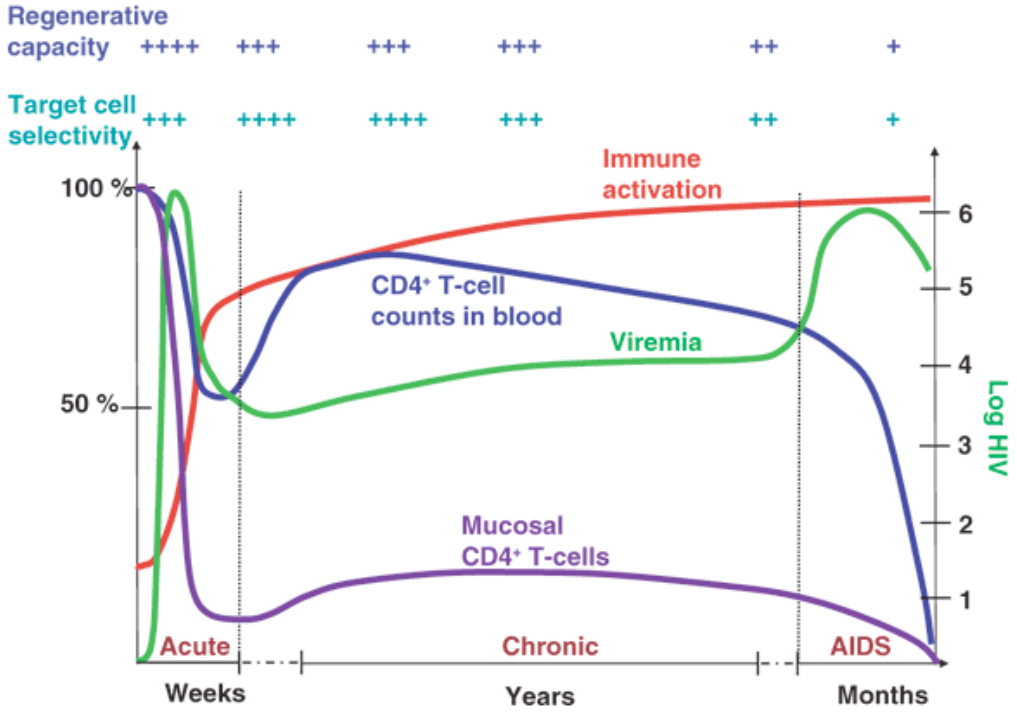

Figure 4: The clinic phases of HIV-1 pathogenesis. Shown are the three major clinical phases of HIV-1 disease progression. Changes in mucosal and blood $CD4^+$ T-cell counts, as well as levels of immune activation and viremia are illustrated. The figure is reproduced with the permission of Macmillan Publisher Limited: Nature Medicine (43), author copyrights 2006.

1.1.6.1 THE ACUTE PHASE

The HIV-1 mainly targets for infection $CD4^+$ T-cells located in the gastrointestinal and/or reproductive tract, leading to an important active viral replication in cells of these affected tissues (Figure 4). Active viral replication is generally associated with flu-like symptoms including fever, headaches and weight loss. The gastrointestinal tract is the lymphoid organ containing the majority (60%) of the T-lymphocytes of the body and is the main anatomic site of viral replication. During the acute phase, the infection initially affects activated $CD4^+$ T-cells expressing CCR5 leading to their massive depletion with the transmitted viruses being reported to exhibit a CCR5 tropism (R5 strains) (44, 45). This depletion is also observed in the subsequent phases of infection. Indeed, the majority of $CD4^+$ T-cells from mucosal tissues express CCR5 (>50%) with only ~15% of $CD4^+CCR5^+$ circulating in the peripheral blood (42). Viruses using CXCR4 as co-receptors

emerge later and expand the repertoire of target cells as the majority of $CD4^+$ T-cells express this chemokine receptor (46). The usage of CXCR4 is correlated to an accelerated progression to the AIDS phase. Variations in the peripheral blood $CD4^+$ T-cells do not always accurately reflect the true proportion of cells depleted in mucosal tissues (42). This large depletion of $CD4^+CCR5^+$ cells in the mucosa occurs within the first three weeks following infection and is associated with viral cytopathic effects that subsequently cause the death of infected cells. An impaired functionality of the innate response is also observed during the early phases of HIV-1 infection. The cytokine production by DCs is altered and the phagocytic activity of macrophages is exhausted (47, 48). The structural aspect of the gastrointestinal tract is significantly impaired following HIV-1 infection. Apoptosis of enterocytes and the disruption of tight junction are observed during acute infection and throughout the course of HIV-1 disease progression (48, 49).

The activation state of the $CD4^+CCR5^+$T-cells makes them susceptible to infection. Indeed, these target cells express early tissue-resident marker CD69 (50, 51) as well as other activation markers such as CD25, and Human Leukocyte Antigen- DR (HLA-DR) (42, 52 , 53 , 54). Cellular activation may be due to the increased presence of pro-inflammatory cytokines in the local environment. Furthermore, Nef, Tat, Vpr and Rev have the capacity to activate cells independently of signals coming from the T-cell receptor (TCR) (42). In quiescent cells, the virus can establish latency thus creating long-lasting cellular reservoirs for HIV-1. The establishment of cellular reservoirs occurs within the first weeks of acute infection. Among total $CD4^+$ T-cells, our group demonstrated that long-lived central memory (T_{CM}) and transitional memory (T_{TM}) $CD4^+$ T-cells are major HIV-1 reservoirs in subjects receiving viral suppressive antiretroviral therapy (ART) (55). At the end of the acute phase, viral replication is controlled by the development of the specific immune responses involving the $CD8^+$ T-cells and B-lymphocytes; this leads to a slight increase of the $CD4^+$ T-cell counts in the peripheral blood but not mucosal tissues in the absence of treatment (43).

1.1.6.2 THE CHRONIC PHASE

The chronic phase is mainly characterized by a persistent viral replication, increased levels of $CD4^+$ and $CD8^+$T-cell activation, and large production of pro-inflammatory cytokines (42, 43)

(Figure 4). Despite the viral load being at lower magnitude compared to observations in the acute phase, the $CD4^+$ T-cell count restoration is only partial in peripheral blood and in the mucosal tissues. The cellular activation level is thought to be a better forecast of disease progression rather than levels of viral replication (42, 56). Viral replication does not seem to be the sole responsible factor for cell depletion as only a small fraction of $CD4^+$ T-lymphocytes are infected (estimated range: 0.01-1%). Indeed, most depleted cells are not productively infected. Studies by *Greene et al.* demonstrate that integrative infection is compatible with survival, while abortive infection leads to cell death by pyroptosis (57). In contrast, reports by *Cooper et al.* support the opposite concept that integrative infection causes cell death (58). Unpublished observations in our laboratory demonstrate that while a small fraction of $CD4^+$ T-cells carry integrated HIV-DNA, a significant fraction of both naive and memory $CD4^+$ T-cells carry early HIV reverse transcripts in aviremic subjects receiving ART (*Niessl et al.,* manuscript in preparation). The later findings support the idea that abortive infection contributes to alterations in $CD4^+$ T-cell counts and functions despite viral suppressive ART (59). In addition to infection *per se*, recent findings suggest that chronic activation of the immune system leads to rapid T-cell turnover, clonal exhaustion and cell death. Evidence showing that chronic immune activation is a key pathogenic factor of disease progression comes from findings in primate models of SIV pathogenesis (60-62). Infection with SIV in natural hosts, such as Sooty mangabeys, does not progress into AIDS as opposed to the Asian or Indian rhesus macaques, known as non-natural hosts. Despite the observed high viremia, the activation and inflammation level in SIV natural hosts is relatively low. The $CCR5^+CD4^+$ T-cells are preserved. The integrity of mucosal barrier is maintained, preventing microbial translocation. Furthermore, the viral burden in tissues is low. Microbial translocation was designated as one of the key factors driving chronic immune activation (49, 56, 63). The increased enterocyte apoptosis, together with the disruption of the intestinal epithelial tight junctions and the loss of Th17 cells conferring protection against bacterial infections, were reported to promote microbial translocation in HIV-infected subjects. Several mechanisms leading to cell depletion involve: *i)* the gradual reduction of the T memory pool caused by the continual cellular activation, *ii)* the increased levels of broad naive T-cells differentiating into memory T-cells, *iii)* the decrease in the frequency of resting T-cells due to constant activation state, and *iv)* the reduced ability to generate naive T-cells pools from lymphopoietic sources (42). Moreover, HIV infection creates dysfunction in the thymus leading to a reduced output in the generation of

naïve $CD4^+$ lymphocytes (64, 65)). Furthermore, viral replication and chronic immune activation may be responsible for the observed abnormal structure in lymph nodes associated with the loss of $CD4^+$ T-cells and collagen deposition (66, 67). Abnormal structures of the thymus and bone marrow were also documented (42). The CD4/CD8 ratio is altered as the $CD8^+$ population is expanded and the frequency of $CD4^+$ T-cells is diminished (42, 68). Indeed the CD4/CD8 ratio is a useful marker to predict disease progression, $CD4^+$ T-cell depletion, and the size of HIV reservoirs (55, 69).

1.1.6.3 THE AIDS PHASE

The AIDS status is declared when the total CD4 count in the peripheral blood is lower than 200 cells/µl (68). This final phase is characterized by an increased viremia and massive depletion in peripheral blood $CD4^+$ T-cells (Figure 4). The immune system becomes weak and susceptible to several pathogens that are normally contained under homeostatic conditions. The opportunistic infections related to AIDS include pulmonary and esophageal candidiasis by *Candida albicans*, pulmonary infections by *Pneumocystis jirovecii*, *Pneumocystis carinii*, *Mycobacterium avium*, *Staphylococcus aureus*, *Escherichia coli* and *Pseudomonas aeruginosa*, viral infection by Cytomegalovirus (CMV), Human papilloma virus (HPV) and herpes simplex virus (HSV), encephalopathies by protozoan infections, and neoplasm such as cervical cancer and rectal Kaposi sarcoma (26). In the absence of antiretroviral treatment, the HIV-infected individuals develop AIDS and die within 10 years following primary infection.

1.1.7 TRANSMITTER FOUNDER VIRUSES

Transmission of HIV is mostly the result of heterosexual or homosexual intercourse. The establishment of primary infection is due to a single HIV-1 variant, referred to as transmitter/founder (T/F) viruses (70). During primary infection, the viral population is homogenous since the establishment of the infection results from one single T/F viral genotype. Once in the chronic phase, the HIV-infected individuals exhibit genetically heterogeneous viral population in their blood and tissues. The T/F viruses appear to have distinct features compared to the global viral population circulating in the periphery. The T/F viruses are thought to be compartmentalized in the genital tract where they undergo clonal amplification. In addition, T/F

viruses differ in their level of glycosylation. The T/F HIV from subtypes A, C, and D has few N-linked glycosylation in their envelope (71-73). An interesting study from *Ping et al.* observed that weakly glycosylated viruses were frequent during female to male transmission (73). Highly glycosylated viruses are unlikely to be sexually transmitted because they can be trapped in the transmission fluid or can be inhibited by host factors (70). The T/F viruses appear to have less glycosylation in the highly variable region of Env and are thus sensitive like other HIV variants to a broadly neutralizing antibody that normally targets the conserved region of Env (73). Furthermore, T/F viruses are mostly R5 strains as they use exclusively CCR5 for viral entry (70). Also, T/F viruses require high expression of CD4, which is found in CD4+T-cells. In fact, T/F viruses are less capable of infecting monocytes/macrophages. Moreover, compared to viruses in the chronic phase of infection, T/F viruses express more than two fold of the *Env* protein, indicating their efficient capacity for transmission (74). The T/F viruses also exhibit an increased binding to DC and are thus transmitted efficiently to $CD4^+$ T-cells. Selective pressure appears to induce T/F viruses that are highly replicative competent.

1.1.8 RESTRICTION FACTORS

During the course of viral replication, host innate immune defenses generate antiviral responses aimed at blocking critical steps of HIV-1 life cycle. These antiviral responses are mediated *via* specific proteins, referred to as restriction factors (75, 76). To date, four restriction factors have been reported and mechanistically characterized: Apolipoprotein B editing catalytic polypeptide-like 3G (APOBEC3G) (77), tripartite motif5 (TRIM5) (78), bone marrow stromal cell antigen 2 (BST-2) (79, 80), and Sterile alpha motif domain- and HD domain-containing protein 1 (SAMHD1) (81, 82) (Figure 3). Very recent studies identified a cellular membrane bound protein, SERINC5, as being a target for HIV Nef (83, 84), thus extending the panel of cellular restriction factors counteracted by viral proteins.

As part of an effort to determine the role of viral protein Vif, APOBEC3G was discovered (77) through experiments involving cell fusion of cells susceptible and resistant to HIV. The use of a cDNA screen database identified ABOBEC3G. The APOBEC3G is a cytidine deaminase targeting the reverse transcription step in resting $CD4^+$ T-cells and macrophages (76, 85-87). The enzyme is

incorporated into virions and causes deamination of cytidine residues leading to the production and insertion of deoxyuridine (dU) in the first strand of cDNA. The reverse transcriptase misreads the insertion of dU for thymidine during the synthesis of the second strand of cDNA resulting in the incorporation of adenine instead of guanine. This mutation consequently reduces the viral fitness. The insertion of dU in the first strand of cDNA itself can also lead to the activation of the cellular DNA repair machinery, specifically the uracil inducing total destruction of viral DNA. Independent of its deaminase activity, several studies suggest that ABOBEC3G can still block viral replication as shown in catalytically inactive mutants (88, 89). Indeed, ABOBEC3G was reported to inhibit steps of reverse transcription and integration by: *1)* decreasing the efficiency of viral RNA strand transfer; *2)* decreasing the interaction between tRNA and viral RNA, representing the first step of reverse transcription; *3)* preventing DNA elongation; and *4)* interacting with integrase, thereby preventing viral integration (86). Vif prevents APOBEC3G encapsidation in virions thus allowing for normal replication to occur (76, 85-87). Precisely, Vif simultaneously interacts with the restriction factor and an E3 ubiquitin ligase complex resulting in the ubiquitination and the subsequent degradation of APOBEC3G. Vif preferentially acts on newly synthesized APOBEC3G as pre-existing APOBEC3G are insensitive to Vif due to complex formations with other cell host proteins (90).

The TRIM5α was discovered using cDNA screen assays (78). Prior to the discovery, studies by *Hoffman et al*. using a pseudotyped HIV-1 virus bypassing viral entry demonstrated a blocking of HIV-1 replication in Old World monkey. Also, SIV infection was restricted in New World monkeys. This restriction was originally defined as genetic barrier and was called lentivirus susceptibility factor 1. TRIM5 belongs to the TRIM family characterized for their conserved motif structured known as the RBCC motif (86). The TRIM5 can be expressed in many isoforms among which only TRIM5α and TRIM5-Cyclophilin A (TRIM5Cyp) exhibit antiviral activity. TRIM5Cyp was discovered after TRIM5α by *Sayah et al.* in Old World monkeys (91). These researchers wanted to identify the restriction factor blocking viral replication in monkeys and found that TRIM5 was fused with cyclophilin A. TRIM5 inhibits viral replication at the early stages of the viral life cycle. TRIM5 binds to the viral capsid and induces premature disassembly thereby preventing reverse transcription (78). In addition, TRIM5 functions as a pattern recognition receptor and senses the viral capsid then alerts the innate immune response (92). Both

TRIM5α and TRIM5Cyp contain a RING (for *Really Interesting New Gene*) domain with E3-ubiquitin ligase activity (85, 86). The C-lectin domain, conferring capsid binding and specificity, differs in the two isoforms. The cyclophilin A domain is expressed in TRIM5Cyp instead of the PRYSPRY found in TRIM5α. The TRIM5 is species-specific and is not efficient against viruses infecting their natural host (86). For example, primate TRIM5α inhibits efficiently HIV-1 infection but fails to block SIV replication in monkey cells. Human TRIM5α is efficient against N-tropic murine leukemia virus but poorly blocks HIV-1 (86). Engineering a human TRIM5α mimicking primate TRIM5α functions is an avenue for generating new therapeutic approaches against HIV-1. Nevertheless, the delivery of such genes into human cells remains a challenge.

Other members of the TRIM family were reported to exhibit antiviral functions, including TRIM1, TRIM19, TRIM22, TRIM32, and TRIM34 (93); however, TRIM15 was identified as an adhesion molecule (94).

The BST-2 (for *Bone Marrow Stromal Cell Antigen 2*) also known as tetherin or CD317 is a trans membrane protein and targets the end stage of viral replication (85, 86). It was discovered that BST-2 physically binds and retains virions at the host surface membrane thereby inhibiting viral budding. Tethered virions have the fate to remain at the cell surface or to be degraded by a series of process involving the E3 ubiquitin ligase, BCA2 (95). Similar to TRIM5, BST-2 also triggers the innate immune response by inducing activation of the NF-κB signaling pathway (96, 97). HIV-1 evades the host's attempts to prevent viral release by expressing viral protein Vpu (85, 86). The accessory protein Vpu interacts with BST-2, leading to its degradation through proteosomal or lysosomal pathway (98-103).

The SAMHD1 is a Deoxynucleoside triphosphate triphosphohydrolase (dNTPase) that normally functions as a regulator of dNTP levels and DNA damage response (85, 86). SAMHD1 was discovered based on studies performed with SIV Vpx showing that expression of Vpx in human myeloid cells increased their permissiveness to HIV infection (82). Thus, Vpx, absent in HIV, was able to overcome a HIV restriction factor in these cells. In 2011, the teams of Benkirane and Skowronski discovered independently the HIV restrictive activity of SAMHD1 (81, 82). This restriction factor is ubiquitously expressed in various cell types including resting CD4+ T-cells,

macrophages, monocytes and DCs (86, 87). This restriction factor restricts viral replication by cleaving dNTPs into deoxyribonucleoside and triphosphate residues thus depleting the dNTP pools available for reverse transcription. Consequently, the HIV-1 genome is not reverse transcribed thus blocking viral replication. A second mechanism of action involves RNA degradation (76). The functions of SAMHD1 seemed to also evade the innate immune response involving the activation of IFN responses (86). Indeed, defects in SAMHD1 have been associated with Aicardi-Goutières syndrome (AGs), a genetic disorder characterized by the excessive production of type I interferon, which is responsible for the increase of unneeded immune responses (76). SAMHD1 is counteracted in HIV-2 by Vpx and in Rhesus macaque by Vpr. Of note, Vpx seems to be derived from Vpr gene duplication (76, 86). Vpx is also expressed in SIV strains infecting macaques (SIVmac) as well as red-capped (SIVrcm) and sooty mangabeys (SIVsm). The SIV Vpx is packaged into virions during assembly and interacts with SAMHD1 leading to its degradation by a process involving the E3 ubiquitin ligase complex and thereby allowing reverse transcription to occur. Vpx only acts on SAMHD1 in the nucleus but not in the cytoplasm (104). SAMHD1 is effective only in non-dividing cells such as macrophages, DCs and $CD4^+$ T resting cells. Because SAMHD1 fails to restrict replication in activated $CD4^+$T-cells (105), it has been suggested that the antiviral activity of SAMHD1 acts in combination with other unidentified cellular proteins or is regulated post-translation (87). The viral protein counteracting SAMHD1 during HIV-1 infection has so far not been identified. Studies indicate that HIV-1 uses host protein cyclin L2 to degrade SAMHD1 (106). Recently, *Ruffin et al.* demonstrated that the expression of SAMHD1 is decreased following activation of memory $CD4^+$ T-cells, leading to an increase susceptibility to infection *in vitro* (107).

1.1.9 HIV PERMISSIVENESS FACTORS

Similar to all viruses, HIV-1 exploits the host cell functions for its own survival. Several studies using multiple techniques (*i.e.,* siRNA screens, bioinformatics analysis, cDNA cloning, etc.) identified host proteins essential for specific steps of HIV-1 replication cycle (108). Blocking the expression of these proteins, known as permissiveness factors (or HIV-dependency factors, HDFs), inhibits viral infection. First, HIV-1 depends on the cellular glycoprotein CD4 and the chemokine receptors CCR5 or CXCR4 for entry (40) (Figure 3). Fusion does not only depend on

viral glycoprotein gp41 but also requires Rab6, a regulator of retrograde transport of the Golgi apparatus (109). Other factors, including glycosphingolipids which function as mediators of cell adhesion, were also reported to participate in this step (110-112). Once fusion is completed, the reverse transcription complex is released into the cytoplasm and binds to actin (40). The transport of the pre-integration complex (PIC) to the nucleus requires interaction with microtubules. HIV also uses the nuclear import factors Transportin 3 (TNPO3) and the RAN (*for RAs-related Nuclear protein*) binding protein 2 (RANBP2), along with nuclear complex component Nup153 for entry of the pre-integration complex into the nucleus (109, 113). Interaction of viral integrase with host TNPO3 and lens epithelium-derived growth factor (LEDGF) is needed prior to integration (40). Proviral transcription requires the viral regulatory protein Tat, which will form a complex with host cyclin-dependent protein kinase (Cdk9) and HIV-1 Tat specific factor (40), positive transcription elongation factor B (PTEFB), and the nuclear factor of activated T cells (NFAT) (114). HIV transcription also depends on mediator complex component Med28, consistent with its functions as a regulator of the RNA polymerase II transcripts (109). Furthermore, NF-κB binding sites within the viral promoter appear to be essential for transcription. HIV interacts with host class E Vps proteins as well as the late endosome trans-Golgi network transport factor Rab9 p40 in order to bud from cell plasma membrane (115, 116). Other proteins including those associated to autophagy, NF-κB signaling, vesicular transport, DNA-damage response, energy metabolism, mitochondrial functions, ubiquitination/proteasome pathway, nucleic acid, and cytoskeleton proteins seem to be implicated in viral replication (108). Validation assays aimed at confirming the role of this protein during HIV replication cycle will need to be performed. All of these proteins may be used as targets for novel therapies to block HIV infection.

1.1.10 FACTORS CONTRIBUTING TO HIV PERSISTENCE

Despite the discovery and use of the anti-viral therapy, which reduces significantly the viral load, HIV-1 continues to persist during the chronic phase of viral infection in cellular and anatomic reservoirs that are not completely characterized (117). A relationship between HIV and the immune system is established once the virus infects its host. HIV reservoirs are established in the very early stages of the infection (118). Studies in SIV models of infection demonstrate that viral reservoirs into the brain are established a few days upon SIV exposure (119). By extrapolation, the

early establishment of HIV reservoirs into distal tissues represents a major challenge for HIV eradication (120). So far, there is no identified surface biomarker to distinguish infected cells from uninfected cells (117). It is well established that HIV infection induces chronic immune activation and dysfunction, which in turn will lead to viral persistence thus creating a vicious cycle that is hard to break (42, 56, 117, 121). Several factors contributing to viral persistence have been identified. HIV preferentially infects activated $CD4^+$ T-cells as studies demonstrate that activated cells harbor higher levels of HIV-DNA compared to resting cells (122). The continuous presence of viral antigens stimulates the generation of HIV-specific $CD4^+$ T-cells that are prone to migrate into the replication site resulting in further infection. Indeed, *Douek et al.* demonstrated that HIV-specific $CD4^+$T cells are susceptible to HIV infection (123). Interestingly, activated cells during HIV infection are mostly specific for herpes viruses (121). The frequency of CMV-specific $CD4^+$ and $CD8^+$T-cells was found to be superior in HIV-infected individuals compared to age-matched HIV-uninfected subjects (124). Of note, CMV-specific $CD4^+$ T-cells were found to be relatively resistant to HIV infection as opposed to *Mycobacterium tuberculosis* in part due to the production of CCR5 ligands (125). Nevertheless, studies of PBMCs from untreated subjects with acute infection showed a positive association between CMV replication, immune activation, and HIV disease progression (126). Therefore, CMV infection is causing cell activation, immune dysfunction, and viral persistence. The damage in mucosal barriers induced by HIV is a source of inflammation that may also drive the migration $CD4^+$ T-cells into inflamed tissues, allowing further viral replication. Resting $CD4^+$ T-cells are poorly infected (121) probably due to SAMHD1 activity (105). HIV infection leads to increased production of pro-inflammatory cytokines and chemokines (*i.e.,* IL-2, IL-6, IL-12, IL-18, TNF, CCL19 and CCL21), which can act in combination, engendering viral susceptibility in resting $CD4^+$ T-cells and establishing latency (127-131). The production of anti-inflammatory cytokines such as IL-10 might also increase the establishment of latency (121). Known to restrain T-cell activation, IL-10 can act on activated cells that harbor HIV DNA and help cells return to a resting state thus contributing to viral persistence (132). Negative regulators of cell activation, including PD-1 and CTLA4, may also promote viral persistence by preventing cell apoptosis (121). PD-1 expression in $CD4^+$ T-cells was observed to be positively correlated with HIV-DNA (55, 133). Indeed, follicular helper T-cells (Tfh) characterized by the expression of CXCR5 and PD-1 are present in increased numbers during HIV infection in lymph nodes and harbor HIV-DNA (134-136). The $CD4^+$ T-cells,

identified as HIV cellular reservoirs, are the T_{CM} and T_{TM} (55). These cells have self-renewal capacities upon antigenic exposure and are long lived (137). Signals transduction pathways involving STAT5 and FOXO3a as well as the IL-7 signaling are required for the survival of T_{CM}. Furthermore, IL-7 and its role in the maintenance of homeostatic proliferation were reported to be the main mechanism promoting latency in T_{TM} and resting cells (121, 138). Effector memory cells (T_{EM}) of treated HIV-infected individuals are prone to harbor residual HIV-DNA. T_{EM} represent only 15% of total reservoir compared to T_{CM} and T_{TM} that comprise 85% of cells harboring HIV-DNA (121) Other T-cell subsets including the newly described stem T-cell memory (T_{SCM}), naive cells, hematopoietic precursors, as well as the γδ T-cells, may also represent alternative viral reservoirs (117, 120, 121). In addition to T-cells, antigen-presenting cells (APCs) may also contribute to HIV-1 persistence. Although still controversial, macrophages may represent a long-lasting viral reservoir (139-141). Novel therapies aimed at addressing these different factors responsible for the maintenance of viral dissemination need to be found.

1.1.11 HIV-1 TREATMENT AND CURRENT CHALLENGES

1.1.11.1 ANTIRETROVIRAL THERAPY

The introduction of antiretroviral drugs as treatment against HIV was a major breakthrough in an attempt to stop the numerous deaths caused by the AIDS pandemic. At the time when HIV was first discovered (2), the only drug available was the nucleoside analogue acyclovir, which was used against the herpes simplex virus (142, 143). Once phosphorylated, nucleoside/nucleotide analogues resemble cellular nucleotides and can be incorporated into the ongoing synthesis of the DNA strand. They act as chain terminators of DNA synthesis, blocking viral replication, and were considered good candidates to prevent HIV infection. In 1987, zidovudine (also known as AZT) became the first nucleoside reverse transcriptase inhibitor (NRTI) approved by the USA regulatory authorities (FDA, Food and Drug Administration) as a treatment against HIV-1 (144, 145). Originally synthesized in 1964, AZT was used as an anti-cancer drug, but the research quickly ceased due to deleterious effects observed on mice (146, 147). Strong activism and increased pressure by the gay community on government, pharmaceutical companies, and research agencies resulted in the rapid approval of AZT for the treatment of AIDS patients (148). Indeed, the clinical

trial was prematurely terminated after the observed beneficial effect on the survival of patients treated with this drug. Unfortunately, the benefits of AZT were short lived with the emergence of viral resistance (149). Following AZT, other NRTIs, such as didanosine and zalcitabine, were approved, in 1991 and 1992, respectively (148, 150). The scientific community sadly did not take into consideration lessons obtained from the development of tuberculosis treatments, and the antiviral drugs were not given in combination but as monotherapy. After extensive studies showing better effects compared to immunotherapy, dual therapies of two NRTIs were adopted. Nevertheless, the effects were only temporary due to the development of viral resistance. The treatments became durable with the use of a triple antiretroviral drug regimen, known as highly active antiretroviral (HAART), which was introduced in 1996 (151, 152). This new therapeutic strategy was possible due to the appearance of new classes of drugs: the protease inhibitor (PIs) in 1995 and the non-nucleoside analogue reverse transcriptase inhibitor (NNRTIs) in 1996 (148). Also, the discovery of new molecular technologies such as the polymerase chain reaction (PCR) served as a tool for the quantification of HIV-DNA and provided vital insights on viral dynamics (153). It was reported by using novel experimental techniques that HAART reduced the plasma viral load to undetectable levels. The HAART originally consisted of two NRTIs and one PI and was shown to prolong the lives of HIV infected subjects (151, 154, 155). The approval of non-nucleoside reverse transcriptase inhibitors (NNRTIs) offered an alternative option to PIs. In addition, NNRTIs production cost was less expensive than the one for PIs and could consequently be distributed in resource-poor countries (148). The entry of generics for antiretroviral drugs led to the availability of these drugs to African countries, where the disease burden is the greatest worldwide. The 2000 era brought new classes of antiretroviral drugs. The fusion inhibitor T20 was approved in 2003 (156, 157) and was followed by the introduction of Maraviroc, a CCR5-blocker inhibiting viral entry (158, 159) as well as the integrase inhibitor Raltegravir in 2007 (160, 161). The most recently released treatment, introduced in 2013, is another integrase inhibitor known as Dolutegravir (162, 163). The emergence of the new classes of drugs allowed for the maintenance of undetectable plasma viral loads in patients that developed a resistance to a

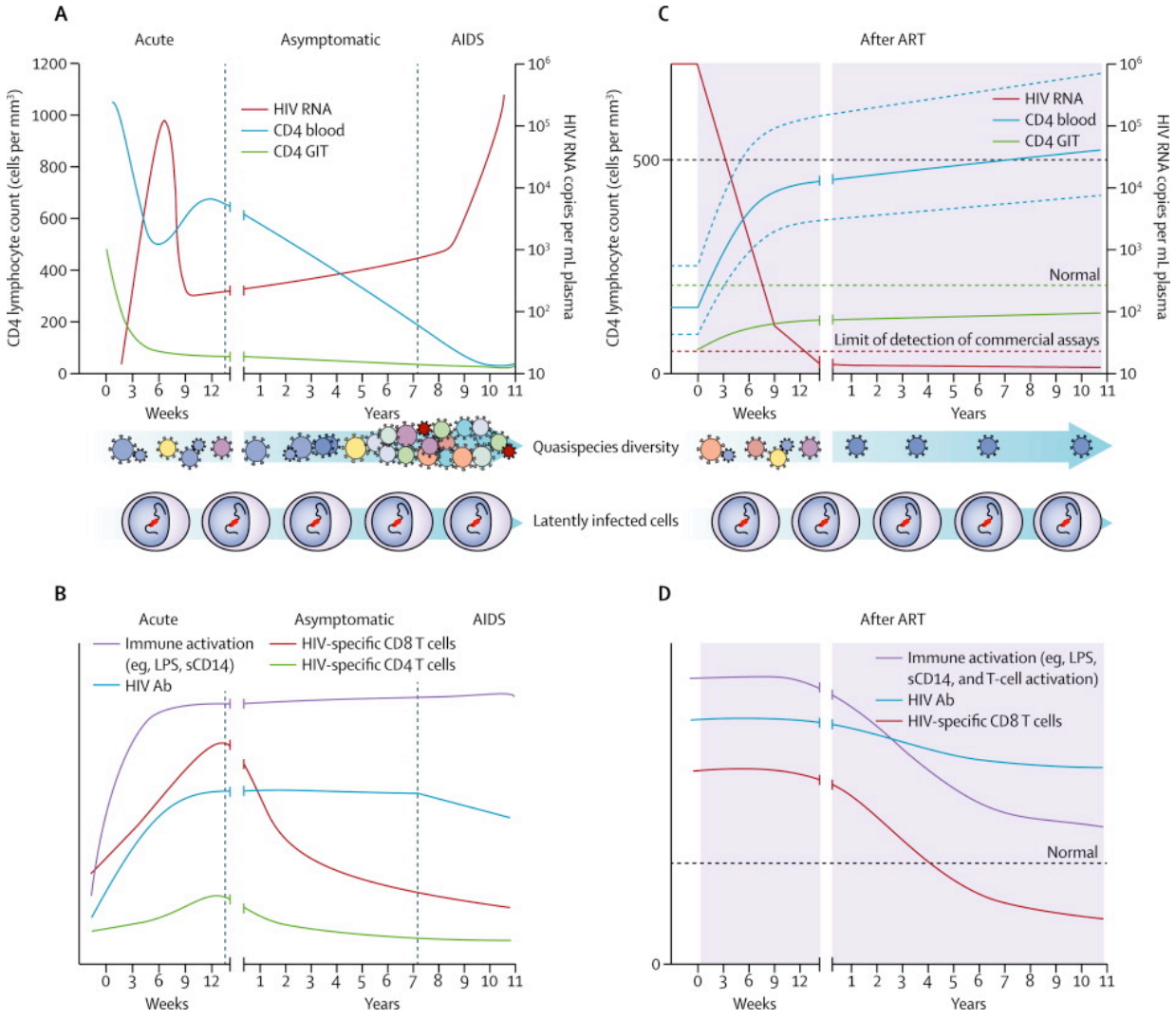

Figure 5: The effect in the absence or presence of ART. Shown in A and B are the dynamics of HIV pathogenesis in terms of viral load, CD4 count and chronic activation of the immune system. Shown in C and D are changes in HIV pathogenesis in the presence of ART. This figure is reproduced with the permission of The Lancet (164), author copyrights 2014.

particular treatment (148). There are now a total of 25 antiviral drugs available for treatment against HIV, drugs of six distinct classes targeting each step of the HIV replication cycle (Figure 3). Over the years, only two drugs, including the NRTI zalcitabine, were withdrawn because the clinicians no longer used them. Due to the efficacy, safety profiles and fixed-dose combinations of the ARV, the investment of pharmaceutical companies in the development of new classes of drugs has slowed down. Developing treatments focusing on new targets seems much more difficult. For example, drugs targeting viral attachment to CD4 and the step of maturation were not efficient enough to generate viral susceptibility (148, 165). Still, GlaxoSmithKline is in the process of

developing news NNRTIs and integrase inhibitors. Recently, the pharmacological booster cobicistat was added to the regimen for improved effectiveness (166). In addition, clinical practice guidelines have changed. In the early years following the discovery of the antiretroviral drugs, the infected patient would wait until their CD4 count reached 200µl/cells to receive treatments. Currently, a consensus was reached among the scientific community where diagnosed patients with HIV are treated as soon as possible (41). The discovery of ART has completely changed the health on HIV-infected individuals with the decrease of viral load, partial restoration of $CD4^+$ T-cells, and lower risk for opportunistic infections (Figure 5). Interestingly, antiretroviral drugs are also used to protect uninfected individuals at risk of being exposed to HIV, thereby preventing establishment of viral infection. This concept is known as pre-exposure prophylaxis (PrEP) (167). The regulatory authorities recently approved a PrEP that consists of two NRTIs, Tenofovir disoproxil fumarate and emtricitabine. The aim is to prevent and contain HIV transmission. Clinical trials reported that patients taking PrEP before participation in sexual activities are 86% protected.

Despite the major benefits of antiretroviral drugs in prolonging lives, the therapy does not cure HIV (117, 120). Treatments need to be taken regularly as interruption leads to a reemergence of viral replication. The virus still remains latent in cellular reservoirs (Figure 5). The HAART cannot prevent the establishment of cellular reservoir as this event occurs within the first few days following viral infection. Not all patients can tolerate HAART, which is associated with side effects. The possibility of developing drug resistance regiments remains an important issue. There is also a strong belief that HAART does not reach all anatomical sites where ongoing viral replication may occur. The brain is a perfect example. Several studies reported the presence of HIV genome in astrocytes and microglia (117, 168, 169). The antiviral drugs have difficulty in crossing the blood brain barrier (BBB) that acts as a filter blocking bacterial infections (170). Furthermore, HAART does not restore complete health in HIV-infected individuals (117, 120). The immune system is chronically activated and has not recovered from the massive loss of mucosal CD4+ T-cells. Importantly, HAART-treated HIV-infected individuals die from non-AIDS related morbidities including cardiovascular and renal disease, cognitive impairment, bone disorders, and cancers (171). Although the cost production and delivery of antivirals were significantly reduced over the years, they still represent an economic burden for many

organizations and the public health system of resource-poor countries (120). Thus, the need to find a cure is pressing. The characteristics of an HIV cure involve targeting the cellular reservoir as well as safety and low production cost for availability to all countries. Several strategies aiming at finding a cure were extensively researched, including the development of effective preventive and/or therapeutic vaccines.

1.1.11.2 VACCINES

The main goal of an HIV vaccine is to block acute viral infection, allowing sterilizing immunity in previously uninfected subjects. Another goal would be to decrease the viral load set point and peak in order to control ongoing replication in HIV infected individuals this providing an alternative to ART. The first clinical trial for a HIV vaccine began in 1986 (172). Since then, more than 250 reposted clinical trials have been conducted (173). The original concept for an HIV vaccine involved the development of neutralizing antibodies (174, 175). Thus, the first 10 years in this field were spent studying humoral anti-HIV immunity. Viral glycoprotein gp120 was used as target for the induction of broadly neutralizing antibodies (bNABs). The use of gp120 as immunogenic in clinical trials such as Vax003 and Vax004 was a complete failure in providing protection against viral infection and progression (176, 177). This disappointment led the scientific community to reevaluate the vaccine approach and instead direct their focus on HIV cellular immune responses. Evidence of the potential benefits of a vaccine targeting cellular immune protection came from studies in rhesus macaques in the context of SIV. In these studies, the T-lymphocyte immune responses generated following vaccination prior infection was critical in controlling viral replication (178, 179). The most promising clinical trial determining whether a vaccine promoting cell-mediated immunity could prevent or reduce viral infection was initiated by Merck in collaboration with the NIH and is known as HIV-1 Vaccine Trials Network (HVTN) 502/503 or STEP trials (174, 180). The HVTN is made up of a replication-defective adenovirus 5 vector expressing HIV-1 subtype B Gag, Pol and Nef. The vaccine was successful in preclinical and phase 1 trial and led to early decrease of viral load in primates challenged with HIV-SIV hybrid virus (SHIV) (179, 181, 182). Nevertheless, the clinical trial was abruptly terminated in 2007 because no effect on the prevention of infection or decreased viral load was observed when compared to placebo (183, 184). Unexpectedly, excess HIV infection was observed in patients

receiving the vaccine (174). Two years later, an interesting clinical trial known as the RV144 Thai trial consisted of a combination of two previously tested vaccines: the vC1521 canarypox vectored vaccine from Sanofi Pasteur and the AIDSVAX B/E gp120 subunit vaccine, which was included in the Vax003 and Vax004 trials. The vC1521vectored vaccine is composed of recombinant canarypox virus that expresses viral glycoprotein gp160 (185). A booster consisting of gp160 is also added to the regimen. Canarypox viruses restrictively infect avian species with poor effects on humans, and the recombinant form was reported to induce humoral and cell-mediated immunity in animals (186). The RV144 clinical trial was 31.2% effective in the prevention of HIV-1 infection thereby providing for the first time evidence of the ability of a vaccine to offer protection against HIV-1 acquisition (187). Antibodies against the variable region 1 and 2 (V1\V2) of gp120 with the production of env-specific IgA may contribute to the efficiency of the vaccine (188). Interestingly, the production of non-neutralizing antibodies involved in the antibody-dependent cell-mediated cytotoxicity (ADCC) process may also play an important role in the prevention of HIV infection. Based on the RV144 clinical trial, the scientific community believes that conceiving an HIV preventive vaccine is achievable (174). Still, key challenges preventing the establishment of an effective HIV vaccine will have to be addressed. For instance, the numerous viral subtypes and sequence diversity represent an issue in generating a protective vaccine. The fact that the HIV-1 reverse transcriptase is a highly error-prone enzyme may lead to changes in the Env sequence that can reach up to difference of 20% (189, 190) resulting in the lack of efficient neutralizing antibodies. Also, HIV envelope displays several N-linked glycosylation that shield the conserved epitopes, preventing antibody recognition (191-193). Furthermore, viral mutation can evade the established cellular immune response involving the HIV-specific $CD8^+$ T-lymphocytes capable of killing the infected cells upon interaction with viral antigens (171). Importantly, immune correlates of protection are still currently unknown and need further investigations (117).

1.1.11.3 ALTERNATIVE HIV CURE STRATEGIES

New approaches creating unique vaccine strategies are now being considered; this includes gene therapy as a curative intervention. The belief that HIV can be cured came from a case report in 2009 (120). A chronically HIV-infected patient treated with ART, by the name of Timothy Brown, also known as the Berlin patient, developed acute myeloid leukemia and successfully received an

allogeneic bone marrow transplant from a matched donor who was homozygous for the CCR5Δ32 allele (194). The CCR5 is a major HIV co-receptor (42). The CCR5Δ32 is a thirty-two base pair deletion mutation of CCR5 in which the cells do not express the chemokine receptor (195). Therefore, viral entry is blocked in individuals expressing the mutation because of the incapacity of gp120 to interact with CCR5 (195). Mr. Brown stopped ART following this transplant and was declared cured of HIV since no detectable viremia was observed in lymphoid tissues for four consecutive years (120). Similar interventions were performed on two HIV-infected patients known as the Boston patients (196). Unlike Mr. Brown, the Boston patients received bone marrow transplant from donors that expressed wt CCR5. Unfortunately, viremia reappeared following the intervention in the absence of ART. This failure clearly demonstrates the critical role played by CCR5 in HIV. Therefore, gene therapy appears as a promising strategy to eradicate HIV infection. Studies on inhibiting CCR5 expression or engineering cytotoxic $CD8^+$ T-lymphocytes capable of killing efficiently the infected cells are in progress (197).

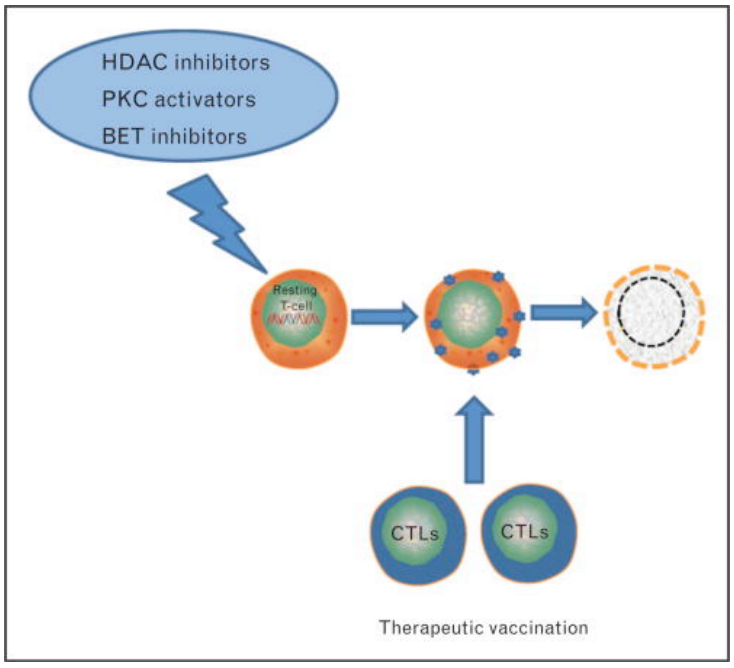

Figure 6: The *"shock and kill"* HIV eradication strategy. Shown is the schematic representation of the molecular and cellular events that may occur during *"shock and kill"* strategies aimed at HIV reservoir eradication. Reproduced with the permission of Lippincott Williams & Wilkins, Inc. (198), author copyrights 2014.

Another concept developed with the goal of eradicating HIV consists of the reactivation of the

latent virus in resting $CD4^+$ T-cells. This strategy is known as "*shock and kill*" or "*kick and kill*". Potential candidates to act as reactivation agents are histone deacetylase inhibitors (HDACi), bromodomain, extra terminal proteins inhibitors, and protein kinase C (PKC) (198). The HDACs play a role in the maintenance of viral latency. They are highly recruited in the promoter of the HIV genome (199). Studies on HDACis, such as vorinostat, were shown to disrupt viral latency and promote HIV transcription (200). Bromodomains are proteins that interact with acetylated lysine residues on histone and non-histone proteins (201). This function of bromodomains leads to histone acetylation, a process involving in HIV genome transcription. Recently, it was demonstrated that bromodomain containing 4 (BRD4) competes with viral Tat for binding with PTEFB thus delaying viral transcription (202-205). A bromodomain inhibitor molecule, JQ1, favors Tat and PTEFB interaction, resulting in efficient viral transcription. The effect was enhanced in the presence of HDACi (198). The PKC is involved in many biological processes, including cell proliferation and HIV replication (206). Activators of proteins such as prostratin and bryostatin was demonstrated to activate NFκB, that translocate into the nucleus where it will interact with NFκB binding site at the HIV promoter leading to viral transcription (198). The quantity and the cost in producing these PKC activators remain an issue. Further studies on the different potential reactivation agent will need to be performed before approval for use. The "*shock and kill*" strategy will not be efficient alone to eradicate HIV and so will probably be used in combination with an efficient vaccine or HAART on HIV-infected individuals (Figure 6). As an alternative to HIV reactivation studies, other groups are working on the opposite phenomenon to avoid viral reactivation by inducing latency. One example in this sense is the use of Tat inhibitors (207).

Since 1983, the scientific field of HIV research has significantly evolved with the currently available antiretroviral drugs able to prolong the lives of HIV-infected individuals. Finding a permanent cure remains the ultimate goal and hopefully will be achieved one day. The challenge of HIV eradication is amplified by our limited knowledge of the heterogeneity of HIV reservoirs in functionally distinct cell subsets where viral integration and latency may be regulated by complex and yet poorly understood transcriptional mechanisms.

1.2 BIOLOGY OF THE TH17 CELLS

1.2.1 HISTORY OF TH17 CELL DISCOVERY

The Th17 lineage is defined as $CD4^+$ T-cells producing mainly IL-17A and as the first line of defense against pathogens at barrier surfaces (208-210). The discovery of Th17 cells changed the Th1/Th2 paradigm that was in place for more than 20 years (211). In the 1970s, the basis for the Th1/Th2 paradigm was created with the studies of Christopher Parish that focused on understanding the capacity of the adaptive immune system to generate a specific response against a particular pathogen while being able to maintain tolerance to self-component and foreign antigens, such as commensal bacteria and food. Parish used the technique of acetoacetylation to induce tolerance to flagellin from *Salmonella adelaide* (212). Modifying the antigen decreased the primary immune response based on antibody production but resulted in an increased delayed-type hypersensitivity (DTH) reaction (213). The DTH was described as a reaction induced by cell-mediated immune responses and was associated with swelling, induration, and redness following the first few days of post-antigenic challenge (214). These studies provided the first evidence of cross regulation between humoral and cell-mediated immune response (215). Due to the lack of novel and appropriate technology, Parish and colleagues failed to ultimately prove the existence of at least two distinct T-cell populations responsible for the induction of humoral or cell-mediated immune response (211). The proof for this came in the mid-1980s when new techniques such as T-cell cloning and antibody-neutralizing assays were developed.

Tim Mossman's laboratory took advantage of these new techniques and identified two different types of T-cells capable of producing distinct cytokines (216). The Th1 cells were found to produce IL-2, whereas Th2 produced IL-4 known at the time as B-cell stimulatory factor-1 (BSF-1). In parallel, Bob Coffman's laboratory developed a specific assay detecting IgE production (211). Collaboration between the two groups led to the discovery that supernatants from Th2 but not Th1 helped B-cells produced IgE (217). The addition of both supernatants did not yield production of IgE suggesting that Th1 cells could block Th2 immune responses. Neutralizing antibody assays identified IFN-γ as the Th1 factor preventing Th2-mediated IgE production by B-cells and IL-4 as the Th2-associated growth factor responsible for the induction of IgE responses

(218). One year later, Mossman's lab discovered using a footpad-swelling assay that Th1 but not Th2 cells were the mediators of DTH reactions (219). The sum of all those discoveries led in 1986 to the description of the Th1/Th2 paradigm that involved the identification of two T-cell subsets with distinct immune responses (220). Th1 were described as lymphocytes producing IL-2 and IFN-γ involved mainly in cellular-mediated immunity against intracellular pathogens and responsible for causing tissue damage as well as the induction of IgG2a production by B-cells. Th2 were characterized as cells producing IL-4 that mainly mediate the humoral immune response involving allergies, eosinophilic inflammation, IgE production, and clearance of extracellular pathogens. Both Th1 and Th2 cells, *via* their respective cytokines, were shown to cross-inhibit each other. The paradigm was further developed with the emergence of new findings. Produced by antigen-presenting cells (APCs), IL-12 was reported to be critical for Th1 differentiation (211). Indeed, IL-12 signals through Signal transducer and activator of transcription (STAT)4 and T-box expressed in T-cells (T-bet) leading to the production of the Th1 key cytokine IFN-γ and the inhibition of IL-4 expression (221-223). Th2 cells were found to be under the transcriptional control of STAT6 and Gata3, leading to IL-4 production and down regulation of IFN-γ (221, 222). The IL-4 was identified as the key cytokine critical for initiation of Th2 differentiation.

The Th1/Th2 paradigm changed in a remarkable way the perception of immunological processes, especially after failed attempts at proving the existence of suppressor cells causing inhibition of effector cell functions (224). The Th1/Th2 paradigm allowed for a better understanding of the reciprocal interaction between two T-cell subsets that are part of the adaptive immune system (211). It also provided further understanding of the peripheral tolerance to self-antigen, regulation of atopic disease, and the resistance versus susceptibility of the host upon interaction with intracellular pathogens such as *Leishmania major* (225). Unfortunately, there were flaws in the Th1/Th2 paradigm (211, 214). It could not explain events occurring in autoimmune diseases including arthritis and experimental autoimmune encephalomyelitis (EAE), a model used in mice to study human multiple sclerosis (MS). Based on the Th1/Th2 paradigm, administration of IFN-γ in a mouse suffering from EAE would worsen the disease. Conversely, blockade of IFN-γ would attenuate symptoms and improve the health of these animals. These predicted assumptions could not be confirmed using the EAE mouse model, and in fact experiments suggested the opposite. Injection of IFN-γ in the EAE mouse model decreased the symptoms associated to the disease

(226). In parallel, the administration of a neutralizing antibody against IFN-γ into EAE-resistant mice rendered the animals susceptible to the disease (227). Disruption or deletion of the IFN-γ or IFN-γ-receptor gene in mice resistant to EAE led to severe susceptibility to the disease (228, 229). Animals depleted of other molecules associated with Th1 differentiation such as STAT1 and IL-12β2 receptor were also shown to develop severe symptoms related to the disease (230, 231). Additionally, contradictory data regarding the Th1/Th2 paradigm came from studies using T-bet deficient mice and adoptive transfer. Preventing T-bet expression led to resistance to EAE in mice previously immunized with MOG peptide, an inducer of the disease (230). Adoptive transfer of Th1 cells into mice or rats immunized with MOG peptides resulted in the induction of EAE. In addition, inhibition of IL-12 expression by the use of neutralizing Abs against IL-12p40 or IL-12p40 knockout mice suggested that IL-12 was essential in promoting EAE (232, 233). These findings led to the conclusion that there were pieces missing to the puzzle, and an unknown factor other than Th1 cells may be causing tissue-damage in the context of autoimmune disease.

The discovery in 2000 of a cytokine chain called p19 that associates with IL-12p40 helped answer questions surrounding the links between the Th1/Th2 paradigm and autoimmune disease (234). The association of p19 and IL-12p40 formed a distinct cytokine from IL-12 and was named IL-23. The IL-12 consists of an interaction with subunit p35 as opposed to p19 and IL-12p40 (211). Furthermore, differences in receptor interaction distinguished IL-23 from IL-12. The IL-23 interacts with IL-23R and IL-12Rβ1, referred to as the IL-23R complex, whereas IL-12 interacts with its receptor consisting of IL-12Rβ1 and IL-12Rβ2 chains. It was originally believed that IL-12 and IL-23 complemented each other and acted at different time points during Th1 differentiation. Moreover, distinct stimuli induced production of IL-23 and IL-12 from DCs. While microbial products could induce IL-12 production, anti-CD40, Adenosine Triphosphate (ATP), and PGE2 stimulation on DCs were reported to induce the production of IL-23 (235, 236). In 2003, *Aggarwal et al.* showed that IL-23 acts on $CD4^+$ T-cells and triggers the production of IL-17, a cytokine that was not expressed by Th1 and Th2 clones (237) (Figure 7). A month later, experiments performed by *Cua et al.* demonstrated that IL-23 but not IL-12 was responsible for the induction of EAE (238). A series of studies showed that IL-17 producing cells, driven by IL-23, were responsible for the induction of EAE (239, 240). Interestingly, cells producing IL-17 conferred protection against extracellular pathogens such as *Klebsiella pneumonia* (241). In 2005,

the scientific community agreed on the identification of a new subset of $CD4^+$ T-cells distinct from Th1 and Th2 lineages with the ability to produce IL-17, and this novel lineage was referred to as Th17 cells (242, 243) (Figure 7). At this time, many other T cell lineages have been described including regulatory T cells, Th9, and Th22 (244-246), but they do not represent the focus of the current thesis. It is to be anticipated that the constantly evolving technological advances will allow in the future the identification at the single cell level of other novel T-cell lineages.

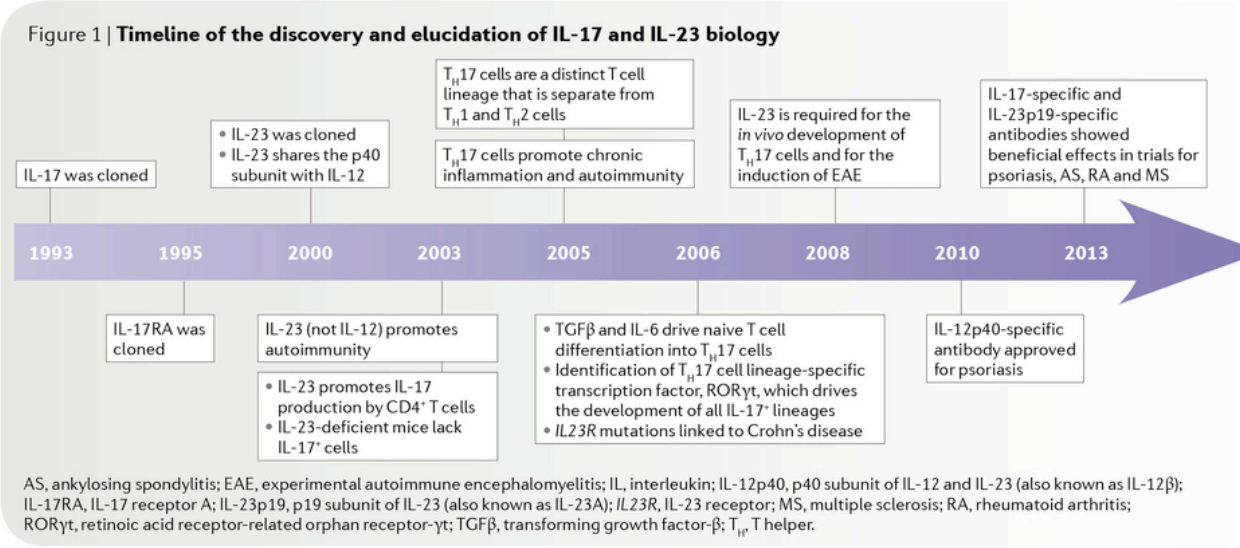

Figure 7: History of Th17 lineage discovery. Shown are the main discoveries from the cloning of IL-17 to the design of therapeutic strategies against autoimmune conditions, therapies aimed at blocking effector cytokine produced by Th17 cells (IL-17) or cytokines involved in Th17 differentiation (IL-23). This figure is reproduced with the permission of Macmillan Publisher Limited: Nature Review Immunology (210), author copyrights 2014.

1.2.2 TRANSCRIPTIONAL REGULATION OF TH17 DIFFERENTIATION

A T-cell population is considered a distinct lineage when it expresses specific effector functions under the control of unique transcriptional regulators. In addition to IL-17A, Th17 cells produce IL-17F, IL-21, IL-22, IL-26, IL-8, and CCL20 (210) (Figure 8). In 2006, shortly after the acknowledgement of the existence of Th17 (242, 243), associated transcription factors characterizing this newly found lineage of effector cells were identified (Figure 7). Two different approaches led to the identification of RA-related orphan receptor (ROR) gamma t (RORγt) as the master transcriptional regulator for Th17 cells (247, 248). The first approach involved genome-wide transcriptional profiling of activated splenocytes stimulated with IL-23 in comparison to

generated Th1 cells (247). The second approach consisted of the use of engineered mice linking GFP to RORγt expression (248). Only cells positive for GFP were shown to express IL-17A. Furthermore, mice deficient for RORC, the gene encoding RORγt, could not generate Th17 cells and showed less susceptibility to EAE (248). Conversely, overexpression of RORC in naive cells led to increased expression of Th17 lineage-specific cytokines. The RORγt is expressed in mice, whereas its homologue RORC2 is the master regulator for human Th17 cells (249). Although RORγt is the master regulator for Th17 differentiation, other transcription factors were later found to be essential for the development of the Th17 cells, including STAT3, Basic leucine zipper transcription factor ATF-like (BATF), interferon regulatory factor 4 (IFR4), aryl hydrocarbon receptor (AhR), and RORα (250-255) (Figure 8).

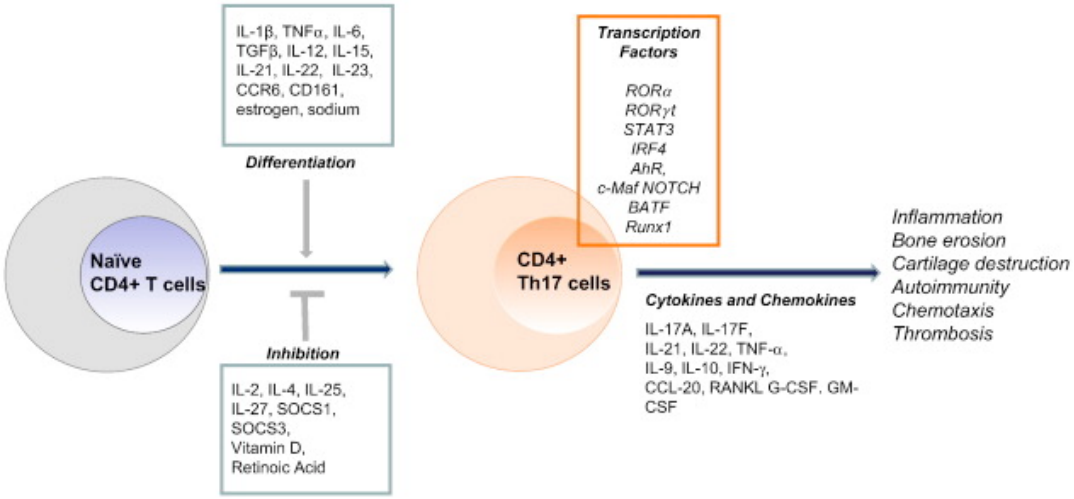

Figure 8: The Th17 differentiation program. Shown are molecular mechanisms involved Th17 differentiation from naïve $CD4^+$ T-cells and effector cytokines produced by Th17 cells that are involved in the pathogenesis of various pathological conditions. This figure is reproduced with the permission of Elsevier: Autoimmunity Reviews (256), author copyrights 2014.

Among cytokines involved in Th17 polarization, TGFβ and IL-6 were originally identified as being critical for Th17 development in mice (210). In fact, IL-6 was shown to signal through STAT3, leading to the production of IL-17A, IL-17F, and IL-21 (250, 257). This STAT3 is also one of the first transcription factors to be up regulated within the first hours of Th17 polarization (258). Using chromatin immunoprecipitation followed by sequencing (CHIP-seq), *Durant et al.* demonstrated that STAT3 directly regulates the gene of IL-17A, IL-17F, and IL-23R and controls the expression of RORC, BATF and IRF4 (257). The STAT3 is known to increase RORγt expression (248). In addition, STAT3 was shown to interact with the promoter regions of *il17a*

and *il17f,* as well as their intergenic regions that have enhancer elements undergoing histone modification during differentiation. Studies in the context of autosomal dominant hyper-IgE syndrome (HIES, also called Job's syndrome) characterized by mutations in STAT3, demonstrated the critical role played by this transcription factor in regulating IL-17A/IL-17F production (259, 260). The HIES is characterized by a dominant negative mutations in *stat3* gene, resulting in the deficiency of Th17 lymphocytes and impaired host defense against pathogens controlled by Th17 immune responses including *Candida albicans* and *Staphylococcus aureus*. BATF belongs to the FOS-like AP1 family of transcription factors and acts as a positive regulator for RORγt, IL-17, and IL-23R expression (210). Although mice deficient for BATF express similar levels of RORγt compared to wild-type (WT) at early stages of Th17 differentiation, RORγt expression is only temporary and is not maintained during complete Th17 development (251). Partial restoration of IL-17-producing cells in BATF$^{-/-}$ animals was observed with overexpression of RORγt, suggesting that both BATF and RORγt drive Th17 differentiation. BATF dimerizes with the transcription factor AP-1 and binds to the promoter regions of *il17a, il21* and *il22* genes. Originally described as a Th2 regulator, IRF4 was found to contribute to Th17 development (252). Mice deficient in IRF4 showed resistance to EAE linked to defect in Th17 differentiation, a defect independent of RORγt expression. Similar to BATF, overexpression of RORγt in IRF4$^{-/-}$ mice partially restored Th17 development, indicating that RORγt and IRF4 cooperatively control Th17 differentiation. *Ciofani et al.* observed that BATF and IRF4 function as pioneer transcription factors, governing initial chromatin accessibility that allows RORγt recruitment and interaction with Th17-relevant genes (261). STAT3 forms a complex with BATF and IRF4, resulting in the recruitment of RORγt that up regulates Th17-related genes while suppressing the fate of Th1 and Th2 lineage. Of note, the transcription factors included in the complex regulate DNA-binding activities of each other and together control cell fate commitment (210, 262). Therefore, RORγt is not the sole regulator of Th17 development. The association between BATF and IRF4 occurs only in TCR-activated cells (261). Dependent on its interaction with specific agonist FICZ, AhR acts as a booster for Th17 differentiation (253, 254). Although AhR-/- mice still comprise Th17 cells, they lack the ability to produce IL-22 (254). RORα was also shown to interact with RORγt (255). However, the function of RORα in Th17 development remains unknown. Recently, other transcription factors were found to be positive regulators of Th17 differentiation; these include c-Maf, SRY-related high-mobility-group-box (Sox5), Aiolos, Ikaros, IκBζ, inhibitor of nuclear factor-κB kinase-α (IKKα), Runx1,

hypoxia-inducible factor 1 alpha (HIF-1α), and promyelocytic leukemia zinc finger protein (PLZ) (263-265). Apparently, c-Maf is required for the maintenance of the Th17 lineage and production of IL-21 (266, 267). Also, *Tanaka et al.* demonstrated that in combination with Sox5, c-Maf induces Th17 differentiation downstream of STAT3 (263). Aiolos is up regulated by STAT3 and Ahr following Th17 polarization (268). Aiolos promotes Th17 differentiation by silencing the *il2* locus, and IL-2 was found to inhibit Th17 development (269, 270). Ikaros prevents repressive chromatin modifications of *ahr*, *rorc, il17a* and *il22*, thereby promoting Th17-related gene expression upon polarizing cues (271). Also, Ikaros represses T-bet and the regulatory T-cell (Tregs)-specific transcription factor Foxp3. The IκBζ, is encoded by the Nfkbiz gene and is up regulated following IL-6 and TGF-β stimulation (272). The IκBζ interacts with RORγt and RORα, increasing IL-17 production. The Nfkbiz-/- mice are resistant to EAE due to a defect in Th17 differentiation. IKKα binds to the *il17a* locus and subsequently promotes gene transcription leading to IL-17A production upon Th17 polarization (273). The non-activated form of IKKα leads to reduced frequency of IL-17A producing lymphocytes. RUNX positively regulates Th17 lineage by inducing RORγt expression, interacting with this master regulator and the promoter region of *il17a* (274). HIFα functions as a sensor to hypoxia and is up regulated under hypoxic conditions and IL-6 signaling pathways involving STAT3 (210, 275). HIFα interacts and promotes *rorc* gene transcription and associates with RORγt to drive *il17a* transcription (275). PLZ was demonstrated to be important for Th17 differentiation and in the maintenance of CCR6 expression at the surface of Th17 cells (265). Most recently, the double susceptibility to *Candida albicans* and *Mycobacterium* species was associated with RORγt mutations in humans (276). Of note, in these human subjects, Th17 effector functions, but not CCR6 expression, were altered indicating that CCR6 expression is not dependent on RORγt (276). CCR6 is a well-established marker for Th17 cells, and its independence from RORγt demonstrates the complexity of the Th17 polarization program. All these advances in the molecular determinism of Th17 polarization provide a detailed understanding of the multiple mechanisms involved in this process, mechanisms that can be separated into at least two major steps: *(i)* **specification** of the polarization profile, and *(ii)* **induction** of effector functions (Dan Littman, Cell Symposium on Microbiota). Indeed, in humans, the existence of these two steps was first revealed by the demonstration that $CCR6^{+}IL\text{-}17A^{-}$ but not CCR6- T-cells can become $IL\text{-}17A^{+}$ under specific culturing conditions *in vitro* (277).

In contrast to positive regulators for Th17 differentiation, negative regulators such as lineage-specific transcription factor for Th1 (T-bet) and Treg (FOXP3) have been reported to suppress Th17 development. T-bet suppresses the Th17 lineage by inhibiting IRF4 expression and by competing with RORγt for RUNX1 binding (278, 279). FOXP3 directly binds to RORγt to prevent Th17 differentiation (280). It was also found that FOXP3 binding to RUNX1 also prevents Th17 development (274). The extensive list of negative regulators includes: T-cell factor 1 (TCF-1), Growth factor independent 1 (GFI-1), Interferon regulatory factor 8 (IRF8), Twist Family BHLH Transcription Factor 1 (TWIST1), peroxisome proliferator-activated receptor gamma (PPARγ), E-twenty six 1 (ETS1), E74-like factor 4 (ELF4), inhibitor of DNA-binding 3 (ID3), and Early growth response gene (EGR2) (264). TCF-1 interacts with the *il17a* locus, leading to gene silencing (281). TCF-1 also inhibits IL-7R expression, affecting Th17 survival capacity. GFI-1 suppresses Th17-related genes expression to promote Th2 differentiation (282), and IRF8 interacts with RORγt to shut down Th17 development (283). The complete mechanism used by IRF8 to suppress Th17 differentiation is still unknown. TWIST1 is induced following activation of the IL-6-STAT3 signaling pathways and acts as a regulator of Th17 differentiation by repressing *il6ra* gene expression (284). TWIST1-/- mice exhibit higher frequency of Th17 cells. Activation of PPARγ prevents the removal of repressor on the promoter region of RORγt (285), inhibiting Th17 differentiation without affecting Th1 or Th2 lineage development. In mice, ETS1 was shown to favor IL-2-STAT5 axis, shutting down Th17 differentiation (286). Another member of the ETS transcription factor family, ELF4, was also shown to regulate Th17 development in a different manner than ETS (287). The IL-6 and TGF-β signaling threshold to initiate Th17 differentiation was decreased in mice deficient in ELF4. Through unknown mechanisms, ID3 also repress Th17 differentiation as $ID3^{-/-}$ animals expressed increased frequency in Th17 cells (288). EGR2 interaction with BATF prevents the formation of the transcriptional complex involved in the initiation of Th17 differentiation (289). Most of the studies cited above were performed using mouse models. Transcriptional regulators shown to be involved in human Th17 development include the positive regulators AHR, IRF4, c-Maf, BATF, and PLZ (261, 264, 265, 290, 291) and the negative regulators TWIST1, PPARγ, and EGR-2 (284, 285, 289). In conclusion, the modulation of Th17 development is tightly regulated and involves a set of transcription factors with specific functions at different levels.

1.2.3 SURFACE MARKERS DEFINING HUMAN TH17 SUBSETS

Pioneering studies by *Sallusto, Lanzaveccia et al.* demonstrated in 1997 that the chemokine receptor CCR3 was preferentially expressed on Th2 cells (292). Two years later, this same group reported that differential expression of CCR7, a chemokine receptor mediating trafficking into lymph nodes (293), together with CD45RA, a receptor-linked protein tyrosine phosphatase (294), identify subsets of $CD4^+$ and $CD8^+$ T-cell subsets with naive ($CCR7^+CD45RA^+$), central ($CCR7^+CD45RA^-$), and effector memory features ($CCR7^-CD45RA^-$) (295). In 2004, CXCR3 and CCR4 chemokine receptors were further reported to identify $CD4^+$ T-cell lineages with distinct polarization profiles and antigenic specificities (296): CXCR3 identified Th1 cells, while CCR4 expression characterized Th2 cells. The CXCR3 mediates cell migration into inflammatory sites, whereas CCR4 is a skin-homing marker. In 2007, two years after the official identification of human Th17 cells (242, 243), the chemokine receptor CCR6 was identified as the main surface marker characterizing the Th17 lineage (297-299). Murine Th17 cells were found to express CCR6 as well (300). The CCR6 plays a critical role in regulating Th17 trafficking into the gut (301)). Differential expression of CCR4, CCR6 and CXCR3 distinguishes functionally distinct Th17 subsets. The co-expression of CCR6 and CCR4 identifies human Th17 cells that homogenously produce IL-17A and proliferate in response to *C.albicans* and *S.aureus* (298, 302). The co-expression of CCR6 and CXCR3 identifies a heterogeneous population, known as Th1Th17 that produces both IL-17A and IFNγ (298). Precisely, Th1Th17 cells, also known as non-classical Th1 cells or Th1*, express RORC as well as T-bet and comprise a major fraction of Th1 cell producing IFN-γ and a minor population of cells expressing both IL-17A and IFN-γ (298, 303, 304). Th1Th17 cells were originally found to mediate immune responses against *M. tuberculosis* but were later reported to proliferate in response to *C.albicans* and *S.aureus* as well (298, 304, 305). Both human Th17 and Th1Th17 cells also express IL-23R, IL-1R, CD26 and CD161 at their surface (306, 307). Originally found to be expressed in natural-killer (NK) and NKT cells, the C-type lectin CD161 was also shown to identify Th17 precursors (308). As opposed to Th17 lymphocytes, Th1Th17 cells express at their surface the IL-12 receptor (303), suggesting their ability to respond to this polarizing cytokine. The fact that Th1Th17 shares features of Th17 and Th1 cells suggests the existence of a developmental relationship between the Th17 and Th1 lymphocytes.

The use of surface markers for the identification of Th17 subsets is instrumental in immune monitoring studies during disease pathogenesis and in response to treatment. However, the fact that not all $CCR4^{+}CCR6^{+}$ or $CXCR3^{+}CCR6^{+}$ T-cells produce IL-17A raised questions in the field regarding the possibility of overestimating the frequency of Th17 cells by using surface markers. Nevertheless the current understanding that Th17 polarization is a multistep process that can be grouped into at least two big steps: *(i)* specification of polarizing profile, and *(ii)* induction of effector functions, supports the finding that the use of effector functions (i.e., IL-17A production) leads to the underestimation of Th17 frequency. Indeed, studies by *Unutmaz et al.* demonstrated that sorted CCR6+IL-17A- have the ability to produce IL-17A upon signaling via cytokines (*i.e.,* IL-2, IL-7, IL-15) (277) further strengthening the use surface markers for the identification of Th17 subsets.

1.2.4 TH17 DIFFERENTIATION PROGRAM AND PLASTICITY

The IL-23 was originally described as the key inducer of pathogenic $CD4^{+}$ T-cells producing IL-17A (239, 240). However, it was later found that IL-23 alone does not drive Th17 differentiation but rather has a role in the lineage expansion, maintenance, and survival (309-311). This observation indicated that other components are involved in the induction of IL-17-producing cells from naive precursors. Several laboratories including the groups of Stockinger, Weaver and Kuchroo demonstrated that the presence of both TGF-β and IL-6 in the context of antigenic presentation promoted murine Th17 development (310, 312, 313). As mentioned previously, IL-6 signaling activates STAT3, which subsequently drives Th17 differentiation (250). The $IL\text{-}6^{-/-}$ mice are unable to generate Th17 cells and are resistant to EAE (210). IL-6 is currently being used as a target for treatment against RA and other inflammatory conditions. The need of TGF-β for Th17 differentiation remains controversial. Experiments involving inhibition of the TGF-β signaling complex and deletion of TGF-β gene on T-cells indicate that TGF-β is essential for Th17 development in mice (314-316). Nevertheless, deletion of TGF-β led to the substantial increase of IFN-γ and IL-4 production, suggesting that TGF-β shuts down Th1 and Th2 differentiation pathways (314, 315), allowing for Th17 development. In the absence of TGF-β, IL-6 alone can promote Th17 differentiation in cells deficient for T-bet and STAT6 (317), indicating that TGF-β indirectly induces Th17 development by restraining T-bet and GATA3 expression. The

controversial requirement of TGF-β in Th17 differentiation is further highlighted in human studies. Indeed, several groups demonstrated that a combination of IL-6, IL-1β and IL-23 is sufficient for the development of human Th17 cells (306, 318, 319) and that the requirement of TGF-β is not essential (247, 320). Similar findings were also reported in mice (321). The addition of anti-IL-4 and anti-IFN-γ Abs is important for Th17 polarizing studies from naive T-cells, consistent with IL-4 and IFN-γ being shown to inhibit IL-17A production (314, 315). In contrast, other researchers reported that TGF-β was essential for human Th17 differentiation (322-324), especially for the induction of T-cells producing homogenously IL-17A (323). In fact, the absence of TGF-β led to Th1Th17 generation (323). Other studies reported that the addition of TGFβ was needed for up regulation of RORγt expression but not IL-17A production (322, 325). Some researchers argue that it is difficult to exclude the importance of TGF-β in experiments involving *in vitro* induction of Th17 cells from naive precursors since low levels of TGF-β are known to be present in serum (322). TGF-β was previously shown to be a key factor in the generation of inducible T-reg (iT-reg) (326). The involvement of TGF-β in the development iTregs and Th17 cells appears to be counterintuitive. The current understanding is that high doses of TGF-β promote expression of FOXP3 that will repress RORγt, whereas low doses of TGF-β combined with IL-6 overcome FOXP3 repression of RORγt (209). Of note, the combination of TGF-β and IL-6 does not induce pathogenic Th17 cells (210). Subsequent cell exposure to IL-23 drives pathogenicity in Th17 cells (321, 327, 328). The IL-1β signaling is critical in Th17 differentiation as *il1r*-/- mice fail to generate antigen-specific Th17 cells and are protected from EAE (329). The expression of IL-R1 is induced in Th17 cells by IL-6, and signaling through this receptor leads to the expression of IRF4, which will strengthen RORγt function (330). IL-1β is important for the phosphorylation of mammalian targets of rapamycin (mTOR) that will increase the metabolic fitness of newly dividing Th17 cells under inflammatory conditions (331). Therefore, the presence of IL-1β is important for the expansion of the Th17 lineage in a cytokine environment where the differentiation of other lineage can occur. IL-21 is another important cytokine for the expansion of Th17 cells (267). In fact, IL-21 represents a key survival factor for Th17 cells (332) and may compensate for the intrinsic inability of Th17 cells to produce IL-2 (333). Studies by *Pallikkuth et al.* demonstrated that supplementation with IL-21 contributes to the restoration of Th17 cells in a simian model of AIDS (334). Of note, IL-21 is recognized as a key marker for follicular helper T-cells (Tfh)(335, 336), and thus IL-21 being produced by fractions of Th17 cells with Tfh features

remains one possibility.

The Th17 lineage plasticity is described as the ability of Th17 cells to acquire new effector features while losing their original identity as defined by the expression of RORγt and IL-17A (210). The plasticity of Th lineages depends on epigenetic modifications dictating the expression or repression of lineage-specific transcription factors (337). The epigenetic modification basically consists of permissive (H3K4me3) *versus* repressive (H3K27me3) histone marks (210). Although Th1 and Th2 cells are enriched in repressive histone marks for the *rorc* and *il17a* loci, Th17 cells exhibit both permissive and repressive marks on *tbet* and *gata3* (338). This observation suggests that Th17 cells have the capacity to acquire Th1 or Th2 features when exposed to specific polarization stimuli within their environment. Indeed, the plasticity of Th17 cells towards the Th1 program is well documented (209, 210, 339). Studies performed in mice and humans demonstrated the down regulation of RORγt/RORC, IL-17A, IL-17F, IL-22 and CCR6 as well as the up regulation of T-bet and IFN-γ in Th17 cells when cultured in the presence of IL-12 (297, 340-343). Th17 cells exposed to IL-12 co-express T-bet and at lower levels, RORγt as well as IL-17A$^+$IFN-γ$^+$ double positive cells (Th1Th17 profile). These Th17 cells with Th1 features are referred to as Th1Th17 (298) or most recently Th1* cells (276, 304) as mentioned earlier. Th1Th17 cells are considered pathogenic as they produce high levels of TNF-α and GM-CSF (239, 344). They are the main tissue-infiltrating CD4$^+$ T-cells in several inflammatory disorders such as RA, MS, and Crohn's disease (344, 345). Furthermore, fate-mapping reporter mice experiments demonstrated that IL-17A$^+$ producing cells became IL17A$^+$IFNγ$^+$ under EAE-associated inflammatory conditions (346). This shift was mainly mediated by IL-23. In humans, epigenetic studies also suggested that the Th1Th17 cells originate from Th17 cells (347). Nevertheless, other findings using TCRβ deep sequencing techniques in the context of antigenic presentation indicate that a fraction of Th1Th17 cells may originate directly from naive precursors without any transition through an initial Th17 stage (304).

Similar to IL-12 and IL-23, IL-1β was found to induce IFN-γ in Th17 cells. *Zielinski et al*. demonstrated that *C.albicans* but not *S.aureus* generated IL17A$^+$IFNγ$^+$ populations in humans Th17 cells and that priming of IL-17A and IFN-γ double-producing cells was mediated by IL-1β (302). Recently, TNF-α was also found to drive the shift of Th17 cells towards the Th1/Th17

subsets (348). The Th17 plasticity is not limited only to the Th1 axis as these cells were also shown to shift toward other lineages, including Th2, Tfh and Tregs (349-351). Memory $CCR6^{+}CD161^{+}$ Th17 cells exposed to a rich IL-4 microenvironment acquired the ability to produce Th2 lineage-specific cytokines including IL-4 and IL-5 while maintaining their ability to express IL-17A, IL-21, and IL-22 (349). These cells were referred to as Th17/Th2 cells and were detected in the peripheral blood of patients with chronic asthma. The Tfh development is still controversial and one of the proposed models involve the concept that a naive $CD4^{+}$ T-cell initially undergoes a Th1, Th2, or Th17 differentiation program before becoming a Tfh lymphocyte (335). In line with this model, fate-mapping reporter mice experiments demonstrated the shift of Th17 cells acquiring Tfh properties and thereby becoming able to help B-cell produce IgA (350). Although the shift of Treg towards the Th17 progeny has been observed (352, 353), only two studies found the ability of Th17 cells to transition into iTreg (351, 354). This conversion was dependent on a specific type of monocyte being able to produce high levels of TGFβ and retinoic acid (351). Pathogenic Th17 cells have been extensively described in the context of autoimmunity as being involved in the production of TNFα and GM-CSF (239, 355, 356). Recently, several reports performed in mice have described the presence of non-pathogenic Th17 cells that produce IL-10 and display immune-suppressive properties limiting tissue inflammation (355-360). There is growing experimental evidence supporting the concept that pathogenic Th17 cells can convert into nonpathogenic cells (355). Furthermore, a new study suggests that during the resolution of an immune response, Th17 cells lose their capacity to produce IL-17A as well as the expression of high levels of RORγt (354). These Th17 cells undergo transdifferentiation into T regulatory type 1 cells (T_R1) and acquire the ability to express IL-10 and T_R1 surface marker LAG-3. Therefore, accumulating data indicate that Th17 cells homogenously producing IL-17A do not represent end stages of memory T cell differentiation as they can further gain other effector functions associated with other T-cell lineages. This plasticity displayed by Th17 cells broadens their function and allows them to traffic in several anatomic locations to efficiently promote diversity in host defense.

1.2.5 ROLE OF TH17 CELLS IN IMMUNITY AT BARRIER SURFACES

Th17 cells play an important role in the induction of protective immunity against bacterial and

fungal infection at mucosal sites such as the gut, lung and the oral cavity. The number of Th17 cells in humans and mice is small under non-pathological conditions. Murine Th17 cells under a steady state reside within the intestine where they are generated due to the presence of specific members of the commensal microbiota, including the segmented filamentous bacteria (SFB) (361-363). SFB promote the production of serum amyloid A (SAA) and ATP, activating the lamina propria APCs to induce Th17 differentiation (361, 364, 365). The Th17-associated protective functions involve primarily the secretion of several cytokines such as IL-17A, IL-17F, IL-22, and IL-26.

IL-17A signals through its receptors IL-17RA and IL-17RC that are mostly expressed in non-hematopoietic cells such as the epithelial and mesenchymal cells (210). The IL-17 receptors are made up of conserved cytoplasmic motifs termed SEF/IL-17R (SEFIR) that interact with adaptor protein ACT1, activating downstream the NF-κB and MAPK pathways (Figure 9). The IL-17A signaling induces the production of the chemokines CXCL1, CXCL2, CXCL5, CXCL8 (also known as IL-8), which will result in recruitment of neutrophils. In addition, IL-17A leads to the production of CCL20 that will promote the recruitment of cells expressing CCR6. Th17 cells themselves produce CCL20 and CXCL8, attracting even more Th17 lymphocytes and neutrophils, respectively, at inflammatory sites (210, 366). Downstream IL-17A effector molecules also include IL-6, TNF-α, and G-SCF that regulate the biological functions of myeloid cell lineages, especially neutrophils. Interestingly, IL-6 acts in a positive feedback loop, amplifying Th17 differentiation. Furthermore, IL-17A is an inducer of antimicrobial peptides including the β-defensins and lipocalin 2 (LCN2) that prevent infection at mucosal surfaces (210, 367). Although IL-17A is a weak activator of signaling pathways, its activity is increased when combined with other cytokines/factors including TNF-α, IL-6, IL-22, IL-1β, IFN-γ, CD40 and LPS, for the regulation of target genes. The complete molecular basis explaining this synergy is still not well understood. However, studies suggest that the mechanism of synergy involves increase in the expression of IL-17R and stabilization of the induced cytokines mRNA (368, 369). Another function of IL-17A is the activation of B-cell germinal center formation and antibody responses (370).

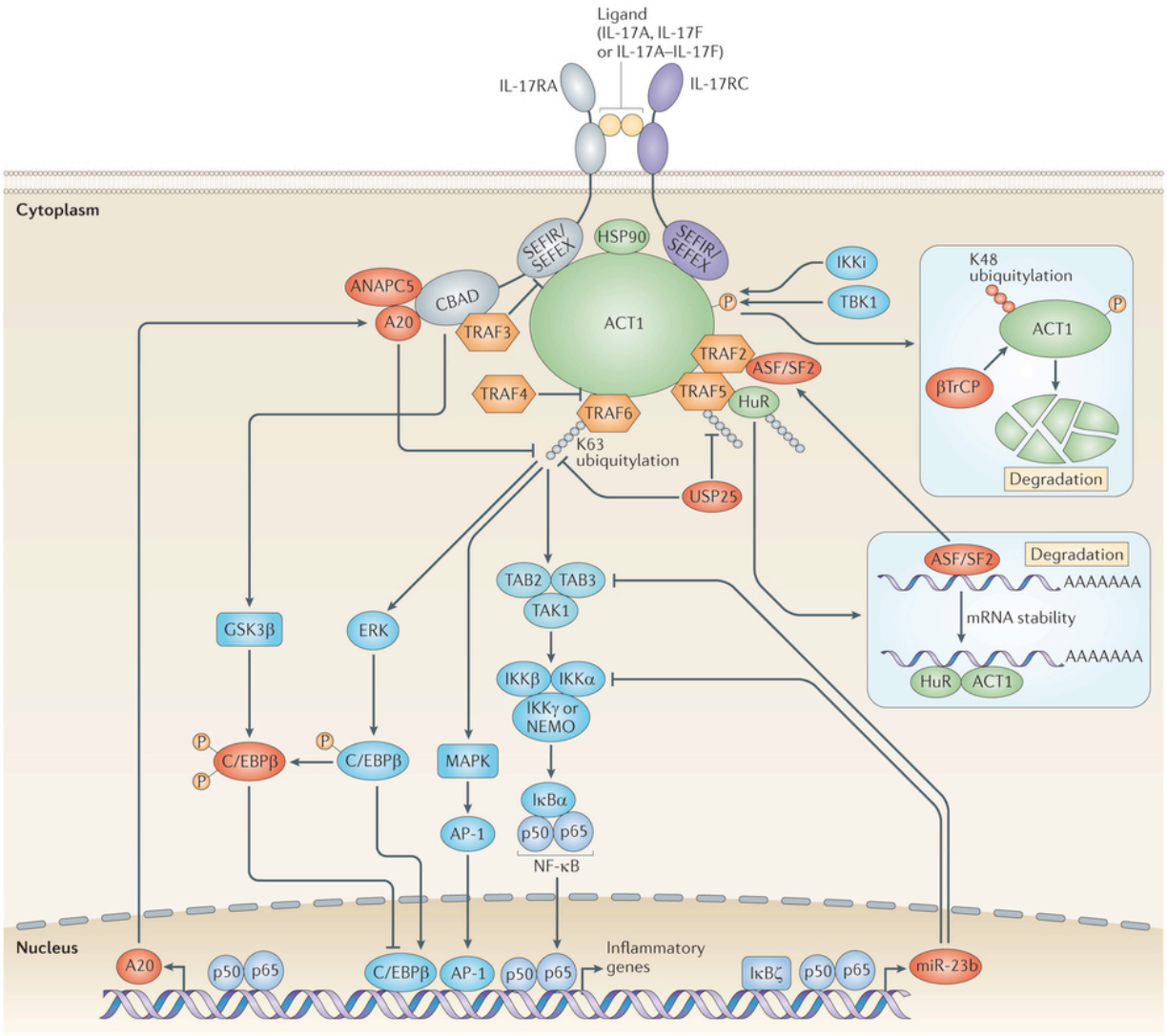

Figure 9: IL-17A and IL-17F signaling pathway. Shown is the signaling cascade downstream the IL-17 receptors RA and RC including molecules involved in the positive as well the negative (*e.g.,* A20) regulation of the IL-17A/F-mediated cellular activation. Reproduced with the permission of Macmillan Publisher Limited: Nature Reviews in Immunology (210), author copyrights 2014.

IL-17F shares ~50% homology with IL-17A, and both have overlapping functions (371). However, IL-17F is less potent than IL-17A in the induction of downstream signaling *via* IL-17RA/RC (Figure 9). Interestingly, cell fate mapping experiments demonstrated that the IL-17F but not the IL-17A homodimer is highly expressed in naive T-cells differentiating towards the Th17 cell-line (372, 373). IL-17F is thus considered as an early marker of Th17 differentiation.

IL-22, similar to IL-17A, induces production of antimicrobial peptide from epithelial cells.

Moreover, IL-22 contributes to epithelial cell proliferation, survival, and tissue repair in the intestine (374). IL-22 has a dual role in immunity as it can confer protection or induce inflammation (375). As well, IL-22 stimulating keratinocytes lead to the production of pro-inflammatory molecules promoting psoriasis (376). Also, IL-22 provides protection against hepatitis and inflammatory bowel disease (IBD) (377-379).

IL-26 is a cytokine specifically produced by Th17 cells with a role that currently remains unclear. Very recent studies demonstrated that IL-26 is an antimicrobial factor that mediates sensing of bacterial and host-cell debris (380). Through IL-26, Th17 cells *via* IL-26 can kill extracellular bacteria by inducing pores in cell membrane. Furthermore, IL-26 can interact with the bacterial and self-genome, which will lead to production of type 1 IFN by plasmacytoid DCs (pDCs). Of note, IL-26 was identified and studied in humans but its role remains to be examined in more detail in murine models.

The mechanism of action of Th17 cells is pathogen-specific. For example, Th17 immune response against *Klebsiella pneumonia*, mediated by IL-17A and IL-22 includes the induction of CXCL1, CXCL2, CXCL5 causing neutrophil infiltration and LCN2, restricting bacterial growth by preventing access to dietary iron (367). However, induction of β-defensins 1, 2, 3, and 4 by Th17 cells is sufficient for the clearance of *Citrobacter rodentium*, infecting the gut mucosa. Interestingly, vaccine-induced responses to Mycobacterium tuberculosis reveal that IL-17A recruits Th1 cells *via* the regulation of CXCR3 ligands CXCL9, CXCL10 and CXCL11 (381). The list of pathogens inducing Th17 responses also includes *C.albicans*, *S.aureus*, *Salmonella enterica*, *E.coli*, *H.pilori*, *Bordetella pertussis*, *Blastomyces dermatitidis*, *Coccidioides posadasii*, *Porphyromonas gingivalis*, *Listeria monocytogenes*, *Pneumocystis carinii*, *Aspergillus fumigatus,* and *Toxoplasma gondii* (382). In conclusion, Th17 cells act at the interface between innate and adaptive immunity at barrier surfaces with their role in mediating the cognate immunity against various pathogens being increasingly documented.

1.2.6 TH17 REGULATION MECHANISM

Regulation of Th17 cell polarization and functions is primordial for the maintenance of

homeostasis and for avoiding chronic inflammatory episodes once a pathogen is cleared. Restricting either IL-17 signaling or *de novo* Th17 differentiation are ways to stop exacerbated Th17 immune responses. Ubiquitination of components involved in IL-17A signaling transduction pathway is one of the mechanisms used by the immune system to inhibit expression of IL-17A target genes (210). Reported molecules implicated in the negative regulation of IL-17 signaling include deubiquitinating enzymes, A20, ubiquitination adaptor proteins, micro-RNA (miR)-23b and CCAAT/enhancer-binding protein transcription factors (C/EBPs) (210) (Figure 9). Interestingly, A20 and C/EBPs are induced by IL-17 signaling and can act separately or in combination to repress IL-17A targeted genes.

Inhibition of *de novo* Th17 differentiation in mucosal tissues is dependent on the specific cues present in local environment. For example, the presence of high levels of TGF-β and/or retinoic acid promotes the differentiation $Foxp3^+$ Tregs thus shutting down Th17 development. IL-2 also inhibits Th17 differentiation by activating STAT5 that will compete with STAT3 for binding sites across the *il17a* locus (269, 270). In addition, IL-2 can function jointly with TGF-β to induce iTregs. Through the interaction with AhR and c-Maf, IL-27 promotes the generation of T_R1 cells producing IL-10 and is dependent on STAT1 expression (374, 383). As well, IL-27 can directly inhibit RORγt expression in both mice and humans (384) thereby blocking Th17 development. Of note, IL-27 has an effect on naive cells undergoing Th17 differentiation (374). The host defense can also control Th17 immune responses after pathogen clearance (Figure 10). Results generated by the group of Richard Flavell support the concept that once the immune response is resolved, Th17 cells leave the site of inflammation and migrate towards the duodenum (355). This trafficking process is mediated by the CCL20-CCR6 axis. Once in the duodenum, Th17 cells are eliminated by unknown mechanisms or acquire features of Tregs (e.g., IL-10 production). These regulatory Th17 cells are immunosuppressive as they have the ability to prevent cell proliferation. The Tregs can also control and stop Th17 immune responses. In summary, the immune host defense employs several mechanisms to avoid deregulation by Th17 cells and promote homeostasis.

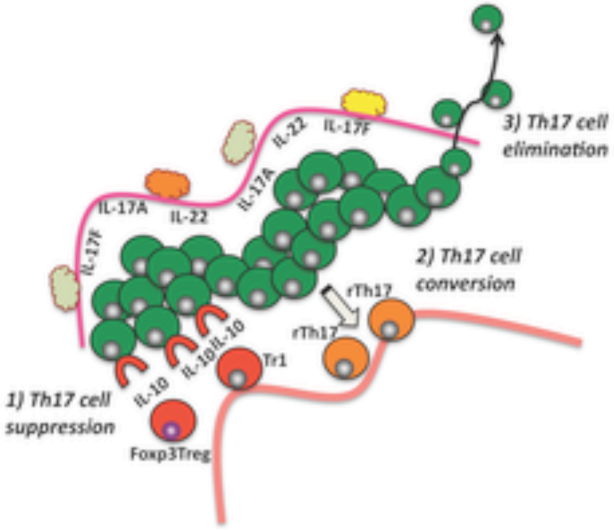

Figure 10: Mechanisms involved in the regulation of Th17 cell functions. Shown are mechanisms that limit the Th17 effector functions including ***1)*** the inhibition by FoxP3$^+$ T_{regs}, Tr1, and rTh17, ***2)*** the de differentiation of Th17 cells, and ***3)*** the elimination of Th17 cells by clonal contraction. Reproduced with the permission of European Journal of Immunology (374), author copyrights 2012.

1.2.7 NATURAL TH17 CELLS

Originally discovered in 2009 with the use of mice models, natural Th17 (nTh17) cells represent a population of IL-17A producing αβ CD4$^+$ T-cells that undergo maturation and functional priming exclusively in the thymus, similar to natural Tregs (nTregs) (385).The nTh17 cells exit the thymus and enter the periphery where they acquire a memory-like phenotype in spite of being naive in terms of antigen recognition. It has been proposed that these cells respond to tissue injuries prior to the activation of conventional/inducible Th17 cells that are generated following antigen recognition (386). Both nTh17 and inducible Th17 cells share common characteristics including the expression on RORγt, CCR6, IL-23R and the production of IL-17A as well as IL-22 (386). Similar to inducible Th17 cells, nTh17 cells also exhibit immune responses against *C.albicans* and play a pathogenic role in autoimmunity (387-389). Nevertheless, nTh17 differ from inducible Th17 cells in their development pathway and in their ability to produce IL-17A and IL-22, following Toll-like receptor (TLR) stimulation without TCR engagement (386, 388). TGF-β and

IL-23/STAT3 axis were reported to be important factors in nTh17 development and survival, whereas IL-6 was found to be dispensable for the expansion of this subset in the periphery (386). The mechanism regulating the development of nTh17 cells as well as their extended contribution in protective immunity remains to be investigated. Also, the existence of this subset of Th17 cells in humans remains to be confirmed.

1.2.8 ROLE OF TH17 CELLS IN AUTOIMMUNITY

The deregulation of the immune system is often the cause of inflammatory disorders. For example, prolonged and uncontrolled exposure to IL-1β and IL-23 in local environments results in Th17 cell-mediated myeloid cell recruitment and tissue damage (330, 390). In the context of autoimmunity, Th17 cells are considered pathogenic due to their strong capacities to produce inflammatory cytokines, which leads to severe tissue injury. Experimental approaches using mice deficient in IL-17A, IL-22, IL-23 or IL-23RA confirmed the importance of these Th17-associated key components in autoimmune disorders such as psoriasis, IBD and EAE (210).

Psoriasis is an inflammatory disorder affecting the skin and causing dermal hyperplasia. The presence of Th17 cells was observed in psoriatic lesions (391). The IL-23/IL-17 axis plays a critical role in the pathogenicity of psoriasis. The IL-23 signaling in Th17 cells induces the production of IL-17A and IL-22 (210). These two cytokines act in a synergistic manner, increasing the levels of skin antimicrobial peptides. Indeed, the levels of antimicrobial peptides, including S100A7, correlated with the disease onset (392). Of note, patients suffering from psoriasis are resistant to bacterial infections in the skin, possibly due to the high levels of antimicrobial peptides. Also, the induction of angiogenic chemokines (*i.e.,* CXCL1, CXCL3, CXCL5, CXCL8) by IL-17A seems to be responsible for the enhanced vascularity seen in psoriatic legions (210, 367).

The IBD is a relapsing disorder affecting the intestinal tract that includes Crohn's disease and ulcerative colitis (367). This disease is partly caused by unregulated immune response against intestinal bacteria. Several experimental approaches, including adoptive transfer of Th17 cells into lymphopenic mice, demonstrated the importance of this lineage in the disease progression (310).

The Th17-genes associated with the pathogenicity of IBD include IL-12B, STAT3 and CCR6 (367). Also, polymorphism in the IL-23R gene is associated with susceptibility to IBD. The role of IL-17A in IBD remains controversial. Mice deficient in IL-17RA were protected from trinitrobenzene sulfonic acid (TNBS) chemically–induced IBD, partly due to low levels of IL-6 and CXCL2 (393). However, IL-17A was observed to have a protective role in dextran sulfate sodium (DSS)-induced colitis (394). IL-22 produced by Th17 cells is involved in the induction of hyperplasia in animal models of IBD (374). As well, TNF-α is abundantly produced by Th17 cells and has been shown to play an important role in the development of the disease. In fact, Abs against TNF-α were approved for treatment against IBD (395). Nevertheless, the production of TNF-α is minor compared to that of non-T cells. The role of TNF-α produced by Th17 cells remains unclear. Furthermore, the plasticity of Th17 cells towards the Th1 lineage may be a factor contributing to IBD progression. Th1Th17 cells have been observed in the colon of patients suffering from Crohn's disease (297, 396, 397). As well, CD161 in addition to CCR6 was confirmed to be a surface marker of these pathogenic cells (396). Recently, *Ramesh et al.* demonstrated that a fraction of Th1Th17 cells expressing the P-glycoprotein (P-gp) or multi-drug resistance type-1 (MDR-1) represent the human pathogenic Th17 cells and also demonstrated that in the context of Crohn's disease these cells are resistant to glucocorticoids (344). MDR-1 is an ATP-dependent membrane efflux pump and has been reported to promote tumor resistance upon chemotherapy (398). These findings are of high relevance as they explain why subjects with Th17-mediated autoimmune disorders are resistant to anti-inflammatory drugs.

As mentioned earlier, pathogenic Th17 cells were originally discovered in EAE, a model of MS (367). The MS is a degenerative disease affecting the nerve cells of the brain and spinal cord. In mice, EAE is mainly induced by immunization of neuroantigens, including myelin basic and proteolipid proteins. Pathogenic Th17 cells induced by IL-23 are responsible for EAE development (210). In fact, IL-23 has been reported to induce the production of GM-CSF (399), which has been identified as the key factor involved in the in the induction of EAE and an essential component of Th17 pathogenicity (356, 399, 400). Also, the presence of human Th17 cells has been detected in areas of brain lesions of patients with MS (401, 402). In fact, the receptors for IL-17 and IL-22 are expressed on blood-brain barrier (BBB) endothelial cells, and the secretion of IL-17A and IL-22 by Th17 cells leads to disruption of the BBB tight junctions

(403). Finally, the infiltration of Th17 cells in the brain leads to the killing of the neurons and further inflammation due to the recruitment of effector $CD4^+$ T-cells.

Th17 cells also contribute to the pathogenesis of other autoimmune disease including RA and systemic lupus erythematosus (SLE) (256, 367). The frequency of Th17 cells was observed to be increased in patients with RA compared to healthy individuals (404). Also, levels of IL-17A were elevated in synovial fluid of RA patients (367). IL-17A promotes inflammation by inducing IL-1β and TNFα in APCs, bone cells and synoviocytes as well as recruiting neutrophils and effector CD4+ T-cells in the synovium (405). Not only does IL-17A stimulates inflammation but is also directly involved in bone and cartilage damage (367). The frequency of Th17 cells is also increased in SLE patients, a disorder characterized by excessive autoantibody production (406). In fact, a correlation between the frequency of Th17 cells and the onset of this disease has been reported (407). A correlation between IL-22 and the onset of SLE has also been reported (408). IL-17A seems to act in synergy with the TNF super family member, B-cell activating factor (BAFF) to inhibit apoptosis of B-cells (409) thus explaining exacerbated B cell activation during these autoimmune conditions.

Based on these findings, it is clear that Th17 cells have an impact on various autoimmune diseases. The mechanisms of action of Th17 and associated cytokines appear to be disease-specific. However, common pathogenic factors exist in all disorders. The extensive studies on Th17 cells and associated cytokines in the context of pathogenicity led to the approval of an IL-12p40-specific antibody as treatment for psoriasis (210). Furthermore, ongoing clinical trials show the beneficial effects of the use of IL-17 and IL-23 Abs in psoriasis, RA, and MS. It is important to acknowledge that the impact of IL-17 and IL-23 Abs-based therapies is disease-specific. For example, the clinical outcome of secukinumab treatment, an IL-17A-specific Abs, is different for patients treated for psoriasis *versus* Crohn's disease. Following the administration of secukinumab, a higher frequency of fungal infections was observed in patients suffering from Crohn's disease but not psoriasis (210). Both diseases target different anatomical site. Psoriasis targets the skin whereas Crohn's disease affects intestinal tissues (367). The increased presence of fungal infection may be due to gut mucosal permeability (210). Interestingly, very recent studies demonstrated that role of IL-17A in limiting the permeability of the intestinal mucosa (410, 411), as blockade of IL-

17A results in the weakening of gut mucosal tissue and increased inflammation. Therefore, defining the complete impact of Th17 lineage on autoimmunity has yet to be achieved (412). Therapies intending to block IL-17 should take into consideration beneficial functions of IL-17A in maintaining barrier functions at the intestinal level.

1.2.9 ROLE OF TH17 CELLS IN CANCER

Th17 cells in cancer have poorly been described compared to the extensive studies characterizing these cells in the context of autoimmunity. In addition, the role of Th17 cells in cancer remains controversial and likely dependent on the type of cancer. Th17 cells appear to promote disease progression in hepatocellular carcinoma and gastric cancer (413, 414). Th17 cells are known to be present in the vicinity of several malignancies including ovarian (415), gastric (416), colorectal (417), breast (418), pancreatic carcinomas (419), and melanomas (417). Tumors secrete monocyte chemoattractant protein 1 (MCP-1) that attracts monocytes and RANTES that attracts Th17 cells (418). Nevertheless, Th17 cells were reported to provide protective immunity in melanomas and ovarian cancer (420-424). In melanomas, tumor-specific Th17 cells led to the recruitment on $CD8\alpha^+$ DCs and activation of tumor-specific $CD8^+$ T-cells, which were crucial for the prevention of tumor development (420). Th17 cells conferred protection against ovarian cancer by the recruitment of effector cells through the production of CXCL9 and CXCL10 (422). The production of IFN-γ by Th17 cells was reported to be essential for an efficient immune response against both melanomas and ovarian cancers (421, 422, 424). Interestingly, studies in mice and humans in the context of cancer revealed the existence of Th17 cells with features of a newly characterized population of T lymphocytes with self-renewal properties (423, 424) known as stem memory T cells (T_{SCM}) (425). These Th17 cells were referred to as long-lived Th17 cells. The T_{SCM} were originally observed in mice in the context of graft-versus-host disease (426) and were later rediscovered in the context of cancer (427, 428). The T_{SCM} were described not only for their robust self-renewal and expansion capacity but also for their ability to be progenitors for effector T-cells as well as central and effector memory T-cells. Therefore, T_{SCM} have characteristics of hematopoietic stem cells (429). Long-lived Th17 cells were described in mice and in humans as Th17 cells expressing molecules of the Wnt-β catenin signaling axis (423, 424), a pathway associated with self-renewal and survival capacity in stem cells (430). In humans, long-lived Th17

cell express stem cell related genes such as Nanog, OCT4, Bcl2, Notch, and SOX2 (423). Survival and apoptosis of human long-lived Th17 cells are controlled by the HIF-1α/Notch/Bcl-2 signaling pathway. Both murine and human long-lived Th17 cells express both IL-17A and IFN-γ (Th1Th17 profile) and exhibit a phenotype of terminally differentiated memory T-cells due to their low level of CD27 expression (423, 424). Adoptive T-cell transfer in mice demonstrated that $CD4^+$ T-cells producing IL-17A are progenitors of long-lived Th17 cells (424). The discovery that specific Th17 subsets display stem-cell features may explain the fact that a fraction of them persist in diverse pathologies including cancer and HIV.

1.2.10 ROLE OF TH17 CELLS IN HIV-1 PATHOGENESIS

The role of Th17 cells in HIV pathogenesis is quite different from autoimmune diseases and cancer. As mentioned earlier (Section 1.1.6: HIV-1 pathogenesis), HIV infection induces massive depletion of $CD4^+$ T-cells in the gastrointestinal tract. The loss of Th17 cells contributes to HIV and SIV pathogenesis (49, 431). The loss of Th17 cells in mucosal tissues of SIV-infected primates was associated with increased viremia (432). Depletion of Th17 cells is associated with microbial translocation leading to chronic immune activation and disease progression as originally shown in primate models studying SIV pathogenesis. The deficiency of Th17 cells was associated with translocation of the pathogen *Salmonella typhimurium* and enhanced bacterial dissemination (433). This depletion occurs within weeks following primary infection and persists during the chronic phase of SIV infection (432). Of note, the natural host of SIV infection, the sooty mangabeys, conserved their Th17 cells following primary infection and exhibited little immune activation (434).

Although the complete mechanisms explaining the loss of Th17 cells during HIV/SIV infections are still under investigation, well-established mechanisms include: *(i)* HIV *per se*, *(ii)* deficient expression of Th17 polarizing cytokines, *(iii)* altered Th17 trafficking into the gut, *(iv)* expansion of Tregs, *(v)* overexpression of factors inhibiting of Th17 differentiation program *(vi)* depletion of $CD103^+$ DC from the gut, and *(vii)* depletion of naive Th17 precursors.

In the gut mucosa, Th17 cells express at high levels the major HIV co-receptor CCR5. The $CCR5^+$ Th17 cells were shown to be preferentially depleted in the gastrointestinal tract of HIV-infected

individuals (434). It was also showed peripheral blood Th17 cells co-expressing CCR6 and CCR5 are significantly depleted in HIV-infected individuals (435). While the depletion of gut Th17 cells is accepted in the field, the depletion of blood Th17 cells is controversial. We previously reported a decreased in the frequency of peripheral blood $CCR4^{+}CCR6^{+}$ Th17 and $CXCR3^{+}CCR6^{+}$ Th1Th17 cells of chronically HIV-infected individuals during ART (CI on ART) compared to uninfected controls (436). Consistently, studies from *El-Hed et al.* reported a decrease in the frequency of CD4+ T-cells producing IL-17A in HIV-infected individuals compared to uninfected controls (435). The decrease observed from both studies was minimal in terms of percentages but the results were statistically significant (435, 436). Minimal secretion of IL-17A from CD4+ T-cells was observed in HIV-infected children with detectable viremia (437). Furthermore, the studies performed by our group and others reported the drastic depletion of CD4+ T-cells producing IL-17A, with the reduction going up to 10-fold (59, 438). Nevertheless, *Ciccone et al* as well as *Brenchley et al.* reported no depletion of blood Th17 in HIV-infected individuals (434, 439).

Although *Brenchley et al.* claimed that Th17 cells are not preferentially infected (434), our group and others showed the preferential infection of Th17 cells *in vitro* and *ex vivo* (435, 436, 440). *Brenchley et al.* quantified HIV-DNA expression in cells exhibiting Th17 effector functions (IL-17A) to make their observation (434), whereas studies by our group and others used surface markers for Th17 identification (435, 436, 440), including CCR6, CCR4, and CXCR3 (297, 298). We previously demonstrated that memory $CCR6^{+}$ T-cells harbored higher levels of integrated HIV-DNA compared to the $CCR6^{-}$ counterpart population (436, 441). The preferential infection of Th17 cells was also confirmed in SIV-infected rhesus macaques (442). Together, these findings suggest that the permissiveness of Th17 cells to HIV/SIV infection is a major cause for their depletion. Of note, Th17 cells from the female reproductive tract were found to co-express CCR5 and CD90 and to be susceptible to HIV infection (443). Nevertheless, a fraction but not all Th17 cells are infected *in vitro* (440). Also, Th17 appear to be preferentially depleted from the gut but not from the lung (434). Thus, in addition to HIV infection *per se*, other mechanisms contribute to Th17 depletion from the gut as discussed below.

It is possible to anticipate that impairment of Th17 cells involve a lack of Th17 polarizing cytokine

in the local environment. Levels of IL-6 and TGF-β1 but not IL-21 in the course of HIV and SIV infection are relatively high (431). The decrease in IL-21 producing $CD4^+$ T-cells is directly associated with the loss of Th17 cells in the blood and rectal mucosa of SIV-infected primates (332). Conversely, treatment of IL-21 in SIV-infected primates increased Th17 frequency (332, 334). Recently, administration of IL-21 combined with pro-antibiotics to SIV-infected macaques treated with antiretroviral treatment led to an increase in the frequency of poly-functional Th17 cells capable of producing IL-2, IL-22 and TNF-α (444).

Impairment in the trafficking of gut-homing cells may also be involved the incomplete reconstitution of mucosal immunity. *Mavinger et al.* showed that gut-homing $CD4^+$ T-cells expressing CCR9 and integrin β7, including the Th17 cells, remained in the peripheral blood of CI of ART patients and failed to migrate into the intestine (445). This altered trafficking phenomenon was due to decreased levels of CCR9 ligand CCL25 in the intestines of HIV-infected individuals. Lack of $CD4^+CCR9^+\beta7^+$ T-cells was linked to microbial translocation and systemic immune activation. Furthermore, reports revealed a reduction in CCL20 levels in the gut of SIV-infected primates (433, 446) thereby preventing migration of circulating $CCR6^+$ Th17 cells. Recent studies demonstrated the impairment of the CCR6-CCL20 axis in treated HIV-infected individuals resulting in the inability of the Th17 cells to migrate in intestinal mucosa (447). This alteration is due to an increased frequency of $CCR6^-$Tregs that blunt the production of CCL20 from the enterocytes (447).

The depletion of Th17 cells was also shown to be associated with expansion of Tregs during HIV and SIV infection (448). Expression of Foxp3 was increased in untreated HIV-infected individuals (121, 446). The imbalance of the Th17/Treg ratio is due to the accumulation of byproducts of tryptophan metabolism. Tryptophan catabolites promote the expression of FoxP3 in T-cells resulting in the down regulation of RORγt and subsequent inhibition of Th17 generation (449, 450). Also, deprivation of tryptophan and amino acid can enhance Treg development to the detriment of Th17 differentiation. Catabolism of tryptophan is mediated by enzyme indoleamine dioxygenase, expressed in mucosal DC, and was found to be up regulated during HIV and SIV infection (446, 451). Indeed, *Favre et al.* discovered that DCs produce high levels of indoleamine 2,3-dioxygenase 1 (IDO-1); this promotes the generation of T regulatory (Treg) cells as opposed to

Th17 cells and thereby shifts the Th17/Treg ratio in the gut (446, 451). Interestingly, the Th17/Treg ratio was maintained in the natural host of SIV and also in HIV-infected individuals with undetectable viral loads and high CD4 counts that are not under therapy treatment, also known as elite controllers (452).

Overexpression of negative regulators of Th17 differentiation program may also explain the depletion of Th17 cells in HIV infection. Suppressor of cytokine signaling-3 (SOCS3), protein inhibitor of activated STAT3 (PIAS3), and protein tyrosine phosphatase (SHP-2) are negative regulators of STAT3 (431). The expression of SOCS3 mRNA is increased in HIV-infected individuals. The high levels of SOCS3 in mucosal tissues were associated with the increased permissiveness to HIV infection (453). In the context of SIV-pathogenesis, the up regulation expression of SOCS3, PIAS3 and SHP-2 was correlated to the suppression of IL-17 (454). The suppression of Th17 cells in these animals led to increase of soluble CD14, a marker of microbial translocation (454). Whether negative regulators of Th17 polarization are also increased in cells from HIV-infected subjects remains unknown.

Studies reported that acute HIV infection induces specific Th17 responses that are lost during the chronic phase of infection. The impact of ART in restoring the numbers of gut and peripheral Th17 remains controversial. *Kim et al.* reported that short-term ART restore the number of gut Th17 cells but not their function during chronic infection (455). Furthermore, studies by *Ciccone et al.* as well as *Chege et al.* reported similar frequencies of gut and/or peripheral blood Th17 cells between ART-treated HIV-infected and uninfected individuals (439, 456). Nevertheless several groups reported that antiretroviral therapy only led to partial restoration of Th17 cells (445, 457, 458). The mechanism involved may include the alteration in the trafficking of gut-homing cells via the CCR6-CCL20 and/or the CCR9-CCL25 axis (445, 447). Increased frequency of total $CD4^+$ T-cells in the gastrointestinal tract following treatment was correlated with the partial restoration of Th17 cells (459). Interestingly, *Schuetz et al.* demonstrated that early administration of the antiretroviral therapy during acute infection led to the preservation of Th17 function and numbers (460). Although ART does not completely restore Th17 cells at the stage of chronic infection, the addition of probiotics may increase the levels of $CD4^+$ T-cells and also the frequency of Th17 cells, in the mucosa. Indeed, treatment with probiotics along with HAART in SIV-infected pigtail

macaques was reported to increase the levels of IL-23 which was accompanied with the enhancement of Th17 cells when compared to animals that were only treated with HAART (461). Other findings showed that the addition of prebiotics and probiotics led to a reduction of microbial translocation and chronic immune inflammation, improving the health of patients (462). Not all studies succeeded in demonstrating the benefits of probiotics on HIV infection (431). Nevertheless, *Ortiz et al.* recently demonstrated that combined administration of IL-21 and probiotics led to Th17 expansion and a decrease in markers of microbial translocation in SIV-infected pigtail macaques treated with antiretroviral drugs (444). Future investigations should further determine the beneficial effects of the use of probiotics in the context of HIV infection as this concept still remains controversial. Also, the timing in which ART is administered may play a role in the maintenance *versus* depletion of the Th17 population. *Schuetz et al* demonstrated that early administration of treatment on HIV-infected subjects at stages I and II of acute infection prevented the depletion of mucosal Th17 cells (460). Administration of ART at stage III of infection allowed a restoration of only the frequency and not the poly-functionality of Th17 cells. Studies aiming at finding alternatives to restore Th17 cells in HIV-infected subjects are necessary.

Possible impairments in the Th17 differentiation program may occur during HIV infection. Studies in the context of SIV observed the depletion of $CD103^+$ DCs, which are responsible for the induction of Th17 differentiation (463). The loss of $CD103^+$ DCs was associated with the reduced frequency of Th17 cells in the gut of HIV-infected individuals. Recently, our group demonstrated the depletion of Th17 precursors in the CI of ART patients, including the naive Tregs (nTregs: $CD25^{high}CD127^-FoxP3^+$) and naive cells expressing CD25 and CD27 but lacking the expression of FoxP3, called double positive cells (DP) (59). The decrease of Th17 precursors was associated with the reduced proportion of Th17 memory cells. Of note, nTregs and DPs harbored higher levels of integrated HIV-DNA compared to classical naive CD25-CD127-FoxP3- T-cells, indicating that these cells are permissive to HIV infection. Another study demonstrated the depletion of a population derived from naïve CCR6+ precursors, expressing IL-17A, FOXP3 and CD25 (IL-17A-Tregs) in HIV-infected subjects(464). Whether the $CCR6^+$ naive precursors are depleted from HIV-infected patients remains to be determined. If proven to be the case, it would further explain the incapacity of the host to restore Th17 cells during HIV infection. In this sense, our group already has demonstrated that bulk naive cells from the CI of ART subjects have an

inability to generate Th17 cells compared to uninfected individuals (59).

1.2.11 PATHOGENIC *VERSUS* NON-PATHOGENIC TH17 CELLS DURING HIV/SIV INFECTION

The pathogenicity of Th17 cells appears to be disease specific. Even in the context of autoimmunity, the role Th17 cells appear to be distinct in several autoimmune diseases. While the increased presence of Th17 cells is deleterious in multiple sclerosis and psoriasis (210, 465), the absence of cells producing IL-17A may lead to the exacerbation of Crohn's disease (411). Very recent studies demonstrated the critical role of IL-17A in the maintenance of barrier function at epithelial cell level (410, 411), which may influence the outcome of IBD pathogenesis in patients. In the context of HIV pathogenesis, the loss of Th17 cells is detrimental. The depletion of Th17 cells lead to microbial translocation`, chronic immune activation and contribute to the emergence of opportunistic infections including candidiasis (466). Therefore, their loss during HIV disease progression is a direct pathogenic consequence. Of interest, Th17 cells have been reported to be depleted in the gut but not in the lungs of HIV-infected individuals (434), thus suggesting the functional heterogeneity of Th17 subsets in different anatomic sites. Pathogenic Th17 cells during HIV infection can be described as cells that are permissive to HIV replication. The phenotypic characterization of pathogenic Th17 cells in the context of HIV remains to be determined. The concept of pathogenic Th17 in terms of HIV infection is complex, not well documented and opens an area of research that involves detailed characterization of Th17 biology. In the context of autoimmunity, MDR1 was identified as a marker of human pathogenic of IL-17A producing $CD4^+$ T-cells (344). Precisely, MDR1 is highly expressed in $CCR6^+CXCR3^+$ Th1Th17 cells compared to $CCR6^+CCR4^+$ Th17 cells. Our group has demonstrated that both Th17 and Th1Th17 cells are permissive to HIV infection (436). One of the reasons why Th1Th17 may be considered more pathogenic in the context of HIV infection is that these cells express the highest levels of CCR5 and integrin β7 as well as producing TNF-α (436). The definition of pathogenic Th17 cells in the context of HIV needs further investigation. Currently, the marker of pathogenic Th17 cells identified is Th17 main surface marker CCR6 as studies demonstrated that HIV-DNA is mostly enriched in $CCR6^+$ cells as opposed to $CCR6^-$ cells (436, 441, 467).

Nonpathogenic Th17 cells have been described, as mentioned earlier (section 1.2.4).

Nonpathogenic Th17 cells resistant to HIV infection have not yet been described, but studies in our laboratory (unpublished observations) and published by others demonstrated that not all Th17 cells are infected with HIV (435, 440). Investigations of nonpathogenic Th17 cells are important and may lead to discoveries of new therapies to eradicate HIV. Whether MDR1 is a marker for pathogenic Th17 cells in the context of HIV-1 infection (permissive to infection and/or resistant to antiretroviral drugs) is currently under investigation in our laboratory. The possibility that Th17 cells expressing MDR-1 escape antiretroviral drugs and contribute to HIV reservoir persistence under ART is supported by published evidence that certain antiretroviral drugs are MDR1 substrates (468, 469).

Taking into consideration the finding presented in Chapter 1.2, in the first part of the Ph.D. work presented in this dissertation (Chapter 3) we focused on the transcriptional and functional characterization of two newly identified *versus* two previously characterized Th17 subsets in terms of immunological function and contribution to HIV persistence under ART. These studies were based on the recent identification of long-lived Th17 cells that exhibit stem cell features (423, 424). To the best of our knowledge, we provide the first evidence that long-lived Th17 cells exist in humans and harbor replication competent HIV-DNA (*Wacleche et al.,* Manuscript #1, (470).

1.3 BIOLOGY OF MONOCYTE-DERIVED DENDRITIC CELLS

1.3.1 HERETOGENEITY OF MONOCYTES

Monocytes are bone marrow-derived phagocytes that circulate in the blood where they display a half-life of one to two days (471). They are a conserved population of mononuclear phagocytes as they are present in all vertebrates (472). A similar population has also been detected in fly hemolymph (473). Monocytes represent approximately 10% and 4% of leukocytes in the human and mice peripheral blood, respectively, with a considerable pool located at the spleen and lungs as well as trafficking into inflammatory sites in response to specific chemokines (472). Monocytes belong to the innate arc of the immune system providing responses against viral, bacterial, fungal or parasitic infections (474, 475). Their functions include the killing of pathogens *via* phagocytosis, the production of reactive oxygen species (ROS), nitric oxide (NO), myeloidperoxydase, and inflammatory cytokines (475). Under specific conditions, monocytes can stimulate or inhibit T-cell responses during cancer as well as infectious and autoimmune diseases. They are also involved in tissue repair and neovascularization (476). The expression of various chemokine receptors and cell adhesion molecules at the surface allows the monocytes to circulate from the blood to tissues during inflammation (477). Monocytes exhibit well-established developmental plasticity as they can differentiate into macrophage, dendritic cells (DCs), and osteoclasts depending on the inflammatory milieu (478). Monocytes were originally considered as circulating precursors of macrophages and DCs (472, 477). However, it was later observed that specific subsets of DCs and macrophages can directly originate from bone marrow progenitors that are maintained independently of monocytes (479). In the brain, microglia can be generated from monocytes under specific conditions where brain tissues are damaged but not under homeostatic conditions (480). In the intestine, however, the majority of macrophages and DCs derive from blood monocytes (472). Also, monocytes contribute to the replenishment of cardiac macrophages following local inflammation (481). Of note, recently it was demonstrated that at steady state, monocytes traffic into tissues, capture antigens, and return into the blood stream while retaining their phenotype (482).

Both human and mice monocytes have particular morphology features that include: *a)* an irregular cell shape, *b)* a nucleus with oval or kidney-like shape, *c)* cytoplasmic vesicles, and *d)* high cytoplasm/nucleus ratio (483). The original identification of monocytes was based on their

morphology and cytochemistry. Monocytes are difficult to differentiate from blood DCs, activated lymphocytes, NK cells by morphology or light scatter analysis based on their heterogeneous size and shape. Nevertheless, the technology of flow cytometry based on light scatter cycler and fluorochrome attached to an anti-CD14 antibody allows the identification of human monocytes (484). Flow cytometry also provided knowledge on the heterogeneity of the monocyte population. Human monocytes can be classified into three subtypes based on the differential expression of CD14 and CD16: classical $CD14^{++}CD16^{-}$ (also referred as $CD14^{+}$ or $CD14^{+}CD16^{-}$), intermediate $CD14^{++}CD16^{+}$ (also referred as $CD14^{+}CD16^{+}$ or $CD14^{+}CD16^{int/low}$), and non-classical $CD14^{+}CD16^{++}$ (also referred as $CD14^{Low}CD16^{+}$ or $CD14^{dim}CD16^{+}$) monocytes (472, 483, 485, 486). The "+" sign defines the expression levels which is ~ 10 fold higher than the isotype control in cytometry (485). The main marker of the human monocytes CD14 is a glycoprotein and myelomonocytic differentiation antigen that functions as an accessory protein to Toll-Like receptor (TLR)-4 (26, 487). The CD16 (or the Fcγ receptor III) is a molecule of the Ig superfamily that is implicated in antibody-dependent-cellular cytotoxicity (ADCC) (487). Originally, it was reported that CD16 is expressed on NK cells and trigger target-cell lysis (488). In addition, CD16 is expressed on macrophages and neutrophils where it is involved in the uptake and clearance of antibody-bound pathogen (487). The classical $CD16^{-}$ and $CD16^{+}$ monocytes that include the intermediate as well as the non-classical monocytes (Figure 11) represent ~90%, and 10% of total monocytes (471, 489), respectively. Until the discovery of $CD16^{+}$ monocytes in 1989 (484), classical monocytes were viewed as a homogeneous population (485).

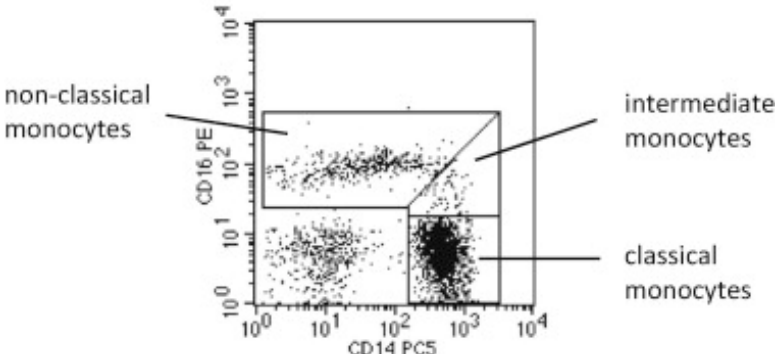

Figure 11: Heterogeneity of human peripheral blood monocytes. Shown is the gating strategy for the identification of three monocyte subsets based on the differential expression of CD14 and CD16: classical ($CD14^{++}CD16^{-}$), intermediate ($CD14^{++}CD16^{+}$), and non-classical ($CD14^{+}CD16^{++}$) monocytes. This figure is reproduced with the permission of Elsevier: Cellular Immunology (471), author copyrights 2014.

For several years, the mechanisms regulating recruitment of $CD16^+$ monocytes into the tissues where unknown; therefore, their functional role in immunity was poorly understood. Indeed, it was reported that $CD16^-$ but not $CD16^+$ monocytes expressed the MCP-1/CCL2 receptor CCR2, known to be a major regulator of monocyte trafficking (490). In 2003, studies by *Ancuta et al.* (491) and then by *Geissmann et al.* (492) independently identified the fractalkine/CX3CL1 receptor CX3CR1 as a major regulator of $CD16^+$ monocyte trafficking. Of note, CX3CR1 levels are higher on non-classical compared to intermediate monocytes, while classical monocytes expressed CCR2 but low/undetectable levels of CX3CR1 (491). The $CD16^+CX3CR1^+$ monocytes migrate in response to soluble CX3CL1 but also attach under shear stress conditions to the CX3CL1 expressed by inflamed endothelial cells (491, 493). This interaction leads to the production of pro-inflammatory cytokines thus explaining the involvement of $CD16^+$ monocytes in the pathogenesis of multiple diseases (494). Subsequent genome-wide analysis of gene expression confirmed the preferential expression of CX3CR1 and CCR2 in $CD16^+$ and $CD16^-$ monocytes, respectively (495). These findings opened the way for major advances in the field of monocyte biology and disease pathogenesis (496). It is now well established that monocytes subsets exhibit unique features. Classical monocytes express high levels of CCR2, CD62L, CD11b, and TLR-4 but low levels of CX_3CR_1 (478, 483). In addition, a meta-analysis merging several transcriptional studies on monocyte subsets indicate that classical monocytes highly express low density lipoprotein receptor (LDLR), scavenger receptor class B type-1 (SCARB1), and Stabilin-1 (STAB1) genes that may make the classical monocytes efficient scavenging cells (478, 495). Classical compared to intermediate and non-classical monocytes exhibit superior phagocytic and myeloperoxidase activities (483). They also release superior levels of superoxide. Following lipopolysaccharide (LPS) stimulation, classical monocytes produce high levels of IL-10 but lower levels of TNF-α and IL-1. Non-classical monocytes are less granular, express high levels of the chemokine fractalkine receptors CX_3CR_1, CXCR4, and HLA-DR, Lymphocyte function-associated antigen 1 (LFA-1) but low to undetectable levels of CCR2 and CD11b (485, 490, 491, 497). The different expression of chemokine receptors suggests that classical and non-classical monocytes traffic in different anatomical locations. In contrast to classical monocytes, non-classical monocytes produce very high amounts of TNF-α in response to LPS and TLR-2 agonist Pam3Cys (498). Also, higher levels of TNF-α was detected in monocytic cultures of HIV-infected

individuals (499). Non-classical monocytes appear to represent a more advanced stage of monocytes differentiation as they show a transcriptional program common to macrophages and DCs (495). Also, a transcription network meta-analysis suggested that non-classical monocytes are highly migratory cells since they exhibit elevated expression of genes involved in the cytoskeletal dynamic (478). The expression of CD16 itself makes the non-classical monocytes a unique population. CD16 is known to activate the negative regulators of the TLR-MyD88-dependent pathway, rendering monocytes tolerant to sepsis (500). Within the pool of $CD16^{+}$ monocytes, the monoclonal antibody M-DC8 can differentiate non-classical $CD14^{+}CD16^{++}$ monocytes from the intermediate $CD14^{++}CD16^{+}$ monocytes (501). It was found that the M-DC8 Abs binds to 6-sulfo LacNAc (SLAN) (502), a carbohydrate modification of the P-selectin glycoprotein ligand 1 (PSGL-1) or CD162) (503, 504). The $M\text{-}DC8^{+}$ population represents 40% of the non-classical monocytes. Of note, the highest production of TNF-α was detected in the M-DC8+ fraction within the non-classical monocytes following LPS stimulation (505). Although non-classical $CD14^{+}CD16^{++}$ monocytes represent a low fraction of the total monocyte population in healthy people, this subset is significantly expanded in the blood of individuals with inflammatory conditions (483, 485). Furthermore, excessive exercise and stress also leads to increased numbers of non-classical monocytes in the peripheral blood (506). Intermediate monocytes are a population that exhibits phenotypic and functional characteristics in between those of classical and non-classical monocytes. Intermediate monocytes were not initially considered as a separate population and were originally allocated to classical or non-classical monocytes depending on the gating positioning in flow cytometry. Nevertheless, intermediate monocytes were later recognized as a distinct population from the two subsets previously found (485, 489). In fact, genome-wide transcriptional profiling demonstrated 90% of genes highly expressed in classical or non-classical monocytes were observed at intermediate levels on intermediate $CD14^{++}CD16^{+}$ monocytes (507). Nevertheless, intermediate monocytes were shown to express higher levels of major histocompatibility complex (MHC)-class II including HLA-DR and transmembrane receptor CD74, scavenger receptor CD163, the C-type lectin/C-type lectin-like domain member CLEC10A, and Glial cell line-derived neurotrophic factor family receptor-α2 (GFRA2) (507-510). Also, studies by *Zawada et al.* identified a higher expression of the angiopoietin receptor Tie2 (508). The Tie2-expressing monocytes (TEM) were previously characterized as a subset of monocyte promoting angiogenesis (511, 512). The fact that intermediate $CD14^{++}CD16^{+}$ cells express the

highest levels of Tie2 among the monocyte subsets indicates that this population may overlap with TEM (489). Following LPS or zymosan stimulation, intermediate monocytes were shown to produce the highest levels of IL-10 (513). Other studies demonstrated that intermediate monocyte produce the highest level of IL-12 and IFN-γ in the context of antigenic presentation and have an increased ability to induce superantigen mediated T-cell proliferation (508). This is in contrast to previous studies by *Schakel et al.* that reported IL-12 production as being associated with M-DC8^{+} monocytes (514), which are non-classical.

The nomenclature of murine monocytes is quite different from human homologues. In contrast to humans, murine monocytes are classified in two subsets: the Gr1^{+}Ly6C^{high} and Gr1^{-}/Ly-6C^{low}. Of note, similar to human monocytes, CX3CR1 is mainly expressed on Gr1^{-}/Ly-6C^{low}, while CCR2 is highly expressed on Gr1^{+}Ly6C^{high} monocytes (492, 496). The classical and intermediate monocytes are closely related to Gr1^{+}Ly6C^{high}, whereas the non-classical monocytes are equivalent to the Gr1^{-}/Ly-6C^{low} (475, 483). Based on the fact that only Gr1^{+}Ly6C^{high} monocytes migrated in the peritoneal cavity in response to thioglycolate, while Gr1^{-}/Ly-6C^{low} monocytes were found infiltrating different tissues, *Geissmann et al.* proposed the term "inflammatory" for Gr1^{+}Ly6C^{high} monocytes and "resident" for Gr1^{-}/Ly-6C^{low} monocytes (515). This classification is in part misleading because it implies that Gr1^{-}Ly6C^{Low} monocytes are not inflammatory; this contradicts a whole body of literature on the inflammatory potential of human CD16^{+} monocytes. It is well established that monocyte migration into the peritoneal cavity is dependent on CCR2; therefore, it is normal that only monocytes expressing CCR2 migrate into this specific cavity. In fact, subsequent elegant studies by the group of Geissmann demonstrated that Gr1^{-}/Ly-6C^{low} monocytes are the first line of defense against pathogens *via* the production of TNF-α and other pro-inflammatory cytokines as well as acting as "patrolling" cells on endothelial beds (497). Therefore, the classification of monocyte subsets into "inflammatory" *versus* "resident" is confusing and requires revision because all monocyte subsets can be either "inflammatory" or "resident" depending on the specific chemotactic and activator stimuli they receive from specific tissues.

Accumulating evidence indicates that the role of mouse Gr1^{-}/Ly-6C^{low} and their human non-classical CD14^{+}CD16^{++} monocyte homologues is the surveillance of endothelial integrity. Indeed,

intravital microscopy studies demonstrated the CX3CR1-mediated crawling of $Gr1^{-}/Ly\text{-}6C^{low}$ monocytes on the luminal side of the endothelium (497, 516). Also, $Gr1^{-}/Ly\text{-}6C^{low}$ cells were shown to be involved in the coordination of intraluminal stress response. These monocytes induce the recruitment of neutrophils that will promote endothelial necrosis and afterwards are involved in the clearance of the neutrophil-induced cellular debris. In contrast, the function of mouse $Gr1^{+}Ly6C^{high}$ and human classical monocytes in the peripheral blood is poorly documented and is associated with their high phagocytic and scavenger activity (472). Interestingly, it was recently demonstrated that $Gr1{+}Ly6C^{high}$ monocyte expression is under the control of circadian marker Bmal1 (517). The same study also showed that these monocytes exit the bone marrow in diurnal rhythmic waves. Many scientists accept the idea that the establishment of a development relationship between the classical and non-classical monocytes, including the fraction expressing M-DC8 (505, 507, 518, 519). Furthermore, gene expression profiling studies indicate that intermediate monocytes must be regarded as a transition population between classical and non-classical monocytes (507).

1.3.2 MONOCYTES AND HIV-1

During HIV/SIV infection, monocytes undergo changes in their phenotype such as modulation in MHC expression and up regulation of CCR2 at T-cell surface, in addition to being primed to apoptosis (520). The frequency of monocyte subsets is also altered during HIV pathogenesis. Indeed, monocytes expressing CD16 were first found to expand during AIDS, the late-stage of HIV infection (521-523). The expansion of $CD16^{+}$ monocytes was later reported in the chronic phase of infection (499, 524). This increase ranges from 30 to 50% within the total monocytic population of HIV-chronically infected and AIDS patients (63, 499, 521, 524, 525) as opposed to the 5 to 10 % observed in healthy individuals. This expansion may be due to high levels of monocyte/macrophage growth factor (M-CSF) observed in HIV-infected subjects (518), which was reported to induce monocytic maturation including the acquisition of CD16 expression (526, 527). The increase of $CD16^{+}$ monocytes was reported to affect HIV-infected viremic groups but not individuals undergoing successful treatments (499, 505, 528, 529). The initial reports did not dissociate the intermediate from the non-classical monocytes. However, one study reported that expansion of monocytes affected the non-classical population (530). In contrast, *Ancuta et al.*

observed the expansion of intermediate monocytes in a cohort of AIDS subjects with HIV-associated dementia (HAD) (63). Recently, emerging data confirmed the expansion of the intermediate monocytes in HIV-infected treatment-naive individuals and SIV-infected primates (505, 531, 532) and further documented their role during HIV pathogenesis (526, 533, 534). Interestingly, levels of intermediate monocytes expressing CD163, a scavenger receptor, are increased in HIV-infected individuals with detectable viral loads but not in uninfected or in HIV-infected subjects with undetectable viremia (535). The frequency of $CD16^{+}CD163^{+}$ monocytes is positively correlated with the viral load. The frequency of intermediate monocytes positively correlated with levels of plasma inflammation markers including IL-6 and high-sensitivity C-reactive protein (hs-CRP) as well as the monocyte activation marker soluble CD14 (sCD14) (536). Therefore, this intermediate population may represent a biomarker for AIDS progression as well as non-AIDS related pathologies. The numbers of $CD14^{+}CD16^{++}$ cells are also increased during the acute and chronic phases of SIV infection (537). Within the non-classical monocytes, the $M\text{-}DC8^{+}$ fraction represented the most expanded population (505). The non-classical $M\text{-}DC8^{+}$ monocytes contribute to the overproduction of TNF-α observed in HIV^{+} viremic individuals. The expansion and infection of $CD16^{+}$ monocytes can be decreased following Maraviroc intensification (538). Furthermore, glucocorticoid treatment was shown to result in a decreased proportion of the $CD16^{+}$ monocytes during SIV infection (531). $CD16^{+}$ monocytes expressing high levels of TLR4, particularly the non-classical monocytes, are major sources of IL-23 in response to commensal enteric bacteria such as *E.coli* during HIV infection (539). Induction of IL-23 by $CD16^{+}$ monocytes may contribute to systemic immune activation as it correlates with levels of immune activation marker CD27. Of note, the numbers of circulating classical monocytes are found unaltered during HIV infection by certain groups (499, 505). Nevertheless, *Gama et al.* identified the expansion of classical monocytes lacking the expression of CCR2 during HIV and SIV infection (520). This enhancement was observed as early as seven days post primary SIV infection. $CCR2^{Low/neg}$ classical monocytes harbored low levels of SIV DNA compared to $CD16^{+}$ monocytes but had defects in phagocytosis function and CCL2-mediated chemotaxis. In addition, $CCR2^{Low/neg}$ classical monocytes suppress $CD8^{+}$ T-cells proliferation and IFN-γ release indicating that these monocytes may postpone the development of the antiviral response. The emergence of $CCR2^{Low/neg}$ classical monocytes appears to be linked to viral replication as the ART in infected primates and individuals resulted in their decline. However, *Ancuta et al.* reported a decreased

frequency of classical monocytes in AIDS subjects with neurocognitive impairment but an increased expression of the HIV co-receptor CCR5 on these cells (63).

Studies by groups including that of Suzanne Crowe demonstrated that $CD16^+$ monocytes are more permissive to HIV infection and harbored preferentially HIV-DNA compared to $CD14^{++}CD16^-$ monocytes even with successful HAART (530, 540, 541). Furthermore, $CD16^+$ *versus* $CD16^-$ monocytes express higher levels of CCR5, which may promote HIV permissiveness (63, 541). Monocytes were previously reported to be resistant to HIV infection *in vitro* (542-545). Monocytes were shown to block infection at the level of viral entry (544) and post-entry by their limited ability to support HIV reverse transcription (546). This restriction is linked to low levels of dNTP available in monocytes for reverse transcription, a restriction mechanism abrogated upon monocyte differentiation into macrophages (543). The function of SAMHD1 in cleaving in dNTPs may also explain the resistance of monocytes toward HIV infection (86, 87). The small frequency of $CD16^+$ monocytes in the peripheral blood of uninfected individuals, together with the difficulties in working with such cell subsets, explains the limited knowledge in the field (527). Permissiveness to HIV increases during monocyte differentiation (494, 526, 547, 548). Indeed, the induction of monocyte maturation leads to increased HIV permissiveness as opposed to freshly isolated monocytes (526, 543). Also, $CD16^+$ monocytes differentiating into macrophages were shown to promote HIV infection in $CD4^+$ T-cells (549). Genome-wide transcriptional profiling of $CD16^+$ *versus* $CD16^-$ monocytes showed increased expression of syndecan-2 and fibronectin transcripts (526), two proteins previously reported to interact with HIV (550, 551). Syndecan-2 may promote viral entry as it acts as a *trans* attachment receptor for HIV (550). Fibronectin was reported to interact with the HIV-gp120 protein thus facilitating virus-cell interaction (551).

Monocytes, particularly those expressing CD16, were reported to cause in part the initiation and the persistence of neuroAIDS, a cognitive, motor and behavioral deficit pathology affecting the brain during HIV infection, also referred to as HIV-associated neurocognitive disorder (HAND) (527, 552). A correlation between the increased levels of circulating $CD16^+$ monocytes expressing CD69 and HIV-related dementia was first revealed in the late 1990's (525, 553). Despite the success of HAART, HAND occurs in 40 to 60% of HIV-infected individuals (554, 555). In fact, infection of monocytes correlates with HAND during successful antiretroviral therapy (556). The

expansion of $CD16^+$ monocytes persists even after one year of treatment (556). Several lines of evidence support a model in which infected $CD16^+$ monocytes migrate into the central nervous system (CNS) where they will differentiate into macrophages and act as cellular reservoirs for HIV in the brain (552). Indeed, levels of FKN/CX3CL1 are elevated in the brain of HIV-infected subsets and correlated with neurocognitive impairment (557). Also, $CD16^+$ monocyte recruitment into the brain is highly likely mediated *via* the FKN receptor CX3CR1 (491, 515). $CD16^+$ mononuclear phagocytes expressing HIV antigens were observed in the perivascular space and within the brain parenchyma of HIV-infected subjects (558, 559); this supports the contribution of these monocytes to HIV infection in the CNS. Myeloid cells are resistant to the HIV cytopathic effects affecting the $CD4^+$ T-cells and monocyte-derived macrophages represent long-lived cells (560). The infiltration of infected monocytes leads to chronic immune activation and inflammation within the CNS (552). In addition, the transmigration of infected monocytes results in further infection of CNS associated cells including microglia, macrophages and, at low levels, astrocytes (527). Although HIV does not productively infect neurons, they are affected by the consequences of HIV infection in the CNS. HIV-infected cells can release viral proteins such as Tat and gp120, which results in the activation of surrounding cells including the macrophages, microglia, and astrocytes (561). The activated cells will in turn secrete cytokines such as IL-1β, IL-6, and TNFα as well as CCL2 and CXCL12 chemo-attractants recruiting more $CD16^+$ monocytes in the CNS that will amplify neuro-inflammation (527, 552); neuro-toxic host factors such as arachidonic acid, quinolinic acid, and NO will also be produced. The presence of all these factors leads to deregulation of the BBB permeability and astrocytic glutamate uptake; this will result in neuronal cell damage and death related to HAND. The transmigration of $CD16^+$ monocytes is partly due to the increased expression of CCR2 (534). The ligand of CCR2, CCL2 (or monocyte chemotactic protein 1 (MCP-1) is elevated in brain tissues of individuals suffering from HAND (562). Infected $CD16^+$ monocytes appear to be highly sensitive to CCL2 in the induction of chemotaxis (534). As mentioned earlier, the non-classical monocytes were previously reported to express low levels of CCR2 (485, 491). With the goal of amplifying $CD16^+$ cells from the total monocytic population, *Williams et al.* established a protocol in which monocytes expressing CD14 and CD16 were generated following three days culture with M-CSF (526, 534, 552). M-CSF functions as a factor differentiating monocytes into macrophages (563). The cells generated following culture, which may be perceived as intermediate monocytes, express CCR2 and were found *in vitro* to

transmigrate across the BBB in response to CCL2 (526, 527, 534). In fact, the intermediate monocytes from the peripheral blood of HIV-infected individuals suffering with HAND expressed higher levels of CCR2 compared with HIV-infected subjects with unaltered cognition (533). CCR2 levels were similarly high on classical or non-classical monocytes in the two groups of HIV-infected individuals. The enhancement of CCR2 on the intermediate monocytes was independent on HARRT, the severity of dementia, viremia, and $CD4^+$ T-cell counts/nadir. Furthermore, this increase of CCR2 observed in patients with HAND led to higher CCL2-mediated trafficking of intermediate monocytes into the BBB compared to counterpart monocytes from HIV-infected subjects with normal cognition. These results suggest that the intermediate monocytes play an important role in neurocognitive disorders and may be regarded as a biomarker for HAND (533). This is consistent with findings by *Ancuta et al.* that reported the preferential expansion of intermediate monocytes in AIDS subjects with dementia (63). Another mechanism contributing to the intermediate monocytes entering the brain involved the expression of junctional proteins at cell surfaces interacting with the brain microvascular endothelial cells (BMVEC) of the BBB (527). As the monocytes mature, they acquire increased expression of the junctional proteins such as junctional adhesion molecule-A (JAM-A), activated leukocyte cell adhesion molecule (ALCAM), CD99, and platelet endothelial cell adhesion molecule 1 (PECAM-1) (534). HIV infection of intermediate monocytes results in an elevation of JAM-A and ALCAM, which, together with CCR2, were reported to mediate transmigration of intermediate monocytes across the BBB. Other factors including osteopontin, an activation marker with chemotactic properties (564), may contribute to the maintenance of intermediate monocytes in the CNS. Osteopontin levels are elevated in HIV-infected individuals with dementia and also in intermediate monocytes (526, 565). Osteopontin was reported to decrease *in vitro* reverse transmigration across the BBB of $CD16^+$ but not that of $CD16^-$ monocytes (566) potentially promoting selective retention of these $CD16^+$ monocytes in the CNS during HIV infection. Targeting these surface molecules therapeutically may limit neuroinflammation during HIV infection.

The pro-inflammatory environment induced by HIV resembles that observed during the natural biological process of aging. Both HIV infection and aging affect the functions of the innate immune system (528). Indeed, studies from the group of Crowe showed that HIV infection leads to premature aged-related changes to monocytes (528). The frequency, phenotype, and functions

of monocytes from young HIV-infected individuals are similar to those displayed by healthy elderly people (528). First, both groups have similar increased levels of $CD16^+$ monocytes. Also, monocytes from young HIV-infected individuals and elderly controls showed increased expression in CD11b and decreased levels of CD62L and M-CSF receptor CD115. Exposure of monocytes to TNF-α and LPS leads to decreased CD62L and enhanced CD11b expression at the cell surface, suggesting that the pro-inflammatory conditions induced during HIV-infection and aging may result in changes in the monocyte phenotype. The decrease in CD115 may be due to the high M-CSF levels observed in HIV-infected subjects leading to CD115 internalization and degradation. Furthermore, monocytes from elderly and young HIV-infected subjects have impairment in their phagocytic functions and displayed telomere shortening compared to the counterpart cells from young uninfected controls (528). Telomere shortening appears to reflect the increase turnover of monocytic precursors, as monocytes do not typically undergo cell division. Indeed, monocyte turnover in SIV-infected primates is correlated to the innate immune activation marker soluble CD163 (sCD163) (567). The increased $CD16^+$ monocytes, telomere shortening, and changes in monocytes phenotype correlated with another innate immune activation marker, CXCL10 (528); this indicates that CXCL10 may represent a biomarker for aging. The immune impairments and phenotypic changes in monocytes observed in HIV-infected individuals are not reversed by ART.

Together, these lines of evidence reveal major alterations in the monocyte compartment during HIV/SIV infection. They raise questions concerning the impact these alterations have on the quality of the immune responses since monocytes are well-established precursors for DCs.

1.3.3 DISCOVERY OF DENDRITIC CELLS

Dendritic cells represent a heterogeneous group of specialized antigen sensing and presenting cells that are essential for the induction and regulation of immune responses. DCs were originally described in 1973 at a conference in Leiden by Ralph Steinman, an M.D., Ph.D. candidate in the laboratory of Dr. Zanvil Cohn (568). At that time, macrophages and lymphocytes were already discovered as cells of the immune system. These cell types could be distinguished by their differential adherence in culture dishes. Adherent cells included macrophages, whereas lymphocytes were the non-adherent cells. Steinman originally wanted to understand the

immunogenicity of specific macrophages that retain whole antigens on their surfaces, first termed dendritic macrophages but now known as follicular DCs. The identification of these dendritic macrophages *in vitro* was difficult since the cells would degrade the antigen upon exposure. He then turned his focus to the identification of immune cells from the mouse spleen. Previous studies by Mitchell and Dutton demonstrated that antibody responses would not be induced without the presence of "*accessory cells*" in the T: B mixture (569). Steinman sought to identify these "*accessory cells*" in the mouse spleen. Surprisingly, these cells had a different morphology and function than macrophages, T and B cells. Furthermore, these cells would tend to extend or contract their dendrites. The cells were named DCs from the Greek word *dendron* that stands for tree. The first immunological role for DCs as a stimulator of graft rejection was found in 1978 by *Steinman et al.* (570). Later on, Steinman and colleagues discovered the role of DCs as antigen-presenting cells, and characterized the process of DC maturation (571). Although the concept of DCs as a distinct type of myeloid cells was not accepted at first by the immunology community (568), Steinman was the driving force in convincing the world of the importance of DCs in immunity. In recognition for his discovery, he received prestigious honors including the 2003 Gairdner Foundation Award and the 2007 Albert Lasker Award. Furthermore, Steinman was the first scientist to receive posthumously in 2011, the Nobel Prize for Medicine or Physiology (568, 572, 573).

1.3.4 DENDRITIC CELLS TYPES AND ASSOCIATED FUNCTIONS

In the years following the original discovery, many types of DCs were described in mice as well as in humans. Several genetic comparisons succeeded in aligning mouse and human DCs, supporting the hypothesis that human and mice have a similar organization of the DC system. In the peripheral blood, human DCs are characterized as cells lacking the T-cells (CD3, CD4, CD8), the B cells (CD19, CD20), and the monocyte markers (CD14, CD16) but highly express HLA-DR (487). Similar to mice DCs, human DCs are divided into three major subsets: plasmacytoid DCs (pDCs), myeloid DCs (mDCs), and monocyte-derived DCs (MDDCs).

1.3.4.1 PLASMACYTOID DENDRITIC CELLS

The pDCs are distinct from mDCs because they are long-lived specialized cells that massively

produce type 1 interferons (IFNs) upon infection (477, 574). In addition to inducing a wide immune response affecting APCs, T- and B-cells, type 1 IFN can also then block viral infections, resulting in pathogen clearance (574). The pDCs also can function as APCs and regulate T-cell responses less potently than mDCs. Human pDCs can be detected by the expression of BDCA-2 and -4, leukocyte immunoglobulin-like receptor subfamily A member 4 (LILRA4-ILT7), and IL-3 receptor α-chain CD123 at the cell surface (575). Under steady-state conditions, pDCs has the morphology of an antibody-secreting plasma cell as indicated by their name (574, 576). As opposed to mDCs, pDCs have a narrow range of TLR expressions. The pDCs highly express TLR-7 and TLR-9 that detect viral and bacterial nucleic acid. Once activated *via* TLR-7 or TLR9, the pDCs undergo changes in morphology with the acquisition of dendrites and up regulate the expression of MHC molecules and activation markers that will allow antigenic presentation to T-cells (577, 578). Indeed, pDCs were reported to activate $CD8^+$T-cells (578). However, pDCs were shown to exhibit a low ability to activate $CD4^+$ T-cells (574, 579) possibly due to the difference in pDC antigen uptake and presentation compared to mDCs. The pDCs can be divided in two subsets, pDC1 and pDC2 (574). The pDC1 display an immature phenotype with low to undetectable expression of MHCII and activation markers, whereas pDC2 express highly MHCII and CD86. The pDC1 were reported to induce T-reg while pDC2 promote the differentiation of pro-inflammatory T-cells. Nevertheless, pDC1 and pDC2 are not stable lineages and can display plasticity between each other depending on local environment. Furthermore, ligation of CD123 on pDCs has been found to result in the induction of iTreg producing IL-10. Interestingly, pDCs were shown to promote Th17 differentiation (579). Therefore, similar to mDCs, pDCs represent a distinct class of DCs with a critical role in shaping immunity.

1.3.4.2 MYELOID DENDRITIC CELLS

Often termed classical or conventional DCs (cDCs), mDCs are specialized antigen processing and presenting cells (477). The mDCs express CD4 but at lower levels compared to $CD4^+$ T-cells (487). Immature mDCs have high phagocytic abilities, while mature mDCs have an increased capacity to produce cytokines. Unlike mice mDCs, human mDCs can be detected in the peripheral blood (477). The mDCs are short-lived and constantly replaced by blood-derived precursors (580, 581). The mDCs are highly migratory and regularly traffic from the periphery into T-cell and B-

cell zones of lymphoid organs. At steady state or during infection, mDCs regulate T-cell functions. The mDCs are classified in two major populations based on the expression of CD141 (or blood DC antigen 3, BDCA-3) and CD1c (or BDCA-1): $CD141^+$ DCs (or cDC1) and $CD1c^+$ DC (or cDC2) (485, 582).

Human $CD141^+$ mDCs are found in peripheral tissues such as the lungs, skin, intestinal lamina propria, and peripheral blood (582). The $CD141^+$ DCs represent the mDC subsets with the highest capacity for cross-presentation (583, 584). Human $CD141^+$ mDCs are the homologues for mouse $CD8\alpha^+CD103^+$ mDCs that exclusively express the chemokine receptor XCR1 and the transcription factor IRF8. Both mice $CD8\alpha^+CD103^+$ mDCs and human $CD141^+$ DCs also express cell adhesion molecule 1 (CAM1), activation receptor CLEC92A, and TLR3. Also, human $CD141^+$ DCs conserved their function of being large producers of type III interferons. Although CD141 is also expressed in pDCs, dermal $CD14^+$ cells and $CD1c^+$DCs, $CD141^+$DCs are distinguished by their low to undetectable expression of cytosolic RNA or DNA sensors RIG-1 and MDA5 as well as surface molecules CD14, SIRPα, CD11b, CD1c and CD11c (582, 585). In addition, human $CD141^+$ mDCs express at high levels CD26 (or dipeptidyl peptidase 4) (582), a receptor for the enzyme adenosine deaminase and costimulatory molecules (586, 587). In fact, the combination of CD26, IRF8, and CAM1 are sufficient for the identification of $CD141^+$ DCs (582). Anatomic locations can further define $CD141^+$ DCs. For example, intestinal $CD141^+$DCs express CD103 (integrin α_E). $CD103^+$mDCs represent an important migratory intestinal population well characterized in mice; in addition to the intestine, these cells can also be located in other peripheral organs and lymph nodes. The $CD141^+$ DCs are known to express co-stimulatory molecules CD40, CD80, CD86 and upon maturation acquire the expression of CCR7 and CXCR3 (588). The $CD141^+$ DCs migrate into the draining lymph nodes where they are specifically localized in paracortical regions.

Human $CD1c^+$ DCs are the most abundant mDCs in the human peripheral blood (577). The $CD1c^+$ DCs were also detected in lymphoid and non-lymphoid organs (582). Human $CD1c^+$ DCs are the homologues of mouse $CD11b^+$ DCs (576, 582). Although all $CD1c^+$ DCs express considerable levels of CD1c, CD11c, and SIRPα, the expression of several markers are dependent on their anatomic location. For instance, dermal $CD1c^+$ DCs express langerin, a marker of Langerhans

cells (589), a type of antigen-presenting cell located in the skin. Also, dermal $CD1c^+$ DCs when compared to peripheral blood $CD1c^+$ DCs exclusively express CD1a and CD141 and down regulate the skin-homing epitope cutaneous lymphocyte antigens (CLA) (582). In the same manner, lamina propria $CD1c^+$ DCs are distinguished from peripheral blood $CD1c^+$ DCs by their high expression of CD103 and CCR6 and lower expression of CX3CR1 as well as membrane glycoprotein CD64. Similar to $CD141^+$ DCs, $CD1c^+$ DCs express the co-stimulatory molecules CD40, CD80 and CD86 at cell surface and acquire CCR7 expression upon maturation. The $CD1c^+$ DCs are distinguished from $CD141^+$ DCs by their expression of various TLR including TLR1-8 Whereas $CD141^+$ DCs were shown to induce Th1 and $CD8^+$ T-cell differentiation (582, 590), $CD1c^+$ DCs were found to generate not only Th1 but also Th2, Th17, and iTreg immune responses (582). Indeed, cDC2 cells were reported as the primary inducers of Th2 and Th17 immune response following antigenic stimulation (591, 592). The cDC2 produce IL-23 under steady state and during infection whether they are located in the lungs, skin, or within the intestine (591, 593, 594). Therefore, each subset has a distinct role during host defense.

1.3.4.3 MONOCYTE-DERIVED DENDRITIC CELLS

The discovery of monocytes as precursors of DCs was made by studies from Frederica Sallusto and Anthony Lanzavecchia and Romani in 1994 (595, 596). Previous studies by the group of Jacques Banchereau provided evidence supporting the possibility that DCs from the skin derive from hematopoietic progenitor such as monocytes (597). It was originally thought that monocytes were the precursors of mDCs. Indeed, MDDCs have similar transcriptomic features as $CD1c^+$DCs (598). Both human and mice have MDDCs (477, 576, 582). However, under steady state conditions, DC induction is independent from monocytes. In fact, upon infection, murine classical monocytes are recruited to the site of inflammation to be converted into "*inflammatory*" DCs (inf-DCs). The inf-DCs have a large capacity to produce microbicidal compounds and appear to perform functions distinct from those of DC that are present under steady-state conditions (585). It is thought that DCs are shaped to induce tolerance during homeostasis thus preventing inflammatory responses from Th1 cells (599). The inf-DCs are thought to bypass this conditioning to become one of the first APCs capable of activating effector T-cells at the local site of infection (585). Indeed, many research groups provided evidence that the immune system uses monocytes

as precursors of DCs for efficient antigenic presentation in the periphery during inflammation (600-602). The MDDCs are thus recognized as specialized APCs that potentially serve as an emergency plan in peripheral organs in unexpected hostile inflammatory settings. The inf-DCs are cleared from immune system once the inflammation is resolved (576). The inf-DCs produce large amounts of IL-23 upon specific stimulation leading to the differentiation of Th17 cells (603). Following ligation of TLR-4, TLR-8, or Nucleotide-binding oligomerization domain-containing (NOD) family members, inf-DCs become a source of TNF and inducible NO synthase (iNOS)-producing DCs (Tip-DC) with effective antimicrobial effector properties (576, 585). The MDDCs can be generated *in vitro* from human and mouse monocyte precursors in the presence of IL-4 and GM-CSF (or CFS-2) (595, 604). The inf-DCs are homologous to mouse and human MDDCs generated *in vitro* (585). Although not well described, inf-DCs and Tip-DCs were identified in humans with similar characteristics (605). Both human $CD16^-$ and $CD16^+$ monocytes can differentiate into DCs *in vitro* (483). Both MDDCs subsets internalize soluble antigen and induce effector T-cells proliferation in similar manners (606). In addition, human MDDCs express at the cell surface CD11b, CD11c, MHC-II, Dendritic Cell-Specific Intercellular adhesion molecule-3-Grabbing Non-integrin (DC-SIGN), cell adhesion molecule CD24, SIRPα, and macrophage markers CD107b and LAMP2 (483). Indeed, DC-SIGN can distinguish MDDCs from other subsets of DCs (607). Compared to $CD16^-$ MDDCs, $CD16^+$ MDDCs express higher levels of CD86, CD11a, and CD11c as well as lower levels of CD1a and B cell co-receptors CD32 (606). Also, $CD16^+$ *versus* CD16- MDDCs express higher levels of TGF-β1. The $CD16^+$ MDDCs were reported to represent migratory DCs that transiently traffic to lymphoid and non-lymphoid organ to perform immunosurveillance (608). Furthermore, $CD16^+$ MDDCs induce the production of IL-4 following stimulation with TLR-2 ligand peptidoglycan, TLR-3 ligand poly-IC, and TLR4 ligand LPS (609). Conversely, $CD16^-$ moDCs primed with LPS express increase mRNA levels of IL-12p40 mRNA and produce higher secretion of IL-12 compared to $CD16^+$ moDCs counterpart (606). The $CD16^-$ moDCs also express higher levels of DC maturation marker CD83 following ligation of TLR2, TLR3 and TLR4 (609) suggesting possible differences in the activation of signal transduction molecules between the two subsets of MDDCs. Interestingly, a subset of DCs distinct from $CD1c^+$DCs and $CD141^+$DCs referred to as Slan DCs was identified in human peripheral blood (503). These Slan DCs are identified as $CD1c^-CD11c^+CD16^+CD14^-$ cells that massively produce TNF-α, IL-12, and iNOS as well as highly expressing TLR7 and TLR8 (610). The group

of Schäkel found that Slan DCs produce high levels of IL-23, IL-1β, and IL-6, which leads to the development of Th1/Th17 cells (611). By being inducers of Th1/Th17 cells, slan DCs are thought as pro-inflammatory DCs that contribute to the pathogenesis of autoimmune diseases such as psoriasis. However, the identity of Slan DCs as a distinct DC subset is still controversial since these cells are not detected in peripheral tissues and are genetically close to the monocyte lineage (612, 613). They are thought to be monocytes with DC properties (612); slan DCs are derived from this subset of monocytes (612). In addition, MDDCs were reported to possess the capacity of cross-presentation to naive T-cells and the ability to transfer peptides from MHC-I to lymphoid resident DCs (614). Peripheral blood monocytes represent an important pool of DC precursors that traffic to sites of infection. Monocytes are numerous in the blood and constitute an essential component in the induction of T-cell immunity. In fact, MDDCs generated *in vitro* are the most common type of DCs used in vaccine-based therapies (483).

1.3.5 ONTOGENY OF DENDRITIC CELLS

Similar to macrophages and monocytes, DCs originate and develop from common hematopoietic stem cell-derived progenitors in the bone marrow (477). The progenitors of DCs differ from those of the Langerhans cells, which are derived from embryonic precursors (615). Cytokines that control the development of the DC lineage include Flt3L, M-CSF, GM-CSF, lymphotoxin-β, and TGF-β1 (483). Early hematopoietic stem cells will give rise to lymphoid (LP) and myeloid (MP) committed precursors. The MPs will proliferate and differentiate into macrophage/DC precursors (MDPs) (477). The MDPs are precursors of myeloid cells, excluding the granulocytes. The MDPs will then generate the monocytes and the common DC precursors (CDPs). At this stage, the CDPs derived from MDPs cannot give rise to monocytes and differentiate into pDCs or the precursors of classical DCs (pre-cDCs) (580, 616, 617). Two subsets of CDPs have been characterized based on the expression of colony-stimulator factor 1 receptor (CSF1-R). The CSF1-R^+CDPs gives rise to mDCs, whereas CSF1-R^-CDPs differentiate into pDCs (618). Recent findings indicate that pDCs can be generated from lymphoid-primed multipotent progenitor (LMPP), a more primitive progenitor (618). Pre-cDCs exit the bone marrow to circulate into the bloodstream via the high endothelial venules and migrate into the lymphoid and non-lymphoid organs where they will differentiate into mDCs ($CD1c^+$DCs or $CD141^+$DCs) and undergo maturation in surface

phenotype and morphology. Also, the development of mDCs continues in lymphoid organs that are controlled partly by Tregs, cytokine receptor Flt3 and lymphotoxin-β receptor. The transcription factor Zbtb46 is uniquely expressed by mDCs, as well as associated progenitors, and defines this lineage. Interestingly, recent studies by *Schlitzer et al.* argue that $CD1c^{+}$DCs and $CD141^{+}$DCs commitment occurs in the bone marrow and not in peripheral organs (619). Both cDC1 and cDC2 appear to have distinct established lineage markers at the CDP stage. At steady state, the pDCs also exit the bone marrow to migrate into the thymus and secondary lymphoid organs. Only upon inflammation will the pDCs migrate and accumulate into non-lymphoid organs. The development of pDCs is dependent on the expression of specific transcription factors E protein E2-2 and Spi-B (Schotte R and J ex med 2004) (620). The E2-2 binds to the promoter of pDCs associated genes, including BDCA2 and LILRA4-ILT7 (621). In the presence of specific inflammatory environment, monocytes will give rise to DCs that are distinct from pDCs and cDCs. In contrast to pDCs and cDCs, MDDCs development is independent of the key regulator of DC commitment, Flt3L. Of note, the associated receptor Flt3 is absent in MDDCs (483). The DC ontogeny was mostly characterized in the mice model. Although Gata2 and IRF8 were identified as potential transcription factors involved in the development of human DCs, the complete list of components, as well as the equivalents transcription factors for murine DC progenitors, remains to be identified in humans.

1.3.6 DENDRITIC CELL MATURATION

Cellular maturation is a crucial biological process in which DCs acquire immunogenic properties that will drive subsequent T-cell differentiation. Maturation is complex and involves a series of steps in which the DCs process and present the antigen, migrate toward lymphoid tissues, and provide co-stimulatory signals to T-cells (576). Also, maturation is a heterogeneous process in which DCs acquire distinct properties dictating the quality of subsequent adaptive immune responses. Under steady state conditions, DCs are considered immature or in a resting mode. Immature DCs express low level of MHC-II and co-stimulatory molecules such as CD80 and CD86. Recognition of pathogen components *via* interaction with pattern recognition receptors (PRRs) will trigger a series of intracellular events in DCs leading to maturation. The PRRs include TLRs, C-lectin receptors (CLRs) and NOD-like receptors (NLRs) that are essential in inducing

effector Th1, Th2 or Th17 type responses (622). The TLRs were the first group of PRRs identified; they recognize a variety of bacterial/viral/fungal components ranging from RNA/DNA genome to cell wall features. The discovery of TLR helped in better understanding the way the immune system distinguishes between self and non-self and initiates immune responses (623) (624-626). The CLRs recognize carbohydrate from pathogen cell membrane. The NLRs are characterized by their conserved NOD domain and sense intracellular microbial features. Following capture through interaction with PRRs expressed on immature DCs, pathogen-derived components are phagocytized and processed into fragmented peptides, leading to subsequent antigen presentation via MHC class II molecules (487). In addition, interaction with distinct PRRs will trigger the activation of specific signaling pathways. All TLRs, except TLR3, signal through MYD88 adapter that triggers the NF-κB and the mitogen-activated protein kinase (MAPK) signaling pathway (576). The TLR3 triggering leads to the stimulation of the IRF signaling pathway. The CLRs activates the Syk protein kinase pathway, whereas the NLRs signal through the NFκB (622). The activation of these signaling pathway leads to the up regulation of co-stimulatory as well as adhesion molecules and production of cytokines. Furthermore, PRR signaling results in serious alteration in the expression of DC chemokine receptors such as the up regulation of CCR7, which promotes trafficking into peripheral lymphoid tissues (487, 627). This behavioral change is termed licensing in which DCs undergo a differentiation program that will allow them to interact and activate naive and/or memory $CD4^+$ T-cells. Mature DCs highly express MHC-II, adhesion proteins (i.e. CD54, DC-SIGN), maturation markers (i.e. CD83), co-stimulatory molecules (i.e. CD80, CD86), and lymph-node homing markers (i.e. CCR7). Also, mature DCs secrete chemokine CCL18 to attract naive $CD4^+$ T-cells. Together, these newly acquired properties will shape a proper adaptive immune response against a specific pathogen.

1.3.7 REGULATION OF TH17 DEVELOPMENT BY DENDRITIC CELLS

The fate of a naive $CD4^+$ T-cell depends largely on three signals provided by the APCs (622). Signal #1 is delivered following engagement of the TCR on naive-$CD4^+$ T-cells upon interaction with the MHC complex carrying immunogenic peptides at the surface of DCs to TCR. Signal #2 involves the interaction between co-stimulation molecules (*i.e.,* CD80, CD86, ICOSL) up regulated at the surface of APCs upon pathogen recognition and the counter-receptors expressed

on T-cells. Signal #2 is crucial for the subsequent T-cell survival and proliferation. Signal #3 is provided by APCs and consists of specific cytokines and non-cytokine mediators produced following engagement of a PRR signaling pathway; signal #3 shapes the polarization of naive T-cells into Th1, Th2 or Th17 cells. The quality and/or strength of each signal will influence the ultimate induction of the Th17 differentiation program. Studies in 2009 implied that strong but not intermediate or low TCR signaling leads to the development of Th17 cells (628). The strong antigenic stimulation results in the massive up regulation of CD40L expression on T-cells, which acts in combination with IL-6 produced by DCs to trigger Th17 differentiation. Of note, the indicated strength of TCR signaling essential for Th17 differentiation is stronger than the one required for Th1 or Th2 development. This is in contrast with recent publications demonstrating that Th17 differentiation depended on low-strength T-cell activation (629, 630). Indeed, *Kastirr et al.* demonstrated that uncommitted naive T-cells required sustained and low CD3 concentrations to induce higher levels of IL-17A (630). Interestingly, memory Th17 cells were also reported to require low antigenic stimulation to induce proliferation due to the up regulation of miR-181a (631). CD86 expression on DCs was reported to be primordial for the generation of Th17 cells as blockage of CD86 but not CD80 expression leads to inhibition of IL-17A-producing T-cells (632, 633). Ligation through inducible costimulator (ICOS) on T-cell surface is critical for the induction and expansion of human Th17 as well as Th1Th17 cells (634). The DC-$CD4^+$ T-cell interaction through ICOSL and ICOS leads to increased expression of IL-21, IL-17A, IL-17F, IFN-γ, c-Maf, RORC, and T-bet. The Th17 differentiation also depends on DC secretion of IL-6, IL-1β, and IL-23 (298, 622). Because naive T-cells do not express IL-23R, the effect of IL-23 is observed at later stages of Th17 differentiation. Furthermore, DCs can produce cytokines that limit Th17 differentiation. For example, IL-27 appears to be the most potent cytokine in the inhibition of Th17 cell development (384, 635). The DCs also produce IL-10 that restrains in an autocrine manner the ability of DCs to produce IL-1β (636).

Segmented filamentous bacteria (SFB) have been reported to induce intestinal murine Th17 cells (361, 362). Recently, the group of Ivanov extended their original studies and showed that the induction of SFB-specific Th17 cells was dependent on MHC-II expression on DCs (637). Presentation of SFB by DCs through MHC-II was crucial for the induction of Th17 cells. Of note, ablation of MHC-II did not affect the production of polarizing cytokines such as IL-6, TGFβ, and

IL-1β in the environment; this indicates that other cells were responsible for their induction. Besides the influence of polarizing cytokines, SFB induced the expression of serum amyloid A (SAA) in epithelial cells (365), which can act on lamina propria DCs for the induction of Th17 cells (361, 638). Also, the generation of SFB-specific Th17 cells did not require migration towards LN or GALT but could occur locally in the lamina propria (637).

The production of Th17 polarizing cytokines by DCs is largely mediated through interaction between specific pathogens and particular PRRs. Among various microorganisms, *C. albicans* has been reported to be by far the most potent inductor of Th17 immune responses (639). The DCs sense the presence of *C. albicans* or other fungus *via* their cell wall composed of the polysaccharides zymosan and mannan (622). Zymosan is rich in β-glucans, which are recognized by CLRs expressed on DCs. The CLR β-glucan receptor dectin-1, also referred to as CLeC7A, was reported to stimulate DC maturation, leading to Th17 cell development (640). Indeed, ligation of dectin-1 on DCs activates the kinase Syk and the adaptor caspase recruitment domain (CARD) 9, which leads to the production of Th17 polarizing cytokines such as IL-6, TNF-α, and IL-23 that will instruct a T-cell to become an effector Th17 cell. The *C. albicans* infection leads to the activation of CARD9 signaling pathway and subsequent Th17 immune responses. Similar to dectin-1, ligation of dectin-2 (known as CleC6A) was also described as inducing Syk-CARD9 signaling (641, 642). However, dectin-2 was shown to be a potent inducer of Th17 differentiation and mediator of immune protection against both the yeast and hyphal form of *C. albicans* (642). The CLR mannose receptor also interacts with *C.albicans* and resulting in the production of IL-17A on T-cells (639). Although TLRs have a role in the induction of Th17 differentiation, their impact is weaker when compared to CLRs (622). Ligation with all human TLRs can drive DCs to induce Th17 responses (643). Interestingly, the effect of TLR on the regulation of Th17 differentiation appears to be dependent on the type of DCs. Indeed, zymosan binding to TLR2 on mice splenic DCs was reported to promote the generation of T-regs, whereas zymosan-TLR2 interaction on murine bone-marrow derived DCs and human MDDCs led to IL-6, IL-1β, and IL-23 production as well as priming of Th17 responses (643-645). Among all TLRs expressed on MDDCs, TLR2 was reported to be the larger inducer of Th17 cell development (643). The TLR2 was also described to act in combination with other PRRs on DCs for the induction of Th17-polarizing cytokines, following pathogen recognition. Studies from *Gerosa et al.* demonstrated

that ligation of TLR-2 and dectin-1 on human MDDCs mimicked the zymosan triggering of IL-23 with low expression of IL-12 (645). Up regulation of IL-12 production with no effect on IL-23 expression by zymosan required IFN-γ or TLR7 ligation. Interestingly, IL-12 was efficiently triggered in the presence of low but not high doses of zymosan in combination with TLR7 ligands or IFN-γ; this indicated that the level of PRR engagement dictated the quality of DC cytokine production. *Gerosa et al.* also demonstrated that supernatant from MDDCs primed with zymosan or β-glucans induced differentiation of naive $CD4^+$ T-cells into effector Th17 lymphocytes (645). This differentiation required the production of IL-1β as the activation of MDDCs with the combination of LPS and TLR7 ligand triggered IL-23 but not IL-1β production and subsequently failed to generate Th17 cells. In addition to the antifungal immunity, the antibacterial response, including the one against *S. aureus* and *M. tuberculosis,* also involves the induction of Th17 differentiation (643, 645). Intracellular NLR NOD2 in combination with TLRs such as TLR2 and TLR4 mediates this mechanism. The bacterial component is metabolized following its internalization *via* TLR in DCs thus allowing for interaction with NOD2 that will enhance the IL-23 and IL-1β production originally initiated by TLR signaling (643). Crohn's disease patients deficient in NOD2 lack the ability to activate the IL-23/IL-1βI/L-17 axis. Furthermore, the NLRP3-mediated inflammasome complex is also triggered in DCs leading to IL-1β and subsequent Th17 immune responses. Uric acid from apoptotic cells, a damage-associated molecular pattern (DAMP), combined with NOD2 activates the NF-κB cascade on DCs for the production of IL-6, IL-23 as well as inflammasome-dependent cytokines IL-1α/β and IL-18; this drives Th17 cell development (646). The role of the NLRP3-mediated inflammasome complex in DCs has been observed as a response to infection with *Bordetella pertussis* and *C.albicans* (622). The DCs triggering Th17 responses mainly depend on downstream activation of p38α MAPK following sensing of fungal and bacterial component *via* PRRs (633). Ligation on CD40 was also reported to be involved in the up regulation of p38α MAPK activity. Subsequent activation of p38α MAPK led to higher expression of CD86 and production of IL-6 as well as IL-27. The role of p38α MAPK in programming DC to promote Th17 cell development was observed in murine DCs and human MDDCs (633).

In addition to PRR, other factors may influence DC-dependent Th17 response. For example, TNF-α acts on DCs to promote IL-23 production whereas blockade of TNF-α inhibits Th17 responses in

psoriasis patients (647). Allergen stimuli trigger the up regulation of stem cell marker c-kit that will lead to PI3K activation and subsequent production of IL-6. Stimulation of DCs via CCR7 also triggers IL-23 production and the subsequent generation of pathogenic Th17 cells (648). ATP produced by leukocytes is considered as an "alarmin" (649). Signaling through adenosine receptors such as adenosine receptor A (2B)AR) induces IL-6 and generation of Th17 cells (650). Ligation of EP2/EP4 receptor on DCs with lipid mediator PGE2 favors IL-23 as opposed to IL-12 production, promoting Th17 generation during EAE (651). Conversely, triggering of IFN-γ receptor leads to inhibition of DC-mediated Th17 induction and promotes the production of IL-10, a mechanism in which IL-27 is involved (652). Expression of galectin-3 on DCs also results in suppression of Th17 differentiation (653). Therefore, several factors, including the nature of antigen and the surface expression of specific molecules, will dictate the activation of signaling pathways leading to the production by DCs of polarizing cues that instruct a naive T-cell to undergo Th17 differentiation.

1.3.8 DENDRITIC CELLS AND HUMAN IMMUNODEFICIENCY VIRUS

Primary HIV infection generally occurs *via* vaginal or rectal routes (654). These sub-mucosal tissues comprise a variety of DC subsets ready to encounter the virus. Due to their localization, DCs play an important role in disseminating viral infection to $CD4^+$ T-cells (655). During early SIV infection, pDCs are recruited to the site of infection following viral challenge (656). This recruitment is mediated by CCL20 produced by endocervical epithelial cells. The pDCs, in turn, secrete CCL3 and CCL4 leading to the trafficking of $CCR5^+CD4^+$ T-cells into the endocervix (656). Furthermore, endocervical epithelial cells were demonstrated to secrete *in vitro* thymic stromal lymphopoietin (TSLP) resulting in the activation of mDCs that subsequently produce CCL17 and CCL22, attracting naive $CD4^+$T-cells for expansion and infection (657). Elevated levels of TSLP associated with high viral replication are found in rhesus macaques' vaginal tissues during the first two weeks of SIV infection (657). Compared to $CD4^+$ T-cells, DCs are poorly infected (658). Studies on early SIV infection demonstrated that resting $CD4^+$ T-cells, but not DCs, represent the initial SIV-infected population in mucosal tissues (659, 660). Nevertheless, DCs were found to sequester virus for several days before efficiently spreading the infection to $CD4^+$ T-cells (661-664). The DCs express high levels of HIV-1 co-receptors CCR5 and CXCR4

and low levels of CD4, allowing attachment of viral glycoprotein gp120 to target cells (665, 666). In addition to the expression of these key molecules for HIV entry, DCs express other receptors capable of binding to the envelope protein HIV-gp120. Indeed, myeloid dermal DCs and MDDCs express C-type lectin (CLR) receptor DC-SIGN as well as the mannose receptor (667-670). Initially, studies by the group of Littman (671) demonstrated that DC-SIGN allowed HIV internalization into low pH sub-membrane vesicles thus preserving virion virulence (672). The same group later published contradictory results that DC-SIGN was not essential for HIV *trans* infection by DC (673). The MDDCs also express DC immunoreceptor (DCIR) that binds HIV-gp120 and contributes to HIV dissemination by DC to T-cells (674). Other receptors such as syndecan-3 attach to gp120 and subsequently contribute to viral transmission (675). Although pDCs express the CLR BDCA2 and DEC-205, recognition and binding of HIV-gp120 is mediated by CD4 followed by the endocytosis of viral particles (676). The HIV can also enter in DCs independently of HIV-gp120. Interaction between glycosphingolipids in the virus lipid bilayer and an unknown receptor at the DC surface membrane were reported to occur (677-679). Lipid content on DC membrane surface may affect envelope-independent HIV capture. Indeed, peroxisome proliferator-activated receptor (PPAR)γ and liver X receptor (LXR) prevent HIV uptake by triggering cholesterol efflux, which diminishes the lipid content (680). The maturation of both MDDCs and mDCs results in an increased *trans* infection (681). The DCs play a dual role in HIV infection: *cis*- and *trans* infection. *Cis*-infection occurs when HIV infects DCs as target cells, generating *de novo* virions (682). This phase lasts 24 to 72 hours after HIV exposure (654). The transfer of virus from DC to $CD4^+$ T-cells is referred to as *trans* infection. Transmission of viral particles from DC to $CD4^+$ T-cells involves exosome secretion pathway or structures called virological/infectious synapse (683-687). More precisely, the virological synapse is defined as an adhesive junction between two cells (one infected and one uninfected) involving the cytoskeleton and lipid rafts that allow transmission of a virus from a donor to a recipient cell. Viral transmission occurs when a DC is in the proximity of a T-cell allowing for cell-contact. The virological synapse is strengthened by molecules such as DC-SIGN, ICAM-1, LFA-1, and CD4. These molecules are found in large numbers at the interface between DC and $CD4^+$ T-cells. During *trans* infection, DC may interact with the virus through DC-SIGN, leading to the formation of a pocket structure at cell surface. Once cell contact with $CD4^+$ T-cells occurs, a virological synapse is established. In immature DCs, HIV induces membrane extensions through the

activation of the Rho-GTPases Cdc42 and promotes viral transfer in $CD4^+$ T-cells (688). Conversely, *trans* infection involving LPS-matured DCs leads to filopodial extensions of the $CD4^+$ T-cells into the structured pocket of DCs (689). Viral transfer in this context depends on the activation of CD4 molecules at the T-cell surface. Mature DCs are more efficient in HIV trans infection compared to immature DCs (545). Of note, a specific DC subset expressing both CD14 and CD16 was demonstrated to have a high capacity to transmit infection to $CD4^+$ T-cells through DC-SIGN expression (690). Cell-to-cell viral transmission favors HIV dissemination and persistence, as it is less sensitive to the presence of antiretroviral drugs such as the nucleotide reverse transcriptase inhibitor tenofovir and the non-nucleoside reverse transcriptase inhibitor efavirenz (691). Studies in humanized mice also emphasized the importance of DC-mediated *trans* infection of T-cells in promoting viral persistence (692).

Once the virus interacts with DCs, its fate is dependent on the bound receptor, the subset of DCs, the stage of maturation, and the cell interaction (665). The majority of virions captured are in part degraded in DCs. However, interaction with DC-SIGN does not result in complete viral degradation. Virions bound to DC-SIGN are retained in early endosome compartments, and this may promote the *trans* infection of T-cells (663, 672). Once captured in mature MDDCs, HIV is localized within the cholesterol-enriched and tetraspanin-containing compartments where it may be subsequently delivered to target $CD4^+$ T-cells through the exosome pathway (677, 693). Retention of virions in pDC non-acidic early endosomes will activate IRF7, triggering IFN-α production (694). The pDCS up regulate CD83 as well as CCR7 following viral interaction and respond to CCL19-mediated chemotaxis (695). Nevertheless, HIV infection in pDCs does not lead to complete maturation. The pDCs stimulated with HIV do not result in high expression of CCR7, CD40, and CD86 compared to pDCs activated with TLR7 agonists (694). In addition, pDCs partially matured by HIV induce low levels of $CD4^+$ and $CD8^+$ T-cell proliferation as opposed to pDCs stimulated with TLR7 or TLR9 agonists (694). Furthermore, HIV-exposed pDCs produce inferior levels of IL-6 and TNF-α compared to other stimuli. In contrast to ligands that can traffic to late endosome/lysosome, HIV retention in early endosomes leads to poor activation of the NF-κB signaling resulting in incomplete maturation and lack of MHC expression. Therefore, pDCs are not able to efficiently present antigens. The induction of the NF-κB signaling pathway leading to complete maturation is closely associated to TLR regulation in which previously activated pDCs

become resistant to further stimuli that would lead to additional production of IFN-α (665). Therefore, the lack of maturation in HIV-exposed DCs leads to unregulated, persistent production of IFN-α due to repetitive stimulation, and this increase in the levels of IFN-α can induce serious immunological consequences including cell exhaustion (665, 694). Similar to pDCs, mDCs exposed to HIV exhibit a certain level of activation but do not fully mature (47). Early studies demonstrated that HIV exposure impairs the immunogenic potential of DCs (696). In contrast to pDCs, TLR7-mediated immune response is poorly induced in MDDCs following HIV exposition (697). Partially matured mDCs lead to the generation of Tregs, which will attenuate the pro-inflammatory antiviral response. Also, alterations of the crosstalk between mDCs and NK cells lead to poor DCs maturation. Immature MDDCs exposed to HIV secrete considerable levels of IL-10 leading to resistance of NK-cell mediated lysis and accumulation of poorly immunogenic DCs in lymph nodes of HIV-infected individuals (698).

Evidence provided by various groups including that of Dan Littman support the concept that mDCs and MDDCs are unable to appropriately sense HIV because viral replication is restricted in these cells; this impedes their maturation process and immunogenic potential (671). The HIV capsid includes motifs able to block sensing of viral cDNA (699). Studies by *Manel et al*. demonstrated that increased HIV replication by ectopic SIV-Vpx expression in human DCs results in increased viral replication and immunogenic potential (700). In contrast, other lines of evidence provided by the groups including that of Vincent Piguet suggest that a decreased immunogenic potential in DCs during HIV infection is explained by HIV altering cellular metabolic processes important for antiviral responses (701). Indeed, autophagy, a process required for TLR-induced immune response, was shown to be exhausted in MDDCs during HIV-infection (701). Interaction with HIV envelops leads to the activation of mTOR in MDDCs; this results in suppression of autophagy and impaired TLR signaling. Also, the defect in autophagy upon HIV exposition leads to altered antigen processing and presentation (701).

The fact that DCs are poorly infected with HIV compared to $CD4^+$ T-cells is explained by the presence of several host factors shutting down HIV replication. Several restriction factors including TRIM5α, APOBEC3G, BST-2, and SAMHD1 are expressed in DCs (47, 665) (81, 82). The ABOBEC3G is up regulated in immature MDDCs following stimulation with type 1 IFN,

preventing viral infection (702). The most effective restriction factor probably remains SAMHD1 (81). The pDCs and mDCs were reported to express high levels of SAMHD1 that is not degraded by HIV, and this leads to inhibition of viral replication (703). Furthermore, before the discovery of SAMHD1, it was well established that SIV-Vpx overexpression induces MDDCs maturation and production of type 1 interferon (700, 704). The immune activation induced by the presence of Vpx is dependent on interaction of *de novo* synthesis of viral capsid protein with cellular cyclophilin A leading to subsequent activation of IRF3 (700). The innate sensor involved in this pathway has been proposed to be cyclic GMP-AMP (cGAMP) synthase (cGAS) as this is a factor sensing reverse-transcribed HIV-DNA (699, 705). Nevertheless, the viral capsid prevents sensing of HIV-DNA by cGAS, after reverse transcription (699, 706). Recognition of HIV components by cGAS is the only sensing mechanism discovered in MDDCs (697). The lack of Vpx in HIV-1 may in part explain the inability of mDCs to accurately induce priming and expansion of HIV-specific T-cell responses. A recent study on HIV-2 that express Vpx, demonstrated that infected individuals show higher mDC activation that may contribute to effective viral control (707). The effect of Vpx in the activation of mDCs appears to be difficult to observe as mDCs expressed by 30-fold higher levels of SAMHD1 compared to MDDCs (47). Independently of induction by Vpx, type 1 IFN production itself can inhibit early and late stages of HIV replication (708). The host exonuclease TREX1 also contributes to viral evasion by degrading reverse transcribed HIV-DNA thus preventing sensing by PRRs (709). Deletion of TREX1 triggers innate immune responses. Therefore, impaired viral immune recognition and blocking of infection at different stages of replication may allow HIV to escape detection by DCs.

The impact of HIV on DCs is also observed quantitatively. Both pDC and mDC frequency is reduced, starting during early stages of infection and throughout the chronic phase of HIV pathogenesis (710, 711). Nevertheless, it appears that $CD163^+$ DCs lacking CD16 expression are increased in frequency during HIV infection compared to $CD163^-$ DCs expressing CD16 (712). The frequency of DCs is inversely associated with viral load. The decrease in peripheral blood pDC numbers may indicate enhanced recruitment into lymph nodes or other tissues, early death, or a defect in precursor differentiation in the bone marrow (47). Indeed, during primary SIV infection in rhesus macaques, elevated frequencies of pDCs tend to migrate into lymph nodes where they subsequently undergo cell death (713). The number of peripheral blood pDCs is positively

correlated to $CD4^+$ T-cells rate (47). The antiviral therapy only partially restores the number of pDCs (711). During the acute phase of HIV infection, pDCs appear to be in a hyperactive mode as they produce superior levels of pro-inflammatory cytokines including IL-6, TNF-α, and chemokine ligands of CCR5 following stimulation with TLR-7 agonist (710). Throughout the acute and chronic phase of infection, pDCs constantly persist in being large producers of IFN-α; this is possibly due to impairment in type 1 interferon regulation as these cells partially mature (47). The HIV does not trigger the signaling pathway involved in shutting down IFN-α expression. In fact, HIV-exposed pDCs continuously up regulate IRF7 that is associated with the persistent production of type 1 IFN. High levels of IFN-α in infected primates and humans are correlated with immune activation and disease progression. Persistent production of type 1 IFN is also associated with the T-cell exhaustion reflected by the up regulation of PD-1 and CTLA-4 (714-716). Interestingly, studies by *Sandler et al.* demonstrated that blockade of type 1 interferon receptor led to a reduced in antiviral responses, an increase in viral reservoir size and SIV disease progression (717). Furthermore, acute but not persistent administration of IFN, preferentially IFN-α2a triggered an upregulation of antiviral response and prevented infection. Therefore, the timing of IFN-associated response in SIV infection can affect the overall course of disease progression. Compared to the non-pathogenic primate model in which the intense expression of IFN-α and IFN-stimulated genes is resolved following primary SIV infection, the pathogenic model of SIV is characterized by sustained levels of type 1 IFN (718, 719). Whether the IFN signature mirrors SIV replication or the control of SIV replication in pathogenic *versus* non-pathogenic SIV models remains unclear (717, 720). However, several studies report that HIV-exposed pDCs produced reduced levels of IFN-α following stimulation by TLR-7 and TLR-9 agonists and display decreased capacity to activate NK cells (721-723). Recent studies demonstrated that Vpu interacts with BST2 and inhibits TLR-7 mediated IFN-α production in pDCs (724). Persistent production of IFN-α can result in enhanced apoptosis of uninfected $CD4^+$ T-cells with the up regulation of the TNF-mediated cell death pathway (725). Furthermore, sustained type 1 IFN signaling during chronic infection leads to up regulation of PD-1 on DCs, production of IL-10, and reduced frequency of $CD4^+$ T-cells producing IFN-γ (726, 727).

The effects of type 1 IFN on Th17 polarization are controversial. Although, pDC and IFN trigger exacerbated Th17 responses in a model of psoriasis (728), it was also reported that type 1 IFN

decreases the development Th17 responses (729). The HIV-exposed pDCs can induce the generation of Tregs from naive $CD4^+$ T-cells (730). This induction of Tregs involved the production of IDO that is triggered following CD4-mediated endocytosis of HIV and TLR7 activation. The generated Tregs by pDCs were shown to suppress $CD4^+$ T-cell responses and inhibit maturation of mDCs upon stimulation with TLR4 and TLR7 agonist thus reducing antigen-presentation (731). This finding reflects the dichotomous impact of pDCs during HIV infection as previous studies demonstrated that pDCs could also induce bystander activation and maturation of mDCs through the production of TNFα (695). Growing evidence indicates that mDCs functions are altered within weeks following HIV infection where viremia is still undetectable. During early stages of acute HIV infection, mDCs lose the capacity to produce high levels of IL-12 and TNF-α following stimulation with TLR-7 agonist (732). The MDDCs from uninfected individuals exposed to plasma from acutely HIV infected subjects had a reduced ability to secrete pro-inflammatory cytokines. Also, culture with plasma from acutely HIV-infected individuals inhibited NK and T-cell activation induced by MDDCs (732). The HIV itself does not seem to be directly involved in DCs suppressed cytokine production. Conversely, non-viral components including apoptotic microparticles seem to affect mDC function, preventing the establishment of much needed innate and adaptive immune response at early stage of infection (732). As opposed to the early stages of acute HIV infection, mDCs from later stages are hyper-responsive to TLR7 agonist and produce strong levels of IL-12, IP-10, TNFα, and ligands of CCR5 (710). These findings indicate that the alteration in mDC function during acute HIV infection is time specific as it transitions from an absence to a massive production of pro-inflammatory cytokine, which affects the course of immune response. The impairment in mDC functions continues during the chronic phase of HIV infection (47). The MDDCs from chronically HIV-infected individuals produce lower levels of IL-12 upon stimulation of lipopolysaccharide and CD40 ligand (733). The IL-12 is essential for the activation of NK cells and generation of Th1 cells. Furthermore, MDDCs from infected individuals exposed to plasma from untreated viremic subjects have a reduced ability to produce IL-12, IL-6, and TNF-α after stimulation with TLR3 and TLR7 ligands (734). Again, non-viral components seem to be responsible for the altered functions of MDDCs. The direct effect of HIV on MDDC function was shown to involve production of IL-10 that inhibits cell maturation (47).

Taking into consideration the findings summarized in Chapter 1.3, in the second part of my Ph.D. work (Chapter 5), I focused on the transcriptional and functional characterization of DC derived from $CD16^+$ *versus* $CD16^-$ monocytes in terms of immunogenic potential and HIV *trans* infection capacity. The goal of these studies was to determine the effect of the well-documented expansion of $CD16^+$ monocytes in HIV-infected subjects on the quality of immune responses and HIV dissemination. We provide evidence that $CD16^+$ and $CD16^-$ monocytes differentiate into DCs with distinct trafficking potential, immunological function, and ability to propagate HIV to T-cells (*Wacleche et al.,* Manuscript #2 (in preparation for submission at ***eBlood***) and Manuscript #3 (in preparation for submission at ***The Journal of Immunology***)).

CHAPTER 2:
HYPOTHESIS AND OBJECTIVES

The chapter 2 of my thesis is divided in two sections. The first section (Section 2.1) focuses on defining and characterizing novel population of the Th17 lineage as well as their contribution to HIV-1 pathogenesis. The second section (Section 2.2) aims to identify transcriptional and functional differences between two DC subtypes derived from monocytes with differential expression of the FcγRIII/CD16 ($CD16^-$ and $CD16^+$ monocytes) in terms of immunogenic potential and ability to disseminate HIV-1.

2.1 IDENTIFICATION OF TWO NEW TH17 SUBSETS WITH UNIQUE IMMUNOLOGICAL FEATURES AND CONTRIBUTION TO HIV-1 PATHOGENESIS

The gut-homing marker CCR6 together with CCR4 or CXCR3 identify two previously characterized subsets of T-cells (298, 436): $CCR4^+CCR6^+$ T-cells producing IL-17 and being specific for *C. albicans* (Th17 polarization) and $CXCR3^+CCR6^+$ T-cells producing IL-17 and IFN-γ and being specific for *M. tuberculosis* (Th1Th17 polarization) (436). In the laboratory, we previously demonstrated that *i)* both $CCR4^+CCR6^+$ Th17 and $CXCR3^+CCR6^+$ Th1Th17 cells are highly permissive to CCR5- (R5) and CXCR4- (X4)-using HIV strains; *ii)* $CCR4^+CCR6^-$ Th2 cells are permissive to X4 HIV only; and that *iii)* $CXCR3^+CCR6^-$ Th1 cells are relatively resistant to R5 and X4 HIV strains despite their expression of CCR5 and CXCR4 HIV co-receptors (436) (Figure 12). Accordingly, we demonstrated that in HIV-infected untreated subjects, CCR6 is a marker for memory $CD4^+$ T-cells enriched in integrated HIV-DNA (436). Thus, the differential expression of CCR4, CCR6, and CXCR3 identifies memory $CD4^+$ T-cells with distinct trafficking potential, polarization profile, antigenic specificity and permissiveness to HIV infection.

Pathogenic Th17 cells have been well characterized in the context of autoimmunity (344, 355, 356). Their presence exacerbates many pathological conditions, including multiple sclerosis and IBD (307, 344, 396). Nevertheless, the definition of pathogenic Th17 cells seems to be disease specific. In the context of HIV, pathogenic Th17 cells may be defined as cells that are permissive to infection. Their depletion during HIV disease progression is a direct pathogenic consequence. The definition of pathogenic Th17 cells in the context of HIV is well understood and requires further investigations. The concept of pathogenic Th17 cells in the context of HIV implies distinct characterization of Th17 lymphocytes and opens an area of research that is currently in progress. At the opposite, non-pathogenic Th17 cells may be defined as cells resistant to HIV infection and contribution to the maintenance of mucosal immunity. Reports from *Brenchley et al* revealed that Th17 cells are depleted in the gut but not in the lungs of HIV-infected individuals, supporting the differential alterations in the mucosal immune milieu during the course of HIV pathogenesis as well as the functional heterogeneity of Th17 subsets in different anatomic sites (735). The possibility that Th17 cells are not depleted in the lungs during HIV infection remains

intriguing considering that the lungs represent an important site of HIV replication and persistence as documented in macrophages (736-738). Whether fractions of long-lived Th17 cells carry replication competent HIV-DNA but are resistant to the cytopathic effects of the virus and contribute to HIV persistence under ART remains unknown.

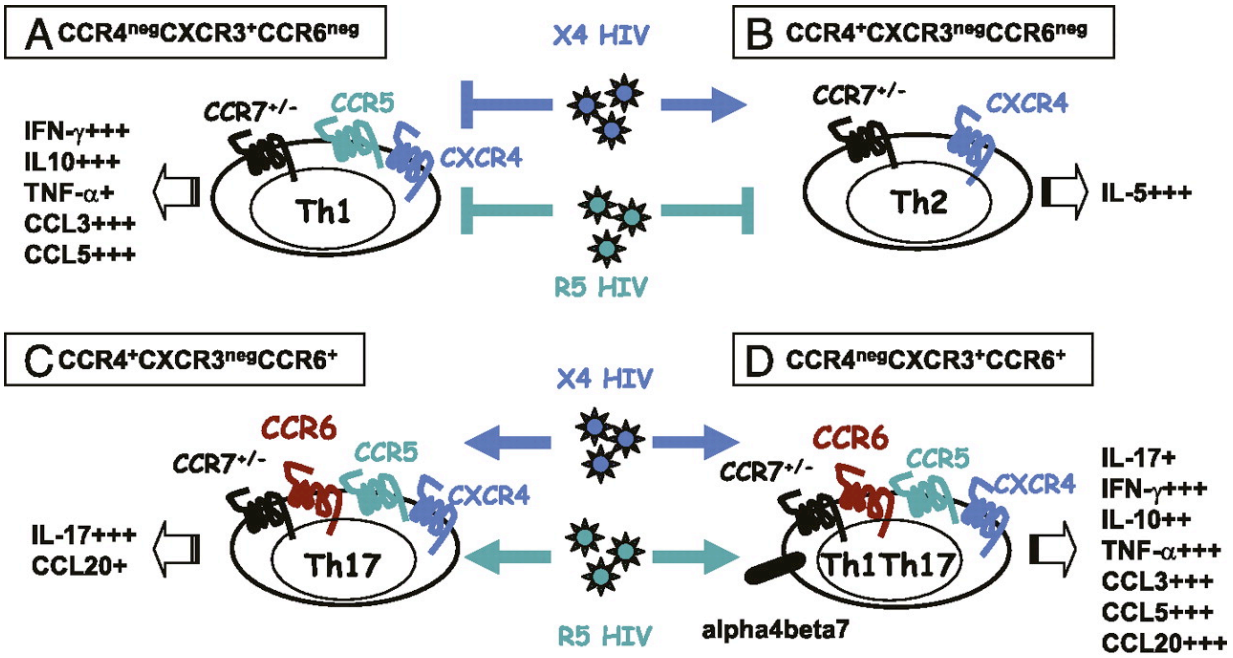

Figure 12: Differential HIV permissiveness in Th1, Th2, Th17, and Th1Th17 subsets. Shown are effector cytokines and the antigenic specificity of $CD4^+$ T-cell subsets identified based on their differential expression of the chemokine receptors CCR4, CCR6 and CXCR3, as well as their permissiveness to infection with R5 and X4 HIV-1 strains. This figure is reproduced with the permission of the Journal of Immunology (436), author copyrights 2010.

We demonstrated that the $CCR4^+CCR6^+$ Th17 and $CXCR3^+CCR6^+$ Th1Th17 cells are not only permissive to HIV infection but also are depleted in the peripheral blood of HIV-infected individuals (436), thus indicating that these cells represent pathogenic Th17 cells. Not all Th17 cells are infected by HIV (435, 440), suggesting the existence of non-pathogenic Th17 cells resistant to viral replication. The $CCR6^+$ cells remain a heterogeneous population. Based on the differential expression of CCR4 and CXCR3 one identifies four $CCR6^+$ T-cell subsets (Figure 12). Among these four subsets, two remain to be characterized: the double negative (DN) ($CCR4^-CXCR3^-$) $CCR6^+$ ($CCR6^+$DN) T-cells and the double positive ($CCR4^+CXCR3^+$) $CCR6^+$ ($CCR6^+$DP,) T-cells (Figure 13). Preliminary results generated by former post-doctoral fellow

Dr. Patricia Monteiro demonstrated that both CCR6^{+}DN and CCR6^{+}DP cells express the Th17-specific transcription factor RORγt (Figure 14). Knowing that CCR6 is a marker of Th17 cells (297-299), there is a possibility that both CCR6^{+}DN and CCR6^{+} DP cells expressing RORγt are part of the Th17 development program.

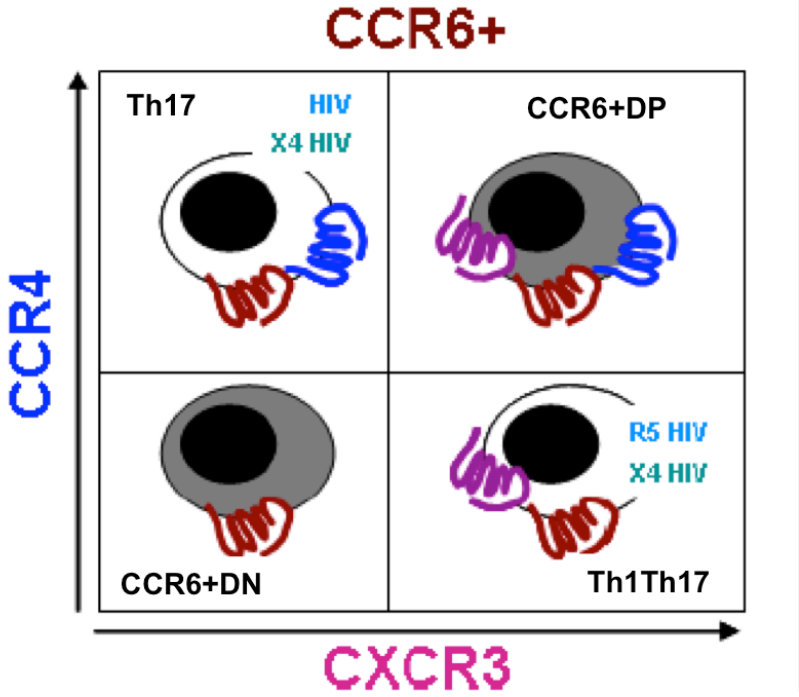

Figure 13: Heterogeneity of memory CD4^{+}CCR6^{+} T-cells. Shown are four CCR6^{+} T-cell subsets identified based on their differential expression of CCR4 and CXCR3. Our group and others previously characterized two CCR6+ T-cell subsets: CCR4^{+}CXCR3^{-} (Th17 profile) and CCR4^{-}CXCR3^{+} (Th1Th17 profile) ((298, 436)). Two other subsets remain to be characterized and represent the object of study of this thesis: double negative (CCR4^{-}CXCR3^{-}) CCR6^{+} T-cells (CCR6^{+}DN) and double positive (CCR4^{-}CXCR3^{+}) CCR6^{+} T-cells (CCR6^{+}DP).

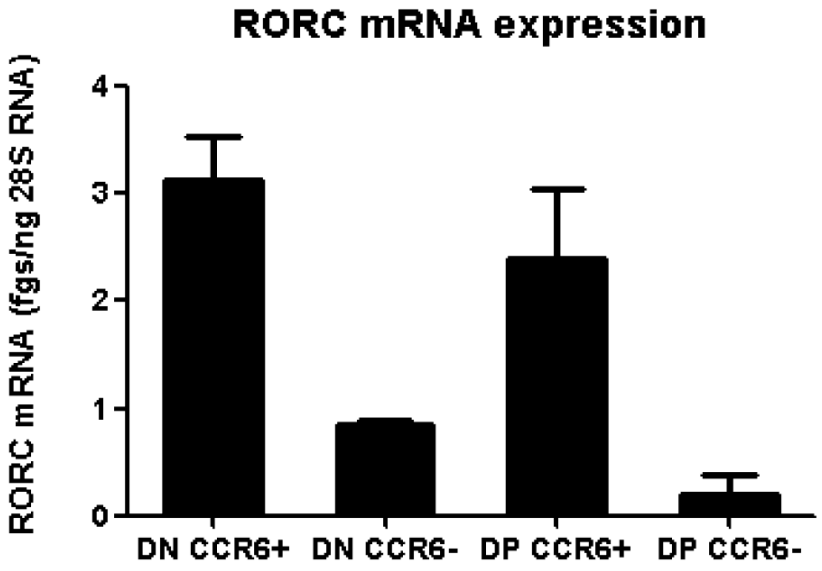

Figure 14: The expression of RORγt mRNA by CCR6$^+$DN and CCR6$^+$DP subsets. Cells were sorted by FACS and stimulated *via* CD3/CD28 using specific Abs for 3 days. Cellular RNA was extracted and levels of RORγt mRNA were measured by quantitative RT-PCR, as previously described (436). Results are from one donor representative of experiments performed with cells form two different donors.

We **hypothesized** that the CCR6$^+$DN and CCR6$^+$DP T-cells represent two previously uncharacterized new subset of Th17 cells with distinct contribution to HIV infection.

This first part of my Ph.D. **project aimed** to study the expression lineage commitment, and susceptibility *versus* resistance to HIV in two new previously uncharacterized memory CD4$^+$ T-cell subsets using state-of-the-art approaches in polychromatic flow cytometry, cDNA microarrays, and real-time PCR. Understanding the mechanism and cellular determinants exploited by HIV for its own dissemination is important to design targeted strategies to eradicate HIV infection. Precisely, the **objectives** of this study were to: **1)** determine the differentiation relationship between CCR6$^+$DN and CCR6$^+$DP T-cells compared to CCR4$^+$CCR6$^+$ Th17 and CXCR3$^+$CCR6$^+$ Th1Th17 cells and to **2)** to investigate the contribution of CCR6$^+$DN and CCR6$^+$DP T-cells to HIV persistence. For the **objective #1**, we sought to explore ***i)*** the Th lineage polarization of CCR6$^+$DN and CCR6$^+$DP T-cells; ***ii)*** the transcriptional profiles of CCR6$^+$DN and CCR6$^+$DP T-cells; ***iii)*** the antigenic specificity of CCR6$^+$DN and CCR6$^+$DP T-cells; and ***iv)*** determine the stability *versus* flexibility of Th17 lineage polarization of CCR6$^+$DN and CCR6$^+$DP T-cells. The **objective #2** aimed to evaluate CCR6$^+$DN and CCR6$^+$DP T-cells in

terms of ***i)*** expression of the HIV-1 co-receptors CCR5 and CXCR4; ii) frequency of circulating populations in chronically HIV-infected subjects receiving viral suppressive ART (CI on ART) compared to HIV-uninfected individuals; ***iii)*** dynamics in relationship with plasma viral load at different time-points post-infection, before and after ART initiation; ***iv)*** permissiveness to HIV-1 infection *in vitro*; ***v)*** ability to carry replication competent integrated HIV-DNA in CI on ART subjects.

To fulfill these objectives, we had access to large numbers of PBMC through leukapheresis from HIV-uninfected and CI on ART subjects, in collaboration with Dr Jean-Pierre Routy from McGill University and *via* the FRQ-S HIV/AIDS Network. Access to leukapheresis provided us the opportunity to work with a sufficient number of PBMC required for these studies on discrete cell subsets. This was very important since each of the four $CCR6^+$ subsets represent less that 0.5% of total PBMCs. The majority of our experiments relied on cell staining and sorting using the technology of flow cytometry. Globally, the ultimate purpose of this study was to further understand how HIV exploits the heterogeneity of Th17 cells for its persistence under ART and to explore the definition of pathogenic Th17 cells in the context of HIV infection. The knowledge we generated will be highly relevant for the design of novel targeted therapies to eradicate HIV.

2.2 DISTINCT IMMUNOLOGICAL FEATURES OF DENDRITIC CELLS DERIVED FROM CD16$^+$ AND CD16$^-$ MONOCYTES AND CONTRIBUTION TO HIV-1 PATHOGENESIS

HIV-1 exploits DCs for its own replicative advantage. A large body of literature demonstrated that mDCs are efficient in transmitting HIV to CD4$^+$ T-cells (661-664, 669, 683-687, 739). In addition, mDCs sense HIV poorly and subsequently are unable to efficiently induce a potent anti-viral response (671, 697). Of note, only a fraction of myeloid DCs is responsible for viral transmission (740) but that fraction has not been yet identified. Whether there is a division of labor among mDCs, with subsets displaying an immunogenic potential *versus* those contributing to viral dissemination remains unknown. Monocytes are major precursors for human and murine DCs, especially under hostile inflammatory settings (483, 576, 585, 600-602). Monocytes represent a heterogeneous population in terms of stage of differentiation and immunological function (471, 477, 485, 489). Human monocytes are classified into two major subtypes based on the differential expression of CD14 and CD16. Early studies demonstrated the dramatic expansion of CD16$^+$ monocytes during HIV disease progression, with their frequency remaining above normal values upon viral suppressive ART (63, 499, 521-525). Compared to CD16$^-$ monocytes, CD16$^+$ monocytes were reported to be more permissive to HIV infection and harbored preferentially HIV-DNA (530, 540, 541). Interestingly, CD16$^+$monocytes differentiating into macrophages were shown to promote higher HIV infection in CD4$^+$ T-cells (494, 549). Also, CD16$^+$ monocytes express chemokine receptors such as CX3CR1 that can mediate migration into anatomical HIV replication sites including the intestine and brain (557, 741). To the best of our knowledge, it remains unknown whether the CD16$^-$ and CD16$^+$ monocyte subsets give rise to DCs with distinct immunologic features (e.g., Th17 polarization) and contribution to HIV pathogenesis.

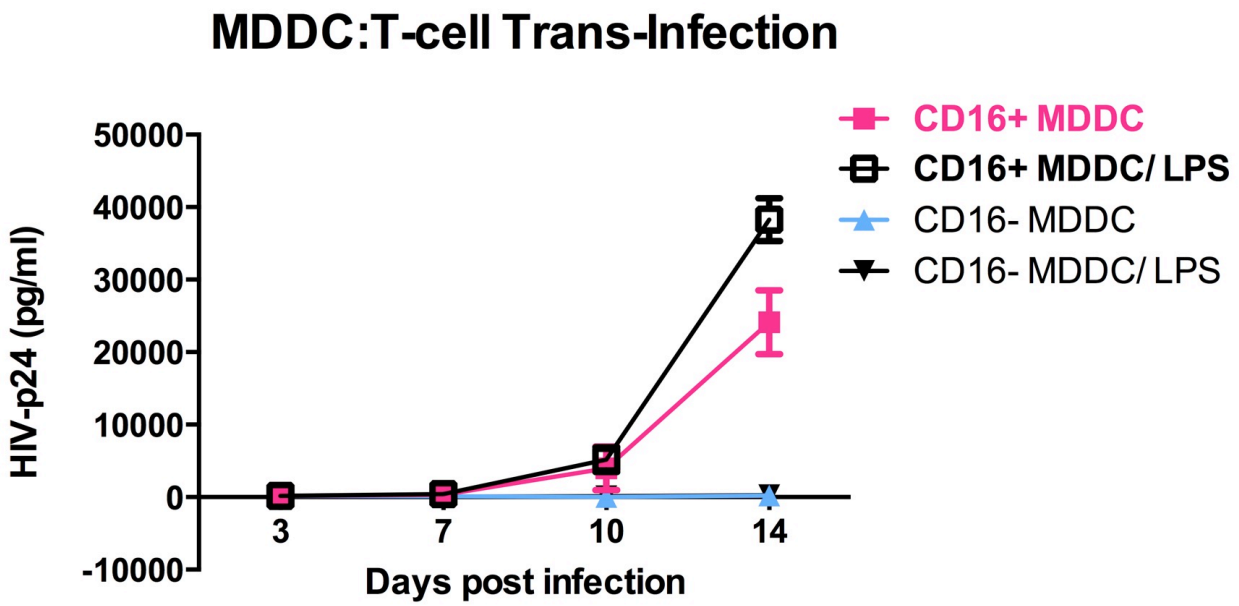

Figure 15: CD16$^+$ MDDC selectively promote HIV replication in autologous CD4$^+$ T-cells. Sorted CD16$^+$ and CD16$^-$ monocytes were differentiated into immature DC for a period of 6 days. The generated MDDC subsets were exposed to HIV-1 NL4.3BaL (50 ng/10^6 cells) for 2 hours at 37 ºC, and subsequently co-cultured with autologous CD4$^+$ T-cells purified by MACS negative selection at a MDDC: T ratio 1:2 in the presence or absence of E. coli LPS (100 ng/ml). Supernatants were harvested at days 3, 7, 10 and 14 post-infection, and HIV-p24 levels were quantified by ELISA.

Based on all these scientific evidences and knowledge gaps, in this second part of my Ph.D. project we **hypothesized** that CD16$^+$ and CD16$^-$ monocyte-derived DCs (MDDCs) play distinct immunological roles at homeostasis and during HIV-infection. Indeed, preliminary results generated in our lab indicate that the CD16$^+$ MDDC compared to C16$^-$ MDCC have superior capacity to *trans* infect CD4$^+$ T-cells (Figure 15). Our model is that CD16$^+$ monocytes are recruited into major sites of HIV replication where they differentiate into DCs with superior capacity to disseminate HIV infection, while CD16$^-$ MDDCs promote a more robust immunity against HIV and other pathogens. This **project aimed** to investigate immunological differences between CD16$^+$ and CD16$^-$ MDDCs at homeostasis and upon HIV-infection. Precisely, the **objectives** of this study were 1) to identify transcriptional and functional properties of CD16$^+$ and CD16$^-$ MDDCs in healthy human subjects, 2) to determine the alteration of their immunological functions upon HIV-infection and 3) to determine the role of both subsets of MDDCs in HIV dissemination. For the **objectives #1 and #2**, we sought ***i)*** to perform genome-wide transcriptional analysis of CD16$^+$ and CD16$^-$ MDDCs and ***ii)*** to characterize the immunological

potential of each MDDC subsets in terms of Th1 and Th17 polarization in the presence of antigens such as LPS and several antigens/pathogens including CMV, *C.albicans* and *S.aureus*. For the **objective #2**, the immunological potential of MDDC subsets was measured upon HIV exposure *in vitro*. For the **objective #3**, we ***i)*** investigated the *trans*-infection ability of both MDDC subsets to activated or resting $CD4^+$ T-cells, ***ii)*** measured the capacity of $CD16^+$ and $CD16^-$ MDDCs to harbor integrated HIV-DNA; and ***iii)*** identified transcriptional and functional signatures associated with HIV permissiveness/dissemination.

To fulfill these objectives, we again had access to leukapheresis of HIV-uninfected individuals. The majority of our experiments relied on cell staining and sorting using the technology of flow cytometry. The isolation of viable $CD16^+$ and $CD16^-$monocytes was challenging and required an expert assistance by Dr. Dominique Gauchat for cell sorting in low pressure at the Flow Cytometry Core Facility at the CRCHUM. The purpose of this study was to determine whether the expansion of $CD16^+$ monocytes in HIV-infected individuals, and their subsequent differentiation into DC, promotes HIV dissemination and disease progression, with a negative impact on the quality of antifungal and antiviral immunity; and to characterize the quality of immune response generated by CD16- MDDCS in response to HIV. The sum of this study will provide a better understanding of the impact of HIV-1 infection on the quality of innate immune responses.

CHAPTER 3:

NEW INSIGHTS INTO THE HETEROGENEITY OF TH17 SUBSETS CONTRIBUTING TO HIV -1 PERSISTENCE DURING ANTIRETROVIRAL THERAPY (MANUSCRIPT #1)

Authors Contribution of Manuscript entitled:

New insights into the heterogeneity of Th17 subsets contributing to HIV-1 persistence during antiretroviral therapy

Retrovirology 2016 Aug 24;13(1):59. doi: 10.1186/s12977-016-0293-6.

Vanessa Sue Wacleche performed research, analyzed data, and wrote the manuscript. Concerning the experimental approach, VSW performed the isolation and staining for cell sorting. She also performed all experiments involving cell stimulation, antigen presentation, polarisation assay, RT-PCR, infection and HIV reactivation assays. Figures involved include Figure 1 to 10 as well as supplemental 1 to 8.

Jean-Philippe Goulet performed microarray analysis and generated figures including Figure 1F, Figure 2A-D, Supplemental figure 2 and Table 1.

Annie Gosselin performed experiments of staining shown in Figures 1B and Figure 6A-B and Figure 7.

Patricia Monteiro performed experiments performed experiments of staining involving Figure 6A-B.

Hugo Soudeyns contributed to research design and manuscript writing.

Rémi Fromentin performed experiments of staining shown Figure 7.

Mohammad-Ali Jenabian ensured access to clinical samples/information and/or provided experimental protocols concerning figures 1-8 and 9 as well as figure supplemental

Shant Vartanian ensured access to clinical samples/information and/or provided experimental protocols concerning figures 7.

Steven G. Deeks ensured access to clinical samples/information and/or provided experimental protocols concerning figures 7.

Nicolas Chomont ensured access to clinical samples/information and/ provided experimental protocols concerning figures 7.

Jean-Pierre Routy ensured access to clinical samples/information and/or provided experimental protocols figures 1-8 and 9 as well as figure supplemental.

Petronela Ancuta designed research, analyzed data, and wrote the manuscript. This includes all the figures, tables and supplemental figures.

New Insights into the Heterogeneity of Th17 Subsets Contributing to HIV-1 Persistence during Antiretroviral Therapy

Vanessa Sue Wacleche[1,2], Jean-Philippe Goulet[3], Annie Gosselin[2], Patricia Monteiro[1,2], Hugo Soudeyns[1,4], Rémi Fromentin[2], Mohammad-Ali Jenabian[5], Shant Vartanian[6], Steven G. Deeks[6], Nicolas Chomont[1,2], Jean-Pierre Routy[7,8], and Petronela Ancuta[1, 2,*]

[1]Université de Montréal, Faculté de Médecine, Département of microbiologie, infectiologie et immunologie, Montreal, QC, Canada.

[2]Centre de recherche du CHUM, Montreal, QC, Canada.

[3]Caprion, Montreal, QC, Canada.

[4]Unité d'immunopathologie virale, Centre de recherche du CHU Sainte-Justine, Montreal, QC, Canada.

[5]Département des sciences biologiques, Université du Québec à Montréal, Montreal, QC, Canada.

[6]Department of Medicine, University of California San Francisco, San Francisco, CA, USA

[7]Chronic Viral Illness Service and Research Institute, McGill University Health Centre, Montreal, QC, Canada.

[8]Division of Hematology, McGill University Health Centre, Montreal, QC, Canada.

ABSTRACT

Background: Th17 cells are permissive to HIV-1 infection and their depletion from the gut of infected individuals leads to microbial translocation, a major cause for non-AIDS co-morbidities. Most recent evidence supports the contribution of long-lived Th17 cells to HIV persistence during antiretroviral therapy (ART). However, the identity of long-lived Th17 cells remains unknown. **Results**: Here, we performed an in-depth transcriptional and functional characterization of four distinct Th17 subsets and investigated their contribution to HIV reservoir persistence during ART. In addition to the previously characterized $CCR6^+CCR4^+$ (Th17) and $CCR6^+CXCR3^+$ (Th1Th17) subsets, we reveal the existence of two novel $CCR6^+$ subsets, lacking (double negative, $CCR6^+$DN) or co-expressing CXCR3 and CCR4 (double positive, $CCR6^+$DP). The four subsets shared multiple Th17-polarization markers, a fraction proliferated in response to *C. albicans,* and exhibited lineage commitment and plasticity when cultured under Th17 and Th1 conditions, respectively. Of note, fractions of $CCR6^+$DN and Th17 demonstrated stable Th17-lineage commitment under Th1-polarization conditions. Among the four subsets, $CCR6^+$DN expressed a unique transcriptional signature indicative of early Th17 development (IL-17F, STAT3), lymph-node homing (CCR7, CD62L), follicular help (CXCR5, BCL6, ASCL2), and self-renewal (LEFI, MYC, TERC). Cross sectional and longitudinal studies demonstrated that $CCR6^+$DN cells were the most predominant $CCR6^+$ subset in the blood before and after ART initiation; high frequencies of these cells were similarly observed in inguinal lymph nodes of individuals receiving long-term ART. Importantly, replication competent HIV was isolated from $CCR6^+$DN of ART-treated individuals.

Conclusions: Together, these results provide new insights into the functional heterogeneity of Th17-polarized $CCR6^+CD4^+$ T-cells and support the major contribution of $CCR6^+$DN cells to HIV persistence during ART.

Key words: human, Th17, CCR6, CCR4, CXCR3, HIV reservoirs, ART

BACKGROUND

The Th17 cells represent a subset of $CD4^+$ T-cells that act as the first line of defense against pathogens at barrier surfaces [1]. Th17 cells are defined by the production of unique effector cytokines (IL-17A, IL-17F, IL-21, IL-22, IL-26, CCL20) under the transcriptional regulation of multiple lineage-specific transcription factors (IRF4, BATF, STAT3, RORγt) [2, 3]. Their anatomic localization and effector functions, together with their unique developmental plasticity, position Th17 cells at the very core of the immune system [2, 4]. CCR6 is a well-established marker for Th17 cells [5, 6]. CCR6 mediates recruitment into specific tissues including Peyer's patches (CCR6 [7]), skin [8] and brain [9]. Although not all $CCR6^+$ T-cells produce IL-17A upon stimulation *ex vivo*, the majority of these cells are prone to acquire Th17 effector functions [10]. The co-expression of CCR6 and CCR4 identifies cells producing IL-17A (Th17 profile) specific to *Candida albicans* and *Staphylococcus aureus* [5, 11], while $CCR6^+CXCR3^+$ cells produce both IL-17A and IFN-γ (Th1Th17 profile) in response to *Mycobacterium tuberculosis* or upon polyclonal stimulation [5] [12]. These advances in the identification of surface markers for functionally distinct $CD4^+$ T-cell subsets proved to be instrumental for understanding the contribution of Th17 cells to human pathologies including rheumatoid arthritis [13], multiple sclerosis [9], cancer [14], and HIV-infection [15, 16].

The existence of functionally distinct IL-17A-producing $CD4^+$ T-cells cells was originally reported in the context of autoimmunity, with $CCR6^+CXCR3^+$Th1Th17 and $CCR6^+CCR4^+$Th17 cells being considered pathogenic and non-pathogenic, respectively [3, 17]. This discovery led to the identification of molecular signatures associated with Th17 pathogenicity in mice [18-20] and most recently in humans [21]. In contrast, during HIV-1 infection, we previously demonstrated that both

$CCR6^+CCR4^+$Th17 and $CCR6^+CXCR3^+$Th1Th17 cells are pathogenic since they are permissive to viral infection *in vitro*, carry integrated HIV-DNA *in vivo*, and their frequency is significantly reduced in HIV-infected individuals, including those with undetectable plasma viral load under antiretroviral therapy (ART) [15]. Considering the fact that IL-17A plays a critical role in maintaining epithelial barrier integrity at intestinal level [22, 23], the depletion of Th17 and Th1Th17 cells from gut-associated lymphoid tissues (GALT) is considered as a major cause for microbial translocation, chronic immune activation and occurrence of non-AIDS co-morbidities in HIV-infected individuals [24]. Thus, features of Th17 pathogenicity are unique in the context of HIV infection. In addition, long-lived Th17 cells exist and were reported to promote cancer progression [25]. The possibility that long-lived Th17 cells contribute to HIV reservoir persistence under ART, as supported by recent findings by our group (Gosselin *et al.,* unpublished observations) and others [26], adds to the complexity of Th17 pathogenicity concept and position these cells as a major barrier for HIV eradication.

In this study, we used a systems biology approach an revealed phenotypic, functional and transcriptional features of two previously uncharacterized human $CD4^+$ T-cell subsets expressing the Th17 marker CCR6 and lacking or co-expressing the homing receptors CCR4 and CXCR3: $CCR4^-$ $CXCR3^-$ (double negative; $CCR6^+$DN) and $CCR4^+CXCR3^+$ (double positive; $CCR6^+$DP). Our results provide new insights into the diversity of Th17 subsets during homeostasis and HIV-1 infection, thus adding a novel piece of complexity to the recent understanding of Th17 functional heterogeneity and clonotype sharing in humans [27]. We reveal that $CCR6^+$DN are distinguished from Th17, Th1Th17 and $CCR6^+$DP by their expression of markers of early Th17 development, lymph node trafficking, follicular help and self-renewal. We also demonstrate that $CCR6^+$DN

represent the most predominant Th17 subset in the blood and lymph nodes of HIV-infected ART-treated individuals and carry replication-competent integrated HIV-DNA. These findings support the newly emerged concept that HIV takes advantage of the long-lived properties of specific Th17 subsets [25, 28, 29] to ensure its persistence during ART. Thus, permissiveness to HIV-DNA integration compatible with survival represents a new previously unrecognized feature of pathogenic Th17 cells during HIV infection

RESULTS

Two novel subsets of memory CCR6$^+$ T-cells exhibit Th17-features

Differential expression of CCR4 and CXCR3 identifies four memory (CD45RA$^-$) CCR6$^+$ and four CCR6$^-$ subsets. The following four subsets were previously demonstrated to be enriched in cells with specific polarization features: CCR6$^+$CCR4$^+$ (Th17) and CCR6$^+$CXCR3$^+$ (Th1Th17), CCR6$^-$CXCR3$^+$ (Th1), and CCR6$^-$CCR4$^+$ (Th2) [5, 15, 27]. While acknowledging the fact that these subsets are heterogeneous, for simplicity, these subsets are typically identified as Th17, Th1Th17 (or Th1*), Th1, or Th2 cells [5, 12, 21, 27]. We previously demonstrated that Th17 and Th1Th17 subsets are highly permissive to R5 and X4 HIV-1 infection *in vitro* [15]. Among CCR6$^+$ T-cells, two subsets remain uncharacterized in terms of polarization profile and contribution to HIV-1 pathogenesis: CCR4$^-$CXCR3$^-$ (double negative; CCR6$^+$DN) and CCR4$^+$CXCR3$^+$ (double positive; CCR6$^+$DP) (Figure 1A). In HIV-uninfected individuals, the frequency of blood CCR6$^+$DN was similar to that of Th17 and Th1Th17, while the frequency of CCR6$^+$DP was slightly lower (Figure 1B). The CCR6$^-$ population also included two previously uncharacterized subsets, CCR6$^-$DN and CCR6$^-$DP, with CCR6$^-$DN being the most predominant (Figure 1A-B). CCR6$^+$DN and CCR6$^+$DP expressed the Th17 marker CD161 [30] at levels higher and similar compared to Th17 and Th1Th17, respectively (Figure 1C). The frequency of CD161 was relatively low on CCR6$^-$ subsets (Figure 1C). CCR7 and CD27 identify distinct memory subsets [31, 32]: CCR7$^+$CD27$^+$ (CM, central memory), CCR7$^-$CD27$^-$ (EM, effector memory), CCR7$^-$CD27$^+$ (TM, transitional memory) and CCR7$^+$CD27$^-$ subset. CM predominated over EM and TM in all CCR6$^+$ subsets, with the highest % of CM in Th1Th17 and CCR6$^+$DP (Figure 1D).

For subsequent functional studies, sufficient numbers of highly pure $CCR6^+$ and $CCR6^-$ cells with differential CCR4 and CXCR3 expression were sorted by flow cytometry from large numbers of PBMCs (10^9) obtained by leukapheresis (S1 Figure) from HIV-uninfected individuals. To determine the polarization profile of $CCR6^+$DN and $CCR6^+$DP, the expression of lineage-specific cytokines was measured in FACS-sorted cells exposed to CD3/CD28 triggering. Compared to Th17 and Th1Th17, $CCR6^+$DN and $CCR6^+$DP produced high and low levels of IL-17A, respectively. In contrast to Th17, $CCR6^+$DN and $CCR6^+$DP produced IFN-γ but at significantly lower levels compared to Th1Th17; as expected, the Th2 cytokine IL-5 was produced by $CCR6^-$ but not $CCR6^+$ cells (Figure 1E).

To further investigate the Th17 polarization profile of $CCR6^+$DN and $CCR6^+$DP, their transcriptome was compared to that of Th17 and $CCR6^-$DN using the Illumina technology. The list of 1,020 transcripts differentially expressed in $CCR6^+$DN *vs*. $CCR6^-$DN (adjusted p-value>0.05; FC cut-off 1.3), included well-established markers for Th17 (IL-17F, KLRB1/CD161, CCL20, KLF2, CTSH, IL-22, CCR6, RORA, IL-23R, RORC, PTPN13, IL-26, S100A4, ARNTL, IL-6R) and Th1 lineages (CCL3L3, CCL3, CCL3L1, CCL5, CD300a), potentially new Th17 markers (CD96, LGMN, ANTXR2, CXCR6, MAP3K4, TNFSF25, LY9, S1PR1), together with negative regulators of Th17 polarization (IL-9, IFITM3, OSM, IRF8, MX1, NFIL3, PTK2, IL4R, SOCS1) (Figure 1F). Clustering analysis of these transcripts grouped all $CCR6^+$ subsets together, indicative of their common Th17 polarization. These results identify $CCR6^+$DN and $CCR6^+$DP as two novel Th17 subsets, with $CCR6^+$DN producing high levels of IL-17A and being as preponderant as the previously described Th17 and Th1Th17 in the peripheral blood of healthy humans [5].

Th17-polarized CCR6$^+$DN and CCR6$^+$DP subsets exhibit unique transcriptional profiles

Further analysis of transcriptional profiles identified 344, 1,407 and 3,148 probe-sets differentially expressed by CCR6$^+$DN *vs.* Th17, CCR6$^+$DP *vs.* Th17, and CCR6$^+$DN *vs.* CCR6$^+$DP (p-value <0.05; FC cut-off 1.3), respectively (Figure 2A). Differences in gene expression in CCR6$^+$DN *vs.* Th17 (13 up; 13 down) were also found inferior to differences in CCR6$^+$DP *vs.* Th17 (368 up; 357 down) and CCR6$^+$DN *vs.* CCR6$^+$DP (1,537 up; 1,417 down), when transcripts with adjusted p-values <0.05 were considered (Table S1, data not shown). These results reveal the transcriptome of CCR6$^+$DN is similar to that of Th17, but highly distinct from that of CCR6$^+$DP. Of note, IL-17F, a cytokine associated with early Th17 development [33], was included among the top up-regulated transcripts in CCR6$^+$DN *vs.* Th17 (FC: 7.8) and CCR6$^+$DN *vs.* CCR6$^+$DP (FC: 12.8) (Table S1). In contrast, LMNA, a senescence marker [34], was included among the top down-regulated genes in CCR6$^+$DN *vs.* Th17 (FC: -2.2) and CCR6$^+$DN *vs.* CCR6$^+$DP (FC: -4).

To extract functional meaning from these transcriptional dissimilarities, Ingenuity Pathway Analysis (IPA), Gene Set Variation Analysis (GSVA), and Gene Ontology (GO) tools were used to identify differentially expressed pathways and biological functions. IPA identified the most significant differences for the CCR6$^+$DN *vs.* CCR6$^+$DP and Th17 *vs.* CCR6$^+$DP contrasts, and revealed similarities between CCR6$^+$DN and Th17 (Figure 2B). Among top modulated pathways, PPAR/RXR (previously associated with the negative regulation of Th17 polarization [35]), cyclin and cell cycle regulation, and apoptosis pathways were under represented in CCR6$^+$DN *vs.* CCR6$^+$DP. In contrast, IL-6, phospholipase C (both involved in Th17 differentiation [29] CXCR4, thrombin, p38/ERK/MAPK (involved in cell activation/proliferation [36]) and Tec Kinase (involved in TCR signaling [37]) were over expressed in CCR6$^+$DN *vs.* CCR6$^+$DP and in CCR6$^+$DN *vs.* Th17.

Other pathways specifically up-regulated in CCR6$^+$DN *vs.* CCR6$^+$DP and Th17 *vs.* CCR6$^+$DP included IL-2, Jak/STAT, PKC, sphingosine-1-phosphate (involved in cell migration [38]), NANOG (implicated in the maintenance of stem cells [39]), IL-3 (involved in lymphopoiesis [40]), PI3K (involved in Th17 differentiation [10], April (involved in Th17 polarization [41], and NFAT (involved in IL-17A production [42]) (Figure 2B).

GSVA identified canonical pathways (C2) and biological processes (C5) differentially expressed in CCR6$^+$DN *vs*. CCR6$^+$DP and Th17 *vs*. CCR6$^+$DP (S2A-B Figure). Among the top 50 differentially-expressed canonical pathways, the IL-23 pathway, which is key for Th17 polarization [43], was found to be enriched in CCR6$^+$DN (Figure 2C). Among the top 50 differentially-expressed biological processes, the expression of pathways such as lymphocyte differentiation, protease inhibitor and response to steroid hormone receptor were over represented in CCR6$^+$DN (Figure 2D).

GO identified differentially-expressed genes in CCR6$^+$DN *vs.* CCR6$^+$DP ($p<0.05$, cut-off 1.3-fold) involved in cell migration, chemotaxis, cell differentiation, and transcription. Transcripts associated with migration/chemotaxis into/outside lymph nodes, including CCR7, CXCR5, the CXCR5 ligand CXCL13, SELL, SIRP1, JAM3 and AIF1 were enriched in CCR6$^+$DN, whereas adhesion molecules/chemokine receptors mediating homing into peripheral tissues such as integrin β7 (gut), CXCR3 (inflammatory sites), CCR2 and CCR4 (skin), and integrin β1 (cervix) were enriched in both Th17 and/or CCR6$^+$DP (S2C-D Figure). Well-established markers of Th17 (IL-8, IL-23R, SOSC3, TIM3, CD26/DPP4) and follicular helper T cells (Tfh) (CXCR5, ICOS) were enriched in CCR6$^+$DN (S2E Figure). Also, transcription factors related to the control of Th17 (STAT3, RORA) and Tfh (BLC6, ASCL2 [44, 45]) polarization/function were enriched in CCR6$^+$DN (S2E-F Figure).

In addition, other transcripts enriched in CCR6$^+$DN *vs.* CCR6$^+$DP include LEF1 and MYC, key markers of human stem-cells and long-lived Th17 cells [25], together with the anti-senescence marker TERC [46] (Table S1). RT-PCR quantifications confirmed superior expression of STAT3, BCL6, LEF1 and TERC in CCR6$^+$DN *vs.* Th17 and CCR6$^+$DP (Figure 2E). These transcriptional analyses suggest that CCR6$^+$DN, Th17 and CCR6$^+$DP represent distinct stages of Th17 differentiation with specific migration potential, immunological functions, and transcriptional regulation. Among these subsets, CCR6$^+$DN exhibit markers of early Th17 commitment, lymph-node tropism, follicular help, and self-renewal.

CCR6$^+$DN are a major source of IL-17F, IL-8 and IL-21

A Cytokine Array was used to screen for the presence of 34 lineage-specific cytokines produced by CD3/CD28-activated CCR6$^+$ subsets of HIV-uninfected individuals. CCR6$^+$DN were distinguished from Th17 by increased IFN-γ, IL-17A, IL-17F, MIP-3α/CCL20 and TNF-α and decreased IL-13 (Figure 3A), and from Th1Th17, by increased IL-17A and IL-17F, and decreased IFN-γ and TNF-α production (Figure 3B). Levels of GM-CSF, IL-10 and IL-22 were similarly high in CCR6$^+$DN, Th17 and Th1Th17 (Figure 3A-B). ELISA quantifications demonstrated that CCR6$^+$DN were the major source of IL-17F, produced IL-22 at levels similar to Th17 and Th1Th17, and CCL20 at levels higher and similar compared to Th17 and Th1Th17, respectively. In contrast, CCR6$^+$DP produced low/undetectable levels of IL-17F, IL-22 and CCL20. Regarding the pro/anti-inflammatory profiles, Th1Th17 were major TNF-α and IL-10 producers [5, 15, 27], while CCR6$^+$DN and CCR6$^+$DP produced low levels of TNF-α and moderate levels of IL-10 and IL-13. Nevertheless, CCR6$^+$DN produced slightly more TNF-α compared to Th17 or CCR6$^+$DP (Figure 3C). Although not detected in our cytokine screen, IL-8, IL-21, and IL-2 were quantified by ELISA.

The highest levels of IL-8 and IL-21 were detected in CCR6$^+$DN, while the highest levels of IL-2 were detected in Th1Th17 (Figure 3D). Thus, in contrast to CCR6$^+$DP which exhibit modest Th17 features, CCR6$^+$DN are a major source of IL-17F, IL-8 and IL-21 and their pro-inflammatory profile is intermediate between that of Th17 and Th1Th17. Similar to CCR6$^+$DP, CCR6$^+$DN produce low IL-2 levels, a typical property of Th17 cells [15, 47].

CCR6$^+$DN proliferate and produce IL-17A in response to *C. albicans*

We further examined proliferation in response to typical Th17 (*C. albicans*) *vs.* Th1 (CMV) antigens [5, 48] using a monocyte-derived dendritic cell (MDDC)-based antigen presentation assay (Figure 4A). SEB was used to induce polyclonal proliferation. Sufficient numbers of CCR6$^+$DP could not be sorted for these studies. Th17 and Th1Th17 proliferated in response to *C.albicans* at levels superior to Th1, while Th1Th17 and Th1 but not Th17 proliferated in response to CMV. Similar to Th17, CCR6$^+$DN proliferated in response to *C. albicans* but not CMV. All subsets proliferated similarly well in response to SEB (Figure 4B). In response to *C. albicans*, the frequency of IL-17A$^+$ cells was similarly high in CCR6$^+$DN and Th17, low in Th1Th17, and background in Th1 (Figure 4C). The frequency of IFN-γ^+ within *C. albicans*-specific CCR6$^+$DN was lower compared to Th1Th17 and Th1 and higher compared to Th17. TNF-α was produced by all subsets at similarly high frequencies. The frequency of IL-17A$^+$ cells co-expressing IFN-γ was different between the three *C. albicans*-specific CCR6$^+$ subsets, while the majority of IL-17A$^+$ cells in all subsets co-expressed TNF-α (Figure 4D). Notably, *C. albicans*-specific CCR6$^+$DN included relatively high frequencies of IL-17A$^+$IFN-γ^- and IL-17A$^+$IFN-γ^+ cells (Figure 4E-F). Thus, CCR6$^+$DN share antigenic specificity and cytokine profiles with the previously characterized Th17 and Th1Th17.

CCR6$^+$DN and CCR6$^+$DP exhibit Th17-commitment and lineage plasticity

The Th17 polarization flexibility/plasticity is well documented [2, 29], with Th17 being able to down-regulate RORγt and acquire Th1 features in response to Th1-specific polarizing cues [6]. Therefore, we investigated the Th17-lineage commitment *vs.* plasticity of the four CCR6$^+$ subsets upon short (4 days) and long-term (14 days) culture under Th17- *vs.* Th1-polarizing conditions (Figure 5A). It is well-established that CM *vs.* EM/TM are long-lived and acquire robust effector functions upon TCR triggering [32, 49]. Considering the superior production of Th17 cytokines by Th17-polarized CM *vs.* EM/TM (S3 Figure) as well as the preponderance of CM cells (Figure 1D), subsequent experiments were performed using CM isolated from HIV-uninfected individuals. Under Th17-conditions, all four CCR6$^+$ subsets produced IL-17A, IL-17F, IL-22 and TNF-α, while IFN-γ was highly expressed by Th1Th17, CCR6$^+$DP and Th1 (Figure 5B-C). The culture under Th17-conditions for 14 *versus* 4 days resulted in a remarkable increase in the proportion of cells producing Th17 effector cytokines. The culture under Th1- *vs.* Th17-conditions resulted in a significant decrease in IL-17A, IL-17F and/or IL-22 expression by all CCR6$^+$ subsets, with differences being more significant at day 14 *vs.* 4. This was associated with increased IFN-γ and TNF-α expression by CCR6$^+$ subsets at day 4 (Figure 5B) and increased IFN-γ within Th17 at day 14 (Figure 5C). As expected [29], Th1 did not acquire Th17-features under Th17-conditions (Figure 5B-C). Changes in the poly-functionality of CM subsets cultured long-term under Th17 *vs.* Th1-conditions (S4 Figure) were further evaluated using SPICE [50] (S5 Figure). Under Th17-conditions, CCR6$^+$ subsets expressed 1-5 cytokines simultaneously. Th17 and CCR6$^+$DN expressed IL-17A mainly in combination with TNF-α alone or with TNF-α and IL-17F and/or IL-22, but at relatively low frequency in combination with IFN-γ. Th1Th17 and CCR6$^+$DP expressed IL-17A mainly in combination with IFN-γ and TNF-α, in the presence or absence of IL-17F or IL-22. The poly-

functionality of CCR6$^+$ subsets decreased under Th1- *vs.* Th17-conditions and was associated with diminished expression of Th17-cytokines and expansion of IFN-γ^+TNF-α^+ cells, representative of a Th1 profile. Thus, similar to Th17 and Th1Th17, CCR6$^+$DN and CCR6$^+$DP amplified their Th17-features under Th17-conditions and acquired Th1-features under Th1-conditions. Nevertheless, fractions of Th17 and CCR6$^+$DN preserved their Th17 features under Th1-conditions, indicative that stably-committed Th17 exist in humans.

CCR6$^+$DN acquire CCR4/CXCR3 expression in response to Th17- or Th1-polarizing signals

Finally, we investigated the stability/plasticity of CCR6, CCR4, and CXCR3 expression on CM Th17-subsets upon long-term exposure to Th17-/Th1-polarizing signals (S6 Figure). Under Th17-conditions, CCR6 was significantly down-regulated compared to Day 0, while culture under Th1-*versus* Th17-conditions was associated with a further decrease in CCR6 expression, mainly on CXCR3$^+$Th1Th17 (S6A Figure). However, CCR6 expression was preserved at >70% and >50% under Th17- and Th1-conditions, respectively (S6A Figure). CCR4 expression was acquired by CXCR3$^+$Th1Th17, CCR6$^+$DN, and Th1 under Th17- or Th1-conditions (S6B Figure). Notably, CCR6$^+$DN cultured under Th17- or Th1-conditions acquired CCR4 at levels similar to CCR4$^+$Th17 (S6B Figure). In contrast, CCR4 expression decreased on CCR6$^+$DP and CCR4$^+$Th17 under Th17- or Th1-conditions (S6B Figure). CXCR3 expression was decreased on CXCR3$^+$Th1Th17, CCR6$^+$DP, and Th1 under Th17- or Th1-conditions, but increased on CCR6$^+$DN and CCR4$^+$Th17 under Th17-, and even more dramatically Th1-conditions. However, CXCR3 levels remained inferior to those detected on CXCR3$^+$Th1Th17 and CCR6$^+$DP (S6C Figure). Analysis of CCR6 co-expression with CCR4 or CXCR3 revealed that ~70% of CCR4$^+$Th17 and CXCR3$^+$Th1Th17 maintained their original phenotype under Th17-conditions (S6D-E Figure). Fractions of

CXCR3$^+$Th1Th17 (mean: 21%) and CCR6$^+$DN (mean: 48%) acquired a CCR6$^+$CCR4$^+$ phenotype (Figure 6D), while Th17 (mean: 29%) and CCR6$^+$DN (mean: 24%) acquired a CCR6$^+$CXCR3$^+$ phenotype (S6E Figure). The CCR6$^+$CCR4$^+$ and CCR6$^+$CXCR3$^+$ phenotype was dramatically reduced within CCR6$^+$DP under Th17- or Th1-condititions (S6D-E Figure), with CCR6$^+$DP acquiring a CCR4$^-$CXCR3$^+$ but not CCR4$^+$CXCR3$^-$ phenotype. These results reveal the remarkable flexibility of CCR6/CCR4/CXCR3 expression on Th17-subsets upon TCR triggering and in relation with the cytokinic environment. Nevertheless, CCR6 expression was maintained on the majority of the four Th17-subsets, supporting the key role played by CCR6 in regulating tissue-specific homing of Th17-cells.

Th17-polarized CCR6$^+$DN and CCR6$^+$DP are present in the blood of HIV-infected individuals. To determine whether CCR6$^+$DN and CCR6$^+$DP exist in the blood of HIV-infected individuals and are stably Th17-polarized, the four memory CCR6$^+$ T-cell subsets as well as Th1 cells were identified and then sorted by flow cytometry (as in S1 Figure) from three chronically infected aviremic ART-treated individuals (CI on ART) (Table S2). The intracellular expression of IL-17A and IFN-γ was assessed upon long-term culture *in vitro*. Briefly, cells were stimulated *via* CD3/CD28 for 4 days and then cultured in the presence of IL-2 (Th0 polarizing conditions) for additional 9 days (S7A Figure). Similar to HIV-uninfected donors, Th17 and CCR6$^+$DN subsets from CI on ART individuals included a major fraction of IL-17A$^+$IFN-γ$^-$ cells, while Th1Th17, CCR6$^+$DN, and CCR6$^+$DP exhibited a similar frequency of IL-17A$^+$IFN-γ$^+$ cells (S6B-C Figure). Of note, similar to Th1, Th1Th17 and CCR6$^+$DP included a major fraction of IL-17A$^-$IFN-γ$^+$ cells (S7B-C Figure). In conclusion, the two newly identified Th17-polarized subsets, CCR6$^+$DN and

CCR6$^+$DP, exist in the peripheral blood of HIV-infected individuals and exhibit a Th17- and Th1Th17-polarization profile.

CCR6$^+$DN predominate in the blood of HIV-infected individuals during ART

Circulating Th17 and Th1Th17 are depleted upon HIV-infection and their frequency is not restored with viral-suppressive ART [15, 16]. Thus, we investigated alterations in the frequencies of CCR6$^+$DN and CCR6$^+$DP, relative to Th17 and Th17Th17, during HIV infection. In contrast to uninfected controls (Figure 1B), the frequency of CCR6$^+$DN in CI on ART individuals (Table S2) was superior to that of Th17 and Th1Th17, while CCR6$^+$DP were the least preponderant subset (Figure 6A). As in uninfected controls (Figure 1D), the four CCR6$^+$ subsets from CI on ART individuals were enriched in cells with a CM phenotype (Figure 6B). Similar to Th17 and Th1Th17 [15], the frequency of memory CCR6$^+$DP was significantly reduced in CI on ART *vs.* uninfected individuals (Figure 6C). In contrast, no significant differences were observed in the frequency of CCR6$^+$DN in CI on ART *vs.* uninfected individuals. Similar observations were made when absolute cell counts were compared (Figure 6D), indicative that CCR6$^+$DN are preserved during HIV infection.

To further explore the preservation of CCR6$^+$DN during HIV infection, we performed longitudinal studies in HIV-infected individuals enrolled in the Montreal HIV Primary Infection (HPI) cohort. The dynamics of the four CCR6$^+$ subsets were studied in relationship with plasma viral load at different time-points post-infection, before and after ART initiation (Figure 6E-F). Of note, in all five HIV$^+$ individuals, CCR6$^+$DN were the most predominant CCR6$^+$ subset before and after ART initiation. ART initiation during the first year of infection efficiently decreased plasma viral load to

undetectable levels in all individuals (Figure 6E) and increased CD4 counts (Table S3). We observed a tendency for increased Th17, Th1Th17 and CCR6$^+$DN counts following treatment (Figure 6E), indicative of the positive effects of ART in increasing Th17 levels during early chronic infection. The counts of CCR6$^+$DP were increased in 4/5 individuals following treatment but remained stable in one individual. Interestingly, the counts of CCR6$^+$DN were superior at all time-points in 4/5 and 5/5 individuals, respectively, when compared to Th17 and CCR6$^+$DP. In contrast, CCR6$^+$DP counts were the lowest in all patients before/after ART initiation. These results demonstrate that CCR6$^+$DP but not CCR6$^+$DN are depleted in CI on ART individuals.

CCR6$^+$DN are enriched in the lymph nodes of HIV-infected individuals on ART

Blood CCR6$^+$DN express Tfh markers as demonstrated by transcriptional profiling (Figure 2) and IL-21 quantification (Figure 3D). Tfh are localized in the B cell follicles of secondary lymphoid organs and are major targets for HIV infection [51, 52]. Access to inguinal lymph nodes from three HIV-infected individuals on ART (Table S2; CI 36, CI 37, CI 38) allowed us to reveal that CCR6$^+$DN represent the most frequent CCR6$^+$ T-cell subset in the lymph nodes (Figure 7). These results suggest that peripheral blood CCR6$^+$DN recirculate preferentially through lymph nodes and may include a fraction of Tfh.

CCR6$^+$DN are permissive to viral infection *in vitro* and in HIV-infected individuals

We and others previously demonstrated that Th17 and Th1Th17 cells are permissive to HIV infection [15, 16]. Thus, CCR6$^+$DN and CCR6$^+$DP were compared to Th17 and Th1Th17 in terms of HIV permissiveness *in vitro* and ability to carry proviral DNA in HIV-infected individuals. The HIV co-receptor CCR5 was expressed at low levels on CCR6$^+$DN, similar to Th17, and high levels

on CCR6^{+}DP, similar to Th1Th17. CXCR4 expression was similarly high on all subsets (Figure 7A). Exposure to replication-competent R5 HIV strain ADA8 demonstrated that CCR6^{+}DN and CCR6^{+}DP, similar to Th17 and Th1Th17, are permissive to HIV infection *in vitro* (Figure 7B). Further, Th17, Th1Th17, CCR6^{+}DN and/or CCR6^{+}DP were isolated from three recently-infected viremics untreated individuals (RI) (Table S2) for integrated HIV-DNA quantification. Results in S8 Figure demonstrate that similar to Th17 and Th1Th17, CCR6^{+}DN carry integrated HIV-DNA in all three donors tested, at relative levels varying between donors but superior to levels in naive T-cells. Thus, CCR6^{+}DN are permissive to HIV infection *in vitro* and *in vivo*.

CCR6^{+}DN carry replication-competent integrated HIV-DNA in CI on ART individuals

Recent evidence from our group (Gosselin *et al.,* unpublished observations) and others [26], support the contribution of long-lived Th17 cells to HIV reservoir persistence under ART. Thus, we sought to determine whether CCR6^{+}DN harbor replication-competent HIV reservoirs in HIV-infected individuals with undetectable viral load under ART (Table S2). The four CCR6^{+} T-cell subsets as well as Th1 cells were sorted by flow cytometry as in S1 Figure. Similar to the other cell subsets, CCR6^{+}DN harbored integrated HIV-DNA *ex vivo* (Figure 9A) and produced measurable levels of viral particles after stimulation *via* CD3/CD28 for 4 days (Figure 9B), indicating that these integrated genomes can be induced to produce HIV virions. To further determine the replication competency of HIV virions, we performed a modified viral outgrowth assay [53] that consisted in the culture of CD3/CD28-activated cells for thirteen days in the presence of IL-2 (as in S7A Figure). Results in Figure 9C demonstrate intracellular expression of HIV-p24 in CCR6^{+}DN from 3/3 CI on ART individuals, as well as the co-expression of HIV-p24 with IL-17A. The HIV-24 expression was also observed at various frequencies in Th17, Th1Th17 and Th1 cells in 2/3 CI on ART individuals

Figure 9C. Interestingly, HIV-p24 was detected in $CCR6^{+}$DP only 1/3 CI on ART individuals. Of note, in preliminary experiments, intracellular HIV-p24 was detected when cells were cultured in the absence but not the presence of antiretroviral drugs (ARVs: AZT (180 nM), Efavirens (100 nM), Raltegravir (200 nM)), suggesting that cell-to-cell HIV spreading occurred in culture (data not shown). Noteworthy, the HIV-$p24^{+}$ $CCR6^{+}$DN cells probed to be highly poly-functional in terms of IL-17A, IL-22, IFN-γ and TNF-α expression (Figure 9D; S9 Figure). Finally, we observed that a fraction of the HIV-$p24^{+}$ $CCR6^{+}$DN cells were able to proliferate when cultured for additional five days in the presence of IL-2 or CD3/CD28 Abs (Figure 9E). Together these results support the contribution of $CCR6^{+}$DN cells to HIV persistence during ART.

DISCUSSION

The concept of Th17 pathogenicity is well defined in the context of autoimmunity [18, 19, 21]. During HIV-1 infection, Th17 cells may be considered pathogenic because they are permissive to HIV-1 and subsequently depleted [15, 16]. Alternatively, long-lived Th17 cells [25, 28, 29] may carry integrated HIV-DNA and contribute to viral reservoir persistence under ART (Gosselin *et al.,* unpublished observations) [26]. In this manuscript we used a systems biology approach to characterize the heterogeneity of memory subsets expressing the Th17 marker CCR6 at homeostasis and during HIV-1 infection. We reveal the existence of two new subsets of Th17-polarized $CCR6^+$ T-cells, $CCR6^+$DN ($CCR4^-CXCR3^-$) and $CCR6^+$DP ($CCR4^+CXCR3^+$), that share functional characteristics with the previously characterized Th17 and Th1Th17 [5, 15, 16] in terms of lineage-specific cytokines, antigenic specificity, lineage specification *vs*. plasticity and HIV permissiveness. Genome-wide transcriptional profiling revealed a unique molecular signature in $CCR6^+$DN, suggesting they represent an early stage of Th17 differentiation. In contrast to the other Th17-polarized subsets, the $CCR6^+$DN was the most predominant in the blood and the lymph nodes of HIV-infected subjects with undetectable plasma viral load under ART. Finally, we demonstrated that $CCR6^+$DN carry replication competent HIV reservoirs in ART-treated individuals. Our results support the concept that long-lived Th17 cells, *i.e.,* $CCR6^+$DN, contribute to HIV persistence during ART.

Similar to Th17 cells, $CCR6^+$DN were a major source of IL-17A, while $CCR6^+$DP and Th1Th17 cells produced low IL-17A levels. Nevertheless, $CCR6^+$DN and $CCR6^+$DP expressed both typical Th17 transcripts (*i.e.,* IL-26, CCL20, IL-22, IL-23R, RORC, IL-17F, RORA, KLRB1/CD161, IL6R

[3]) and potentially new Th17 markers (CXCR6, PTPN13, MAP3K4, S100A4, CD96, Ly9, KLF2, LGMN, TNFRSF25, ANTXR2, and CTSH). PTPN13, a phosphatase associated with Fas [54], was previously identified as Th17-specific [21, 55] and may contribute to the regulation of cell activation/apoptosis. ARNTL, a component of the circadian clock machinery, was proved to regulate RORγt expression and Th17 development in mice [56]. Finally, the expression of ANTXR2 is consistent with recent findings that Th17 cells govern adaptive immune responses against *Bacillus anthracis* [57].

Despite several transcriptional similarities, CCR6$^+$DN, CCR6$^+$DP and Th17 expressed distinct molecular signatures linked to specific pathways and biological processes. CCR6$^+$DN were enriched in molecules associated with lymph node chemotaxis (CCR7, CXCR5, CXCL13, SELL, SIRP1, JAM3, AIF1). In contrast, Th17 and CCR6$^+$DP expressed molecules related to homing into peripheral tissues including the gut (integrin β7 or CXCR3), skin (CCR2, CCR4) and cervix (integrin β1). Several signaling pathways involved in Th17 differentiation, including IL-6, phospholipase C, April and NFAT, were upregulated in CCR6$^+$DN *vs.* Th17 and/or CCR6$^+$DP. CCR6$^+$DN expressed higher levels of STAT3 mRNA and were enriched in other Th17-associated markers including IL-17F, RORA [58], IL-23R [43], SOSC3 [59], TIM3 [60] and CD26/DPP4 [61]. STAT3 is one of the first transcription factors to be up-regulated within the first hours of Th17 polarization [62]. Cell fate mapping experiments demonstrated IL-17F is expressed during early stages of Th17 differentiation [33]. Further, CCR6$^+$DN were found to express a stem-cell-like molecular signature including RORA, STAT3, LEF1, MYC and TERC [25, 46, 63, 64] as well as the NANOG signaling pathway, important for the maintenance of stem cells[39]. LEF1 and MYC characterize long-lived Th17 cells with self-renewal properties [25]. TERC is linked to telomerase

activity, which is up-regulated in stem cells, cancer cells and proliferating lymphocytes [46]. In contrast, CCR6^{+}DP [56] together with Th17 expressed high levels of LMNA, a senescence marker [34]. These findings feed the idea that CCR6^{+}DN *vs*. Th17 and CCR6^{+}DP represent a less advanced stage of Th17 differentiation with superior survival potential.

In addition to IL-17F, CCR6^{+}DN are distinguished from the other CCR6^{+} subsets by their relatively high production of IL-8 and IL-21. IL-8 is critical for neutrophil recruitment at inflammatory sites [65], indicative of superior effector functions for CCR6^{+}DN. IL-21 is the hallmark cytokine for follicular helper T cells (Tfh) [44]. IL-21 up-regulates expression of the Tfh-specific transcription factor BCL6 and the chemokine receptor CXCR5 [66]. Consistently, CCR6^{+}DN express the highest levels of BCL6 and CXCR5 mRNA, and are also enriched in ASCL2 mRNA, another Tfh-specific transcription factor [45]. Thus, CCR6^{+}DN cells share Tfh features. This is in line with a proposed differentiation model in which Tfh development occurs subsequent to Th1, Th2 or Th17 polarization [44]. Similar to Th17 but in contrast to Th1Th17 [15], CCR6^{+}DN and CCR6^{+}DP produce low/undetectable levels of IL-2, a cytokine known to promote cell survival [67]. IL-21 acts as a survival factor for Th17 cells [68]. IL-21 supplementation leads to the restoration of IL-17A-producing cells in SIV-infected macaques [68]. Therefore, IL-21 produced by CCR6^{+}DN may act in autocrine manner to support superior survival of these cells and compensate for their limited IL-2 expression.

Th17 cells mediate immunity against pathogens localized at barrier surfaces including *C. albicans* [3, 5]. Here, we reveal that CCR6^{+}DN, similar to Th17, proliferate and produce IL-17A in response to *C.albicans* but not CMV. We also observed proliferation of Th1Th17 and Th1 in response to *C.*

albicans and CMV. These results are consistent with recent studies from *Becattini et al.* in which Th17, Th1Th17 and Th1 share *C.albicans* clonotypes, while expressing distinct effector cytokines [27]. Clonotype sharing between Th17 subsets is consistent with previous reports on the acquisition of Th1 features by Th17 cells under inflammatory conditions[29]. Whether $CCR6^+$DN and Th17 share *C.albicans* clonotypes remains to be investigated. The antigenic specificity of $CCR6^+$DP was not tested in our study. However, Becattini *et al.* identified a population similar to $CCR6^+$DP that shared with Th1Th17 *M. tuberculosis* clonotypes [27], thus suggesting a potential differentiation relationship between $CCR6^+$DP and Th1Th17.

In contrast to $CCR6^-$, $CCR6^+$ T-cells are prone to express Th17 functions [10]. Consistently, the frequency of cells expressing IL-17A, IL-17F and IL-22 was dramatically increased in all $CCR6^+$ subsets upon long-term exposure to Th17-polarizing signals. Notably, $CCR6^+$DN and Th17 were distinguished from $CCR6^+$DP and Th1Th17 by their superior IL-17A/IL-17F and reduced IFN-γ expression. Th17 cells are known to be extremely plastic and can dedifferentiate into other lineages [29]. As such, all Th17 subsets diminished expression of Th17 cytokines and enhanced IFN-γ expression in response to Th1-polarizing signals. This is consistent with other studies in mice and humans demonstrating suppression of Th17 effector cytokines upon IL-12 exposure [6, 69]. Our results reveal that $CCR6^+$DN and $CCR6^+$DP, together with Th17 and Th1Th17, are four distinct Th17-commited subsets that exhibit lineage plasticity. Noteworthy, a fraction of $CCR6^+$DN and Th17 preserved production of Th17 cytokines under Th1 conditions, providing evidence that stably-committed Th17 cells exist in humans, as previously predicted [2]. Our results also confirm the stability of the Th1 transcriptional program [29].

The chemokine receptors CCR6, CCR4, and CXCR3 mediate T-cell recruitment into gut-associated lymphoid tissues (12, 83), skin (84), and various other inflammatory sites (85). We observed that expression of these receptors represents stable signatures only for a fraction of CM Th17-subsets upon exposure to Th17/Th1-polarization signals. The expression of CCR6 was particularly stable under Th17-polarizing conditions, consistent with the identification of stable epigenetic mechanisms involved in controlling CCR6 expression (86). CCR6 expression was however dramatically decreased upon exposure to Th1-polarizing cytokines, consistent with the reported ability of IL-12 to down-regulate CCR6 (87). The expression of CCR4 and CXCR3 was stable on >70% Th17 and >80% Th1Th17, respectively, regardless of the polarization conditions. Interestingly, $CCR6^{+}$DN cultured under Th17- or Th1-conditions acquired a "classical" Th17-phenotype ($CCR6^{+}CCR4^{+}$), while CXCR3, a marker for Th1Th17 and Th1-cells (10, 21), was similarly acquired by $CCR6^{+}$DN and Th17 under Th17-/Th1-conditions. It is reported that Th1Th17-cells derive from Th17-cells that acquired Th1-features under inflammatory conditions (24, 88, 89). Our results demonstrate that $CCR6^{+}$DN acquire Th17 and/or Th1Th17 phenotypic features. In contrast to $CCR6^{+}$DN, a significant fraction of $CCR6^{+}$DP lost CCR4 and/or CXCR3, regardless of polarization conditions, and acquired a Th1Th17 but not Th17 phenotype. All these findings reveal flexibility in the expression of CCR6, CCR4 and/or CXCR3 by these Th17-subsets, flexibility that may be relevant for their differential recruitment into various tissues. This flexibility suggests a developmental relationship between these four Th17-subsets *via* molecular mechanisms that remain to be further investigated.

Of particular importance, we demonstrate that the four $CCR6^{+}$ T-cell subsets exist in the peripheral blood of HIV-infected individuals and exhibit a Th17-polarization profile similar to subsets from

uninfected individuals. The CCR6$^+$DN were the most preponderant among Th17 subsets in the peripheral blood of ART-treated individuals as their frequency/counts were preserved at levels similar to uninfected individuals. Furthermore, in a longitudinal follow-up in five HIV-infected individuals, CCR6$^+$DN proved to be the most predominant CCR6$^+$ subset before/after ART initiation. This raised the possibility that CCR6$^+$DN are resistant to infection.

In contrast to the above prediction, we demonstrated that all four Th17 subsets, including CCR6$^+$DN, were permissive to HIV infection *in vitro* and *in vivo*. CCR6$^+$DN and CCR6$^+$DP expressed the HIV coreceptors CCR5 and CXCR4 at levels similar to Th17 and Th1Th17, respectively. Accordingly, all Th17 subsets were permissive to HIV *in vitro*. Furthermore, CCR6$^+$DN, Th17 and Th1Th17 harbored proviral HIV-DNA in RI individuals, indicative of their HIV permissiveness *in vivo*. Of particular interest, all four CCR6$^+$ subsets were found to carry relatively high levels of integrated HIV-DNA in virologically suppressed ART-treated individuals. We further demonstrated that viral transcription and production, reflected by the detection of HIV-RNA in cell culture supernatants, occurred in all four Th17 subsets, including CCR6$^+$DN cells. Finally, we demonstrate active viral replication in CCR6$^+$DN cells cultured for 13 days under Th0 polarizing conditions *in vitro*. Of note, HIV-p24$^+$ CCR6$^+$DN cells from CI on ART individuals co-expressed IL-17A and were highly poly-functional, and a fraction of them were able to proliferate in response to repetitive IL-2 stimulation or TCR triggering *in vitro*. These results support the contribution of CCR6$^+$DN cells to HIV reservoir persistence under ART. This is consistent with a model in which integrative infection is compatible with survival [70] and CCR6 triggering *via* CCL20 promotes HIV latency [71] and suggests that permissiveness to HIV integration compatible with survival represents a new previously unrecognized feature of pathogenic Th17 cells during HIV

infection. **Understanding the mechanism and cellular determinants exploited by HIV for its own dissemination is important to design targeted strategies to eradicate HIV infection. Identifying cells being viral reservoir is crucial in the search of a cure. Target cells carrying replication-competent virus including the CCR6+DN cells could be targeted for the shock and kill strategy. Permissivity to HIV appears to be a characteristic of the Th17 lineage. A strategy to target the Th17 cells carrying replication-competent virus might involved engineering a molecule with the CCL20 sequence. However, not all Th17 cells are permissive to HIV. HIV**

Our results that $CCR6^{+}$DN express Tfh markers are in line with a recent study demonstrating the restoration of $CCR6^{+}$ T cells expressing a Tfh signature ($CCR7^{high}CXCR5^{high}PD\text{-}1^{high}$) under ART [72]. $CD4^{+}$ T cells with CM features constitute the main reservoir of latent HIV [73]. Indeed, we demonstrate that $CCR6^{+}$DN are enriched in cells with CM phenotype and they are the most predominant $CCR6^{+}$ T-cell subset in the inguinal lymph nodes of three ART-treated individuals. Future studies are required to determine whether $CCR6^{+}$DN from lymph nodes exhibit Tfh features and carry replication-competent HIV reservoirs.

CONCLUSIONS

In summary, we demonstrated the existence in humans of four distinct Th17-polarized $CCR6^{+}$ $CD4^{+}$ T-cell subsets with differential expression of CCR4 and CXCR3, including two newly characterized $CCR6^{+}$DN and $CCR6^{+}$DP populations (Figure 10). The existence of multiple Th17 subsets with distinct trafficking potential and functional properties might allow defenses at barrier surfaces including the gut, while maintaining a pool of long-lived CM Th17 cells, *i.e.,* $CCR6^{+}$DN, that

recirculate across lymph nodes. HIV-1 appears to exploit this heterogeneity for its replication and persistence. Considering alterations in the Th17 pool during early acute phases of HIV-1 infection [74], together with the long-lived properties of some Th17 cells [25, 28, 29], new Th17-specific therapeutic strategies are needed to prevent HIV reservoir establishment during primary infection and to induce latency reversal during the chronic phase. Outside the HIV field, this work provides a new original understanding of the functional heterogeneity of Th17 cells at molecular level that is critical for designing new therapeutic strategies to manipulate cellular features during other pathological conditions associated with impaired or exacerbated Th17 responses.

MATERIAL AND METHODS

Study individuals and biological samples

Human individuals were recruited at the Montreal Chest Institute, McGill University Health Centre, and the Universite de Montreal Hospital Centre (CHUM), Montreal, Quebec. Peripheral blood mononuclear cells (PBMCs) were collected by leukapheresis and cryopreserved until use [15]. Cytomegalovirus (CMV) infection was determined upon detection of CMV-specific Abs using chemiluminescent microparticle immunoassay (CMIA){Juhl, 2013 #3173}. In parallel, matched blood and inguinal lymph node samples were collected from three HIV-infected individuals from the SCOPE study (UCSF School of Medicine, CA, USA) who were on stable ART with undetectable viremia (<40 HIV RNA copies/ml) for at least 8 years. After careful removal of the surrounding fatty tissue, lymph nodes were mechanically disrupted using frosted glass slides. The single cell suspension obtained was filtered and benzonase digested (25 U/mL) before to be used for flow cytometry analysis.

Antibodies and polychromatic flow cytometry analysis

Detailed description available in Online supplemental material.

Magnetic (MACS) and fluorescence activated cell sorting (FACS)

Total $CD4^+$ T-cells were sorted from PBMCs by negative selection using magnetic beads (Miltenyi Biotec) [15], and stained with CD45RA, CCR4, CXCR3 and CCR6 Abs, and a cocktail of FITC-conjugated CD8, CD19, and CD56 Abs. Memory $CD4^+$ T-cells ($CD45RA^-$) with differential expression of CCR6, CCR4 and/or CXCR3 were sorted by FACS (BDAria II; BD Biosciences):

$CXCR3^-CCR4^+$ ($CCR4^+$Th17[5, 15]), $CXCR3^+CCR4^-$ ($CXCR3^+$Th1Th17[5, 15]), $CXCR3^-CCR4^-$ ($CCR6^+$DN), and $CXCR3^-CCR4^-$ ($CCR6^+$DP). Total $CCR6^-$ or $CXCR3^+CCR4^-$ (Th1 [5, 15]) subsets were sorted in parallel. Sorting gates were set on FITC- to exclude $CD8^+$ T-cells, $CD19^+$ B-cells, and $CD56^+$ NK-cells. For specific experiments, central (CM, $CD45RA^-CCR7^+$) and effector memory (EM, $CD45RA^-CCR7^-$) subsets with differential expression of CCR6, CCR4 and/or CXCR3 were sorted. Sorting gates were set based on FMO controls [15]. Quality control analysis post-sort indicated an average purity >95% (S1 Figure).

Genome-wide transcription profiling

Matched memory $CD4^+$ T-cell subsets were isolated by FACS from different HIV-uninfected donors stimulated with immobilized CD3 and soluble CD28 (1μg/ml) for 4 days. Total RNA was isolated using RNeasy columns kit (Qiagen) according to the manufacturer's protocol. RNA quantity was determined by Pearl nanophotometer (Implen, Germany) (10^6 cells yielded 1-5 μg RNA). Genome-wide analysis of gene expression was performed on total RNA by Génome Québec Innovation Centre (Montreal, Qc, Canada). Briefly, the quality of total RNA was tested using the Agilent 2100 Bioanalyzer chip. High quality RNA was reverse transcribed and hybridized on the Illumina HumanHT-12 v4 Expression BeadChip providing coverage for more then 47,000 transcripts and known splice variants across the human transcriptome. The expression of differentially expressed genes was identified as previously described[55]. The entire microarray dataset and technical information requested by Minimum Information About a Microarray Experiment (MIAME) are available at the Gene Expression Omnibus (GEO) database under accession number GSE66972. Differentially expressed genes (cut-off 1.3-fold; $p < 0.05$) were classified through Gene Ontology using the NetAffx web-based application (Affymetrix), while

differentially expressed pathways were identified using *Ingenuity Pathway Analysis* (IPA) and *Gene Set Variation Analysis* (GSVA). Corresponding heat maps for biological function categories were generated using programming language R [55].

Real-time RT-PCR

One step SYBR Green real-time RT-PCR was carried out in a LightCycler 480 II (Roche) using Qiagen reagents according to manufacturer's recommendations, as previously described [55, 75]. Briefly, STAT3, BCL-6, Lef1, and Terc primers were purchased from Qiagen (QuantiTect Primer Assay). The expression of each gene was normalized relative to the internal control 28S rRNA levels (forward 5'-CGAGATTCCTGTCCCCACTA-3'; reverse 5'-GGGGCCACCTCCTTATTCTA-3' (IDT[75]). Samples without template or without reverse transcriptase were used as negative controls. Each RT-PCR reaction was performed in triplicata.

Cytokine screening and ELISA quantification

Cell culture supernatants were screened for the expression of 34 cytokines using the Human Th1/Th2/Th17 Antibody Array C series (RayBiotec, Norcross, GA), as previously described [76]. Cytokine levels were quantified by ELISA using commercial kits for IL-10, IL-13, IL-17A, IL-17F, IL-21, IL-22, IFN-γ, TNF-α (Ebioscience) as well as CXCL8/IL-8 and CCL20 (R&D Systems).

Intracellular cytokine staining

Intracellular expression of cytokines was measured by FACS [77] using the BD Cytofix/Cytoperm kit (BD Biosciences) and specific Abs (See table above). Analysis was performed using Diva and

FlowJo. Polyfunctional profiles were analyzed using the SPICE (version 5.3; provided by Mario Roederer, VRC/NIAID/NIH) [50].

Antigen presentation assay

Cell proliferation was measured using the carboxy fluoroscein succinimidyl ester (CFSE) dilution assay[77], following co-culture with antigen-loaded autologous monocyte-derived dendritic cells (MDDC). Briefly, monocytes isolated from PBMCs by negative selection using magnetic beads (Miltenyi Biotec) [76] were differentiated into MDDC in the presence of GM-CSF and IL-4 (20 ng/ml; R&D Systems). MDDCs were loaded with SEB (25 ng/ml; Toxin Technologies), CMV-pp65 peptide pool (1 μg/ml; Miltenyi) or *Candida albicans* hyphae LAM-1 [78] (25 μl protein lysate[77]) for one hour at 37°C and cocultured with FACS-sorted CFSE-loaded T-cell subsets. MDDC:T-cell cocultures (1:4 ratio) were maintained for 5 days at 37 °C. MDDC:T-cell co-cultures were stained with CD3 (T-cell marker) and CD1c (DC marker). Proliferating T-cells were identified as cells with a $CFSE^{low}CD3^{+}CD1c^{-}$ phenotype. In parallel, MDDC:T-cell co-cultures were stimulated with PMA and Ionomycin in the presence of brefeldin A and the expression of cytokines in proliferating T-cell subsets was quantified by FACS upon intracellular staining with specific anti-cytokine Abs (See table above). Intracellular expression of cytokines was quantified by FACS [77].

Th17 *versus* Th1 polarization

Cells were stimulated *via* CD3/CD28 and cultured under Th17-polarizing conditions (IL-1β (10 ng/ml), IL-6 (50 ng/ml), and IL-23 (40 ng/ml), and anti-IL-4 (1 μg/ml) and anti-IFN-γ Abs (10 μg/ml) (R&D Systems)) or Th1-polarizing conditions (IL-12 (5 ng/ml) (R&D Systems) and anti-IL-4 Abs (1 μg/ml)) for 4 days. Cells were washed and plated in media containing the Th17- or Th1-

polarization cocktails together with recombinant IL-2 (5 ng/ml) for 10 additional days. Polarizing cytokines were replenished every 2-3 days and cells were split to optimal density (<$2x10^6$ cells/ml).

HIV infection *in vitro*

FACS-sorted memory $CCR6^+$ T-cell subsets were activated for 4 days *via* CD3/CD28 (1μg/ml) and then exposed to HIV-1 ADA8 (50 ng HIV-p24 *per* 10^6 cells) for 3 h at 37°C. Extensive washing was performed to remove unbound HIV. Cells (10^6 cells *per* ml) were cultured in media containing FBS (10%) and IL-2 (5 ng/ml; R&D Systems). Cell culture supernatants were harvested at day 3 post-infection and HIV replication was measured by HIV-p24 ELISA.

Real-time PCR quantification of integrated HIV-DNA

The quantification of integrated HIV-DNA was performed as we previously described[15, 73]. Briefly, cells were digested in a proteinase K buffer (Invitrogen), and 10^5 cells/15 μl lysate were used *per* amplification. Integrated HIV-DNA was amplified first (12 cycles) using two outward-facing *Alu* primers and one HIV LTR primer tagged with a lambda sequence; the CD3 gene was amplified in the same reaction. The HIV and CD3 amplicons were then amplified in separate reactions (Light Cycler 480, Roche Diagnostics). The HIV-DNA was amplified using a lambda-specific primer and an inner LTR primer in the presence of two fluorescent probes specific for HIV LTR. The CD3 DNA was amplified using inner primers and two fluorescent probes specific for CD3. Amplification reactions were carried out with Light Cycler 480 Probe Master Mix (Roche) and Taq Polymerase (Invitrogen). The ACH2 cells carrying one copy of integrated HIV-DNA per cell (NIAIDS reagent program) were used as standard curve.

HIV reactivation assay

Highly pure matched memory $CD4^+$ T-cell subsets were isolated by FACS from different CI on ART individuals and stimulated with immobilized CD3 and soluble CD28 Abs (1µg/ml) for 4 days. Cells were washed and plated in media containing recombinant IL-2 (5 ng/ml) for 9 additional days. IL-2 was replenished and cells were split to optimal density ($<2x10^6$ cells/ml) every 3 days. At day 13, cells were stimulated with PMA and Ionomycin in the presence of Brefeldin A for 6 hours. Intracellular staining was performed with cytokine-specific Abs and HIV-p24. Cell culture supernatants were collected at day 4, 7, 11, and 13 post-TCR triggering and used for the quantification of HIV-RNA and/or HIV-p24 levels.

Real-time RT-PCR quantification for HIV-RNA

Viral RNA was isolated from cell-culture supernatants using the QIAmp viral RNA mini kit (Qiagen) according to the manufacturer's protocol. Collected RNA was treated with DNase, reverse transcribe and then amplified for 20 cycles using primers specific for HIV-LTR (tagged with a lambda sequence) and HIV-GAG. The HIV-DNA was further amplified using a lambda-specific primer and an inner HIV-LTR primer as well as two fluorescent probes specific for HIV-LTR, using a protocol adapted from [73].

Statistics

Statistical analyses were performed using the GraphPad Prism 5. Details are included in Figure legends.

Accession numbers

The entire microarray dataset and technical information requested by Minimum Information About a Microarray Experiment (MIAME) are available at the Gene Expression Omnibus (GEO) database under accession number GSE66972.

Online supplemental material

Supplemental information includes Supplemental Table 1 legend, Supplemental Tables 2-3, Supplemental Figure 1-9 legends, Supplemental Material and Methods, and Supplemental references.

Ethics approval and consent to participate

Written informed consents and Institutional Review Board approvals were obtained from all HIV-infected and uninfected individuals included in this study, in compliance with the Declaration of Helsinki principles.

Competing interests

The authors declare no financial and non-financial competing interests.

Authors' contributions

VSW performed research, analyzed data, and wrote the manuscript. JPG performed microarray data analysis and generated figures. AG and PM performed experiments. HS contributed to research design and manuscript writing. RF performed experiments. MAJ, SV, SGD, NC, and JPR ensured access to clinical samples/information and/or provided experimental protocols. PA designed research, analyzed data, and wrote the manuscript. All authors reviewed and accepted the manuscript.

Funding

This work was supported by grants to PA from the CIHR (MOP-82849; MOP-114957). VSW received a CIHR Ph.D. Fellowships. JPR holds a Louis-Lowenstein Chair in Hematology and Oncology, McGill University. Human cohorts were supported by the FRQ-S/AIDS and Infectious Diseases Network.

Acknowledgements

The authors thank Laurence Lejeune and Dr. Dominique Gauchat for expert technical support in FACS analysis and cell sorting (the CHUM-Research Centre FACS Core Facility), Anne Vassal and Mario Legault (HIV/AIDS and Infectious Diseases Network of the Fonds de Recherche Québec-Santé (FRQ-S)) for help with ethical approvals and informed consents, Dr. Louis de Repentigny and Mathieu Goupil for *Candida albicans* LAM-1 strain preparation, Dr. Dana Gabuzda (Dana-Farber Cancer Institute, Boston, MA, USA) for the HIV-ADA8 molecular clone, Dr. Mohamed Salah and Tomas Fabre for technical assistance with SPICE, and Dr. Shoukry and Dr. El-Far for critical reading of the manuscript. We thank Josée Girouard and Angie Massicotte (McGill University Health Centre) for their involvement in patient recruitment and leukapheresis collection, and Amélie Pagliuzza and Marion Pardons for assistance with lymph node sample treatment. We finally acknowledge the major contribution to this work of all human donors *via* their gift of leukapheresis.

REFERENCES

1. van der Meer JW, Netea MG: **A salty taste to autoimmunity.** *N Engl J Med* 2013, **368:**2520-2521.
2. Basu R, Hatton RD, Weaver CT: **The Th17 family: flexibility follows function.** *Immunol Rev* 2013, **252:**89-103.
3. Gaffen SL, Jain R, Garg AV, Cua DJ: **The IL-23-IL-17 immune axis: from mechanisms to therapeutic testing.** *Nat Rev Immunol* 2014, **14:**585-600.
4. Gagliani N, Vesely MC, Iseppon A, Brockmann L, Xu H, Palm NW, de Zoete MR, Licona-Limon P, Paiva RS, Ching T, et al: **Th17 cells transdifferentiate into regulatory T cells during resolution of inflammation.** *Nature* 2015, **523:**221-225.
5. Acosta-Rodriguez EV, Rivino L, Geginat J, Jarrossay D, Gattorno M, Lanzavecchia A, Sallusto F, Napolitani G: **Surface phenotype and antigenic specificity of human interleukin 17-producing T helper memory cells.** *Nat Immunol* 2007, **8:**639-646.
6. Annunziato F, Cosmi L, Santarlasci V, Maggi L, Liotta F, Mazzinghi B, Parente E, Fili L, Ferri S, Frosali F, et al: **Phenotypic and functional features of human Th17 cells.** *J Exp Med* 2007, **204:**1849-1861.
7. Kunkel EJ, Campbell DJ, Butcher EC: **Chemokines in lymphocyte trafficking and intestinal immunity.** *Microcirculation* 2003, **10:**313-323.
8. Lowes MA, Suarez-Farinas M, Krueger JG: **Immunology of psoriasis.** *Annu Rev Immunol* 2014, **32:**227-255.
9. Reboldi A, Coisne C, Baumjohann D, Benvenuto F, Bottinelli D, Lira S, Uccelli A, Lanzavecchia A, Engelhardt B, Sallusto F: **C-C chemokine receptor 6-regulated entry of**

TH-17 cells into the CNS through the choroid plexus is required for the initiation of EAE. *Nat Immunol* 2009, **10:**514-523.

10. Wan Q, Kozhaya L, ElHed A, Ramesh R, Carlson TJ, Djuretic IM, Sundrud MS, Unutmaz D: **Cytokine signals through PI-3 kinase pathway modulate Th17 cytokine production by CCR6+ human memory T cells.** *J Exp Med* 2011, **208:**1875-1887.

11. Zielinski CE, Mele F, Aschenbrenner D, Jarrossay D, Ronchi F, Gattorno M, Monticelli S, Lanzavecchia A, Sallusto F: **Pathogen-induced human TH17 cells produce IFN-gamma or IL-10 and are regulated by IL-1beta.** *Nature* 2012, **484:**514-518.

12. Okada S, Markle JG, Deenick EK, Mele F, Averbuch D, Lagos M, Alzahrani M, Al-Muhsen S, Halwani R, Ma CS, et al: **IMMUNODEFICIENCIES. Impairment of immunity to Candida and Mycobacterium in humans with bi-allelic RORC mutations.** *Science* 2015, **349:**606-613.

13. Kochi Y, Okada Y, Suzuki A, Ikari K, Terao C, Takahashi A, Yamazaki K, Hosono N, Myouzen K, Tsunoda T, et al: **A regulatory variant in CCR6 is associated with rheumatoid arthritis susceptibility.** *Nat Genet* 2010, **42:**515-519.

14. Zhao F, Hoechst B, Gamrekelashvili J, Ormandy LA, Voigtlander T, Wedemeyer H, Ylaya K, Wang XW, Hewitt SM, Manns MP, et al: **Human CCR4+ CCR6+ Th17 cells suppress autologous CD8+ T cell responses.** *J Immunol* 2012, **188:**6055-6062.

15. Gosselin A, Monteiro P, Chomont N, Diaz-Griffero F, Said EA, Fonseca S, Wacleche V, El-Far M, Boulassel MR, Routy JP, et al: **Peripheral blood CCR4+CCR6+ and CXCR3+CCR6+CD4+ T cells are highly permissive to HIV-1 infection.** *J Immunol* 2010, **184:**1604-1616.

16. El Hed A, Khaitan A, Kozhaya L, Manel N, Daskalakis D, Borkowsky W, Valentine F, Littman DR, Unutmaz D: **Susceptibility of human Th17 cells to human immunodeficiency virus and their perturbation during infection.** *J Infect Dis* 2010, **201:**843-854.

17. Langrish CL, Chen Y, Blumenschein WM, Mattson J, Basham B, Sedgwick JD, McClanahan T, Kastelein RA, Cua DJ: **IL-23 drives a pathogenic T cell population that induces autoimmune inflammation.** *J Exp Med* 2005, **201:**233-240.

18. Lee Y, Awasthi A, Yosef N, Quintana FJ, Xiao S, Peters A, Wu C, Kleinewietfeld M, Kunder S, Hafler DA, et al: **Induction and molecular signature of pathogenic TH17 cells.** *Nat Immunol* 2012, **13:**991-999.

19. Esplugues E, Huber S, Gagliani N, Hauser AE, Town T, Wan YY, O'Connor W, Jr., Rongvaux A, Van Rooijen N, Haberman AM, et al: **Control of TH17 cells occurs in the small intestine.** *Nature* 2011, **475:**514-518.

20. Peters A, Pitcher LA, Sullivan JM, Mitsdoerffer M, Acton SE, Franz B, Wucherpfennig K, Turley S, Carroll MC, Sobel RA, et al: **Th17 cells induce ectopic lymphoid follicles in central nervous system tissue inflammation.** *Immunity* 2011, **35:**986-996.

21. Ramesh R, Kozhaya L, McKevitt K, Djuretic IM, Carlson TJ, Quintero MA, McCauley JL, Abreu MT, Unutmaz D, Sundrud MS: **Pro-inflammatory human Th17 cells selectively express P-glycoprotein and are refractory to glucocorticoids.** *J Exp Med* 2014, **211:**89-104.

22. Lee JS, Tato CM, Joyce-Shaikh B, Gulan F, Cayatte C, Chen Y, Blumenschein WM, Judo M, Ayanoglu G, McClanahan TK, et al: **Interleukin-23-Independent IL-17 Production Regulates Intestinal Epithelial Permeability.** *Immunity* 2015.

23. Maxwell JR, Zhang Y, Brown WA, Smith CL, Byrne FR, Fiorino M, Stevens E, Bigler J, Davis JA, Rottman JB, et al: **Differential Roles for Interleukin-23 and Interleukin-17 in Intestinal Immunoregulation.** *Immunity* 2015.

24. Sandler NG, Douek DC: **Microbial translocation in HIV infection: causes, consequences and treatment opportunities.** *Nat Rev Microbiol* 2012, **10:**655-666.

25. Kryczek I, Zhao E, Liu Y, Wang Y, Vatan L, Szeliga W, Moyer J, Klimczak A, Lange A, Zou W: **Human TH17 cells are long-lived effector memory cells.** *Sci Transl Med* 2011, **3:**104ra100.

26. Sun H, Kim D, Li X, Kiselinova M, Ouyang Z, Vandekerckhove L, Shang H, Rosenberg ES, Yu XG, Lichterfeld M: **Th1/17 Polarization of CD4 T Cells Supports HIV-1 Persistence during Antiretroviral Therapy.** *J Virol* 2015, **89:**11284-11293.

27. Becattini S, Latorre D, Mele F, Foglierini M, De Gregorio C, Cassotta A, Fernandez B, Kelderman S, Schumacher TN, Corti D, et al: **T cell immunity. Functional heterogeneity of human memory CD4(+) T cell clones primed by pathogens or vaccines.** *Science* 2015, **347:**400-406.

28. Muranski P, Borman ZA, Kerkar SP, Klebanoff CA, Ji Y, Sanchez-Perez L, Sukumar M, Reger RN, Yu Z, Kern SJ, et al: **Th17 cells are long lived and retain a stem cell-like molecular signature.** *Immunity* 2011, **35:**972-985.

29. Muranski P, Restifo NP: **Essentials of Th17 cell commitment and plasticity.** *Blood* 2013, **121:**2402-2414.

30. Cosmi L, De Palma R, Santarlasci V, Maggi L, Capone M, Frosali F, Rodolico G, Querci V, Abbate G, Angeli R, et al: **Human interleukin 17-producing cells originate from a CD161+CD4+ T cell precursor.** *J Exp Med* 2008, **205:**1903-1916.

31. Sallusto F, Palermo B, Lenig D, Miettinen M, Matikainen S, Julkunen I, Forster R, Burgstahler R, Lipp M, Lanzavecchia A: **Distinct patterns and kinetics of chemokine production regulate dendritic cell function.** *Eur J Immunol* 1999, **29:**1617-1625.

32. Riou C, Yassine-Diab B, Van grevenynghe J, Somogyi R, Greller LD, Gagnon D, Gimmig S, Wilkinson P, Shi Y, Cameron MJ, et al: **Convergence of TCR and cytokine signaling leads to FOXO3a phosphorylation and drives the survival of CD4+ central memory T cells.** *J Exp Med* 2007, **204:**79-91.

33. Lee YK, Turner H, Maynard CL, Oliver JR, Chen D, Elson CO, Weaver CT: **Late developmental plasticity in the T helper 17 lineage.** *Immunity* 2009, **30:**92-107.

34. Bonello-Palot N, Simoncini S, Robert S, Bourgeois P, Sabatier F, Levy N, Dignat-George F, Badens C: **Prelamin A accumulation in endothelial cells induces premature senescence and functional impairment.** *Atherosclerosis* 2014, **237:**45-52.

35. Klotz L, Burgdorf S, Dani I, Saijo K, Flossdorf J, Hucke S, Alferink J, Nowak N, Beyer M, Mayer G, et al: **The nuclear receptor PPAR gamma selectively inhibits Th17 differentiation in a T cell-intrinsic fashion and suppresses CNS autoimmunity.** *J Exp Med* 2009, **206:**2079-2089.

36. Dong C, Davis RJ, Flavell RA: **MAP kinases in the immune response.** *Annu Rev Immunol* 2002, **20:**55-72.

37. Berg LJ, Finkelstein LD, Lucas JA, Schwartzberg PL: **Tec family kinases in T lymphocyte development and function.** *Annu Rev Immunol* 2005, **23:**549-600.

38. Cyster JG, Schwab SR: **Sphingosine-1-phosphate and lymphocyte egress from lymphoid organs.** *Annu Rev Immunol* 2012, **30:**69-94.

39. Chambers I, Colby D, Robertson M, Nichols J, Lee S, Tweedie S, Smith A: **Functional expression cloning of Nanog, a pluripotency sustaining factor in embryonic stem cells.** *Cell* 2003, **113:**643-655.

40. Brown MP, Nosaka T, Tripp RA, Brooks J, van Deursen JM, Brenner MK, Doherty PC, Ihle JN: **Reconstitution of early lymphoid proliferation and immune function in Jak3-deficient mice by interleukin-3.** *Blood* 1999, **94:**1906-1914.

41. Xiao Y, Motomura S, Podack ER: **APRIL (TNFSF13) regulates collagen-induced arthritis, IL-17 production and Th2 response.** *Eur J Immunol* 2008, **38:**3450-3458.

42. Hermann-Kleiter N, Baier G: **NFAT pulls the strings during CD4+ T helper cell effector functions.** *Blood* 2010, **115:**2989-2997.

43. Zhou L, Ivanov, II, Spolski R, Min R, Shenderov K, Egawa T, Levy DE, Leonard WJ, Littman DR: **IL-6 programs T(H)-17 cell differentiation by promoting sequential engagement of the IL-21 and IL-23 pathways.** *Nat Immunol* 2007, **8:**967-974.

44. Crotty S: **T follicular helper cell differentiation, function, and roles in disease.** *Immunity* 2014, **41:**529-542.

45. Liu X, Chen X, Zhong B, Wang A, Wang X, Chu F, Nurieva RI, Yan X, Chen P, van der Flier LG, et al: **Transcription factor achaete-scute homologue 2 initiates follicular T-helper-cell development.** *Nature* 2014, **507:**513-518.

46. Hiyama E, Hiyama K: **Telomere and telomerase in stem cells.** *Br J Cancer* 2007, **96:**1020-1024.

47. Santarlasci V, Maggi L, Capone M, Querci V, Beltrame L, Cavalieri D, D'Aiuto E, Cimaz R, Nebbioso A, Liotta F, et al: **Rarity of human T helper 17 cells is due to retinoic acid**

orphan receptor-dependent mechanisms that limit their expansion. *Immunity* 2012, **36:**201-214.

48. Rivino L, Messi M, Jarrossay D, Lanzavecchia A, Sallusto F, Geginat J: **Chemokine receptor expression identifies Pre-T helper (Th)1, Pre-Th2, and nonpolarized cells among human CD4+ central memory T cells.** *J Exp Med* 2004, **200:**725-735.

49. Sallusto F, Lenig D, Forster R, Lipp M, Lanzavecchia A: **Two subsets of memory T lymphocytes with distinct homing potentials and effector functions.** *Nature* 1999, **401:**708-712.

50. Roederer M, Nozzi JL, Nason MC: **SPICE: exploration and analysis of post-cytometric complex multivariate datasets.** *Cytometry A* 2011, **79:**167-174.

51. Perreau M, Savoye AL, De Crignis E, Corpataux JM, Cubas R, Haddad EK, De Leval L, Graziosi C, Pantaleo G: **Follicular helper T cells serve as the major CD4 T cell compartment for HIV-1 infection, replication, and production.** *J Exp Med* 2013, **210:**143-156.

52. Xu Y, Weatherall C, Bailey M, Alcantara S, De Rose R, Estaquier J, Wilson K, Suzuki K, Corbeil J, Cooper DA, et al: **Simian immunodeficiency virus infects follicular helper CD4 T cells in lymphoid tissues during pathogenic infection of pigtail macaques.** *J Virol* 2013, **87:**3760-3773.

53. Bruner KM, Hosmane NN, Siliciano RF: **Towards an HIV-1 cure: measuring the latent reservoir.** *Trends Microbiol* 2015, **23:**192-203.

54. Zhou YW, Komada Y, Inaba H, Azuma E, Sakurai M: **Down-regulation of Fas-associated phosphatase-1 (FAP-1) in interleukin-2-activated T cells.** *Cell Immunol* 1998, **186:**103-110.

55. Bernier A, Cleret-Buhot A, Zhang Y, Goulet JP, Monteiro P, Gosselin A, DaFonseca S, Wacleche VS, Jenabian MA, Routy JP, et al: **Transcriptional profiling reveals molecular signatures associated with HIV permissiveness in Th1Th17 cells and identifies peroxisome proliferator-activated receptor gamma as an intrinsic negative regulator of viral replication.** *Retrovirology* 2013, **10:**160.

56. Yu KR, Kang KS: **Aging-related genes in mesenchymal stem cells: a mini-review.** *Gerontology* 2013, **59:**557-563.

57. Harris KM, Ramachandran G, Basu S, Rollins S, Mann D, Cross AS: **The IL-23/Th17 axis is involved in the adaptive immune response to Bacillus anthracis in humans.** *Eur J Immunol* 2014, **44:**752-762.

58. Yang XO, Pappu BP, Nurieva R, Akimzhanov A, Kang HS, Chung Y, Ma L, Shah B, Panopoulos AD, Schluns KS, et al: **T helper 17 lineage differentiation is programmed by orphan nuclear receptors ROR alpha and ROR gamma.** *Immunity* 2008, **28:**29-39.

59. Kleinsteuber K, Heesch K, Schattling S, Sander-Juelch C, Mock U, Riecken K, Fehse B, Fleischer B, Jacobsen M: **SOCS3 promotes interleukin-17 expression of human T cells.** *Blood* 2012, **120:**4374-4382.

60. Hastings WD, Anderson DE, Kassam N, Koguchi K, Greenfield EA, Kent SC, Zheng XX, Strom TB, Hafler DA, Kuchroo VK: **TIM-3 is expressed on activated human CD4+ T cells and regulates Th1 and Th17 cytokines.** *Eur J Immunol* 2009, **39:**2492-2501.

61. Bengsch B, Seigel B, Flecken T, Wolanski J, Blum HE, Thimme R: **Human Th17 cells express high levels of enzymatically active dipeptidylpeptidase IV (CD26).** *J Immunol* 2012, **188:**5438-5447.

62. Yosef N, Shalek AK, Gaublomme JT, Jin H, Lee Y, Awasthi A, Wu C, Karwacz K, Xiao S, Jorgolli M, et al: **Dynamic regulatory network controlling TH17 cell differentiation.** *Nature* 2013, **496:**461-468.

63. Doulatov S, Vo LT, Chou SS, Kim PG, Arora N, Li H, Hadland BK, Bernstein ID, Collins JJ, Zon LI, Daley GQ: **Induction of multipotential hematopoietic progenitors from human pluripotent stem cells via respecification of lineage-restricted precursors.** *Cell Stem Cell* 2013, **13:**459-470.

64. Niwa H, Burdon T, Chambers I, Smith A: **Self-renewal of pluripotent embryonic stem cells is mediated via activation of STAT3.** *Genes Dev* 1998, **12:**2048-2060.

65. Pelletier M, Maggi L, Micheletti A, Lazzeri E, Tamassia N, Costantini C, Cosmi L, Lunardi C, Annunziato F, Romagnani S, Cassatella MA: **Evidence for a cross-talk between human neutrophils and Th17 cells.** *Blood* 2009.

66. Spolski R, Leonard WJ: **IL-21 and T follicular helper cells.** *Int Immunol* 2010, **22:**7-12.

67. Liao W, Lin JX, Leonard WJ: **IL-2 family cytokines: new insights into the complex roles of IL-2 as a broad regulator of T helper cell differentiation.** *Curr Opin Immunol* 2011, **23:**598-604.

68. Micci L, Cervasi B, Ende ZS, Iriele RI, Reyes-Aviles E, Vinton C, Else J, Silvestri G, Ansari AA, Villinger F, et al: **Paucity of IL-21-producing CD4(+) T cells is associated with Th17 cell depletion in SIV infection of rhesus macaques.** *Blood* 2012, **120:**3925-3935.

69. Bending D, Newland S, Krejci A, Phillips JM, Bray S, Cooke A: **Epigenetic changes at Il12rb2 and Tbx21 in relation to plasticity behavior of Th17 cells.** *J Immunol* 2011, **186:**3373-3382.

70. Doitsh G, Cavrois M, Lassen KG, Zepeda O, Yang Z, Santiago ML, Hebbeler AM, Greene WC: **Abortive HIV infection mediates CD4 T cell depletion and inflammation in human lymphoid tissue.** *Cell* 2010, **143:**789-801.

71. Cameron PU, Saleh S, Sallmann G, Solomon A, Wightman F, Evans VA, Boucher G, Haddad EK, Sekaly RP, Harman AN, et al: **Establishment of HIV-1 latency in resting CD4+ T cells depends on chemokine-induced changes in the actin cytoskeleton.** *Proc Natl Acad Sci U S A* 2010, **107:**16934-16939.

72. Boswell KL, Paris R, Boritz E, Ambrozak D, Yamamoto T, Darko S, Wloka K, Wheatley A, Narpala S, McDermott A, et al: **Loss of circulating CD4 T cells with B cell helper function during chronic HIV infection.** *PLoS Pathog* 2014, **10:**e1003853.

73. Chomont N, El-Far M, Ancuta P, Trautmann L, Procopio FA, Yassine-Diab B, Boucher G, Boulassel MR, Ghattas G, Brenchley JM, et al: **HIV reservoir size and persistence are driven by T cell survival and homeostatic proliferation.** *Nat Med* 2009, **15:**893-900.

74. Schuetz A, Deleage C, Sereti I, Rerknimitr R, Phanuphak N, Phuang-Ngern Y, Estes JD, Sandler NG, Sukhumvittaya S, Marovich M, et al: **Initiation of ART during early acute HIV infection preserves mucosal Th17 function and reverses HIV-related immune activation.** *PLoS Pathog* 2014, **10:**e1004543.

75. Ancuta P, Liu KY, Misra V, Wacleche VS, Gosselin A, Zhou X, Gabuzda D: **Transcriptional profiling reveals developmental relationship and distinct biological functions of CD16+ and CD16- monocyte subsets.** *BMC Genomics* 2009, **10:**403.

76. Ancuta P, Autissier P, Wurcel A, Zaman T, Stone D, Gabuzda D: **CD16+ Monocyte-Derived Macrophages Activate Resting T Cells for HIV Infection by Producing CCR3 and CCR4 Ligands.** *J Immunol* 2006, **176:**5760-5771.

77. Wacleche VS, Chomont N, Gosselin A, Monteiro P, Goupil M, Kared H, Tremblay C, Bernard N, Boulassel MR, Routy JP, Ancuta P: **The colocalization potential of HIV-specific CD8+ and CD4+ T-cells is mediated by integrin beta7 but not CCR6 and regulated by retinoic acid.** *PLoS One* 2012, **7:**e32964.

78. Goupil M, Trudelle EB, Dugas V, Racicot-Bergeron C, Aumont F, Senechal S, Hanna Z, Jolicoeur P, de Repentigny L: **Macrophage-mediated responses to Candida albicans in mice expressing the human immunodeficiency virus type 1 transgene.** *Infect Immun* 2009, **77:**4136-4149.

Figure Legends

Figure 1: Two new subsets of memory CD4$^+$ T-cells express Th17 lineage markers. (A-D) (A) Memory CD4$^+$ T-cells (CD3$^+$CD4$^+$CD45RA$^-$) isolated from the peripheral blood of HIV-uninfected individuals were analyzed for their differential expression of CCR6, CCR4, and CXCR3. CCR6$^+$ subsets included: CCR4$^+$CXCR3$^-$ (Th17), CCR4$^-$CXCR3$^-$ (double positive, CCR6$^+$DP), CCR4$^+$CXCR3$^+$ (double negative, CCR6$^+$DN), and CCR4$^-$CXCR3$^+$ (Th1Th17). CCR6$^-$ subsets included: CCR4$^+$CXCR3$^-$ (Th2), CCR4$^+$CXCR3$^+$ (CCR6$^-$DP), CCR4$^-$CXCR3$^-$ (CCR6$^-$DN) and CCR4$^-$CXCR3$^+$ (Th1). Shown is the frequency of CCR6$^+$ and CCR6$^-$ subsets (**B**; n=30) and their expression of CD161 (**C**; n=8). Each symbol represents a distinct subject. Paired t-Test *p*-values are indicated on the figures. Horizontal bars indicate median values. **(D)** Shown are median frequencies of central (CM, CCR7$^+$CD27$^+$), transitional (TM, CCR7$^-$CD27$^+$) and effector (EM, CCR7$^-$CD27$^-$) memory cells per CCR6$^+$ subset (n=10). **(E-G)** FACS-sorted memory subsets (S1 Figure) were stimulated *via* CD3/CD28 for 4 days. **(E)** The production of the lineage-specific cytokines IL-17A, IFN-γ, and IL-5 was quantified by ELISA. Shown are results (mean±SEM) on matched Th17, Th1Th17, CCR6$^+$DN, CCR6$^+$DP, and CCR6- (n=3-7). Paired t-Test *p*-values are indicated on the figures. **(F)** Transcriptional profiling were generated using the HumanHT-12 v4 Expression BeadChip; (Illumina)The heat map depicts differential expression of well-established Th17 and Th1 transcripts (identified as being up/down regulated in Th17 *versus* CCR6$^-$DN, p-value<0.05, fold change cut-off 1.3) in matched CCR6$^-$DN vs.CCR6$^+$DN, CCR6$^+$DP and Th17 (n=4-6; up-regulated genes in red; down-regulated genes in blue).

Figure 2: CCR6$^+$DN and CCR6$^+$DP cells express unique transcriptional signatures. Genome-wide transcriptional profiling was performed on sorted matched Th17, CCR6$^+$DN, and CCR6$^+$DP (n=4-6) isolated from the peripheral blood of HIV-uninfected individuals, as in Figure 1F. Shown are (**A**) volcano representation of differentially expressed probe sets in CCR6$^+$DN *vs.* Th17, CCR6$^+$DP *vs.* Th17, and CCR6$^+$DN *vs.* CCR6$^+$DP (depicted in red: p-values<0.05 and fold change cut-off 1.3). (**B-D**) For the same contrasts, shown are heat maps depicting top modulated pathways identified using *Ingenuity Pathway Analysis* (IPA) **(B)** and *Gene Set Variation Analysis* (GSVA) canonical pathways (**C**) and biological functions (**D**). Genes up and down regulated in different subsets are represented in red and blue, respectively. (**E**) Expression of STAT3, BCL6, LEF1, and TERC mRNA was quantified by real-time RT-PCR (mean±SEM; n=3-4). Paired t-Test *p*-values are indicated on the figures.

Figure 3: CCR6$^+$DN cells are a major source of IL-17F, IL-8, and IL-21. Culture supernatants harvested from Th17, Th1Th17, and CCR6$^+$DN (stimulated as in Figure 1E) isolated from the peripheral blood of HIV-uninfected individuals were screened for the expression of 34 T-helper lineage-specific cytokines using the Human Th1/Th2/Th17 Antibody Array C series (RayBiotec). **(A-B)** Shown are results from one experiment with matched Th17 *vs.* CCR6$^+$DN and Th1Th17 *vs.* CCR6$^+$DN subsets: membrane blot (**left panels**) and relative density quantification (**right panels**). Results are representative of experiments performed with cells from two different donors: (**C-D**) Levels of IL-17F, IL-22, CCL20, IL-10, IL-13, TNF-α, IL-8, and IL-21 were quantified by ELISA. Shown are results on matched Th17, Th1Th17, CCR6$^+$DN, CCR6$^+$DP, and CCR6$^-$ samples from different individuals (n=3-7, mean±SEM). Paired t-Test *p*-values are indicated in the graphs.

Figure 4: CCR6$^+$DN proliferate in response to *C.albicans* but not CMV. (**A**) FACS-sorted T-cell subsets isolated from the peripheral blood of HIV-uninfected individuals were stained with CFSE, co-cultured with antigen-loaded autologous monocyte-derived dendritic cells (MDDC), and analyzed for their ability to proliferate (CFSE^{low}) and produce cytokines. (**B**) Shown is the frequency of T-cells proliferating in response to *C.albicans* hyphae, CMV, or SEB at day 5 post co-culture. **(C)** Shown is the frequency of cytokine-expressing T-cells proliferating in response to *C. albicans* within each subset. (**D-F**) *C. albicans*-specific T-cells were further analyzed for the co-expression of IL-17A with IFN-γ or TNF-α. **(D)** Results are from one donor representative of results obtained with matched subsets from four different donors. **(E-F)** Shown is the frequency and MFI of *C. albicans*-specific T-cells expressing IL-17A either alone (IL-17A$^+$IFN-γ$^-$) (**E**) or in combination with IFN-γ (IL-17A$^+$IFN-γ$^+$) (**F**). **(B-F)** The positivity gates were defined based on FMO controls. (**B-C** and **E-F**) Shown are results (mean±SEM) on matched samples from n=4 different. Paired t-Test *p*-values are indicated in the figures. *ND, not determined*

Figure 5: Lineage commitment *versus* plasticity of the four CM CCR6$^+$ subsets *in vitro*. FACS-sorted CM (CD45RA$^-$CCR7$^+$) subsets isolated from the peripheral blood of HIV-uninfected individuals were analyzed for the expression of lineage-specific cytokines upon Th17/Th1-polarization *in vitro*. (**A**) CM subsets were stimulated *via* CD3/CD28 and cultured under Th17- (IL-1β, IL-6, and IL-23, and anti-IL-4 and anti-IFN-γ Abs) and Th1-polarizing conditions (IL-12 and anti-IL-4 Abs) for 4 and 14 days. Cells were stimulated with PMA and Ionomycin in the presence of Brefeldin A for 16 hours. Intracellular staining was performed with cytokine-specific Abs. (**B-C**) Shown are statistical analyses of cytokines expressed by the distinct CM subsets cultured for 4 (**B**) or 14 days (**C**) under Th17- (black bars) and Th1-polarizing conditions (grey bars). Results

(mean±SEM) were generated with matches samples from n=3 different donors. Paired t-Test *p*-values are indicated on the figures (Th17- *vs.* Th1-polarization).

Figure 6: CCR6$^+$DN distinguish from the other Th17-subsets by superior frequency/counts in CI on ART individuals. (**A**) PBMCs from CI on ART individuals (n=20; Table S2) were stained as in Figure 1. Shown is the relative frequency of the four CCR6$^+$ subsets in CI on ART individuals. Paired t-Test *p*-values are indicated on the figures. Horizontal bars indicate median values. **(B)** Shown are median frequencies of CM, TM, and EM within each CCR6$^+$ subsets from CI on ART (n=10). Shown is the frequency (**C**) and counts (**D**) of the four CCR6$^+$ subsets in CI on ART *vs.* uninfected individuals. Cell counts were calculated taking into account their frequency within the total CD4$^+$ T-cell fraction. (**E**) The dynamics of CCR6$^+$ subset counts were investigated longitudinally in n=5 HIV-infected individuals from the Montreal HIV Primary infection cohort (Table S3), in relationship with plasma viral load, before and after ART initiation (grey). (**F**) Shown are statistical analysis for differences in cell counts between the four CCR6$^+$ subsets (n=5 HIV-infected individuals) using Friedman test and the post-test Dunn's multiple comparison and Wilcoxon t-test.

Figure 7: CCR6$^+$DN are predominant in lymph nodes of HIV-infected individuals receiving ART. (A-B) Matched PBMCs and inguinal lymph node cells from three CI on ART individuals (CI 36, CI 37, CI 38; S2 Table) were stained with a cocktail of fluorochrome-conjugated CD3, CD4, CD45RA, CCR4, CXCR3, CCR6, and CCR7 Abs. A viability staining was used to exclude dead cells. Viable memory CD4$^+$ T-cells (CD3$^+$CD4$^+$CD45RA$^-$) expressing CCR6 were analyzed for their differential expression of CCR4 and CXCR3. The four CCR6$^+$ subsets including Th17, CCR6$^+$DP,

CCR6$^+$DN, and Th1Th17 were identified in both PBMCs and cells from lymph nodes. **(A)** Shown is the phenotype of PBMCs (upper panels) and lymph node cells (lower panels) in one representative donor. **(B)** Shown are statistical analysis of the frequency of CCR6$^+$ subsets in the lymph node (n=3). Paired t-Test *p*-values are indicated on the figures.

Figure 8: CCR6$^+$DN and CCR6$^+$DP subsets are permissive to HIV infection *in vitro*. (A) PBMCs from healthy individuals were stained with a cocktail of fluorochrome-conjugated CD3, CD4, CD45RA, CCR4, CXCR3, CCR6, and CCR5 or CXCR4 Abs. The gating strategy for the identification of distinct CCR6$^+$ and CCR6$^-$ T-cell subsets was designed as in Figure 1A. The frequency of cells expressing CCR5 (left panel) and CXCR4 (right panel) was analyzed within the Th17, Th1Th17, CCR6$^+$DN and CCR6$^+$DP subsets. Paired t-Test *p*-values are indicated on the figures. Horizontal bars indicate median values. (**B**) Memory CCR6$^+$ subsets from three HIV-uninfected subjects were sorted and stimulated *via* CD3/CD28 for 4 days, as in Figure 1E. Cells were exposed to a highly infectious R5 strain HIV-ADA8. Levels of HIV-p24 were quantified by ELISA in cell supernatants at day 3 posy-infection.

Figure 9: CCR6$^+$DN carry replication competent HIV-DNA. (A-B) The four memory CCR6$^+$ subsets as well as Th1 cells from PBMCs of chronically infected receiving viral suppressive ART (CI on ART) individuals were sorted by FACS. (**A**) Levels of integrated HIV-DNA were quantified by nested real-time PCR in sorted cells *ex vivo* (mean±SD of triplicate wells; n=4 CI on ART individuals). (**B-C**) FACS-sorted memory subsets were stimulated *via* CD3/CD28 and cultured as described in S6A Figure legend for up to 14 days. (**B**) HIV-RNA levels were quantified by real-time RT-PCR in culture supernatant of cells stimulated *via* CD3/CD28 for 4 days (n=4 CI on ART

individuals). (**C-D**) At day 13, cells were stimulated with PMA and Ionomycin in the presence of Brefeldin A for 6 hours. Intracellular staining was performed with cytokine-specific Abs and HIV-p24. (**C**) Shown are flow cytometry dot plots illustrating the co-expression of IL-17A and HIV-p24 (n=3). (**D**) Shown are pie charts representations generated with the SPICE software illustrating the poly-functional profile of HIV-p24^{+} CCR6^{+}DN cells; all possible combinations of one (blue), two (green), three (orange) and four (yellow) or no (purple) cytokines are depicted (n=3 CI on ART individuals). (**E**) At day 13, CCR6^{+}DN subsets were stained with CFSE and cultured for 5 additional days in the presence of either IL-2 (5 ng/ml) or CD3/CD28 (1 µg/ml). Cells expressing or not intracellular HIV-p24 were then analyzed for their ability to proliferate (CFSE^{low}).

Figure 10: New insights into the heterogeneity of human Th17 cells at homeostasis and during ART-controlled HIV-1 infection. In this work we identified two new subsets of CCR6^{+} T-cells, CCR6^{+}DN/CCR4^{-}CXCR3^{-} and CCR6^{+}DP/CCR4^{+}CXCR3^{+}, that share Th17 features with the previously described Th17/CCR4^{+}CXCR3^{-} and Th1Th17/CCR4^{-}CXCR3^{+} [5]. Despite these similarities, CCR6^{+}DN distinguished from the other three subsets by superior their ability to produce Th17 effector cytokines (*e.g.,* IL-17F, IL-8, and IL-21) and their predominant frequency/counts in the blood and lymph nodes HIV-infected individuals receiving ART. Finally, we demonstrate that CCR6^{+}DN harbor replication-competent HIV-DNA. Thus, we reveal the existence in humans of four Th17-polarized CCR6^{+} subsets that represent distinct stages of Th17 differentiation, with CCR6^{+}DN being the most predominant and contributing to HIV reservoir persistence under ART.

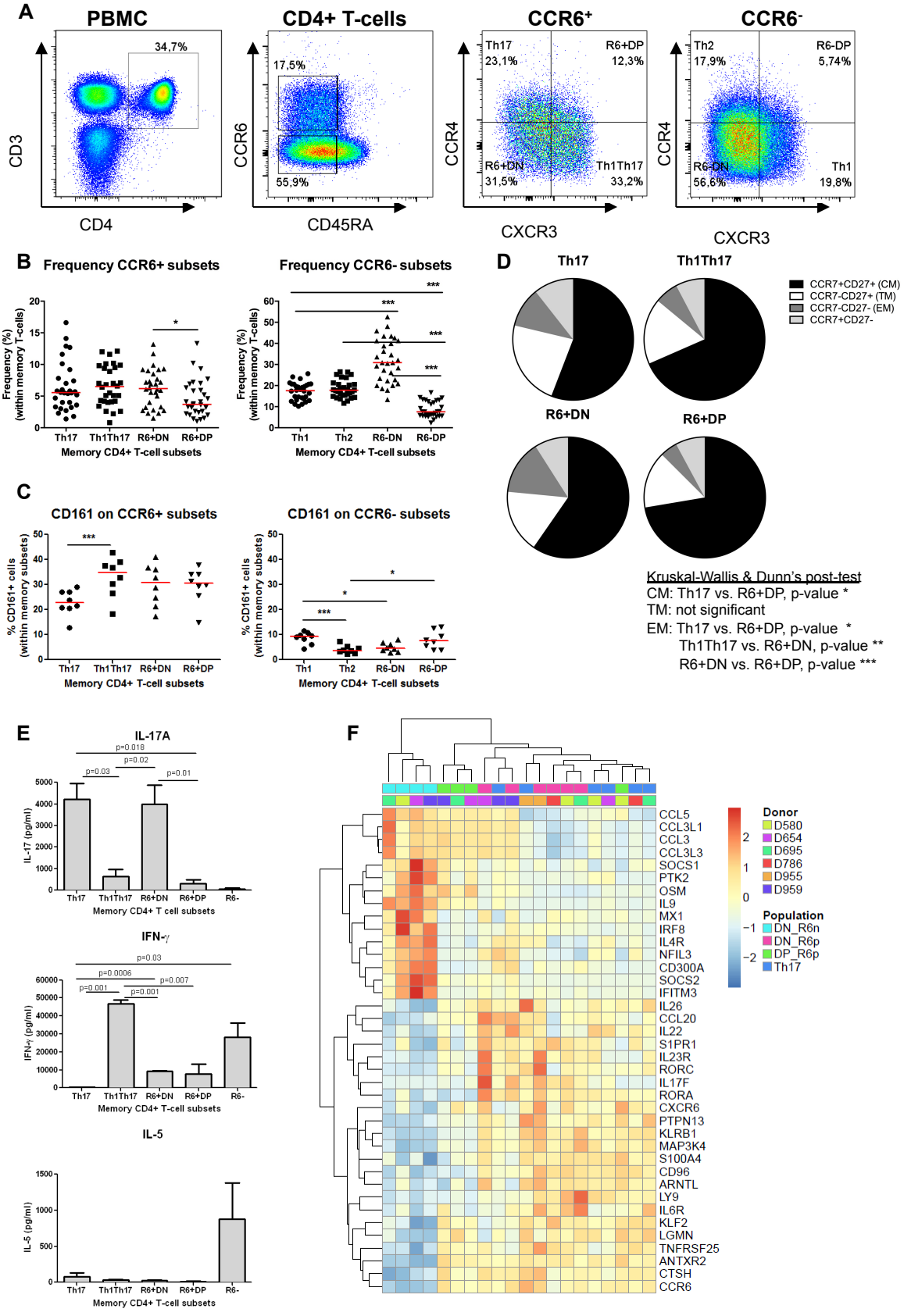

Wacleche et al., Figure 1

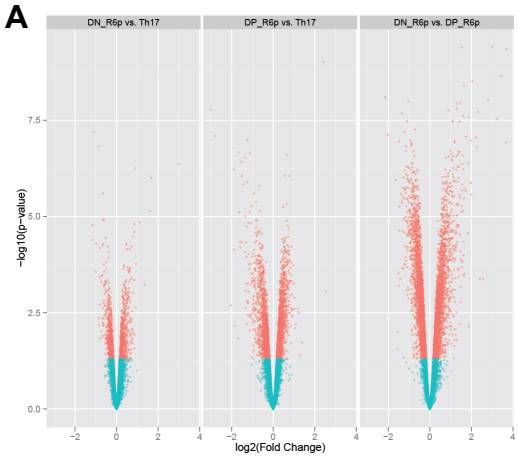

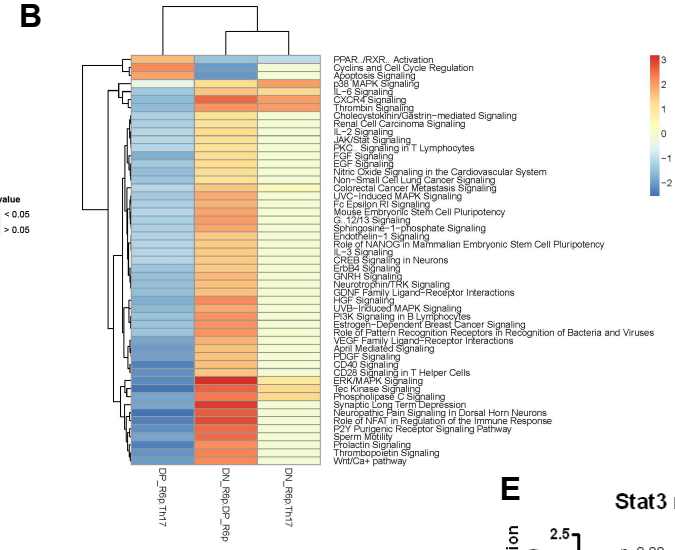

C: Canonical pathways (C2)

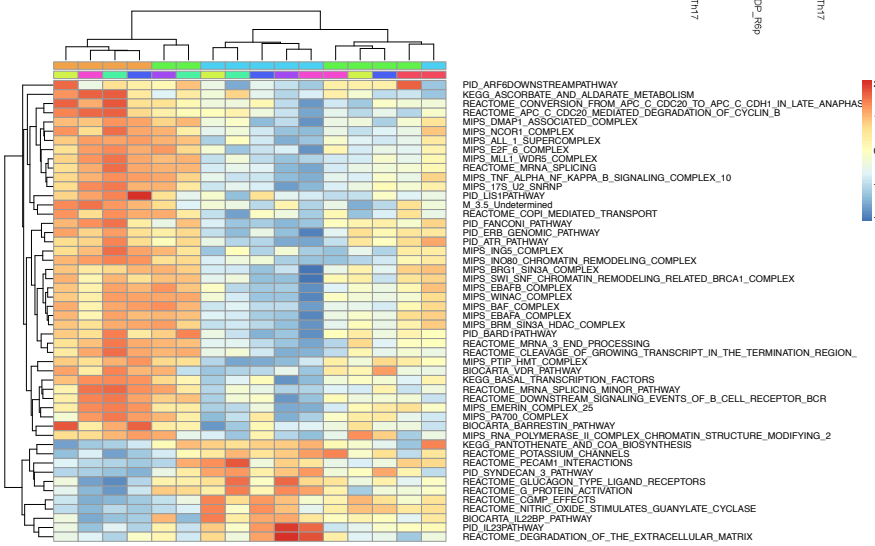

D: Biological Processes (C5)

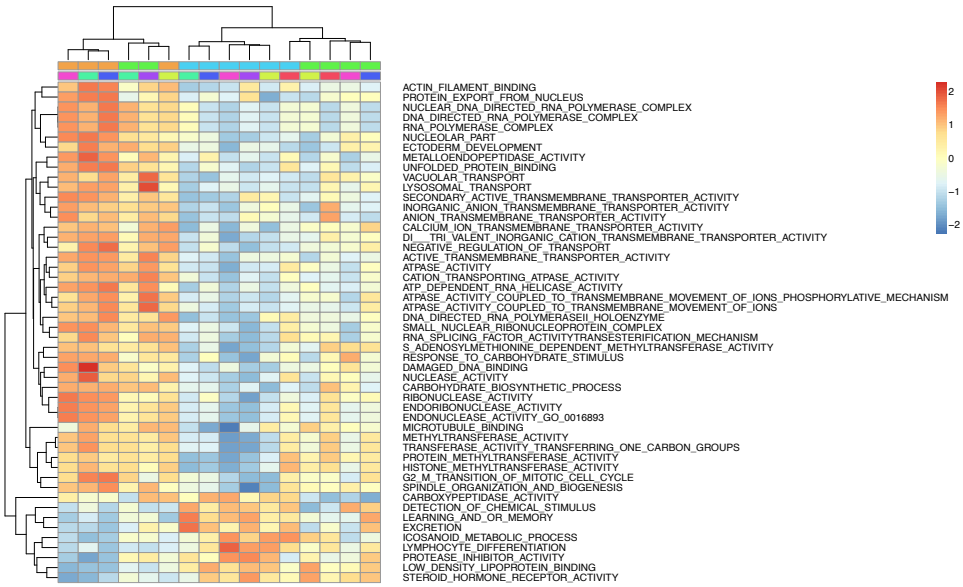

E

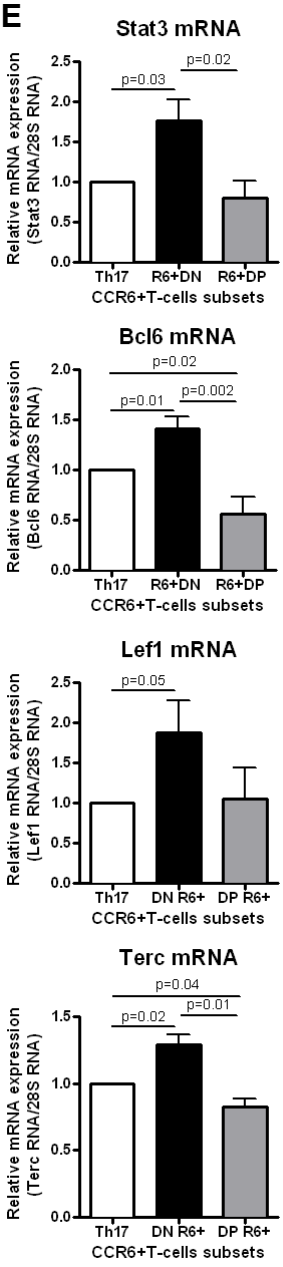

Wacleche et al., Figure 2

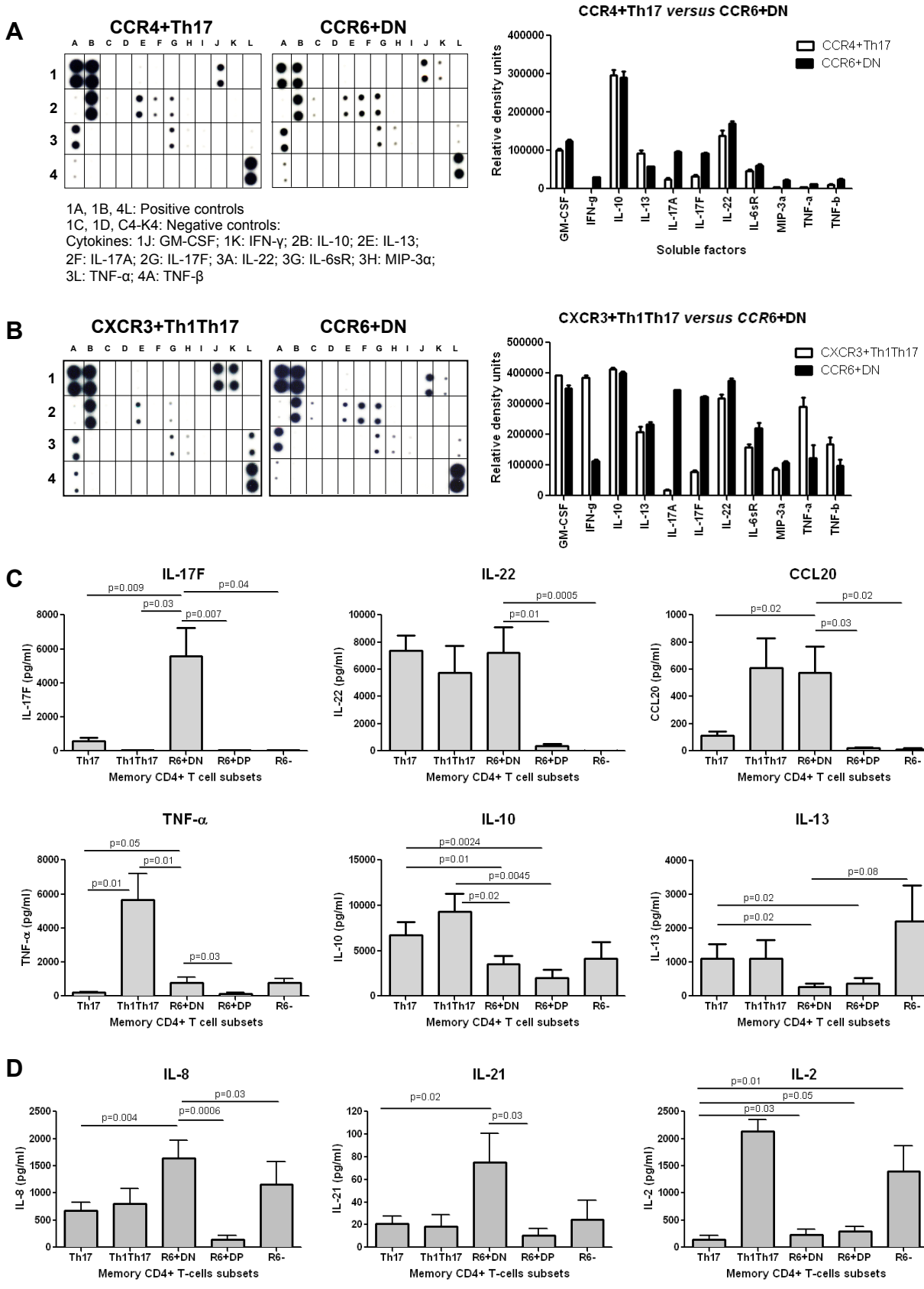

Wacleche et al., Figure 3

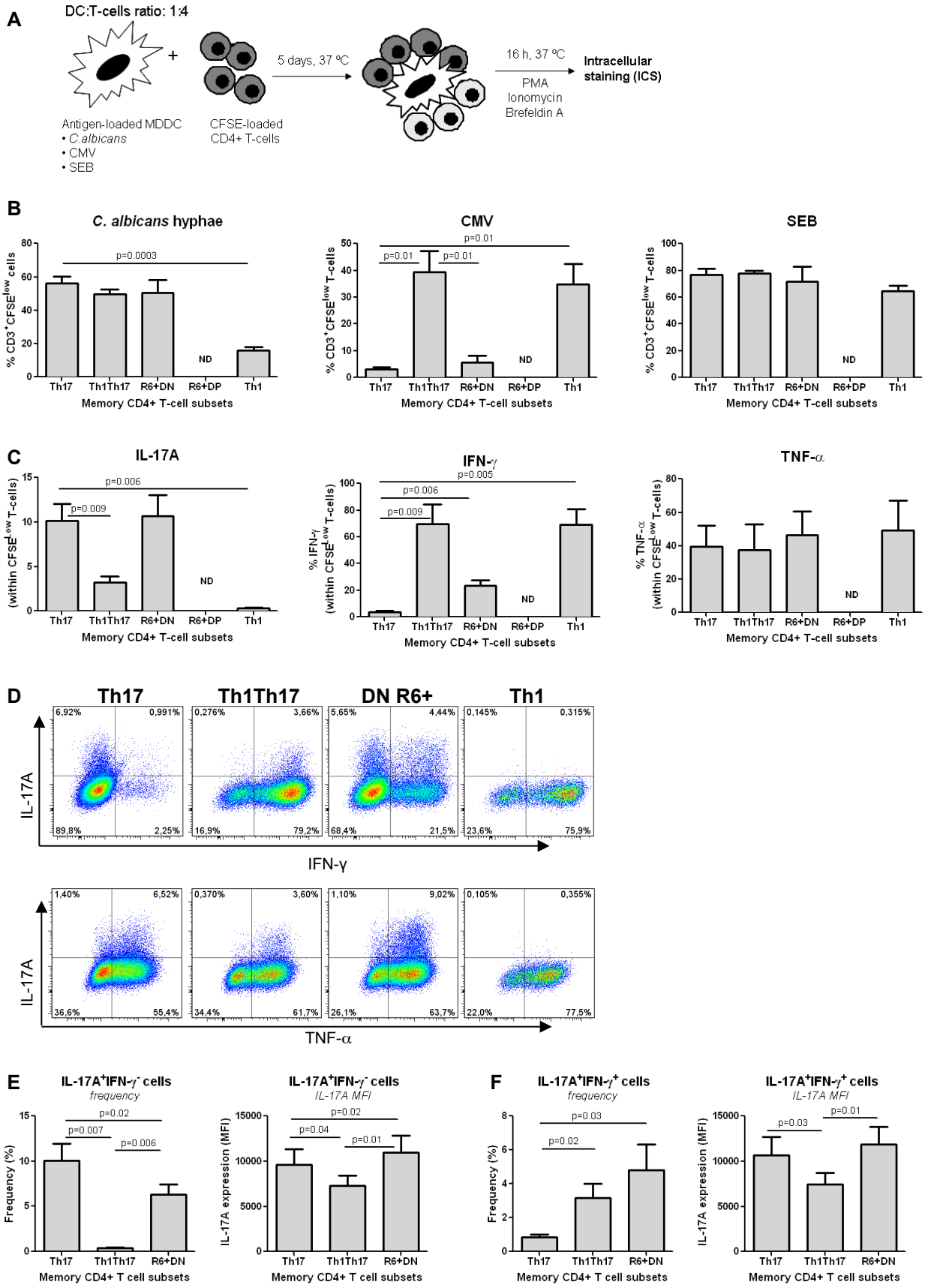

Wacleche et al., Figure 4

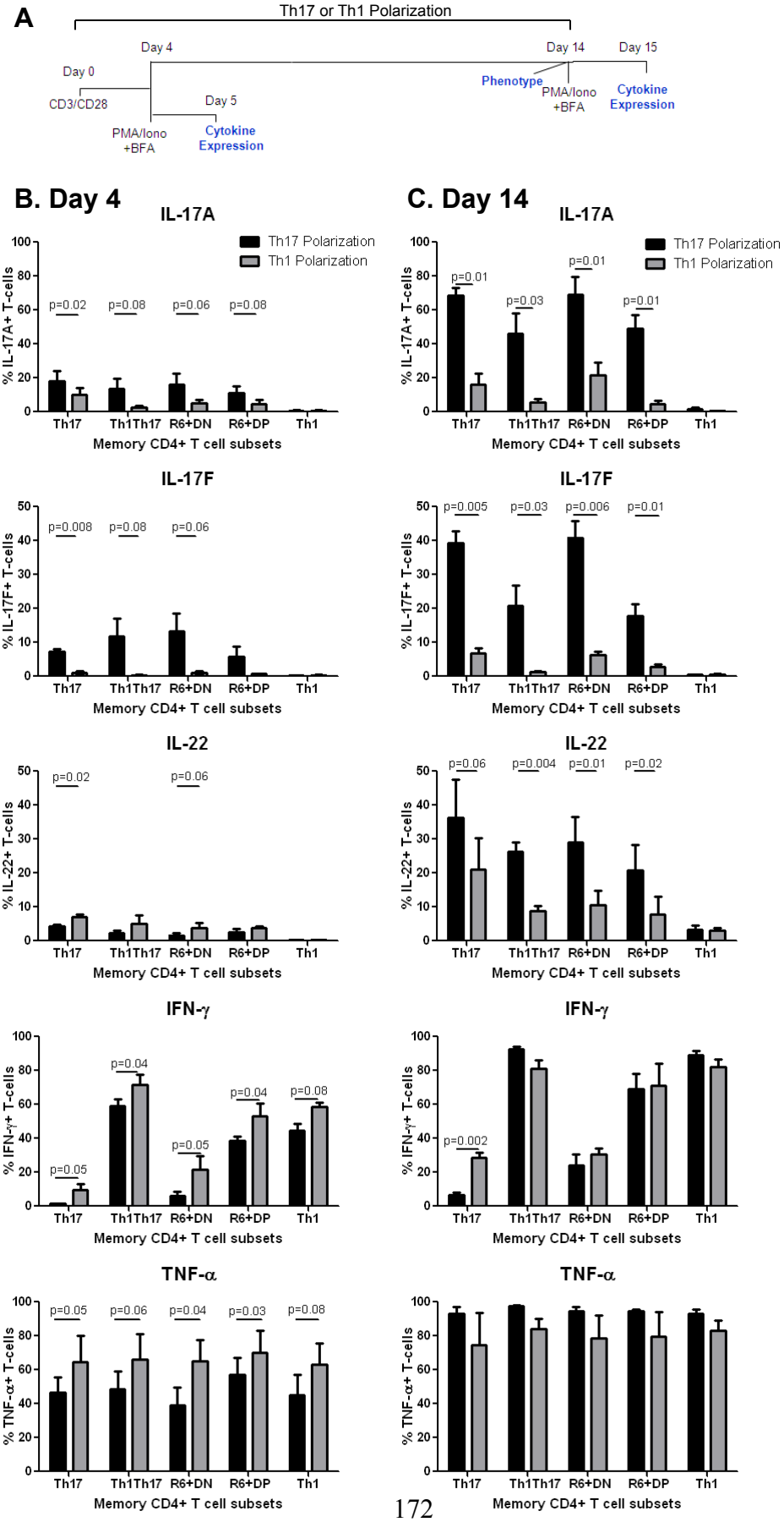

Wacleche et al., Figure 5

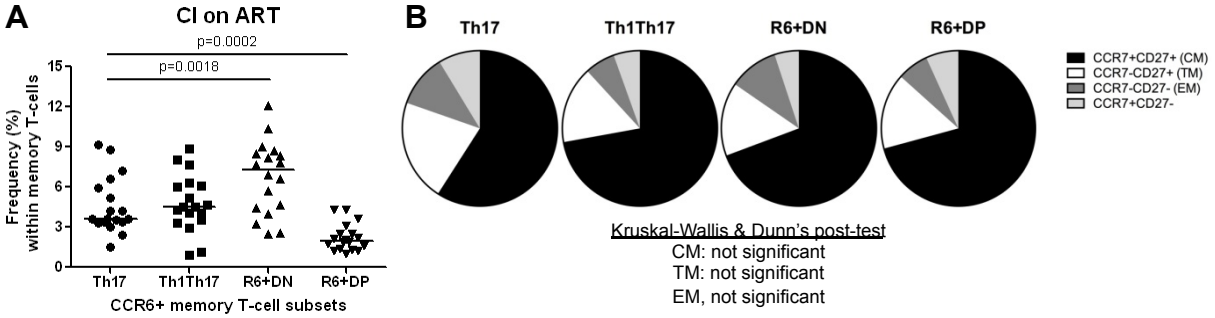

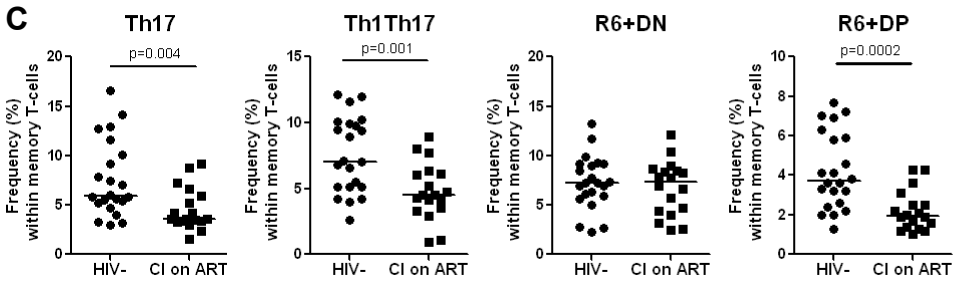

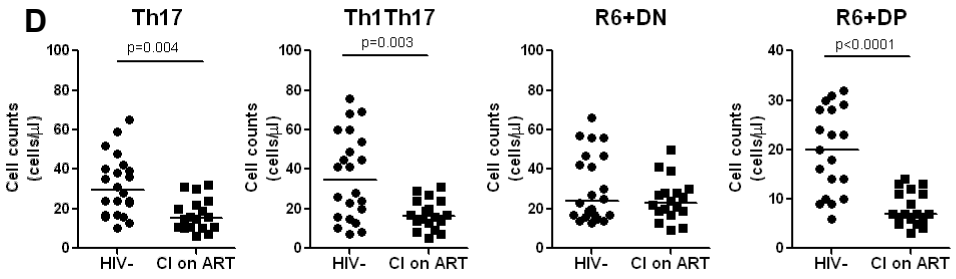

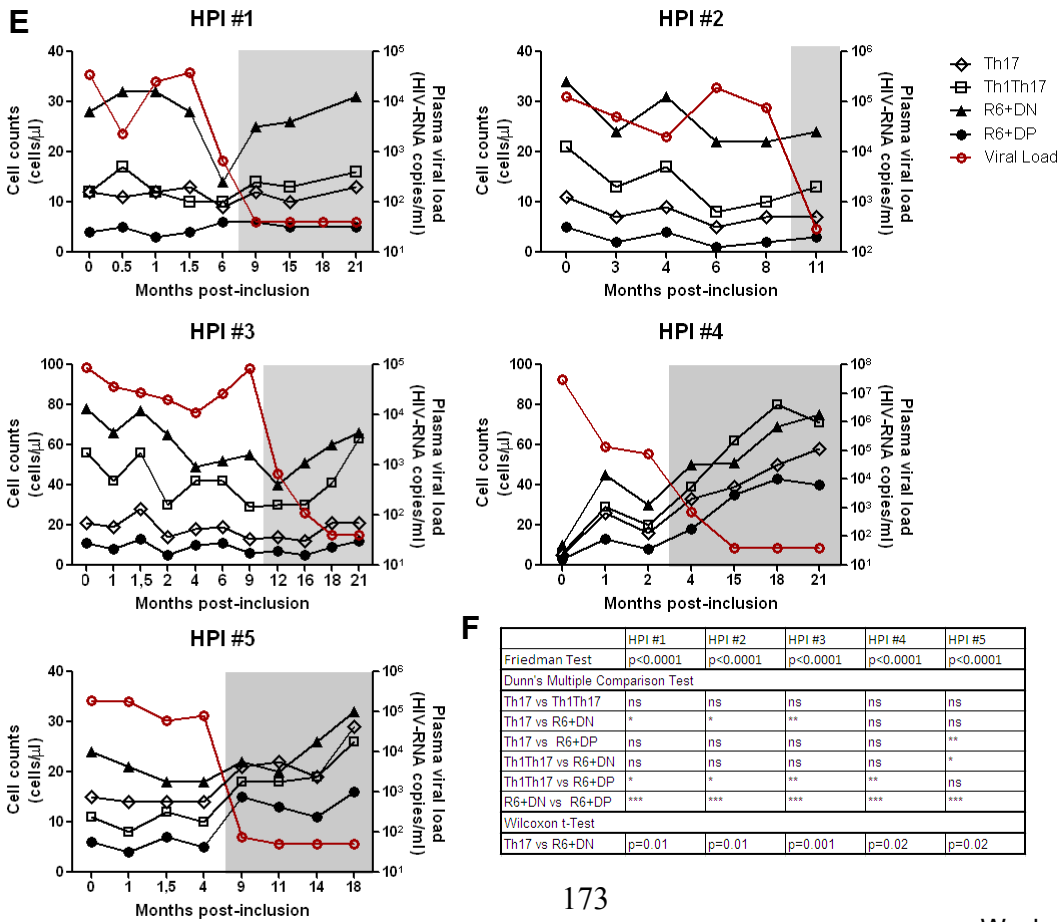

F

	HPI #1	HPI #2	HPI #3	HPI #4	HPI #5
Friedman Test	p<0.0001	p<0.0001	p<0.0001	p<0.0001	p<0.0001
Dunn's Multiple Comparison Test					
Th17 vs Th1Th17	ns	ns	ns	ns	ns
Th17 vs R6+DN	*	*	**	ns	ns
Th17 vs R6+DP	ns	ns	ns	ns	**
Th1Th17 vs R6+DN	ns	ns	ns	ns	*
Th1Th17 vs R6+DP	*	*	**	**	ns
R6+DN vs R6+DP	***	***	***	***	***
Wilcoxon t-Test					
Th17 vs R6+DN	p=0.01	p=0.01	p=0.001	p=0.02	p=0.02

Wacleche et al., Figure 6

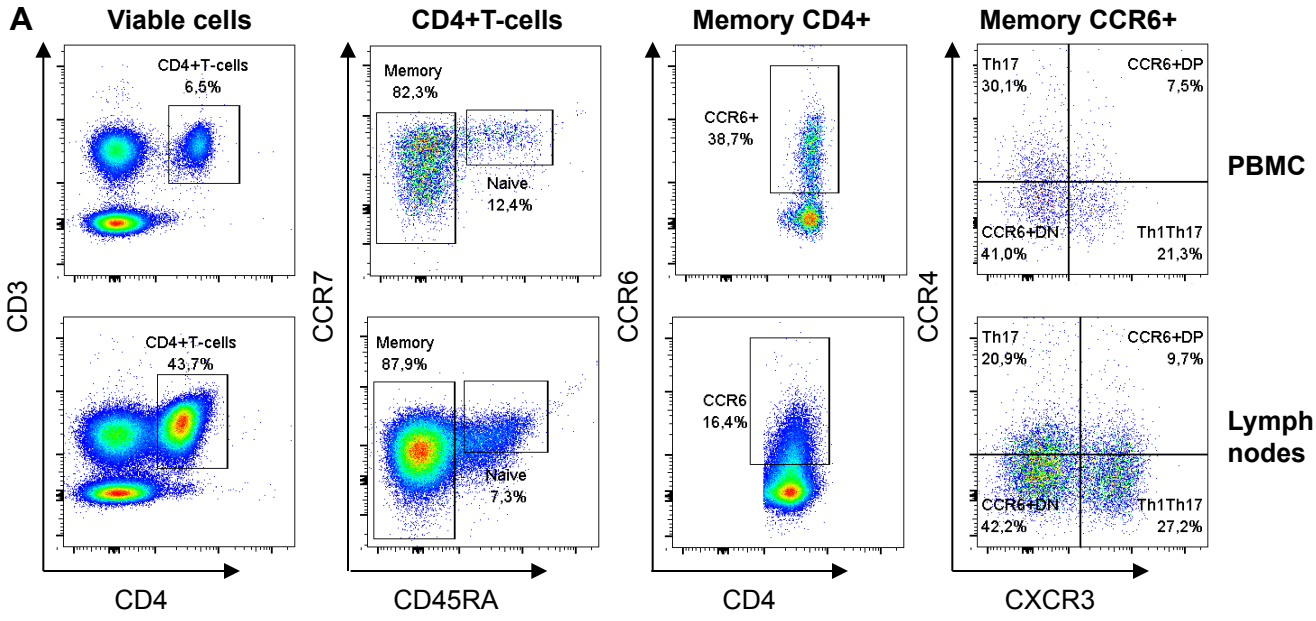

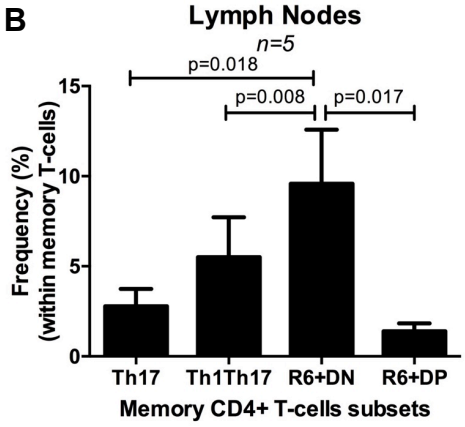

Wacleche *et al.*, Figure 7

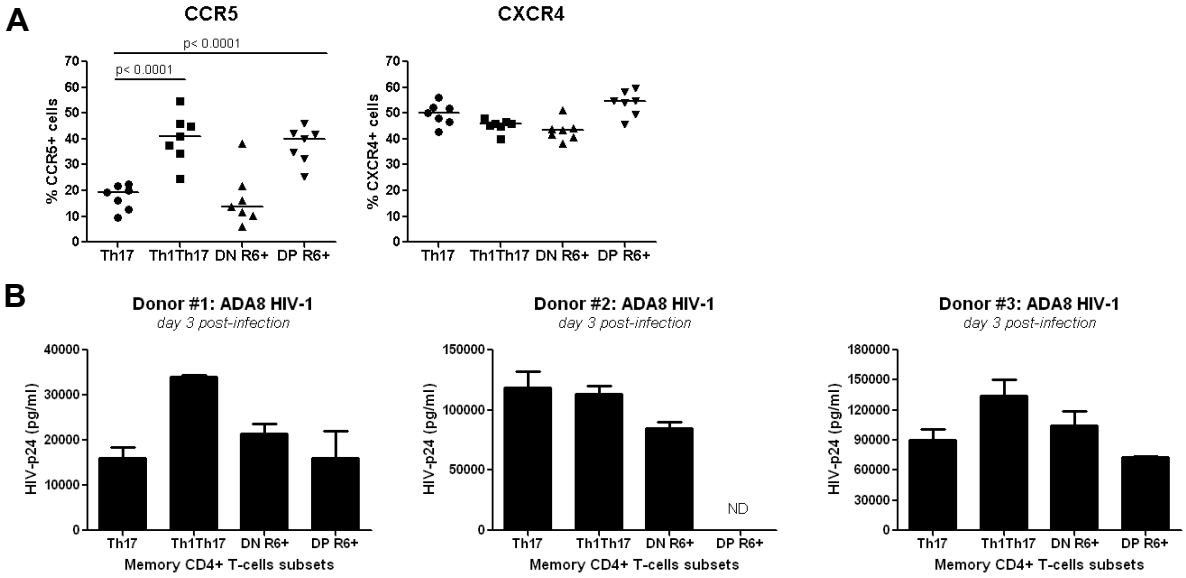

Wacleche *et al.*, Figure 8

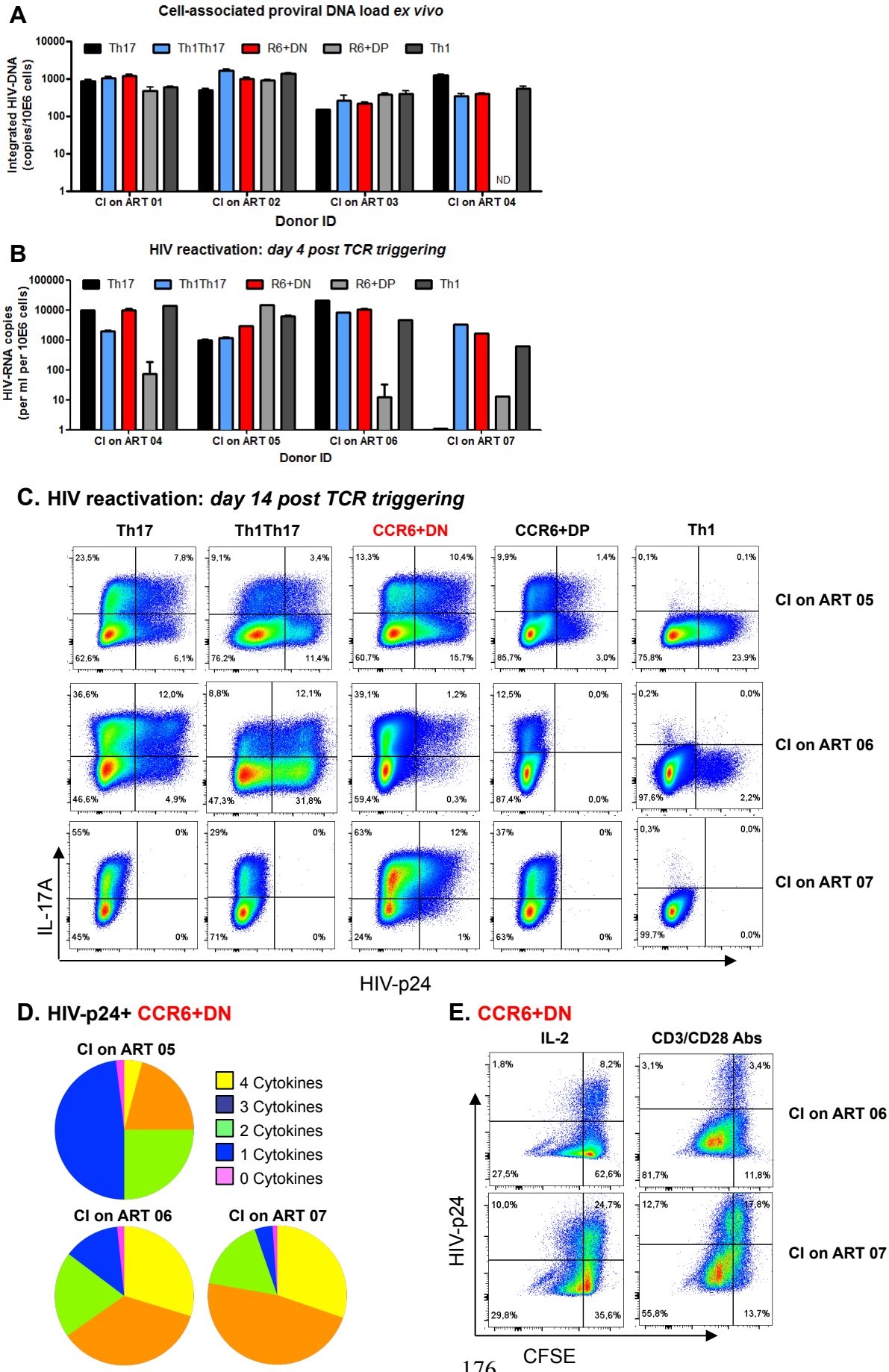

Wacleche *et al.*, Figure 9

Four distinct Th17 subsets in humans

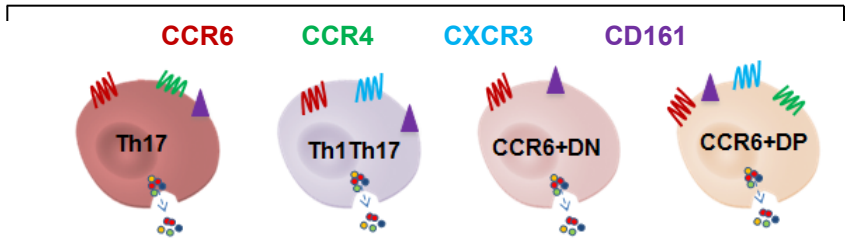

Functional features	Th17	Th1Th17	CCR6+DN	CCR6+DP
IL-17A	+++	+	+++	+
IL-17F	+	+/-	+++	+/-
IL-22	+++	+++	+++	+/-
IL-21	+	+	+++	+
IL-8	++	++	+++	+
CCL20	+	++	++	+/-
IFN-γ	-	+++	+	++
TNF-α	+/-	+++	+	+/-
IL-10	+++	+++	+	+
IL-13	+	+	+/-	+/-
Linage flexibility	Yes	Yes	Yes	Yes
Depleted in HIV-infected individuals	Yes	Yes	No	Yes
Frequency in the lymph nodes of CI on ART individuals	+	++	+++	+/-
Permissive to HIV infection *in vitro* and *in vivo*	Yes	Yes	Yes	Yes
Replication competent HIV reservoirs in CI on ART	Donor-dependent	Donor-dependent	Yes	Donor-dependent

Wacleche et al. Figure 10

Suppemental Table 1: Transcripts differentially expressed by CCR6+DP or Th17 vs. CCR6+DN cells

adjusted p-value <0,05
upregulated transcripts FC cut-off 1.3
downregulated transcripts FC cut-off 1.3

	Adjusted p-value		Fold change (FC)		
SYMBOL	Th17 vs. CCR6+DN	CCR6+DP vs. CCR6+DN	Th17 vs. CCR6+DN	CCR6+DP vs. CCR6+DN	ProbeID
CXCR3	0,59	1,28E-05	-1,21	4,43	4390202
LMNA	0,03	3,62E-05	2,21	4,04	6020424
RRS1	0,24	1,44E-04	1,56	3,10	4120437
CCL4L2	0,92	3,25E-02	1,11	2,90	2970575
OSM	0,69	2,92E-03	1,24	2,84	7560593
IL3	0,78	4,68E-03	1,19	2,78	6040332
SDF2L1	0,15	4,26E-05	1,52	2,78	3120079
CTPS	0,37	6,01E-04	1,44	2,75	6370273
SRM	0,32	2,92E-04	1,45	2,74	5570088
CSF2	0,44	3,63E-03	1,47	2,65	2750196
FER1L3	0,21	2,00E-04	1,52	2,60	3170273
LMNA	0,07	1,67E-05	1,51	2,53	2630768
CCDC86	0,44	2,34E-04	1,28	2,52	650300
BOP1	0,30	2,61E-04	1,42	2,51	1660435
CD70	0,64	2,36E-03	1,23	2,51	4220068
HNRNPAB	0,20	1,68E-04	1,49	2,47	1820398
PROK2	0,21	6,11E-04	1,60	2,47	1030463
GPATCH4	0,37	2,14E-04	1,33	2,44	1820544
ODC1	0,30	4,34E-04	1,44	2,42	4070017
ITGB7	0,03	1,34E-04	1,75	2,39	3990379
IL9	0,57	2,38E-03	1,27	2,38	2120167
HNRNPAB	0,24	6,34E-04	1,54	2,35	3370487
HNRNPAB	0,27	1,69E-04	1,39	2,34	5810440
TGFBR3	0,00	3,14E-05	2,11	2,33	3190379
HSPC111	0,59	1,99E-03	1,24	2,33	380370
DPH2	0,35	2,23E-04	1,32	2,30	6040112
PSME3	0,30	4,10E-04	1,40	2,30	1450064
MSC	0,16	2,06E-03	1,76	2,29	7510377
EIF4G1	0,30	1,06E-04	1,32	2,28	3930189
NOL6	0,37	1,76E-04	1,29	2,28	3180706
HSPH1	0,24	1,04E-03	1,54	2,27	160598
PHB	0,33	4,62E-04	1,36	2,25	4280204

CCL1	0,29	1,56E-03	1,51	2,23	1030204
MB	0,03	5,80E-05	1,60	2,23	4920561
PDCD2L	0,31	3,97E-04	1,37	2,23	4590424
NETO2	0,31	1,90E-04	1,32	2,21	1580161
SLC20A1	0,28	1,69E-04	1,35	2,21	6420731
SLC29A1	0,31	1,19E-04	1,30	2,20	5910424
KIAA1618	0,53	1,76E-03	1,25	2,19	7400743
ZMPSTE24	0,34	2,89E-04	1,31	2,18	5390543
SLC2A8	0,10	4,81E-05	1,45	2,18	5870326
LOC642233	0,27	5,55E-03	1,65	2,18	4200369
PPRC1	0,30	9,99E-05	1,29	2,17	7160100
RPP40	0,31	6,95E-04	1,38	2,14	160204
NOP2	0,31	2,23E-04	1,32	2,13	540221
PUS1	0,20	1,68E-04	1,40	2,13	60092
NOP16	0,45	2,26E-03	1,31	2,13	4780561
LOC727761	0,29	4,62E-04	1,38	2,13	6110470
CDC25A	0,58	6,55E-04	1,18	2,12	2480341
CCR4	0,00	1,85E-05	1,82	2,11	7570154
PSMD1	0,30	1,22E-03	1,43	2,11	5090647
PTGES2	0,25	3,43E-04	1,39	2,11	6110161
SLC5A6	0,71	1,05E-03	1,14	2,11	5050040
IL9	0,73	6,71E-03	1,17	2,10	4180600
EIF4G1	0,39	1,39E-04	1,23	2,10	150577
C16ORF59	0,31	1,26E-04	1,28	2,09	6560725
TOMM40	0,26	1,43E-04	1,32	2,08	1740494
RRP12	0,48	4,80E-04	1,21	2,08	3460687
PSME3	0,40	1,10E-03	1,31	2,08	2470427
PRELID1	0,42	4,57E-04	1,25	2,08	6220379
RPL6	0,56	4,96E-03	1,25	2,07	2630561
GRWD1	0,41	2,31E-04	1,23	2,07	670554
ATP2A2	0,35	9,99E-05	1,24	2,06	770079
UHRF1	0,37	6,82E-04	1,31	2,05	2940110
NOP2	0,43	5,48E-04	1,24	2,05	6960538
ISG20L1	0,32	1,28E-05	1,19	2,04	4480288
LOC644846	0,29	7,70E-03	1,59	2,04	4670615
PTGES2	0,40	5,22E-04	1,26	2,03	870113
HLA-DQA1	0,07	5,48E-03	2,00	2,02	780403
AIMP2	0,27	4,04E-04	1,36	2,02	6960056
SYNCRIP	0,33	6,11E-04	1,32	2,02	4880500
C6ORF153	0,27	1,44E-04	1,30	2,01	3130577

ADCY3	0,12	1,69E-04	1,45	2,01	3800050
PRMT1	0,29	5,98E-04	1,36	2,01	3460669
PGAM5	0,34	2,60E-04	1,27	2,01	1050021
MRPL12	0,44	6,39E-04	1,23	2,00	5080546
PGAM5	0,32	2,11E-04	1,27	2,00	2940274
HOMER2	0,09	7,09E-04	1,64	2,00	3850630
SLC35B1	0,29	1,44E-04	1,28	1,99	5290692
TMEM109	0,37	3,26E-04	1,25	1,99	6130193
C20ORF24	0,23	1,49E-04	1,33	1,98	4560554
SLC39A14	0,40	1,04E-04	1,19	1,98	2630563
METTL1	0,38	6,55E-04	1,28	1,97	650348
ATP2A2	0,35	3,36E-04	1,27	1,96	5810189
DNLZ	0,46	1,51E-03	1,25	1,95	3830605
SLC39A3	0,38	3,70E-04	1,24	1,94	4560671
RRM2	0,37	3,25E-04	1,24	1,94	510731
FAM43A	0,41	9,28E-04	1,26	1,93	1690630
LOC727803	0,24	3,40E-04	1,35	1,93	5290546
CD320	0,37	4,62E-04	1,26	1,93	2340327
PRMT1	0,45	9,11E-04	1,23	1,93	6400138
C12ORF5	0,41	1,21E-03	1,27	1,93	2350762
ATAD3A	0,64	6,19E-04	1,13	1,93	4150086
MAPK6	0,17	5,97E-04	1,45	1,93	7160348
LOC100133328	0,72	2,40E-03	1,13	1,93	7210544
SIGMAR1	0,32	5,83E-04	1,31	1,92	50553
GPR172A	0,44	3,97E-04	1,20	1,92	2140528
PAK1IP1	0,50	1,66E-03	1,22	1,92	4280253
NIPA2	0,21	5,98E-04	1,41	1,92	4670020
NOLC1	0,54	3,86E-03	1,22	1,92	5960132
C20ORF24	0,38	3,40E-04	1,24	1,91	7040176
C20ORF24	0,24	1,05E-04	1,28	1,90	4760537
LOC100133678	0,10	3,73E-03	1,77	1,90	5310224
IRAK1	0,25	4,26E-05	1,24	1,90	4040564
GMPPB	0,42	2,17E-04	1,19	1,90	4830458
POLR3H	0,38	5,06E-04	1,25	1,89	2450634
SIGMAR1	0,38	1,23E-03	1,29	1,89	2940528
MAT2A	0,39	4,97E-04	1,24	1,89	7150176
NOP56	0,56	3,32E-03	1,20	1,88	5560465
CTNS	0,15	4,37E-05	1,30	1,88	5910541
MYOF	0,36	8,75E-04	1,28	1,88	4670592
SNHG3-RCC1	0,42	1,59E-03	1,26	1,87	3710373

PIGW	0,46	9,11E-04	1,21	1,87	5080647
ZMYND19	0,28	1,44E-04	1,26	1,87	4860437
RPL13	0,41	1,06E-03	1,25	1,87	840242
TSSC4	0,51	2,17E-04	1,15	1,87	160309
METTL1	0,37	1,42E-03	1,30	1,86	1990358
POLR3K	0,74	6,38E-03	1,13	1,86	7000703
IFRD2	0,31	1,39E-04	1,23	1,86	4200152
TTLL12	0,53	1,63E-03	1,19	1,86	1430053
SMG5	0,36	4,74E-05	1,18	1,86	5090020
GPR114	0,40	6,55E-04	1,24	1,86	7380273
PSME4	0,18	2,62E-04	1,35	1,85	20671
ABCF2	0,56	7,45E-04	1,16	1,85	5420142
RRP15	0,29	4,90E-04	1,30	1,85	4900484
C9ORF114	0,18	8,80E-05	1,29	1,85	770692
HEATR2	0,58	3,80E-04	1,13	1,85	5290037
GJB2	0,43	1,33E-02	1,36	1,85	5260095
SCRIB	0,66	1,81E-04	1,10	1,85	4290196
MFSD3	0,31	6,48E-04	1,29	1,84	1510703
NOP56	0,40	4,07E-03	1,31	1,84	5910154
TIMM10	0,72	5,30E-03	1,13	1,84	3310376
FAM58A	0,48	5,14E-04	1,18	1,84	1940228
FER1L3	0,39	5,11E-04	1,23	1,84	6510707
MRPL41	0,41	6,85E-04	1,23	1,84	4780040
TBXAS1	0,10	3,08E-03	1,67	1,84	3940390
NOP56	0,45	8,34E-03	1,31	1,84	5550220
TUBG1	0,18	4,57E-04	1,38	1,83	5670180
IL17RB	0,02	7,72E-03	2,21	1,83	1070152
CCND2	0,79	9,51E-03	1,11	1,83	1570348
CTSC	0,31	4,62E-04	1,27	1,83	2640768
POLR2L	0,80	1,66E-03	1,08	1,83	6200017
LOC649553	0,21	4,91E-04	1,35	1,83	1980239
MKI67IP	0,34	1,50E-03	1,30	1,82	1090327
LGMN	0,21	3,15E-02	1,81	1,82	4560129
ITM2C	0,19	1,26E-03	1,44	1,82	2650762
PRMT3	0,17	2,72E-04	1,35	1,82	6760133
ELAC2	0,38	4,10E-04	1,22	1,82	60202
RPL29	0,81	2,91E-02	1,13	1,82	2450167
ATP1B3	0,21	2,74E-04	1,32	1,81	3130092
GPS1	0,27	5,58E-04	1,31	1,81	1990520
NME1	0,50	9,16E-03	1,26	1,81	1820504

GFM1	0,41	1,23E-03	1,24	1,81	3440195
NIP7	0,34	5,87E-04	1,26	1,81	6280482
SNAPC4	0,44	1,42E-03	1,22	1,81	2070195
MT1X	0,74	9,48E-03	1,13	1,81	6620528
DNAJB11	0,41	1,69E-04	1,18	1,80	3190452
JMJD8	0,41	7,59E-04	1,22	1,80	7160246
CTSC	0,13	2,17E-04	1,38	1,80	5270367
ARMET	0,48	7,94E-04	1,18	1,80	4560110
DOLPP1	0,15	4,43E-05	1,28	1,80	1260154
THOC4	0,31	1,75E-03	1,33	1,80	460286
NCLN	0,66	4,65E-04	1,11	1,80	4290687
LYAR	0,49	3,28E-03	1,22	1,80	6220148
ACOT7	0,64	4,55E-03	1,16	1,80	6580639
ILF3	0,31	1,13E-03	1,31	1,80	3360689
AHSA1	0,40	1,19E-03	1,24	1,80	4880561
FLJ23152	0,61	1,49E-04	1,10	1,79	7000575
PUF60	0,26	1,13E-04	1,24	1,79	5050082
LGMN	0,23	1,25E-02	1,58	1,79	1300452
PLEKHG3	0,22	3,97E-04	1,32	1,79	4010397
TNFSF14	0,19	2,00E-03	1,46	1,78	610113
DDX39	0,34	3,71E-04	1,24	1,78	4860673
RUVBL1	0,40	5,95E-04	1,21	1,78	4900465
BYSL	0,57	3,34E-03	1,18	1,78	4860356
HS.430851	0,27	3,80E-04	1,28	1,78	6520553
C14ORF80	0,29	4,07E-04	1,27	1,78	7100008
UCK2	0,36	1,45E-03	1,27	1,78	620725
FAM38A	0,17	1,03E-04	1,28	1,78	4590390
ITM2C	0,18	7,15E-04	1,39	1,78	1110669
TXNDC5	0,35	7,12E-04	1,25	1,77	5050053
ZNF593	0,44	2,95E-03	1,24	1,77	5810201
PFAS	0,45	3,62E-03	1,24	1,77	3840092
GPR55	0,00	8,89E-05	1,56	1,77	2350546
POLR1C	0,60	2,07E-03	1,15	1,77	5700167
LOC389049	0,38	1,68E-04	1,18	1,77	4390367
FANCE	0,16	2,04E-04	1,32	1,77	5720192
C16ORF35	0,20	2,74E-04	1,31	1,76	2640528
DDX21	0,56	1,11E-02	1,22	1,76	2750719
MRTO4	0,45	1,69E-03	1,22	1,76	130220
RIOK1	0,38	4,04E-04	1,21	1,76	60500
QDPR	0,54	2,17E-03	1,18	1,76	6900450

RPL29	0,78	3,68E-02	1,14	1,76	2350465
SLC29A1	0,35	2,09E-04	1,20	1,76	6180687
NOTCH1	0,80	5,58E-04	1,06	1,76	5080167
LTV1	0,24	6,82E-04	1,32	1,75	1230296
ICMT	0,36	1,15E-03	1,26	1,75	5550348
TMEM138	0,30	5,91E-04	1,27	1,75	6290598
YRDC	0,58	5,98E-04	1,13	1,75	3440224
WDR4	0,48	1,55E-02	1,29	1,75	3930703
CD83	0,02	1,69E-04	1,54	1,75	6620026
SIVA	0,31	3,03E-03	1,34	1,74	5550673
MAP7D1	0,47	2,14E-04	1,14	1,74	4880735
FLAD1	0,39	5,38E-04	1,21	1,74	4290014
DKC1	0,42	5,35E-04	1,19	1,74	6980327
UTP14A	0,34	6,55E-04	1,25	1,74	1400008
AEN	0,68	3,18E-04	1,09	1,74	5090438
PHF5A	0,51	4,94E-04	1,15	1,74	450598
MARS2	0,42	3,91E-04	1,18	1,74	10440
NQO1	0,44	1,13E-03	1,20	1,74	5360347
PLD6	0,46	1,85E-04	1,14	1,74	1340707
LYAR	0,64	2,68E-03	1,14	1,74	5310369
UTP14A	0,32	6,06E-04	1,25	1,74	3360377
CSK	0,68	5,19E-04	1,10	1,73	3170239
EMILIN2	0,50	5,80E-05	1,11	1,73	1190142
POLR1C	0,55	2,25E-03	1,17	1,73	1010653
CLPTM1L	0,40	3,47E-03	1,27	1,73	1050750
DNAJA1	0,28	1,49E-04	1,22	1,73	1980632
CENTA1	0,84	6,41E-03	1,07	1,73	830735
DDX56	0,55	4,71E-04	1,13	1,72	7380653
TUBG1	0,31	1,62E-04	1,21	1,72	5390189
CCND2	0,75	7,99E-03	1,11	1,72	3460520
LRRC14	0,38	1,76E-04	1,18	1,72	2810687
TFRC	0,17	3,86E-04	1,33	1,72	2940435
SIVA1	0,43	1,67E-03	1,21	1,72	1450477
ACTR1A	0,23	1,13E-04	1,24	1,72	4280561
POLR3B	0,43	1,63E-04	1,15	1,71	4780253
PIGQ	0,78	7,85E-04	1,07	1,71	6040767
WDR57	0,25	3,05E-04	1,26	1,71	1690348
NOP2	0,33	8,95E-04	1,25	1,71	1010630
KIAA0664	0,40	6,45E-04	1,20	1,71	7400711
EBNA1BP2	0,44	7,56E-03	1,26	1,71	290114

PTS	0,66	1,42E-03	1,12	1,70	4050437
SEC13	0,44	1,25E-03	1,20	1,70	1580017
PTPMT1	0,32	3,12E-04	1,22	1,70	3370142
PRPF19	0,39	4,20E-03	1,28	1,70	7050189
RCC1	0,37	3,60E-04	1,20	1,70	2570292
SIVA1	0,68	3,71E-03	1,12	1,70	5820170
NUP93	0,48	2,12E-03	1,19	1,70	5310068
WDR46	0,59	1,06E-03	1,13	1,70	6980554
RAN	0,15	3,15E-04	1,33	1,70	6250707
TRIP13	0,38	9,51E-04	1,22	1,70	5700373
LOC728666	0,59	3,42E-03	1,15	1,70	7570156
PAQR4	0,16	6,11E-04	1,36	1,69	3460132
ACOT7	0,35	1,22E-03	1,25	1,69	4290050
ATP6V0B	0,32	1,76E-04	1,20	1,69	7160059
NSUN2	0,39	7,12E-04	1,20	1,69	3450093
KPNA4	0,33	6,11E-04	1,23	1,69	2850128
PDXP	0,16	4,62E-04	1,34	1,69	3180273
POP7	0,36	2,23E-04	1,19	1,69	2480554
C7ORF20	0,38	1,13E-04	1,16	1,69	2900504
MGC3731	0,40	6,11E-04	1,19	1,69	4390446
SNORA61	0,69	2,63E-03	1,11	1,69	3990497
RANBP1	0,41	2,59E-03	1,24	1,69	7000735
SIGMAR1	0,48	6,11E-04	1,15	1,69	4050438
TFDP1	0,21	5,35E-04	1,31	1,69	3290435
PDCD2	0,24	5,58E-04	1,29	1,69	4010546
C3ORF26	0,35	3,49E-03	1,29	1,69	520224
E2F2	0,38	1,03E-02	1,33	1,68	5340338
C1QBP	0,27	1,66E-03	1,32	1,68	7200392
FRAP1	0,39	1,46E-03	1,23	1,68	1410243
DCTPP1	0,51	2,49E-03	1,17	1,68	4210192
SNRNP40	0,22	4,62E-04	1,29	1,68	6130220
LOC643856	0,40	4,34E-04	1,18	1,68	6960551
G3BP1	0,31	1,16E-03	1,27	1,68	6520730
MGC40489	0,27	3,95E-04	1,25	1,68	3420400
C17ORF79	0,27	1,49E-03	1,32	1,68	3390477
TMEM118	0,82	6,11E-04	1,05	1,68	4860086
EIF4A1	0,24	6,65E-05	1,20	1,68	3400403
MED22	0,40	1,10E-04	1,14	1,67	6590661
IDE	0,38	1,91E-03	1,24	1,67	2650523
HSD17B10	0,62	6,55E-03	1,16	1,67	6100056

PPIL1	0,47	7,50E-03	1,24	1,67	4200612
UBN1	0,77	1,66E-03	1,08	1,67	7160433
CLCN7	0,52	2,95E-03	1,17	1,67	2060088
SPHK2	0,56	6,70E-04	1,13	1,67	3800725
MRPL20	0,65	2,46E-02	1,19	1,67	520521
CCT6P1	0,40	3,25E-03	1,24	1,67	5420053
MRPL4	0,49	3,73E-03	1,19	1,67	1170121
ABCE1	0,44	8,68E-03	1,26	1,67	1090543
EMG1	0,83	1,30E-02	1,08	1,67	4850091
ASPSCR1	0,32	3,39E-04	1,21	1,67	6940484
NOMO1	0,32	2,61E-04	1,20	1,67	3310056
LOC651816	0,52	2,31E-04	1,12	1,66	1570746
FDX1L	0,44	3,21E-04	1,15	1,66	5090053
TUBG1	0,43	2,24E-03	1,21	1,66	5860411
SEC61A1	0,44	1,68E-04	1,13	1,66	1030471
LETM1	0,51	2,20E-04	1,12	1,66	130270
ATIC	0,42	7,74E-03	1,26	1,66	1770546
IMP4	0,46	7,93E-04	1,16	1,66	6560041
TXNDC5	0,29	8,07E-04	1,26	1,66	4850398
F2R	0,68	4,37E-03	-1,12	1,66	4570398
DCTPP1	0,47	6,30E-03	1,22	1,66	7650435
POLR3E	0,29	5,95E-04	1,25	1,65	4150465
CAD	0,31	5,55E-04	1,23	1,65	3360402
SLBP	0,20	3,82E-04	1,29	1,65	3290291
PDSS1	0,44	1,79E-03	1,19	1,65	430192
LOC399942	0,35	4,41E-03	1,29	1,65	1740673
VCP	0,31	3,36E-04	1,21	1,65	2450093
NUDC	0,37	1,23E-03	1,23	1,65	6110477
NME1	0,49	1,68E-02	1,25	1,65	7560673
ADRM1	0,38	4,71E-04	1,19	1,65	4280136
UHRF1	0,38	3,02E-04	1,18	1,65	1510278
MPDU1	0,50	9,00E-04	1,15	1,65	4890403
TMPO	0,14	2,17E-04	1,31	1,65	3400630
KIAA0020	0,62	4,67E-03	1,14	1,65	1500603
PTPLAD1	0,21	8,67E-04	1,32	1,65	6420349
CIRH1A	0,29	1,19E-03	1,28	1,65	4200162
FAM86B1	0,32	1,08E-03	1,25	1,65	4050646
DHX30	0,49	5,09E-04	1,14	1,65	1340193
CCT3	0,46	2,84E-03	1,20	1,65	7650484
URB2	0,39	8,85E-04	1,20	1,64	1580433

PSMC4	0,41	5,95E-04	1,18	1,64	5360646
CRELD2	0,23	4,62E-04	1,27	1,64	6560390
HMOX1	0,44	3,92E-03	1,22	1,64	6660601
RQCD1	0,30	3,71E-04	1,22	1,64	7050138
HADH2	0,66	1,02E-02	1,15	1,64	620414
MRPL20	0,61	1,79E-02	1,19	1,64	2060646
TUBB2C	0,34	7,20E-04	1,22	1,64	2070368
HNRNPA1	0,41	4,99E-03	1,24	1,64	10209
TSPAN3	0,23	2,10E-04	1,24	1,64	4490615
RHOU	0,29	4,99E-04	1,23	1,64	1230470
RRP9	0,49	3,93E-04	1,13	1,64	3460634
DPP9	0,39	1,66E-04	1,15	1,64	3170332
TXNDC14	0,38	5,58E-04	1,19	1,64	610762
GOT2	0,49	4,12E-03	1,19	1,64	6980048
LIMA1	0,16	9,13E-03	1,53	1,63	4880537
RHBDD2	0,11	3,50E-03	1,51	1,63	510373
RUVBL1	0,46	5,18E-03	1,21	1,63	1780070
STIP1	0,66	3,98E-03	1,12	1,63	620711
FBXL6	0,51	4,84E-04	1,13	1,63	1580215
RPUSD1	0,66	1,91E-03	1,11	1,63	6290181
CCT6A	0,29	2,13E-03	1,29	1,63	2600630
OBFC2B	0,54	4,55E-03	1,17	1,63	270196
CCR2	0,75	2,87E-05	1,04	1,63	580706
C1ORF19	0,07	4,80E-04	1,40	1,63	3870112
C6ORF125	0,64	2,65E-02	1,18	1,63	6520692
LRRC20	0,48	3,62E-03	1,19	1,62	6620379
CYCSL1	0,56	3,60E-02	1,24	1,62	3890008
HRAS	0,71	2,16E-03	1,09	1,62	1770753
BRMS1	0,41	6,48E-04	1,17	1,62	4810129
BRMS1	0,38	7,85E-04	1,20	1,62	4570102
MPDU1	0,29	6,90E-04	1,24	1,62	2710019
PSMC4	0,21	7,85E-04	1,30	1,62	150544
HSPA8	0,46	6,11E-04	1,15	1,62	430672
TACC1	0,25	2,20E-04	1,22	1,62	2940373
LOC652826	0,37	3,82E-04	1,18	1,62	6350148
CCNE1	0,64	7,13E-03	1,14	1,62	3990026
ATP6V0B	0,86	4,84E-03	1,06	1,62	7400673
RCBTB2	0,34	2,75E-02	1,41	1,62	1400035
PSMD2	0,43	2,41E-03	1,20	1,62	450403
RRP7A	0,61	1,10E-02	1,16	1,62	3130598

FAM86A	0,43	4,74E-03	1,22	1,62	580026
SLC38A10	0,35	1,44E-04	1,16	1,62	6590333
LOC100128805	0,48	6,11E-04	1,14	1,62	2070193
UBIAD1	0,40	6,00E-04	1,17	1,62	110121
BRIX1	0,26	1,42E-03	1,29	1,62	2120445
IPO11	0,40	3,19E-04	1,16	1,61	6770202
TFB2M	0,47	2,36E-03	1,18	1,61	5270296
USP39	0,33	1,62E-03	1,24	1,61	6020487
EIF4G2	0,21	7,78E-04	1,30	1,61	4290446
LOC731049	0,63	1,11E-03	1,11	1,61	4610608
FAM136A	0,62	2,66E-03	1,12	1,61	3890671
EEF1B2	0,47	6,04E-03	1,21	1,61	2640554
PTPLAD1	0,41	5,18E-03	1,24	1,61	7150152
TIMM22	0,47	1,24E-03	1,16	1,61	3390373
EI24	0,30	1,19E-04	1,18	1,61	770541
DDX31	0,41	3,45E-04	1,15	1,61	1820133
LOC113386	0,56	1,68E-02	1,20	1,61	6220600
HSPA4	0,29	8,05E-04	1,25	1,61	5090368
DDX19A	0,42	1,04E-03	1,18	1,61	3520689
DDX28	0,63	1,42E-03	1,11	1,61	1300037
STRA13	0,78	1,41E-03	1,07	1,61	270605
RANBP1	0,32	4,41E-03	1,29	1,61	4610047
BCL2L1	0,62	1,67E-03	1,11	1,60	670673
CLPTM1	0,65	4,71E-04	1,09	1,60	770168
UBQLN4	0,51	6,11E-04	1,13	1,60	3610487
BSG	0,78	7,97E-03	1,09	1,60	20673
DNAJC9	0,35	5,37E-04	1,19	1,60	50114
HNRNPC	0,32	1,44E-04	1,17	1,60	5670487
PUS1	0,65	6,05E-03	1,13	1,60	6100735
SLC43A3	0,48	7,18E-03	1,21	1,60	2600431
DHX37	0,51	3,71E-04	1,12	1,60	4260142
PRDX1	0,49	8,19E-03	1,20	1,60	6180446
CLTA	0,26	3,86E-04	1,23	1,60	6380128
LSM4	0,40	1,67E-03	1,20	1,60	3840594
CIRBP	0,57	9,87E-03	1,17	1,60	7560047
EIF3B	0,41	1,13E-03	1,18	1,60	6290603
C6ORF66	0,85	4,03E-03	1,05	1,60	430309
LOC100129673	0,45	1,05E-02	1,24	1,60	4040343
TSPAN17	0,47	8,68E-03	1,22	1,60	3710609
CCDC124	0,57	1,05E-03	1,12	1,60	2070537

ALG1	0,31	5,49E-04	1,21	1,60	5560670
PDSS1	0,52	1,87E-03	1,15	1,59	3120086
REXO4	0,62	4,99E-04	1,09	1,59	1190221
BIRC5	0,37	1,12E-02	1,30	1,59	1230682
GLRX2	0,29	7,85E-04	1,24	1,59	1240414
POLA2	0,20	4,17E-04	1,27	1,59	4920537
CASZ1	0,32	1,02E-03	1,23	1,59	2450047
VARS	0,30	6,80E-03	1,33	1,59	6980100
KIAA1967	0,64	1,18E-03	1,10	1,59	5050047
CGI-96	0,51	9,72E-03	1,19	1,59	3140669
WDR5	0,44	2,67E-04	1,13	1,59	4850079
KIAA0114	0,44	1,76E-02	1,27	1,59	4150110
MRPL49	0,66	1,53E-03	1,10	1,59	620767
LMNB2	0,58	2,14E-04	1,09	1,59	7570148
GPATCH4	0,45	1,10E-03	1,16	1,59	1580341
IPO4	0,89	3,69E-03	1,04	1,58	4830500
C14ORF169	0,51	4,84E-03	1,17	1,58	6510634
JMJD8	0,46	3,09E-03	1,18	1,58	7650315
U2AF2	0,29	7,85E-04	1,23	1,58	1690114
RANGAP1	0,36	8,85E-04	1,20	1,58	2900292
SLC25A22	0,64	6,15E-04	1,09	1,58	4210626
PTS	0,51	1,47E-03	1,14	1,58	6280341
PINX1	0,46	4,58E-03	1,19	1,58	1240452
BRI3BP	0,54	2,09E-03	1,14	1,58	160437
MTHFD1	0,41	1,28E-03	1,18	1,58	1660270
ILKAP	0,44	9,32E-04	1,16	1,58	580114
MRPL38	0,36	1,75E-03	1,22	1,58	4220327
LRWD1	0,52	1,29E-03	1,13	1,58	7100546
LOC400013	0,44	5,17E-03	1,21	1,58	6330343
TARBP2	0,34	6,72E-04	1,20	1,58	7570446
DHX29	0,49	1,56E-03	1,15	1,58	5130458
C14ORF109	0,43	7,78E-04	1,16	1,58	4210553
PRICKLE4	0,73	1,46E-02	1,12	1,57	730114
PRMT5	0,81	1,02E-02	1,08	1,57	3850520
THOC4	0,30	1,41E-02	1,37	1,57	1660309
PRKDC	0,24	7,18E-03	1,38	1,57	770390
ISOC2	0,61	3,99E-03	1,13	1,57	6650692
SRPRB	0,49	2,06E-03	1,15	1,57	4480224
POP5	0,62	1,01E-02	1,15	1,57	4560528
TSTA3	0,45	1,87E-03	1,17	1,57	2350661

NOL7	0,32	5,09E-04	1,19	1,57	1820470
NME1	0,79	5,30E-03	1,07	1,57	3060440
TMEM177	0,63	1,32E-03	1,10	1,57	3930278
TESC	0,51	2,88E-02	1,23	1,57	5050681
LOC644563	0,56	9,79E-03	1,17	1,57	4290102
PUSL1	0,38	4,62E-04	1,17	1,57	3390010
SAC3D1	0,87	1,38E-02	1,06	1,57	4210692
POGK	0,80	5,06E-04	1,05	1,57	6220368
TEX2	0,39	1,01E-03	1,18	1,57	2350333
RRP1	0,83	4,77E-03	1,06	1,57	240154
MFNG	0,39	5,49E-04	1,17	1,57	2000438
PREB	0,43	4,04E-04	1,14	1,57	2060274
LOC100130919	0,39	5,09E-04	1,16	1,57	2760719
C9ORF40	0,14	3,33E-04	1,29	1,57	4810139
CCNE2	0,25	1,44E-03	1,28	1,57	4760154
SLC25A3	0,27	4,64E-04	1,22	1,57	4250204
BAZ1A	0,29	3,43E-03	1,29	1,57	940288
SRF	0,30	4,34E-04	1,20	1,57	20022
CDC20	0,43	2,02E-03	1,18	1,57	1500010
TUBA1C	0,26	3,43E-04	1,22	1,57	6100673
PFN1	0,51	9,84E-04	1,13	1,57	2850402
CTSC	0,39	6,21E-03	1,24	1,57	3450138
SRXN1	0,48	5,47E-04	1,13	1,56	3780717
TMEM93	0,32	3,40E-04	1,18	1,56	3140768
NUDT16L1	0,53	2,11E-04	1,10	1,56	2850180
ACAD9	0,30	1,22E-03	1,24	1,56	5340561
SLC25A11	0,32	4,49E-04	1,19	1,56	2480475
ATP6V0D1	0,49	1,77E-03	1,15	1,56	6330377
SCPEP1	0,10	6,11E-04	1,35	1,56	2690598
ZWILCH	0,41	6,20E-03	1,23	1,56	7000743
RDH10	0,09	1,06E-02	1,61	1,56	7050433
HCFC1	0,48	1,62E-03	1,15	1,56	4850296
AMD1	0,23	1,63E-04	1,20	1,56	50050
MFN2	0,42	4,80E-04	1,15	1,56	5550253
HNRNPM	0,45	5,95E-03	1,20	1,56	2360669
RNASEH1	0,34	6,01E-04	1,19	1,56	1510661
HEATR1	0,41	1,43E-03	1,18	1,56	3460242
LANCL2	0,29	5,31E-04	1,21	1,56	7560301
ARHGDIA	0,66	6,55E-04	1,08	1,55	4760255
IL5	0,84	6,68E-03	1,06	1,55	7040605

BRI3BP	0,40	8,67E-04	1,17	1,55	6450474
ATP1B3	0,44	2,17E-02	1,26	1,55	4220632
ZWINT	0,27	7,12E-04	1,24	1,55	3800474
KAT2A	0,70	2,74E-04	1,06	1,55	4830301
C10ORF2	0,61	2,80E-03	1,12	1,55	2190538
PTPN7	0,48	5,49E-04	1,13	1,55	3610082
CIAPIN1	0,41	1,23E-03	1,17	1,55	5670523
LUC7L	0,34	5,95E-04	1,19	1,55	3610100
UBE2G2	0,46	2,36E-03	1,17	1,55	2750750
C16ORF53	0,46	4,95E-03	1,19	1,55	2340059
MAK16	0,41	3,21E-03	1,20	1,55	3060397
CENPB	0,32	9,04E-04	1,21	1,55	610056
C9ORF140	0,67	1,42E-03	1,09	1,55	1010470
SFXN4	0,52	4,04E-03	1,15	1,55	730092
FEM1A	0,57	2,92E-04	1,09	1,55	5890538
WDR77	0,49	2,32E-03	1,15	1,55	1110440
AP1B1	0,42	1,50E-03	1,17	1,55	2470327
BAX	0,92	7,12E-03	1,03	1,55	3520092
PRPF31	0,71	5,97E-03	1,10	1,55	1190707
CHCHD4	0,38	5,50E-03	1,24	1,55	3850292
MRPS12	0,59	1,62E-03	1,11	1,55	1850370
WDR1	0,49	5,40E-03	1,17	1,55	4860239
GRK6	0,30	3,12E-04	1,19	1,54	7570717
FEN1	0,24	1,57E-03	1,28	1,54	3370703
SOS1	0,20	9,82E-04	1,28	1,54	2140519
FAM86A	0,48	1,18E-03	1,14	1,54	6270201
TCEB2	0,36	3,20E-03	1,23	1,54	3400133
HMBS	0,34	6,37E-03	1,27	1,54	7320021
TTL	0,18	1,68E-04	1,22	1,54	7320386
FHL2	0,50	4,81E-02	1,27	1,54	990288
GTF3C6	0,61	1,90E-02	1,16	1,54	4200110
MUM1	0,69	1,79E-03	1,09	1,54	6100630
TMEM5	0,23	9,69E-04	1,26	1,54	5690358
C16ORF33	0,77	3,77E-02	1,11	1,54	4760450
LOC653119	0,52	1,81E-03	1,13	1,54	6370669
LOC203547	0,35	2,22E-03	1,22	1,54	7550743
GLRX5	0,38	7,48E-04	1,17	1,54	2030484
SLC25A39	0,47	1,09E-03	1,14	1,54	650634
DHX9	0,48	7,43E-03	1,19	1,54	6900725
CHUK	0,39	3,19E-03	1,21	1,54	3520541

NFKBIB	0,36	5,58E-04	1,17	1,54	7560414
C16ORF53	0,49	2,66E-03	1,15	1,53	4230066
SURF6	0,53	2,75E-03	1,14	1,53	2600452
U2AF2	0,25	1,44E-04	1,18	1,53	2360768
AFG3L2	0,25	8,25E-04	1,24	1,53	1170538
KPNA3	0,41	1,58E-02	1,26	1,53	2760451
LOC731314	0,46	2,93E-03	1,16	1,53	4120538
TMEM93	0,88	6,55E-04	1,03	1,53	3990600
HSPA8	0,46	1,46E-03	1,15	1,53	2650619
DPH2	0,66	1,06E-03	1,09	1,53	130239
DUSP4	0,20	1,65E-02	1,46	1,53	2650041
C3ORF14	0,48	5,67E-03	1,18	1,53	6650079
LOC728666	0,61	4,86E-03	1,12	1,53	1110487
NT5DC3	0,56	2,51E-03	1,13	1,53	6330348
LOC647000	0,32	1,49E-03	1,22	1,53	3310288
HSPA4	0,24	3,86E-04	1,21	1,53	2140711
DHCR24	0,31	9,17E-03	1,31	1,53	4480341
SETMAR	0,49	8,71E-03	1,18	1,53	7610097
C1ORF109	0,56	2,24E-03	1,13	1,53	4540039
GEMIN4	0,49	1,36E-03	1,14	1,53	6450300
RASGRP3	0,44	1,80E-02	1,24	1,53	2450400
MRPL27	0,98	1,24E-02	1,01	1,53	2060612
AIFM1	0,38	5,17E-03	1,23	1,53	1500689
ATP1B3	0,27	6,32E-03	1,32	1,53	1510088
CHORDC1	0,40	7,88E-03	1,23	1,53	380528
MFHAS1	0,04	1,05E-04	1,30	1,53	4260243
FAM173A	0,67	4,13E-03	1,10	1,53	1470561
L3MBTL2	0,71	3,73E-03	1,09	1,53	5870646
LOC652903	0,27	3,37E-04	1,20	1,53	2690091
TOMM40L	0,39	7,04E-04	1,16	1,53	4260152
POMGNT1	0,56	5,18E-04	1,10	1,53	2940224
WDR74	0,41	3,47E-03	1,19	1,53	7380368
PDCL3	0,62	2,02E-02	1,16	1,53	3870646
BCCIP	0,44	7,70E-03	1,21	1,53	1450386
DHX30	0,65	1,89E-03	1,10	1,53	6110608
LOC401127	0,35	1,26E-03	1,19	1,53	3360327
ZNF598	0,68	2,07E-03	1,09	1,53	2030070
MAPKAPK3	0,41	7,19E-04	1,15	1,53	1440440
CCT6A	0,63	2,93E-03	1,11	1,53	5820392
CASP3	0,38	9,20E-04	1,17	1,52	2260215

ABCE1	0,50	1,86E-02	1,21	1,52	5310152
CEP55	0,06	9,04E-04	1,40	1,52	7510709
PTRH1	0,63	2,08E-02	1,15	1,52	6370044
RCAN1	0,18	7,15E-04	1,27	1,52	2850551
BANF1	0,50	5,08E-03	1,16	1,52	150767
CLTA	0,44	1,46E-03	1,16	1,52	4390327
CPSF2	0,37	1,04E-03	1,18	1,52	1430110
EFTUD2	0,56	1,42E-03	1,11	1,52	6980475
TAF6L	0,38	1,32E-03	1,18	1,52	7650025
POLRMT	0,83	2,15E-03	1,05	1,52	1990053
RNPS1	0,49	1,87E-03	1,14	1,52	2630022
RAC1	0,40	5,58E-04	1,15	1,52	630204
DOLK	0,53	4,62E-04	1,10	1,52	3390730
TFDP1	0,33	5,72E-03	1,26	1,52	510487
RPUSD2	0,49	4,40E-03	1,16	1,52	5820333
EEF1E1	0,38	1,43E-02	1,27	1,52	50301
RBBP8	0,30	5,09E-03	1,28	1,52	6580672
MRPS26	0,39	1,25E-02	1,26	1,52	3310445
EDARADD	0,35	2,14E-04	1,15	1,52	3710273
GRAP2	0,30	6,81E-03	1,29	1,52	1580184
TCP1	0,29	4,49E-03	1,28	1,52	2750424
HSP90AB1	0,66	2,56E-02	1,14	1,52	4830100
SSSCA1	0,66	1,99E-03	1,09	1,52	6480605
PEPD	0,61	7,54E-03	1,13	1,52	5670400
PRDX1	0,57	2,35E-02	1,18	1,52	6250280
FBXL6	0,49	8,45E-04	1,13	1,52	1470092
CSE1L	0,51	1,19E-02	1,18	1,52	7000634
C8ORF33	0,64	1,80E-03	1,10	1,52	1470397
MCAT	0,49	2,66E-03	1,15	1,51	830215
CHAC2	0,29	4,62E-04	1,19	1,51	2850082
PSMC3	0,32	1,13E-03	1,20	1,51	6960315
RAB11FIP1	0,29	2,23E-02	1,38	1,51	6130156
ARSB	0,40	5,49E-03	1,21	1,51	270215
RAB8A	0,36	4,78E-04	1,16	1,51	7150678
CCT2	0,43	5,15E-03	1,19	1,51	7100288
MAGMAS	0,69	5,81E-03	1,10	1,51	6380220
TDG	0,39	1,28E-03	1,17	1,51	1990253
KIF5B	0,40	1,80E-03	1,17	1,51	2710017
COQ3	0,60	7,86E-03	1,13	1,51	2760181
H2AFY	0,36	9,28E-03	1,26	1,51	2360471

MIIP	0,41	3,36E-04	1,13	1,51	7160750
SEPT11	0,18	2,42E-03	1,33	1,51	20288
FUT7	0,58	1,87E-02	1,17	1,51	5340324
CCT3	0,49	7,72E-03	1,17	1,51	5270717
RER1	0,50	1,74E-03	1,13	1,51	3850431
XPO7	0,38	3,70E-04	1,15	1,51	4560730
EIF4G2	0,49	5,43E-03	1,16	1,51	6220044
SFRS2	0,48	6,22E-03	1,17	1,51	3940414
NPLOC4	0,24	5,76E-04	1,22	1,51	1470154
HLA-DPA1	0,18	3,71E-02	1,57	1,51	1190039
EHD4	0,34	1,58E-02	1,30	1,51	6400647
LOC389873	0,45	4,18E-03	1,17	1,51	2340053
SMARCA4	0,38	6,67E-04	1,16	1,51	6860300
MLEC	0,48	1,45E-03	1,14	1,51	1990546
EIF4G3	0,41	4,67E-04	1,14	1,51	3290551
MPP6	0,30	1,28E-03	1,22	1,51	3370280
TATDN2	0,36	6,00E-04	1,17	1,51	2690753
DDX46	0,33	3,43E-03	1,23	1,51	3890192
CYP1B1	0,73	3,30E-02	1,12	1,51	2120053
SFXN4	0,30	2,13E-03	1,24	1,51	1820706
ACACA	0,34	2,23E-03	1,21	1,51	2190414
HNRPM	0,27	2,67E-03	1,26	1,50	6450646
UTP11L	0,47	1,25E-02	1,20	1,50	6280152
PHF15	0,45	3,08E-03	1,16	1,50	770411
STARD7	0,49	1,32E-03	1,13	1,50	4210750
TMEM97	0,36	5,69E-03	1,23	1,50	3420541
RAB11FIP3	0,47	1,19E-03	1,13	1,50	3610112
LOC652615	0,51	4,73E-03	1,15	1,50	2570553
RPRC1	0,64	1,91E-03	1,09	1,50	2970563
PUS7	0,31	3,63E-03	1,25	1,50	3940615
NUDT3	0,54	1,91E-03	1,12	1,50	3850167
TMEM93	0,48	1,93E-03	1,14	1,50	1500041
HMBS	0,43	1,43E-02	1,23	1,50	6060278
MB	0,23	1,59E-03	1,26	1,50	2600019
TOR3A	0,56	9,05E-04	1,10	1,50	430411
FAM129A	0,11	8,42E-03	1,49	1,50	4230735
PMM2	0,36	1,02E-03	1,18	1,50	1260315
RAN	0,40	7,45E-04	1,15	1,50	1940377
LFNG	0,82	6,70E-03	1,06	1,50	6620392
C10ORF119	0,57	7,05E-04	1,10	1,50	5050112

ANAPC7	0,30	2,27E-03	1,24	1,50	160220
LOC642031	0,51	7,50E-04	1,11	1,50	6770091
PTBP1	0,41	1,04E-03	1,15	1,50	6060332
C8ORF33	0,34	1,13E-03	1,19	1,50	6350671
ZNF142	0,61	1,46E-03	1,10	1,50	150040
E2F6	0,21	1,69E-04	1,19	1,50	7510707
GOLGA3	0,38	1,63E-04	1,12	1,50	6250093
CPSF2	0,36	1,12E-03	1,18	1,50	3830204
TIMM23	0,36	1,83E-03	1,19	1,49	4230050
HS.390407	0,86	2,03E-02	1,06	1,49	5310327
BCS1L	0,51	1,40E-02	1,18	1,49	7100131
ADRM1	0,54	3,62E-03	1,13	1,49	4390121
RRP1B	0,59	1,77E-02	1,16	1,49	6480609
UBP1	0,69	2,07E-03	1,08	1,49	5870600
RCC2	0,60	2,55E-03	1,11	1,49	1340360
CCR2	0,97	1,10E-04	1,01	1,49	6040711
UCHL5IP	0,58	7,45E-03	1,13	1,49	1090370
TPRG1	0,02	1,95E-03	1,55	1,49	6860632
LOC391811	0,45	6,75E-04	1,13	1,49	6020669
LSM10	0,63	3,95E-03	1,11	1,49	160255
C1ORF163	0,45	3,08E-03	1,16	1,49	2810022
OGFOD1	0,47	1,26E-03	1,13	1,49	2510731
CYBASC3	0,53	6,64E-03	1,15	1,49	6940152
DCTD	0,47	1,06E-03	1,13	1,49	2480612
TXNRD1	0,39	2,66E-03	1,19	1,49	730286
NOMO1	0,48	9,85E-04	1,12	1,49	2650040
LOC399988	0,59	1,30E-03	1,10	1,49	4850136
GAR1	0,45	1,37E-02	1,21	1,49	1340647
CD83	0,12	1,66E-03	1,34	1,49	5050162
HNRNPR	0,43	4,86E-03	1,18	1,49	3060035
CHPT1	0,70	1,12E-02	1,10	1,49	2630687
BCL7B	0,12	3,33E-04	1,26	1,49	2850360
JTB	0,59	2,18E-03	1,11	1,49	70044
CCT7	0,41	2,96E-03	1,18	1,49	4290358
IWS1	0,24	2,31E-04	1,19	1,49	4070289
U2AF1	0,43	1,73E-02	1,23	1,49	1450102
ERI1	0,38	4,32E-04	1,14	1,49	5360398
XRCC3	0,34	9,84E-04	1,18	1,49	670014
SNHG9	0,97	3,75E-02	-1,02	1,49	1300608
SLC35F2	0,30	5,80E-04	1,18	1,49	3190685

GMPPB	0,51	2,65E-03	1,13	1,49	6020228
C9ORF69	0,74	8,44E-04	1,06	1,49	7380367
BCCIP	0,30	2,14E-03	1,23	1,48	990598
EXOSC4	0,69	6,62E-03	1,10	1,48	7560253
FUBP3	0,71	1,67E-03	1,07	1,48	2370494
BMS1	0,43	6,14E-04	1,13	1,48	1190717
CALM1	0,46	9,44E-04	1,13	1,48	1660477
PPM1G	0,22	1,13E-03	1,25	1,48	3140008
DNMT1	0,40	4,18E-03	1,19	1,48	1260162
C16ORF91	0,76	3,55E-03	1,07	1,48	4890056
SEPHS1	0,56	2,56E-03	1,12	1,48	5700612
NMT1	0,55	3,86E-04	1,09	1,48	6280037
LOC643446	0,29	2,59E-03	1,24	1,48	290392
ILF3	0,43	2,67E-03	1,16	1,48	1780053
MPHOSPH10	0,30	1,29E-03	1,20	1,48	2350563
TMEM110	0,56	2,29E-03	1,11	1,48	5270681
SNRNP25	0,69	1,82E-02	1,11	1,48	1440639
ABCF1	0,55	2,13E-03	1,11	1,48	7380113
SFRS9	0,41	4,91E-04	1,13	1,48	6420767
TIMM44	0,73	2,24E-03	1,07	1,48	7550402
HSPD1	0,57	3,92E-03	1,12	1,48	4250577
SH2D1A	0,32	1,30E-02	1,29	1,48	5910465
EIF4G2	0,30	2,25E-03	1,23	1,47	2260095
GINS3	0,57	4,03E-03	1,12	1,47	3060192
HNRNPM	0,41	8,32E-03	1,20	1,47	6510437
TFB2M	0,56	2,12E-02	1,17	1,47	990100
NCL	0,67	1,98E-02	1,12	1,47	2600035
TAP2	0,69	2,37E-02	1,12	1,47	3940477
C16ORF57	0,86	2,64E-03	1,04	1,47	2750360
NOLA1	0,49	7,44E-03	1,16	1,47	4120465
NCBP1	0,36	1,06E-03	1,17	1,47	2600612
STT3A	0,24	3,10E-03	1,27	1,47	2570692
PES1	0,56	1,57E-03	1,11	1,47	1500066
DUS3L	0,60	6,31E-03	1,12	1,47	6270475
AGPAT3	0,30	4,62E-04	1,17	1,47	3850435
TIMELESS	0,51	1,09E-02	1,16	1,47	4180050
ANKRD39	0,89	3,66E-03	1,04	1,47	6220553
PSMG3	0,40	3,23E-03	1,18	1,47	2650138
C7ORF50	0,35	8,88E-04	1,17	1,47	5810671
TOR1A	0,52	3,97E-04	1,09	1,47	4890500

PI16	0,16	2,29E-02	1,48	1,47	1410673
C8ORF30B	0,71	4,93E-04	1,06	1,47	6420333
POLDIP2	0,79	4,66E-03	1,06	1,47	7200356
UBE3C	0,51	4,91E-03	1,14	1,47	1690709
KAT2B	0,59	3,64E-03	1,11	1,47	7200703
PRPF8	0,36	1,10E-03	1,17	1,47	6060349
PTBP1	0,46	3,06E-03	1,15	1,47	4260754
LOC441089	0,20	6,77E-04	1,23	1,47	6660086
SSNA1	0,40	1,29E-02	1,23	1,47	3190735
SLC35F2	0,20	2,67E-04	1,20	1,47	5720445
NEK6	0,48	5,06E-04	1,11	1,47	5860463
LOC650515	0,44	9,49E-04	1,13	1,47	1690546
POP1	0,76	3,61E-03	1,07	1,47	3840397
C11ORF48	0,88	1,68E-02	1,05	1,47	7100280
SIVA	0,40	6,71E-03	1,20	1,46	4670487
LOC646531	0,27	1,95E-03	1,24	1,46	3310301
LOC100131336	0,27	1,19E-03	1,22	1,46	1850050
ATP1A1	0,49	8,94E-04	1,11	1,46	3370164
LOC729057	0,71	2,29E-03	1,07	1,46	4760139
HNRPM	0,56	3,52E-03	1,12	1,46	6290246
SH2B3	0,46	1,79E-02	1,21	1,46	6560301
EIF3B	0,62	1,83E-03	1,09	1,46	4390136
LOC644684	0,59	5,38E-03	1,12	1,46	6620382
PSMB6	0,46	8,75E-04	1,12	1,46	2360682
FAM53B	0,46	1,98E-02	1,21	1,46	6380079
SFMBT1	0,26	5,09E-04	1,19	1,46	2650433
FTSJ3	0,65	3,49E-03	1,09	1,46	4210600
ANKRD9	0,63	4,50E-03	1,10	1,46	7050370
NTHL1	0,64	1,03E-02	1,12	1,46	2070184
DYNLL1	0,74	3,16E-02	1,11	1,46	6220086
HNRNPR	0,81	4,57E-04	1,04	1,46	6650762
POLR3G	0,78	2,42E-02	1,09	1,46	3400037
C14ORF156	0,69	2,63E-02	1,12	1,46	5290025
FARSA	0,49	2,17E-03	1,13	1,46	2360167
IDH3A	0,41	4,83E-03	1,18	1,46	3360100
SLC2A4RG	0,51	2,92E-03	1,13	1,46	2070243
TMEM147	0,29	3,99E-03	1,25	1,46	2600324
GPS2	0,71	1,14E-02	1,10	1,46	4900170
HSP90B1	0,53	7,28E-03	1,14	1,46	2480326
ALG13	0,79	6,05E-03	1,06	1,46	6660411

UBAP2	0,31	4,52E-04	1,16	1,46	5490097
REXO1	0,54	1,69E-04	1,08	1,46	5720767
DDX10	0,51	4,16E-03	1,13	1,46	3930553
KIAA1671	0,60	3,30E-03	1,10	1,46	3120474
RPS6KA4	0,70	3,81E-03	1,08	1,46	6060433
MCM4	0,45	3,82E-03	1,16	1,46	6020170
MLEC	0,24	1,90E-03	1,24	1,46	1780601
SLC38A5	0,73	2,35E-03	1,07	1,46	4860181
WDR34	0,67	3,19E-03	1,09	1,46	6200195
TYW3	0,20	2,14E-04	1,19	1,46	4010343
CBX6	0,39	1,13E-03	1,15	1,46	3370288
STARD7	0,62	1,30E-02	1,13	1,46	5720360
AARSD1	0,80	1,18E-02	1,07	1,46	60154
NOC4L	0,64	2,34E-03	1,09	1,46	4570142
XPO5	0,41	4,39E-03	1,18	1,46	6590400
SNX5	0,24	3,37E-03	1,27	1,46	630100
SPNS1	0,81	5,45E-03	1,06	1,46	1230192
PARD6A	0,75	7,45E-03	1,08	1,46	460086
GEMIN6	0,66	1,55E-02	1,12	1,46	5080164
SGTA	0,69	2,13E-03	1,08	1,46	240731
ANAPC1	0,39	1,42E-03	1,16	1,46	730647
SNRNP70	0,29	1,83E-03	1,22	1,46	1430670
ASF1B	0,47	9,30E-03	1,17	1,46	2630673
UBE2D4	0,54	5,29E-03	1,13	1,46	5260632
ALS2CR4	0,38	1,83E-03	1,17	1,46	50348
TRIAP1	0,99	9,32E-03	1,01	1,45	2600184
ARD1A	0,45	4,52E-03	1,16	1,45	6590053
PTPLA	0,34	1,98E-02	1,29	1,45	730221
PRMT5	0,98	4,60E-03	-1,01	1,45	5700520
POLE2	0,44	4,37E-03	1,16	1,45	1170326
PHF19	0,92	1,20E-02	1,03	1,45	5550402
RARA	0,40	2,21E-02	1,25	1,45	7050600
DNCL1	0,62	1,05E-02	1,12	1,45	4230520
HS.348514	0,25	1,43E-03	1,23	1,45	1980088
KLHL22	0,38	1,57E-02	1,25	1,45	5290259
GPS1	0,74	1,40E-03	1,06	1,45	2600279
MRPS12	0,70	6,05E-03	1,09	1,45	5310465
NOMO2	0,72	6,96E-03	1,08	1,45	7210017
GMFB	0,59	3,51E-03	1,11	1,45	5260044
AKIRIN1	0,49	1,63E-03	1,12	1,45	5820133

RBM15B	0,26	3,97E-04	1,18	1,45	5550026
CDC123	0,34	5,29E-03	1,22	1,45	6100301
MINA	0,58	5,72E-03	1,12	1,45	3360544
CTCF	0,49	6,00E-03	1,15	1,45	5220196
FTSJ2	0,44	2,80E-03	1,15	1,45	2030243
CAPN2	0,19	2,89E-04	1,20	1,45	70646
HRB	0,13	2,74E-04	1,23	1,45	6200736
ALG3	0,55	5,17E-03	1,12	1,45	2650167
CEP78	0,38	5,20E-03	1,20	1,45	4760091
ZNF428	0,65	2,24E-02	1,13	1,45	1820543
POLE	0,62	1,42E-03	1,09	1,45	2000010
NFKBIB	0,39	1,66E-03	1,16	1,45	2360537
C19ORF10	0,46	7,49E-03	1,17	1,45	1030458
DHX33	0,85	1,81E-02	1,06	1,45	2450286
PSMB5	0,72	1,37E-02	1,09	1,45	510315
MBD3	0,57	1,21E-03	1,10	1,45	610528
C15ORF53	0,27	5,49E-04	1,18	1,45	4210368
ACACA	0,15	1,45E-03	1,28	1,44	2630692
PITPNB	0,29	4,71E-04	1,17	1,44	1980687
SRPR	0,45	6,13E-04	1,11	1,44	6290112
RBM14	0,28	1,47E-03	1,21	1,44	6660343
POLD2	0,53	7,59E-03	1,14	1,44	580435
HPS1	0,23	7,12E-04	1,21	1,44	2570131
CSE1L	0,57	3,18E-02	1,17	1,44	5130674
STUB1	0,63	2,68E-03	1,09	1,44	4900431
ABCF2	0,29	4,44E-04	1,17	1,44	7100039
GART	0,42	1,38E-02	1,21	1,44	20544
DDX5	0,29	7,87E-03	1,26	1,44	7610138
SLC39A3	0,78	3,38E-03	1,06	1,44	3890167
TOMM22	0,66	1,53E-02	1,11	1,44	4880689
GNL3	0,31	9,23E-03	1,25	1,44	5270167
YARS2	0,41	4,67E-03	1,18	1,44	4570333
ILF2	0,41	3,16E-03	1,16	1,44	5690437
SNORD68	0,68	1,40E-02	1,11	1,44	1980669
FBXL18	0,47	2,32E-03	1,13	1,44	990523
XRCC5	0,27	1,48E-03	1,21	1,44	2900039
SNRPD3	0,29	2,37E-03	1,22	1,44	4290544
GTPBP4	0,58	3,88E-02	1,17	1,44	1090437
SNAPC5	0,41	2,36E-03	1,15	1,44	7610326
EIF3B	0,44	6,74E-03	1,17	1,44	5390280

HSPA5	0,63	1,08E-02	1,11	1,44	870131
TTC27	0,41	3,22E-03	1,16	1,44	3290044
ZNF511	0,32	4,62E-04	1,15	1,44	1260435
ORC6L	0,49	5,49E-03	1,14	1,44	4830343
FKBP4	0,87	1,57E-02	1,05	1,44	2100750
ATP1A1	0,41	1,58E-03	1,14	1,44	5570152
NCL	0,75	3,45E-02	1,10	1,44	3120458
LOC85390	0,48	4,80E-03	1,14	1,44	670181
C17ORF89	0,97	8,60E-03	1,01	1,43	780053
LARP1	0,82	8,85E-03	1,06	1,43	4040376
MCM10	0,34	1,70E-02	1,27	1,43	7570181
GATAD2A	0,74	4,71E-04	1,05	1,43	1570373
TUBA1C	0,37	8,96E-04	1,15	1,43	3830131
C11ORF82	0,52	1,46E-02	1,16	1,43	2570019
C9ORF142	0,71	6,00E-03	1,08	1,43	4180445
MED24	0,84	1,89E-03	1,04	1,43	1980382
LRRC33	0,48	6,87E-03	1,15	1,43	5220678
SHMT1	0,29	1,46E-02	1,29	1,43	2690528
DUS1L	0,66	6,63E-03	1,10	1,43	4040332
HPDL	0,49	8,37E-03	1,15	1,43	6480026
C12ORF43	0,38	6,70E-03	1,20	1,43	580014
LOC728620	0,66	2,38E-02	1,12	1,43	6900762
HIATL1	0,39	6,31E-03	1,19	1,43	4640427
BRIX1	0,51	2,90E-02	1,18	1,43	1110722
SNORD104	0,78	1,30E-02	1,07	1,43	6290091
YIF1A	0,39	8,35E-03	1,20	1,43	4590494
RPN1	0,29	2,54E-03	1,22	1,43	1340689
SF3B4	0,37	1,25E-02	1,23	1,43	990193
TEX261	0,31	3,95E-04	1,15	1,43	5870382
RNU105A	0,40	1,85E-03	1,15	1,43	4570110
DCTD	0,34	7,19E-04	1,15	1,43	4670519
USP13	0,39	5,58E-04	1,13	1,43	3990075
TMEM165	0,32	2,03E-03	1,19	1,43	460672
LOC653375	0,54	5,10E-03	1,12	1,43	6940674
RBM45	0,48	1,27E-02	1,17	1,43	4200035
ACTN4	0,38	5,67E-03	1,19	1,43	270437
MEOX1	0,33	4,53E-03	1,21	1,43	1230594
TOE1	0,41	1,18E-03	1,14	1,43	630673
C1ORF135	0,27	5,59E-03	1,26	1,43	150129
NHP2L1	0,36	2,41E-03	1,18	1,43	2230491

LOC729486	0,23	6,00E-03	1,29	1,43	130497
AFG3L1	0,58	4,42E-03	1,11	1,43	60609
PAFAH1B1	0,54	2,40E-02	1,16	1,43	5670075
AHCTF1	0,40	2,69E-03	1,16	1,43	6040747
DPP3	0,68	2,67E-03	1,08	1,43	4560484
PSMC4	0,63	7,46E-03	1,10	1,43	6180440
LAMP1	0,75	7,15E-03	1,07	1,43	6270100
LOC201175	0,60	7,76E-03	1,12	1,43	7330070
UBTF	0,63	1,81E-03	1,08	1,43	5670296
EXOSC2	0,50	7,50E-03	1,14	1,42	1440451
LAS1L	0,40	3,37E-03	1,17	1,42	240661
TIMM23	0,46	2,41E-02	1,20	1,42	5050608
LZTR1	0,98	1,62E-02	1,01	1,42	290086
ABCF1	0,87	4,91E-03	1,04	1,42	2190273
HNRPR	0,23	1,10E-03	1,22	1,42	6560672
C12ORF31	0,63	9,32E-03	1,11	1,42	2940546
LRP8	0,75	1,25E-02	1,08	1,42	4780411
PA2G4	0,72	3,00E-02	1,11	1,42	5270280
C3ORF26	0,73	3,77E-02	1,11	1,42	3610372
KPNA2	0,40	1,90E-02	1,22	1,42	4230196
PNO1	0,51	2,66E-03	1,12	1,42	2000450
SMARCD1	0,36	1,43E-03	1,16	1,42	3400593
CDC2L1	0,42	7,76E-03	1,18	1,42	4250739
MELK	0,22	2,24E-03	1,24	1,42	2340392
PEMT	0,61	1,05E-03	1,08	1,42	7560113
N-PAC	0,92	4,95E-03	1,03	1,42	7100424
LOC644877	0,74	6,09E-03	1,07	1,42	1110242
REEP5	0,32	1,92E-02	1,28	1,42	520324
LOC654244	0,30	1,67E-03	1,19	1,42	3190070
NOL11	0,56	1,01E-02	1,13	1,42	2630161
SLC25A10	0,46	6,39E-03	1,15	1,42	2900121
STX2	0,32	1,29E-03	1,17	1,42	5910619
ZDHHC16	0,45	2,72E-03	1,14	1,42	5700296
SRP19	0,38	9,25E-03	1,21	1,42	4210431
BOLA2	0,91	3,76E-02	1,04	1,42	60148
HSPA14	0,39	4,15E-03	1,17	1,42	6660497
ARS2	0,45	3,56E-03	1,14	1,42	3420121
LRDD	0,73	1,17E-03	1,06	1,42	580242
DDX19A	0,47	1,42E-03	1,12	1,42	7330519
COQ10B	0,47	7,78E-04	1,11	1,42	6380021

ATP6V0E2	0,34	2,80E-03	1,19	1,42	6180088
L3MBTL2	0,64	3,61E-03	1,09	1,42	450670
SNX11	0,48	4,06E-03	1,13	1,42	130446
FEN1	0,36	1,00E-02	1,22	1,42	1010719
PSPC1	0,39	3,61E-03	1,17	1,42	5690563
UBE2L3	0,34	4,34E-03	1,20	1,42	1230242
NDUFA9	0,38	5,33E-03	1,19	1,42	4810224
TOMM6	0,84	3,47E-02	1,06	1,42	2070564
CCNE1	0,67	2,68E-02	1,12	1,42	870497
SCLY	0,32	5,83E-04	1,15	1,42	1580519
CD40LG	0,32	3,66E-02	1,31	1,42	50706
GAR1	0,67	8,32E-03	1,09	1,42	130326
PPP2CA	0,38	1,69E-03	1,15	1,42	3190647
PHF5A	0,75	2,02E-03	1,06	1,42	130037
COPS7B	0,57	1,63E-03	1,09	1,42	4590661
LOC728908	0,81	2,36E-03	1,05	1,42	4230487
GLT25D1	0,70	1,32E-03	1,06	1,42	7380279
DNAJA3	0,40	3,15E-04	1,11	1,41	6560445
EIF2B2	0,60	4,50E-03	1,10	1,41	3130079
C7ORF26	0,56	1,11E-02	1,13	1,41	3780148
UCRC	0,91	4,58E-02	1,04	1,41	6130332
SNRNP70	0,38	5,23E-03	1,18	1,41	3870010
HS.145049	0,24	5,81E-04	1,19	1,41	5870605
RHBDD2	0,10	8,68E-03	1,41	1,41	6650746
ECE2	0,66	1,31E-02	1,10	1,41	4230368
LOC652864	0,49	1,04E-02	1,15	1,41	770437
MELK	0,32	7,35E-03	1,22	1,41	160097
MRPS10	0,40	4,34E-03	1,17	1,41	2060082
ATP6V0C	0,42	3,45E-03	1,15	1,41	3610397
WDR74	0,57	8,19E-03	1,12	1,41	2190537
LOC728739	0,49	7,11E-04	1,10	1,41	6350048
CCR2	0,97	2,62E-04	1,01	1,41	5960239
MRPS17	0,83	1,78E-02	1,06	1,41	2690400
LOC401238	0,49	2,14E-03	1,12	1,41	6480390
POLA1	0,31	8,74E-03	1,24	1,41	5810253
TWISTNB	0,43	4,04E-03	1,15	1,41	5570343
SMARCA2	0,56	1,73E-02	1,14	1,41	5290474
C12ORF43	0,82	9,91E-03	1,06	1,41	50414
UBE3C	0,76	4,37E-03	1,06	1,41	6560750
UBQLN1	0,30	7,51E-04	1,16	1,41	4880703

TSPAN17	0,61	2,47E-02	1,13	1,41	840403
PAK1IP1	0,49	4,83E-03	1,13	1,41	1990575
H2AFX	0,96	1,19E-02	1,01	1,40	6980497
EFHD2	0,40	9,79E-03	1,19	1,40	1070544
TTPAL	0,37	9,00E-04	1,14	1,40	2370504
EFR3A	0,32	6,40E-03	1,22	1,40	110161
YTHDF1	0,63	1,51E-02	1,11	1,40	2850441
ATP2C1	0,21	3,62E-03	1,26	1,40	780367
TUBGCP5	0,30	5,50E-03	1,22	1,40	430315
MFSD1	0,47	4,11E-03	1,13	1,40	510288
DDX54	0,72	1,97E-03	1,06	1,40	4760301
APRT	0,74	2,02E-02	1,08	1,40	6510603
ZDHHC8	0,72	2,41E-03	1,06	1,40	4590154
FIBP	0,67	5,43E-03	1,09	1,40	6590504
C9ORF37	0,42	2,09E-03	1,14	1,40	4200204
FBXW2	0,49	6,72E-04	1,10	1,40	1660332
LOC642661	0,34	5,14E-04	1,14	1,40	3800577
KLHL8	0,56	6,47E-04	1,08	1,40	7100349
RPS26	0,51	2,15E-03	1,11	1,40	5490066
LOC652388	0,43	8,22E-04	1,12	1,40	5690068
ITPA	0,61	1,48E-02	1,12	1,40	360445
SEPHS2	0,47	1,92E-02	1,18	1,40	2030736
PDCL3	0,90	4,46E-02	1,04	1,40	460750
CLSPN	0,62	3,12E-04	1,06	1,40	4890634
PEA15	0,44	5,35E-04	1,10	1,40	3610228
LOC100134189	0,51	3,03E-03	1,11	1,40	830674
CENPM	0,64	3,41E-02	1,13	1,40	3930324
VPS25	0,69	1,68E-03	1,07	1,40	1090577
C13ORF23	0,45	1,32E-02	1,17	1,40	6660711
GTF2A2	0,73	1,16E-02	1,08	1,40	2450368
LOC400506	0,69	8,27E-03	1,08	1,40	4760113
LOC387882	0,40	4,39E-02	1,26	1,40	5810743
RPP25	0,39	3,77E-03	1,16	1,40	670598
ATAD3B	0,28	2,94E-03	1,21	1,40	7330091
C17ORF96	0,49	3,47E-02	1,19	1,40	6250427
LOC653884	0,25	3,18E-03	1,23	1,40	290687
CCDC85B	0,81	7,28E-03	1,05	1,40	6400646
MRPL35	0,48	1,63E-03	1,11	1,40	5340100
EXOSC6	0,57	6,13E-03	1,11	1,40	6330025
ETF1	0,53	1,28E-02	1,14	1,40	3170181

HSP90AA1	0,78	2,30E-02	1,07	1,40	7050332
PSMD3	0,40	3,21E-03	1,15	1,40	60360
WDR18	0,70	9,84E-03	1,09	1,40	7400554
LMNB1	0,53	4,90E-03	1,12	1,40	3420593
FLNA	0,45	5,25E-03	1,15	1,40	6250242
NSMCE4A	0,52	1,05E-02	1,13	1,40	6510025
PSMD8	0,37	4,80E-03	1,18	1,40	650369
ABL1	0,60	1,96E-03	1,09	1,40	4180088
TRIM26	0,50	2,95E-04	1,08	1,40	6020463
PEMT	0,49	1,76E-03	1,11	1,40	1780411
RPS19BP1	0,86	5,63E-03	-1,04	1,40	6590209
PYGB	0,38	1,98E-03	1,15	1,40	4540326
WDR12	0,49	4,21E-02	1,20	1,40	2350068
CCT5	0,38	4,22E-03	1,17	1,40	540170
LOC730167	0,66	1,24E-02	1,10	1,40	130414
IPO5	0,39	4,95E-03	1,17	1,40	1440632
H2AFY	0,32	9,92E-03	1,23	1,40	4260414
HSP90AA1	0,72	4,02E-02	1,10	1,40	3390544
PINX1	0,74	9,57E-03	1,07	1,40	3130066
RABEPK	0,54	1,52E-02	1,14	1,39	460519
DPP3	0,43	5,09E-03	1,15	1,39	6760274
MCRS1	0,60	2,36E-03	1,09	1,39	1740504
AVEN	0,49	1,18E-03	1,10	1,39	3800634
EIF4A3	0,41	4,19E-03	1,15	1,39	5270110
ME2	0,48	1,71E-02	1,17	1,39	6200408
MPV17L2	0,56	1,98E-03	1,09	1,39	6370278
DPH3	0,38	5,29E-03	1,17	1,39	7380465
FAR2	0,14	3,62E-03	1,30	1,39	6560291
BCCIP	0,45	4,46E-02	1,22	1,39	2940040
CHAF1B	0,43	6,50E-03	1,16	1,39	4610731
WDR43	0,60	5,15E-03	1,10	1,39	3130400
TMEM208	0,99	1,10E-02	-1,00	1,39	4120066
MAP4K1	0,56	1,56E-02	1,13	1,39	4590477
KPNA6	0,53	3,50E-03	1,11	1,39	5340021
NHP2L1	0,69	4,66E-02	1,12	1,39	4230243
ATG7	0,27	2,42E-03	1,21	1,39	5220754
NCAPD3	0,50	2,76E-03	1,11	1,39	1570551
LOC100134189	0,35	6,40E-03	1,20	1,39	5360576
GLIPR2	0,13	3,31E-02	1,48	1,39	830278
CALU	0,56	8,71E-03	1,12	1,39	940431

MCM4	0,72	4,44E-02	1,11	1,39	2630711
SNRNP70	0,75	8,99E-03	1,07	1,39	3120133
ATP6V0C	0,46	5,47E-03	1,14	1,39	2360138
MRPL52	0,51	1,99E-02	1,15	1,39	1240360
LACTB2	0,37	1,86E-02	1,23	1,39	4050711
AIFM1	0,51	2,51E-02	1,16	1,39	3290341
LLPH	0,48	9,76E-03	1,15	1,39	3190274
NAGPA	1,00	1,14E-02	1,00	1,39	6400630
LOC85389	0,63	2,51E-02	1,12	1,39	3610753
ZNF696	0,48	2,33E-03	1,12	1,39	3310523
CDC45L	0,23	9,77E-04	1,19	1,39	2320170
COPS6	0,49	2,76E-03	1,11	1,39	6350114
FAM82A2	0,92	1,44E-02	1,03	1,39	4730184
LAGE3	0,78	5,24E-03	1,06	1,39	1240482
FUS	0,25	3,23E-03	1,22	1,39	6130161
LOC389168	0,60	6,41E-03	1,10	1,39	3060148
DDA1	0,59	7,25E-04	1,07	1,39	7050349
NOC2L	0,32	2,62E-04	1,12	1,39	7570356
NP	0,91	2,26E-02	1,03	1,39	6840075
DHRS11	0,45	7,65E-03	1,15	1,39	6980300
EIF2B3	0,50	3,09E-02	1,17	1,39	5700647
EXO1	0,29	9,84E-04	1,17	1,39	2690458
PRPF40A	0,43	2,78E-03	1,13	1,39	4890209
EWSR1	0,24	6,71E-03	1,26	1,38	670072
MRPL34	0,88	4,34E-03	1,03	1,38	5960114
PAXIP1	0,36	4,07E-03	1,17	1,38	3830372
ACTL6A	0,30	1,27E-02	1,24	1,38	5220358
TMEM167A	0,64	1,05E-02	1,10	1,38	3870008
GTF2H2B	0,44	1,07E-02	1,16	1,38	1510138
TTC4	0,44	2,67E-03	1,13	1,38	3060347
UCHL5IP	0,50	7,12E-04	1,09	1,38	6350750
TMEM4	0,67	2,02E-02	1,10	1,38	1510564
EIF3J	0,41	6,50E-03	1,16	1,38	4280020
TRMT1	0,55	3,69E-03	1,10	1,38	7650278
ACVR1B	0,41	7,00E-03	1,16	1,38	4570240
NOMO3	0,38	6,02E-03	1,18	1,38	6370181
PPP1CA	0,48	1,21E-02	1,15	1,38	3990368
PIGU	0,30	1,03E-03	1,16	1,38	3180554
TRIOBP	0,43	1,42E-03	1,12	1,38	2900246
MKI67	0,41	3,64E-03	1,14	1,38	20364

SNORA73B	0,53	5,43E-03	1,11	1,38	6620039
NARG1	0,41	1,80E-02	1,20	1,38	3140524
BAZ1B	0,34	3,06E-03	1,17	1,38	4280347
NOP14	0,70	3,69E-03	1,07	1,38	5560121
SPRYD3	0,54	1,50E-03	1,09	1,38	3180521
HS.572219	0,47	1,24E-02	1,16	1,38	4200753
WDR4	0,41	1,11E-02	1,18	1,38	4890240
IER5	0,87	2,73E-02	-1,05	1,38	650241
MRPL4	0,85	7,49E-03	1,04	1,38	6220450
COX4NB	0,72	5,62E-03	1,07	1,38	2630553
TXNDC9	0,32	5,59E-03	1,20	1,38	4290521
ITGB1	0,11	2,02E-02	1,44	1,38	110440
MRPL36	0,38	7,10E-03	1,18	1,38	20465
C1ORF216	0,56	4,50E-03	1,10	1,38	4670608
EIF2B1	0,54	2,38E-03	1,10	1,38	6520682
C13ORF27	0,45	1,37E-02	1,16	1,38	1850068
PHCA	0,31	3,12E-03	1,19	1,38	1230017
C1ORF53	0,56	2,68E-03	1,09	1,38	990382
AHCTF1	0,36	5,16E-03	1,18	1,38	1230196
SCO1	0,41	3,95E-03	1,15	1,38	3450563
C19ORF24	0,84	1,68E-03	1,03	1,38	10189
TTF2	0,20	1,02E-02	1,30	1,38	2190220
TOMM34	0,28	1,56E-03	1,18	1,38	1190445
BTBD6	0,49	1,11E-02	1,14	1,38	6900307
CHN1	0,33	1,50E-02	1,23	1,38	610332
MCOLN1	0,85	1,93E-03	1,03	1,38	6450056
HIGD1A	0,39	1,42E-02	1,19	1,38	3780019
CYB561D2	0,58	1,10E-02	1,11	1,37	4830328
DUSP14	0,55	1,77E-02	1,13	1,37	4150278
ESRRA	0,74	3,99E-03	1,06	1,37	1660541
SETD4	0,50	9,84E-04	1,09	1,37	6380709
RGL1	0,43	4,37E-03	1,14	1,37	3180039
CCDC137	0,36	6,11E-04	1,13	1,37	7100681
RBM12	0,43	7,84E-03	1,16	1,37	2850438
GTSE1	0,41	4,35E-03	1,15	1,37	6980382
FBXW5	0,66	2,64E-03	1,07	1,37	1340427
LYRM4	0,50	1,62E-02	1,15	1,37	1240487
CLTB	0,45	9,45E-03	1,15	1,37	1110095
SLC30A1	0,37	5,48E-04	1,12	1,37	5490546
CYTSA	0,70	6,71E-03	1,08	1,37	6020209

RASAL3	0,56	1,68E-02	1,13	1,37	520273
LARS2	0,78	2,68E-03	1,05	1,37	4280767
OGFOD1	0,50	4,35E-03	1,12	1,37	6330242
GADD45G	0,30	3,21E-02	1,30	1,37	5570114
LOC727980	0,70	3,69E-03	1,07	1,37	1240154
SELI	0,20	1,08E-03	1,20	1,37	4280370
EZH2	0,27	2,38E-03	1,20	1,37	4180524
TBRG4	0,79	5,50E-03	1,05	1,37	6420152
C7ORF49	0,35	5,39E-03	1,18	1,37	7150259
ACOT1	0,39	8,20E-03	1,17	1,37	4900438
MSI2	0,16	8,33E-04	1,21	1,37	7040369
QTRTD1	0,29	3,27E-03	1,19	1,37	2490204
NSUN5	0,79	4,58E-03	1,05	1,37	5340458
KLHL18	0,51	3,73E-03	1,11	1,37	4050239
DDX49	0,53	2,96E-03	1,10	1,37	450309
ZNF259	0,55	5,29E-03	1,10	1,37	7050561
GNPTAB	0,87	1,29E-02	-1,04	1,37	2490670
FLJ20718	0,85	1,14E-02	1,04	1,37	5080746
CCT7	0,76	9,20E-03	1,06	1,37	5270500
SEH1L	0,46	7,49E-03	1,14	1,37	580196
CNDP2	0,62	6,26E-03	1,09	1,37	3390017
SLC19A1	0,80	3,02E-03	1,05	1,37	4760014
B3GAT3	0,33	1,76E-03	1,16	1,37	7510563
SFMBT1	0,27	9,11E-04	1,17	1,37	1780152
ME2	0,70	3,23E-02	1,10	1,37	7550521
HSPBAP1	0,20	1,42E-03	1,21	1,37	6420142
ALDH4A1	0,50	1,69E-03	1,10	1,37	1470427
PPP2CA	0,34	8,24E-03	1,20	1,37	1740240
GART	0,29	6,71E-03	1,22	1,37	3780435
MRPL46	0,78	9,32E-03	1,06	1,37	4210762
TUBB	0,30	3,14E-03	1,19	1,37	6580474
SFRS1	0,40	1,70E-02	1,19	1,37	430026
DDX1	0,48	1,14E-02	1,14	1,37	610324
GCN1L1	0,57	5,18E-03	1,10	1,37	6270450
TOP1	0,40	2,68E-03	1,14	1,37	1570537
CHERP	0,67	1,18E-03	1,06	1,37	3130180
CCT7	0,47	3,14E-02	1,18	1,37	7160719
TEX10	0,62	1,77E-02	1,11	1,37	6770044
ORAOV1	0,37	4,38E-03	1,16	1,37	4880053
KPNB1	0,51	1,81E-02	1,14	1,36	6840577

IP6K1	0,65	3,73E-03	1,08	1,36	6040064
TIMM23	0,67	4,85E-02	1,12	1,36	3840446
LOC729148	0,47	5,30E-03	1,13	1,36	5670397
C16ORF61	0,42	3,03E-03	1,13	1,36	6400025
NHP2	0,78	3,23E-02	1,08	1,36	6550291
STAG1	0,40	1,76E-03	1,13	1,36	7570026
BCLAF1	0,49	3,89E-02	1,18	1,36	3870634
MYH9	0,48	7,16E-03	1,13	1,36	6620136
C17ORF85	0,62	3,14E-03	1,08	1,36	3180343
MED27	0,49	6,57E-03	1,12	1,36	5220392
TRIM37	0,40	1,26E-03	1,12	1,36	4730564
C9ORF86	0,79	6,94E-03	1,05	1,36	1780762
GNL3L	0,60	3,54E-02	1,13	1,36	5900746
CHCHD10	0,95	4,77E-02	1,02	1,36	940010
CRK	0,66	1,36E-03	1,06	1,36	6550196
SF3B3	0,72	5,16E-03	1,07	1,36	1090239
RPL7L1	0,91	3,39E-02	1,03	1,36	1770609
WDR1	0,41	1,42E-02	1,18	1,36	7150475
POLR2F	0,99	1,44E-02	-1,01	1,36	6370762
GUF1	0,78	9,71E-03	1,06	1,36	5890338
LOC390557	0,82	6,69E-03	1,05	1,36	6270193
ANKRD35	0,66	1,41E-02	1,09	1,36	4590377
TRMT61A	0,62	3,37E-03	1,08	1,36	4150484
SLC25A3	0,15	2,17E-03	1,24	1,36	4040224
SLC9A3R1	0,38	2,20E-02	1,21	1,36	2450452
UTP15	0,41	2,89E-03	1,14	1,36	1770195
RRP8	0,45	3,54E-03	1,12	1,36	4890537
LOC728263	0,49	1,04E-03	1,09	1,36	4610292
MED24	0,95	3,68E-03	-1,01	1,36	7400411
TXNRD1	0,52	2,02E-02	1,14	1,36	2320133
C13ORF3	0,34	7,77E-03	1,19	1,36	4180133
EXOC6	0,47	3,54E-03	1,12	1,36	7330196
RSC1A1	0,44	3,02E-03	1,12	1,36	1850176
PRMT6	0,53	9,17E-03	1,12	1,36	7200707
STRAP	0,41	2,55E-02	1,20	1,36	4200672
COBRA1	0,74	4,30E-03	1,06	1,36	6860113
MARCH2	0,40	3,08E-03	1,14	1,36	1470196
NSUN5B	0,57	2,56E-02	1,13	1,36	4070367
ZNF668	0,31	2,25E-03	1,17	1,36	5820647
CDK9	0,41	4,50E-03	1,14	1,36	430767

CDK4	0,58	2,40E-02	1,13	1,36	7380110
NASP	0,40	2,24E-02	1,20	1,36	4260682
LOC644584	0,36	6,79E-03	1,18	1,36	2030619
SIGMAR1	0,47	4,64E-03	1,12	1,36	510136
MCM3	0,39	1,18E-02	1,18	1,36	6650053
CHRAC1	0,19	5,80E-04	1,18	1,36	610300
LOC148915	0,47	4,20E-03	1,12	1,36	3310392
ANXA2	0,69	2,09E-02	1,09	1,36	4780615
C5ORF35	0,56	1,76E-02	1,12	1,36	6100239
SDCCAG3	0,43	8,25E-03	1,15	1,36	7040553
ARPC4	0,40	3,82E-03	1,14	1,36	2690601
C19ORF62	0,47	7,11E-03	1,13	1,36	2760259
ARHGAP10	0,16	1,11E-02	1,31	1,36	2000669
TFAM	0,32	1,25E-02	1,22	1,36	650326
HELLS	0,48	3,80E-03	1,11	1,36	4540768
ACSL1	0,74	2,72E-02	1,08	1,36	1030431
CXORF64	0,45	1,53E-02	1,16	1,35	3180242
LOC654174	0,55	5,68E-03	1,10	1,35	6270367
FTSJ1	0,36	2,56E-03	1,15	1,35	1110605
WDR12	0,57	4,60E-02	1,15	1,35	5270315
MRPL17	0,32	1,43E-02	1,22	1,35	6660270
TAF2	1,00	3,81E-03	1,00	1,35	1410341
ARMC6	0,84	3,54E-03	1,04	1,35	2060128
UBE2M	0,52	3,33E-03	1,10	1,35	6180619
TRAPPC4	0,72	3,86E-02	1,10	1,35	1230639
IMPDH1	0,81	1,51E-02	1,06	1,35	3120431
C7ORF20	0,55	1,76E-03	1,08	1,35	6560608
FAM86A	0,42	3,80E-03	1,13	1,35	6480379
CHAF1A	0,41	1,30E-02	1,17	1,35	2120097
SLC25A25	0,51	1,92E-02	1,14	1,35	10487
MAPRE1	0,38	7,40E-03	1,17	1,35	6060731
WDR55	0,56	1,40E-02	1,12	1,35	5700669
CEP78	0,54	1,49E-02	1,12	1,35	5570142
OTUD6B	0,51	4,58E-03	1,11	1,35	5550537
IVD	0,45	8,14E-03	1,14	1,35	6020398
C14ORF109	0,46	7,40E-03	1,13	1,35	1820092
NUBP2	0,84	9,49E-03	1,04	1,35	6960730
KHSRP	0,46	1,31E-02	1,15	1,35	7000470
CCNA2	0,49	1,43E-02	1,14	1,35	2650608
TMEM99	0,75	2,83E-02	1,08	1,35	3310471

DHDDS	0,80	4,02E-03	1,04	1,35	2350576
C22ORF28	0,48	4,37E-03	1,11	1,35	5810632
TSEN2	0,65	3,61E-02	1,11	1,35	6900176
IP6K1	0,73	3,95E-03	1,06	1,35	6130537
SEH1L	0,31	9,23E-03	1,21	1,35	6760504
LOC401115	0,57	1,52E-02	1,12	1,35	6280167
KIF1B	0,39	2,10E-02	1,20	1,35	7040707
VKORC1L1	0,41	3,92E-03	1,14	1,35	6510189
ADCY1	0,67	1,48E-02	1,09	1,35	580561
NUDT21	0,51	7,86E-03	1,12	1,35	3170446
MCM3	0,49	2,31E-02	1,15	1,35	6290494
CCDC90A	0,51	3,35E-02	1,16	1,35	6270373
SEC16A	0,70	1,80E-02	1,08	1,35	2600343
NADK	0,40	1,18E-03	1,12	1,35	6980753
CIITA	0,48	2,25E-03	1,10	1,35	4210167
ACTL6A	0,29	1,80E-02	1,25	1,35	5080603
CMTM6	0,42	2,22E-02	1,18	1,35	1470520
LOC100132418	0,50	7,31E-04	1,08	1,35	5870754
NUTF2	0,40	3,86E-02	1,22	1,35	3140563
NUP210	0,78	4,09E-02	1,08	1,35	2320215
NUDT5	0,37	2,52E-02	1,22	1,35	1470242
MCM10	0,68	2,07E-02	1,09	1,35	6580685
LSG1	0,35	1,09E-02	1,19	1,35	6660619
ZNF828	0,31	2,28E-02	1,25	1,35	4480504
LIG3	0,72	8,08E-03	1,07	1,34	3460431
ANAPC11	0,81	9,36E-03	1,05	1,34	10220
UPF2	0,59	8,19E-03	1,10	1,34	2750189
LOC653888	0,36	3,55E-02	1,24	1,34	4860093
AAGAB	0,65	1,15E-02	1,09	1,34	5490500
DPH3	0,82	2,31E-02	1,06	1,34	6510279
BCLAF1	0,47	3,87E-02	1,18	1,34	3800176
TAP2	0,72	2,61E-02	1,08	1,34	2650156
FAM100A	0,43	2,62E-03	1,12	1,34	1660086
CRK	0,72	1,66E-03	1,05	1,34	4780086
APP	0,36	6,67E-03	1,17	1,34	3370577
HMGN2	0,36	1,13E-02	1,19	1,34	3930577
CKAP5	0,45	1,68E-02	1,16	1,34	670500
UCHL5	0,21	1,54E-02	1,29	1,34	2750746
DHX35	0,46	3,14E-03	1,11	1,34	20192
PDIA6	0,49	1,11E-02	1,13	1,34	10463

EIF4A1	0,51	6,54E-03	1,11	1,34	1450670
TXNRD2	0,89	5,18E-03	1,03	1,34	2230397
RNF126	0,51	2,40E-02	1,14	1,34	6330561
EIF5B	0,49	1,52E-02	1,14	1,34	7330047
APITD1	0,73	4,46E-02	1,09	1,34	5960709
PPIL5	0,38	1,05E-02	1,17	1,34	4830427
EED	0,27	2,68E-03	1,18	1,34	5700743
RFC3	0,32	5,05E-03	1,18	1,34	3890309
RAB35	0,49	2,57E-03	1,10	1,34	3390192
SEC11C	0,24	3,21E-02	1,31	1,34	150082
ZDHHC14	0,41	2,80E-03	1,12	1,34	7610091
AP4E1	0,50	6,74E-03	1,11	1,34	270343
MED27	0,29	3,08E-03	1,18	1,34	5360446
HNRNPK	0,15	1,83E-03	1,22	1,34	7000463
DPP3	0,53	8,53E-03	1,11	1,34	430408
LSM7	0,69	7,79E-03	1,07	1,34	5670315
NAAA	0,36	1,26E-02	1,19	1,34	5130176
COX17	0,84	3,09E-02	1,05	1,34	630735
CACYBP	0,81	1,74E-02	1,05	1,34	5890736
DARS2	0,41	2,86E-02	1,19	1,34	5910097
TRIM28	0,66	2,84E-03	1,07	1,34	3890600
AMD1	0,56	1,55E-02	1,12	1,34	3870619
RAD51C	0,64	4,98E-02	1,12	1,34	5910215
LOC100132918	0,77	2,08E-02	1,07	1,34	3130504
CDC2L2	0,67	8,16E-03	1,08	1,34	5690152
FAM188A	0,89	1,14E-02	1,03	1,34	3060661
HSPBP1	0,59	1,85E-02	1,11	1,34	5360220
PSMD6	0,48	1,68E-02	1,14	1,34	5810070
LSM1	0,51	5,21E-03	1,11	1,34	6590196
FBXO22	0,70	2,07E-02	1,08	1,34	4880685
RPS6KB2	0,48	3,95E-03	1,11	1,34	4150136
SRP9	0,51	1,62E-02	1,13	1,34	3930358
SNORA76	0,48	5,43E-03	1,12	1,34	4230477
LOC100128266	0,51	4,56E-02	1,16	1,34	10152
TSR1	0,54	9,84E-03	1,11	1,34	7550133
NDUFS8	0,23	4,83E-03	1,22	1,34	1070538
NAE1	0,27	1,32E-02	1,24	1,34	4010243
TMEM50B	0,57	3,86E-02	1,14	1,34	3460307
DDX55	0,34	1,18E-02	1,19	1,34	5960672
PIN1	0,49	4,77E-03	1,11	1,34	4640168

GPAA1	0,91	8,28E-03	1,02	1,34	2480288
BRI3BP	0,89	2,13E-02	1,04	1,34	6840348
PIGK	0,33	4,78E-03	1,17	1,34	6180300
E4F1	0,60	3,26E-03	1,08	1,34	3390068
SLC25A20	0,89	5,50E-03	-1,03	1,34	6220161
DPH3	0,92	1,87E-02	1,03	1,34	6250397
NOS3	0,41	2,32E-02	1,18	1,34	2480195
KEAP1	0,80	1,83E-03	1,04	1,33	3420497
SLC4A7	0,34	2,17E-03	1,15	1,33	940035
STOML2	0,94	1,50E-02	1,02	1,33	6650458
C17ORF70	0,87	4,20E-02	1,05	1,33	4540064
TMEM19	0,41	3,52E-03	1,13	1,33	110196
TRMT5	0,42	1,17E-02	1,15	1,33	5960253
KLC1	0,30	6,30E-03	1,19	1,33	1510736
TUFM	0,72	3,61E-02	1,09	1,33	6370097
CNPY2	0,83	1,68E-02	1,05	1,33	4150475
AUH	0,44	3,47E-02	1,18	1,33	7330180
MCM5	0,31	1,31E-02	1,21	1,33	7330253
CFL1	0,46	1,38E-02	1,14	1,33	4250458
STUB1	0,51	3,54E-03	1,10	1,33	1850445
DPYSL2	0,34	1,44E-02	1,20	1,33	3290685
TBRG4	0,87	1,88E-02	1,04	1,33	5810541
GNL3L	0,86	1,49E-03	1,03	1,33	7610408
LMO4	0,07	4,11E-02	1,53	1,33	5910523
ERI3	0,40	7,91E-03	1,15	1,33	4830747
XPO4	0,51	1,31E-03	1,08	1,33	2940343
DYNLL2	0,87	2,91E-02	1,04	1,33	3400551
DDB1	0,46	7,88E-03	1,13	1,33	2370100
PSMC1	0,27	7,50E-04	1,15	1,33	830608
PGD	0,55	3,41E-02	1,14	1,33	2900594
PPP2R4	0,70	4,06E-03	1,06	1,33	6040114
GLRX2	0,50	1,15E-02	1,12	1,33	6980274
CHTF18	0,95	6,32E-03	-1,02	1,33	1770689
EXO1	0,38	1,12E-02	1,17	1,33	1770646
POLR2D	0,72	1,91E-02	1,08	1,33	6900025
TNFSF14	0,39	2,89E-02	1,20	1,33	770592
USP13	0,68	3,80E-03	1,07	1,33	7160037
C13ORF23	0,51	1,06E-02	1,12	1,33	1260575
SET	0,60	1,56E-02	1,10	1,33	4230224
CCDC99	0,44	1,82E-02	1,16	1,33	520528

E2F3	0,47	1,27E-02	1,14	1,33	3930059
XPR1	0,40	1,75E-03	1,12	1,33	5290246
CRY1	0,16	7,23E-03	1,27	1,33	1940253
KIF3B	0,28	9,32E-03	1,22	1,33	450398
SLC25A44	0,31	4,35E-03	1,17	1,33	4810615
MARS	0,56	4,52E-02	1,14	1,33	2690707
TRAPPC2L	0,94	3,23E-02	1,02	1,33	1450082
RAD51L3	0,45	2,36E-03	1,11	1,33	3890347
LAMP2	0,75	6,54E-03	1,06	1,33	6480142
ORC5L	0,37	2,89E-02	1,21	1,33	3800110
SLC20A2	0,49	3,35E-03	1,10	1,33	6590037
CUL2	0,47	8,68E-03	1,13	1,33	2000193
HYOU1	0,46	4,50E-03	1,12	1,33	5700041
COBRA1	0,45	6,48E-03	1,13	1,33	6380044
DPAGT1	0,63	3,92E-03	1,07	1,33	6290719
USP1	0,30	9,47E-03	1,20	1,33	3400008
TMED9	0,68	3,49E-02	1,10	1,33	5390202
HERC2	0,40	3,44E-03	1,13	1,33	6130674
ALG14	0,82	2,21E-02	1,05	1,32	50128
LASS2	0,79	9,00E-03	1,05	1,32	6380154
PITPNA	0,74	5,66E-03	1,06	1,32	6590243
LOC647150	0,35	2,24E-02	1,21	1,32	630360
ZDHHC16	0,41	4,73E-03	1,13	1,32	1770358
PDIA5	0,51	1,27E-02	1,12	1,32	3170491
LOC652672	0,61	1,14E-02	1,09	1,32	6960020
NDUFB2	0,69	3,09E-02	1,09	1,32	4150687
SNORD110	0,69	3,98E-03	1,06	1,32	1240273
TUBA1A	0,39	2,86E-02	1,20	1,32	4490577
PKMYT1	0,81	2,20E-02	1,05	1,32	2510678
SCAP	0,67	1,15E-02	1,08	1,32	3140382
ILF3	0,90	1,11E-02	1,03	1,32	1450075
DBNL	0,51	1,08E-02	1,12	1,32	2140671
SLC4A7	0,41	3,73E-02	1,20	1,32	620543
TMEM185A	0,79	5,52E-03	1,05	1,32	4640196
GATA3	0,29	3,89E-02	1,28	1,32	5910719
VPS33A	0,34	1,24E-02	1,19	1,32	7510541
SPATA5L1	0,93	7,61E-03	1,02	1,32	7400619
HS.104792	0,27	5,36E-03	1,19	1,32	10600
ARPC1B	0,40	4,74E-02	1,21	1,32	130717
RCE1	0,49	5,29E-03	1,11	1,32	3520288

NUP153	0,67	2,33E-02	1,09	1,32	3840131
PLD6	0,36	3,17E-03	1,14	1,32	1980474
LRPAP1	0,96	3,03E-02	1,02	1,32	2650521
URM1	0,84	5,51E-03	1,04	1,32	60390
ASCC3	0,57	1,64E-02	1,11	1,32	650722
GTF3C2	0,92	1,22E-03	1,02	1,32	2640437
SFRS15	0,60	4,13E-03	1,08	1,32	990056
ASCC2	0,49	7,85E-03	1,11	1,32	1570523
LOC732360	1,00	8,67E-03	1,00	1,32	3940274
KIAA0194	0,99	8,52E-03	1,00	1,32	2850743
NBN	0,72	3,58E-02	1,08	1,32	3610343
RBL1	0,41	3,80E-03	1,12	1,32	2900132
LOC441714	0,41	4,37E-03	1,13	1,32	770706
TUBB4Q	0,74	2,40E-02	1,07	1,32	1990327
LOC221710	0,43	7,96E-03	1,14	1,32	4670703
PPP1CA	0,75	4,70E-02	1,08	1,32	4210414
ANKRD54	0,69	1,46E-02	1,08	1,32	2340598
LOC729406	0,86	4,39E-02	1,05	1,32	3440064
SBDSP	0,46	8,28E-03	1,12	1,32	5260717
CHMP6	0,58	4,56E-03	1,08	1,32	5690520
FASTKD1	0,41	1,03E-02	1,15	1,32	4810546
USP5	0,60	1,44E-02	1,10	1,32	6560747
C1ORF144	0,44	5,29E-03	1,12	1,32	2030044
ABHD11	0,57	6,72E-04	1,06	1,32	1940068
SNRPG	0,61	4,86E-02	1,12	1,32	2940168
ARPC4	0,40	1,73E-02	1,17	1,32	2600619
AGPAT9	0,21	2,73E-02	1,30	1,32	2060477
C19ORF48	0,81	4,45E-02	1,06	1,32	2650349
SBDSP	0,63	3,64E-03	1,07	1,32	4900707
WDR40A	0,79	1,06E-02	1,05	1,32	3290091
RNF220	0,47	5,20E-03	1,11	1,32	4540328
TSR2	0,51	1,92E-03	1,09	1,32	6250390
PSMD9	0,43	2,32E-03	1,11	1,32	2140189
UGCGL1	0,27	1,24E-03	1,15	1,32	3170592
POLE3	0,58	2,25E-02	1,11	1,32	1300491
CHEK1	0,37	1,70E-02	1,18	1,32	7200270
BPGM	0,65	3,56E-03	1,07	1,32	3060682
C12ORF49	0,45	1,06E-02	1,13	1,31	3170102
ST7	0,53	1,90E-02	1,12	1,31	4570575
EXOSC3	0,58	1,96E-02	1,11	1,31	6130196

SNORD48	0,64	4,58E-03	1,07	1,31	3190382
SLC39A3	0,81	1,15E-02	1,05	1,31	5670136
CYC1	0,75	2,97E-02	1,07	1,31	1770520
LRPPRC	0,86	9,30E-03	1,04	1,31	6380064
CTU2	0,40	4,73E-03	1,13	1,31	5490086
DHX9	0,56	1,89E-02	1,11	1,31	3930689
SFRS13A	0,31	7,03E-03	1,18	1,31	6110014
VPS24	0,37	1,16E-02	1,17	1,31	2140634
COMTD1	0,55	4,40E-02	1,14	1,31	6960377
PSPC1	0,78	1,97E-02	1,06	1,31	4200414
MRPS12	0,99	1,08E-02	-1,00	1,31	6980487
ELOVL1	0,49	5,77E-03	1,11	1,31	3370722
LMF2	0,94	1,02E-02	1,02	1,31	1740576
HSPA4	0,42	3,89E-02	1,19	1,31	430142
CCT4	0,37	1,56E-02	1,18	1,31	6290014
HSPA9	0,63	3,34E-02	1,11	1,31	430630
C9ORF78	0,55	2,23E-02	1,12	1,31	3890524
HYOU1	0,70	3,40E-02	1,09	1,31	520189
TIMM8A	0,41	1,73E-02	1,16	1,31	3360156
TLCD1	0,50	7,77E-03	1,11	1,31	1430681
DUT	0,25	4,80E-02	1,32	1,31	6330494
NUPL2	0,45	1,68E-02	1,14	1,31	5340209
TCHP	0,34	5,36E-03	1,16	1,31	730687
UBLCP1	0,45	2,79E-02	1,16	1,31	10278
SELS	0,77	2,73E-02	1,06	1,31	6020474
ADAT1	0,41	8,08E-03	1,14	1,31	1710204
MRPS16	0,39	2,41E-02	1,18	1,31	4830577
SLC7A6	0,98	1,09E-02	1,01	1,31	6380364
RB1	0,92	1,31E-02	1,02	1,31	6280474
RFWD3	0,51	2,40E-02	1,13	1,31	5340167
FOXM1	0,66	1,24E-02	1,08	1,31	540053
PXMP2	0,64	3,49E-02	1,10	1,31	5820324
CDCA4	0,82	1,18E-02	1,04	1,31	290333
KIAA0100	0,61	1,09E-02	1,09	1,31	5420204
AZI1	0,54	2,08E-02	1,12	1,31	3390605
FAM168B	0,94	4,50E-03	1,02	1,31	5270187
SNHG3-RCC1	0,44	5,56E-03	1,12	1,31	5810470
PPAT	0,80	1,96E-02	1,05	1,31	4070132
ACAD8	0,58	1,30E-02	1,10	1,31	730671
XRN2	0,48	2,57E-02	1,15	1,31	2570671

HSPC171	0,80	3,54E-02	1,06	1,31	5820255
DDX18	0,48	1,12E-02	1,12	1,31	6060201
CDC34	0,97	1,98E-03	1,01	1,31	1710278
LOC652324	0,72	1,81E-02	1,07	1,31	5360168
PGRMC1	0,35	5,70E-03	1,15	1,31	2970521
DHX15	0,49	2,46E-02	1,14	1,31	4590333
MSTO1	0,30	5,24E-03	1,17	1,31	290554
ORAI1	0,41	4,69E-03	1,12	1,31	5700717
APP	0,29	9,21E-03	1,20	1,31	650110
HS.551538	0,84	7,65E-03	1,04	1,31	5560544
WDR36	0,39	1,16E-02	1,16	1,31	6650100
HNRNPH1	0,40	9,33E-03	1,15	1,31	5270754
EID3	0,87	1,96E-02	1,04	1,31	3190672
PHF19	0,99	1,46E-02	-1,00	1,31	7650474
OSBPL1A	0,05	3,02E-03	1,30	1,31	7650243
PIK3R2	0,96	1,42E-02	-1,01	1,31	2140097
SUPT16H	0,73	1,94E-02	1,07	1,31	780753
NCOA5	0,60	2,78E-02	1,11	1,31	2690292
THOP1	0,60	9,10E-03	1,09	1,31	770672
BRD7	0,92	1,68E-02	1,02	1,31	430040
DHX29	0,66	1,23E-02	1,08	1,31	4850519
TH1L	0,83	2,76E-02	1,05	1,31	6250017
EEF2K	0,46	5,67E-03	1,11	1,31	3420300
CUL1	0,41	1,30E-02	1,15	1,31	70601
XPR1	0,35	5,33E-03	1,15	1,31	4010075
IFFO1	0,71	2,12E-02	1,07	1,31	6620050
LOC387703	0,32	3,43E-02	1,23	1,31	2850356
LBR	0,37	2,46E-02	1,19	1,31	5080524
CAB39	0,49	8,17E-03	1,11	1,31	7000017
ZC3H14	0,57	8,79E-03	1,09	1,31	3940053
RNF167	0,51	2,83E-02	1,13	1,31	1580521
SMARCB1	0,80	4,84E-03	1,04	1,31	130241
DEGS1	0,41	2,98E-02	1,18	1,31	5560398
SNORA73A	0,63	1,29E-02	1,09	1,31	7550593
KIAA0133	0,90	3,29E-03	1,02	1,31	7050075
SNX19	0,60	1,43E-02	1,09	1,31	360673
TRAP1	0,72	3,12E-02	1,08	1,31	4670092
ABHD11	0,58	9,35E-03	1,09	1,31	6110592
TMEM199	0,41	5,43E-03	1,13	1,31	2190056
HS.554608	0,74	1,17E-02	1,06	1,30	5550242

BIRC5	0,70	3,05E-02	1,08	1,30	7550626
ZNF207	0,48	1,36E-02	1,12	1,30	1660632
UBE4B	0,92	3,04E-02	1,03	1,30	2140563
TP63	0,03	4,17E-02	1,55	1,30	1770156
HELLS	0,31	2,21E-02	1,22	1,30	7040161
RAD54L	0,76	2,97E-02	1,07	1,30	1980291
HS.403972	0,37	5,63E-03	1,14	1,30	5260328
SLC7A1	0,33	1,84E-02	1,20	1,30	20241
TNPO1	0,41	1,81E-02	1,16	1,30	5080482
ANKRD41	0,48	3,91E-02	1,15	1,30	4670554
MRPS34	0,69	8,34E-03	1,07	1,30	6110307
RBM12	0,60	3,03E-02	1,11	1,30	4880021
PKP4	0,43	3,17E-03	1,11	1,30	5890440
MTX1	0,82	3,03E-02	1,05	1,30	380725
DNMT3A	0,55	6,47E-03	1,09	1,30	1300592
XRCC6	0,56	1,05E-02	1,10	1,30	6380347
BTBD10	0,65	5,53E-03	1,07	1,30	4250544
ATP5B	0,41	1,71E-02	1,16	1,30	4540021
HOMER2	0,18	5,04E-03	1,22	1,30	1570767
CDKN2A	0,34	1,02E-02	1,17	1,30	5550671
FASTKD5	0,64	2,13E-02	1,09	1,30	6650220
PITRM1	0,99	2,92E-02	-1,00	1,30	1510072
MCRS1	0,51	6,78E-03	1,10	1,30	2600553
RDH13	0,63	9,07E-03	1,08	1,30	1300187
CPSF4	0,32	4,11E-03	1,15	1,30	5560010
RLN2	0,51	5,16E-03	-1,10	-1,30	6040270
LOC642197	0,99	9,75E-03	-1,00	-1,30	5130601
ITGB3BP	0,59	2,13E-02	-1,10	-1,30	5890253
LOC100132345	0,44	4,04E-03	-1,11	-1,30	5260577
CARS	1,00	3,47E-02	1,00	-1,30	7000682
RSL24D1	0,78	2,12E-02	-1,06	-1,30	3420451
JAZF1	0,78	9,19E-03	-1,05	-1,30	3520463
CKB	0,64	4,63E-02	-1,11	-1,30	4150066
ZNF673	0,40	3,49E-03	-1,12	-1,30	870373
LOC390345	0,73	4,83E-02	-1,08	-1,30	2810050
HSPC157	0,89	4,83E-02	-1,04	-1,30	3460022
HSPC268	0,71	1,43E-02	-1,07	-1,30	1240576
ZNHIT3	0,36	4,97E-02	-1,23	-1,30	6650561
FAM10A4	0,83	2,89E-02	-1,05	-1,30	4050195
CRSP9	0,44	1,31E-02	-1,14	-1,30	6060452

FAM24B	0,63	3,69E-02	-1,11	-1,30	6940181
SMARCD3	0,55	5,26E-03	-1,09	-1,30	5910632
TCEAL8	0,94	2,25E-02	1,02	-1,30	7380138
C21ORF33	0,35	8,99E-03	-1,16	-1,30	5050376
C5ORF41	0,86	2,25E-02	-1,04	-1,30	6860228
CDC25C	0,77	9,46E-03	-1,05	-1,30	4200451
RERE	0,51	7,85E-03	-1,10	-1,30	10008
CEP152	0,64	2,48E-02	-1,09	-1,30	990189
TMUB2	0,59	4,24E-02	-1,12	-1,30	4280661
C18ORF1	0,43	5,90E-03	-1,12	-1,30	3060390
LOC650369	0,69	2,75E-02	-1,08	-1,30	1690465
CASP8	0,59	2,76E-02	-1,11	-1,30	1050092
LOC645895	0,94	4,53E-02	1,02	-1,30	1940709
ZSWIM4	0,61	1,42E-02	-1,09	-1,30	1170072
C16ORF86	0,34	1,16E-03	-1,12	-1,30	3140653
ANKRD28	0,72	1,62E-02	-1,07	-1,30	2760563
LOC100131526	0,14	3,08E-03	-1,23	-1,31	2900022
MGEA5	0,88	1,23E-02	-1,03	-1,31	6840356
DBP	0,40	9,64E-03	-1,15	-1,31	7050458
EGR3	0,66	2,98E-02	-1,09	-1,31	2370373
PDCD4	0,99	2,45E-02	-1,01	-1,31	3130168
NUP43	0,30	2,21E-02	-1,22	-1,31	70593
C11ORF54	0,24	1,58E-03	-1,16	-1,31	3360370
TMEM159	0,48	4,53E-03	-1,10	-1,31	2000431
COMMD6	0,46	3,33E-02	-1,16	-1,31	4260484
LOC388556	0,37	1,15E-02	-1,16	-1,31	7550750
THBS3	0,36	2,30E-03	-1,13	-1,31	1260039
LOC646688	0,96	6,78E-03	-1,01	-1,31	5490202
C7ORF47	0,51	1,31E-02	-1,12	-1,31	1240592
C6ORF130	0,71	1,31E-02	-1,07	-1,31	780187
MRFAP1	0,46	1,05E-02	-1,13	-1,31	2340372
DPM3	0,57	2,98E-02	-1,12	-1,31	2850520
N4BP2L2	0,49	1,31E-02	-1,12	-1,31	7200097
PARP3	0,57	9,17E-03	-1,09	-1,31	6130615
HECA	0,92	1,85E-02	-1,02	-1,31	610367
LOC124220	0,72	8,35E-03	-1,06	-1,31	1470014
LOC643949	0,31	4,29E-02	-1,26	-1,31	4290349
PTTG3P	0,63	4,09E-02	-1,11	-1,31	5960224
SEPT3	0,36	1,52E-02	-1,18	-1,31	4890021
DNAH1	0,51	2,49E-02	-1,13	-1,31	4900612

C1ORF57	0,20	5,18E-03	-1,22	-1,31	3460056
ZNF548	0,51	9,30E-03	-1,11	-1,31	2810100
SYF2	0,65	4,61E-03	-1,07	-1,31	4670241
CD72	0,99	2,96E-02	1,00	-1,31	4200546
BRE	0,76	4,29E-02	-1,08	-1,31	4060292
STAMBP	0,92	3,30E-02	-1,03	-1,31	4880671
UBXN1	0,78	5,75E-03	-1,05	-1,31	6290068
PRR7	0,73	1,33E-02	-1,06	-1,31	60653
ZNF671	0,79	2,93E-02	-1,06	-1,31	6450133
CASP4	0,50	4,94E-02	-1,16	-1,31	3850021
UBXN4	0,98	2,16E-02	-1,01	-1,31	1450537
GLCCI1	0,76	1,58E-02	-1,06	-1,31	5290079
LOC649548	0,25	7,40E-03	-1,21	-1,31	4390524
NLGN2	0,53	6,51E-03	-1,10	-1,31	4830477
XPNPEP3	0,99	2,93E-02	1,01	-1,31	2100309
C17ORF95	0,51	4,50E-03	-1,10	-1,31	5090717
STK16	0,43	1,53E-03	-1,10	-1,31	2690102
CLDN12	0,51	2,64E-02	-1,14	-1,31	1070133
LOC100130053	0,70	3,09E-02	-1,09	-1,31	4890519
LOC100130624	0,42	2,84E-02	-1,17	-1,31	7210593
CHD2	0,49	9,55E-03	-1,12	-1,32	7040240
SP110	0,54	2,83E-02	-1,13	-1,32	5870184
BACH2	0,79	6,50E-03	1,05	-1,32	7650440
HEBP1	0,23	4,73E-03	-1,21	-1,32	360689
MXI1	0,72	9,17E-03	-1,06	-1,32	2490463
STAMBP	0,76	2,54E-02	-1,07	-1,32	1740364
TADA3	0,34	4,43E-03	-1,15	-1,32	7210162
TRIM69	0,51	1,46E-02	-1,12	-1,32	1470025
BRSK1	0,47	1,71E-02	-1,14	-1,32	4890598
POLG2	0,38	3,11E-03	-1,13	-1,32	4230133
FDPS	0,97	2,85E-02	1,01	-1,32	6900398
RDH14	0,97	1,75E-02	-1,01	-1,32	6110739
SUPT3H	0,38	1,43E-02	-1,17	-1,32	4540543
ICAM3	0,73	2,83E-02	-1,08	-1,32	5550278
ZC3HAV1	0,60	1,37E-02	-1,10	-1,32	6620750
TAF1D	0,59	8,83E-03	-1,09	-1,32	6580075
HS.13291	0,60	1,46E-02	-1,10	-1,32	4480537
PAN3	0,64	4,62E-04	-1,05	-1,32	3310674
CCBE1	0,47	1,47E-02	-1,14	-1,32	3370300
SYPL1	0,76	4,41E-02	1,08	-1,32	1190452

OPLAH	0,60	4,55E-02	-1,13	-1,32	5050537
LOC645693	0,45	8,50E-03	-1,13	-1,32	5570634
DPF2	0,56	1,79E-02	-1,11	-1,32	3890274
HS.126768	0,71	1,21E-02	-1,07	-1,32	4200463
LOC146439	0,49	5,31E-03	-1,11	-1,32	7560376
C9ORF5	0,99	1,02E-02	-1,00	-1,32	2940687
TMEM59	0,61	8,36E-03	-1,09	-1,32	10725
PPFIBP2	0,28	3,80E-03	-1,18	-1,32	6900053
CDRT4	0,76	1,07E-02	-1,06	-1,32	5050148
TMEM123	0,67	1,68E-02	-1,09	-1,32	4610102
USP37	0,61	2,51E-02	-1,11	-1,32	4150711
HS.554324	0,98	3,23E-02	-1,01	-1,32	580102
RNFT1	0,97	4,73E-03	-1,01	-1,32	780608
TMEM194	0,62	1,33E-02	-1,09	-1,32	1110494
SEPT6	0,38	2,12E-02	-1,19	-1,32	6270020
BBS2	0,32	1,15E-02	-1,19	-1,32	870671
SERF2	0,72	8,82E-03	-1,06	-1,32	1580309
C16ORF63	0,40	7,15E-03	-1,15	-1,32	6520497
CDC14B	0,34	3,19E-03	-1,15	-1,32	540113
INPP4B	0,87	3,43E-02	1,04	-1,32	4860762
KLHL24	0,89	2,84E-02	-1,03	-1,32	6620201
LOC391126	0,80	3,54E-02	-1,06	-1,32	3930239
RNF122	0,70	2,35E-02	-1,08	-1,32	130605
LOC731985	0,45	1,97E-02	-1,15	-1,32	2760475
PPA2	0,85	9,90E-03	-1,04	-1,32	460630
KCTD18	0,79	2,51E-03	-1,04	-1,32	3140048
MAGED1	0,97	1,42E-02	-1,01	-1,32	460113
LOC100131187	0,48	1,88E-02	-1,14	-1,32	2970333
LOC283788	0,84	2,74E-02	-1,05	-1,32	5560523
LYRM5	0,39	1,29E-02	-1,17	-1,32	10435
FLJ16686	0,58	2,66E-02	-1,12	-1,32	6330301
DDT	0,49	1,58E-02	-1,13	-1,32	2360593
ZFAND1	0,57	1,47E-02	-1,11	-1,32	7000037
AKR7A2	0,75	2,95E-02	-1,07	-1,32	6180681
PFKP	0,61	3,50E-03	-1,08	-1,32	2360452
MFSD11	0,31	1,29E-02	-1,21	-1,32	3940593
FAM134B	0,45	5,50E-03	-1,12	-1,32	270114
AZI2	0,45	6,88E-03	-1,12	-1,32	5490348
LOC197135	0,46	2,20E-03	-1,10	-1,32	4230056
MGC29506	0,60	3,97E-02	-1,12	-1,32	770682

LOC100130775	0,55	3,59E-02	-1,14	-1,33	4570301
HLTF	0,46	2,17E-02	-1,15	-1,33	4480520
CCDC23	0,41	2,38E-02	-1,18	-1,33	630086
RAB5B	0,72	1,31E-02	-1,07	-1,33	2850626
BTAF1	0,70	2,95E-02	-1,09	-1,33	2070209
LPIN2	0,61	4,29E-02	-1,12	-1,33	510224
LOC374443	0,62	3,62E-03	-1,07	-1,33	4010681
LOC440280	1,00	4,02E-03	-1,00	-1,33	2850068
P4HTM	0,13	1,84E-03	-1,23	-1,33	2760301
DCDC2B	0,50	4,74E-03	-1,11	-1,33	2120113
UBE2H	0,52	2,19E-03	-1,09	-1,33	4900746
APPBP2	0,66	1,73E-02	-1,09	-1,33	5270333
S100A6	0,99	2,01E-02	1,00	-1,33	2810315
COPA	0,80	1,45E-02	-1,05	-1,33	4150500
TAGLN	0,66	6,00E-03	-1,07	-1,33	650678
PCMTD2	0,64	1,05E-02	-1,09	-1,33	730673
SLC15A4	0,28	1,46E-02	-1,24	-1,33	6650465
SNRK	0,26	7,49E-03	-1,22	-1,33	5820338
LOC646527	0,48	1,88E-02	-1,14	-1,33	6520273
DBNDD2	0,43	1,75E-02	-1,16	-1,33	6420168
ERCC5	0,71	4,58E-03	-1,06	-1,33	5820343
CD4	0,41	2,55E-02	-1,18	-1,33	6770711
CD28	0,59	1,03E-02	-1,10	-1,33	4890722
UFSP2	0,65	8,56E-03	-1,08	-1,33	4250288
PMPCB	0,73	5,04E-03	-1,06	-1,33	4220707
TMEM9	0,14	2,14E-03	-1,23	-1,33	1010110
KIAA1267	0,43	1,58E-02	-1,16	-1,33	1580338
DTWD2	0,84	1,65E-02	-1,04	-1,33	2940372
DIXDC1	0,53	3,89E-02	-1,15	-1,33	6760451
MCL1	0,89	3,85E-02	-1,04	-1,33	7380100
POFUT1	0,67	1,35E-02	-1,08	-1,33	290348
KIAA1370	0,48	6,19E-03	-1,12	-1,33	4180142
RNF113A	0,52	1,54E-02	-1,12	-1,33	6940196
CASP9	0,63	4,84E-03	-1,08	-1,33	4280735
NFATC1	0,94	1,35E-02	1,02	-1,33	940725
TRAPPC2	0,71	1,37E-02	-1,07	-1,33	6060148
C6ORF57	0,59	1,98E-02	-1,11	-1,33	2570068
ARMCX2	0,46	1,74E-02	-1,15	-1,33	3930201
HS.126245	0,41	1,56E-02	-1,17	-1,33	6370082
FAM119B	0,64	2,91E-02	-1,11	-1,33	870056

EDG1	0,84	1,86E-02	-1,05	-1,33	160754
MIOS	0,60	4,44E-03	-1,08	-1,33	2750544
HS.535392	0,63	1,90E-02	-1,10	-1,33	2940341
VAMP4	0,82	1,46E-02	-1,05	-1,33	7100253
GMPR2	0,36	3,43E-03	-1,15	-1,33	5090392
C2ORF56	0,29	6,11E-04	-1,14	-1,34	620228
ZNF419	0,67	6,64E-03	-1,08	-1,34	7320148
JMJD1A	0,90	1,19E-02	-1,03	-1,34	1240504
CD53	0,30	1,17E-02	-1,22	-1,34	520678
KDELR1	0,61	3,61E-02	-1,12	-1,34	2510209
FCF1	0,40	1,03E-02	-1,16	-1,34	1990402
FAM13A	0,69	3,73E-02	-1,10	-1,34	4540376
LRG1	0,41	8,17E-03	-1,15	-1,34	6660162
AIG1	0,48	9,81E-03	-1,13	-1,34	3940056
ARID3A	0,63	4,21E-02	-1,12	-1,34	6510553
LOC100188949	0,50	2,68E-02	-1,15	-1,34	1010707
ZNF337	0,45	5,17E-03	-1,12	-1,34	780324
LOC402175	0,53	8,92E-03	-1,11	-1,34	520468
RPL28	0,33	6,17E-03	-1,18	-1,34	3520121
OXSM	0,96	1,70E-02	-1,02	-1,34	3710746
RFNG	0,29	1,32E-02	-1,23	-1,34	2070376
TMEM49	0,61	4,16E-03	-1,08	-1,34	6280672
TSPAN5	0,89	3,77E-02	-1,04	-1,34	4900168
UBE2E2	0,07	9,58E-04	-1,25	-1,34	5270021
TFB1M	0,89	3,00E-02	-1,04	-1,34	2340626
TMEM45A	0,73	5,69E-03	-1,06	-1,34	6280520
LANCL1	0,43	6,16E-03	-1,14	-1,34	2450612
FAM115A	0,85	2,03E-02	-1,04	-1,34	4540600
ENPP2	0,57	2,86E-02	-1,13	-1,34	2490152
RLF	0,66	1,47E-02	-1,09	-1,34	520309
CUL4B	0,57	1,08E-02	-1,11	-1,34	5860368
LOC728059	0,82	3,44E-02	1,06	-1,34	4040519
NSMCE1	0,92	2,30E-02	-1,03	-1,34	2940020
TMEM43	0,54	1,03E-02	-1,11	-1,34	2510392
PSAP	0,63	4,25E-02	-1,12	-1,34	7650333
GAPDH	0,51	7,72E-03	-1,11	-1,34	2640048
VPS33B	0,29	6,71E-04	-1,14	-1,34	6330243
STX4	0,72	9,58E-03	-1,07	-1,34	7380164
LOC100133516	0,71	8,28E-03	-1,07	-1,34	1190259
MAP3K4	0,62	1,38E-02	-1,10	-1,34	7320731

USP36	0,81	3,52E-02	-1,06	-1,34	7160612
RORA	0,42	7,99E-03	-1,15	-1,34	3940703
PQLC3	0,81	1,20E-02	-1,05	-1,34	7000382
P2RX7	1,00	1,47E-02	1,00	-1,34	3370086
PFDN5	0,31	6,08E-03	-1,19	-1,34	4220630
LOC727865	0,69	2,79E-02	-1,09	-1,34	7050079
RNF149	0,48	1,37E-02	-1,14	-1,34	990735
LOC730288	0,38	3,14E-02	-1,22	-1,34	2640358
OCIAD1	0,85	3,65E-02	-1,05	-1,34	4810739
NR4A2	0,98	3,15E-02	-1,01	-1,34	650639
TRAF5	0,71	1,48E-02	-1,08	-1,35	7610598
BNIP3L	0,89	4,19E-03	1,03	-1,35	620047
C15ORF63	1,00	9,85E-03	1,00	-1,35	6660332
LOC100128975	0,38	1,72E-02	-1,19	-1,35	650162
PLEKHG2	0,72	1,60E-03	-1,05	-1,35	1690170
SNHG6	0,61	9,09E-03	-1,10	-1,35	5720520
UBL3	0,80	1,68E-02	-1,06	-1,35	6620538
CCDC125	1,00	1,12E-02	1,00	-1,35	650564
RGS10	0,67	3,11E-02	-1,10	-1,35	3830092
BSPRY	0,81	2,27E-02	-1,06	-1,35	5560050
B3GALT4	0,59	3,80E-03	-1,09	-1,35	2510161
GNE	0,84	1,51E-02	-1,04	-1,35	6060209
TMEM167B	0,59	1,93E-02	-1,12	-1,35	3130241
RNF5P1	0,47	1,24E-02	-1,14	-1,35	3450377
LOC283174	0,57	1,85E-02	-1,12	-1,35	4640369
FBXO34	0,66	1,42E-02	-1,09	-1,35	2350754
KIAA1751	0,94	2,72E-02	1,02	-1,35	5570593
ANKRD30B	0,74	2,08E-02	-1,07	-1,35	1770273
GLG1	0,88	2,29E-02	-1,04	-1,35	2030376
C10ORF104	0,60	4,70E-03	-1,09	-1,35	7210300
LOC731007	0,93	4,14E-03	-1,02	-1,35	1850402
C9ORF127	0,54	1,07E-02	-1,12	-1,35	3610280
PLAG1	0,37	2,22E-03	-1,14	-1,35	6770497
ZFAND2A	0,81	2,68E-02	-1,06	-1,35	870379
FAM108A2	0,36	1,15E-02	-1,19	-1,35	4850452
ZNF160	0,47	8,69E-03	-1,13	-1,35	6980474
FAM26F	0,23	1,39E-02	-1,28	-1,35	6590646
LOC653438	0,41	1,32E-02	-1,17	-1,35	4010438
LOC729279	0,43	1,64E-02	-1,17	-1,35	20435
TMEM66	0,99	3,18E-02	1,01	-1,35	6280270

CD55	0,43	6,21E-03	-1,14	-1,35	830274
ECH1	0,68	1,28E-02	-1,08	-1,35	5360553
C14ORF132	0,30	4,61E-03	-1,19	-1,35	730358
CHCHD7	0,36	8,16E-03	-1,18	-1,35	5220504
ZC3H3	0,56	3,10E-02	-1,14	-1,35	4760538
UBAC2	0,89	1,76E-02	-1,04	-1,35	6580521
FAM190B	0,40	8,79E-03	-1,16	-1,35	4920327
C10ORF58	0,34	3,62E-03	-1,17	-1,35	5960168
PRRG2	0,33	2,60E-03	-1,16	-1,35	3060605
HS.213541	0,54	3,20E-03	-1,10	-1,35	2940452
SEC31B	0,14	1,24E-03	-1,23	-1,35	6550253
ADM2	0,65	2,83E-02	-1,11	-1,35	3610626
NBL1	0,68	1,80E-02	-1,09	-1,36	7100010
LOC731542	0,82	1,47E-02	-1,05	-1,36	3520315
ING2	0,85	8,14E-03	-1,04	-1,36	7160025
WDR13	0,76	9,36E-03	-1,06	-1,36	2190364
FBXO11	0,79	8,28E-03	-1,05	-1,36	2100427
TP53AP1	0,35	4,95E-03	-1,17	-1,36	3850026
DDX50	0,71	1,71E-02	-1,08	-1,36	430577
CYB5D2	0,48	8,25E-03	-1,13	-1,36	2630333
LOC441019	0,29	9,71E-03	-1,23	-1,36	6860162
LOC729852	0,81	6,16E-03	-1,05	-1,36	6280678
RGS10	0,15	2,25E-03	-1,25	-1,36	1440209
C12ORF76	0,60	1,20E-02	-1,10	-1,36	2510181
IL17RD	0,57	4,91E-03	-1,10	-1,36	4060017
RAB8B	0,48	2,70E-02	1,17	-1,36	1740497
MYL5	0,46	6,97E-03	-1,14	-1,36	6110577
LOC202781	0,81	2,36E-02	-1,06	-1,36	6280102
C1QTNF6	0,38	3,43E-03	-1,15	-1,36	1010446
MXI1	0,49	1,35E-02	-1,14	-1,36	3390241
C13ORF15	0,96	3,41E-02	1,02	-1,36	160242
RAB24	0,34	1,29E-02	-1,21	-1,36	5910300
CD247	0,74	7,60E-03	-1,06	-1,36	6290400
OBFC2A	0,52	1,27E-02	-1,13	-1,36	4260253
SMYD2	0,50	3,47E-03	-1,11	-1,36	5960053
EIF4EBP3	0,21	1,81E-03	-1,21	-1,36	1850360
VEGFB	0,37	1,30E-03	-1,14	-1,36	5890288
ATG12	0,69	1,41E-02	-1,09	-1,36	1410348
INDO	0,15	3,39E-02	-1,43	-1,36	380259
LOC100131672	0,30	1,13E-02	-1,23	-1,36	3930370

CTBS	0,51	6,35E-03	-1,12	-1,36	60504
SORL1	0,45	2,47E-02	-1,18	-1,36	6940039
CD247	0,79	7,45E-03	-1,05	-1,36	3890689
VCPIP1	0,55	1,25E-02	-1,12	-1,36	4040450
TBC1D22A	0,66	5,69E-03	-1,08	-1,36	5490523
LETMD1	0,39	5,97E-03	-1,16	-1,36	2570435
OXR1	1,00	2,40E-02	-1,00	-1,36	730291
GLA	0,53	2,16E-02	-1,14	-1,37	60630
CLUAP1	0,41	2,57E-03	-1,13	-1,37	6980477
RPL21	0,53	2,05E-02	-1,14	-1,37	4920070
EDEM1	0,55	1,10E-02	-1,12	-1,37	2030292
PKIA	0,85	1,94E-02	1,05	-1,37	510435
MGC18216	0,27	7,35E-03	-1,23	-1,37	6400639
SKAP1	1,00	1,46E-02	1,00	-1,37	4220053
LOC100128936	0,95	4,72E-03	-1,02	-1,37	3610053
ZC3H11B	0,41	4,94E-03	-1,15	-1,37	70047
HOOK2	0,31	2,58E-03	-1,17	-1,37	1710520
HS.561747	0,93	1,50E-02	-1,02	-1,37	3370037
CDAN1	0,90	2,24E-02	-1,04	-1,37	5910445
SP140	0,79	3,03E-02	-1,07	-1,37	870193
FDFT1	0,82	4,06E-03	1,04	-1,37	2360630
MVP	0,44	1,95E-02	-1,18	-1,37	160291
LOC728060	0,37	4,62E-02	-1,27	-1,37	5270538
TCTEX1D2	0,62	7,43E-03	-1,10	-1,37	7150433
RPL12	0,66	8,69E-03	-1,09	-1,37	7550458
FAM125B	0,44	9,74E-03	-1,16	-1,37	650619
NUDT2	0,39	1,31E-02	-1,19	-1,37	2750035
ZNF189	0,69	1,38E-03	-1,06	-1,37	630603
FAM139A	0,57	4,20E-03	-1,10	-1,37	2630544
LOC100128084	0,63	2,06E-02	-1,11	-1,37	4280309
FKBP14	0,40	1,07E-02	-1,18	-1,37	4150753
RNMT	0,69	3,06E-03	-1,07	-1,37	4850176
HS.194225	0,33	2,85E-03	-1,17	-1,37	3360446
TMEM156	0,77	3,48E-02	-1,08	-1,37	2000364
LOC388339	0,55	3,38E-03	-1,10	-1,37	6330408
CHMP5	0,39	4,20E-02	-1,24	-1,37	7650347
LOC648470	0,43	1,22E-02	-1,17	-1,37	1450136
AKR7A3	0,44	1,29E-03	-1,11	-1,37	70484
MAX	0,51	1,45E-02	-1,14	-1,37	4640220
P4HTM	0,61	2,07E-02	-1,12	-1,37	5220398

ZNF518B	0,35	9,60E-04	-1,14	-1,37	1050132
FOXO4	0,43	6,85E-03	-1,15	-1,37	4480575
STAMBPL1	0,74	2,88E-02	-1,09	-1,37	7150059
TMEM143	0,30	1,39E-03	-1,17	-1,37	6180678
NHLRC3	0,96	2,20E-03	-1,01	-1,38	6510598
RAC3	0,32	2,56E-03	-1,17	-1,38	5890273
TDP1	0,40	2,79E-03	-1,14	-1,38	2060110
CTSB	0,65	4,22E-02	-1,13	-1,38	240309
LOC100128505	0,93	1,60E-02	-1,02	-1,38	780170
LOC646463	0,96	2,93E-02	-1,02	-1,38	6580402
OGT	0,58	1,81E-02	-1,12	-1,38	1070300
POLR1E	0,32	3,73E-03	-1,18	-1,38	4040504
NPAL3	0,63	2,21E-03	-1,08	-1,38	5090739
HS.363526	0,27	1,62E-02	-1,28	-1,38	3870025
FCAR	0,75	1,30E-02	-1,07	-1,38	4250193
LOC728643	0,48	1,46E-02	-1,15	-1,38	5390500
BIRC2	0,36	7,24E-03	-1,19	-1,38	4920707
MUC1	0,32	3,08E-02	-1,28	-1,38	7200601
LOC100133772	0,87	1,62E-02	1,04	-1,38	450561
MYO1G	0,70	2,28E-02	-1,10	-1,38	3450195
LOC387841	0,98	3,61E-02	-1,01	-1,38	1940296
VIPR1	0,27	6,54E-03	-1,24	-1,38	2690709
SPG11	0,96	1,46E-02	-1,01	-1,38	2100524
ODF2L	0,69	9,90E-03	-1,08	-1,38	6840026
FEM1C	0,40	1,06E-02	-1,18	-1,38	2000228
RPS4Y2	0,41	1,95E-02	-1,20	-1,38	6020273
LOC100133607	0,90	9,32E-03	-1,03	-1,38	5090341
ADD3	0,59	2,89E-02	-1,14	-1,38	3420747
CORO2A	0,94	3,84E-02	-1,03	-1,38	1410609
RPL14L	0,48	6,54E-03	-1,14	-1,38	4040451
GNL1	0,41	1,24E-02	-1,18	-1,38	6370068
ZNF581	0,41	6,87E-03	-1,17	-1,38	3890482
TRIB2	0,95	4,18E-02	-1,03	-1,38	2570328
HRSP12	0,24	5,17E-03	-1,25	-1,38	6420373
MYC	0,50	1,75E-02	-1,16	-1,39	6550600
ADORA2B	0,90	4,37E-03	-1,03	-1,39	2060040
FAM127B	0,15	4,51E-03	-1,30	-1,39	5810373
ANKMY2	0,81	2,41E-03	-1,04	-1,39	4890136
FAM113A	0,45	1,25E-02	-1,17	-1,39	290296
FAM110A	0,58	1,53E-02	-1,12	-1,39	6400402

PNMA3	0,61	2,27E-02	-1,12	-1,39	7320270
C19ORF22	0,44	1,19E-02	-1,17	-1,39	150020
USP48	0,43	2,80E-03	-1,13	-1,39	6980082
EBI2	0,41	1,65E-02	-1,20	-1,39	4040037
MRPL10	0,36	3,09E-03	-1,17	-1,39	6180154
MAGED2	0,40	1,29E-03	-1,13	-1,39	2320368
TRIM69	0,62	1,43E-02	-1,11	-1,39	1030379
SQSTM1	1,00	3,30E-02	1,00	-1,39	4260044
USP49	0,71	1,45E-02	-1,09	-1,39	5550603
RPS4Y1	0,66	1,67E-03	-1,07	-1,39	6100687
TCEAL8	0,61	4,62E-03	-1,09	-1,39	160474
C17ORF44	0,72	3,59E-02	-1,10	-1,39	5810167
FUT11	0,45	2,33E-02	-1,19	-1,39	70553
LOC100130154	0,31	7,86E-03	-1,23	-1,39	2370167
LOC729009	0,51	2,85E-02	-1,17	-1,39	2810463
LOC642828	0,81	1,41E-02	-1,06	-1,39	7000059
LOC729742	0,48	2,15E-02	-1,17	-1,39	5910484
ZMYM3	0,23	2,34E-03	-1,23	-1,39	2340709
DEM1	0,61	5,69E-03	-1,10	-1,39	3870450
LOC728537	0,58	9,03E-03	-1,11	-1,39	160504
LOC100131609	0,90	1,68E-03	1,02	-1,39	1710192
HPCAL4	0,43	1,19E-02	-1,17	-1,39	5220524
LOC100132037	0,38	1,06E-02	-1,20	-1,39	1110343
HS.279842	0,72	1,13E-02	-1,08	-1,39	6960300
ARHGEF7	0,41	5,20E-03	-1,16	-1,39	510554
WDR60	0,47	4,91E-03	-1,14	-1,39	2600470
SLC15A3	0,13	5,16E-03	-1,33	-1,40	4220044
LOC644937	0,47	1,27E-02	-1,16	-1,40	5360307
DNASE2	0,53	6,38E-03	-1,12	-1,40	6200315
ITGAE	0,19	1,13E-02	-1,33	-1,40	4120341
LOC100129657	0,57	2,95E-02	-1,15	-1,40	580626
TMEM156	0,37	8,62E-03	-1,20	-1,40	3390253
SHROOM4	0,55	1,40E-02	-1,14	-1,40	5270064
LOC400027	0,60	2,40E-02	-1,13	-1,40	6650164
NLRP8	0,90	1,18E-02	-1,03	-1,40	6770326
LOC730994	0,45	7,85E-03	-1,15	-1,40	3800273
HAUS4	0,44	5,43E-03	-1,15	-1,40	4810112
GLS	1,00	2,09E-02	-1,00	-1,40	5570427
ARHGAP15	0,75	5,51E-03	-1,07	-1,40	3310463
CA5B	0,56	6,12E-03	-1,11	-1,40	1690044

LANCL1	0,51	3,23E-03	-1,11	-1,40	4150138
SH2D3C	0,47	8,68E-03	-1,15	-1,40	270487
GGPS1	0,82	4,13E-03	-1,05	-1,40	1260520
LOC729843	0,51	7,32E-03	-1,13	-1,40	3890427
LOC100127983	0,42	1,62E-02	-1,19	-1,40	6510685
PSAP	0,64	3,91E-02	-1,14	-1,40	6200086
LOC646785	0,55	1,30E-02	-1,13	-1,40	1170551
TCEAL8	0,75	9,12E-03	-1,07	-1,40	7550468
DGKA	0,48	3,38E-02	-1,20	-1,40	3170020
LOC387825	0,63	2,95E-02	-1,13	-1,40	2230767
ARHGAP9	0,63	4,73E-02	-1,15	-1,40	110180
IL10RB	0,83	1,24E-02	-1,05	-1,40	5670719
LOC550643	0,57	1,08E-02	-1,12	-1,40	1440753
IFI27L2	0,39	2,79E-02	-1,24	-1,40	6940561
ZC3H7A	0,22	7,01E-04	-1,19	-1,40	4830050
LOC441054	0,70	3,35E-03	-1,07	-1,40	4200180
LOC647030	0,47	5,73E-03	-1,14	-1,40	290180
PCCA	0,16	1,30E-03	-1,25	-1,40	4730309
LOC728620	0,56	7,78E-03	-1,12	-1,40	60753
SCAMP1	0,53	5,92E-03	-1,12	-1,40	1050544
FLJ36131	0,44	1,05E-02	-1,17	-1,40	3290537
RNF19A	0,99	3,57E-03	-1,01	-1,40	4590408
LOC253039	0,52	1,20E-02	-1,14	-1,40	5390553
LOC728661	0,89	3,02E-02	-1,05	-1,40	5550592
LOC729208	0,35	2,18E-02	-1,25	-1,40	4640291
KHNYN	0,32	5,17E-03	-1,21	-1,41	4640639
C5ORF21	0,63	7,72E-03	-1,10	-1,41	4860379
WNT10A	0,87	6,02E-03	1,04	-1,41	2710343
KBTBD3	0,48	4,20E-03	-1,13	-1,41	5910274
HS.572538	0,48	2,24E-03	-1,12	-1,41	3400301
C4ORF47	0,65	1,31E-02	-1,11	-1,41	1850066
LOC727826	0,56	1,92E-02	-1,14	-1,41	7100523
C8ORF37	0,62	1,82E-02	-1,12	-1,41	5360390
GMFG	0,71	6,78E-03	-1,08	-1,41	3370452
LOC388532	0,41	1,70E-03	-1,14	-1,41	2900470
TMEM194A	0,84	1,31E-03	-1,04	-1,41	870767
SLU7	0,42	2,63E-03	-1,14	-1,41	50475
PDE6B	0,42	1,25E-03	-1,13	-1,41	3850474
NARF	0,46	5,67E-03	-1,15	-1,41	2360491
KIAA0895L	0,44	1,89E-03	-1,13	-1,41	580463

SLAMF6	0,79	3,52E-02	-1,08	-1,41	7200743
LOC647285	0,42	6,13E-03	-1,17	-1,41	6040110
LOC401098	0,39	3,56E-03	-1,17	-1,41	5490632
CUTA	0,51	7,18E-03	-1,13	-1,41	3120707
CACNA2D4	0,22	3,13E-03	-1,25	-1,41	5810221
MGST3	0,30	7,43E-03	-1,24	-1,41	7160400
GPR65	0,86	1,09E-02	-1,04	-1,41	7570367
ZNF14	0,61	6,96E-03	-1,11	-1,41	7610528
RAB27A	0,31	1,89E-03	-1,18	-1,41	110010
NFX1	0,62	5,53E-03	-1,10	-1,41	4060494
MYL5	0,35	2,49E-03	-1,17	-1,41	3460010
LOC653079	0,46	9,30E-03	-1,16	-1,41	510053
HS.532698	0,56	7,60E-03	-1,12	-1,41	3940762
HCST	0,99	1,46E-02	1,01	-1,41	1580088
GCA	0,47	1,06E-02	-1,16	-1,41	4230619
LOC100131787	0,29	1,01E-02	-1,27	-1,41	4830377
SMYD3	0,35	6,72E-04	-1,15	-1,41	540452
C9ORF80	0,74	1,05E-02	-1,08	-1,41	5090072
LOC100128098	0,83	4,60E-03	1,05	-1,42	3610427
ENPP2	0,34	1,15E-02	-1,24	-1,42	840678
OBFC1	0,52	1,48E-03	-1,10	-1,42	4120750
LDLR	0,65	1,59E-02	1,11	-1,42	1440736
SOCS3	0,20	3,53E-02	-1,44	-1,42	4230102
RAB24	0,41	7,82E-03	-1,18	-1,42	6560373
MAP1LC3B	0,50	4,87E-03	-1,13	-1,42	2490754
CNIH	0,79	1,03E-02	1,06	-1,42	2900187
LOC731777	0,56	6,10E-03	-1,12	-1,42	5390070
BCKDK	0,58	1,26E-02	-1,13	-1,42	5220347
MAPK3	0,52	8,14E-03	-1,14	-1,42	2060561
SNRK	0,51	2,02E-02	-1,16	-1,42	2060095
MEF2D	0,86	4,18E-02	-1,06	-1,42	3940484
SIPA1	0,45	1,83E-02	-1,19	-1,42	5810068
ZSWIM1	0,92	8,71E-03	1,03	-1,42	4230286
RAPGEF6	0,54	8,83E-03	-1,13	-1,42	3390504
N4BP2L1	0,57	2,50E-02	-1,15	-1,42	6550133
TBC1D9B	0,43	2,05E-02	-1,21	-1,42	7550411
BCAS4	0,45	2,20E-02	-1,20	-1,42	4290079
FAM117B	0,54	1,90E-02	-1,15	-1,42	3140632
LOC732165	0,63	6,93E-03	-1,10	-1,42	3390639
RPL13L	0,75	1,20E-02	-1,08	-1,42	6840324

EVI2B	0,97	1,68E-02	-1,01	-1,42	7050152
C21ORF24	0,73	7,00E-03	-1,08	-1,42	6900279
ACTR1B	0,79	6,78E-03	-1,06	-1,42	2120088
DSCR3	0,70	3,10E-03	-1,07	-1,42	7320437
LOC100131196	0,31	4,56E-03	-1,22	-1,42	3140709
OPN3	0,43	5,24E-03	-1,16	-1,42	780021
ASCC1	0,89	1,69E-03	-1,03	-1,42	830528
SIGIRR	0,40	1,43E-02	-1,21	-1,42	4220193
SPAG4	0,50	1,58E-02	-1,17	-1,42	1190670
FSD1	0,17	1,05E-02	-1,36	-1,43	3170019
RPL14	0,67	2,55E-02	-1,12	-1,43	3930008
ALPP	0,94	7,20E-03	-1,02	-1,43	2600133
KIAA0319L	0,56	1,05E-02	-1,13	-1,43	630397
KLHL6	0,74	8,46E-03	-1,08	-1,43	2470338
BLZF1	0,69	1,60E-02	-1,10	-1,43	6130020
FAM84B	0,85	2,83E-02	-1,06	-1,43	60014
GPR65	0,82	7,86E-03	-1,06	-1,43	6550273
C3ORF19	0,62	4,34E-03	-1,10	-1,43	6960170
SNRPN	0,67	4,70E-03	-1,09	-1,43	2480291
GRAMD4	0,48	4,78E-02	-1,23	-1,43	6380112
RPL17	0,42	7,72E-03	-1,18	-1,43	2000593
ZNF430	0,89	8,17E-03	-1,04	-1,43	1450685
GPBP1	0,56	6,61E-03	-1,12	-1,43	6480315
FTHL12	0,38	2,84E-02	-1,26	-1,43	3190133
JMJD1C	0,45	6,70E-03	-1,16	-1,43	6960523
LOC643310	0,51	1,14E-03	-1,10	-1,43	510209
LOC648771	0,51	1,59E-03	-1,11	-1,43	3390170
GPR160	0,47	1,21E-02	-1,17	-1,43	7510367
PSIP1	0,79	1,10E-03	-1,05	-1,43	5310747
MOAP1	0,43	1,58E-03	-1,14	-1,43	270224
ZNF486	0,74	2,06E-02	-1,09	-1,43	3130544
TANC2	0,03	1,12E-03	-1,38	-1,43	1440768
SH3YL1	0,47	2,52E-03	-1,13	-1,43	2570288
FLJ10986	0,26	3,69E-03	-1,25	-1,43	2650164
MIB2	0,73	6,02E-03	-1,08	-1,43	2260619
LOC641848	0,42	9,28E-03	-1,19	-1,43	2640255
S1PR1	0,36	9,81E-03	-1,22	-1,43	4810768
CATSPER2	0,85	1,62E-02	-1,05	-1,43	2600273
LRRFIP1	0,41	1,13E-02	-1,20	-1,43	3400754
GDPD3	0,15	5,80E-04	-1,23	-1,43	5390121

WBP1	0,65	7,00E-03	-1,10	-1,43	6380537
LOC391019	0,48	4,33E-02	-1,22	-1,44	2190630
PLDN	0,74	1,21E-03	-1,06	-1,44	3180746
ZNF558	0,38	9,64E-04	-1,15	-1,44	4070176
ZNF394	0,83	2,06E-02	-1,06	-1,44	3310592
EGLN1	0,49	4,71E-03	-1,14	-1,44	4670102
C17ORF48	0,32	1,83E-03	-1,19	-1,44	6580129
LOC644186	0,18	2,95E-03	-1,29	-1,44	5310593
LOC647673	0,48	2,41E-02	-1,19	-1,44	4220307
SYPL1	0,89	1,94E-03	1,03	-1,44	3170360
LOC339352	0,41	3,61E-03	-1,16	-1,44	6580091
CFD	0,20	4,56E-03	-1,30	-1,44	1240152
RP11-529I10.4	0,39	2,88E-02	-1,27	-1,44	3400687
MAD1L1	0,22	5,77E-03	-1,30	-1,44	2630370
PPME1	0,56	2,62E-03	-1,11	-1,44	830411
ALKBH7	0,38	1,18E-03	-1,15	-1,44	3310324
TSC22D3	0,81	1,08E-03	-1,04	-1,44	770494
LOC100132585	0,42	5,16E-03	-1,17	-1,44	1240669
ATP6V0A4	0,28	7,20E-03	-1,27	-1,44	6110328
LOC391370	0,48	8,68E-03	-1,16	-1,44	3390674
TMEM205	0,71	2,88E-02	-1,11	-1,44	7210528
CCNG2	0,67	3,15E-02	-1,13	-1,44	130215
LOC645452	0,72	1,28E-02	-1,09	-1,44	1230370
MAGED2	0,38	2,53E-03	-1,18	-1,44	3420487
LOC100128288	0,82	1,30E-02	-1,06	-1,44	2630246
LOC81691	0,71	1,19E-02	-1,09	-1,44	3060703
MGC57346	0,47	3,21E-03	-1,14	-1,44	240152
NOL3	0,69	3,98E-02	-1,13	-1,44	430202
C11ORF67	0,19	3,81E-03	-1,30	-1,44	3310228
LOC442454	0,50	9,84E-03	-1,16	-1,44	5890176
LOC388789	0,36	7,35E-03	-1,22	-1,44	650605
PLTP	0,71	5,73E-03	-1,08	-1,44	5690519
PLEKHB1	0,20	6,11E-04	-1,22	-1,44	2690133
CSF2RA	0,45	4,91E-03	-1,16	-1,44	2900053
WDR51B	0,20	6,16E-03	-1,32	-1,44	7160609
HS.521338	0,55	2,12E-02	-1,16	-1,44	2600494
HSD17B11	0,57	9,84E-03	-1,13	-1,44	6580487
RPS28	0,52	1,51E-02	-1,16	-1,44	650349
LOC388621	0,59	6,00E-03	-1,12	-1,44	730379
BLVRB	0,72	3,98E-02	-1,12	-1,45	6620521

MAN1B1	0,44	2,72E-02	-1,23	-1,45	1780661
HIST1H2AC	0,90	3,89E-02	-1,05	-1,45	6590594
PHF21A	0,92	1,46E-02	-1,03	-1,45	6580164
PGRMC2	0,55	8,33E-04	-1,09	-1,45	1690326
KLF12	0,61	2,85E-03	-1,10	-1,45	1430711
SATB1	0,51	9,50E-03	-1,15	-1,45	3130669
ATP6V1G1	0,37	5,38E-03	-1,21	-1,45	6370091
FXYD5	0,43	1,43E-03	-1,14	-1,45	1470332
LOC255783	0,49	1,01E-02	-1,16	-1,45	1300369
VAMP1	0,36	5,43E-03	-1,21	-1,45	6650639
VEGFA	0,65	2,75E-02	-1,13	-1,45	2640224
LOC728903	0,69	2,13E-03	-1,08	-1,45	3940521
CYTH4	0,51	1,11E-02	-1,16	-1,45	1010037
HS.579530	0,82	1,31E-02	-1,06	-1,45	990719
CCDC115	0,23	2,95E-03	-1,26	-1,45	5910095
CNIH	0,91	1,70E-03	-1,03	-1,45	4070088
MTL5	0,30	3,74E-03	-1,23	-1,45	2360121
OR7E156P	0,59	1,73E-02	-1,14	-1,45	3940201
DCP2	0,66	5,67E-03	-1,10	-1,45	6960349
MGC26356	0,51	3,03E-03	-1,12	-1,45	3930255
RAG1AP1	0,63	7,20E-04	-1,08	-1,45	1570619
LOC388076	0,56	8,05E-03	-1,13	-1,45	940653
FCGRT	0,11	7,06E-04	-1,29	-1,45	4200176
NOD2	0,87	4,17E-02	-1,06	-1,45	940220
C10ORF58	0,87	1,21E-02	-1,05	-1,45	2120468
SNRPN	0,56	6,09E-03	-1,13	-1,45	1740273
FTHL8	0,53	4,95E-02	-1,21	-1,45	1980594
ADHFE1	0,60	8,79E-03	-1,12	-1,45	2760121
GFI1	0,40	1,62E-03	-1,16	-1,45	4120379
CFLAR	0,50	2,49E-02	-1,19	-1,45	1240593
APOBEC3F	0,30	1,98E-03	-1,21	-1,45	5340403
RSPH3	0,63	9,29E-03	-1,11	-1,45	2650678
CNIH	0,74	2,36E-03	-1,07	-1,45	3120767
CASP8	0,87	9,66E-03	-1,05	-1,46	2650750
LOC100129599	0,44	1,47E-02	-1,20	-1,46	5290220
LOC285741	0,67	2,15E-02	-1,12	-1,46	2070324
CAST	0,39	3,86E-03	-1,19	-1,46	670161
HS.570988	0,51	9,28E-03	-1,16	-1,46	4010100
LOC644029	0,45	3,82E-02	-1,25	-1,46	160575
OFD1	0,21	3,79E-04	-1,20	-1,46	3610519

LOC88523	0,45	4,44E-03	-1,16	-1,46	1440452
VAMP4	0,63	4,80E-02	-1,17	-1,46	2100722
LOC100129685	0,40	2,05E-02	-1,25	-1,46	7560215
LRAP	0,78	6,55E-03	-1,07	-1,46	1010296
LOC391833	0,41	6,00E-03	-1,19	-1,46	520672
LRRC37B2	0,79	7,57E-03	-1,07	-1,46	60292
TERC	0,07	7,84E-03	-1,49	-1,46	3420678
PATL2	0,62	2,12E-03	-1,10	-1,46	2970494
RPL7	0,34	9,89E-03	-1,25	-1,46	2680082
KCNH6	0,82	9,17E-03	-1,06	-1,46	7000064
AGXT2L2	0,41	5,22E-04	-1,13	-1,46	5690082
LOC346887	0,40	3,54E-03	-1,18	-1,46	7150491
LOC730256	0,73	2,57E-02	-1,11	-1,46	6220762
HS.402146	0,96	2,33E-03	-1,01	-1,46	2510445
LGALS1	0,57	4,51E-02	-1,19	-1,46	1450193
LOC651149	0,79	1,24E-02	-1,07	-1,47	6590446
ACP5	0,42	5,55E-03	-1,18	-1,47	7050082
C10ORF75	0,59	6,67E-03	-1,12	-1,47	6560500
LOC100127975	0,51	6,49E-03	-1,15	-1,47	3310349
HS.72010	0,28	1,29E-03	-1,22	-1,47	6760286
LOC728820	0,55	9,72E-03	-1,14	-1,47	4560669
IRF2BP2	0,42	1,09E-02	-1,21	-1,47	6660768
KRCC1	0,99	6,11E-04	-1,00	-1,47	2370538
M6PRBP1	0,69	1,51E-02	-1,11	-1,47	620008
TMEM194A	0,41	1,66E-03	-1,15	-1,47	4610066
C14ORF153	0,58	5,45E-03	-1,12	-1,47	7160747
HEBP2	0,76	2,17E-02	-1,09	-1,47	3940026
ARAP3	0,17	9,05E-04	-1,26	-1,47	7380255
BCAS4	0,32	2,02E-02	-1,31	-1,47	5560193
LITAF	0,31	6,14E-04	-1,17	-1,47	3180672
MTMR11	0,69	3,19E-02	-1,13	-1,47	3890138
ATM	0,90	2,87E-02	-1,05	-1,47	6840605
HS.544637	0,47	3,36E-03	-1,15	-1,47	2030020
HSPC157	0,44	3,48E-03	-1,16	-1,47	7550427
SNTB1	0,63	1,71E-02	-1,13	-1,47	3420739
LOC90586	0,78	4,05E-03	-1,06	-1,47	7380390
C1ORF97	0,78	1,11E-02	-1,08	-1,47	6510360
DHX58	0,41	3,25E-02	-1,27	-1,47	3930681
LOC100132795	0,79	8,79E-03	-1,07	-1,47	5090326
LPAR2	0,10	1,67E-03	-1,35	-1,47	6650408

CORO1B	0,21	7,62E-03	-1,35	-1,48	3780451
GRIPAP1	0,61	1,40E-03	-1,09	-1,48	6370682
SIT1	0,53	6,36E-04	-1,10	-1,48	4280053
DPM3	0,61	5,09E-03	-1,12	-1,48	7320435
LOC100134018	0,57	1,24E-03	-1,10	-1,48	7560292
LOC100132391	0,50	1,45E-03	-1,12	-1,48	6130576
ZNF615	0,27	3,70E-04	-1,18	-1,48	1570338
PECI	0,41	4,38E-04	-1,13	-1,48	6200133
HSD17B7	0,84	2,40E-03	-1,05	-1,48	3420328
SYNM	0,32	5,81E-03	-1,25	-1,48	2760735
LOC100134504	0,32	4,94E-03	-1,24	-1,48	7050451
SLC44A2	0,62	2,20E-02	-1,15	-1,48	1980521
LOC220433	0,39	2,20E-03	-1,18	-1,48	6200747
S100A10	0,47	3,60E-03	-1,15	-1,48	540681
PGM1	0,84	1,26E-03	-1,04	-1,48	2070291
NUDT14	0,10	1,06E-03	-1,33	-1,48	110092
C8ORF40	0,98	3,31E-03	-1,01	-1,48	6130433
ZBTB25	0,54	2,00E-03	-1,12	-1,48	2690278
C9ORF103	0,70	6,67E-03	-1,09	-1,48	3390129
SNURF	0,32	1,13E-03	-1,19	-1,48	1050408
TBC1D15	0,68	5,95E-04	-1,07	-1,48	240019
C11ORF54	0,45	1,35E-03	-1,14	-1,48	2470463
SLC24A6	0,17	6,05E-03	-1,37	-1,48	2360376
ADD3	0,61	6,00E-03	-1,12	-1,48	1010477
POMC	0,24	2,29E-03	-1,27	-1,48	5260291
LOC653344	0,37	1,15E-02	-1,25	-1,48	5310681
CDC14B	0,23	2,75E-03	-1,28	-1,48	6040037
FLJ35390	0,52	5,77E-03	-1,15	-1,48	1090377
SRPK2	0,53	1,40E-02	-1,17	-1,48	2000468
WDR59	0,31	2,13E-03	-1,22	-1,48	5290403
FAM120B	0,44	2,93E-03	-1,16	-1,48	7610121
CECR5	0,54	7,00E-03	-1,15	-1,49	1340470
PHF3	0,60	1,66E-03	-1,10	-1,49	6400048
MGC87895	0,42	3,98E-03	-1,18	-1,49	2320291
IMMP2L	0,43	3,73E-03	-1,17	-1,49	5870487
CXCR4	0,37	5,57E-03	-1,22	-1,49	7320288
DHRS1	0,26	3,23E-03	-1,27	-1,49	1470017
GRK5	0,29	1,37E-02	-1,32	-1,49	3190239
C12ORF47	0,57	4,55E-03	-1,13	-1,49	3140138
LOC286016	0,81	2,88E-02	-1,08	-1,49	7560053

CHRNA5	0,58	1,12E-02	-1,15	-1,49	6280731
CYTIP	0,48	1,47E-02	-1,19	-1,49	1260523
RAB33A	0,43	2,44E-03	-1,16	-1,49	6270301
DHX40	0,28	2,63E-04	-1,17	-1,49	5670349
EEF1AL7	0,66	1,04E-03	-1,08	-1,49	1410750
ZNF682	0,44	3,14E-03	-1,16	-1,49	3440431
C16ORF68	0,11	3,76E-04	-1,28	-1,49	650626
VAMP5	0,67	1,54E-02	-1,12	-1,49	2630195
SLC15A4	0,48	3,28E-03	-1,15	-1,49	160279
TTC3	0,31	8,33E-04	-1,19	-1,49	290343
WSB1	0,94	2,41E-02	-1,03	-1,49	7400372
CREB1	0,45	1,59E-03	-1,14	-1,49	7510470
RIOK3	0,71	3,80E-03	-1,09	-1,49	4210019
RPLP1	0,31	4,51E-03	-1,25	-1,49	2690561
C6ORF111	0,28	3,12E-04	-1,18	-1,49	2120376
KIAA0319L	0,49	7,48E-04	-1,12	-1,49	4050475
GIMAP2	0,44	9,18E-03	-1,20	-1,50	6110747
NUDT7	0,96	4,20E-03	1,01	-1,50	4120768
HS.534427	0,59	7,62E-03	-1,13	-1,50	5870008
CCNB1IP1	0,51	9,58E-03	-1,17	-1,50	6450397
MUC1	0,30	4,29E-02	-1,41	-1,50	7650026
ELF1	0,99	5,29E-03	-1,00	-1,50	4010020
CDKN2AIPNL	0,70	5,69E-03	1,09	-1,50	7400224
JOSD1	0,52	6,31E-03	-1,15	-1,50	1500711
MKNK2	0,16	9,77E-04	-1,29	-1,50	5050553
BAG3	0,44	5,25E-03	-1,18	-1,50	1340075
ING2	0,95	3,03E-03	-1,02	-1,50	6960382
SIRT5	0,57	9,85E-04	-1,10	-1,50	1580224
LOC645715	0,74	3,88E-04	-1,05	-1,50	4050435
IL10RB	0,32	1,45E-03	-1,20	-1,50	5050368
PLEKHA2	0,99	3,23E-03	-1,00	-1,50	2970437
VDR	0,72	3,64E-02	-1,13	-1,50	5960440
RPS15A	0,36	5,17E-03	-1,23	-1,50	7100717
C8ORF45	0,66	9,32E-03	-1,12	-1,50	4640132
LOC338870	0,43	9,36E-03	-1,21	-1,50	1170441
PLCG1	0,39	2,92E-03	-1,19	-1,50	1030376
ZNF69	0,59	4,50E-03	-1,12	-1,50	2630379
ANKRD12	0,95	3,80E-03	-1,02	-1,50	7040132
LOC645452	0,89	1,71E-02	-1,05	-1,50	3440482
C9ORF95	0,96	4,50E-03	-1,02	-1,50	1980180

LOC728973	0,66	3,55E-03	-1,10	-1,50	3870470
C8ORF59	0,50	4,83E-03	-1,16	-1,50	1510452
ECHDC2	0,78	2,05E-02	-1,09	-1,50	2320653
MED7	0,26	2,24E-04	-1,18	-1,50	2450681
ZDHHC9	0,44	4,71E-03	-1,18	-1,50	610356
LOC387791	0,23	1,01E-03	-1,25	-1,50	6550672
USP3	0,71	2,65E-03	-1,08	-1,50	6220477
CORO1B	0,31	3,31E-03	-1,25	-1,50	5310170
HSCB	0,47	4,73E-03	-1,17	-1,51	2030433
FYN	0,71	1,47E-02	-1,11	-1,51	6290725
PAN2	0,41	1,76E-03	-1,17	-1,51	2490291
DMC1	0,71	4,34E-03	-1,09	-1,51	5670435
LOC727820	0,70	4,14E-03	-1,09	-1,51	460142
AVPI1	0,41	1,56E-03	-1,17	-1,51	990500
LOC439949	0,69	2,77E-02	-1,14	-1,51	4560088
CAPN12	0,29	1,21E-03	-1,22	-1,51	6400022
MYL6B	0,29	9,64E-04	-1,22	-1,51	6840056
CTBS	0,54	5,37E-03	-1,14	-1,51	2850184
PPP3R1	0,39	1,13E-02	-1,25	-1,51	6200768
DDHD2	0,43	1,70E-03	-1,16	-1,51	2070010
HS.572649	0,49	5,83E-03	-1,17	-1,51	6280750
ABCB7	0,56	1,24E-02	-1,16	-1,51	5700286
TMEM134	0,25	2,64E-03	-1,28	-1,51	670671
XRCC6BP1	0,39	8,53E-04	-1,16	-1,51	5290239
DUXAP3	0,90	2,07E-03	-1,03	-1,51	4640402
LY9	0,51	9,23E-03	-1,17	-1,51	5360692
ZBTB4	0,42	1,23E-03	-1,16	-1,52	2900441
RAB2B	0,54	2,93E-03	-1,13	-1,52	670609
SENP7	0,44	3,82E-03	-1,18	-1,52	2350468
STAT2	0,50	3,44E-02	-1,23	-1,52	130519
TMEM219	0,30	2,72E-03	-1,25	-1,52	2490202
ETV6	0,51	9,20E-04	-1,12	-1,52	240064
SUSD3	0,50	1,15E-02	-1,18	-1,52	1770168
SMAP2	0,24	7,65E-03	-1,35	-1,52	3930390
LOC728732	0,53	1,02E-03	-1,12	-1,52	1990328
QRFPR	0,53	1,90E-03	-1,13	-1,52	4010736
TRAPPC6A	0,41	6,48E-03	-1,22	-1,52	6860072
LOC441087	0,47	4,51E-03	-1,17	-1,52	7100307
SFRS18	0,40	9,26E-04	-1,16	-1,52	2060433
JMJD1C	0,51	5,21E-03	-1,16	-1,52	2490687

SEMA3E	0,34	1,29E-03	-1,20	-1,52	1580608
LOC100131387	0,52	6,88E-04	-1,11	-1,52	580170
LOC648210	0,39	3,61E-03	-1,21	-1,52	4760243
OCEL1	0,49	3,45E-03	-1,16	-1,52	3460253
MAP2K1	0,54	7,59E-03	-1,16	-1,52	1050600
NBL1	0,63	7,60E-03	-1,12	-1,52	5090156
PPP1R3E	0,50	1,66E-03	-1,13	-1,52	1710113
C1ORF165	0,77	2,14E-02	-1,10	-1,52	2140059
GCET2	0,41	3,01E-03	-1,19	-1,52	2510082
LOC644790	0,39	8,97E-03	-1,25	-1,53	540280
NOL3	0,35	9,02E-03	-1,27	-1,53	70463
LOC645157	0,35	4,88E-03	-1,24	-1,53	780364
LOC727865	0,39	6,78E-03	-1,23	-1,53	2510630
HBP1	0,53	1,23E-03	-1,12	-1,53	1940647
RSBN1	0,58	1,69E-03	-1,11	-1,53	6370215
MMP7	0,15	2,85E-02	-1,59	-1,53	3800088
TTC39B	0,44	3,15E-03	-1,18	-1,53	2340477
LOC651202	0,39	1,01E-02	-1,25	-1,53	6020066
CDC2L6	0,85	1,80E-02	-1,07	-1,53	3930452
LOC285074	0,49	4,54E-03	-1,16	-1,53	2810093
JARID2	0,76	1,38E-02	1,09	-1,53	2320286
CROP	0,41	1,30E-03	-1,17	-1,53	3140047
PRMT2	0,16	4,39E-03	-1,39	-1,53	1470392
TGFBR2	0,18	4,22E-03	-1,37	-1,53	6560091
SC4MOL	0,96	6,54E-03	1,02	-1,53	5860348
CD48	0,74	1,73E-02	-1,11	-1,53	2030767
POLR3GL	0,42	1,98E-03	-1,17	-1,53	5490703
CMIP	0,72	2,77E-02	-1,13	-1,53	360626
TTC39C	0,50	4,77E-03	-1,16	-1,53	3310142
PFKFB3	0,37	2,93E-03	-1,21	-1,53	1470601
SPNS3	0,29	9,91E-04	-1,22	-1,53	1740022
USP11	0,50	1,66E-03	-1,14	-1,53	1440040
LOC100129379	0,40	1,06E-02	-1,25	-1,53	4250133
FLJ46309	0,50	9,11E-04	-1,13	-1,53	7200519
MUTED	0,59	7,48E-04	-1,10	-1,53	3190164
PRCP	0,45	1,23E-03	-1,15	-1,53	6110386
TTLL3	0,50	1,14E-03	-1,13	-1,53	870500
TMEM116	0,49	6,88E-04	-1,12	-1,54	2070736
LOC389156	0,42	2,40E-02	-1,27	-1,54	2680612
PRMT2	0,18	2,18E-03	-1,33	-1,54	3850615

PELI2	0,38	1,79E-03	-1,20	-1,54	3840491
TMEM134	0,35	2,33E-03	-1,22	-1,54	5690711
ARL16	0,68	3,18E-03	-1,10	-1,54	990154
HIATL2	0,56	3,56E-03	-1,13	-1,54	2070598
WDR67	0,11	4,18E-04	-1,30	-1,54	6040554
PELI1	0,55	1,80E-02	-1,18	-1,54	3450092
WDR26	0,61	1,18E-03	-1,10	-1,54	2030358
LOC729090	0,96	3,78E-03	1,02	-1,54	2900270
MAPK3	0,07	1,49E-04	-1,29	-1,54	3870601
ZSCAN18	0,32	1,06E-02	-1,31	-1,54	6520280
CDKN1B	0,38	3,50E-03	-1,22	-1,54	1030348
NADSYN1	0,31	2,58E-04	-1,17	-1,54	3370575
PDK3	0,14	1,33E-04	-1,23	-1,54	110347
PRKCA	0,49	3,92E-03	-1,16	-1,54	6560564
LOC729776	0,36	3,62E-03	-1,23	-1,54	1260360
PARP3	0,46	4,95E-03	-1,18	-1,54	1470598
AGTPBP1	0,40	2,58E-03	-1,19	-1,54	4760427
CRADD	0,38	8,21E-03	-1,26	-1,54	1990291
WBP2	0,45	3,61E-03	-1,18	-1,54	3890398
AGXT2L2	0,16	4,71E-04	-1,27	-1,54	870139
FEZ1	0,14	6,79E-03	-1,46	-1,55	3290458
LOC729708	0,28	2,23E-04	-1,19	-1,55	7400193
ZMAT3	0,53	1,53E-03	-1,13	-1,55	6560601
UBASH3A	0,89	7,99E-03	-1,04	-1,55	3830220
ACOX3	0,23	9,20E-04	-1,26	-1,55	4540010
LETMD1	0,36	3,80E-04	-1,16	-1,55	1850379
H2AFJ	0,19	1,69E-04	-1,22	-1,55	5310411
HS.547738	0,69	3,68E-03	-1,10	-1,55	2120746
ABI1	0,43	1,28E-03	-1,16	-1,55	5130725
P2RX5	0,14	5,21E-03	-1,45	-1,55	2900427
LOC440595	0,71	4,55E-03	-1,09	-1,55	3990672
CBLN3	0,64	2,96E-03	-1,11	-1,55	6620291
FLJ45244	0,29	4,00E-04	-1,20	-1,55	6330653
DNAJC4	0,43	6,16E-03	-1,21	-1,55	3440288
LOC653232	0,44	1,74E-03	-1,17	-1,55	5050541
RWDD2A	0,51	3,30E-03	-1,15	-1,55	6420368
LOC653773	0,48	1,46E-02	-1,22	-1,55	2230167
MAP3K8	0,50	3,35E-02	-1,25	-1,55	1470215
BTBD2	0,54	1,37E-02	-1,18	-1,56	7610072
PLCG1	0,75	5,60E-03	-1,09	-1,56	2260131

TGFBR2	0,16	3,74E-03	-1,40	-1,56	5490070
STX16	0,60	4,03E-03	-1,13	-1,56	7040315
PDE3B	0,53	1,39E-02	-1,19	-1,56	5130471
C5ORF39	0,56	1,30E-02	-1,17	-1,56	7330523
AMT	0,51	2,80E-03	-1,15	-1,56	940450
DPP4	0,08	4,71E-03	-1,53	-1,56	4830255
POLD4	0,44	1,67E-03	-1,17	-1,56	1050240
FAM149B1	0,49	3,80E-04	-1,12	-1,56	3130035
TMEM17	0,80	2,69E-03	-1,06	-1,56	4670577
LOC645691	0,99	3,93E-03	-1,00	-1,56	6110673
VNN2	0,41	7,25E-03	-1,23	-1,56	2690239
FAM65B	0,68	1,98E-02	-1,14	-1,56	3450201
CPNE3	0,18	3,29E-04	-1,25	-1,56	7570215
MLLT11	0,48	6,42E-03	-1,19	-1,56	2630474
CLK1	0,85	3,24E-02	-1,08	-1,56	3440138
CYB5R2	0,47	1,82E-02	-1,24	-1,56	2940050
RHOC	0,40	1,05E-02	-1,26	-1,56	4390619
LOC255167	0,50	6,08E-03	-1,18	-1,56	4670563
MGAT4A	0,20	1,42E-03	-1,31	-1,56	6220593
LOC728809	0,71	6,07E-03	-1,10	-1,56	4390053
TMPRSS3	0,58	4,41E-03	-1,14	-1,56	540148
LOC645138	0,39	1,23E-03	-1,19	-1,56	1500538
CSDA	0,40	7,70E-03	-1,25	-1,56	2320129
LOC729340	0,32	2,01E-03	-1,24	-1,56	5550113
CD300A	0,50	1,46E-02	-1,21	-1,56	4780196
PCMTD1	0,50	6,45E-04	-1,13	-1,57	3290187
MZF1	0,42	5,36E-03	-1,22	-1,57	1030053
ABTB1	0,60	6,93E-03	-1,14	-1,57	2970044
FAM46C	0,58	2,89E-02	-1,20	-1,57	6860347
FXR1	0,47	1,67E-03	-1,16	-1,57	4180577
CLIC4	0,92	3,72E-02	-1,05	-1,57	3890193
LOC402251	0,83	5,80E-04	-1,04	-1,57	3440670
HS.436879	0,76	5,16E-03	-1,09	-1,57	6580703
LOC653658	0,45	1,04E-03	-1,16	-1,57	4610681
LOC100130070	0,32	7,11E-03	-1,30	-1,57	290370
LOC100131205	0,38	8,25E-03	-1,26	-1,57	5690369
TCEAL3	0,59	1,09E-02	-1,16	-1,57	730739
ITGA5	0,51	1,77E-02	-1,21	-1,57	6330338
C20ORF111	0,39	1,47E-03	-1,19	-1,57	2810082
ZNF75D	0,24	3,25E-04	-1,22	-1,57	460132

LOC100132797	0,51	1,42E-03	-1,14	-1,57	3830139
XKR6	0,24	5,31E-04	-1,24	-1,57	4730672
AHSA2	0,38	1,42E-03	-1,20	-1,57	1170220
LOC100131205	0,56	1,63E-02	-1,19	-1,57	650735
STAG3	0,15	1,76E-03	-1,37	-1,57	4390630
KIAA1147	0,50	4,83E-03	-1,17	-1,57	1050082
TIMP2	0,25	3,02E-04	-1,22	-1,57	780270
RNF19A	0,37	4,51E-03	-1,25	-1,57	1690184
IFNGR1	0,44	6,05E-03	-1,21	-1,57	2470358
METRNL	0,48	1,54E-02	-1,23	-1,57	5810504
LOC646819	0,32	1,49E-04	-1,16	-1,57	70349
C4ORF14	0,48	3,95E-04	-1,12	-1,57	5220068
ACSS2	0,48	3,47E-03	-1,17	-1,58	4490524
PLIN2	0,87	3,16E-02	-1,07	-1,58	460204
CXCR4	0,30	5,29E-03	-1,31	-1,58	1300280
LOC100129362	0,66	7,94E-04	-1,09	-1,58	290095
LOC100134537	0,41	6,06E-03	-1,23	-1,58	2360082
LOC100190938	0,52	2,22E-03	-1,15	-1,58	5260132
ALDH6A1	0,45	6,15E-04	-1,14	-1,58	5820373
YEATS2	0,69	3,80E-03	-1,10	-1,58	5260537
PRCP	0,55	2,53E-03	-1,14	-1,58	1660300
IL11RA	0,29	3,98E-03	-1,30	-1,58	2760148
BTN3A2	0,42	3,55E-03	-1,21	-1,58	4610674
LOC100131785	0,44	5,22E-03	-1,21	-1,58	4200056
CCDC53	0,92	1,95E-03	-1,03	-1,58	7040544
CD37	0,38	3,39E-03	-1,23	-1,58	1510133
GVIN1	0,92	2,22E-02	-1,04	-1,58	1740050
KDM5B	0,56	3,03E-03	-1,14	-1,58	5870482
TSPAN31	0,67	1,48E-02	-1,14	-1,58	5670577
LOC284023	0,39	3,35E-03	-1,23	-1,58	4220241
LOC391656	0,42	6,41E-04	-1,16	-1,58	6770315
HCG2P7	0,34	9,77E-04	-1,21	-1,58	4780470
C16ORF75	0,99	1,83E-02	-1,00	-1,58	4540072
ARID4B	0,63	1,57E-03	-1,11	-1,58	2470603
PARVG	0,30	2,93E-03	-1,28	-1,58	6200685
P4HTM	0,30	1,43E-03	-1,25	-1,58	7000202
RPS27	0,25	2,80E-03	-1,32	-1,58	6650564
GIMAP7	0,27	3,58E-02	-1,52	-1,59	3170091
FAM175A	0,44	1,98E-03	-1,18	-1,59	990332
TC2N	0,50	3,61E-03	-1,17	-1,59	1850300

PIGP	0,47	2,75E-03	-1,17	-1,59	5810630
IL23R	0,21	2,41E-03	-1,34	-1,59	6650722
GIMAP8	0,31	3,21E-02	-1,45	-1,59	1190040
SLC16A5	0,35	3,82E-03	-1,26	-1,59	6860082
ETS1	0,53	1,05E-03	-1,13	-1,59	6370435
IRF9	0,51	4,40E-03	-1,17	-1,59	2000022
MTSS1	0,78	3,69E-03	-1,08	-1,59	1510121
ALOX5AP	0,65	1,98E-02	1,16	-1,59	3930343
EBI2	0,32	2,17E-03	-1,25	-1,59	4490520
SERGEF	0,43	7,85E-04	-1,16	-1,59	6580437
LOC728782	0,31	5,83E-03	-1,31	-1,59	3840471
CACNB3	0,56	8,78E-03	-1,17	-1,59	1980328
RNF181	0,48	2,68E-03	-1,17	-1,59	3440338
LXN	0,72	1,87E-03	-1,09	-1,59	60670
TRADD	0,39	2,02E-03	-1,21	-1,59	2650706
ANKRA2	0,35	7,85E-04	-1,20	-1,59	1170630
LOC100130892	0,29	2,14E-04	-1,19	-1,59	5270735
FAM134B	0,46	2,24E-03	-1,18	-1,59	3180661
ACAP1	0,31	4,50E-03	-1,30	-1,59	7210682
GK	0,80	1,69E-02	-1,09	-1,59	940274
NPC2	0,56	5,31E-04	-1,11	-1,60	540075
CNOT8	0,60	1,08E-03	-1,11	-1,60	4640484
MGC72104	0,43	6,82E-04	-1,16	-1,60	2810044
CRELD1	0,37	1,98E-03	-1,23	-1,60	3400619
SLC38A2	0,52	2,13E-03	-1,15	-1,60	1740136
TAX1BP1	0,87	4,95E-03	-1,05	-1,60	4920739
GBP2	0,61	3,40E-03	-1,13	-1,60	1940162
METRNL	0,43	2,03E-02	-1,29	-1,60	50095
BMS1P5	0,43	1,90E-03	-1,19	-1,60	1260646
LOC653316	0,51	1,08E-02	-1,20	-1,60	3850411
METRNL	0,47	1,16E-02	-1,23	-1,60	10224
EVI2A	0,95	1,10E-03	-1,02	-1,61	4590224
HPCAL1	0,66	7,59E-03	-1,13	-1,61	520184
RPL12P6	0,41	2,89E-03	-1,21	-1,61	6250408
PIK3R1	0,61	2,95E-03	-1,13	-1,61	1470753
PSCD4	0,65	1,05E-02	-1,14	-1,61	6510524
GPR19	0,82	2,16E-03	-1,06	-1,61	6200072
LOC649946	0,16	1,42E-03	-1,36	-1,61	6270605
CBX7	0,76	1,38E-03	-1,07	-1,61	1500747
LOC730255	0,42	4,62E-04	-1,16	-1,61	6420603

LPIN1	0,48	6,71E-04	-1,14	-1,61	6200670
LRRC37B	0,43	1,76E-03	-1,19	-1,61	4200523
CD37	0,47	4,77E-03	-1,20	-1,61	3800373
PYCARD	0,21	4,02E-03	-1,39	-1,61	6860687
LEF1	0,42	2,67E-02	-1,32	-1,61	4570255
SH3PXD2A	0,51	2,28E-03	-1,16	-1,61	3460451
LYN	0,13	2,57E-02	-1,72	-1,61	7320551
LOC400464	0,37	1,28E-03	-1,22	-1,61	5260605
LOC650737	0,43	6,42E-04	-1,16	-1,61	6250114
LEF1	0,44	3,40E-02	-1,32	-1,61	2810601
SLC25A23	0,40	5,67E-03	-1,25	-1,61	6280092
TTC32	0,52	1,04E-03	-1,14	-1,61	5670114
LOC727984	0,66	1,26E-03	-1,10	-1,61	7320722
EPHX2	0,57	9,36E-03	-1,17	-1,62	6960397
SPATA7	0,29	3,08E-04	-1,21	-1,62	380079
ZNF549	0,78	1,67E-03	-1,07	-1,62	3450750
TMEM44	0,66	6,31E-03	-1,13	-1,62	2350279
TAX1BP1	0,55	1,45E-03	-1,14	-1,62	7050470
C18ORF56	0,84	1,30E-02	-1,07	-1,62	1450682
N4BP2L1	0,51	3,80E-03	-1,17	-1,62	620112
NAALADL1	0,26	2,89E-04	-1,23	-1,63	4120626
BIN1	0,62	1,20E-02	-1,16	-1,63	5130440
APH1B	0,24	2,50E-04	-1,24	-1,63	7160224
HIF1A	0,31	2,77E-03	-1,28	-1,63	6220543
FAM127A	0,29	6,11E-04	-1,24	-1,63	6040376
C14ORF85	0,42	2,74E-04	-1,15	-1,63	360373
MCART1	0,96	1,57E-03	-1,02	-1,63	6770286
TMEM149	0,95	3,59E-02	-1,04	-1,63	5670139
RAB3IP	0,14	7,78E-04	-1,37	-1,63	1410603
PTPRM	0,07	1,38E-03	-1,49	-1,63	5860356
C3ORF34	0,43	1,24E-03	-1,19	-1,63	1850040
LOC202134	0,44	8,35E-03	-1,24	-1,64	160280
LOC100129169	0,51	4,95E-04	-1,13	-1,64	4900164
PPIL3	0,78	3,47E-02	-1,12	-1,64	4390390
RAG1AP1	0,53	1,02E-03	-1,14	-1,64	2140008
TGIF1	0,66	6,62E-04	-1,09	-1,64	3140369
AKAP7	0,34	2,20E-03	-1,26	-1,64	5340504
NR4A2	0,94	3,38E-03	-1,03	-1,64	6400364
RRAS	0,51	1,42E-02	-1,23	-1,64	4570670
CD69	0,38	1,02E-03	-1,21	-1,64	6900634

LOC730313	0,70	6,14E-04	-1,08	-1,64	6020743
QSOX2	0,12	3,29E-04	-1,34	-1,64	290441
LOC391075	0,35	9,94E-04	-1,23	-1,64	6550092
LOC728672	0,56	9,23E-04	-1,13	-1,64	7330689
LOC648622	0,46	5,50E-03	-1,22	-1,64	4050377
FAM65A	0,27	2,80E-03	-1,34	-1,64	6480092
SSH3	0,40	4,11E-03	-1,25	-1,64	540608
C14ORF72	0,44	3,03E-03	-1,21	-1,65	2850176
LOC389156	0,44	7,70E-03	-1,25	-1,65	2340736
PECI	0,70	5,58E-04	-1,08	-1,65	10594
MAGT1	0,69	9,79E-04	-1,09	-1,65	3190626
DPEP2	0,15	2,95E-03	-1,45	-1,65	1820681
FBXO15	0,31	2,25E-04	-1,20	-1,65	770044
SYTL1	0,60	2,76E-03	-1,14	-1,65	2760437
LOC339192	0,98	4,45E-02	1,02	-1,65	1230026
BCL2	0,64	6,32E-03	-1,14	-1,65	3180494
TNFAIP3	0,63	2,83E-02	-1,20	-1,65	3360681
TRADD	0,38	1,46E-03	-1,23	-1,65	20347
STAT4	0,92	9,84E-04	-1,03	-1,65	7320370
LMTK3	0,32	1,04E-03	-1,24	-1,65	6980632
FYN	0,72	1,29E-03	-1,09	-1,65	4860050
SAMD9	0,54	1,82E-02	-1,22	-1,65	1240142
SNORA12	0,12	6,11E-04	-1,38	-1,65	6510156
ADD3	0,45	6,55E-04	-1,16	-1,65	1990468
IL23R	0,16	2,16E-03	-1,42	-1,65	3140088
BAIAP2L1	0,40	5,84E-03	-1,26	-1,65	5700343
CMTM8	0,40	1,05E-02	-1,30	-1,66	2480037
LPAR5	0,13	1,49E-04	-1,29	-1,66	2260241
INSIG1	0,96	1,83E-03	-1,02	-1,66	1820332
ABCG1	0,92	1,87E-02	-1,05	-1,66	6060377
GPI	0,40	4,67E-04	-1,18	-1,66	4220064
PGK1	0,73	2,31E-04	-1,07	-1,66	6110400
BIRC2	0,29	1,16E-03	-1,28	-1,66	840280
C6ORF190	0,71	9,72E-03	-1,13	-1,66	4040187
PLIN2	0,79	1,97E-02	-1,11	-1,67	1400446
NPHP3	0,41	1,28E-03	-1,21	-1,67	1820746
SMAD3	0,24	4,62E-04	-1,28	-1,67	6840328
BIN1	0,55	5,04E-03	-1,18	-1,67	650553
BTN3A2	0,62	4,88E-03	-1,15	-1,67	2570253
LOC654096	0,44	9,72E-03	-1,27	-1,67	5050538

IRAK2	0,43	3,54E-03	-1,23	-1,68	3930750
CA9	0,18	7,93E-04	-1,35	-1,68	6040626
SETDB2	0,27	1,05E-04	-1,20	-1,68	5390646
GPR18	0,72	2,07E-03	-1,10	-1,68	4120224
EDG4	0,19	3,97E-04	-1,30	-1,68	1170605
EID2B	0,41	8,14E-04	-1,20	-1,68	2350543
LOC100132795	0,38	5,79E-04	-1,20	-1,68	2600373
SFRS18	0,36	9,54E-04	-1,23	-1,68	1580204
NIPSNAP1	0,35	3,79E-04	-1,20	-1,68	5490131
TUBB3	0,07	1,45E-03	-1,52	-1,68	4050040
LTBP4	0,53	5,50E-04	-1,13	-1,68	4290315
HCFC1R1	0,03	1,69E-04	-1,42	-1,68	5420347
RPL10A	0,61	1,05E-03	-1,12	-1,69	4040100
NGFRAP1	0,49	6,42E-03	-1,22	-1,69	5260349
SNORD3C	0,13	1,67E-03	-1,46	-1,69	580161
PJA2	0,66	1,13E-03	-1,11	-1,69	520431
KLHL3	0,58	2,68E-03	-1,15	-1,69	2810400
MSRB2	0,40	1,81E-03	-1,23	-1,69	2710646
LOC645688	0,55	1,52E-03	-1,15	-1,69	3130736
SAT2	0,15	2,14E-04	-1,31	-1,69	1980762
ARHGEF10	0,14	4,15E-03	-1,53	-1,70	6900703
GPSM3	0,27	6,31E-04	-1,28	-1,70	6420386
XRN1	0,30	1,66E-03	-1,30	-1,70	1990487
SCARNA9	0,25	3,42E-03	-1,39	-1,70	6220112
DUSP16	0,49	3,14E-03	-1,19	-1,70	1470465
WSB1	0,61	5,87E-04	-1,11	-1,70	6110091
S100A10	0,32	1,13E-03	-1,26	-1,70	2490195
ALDOA	0,59	2,20E-03	-1,15	-1,70	2640088
C15ORF48	0,23	1,15E-02	-1,52	-1,70	1110373
HIST2H2AC	0,61	4,28E-03	-1,16	-1,70	6100022
C19ORF36	0,36	4,74E-04	-1,21	-1,70	2000075
BEX4	0,47	3,69E-03	-1,22	-1,70	1110615
CCNB1IP1	0,51	2,94E-03	-1,19	-1,70	510114
ITM2B	0,55	3,50E-02	-1,27	-1,71	6380315
CTH	0,89	4,49E-02	-1,07	-1,71	60138
LOC644237	0,29	1,21E-03	-1,30	-1,71	7550592
CMAH	0,31	4,37E-03	-1,35	-1,71	4250634
GSDMB	0,12	1,79E-04	-1,34	-1,71	5390608
LTA4H	0,38	1,49E-04	-1,17	-1,71	1430524
RAB9A	0,41	1,03E-03	-1,21	-1,72	2940451

CMAH	0,32	7,79E-03	-1,38	-1,72	5550066
RAB11FIP5	0,59	1,09E-02	-1,20	-1,72	1260193
CAMLG	0,51	4,71E-04	-1,14	-1,72	6660092
LOC653156	0,31	6,64E-03	-1,38	-1,73	4010180
GOLGA8B	0,61	1,81E-02	-1,21	-1,73	5690671
MPI	0,30	1,30E-04	-1,20	-1,73	4010041
LOC647349	0,45	2,84E-03	-1,22	-1,73	1980424
P4HA2	0,56	3,50E-03	-1,17	-1,73	270408
C17ORF61	0,28	7,78E-04	-1,29	-1,73	2340521
PAIP2	0,49	6,90E-05	-1,11	-1,73	240725
C20ORF46	0,51	7,03E-03	-1,22	-1,73	6110102
FLOT1	0,03	5,81E-04	-1,55	-1,73	3780181
TRAF3IP2	0,38	4,08E-03	-1,29	-1,73	7510719
ATM	0,95	2,59E-02	-1,04	-1,73	4250008
ANKRA2	0,35	7,88E-04	-1,25	-1,73	7400114
LOC100129028	0,39	2,74E-04	-1,19	-1,73	2900500
ERO1L	0,41	2,95E-03	-1,25	-1,74	4780671
ABLIM1	0,38	6,32E-03	-1,32	-1,74	6400243
CDKN1B	0,53	1,99E-03	-1,17	-1,74	130309
LOC392437	0,35	3,78E-04	-1,22	-1,74	2260196
SLC2A14	0,80	1,52E-02	-1,11	-1,74	3420241
TOX2	0,20	1,21E-03	-1,39	-1,74	1010736
LOC100129742	0,58	4,62E-04	-1,12	-1,74	2490341
FYN	0,51	3,40E-04	-1,14	-1,74	840025
AK1	0,69	5,31E-03	-1,14	-1,74	5130162
GYPC	0,21	1,76E-04	-1,28	-1,74	7000577
SREBF1	0,35	6,11E-04	-1,24	-1,74	3390343
HIST2H2AA3	0,53	1,06E-02	-1,23	-1,75	1820592
ANKZF1	0,30	3,29E-04	-1,25	-1,75	580598
CCR7	0,21	3,86E-04	-1,32	-1,75	5390246
NINJ1	0,89	1,50E-02	-1,06	-1,75	7380706
INSIG1	0,88	1,66E-03	1,05	-1,75	360192
ATP6V0A4	0,15	3,54E-03	-1,54	-1,76	5290243
LOC100133662	0,46	6,47E-04	-1,18	-1,76	6280646
HS.534680	0,44	7,85E-04	-1,20	-1,76	2510403
AP3S1	0,32	1,66E-03	-1,30	-1,76	7200402
ZFP36L2	0,45	2,31E-04	-1,15	-1,76	7050300
DUSP19	0,63	1,90E-04	-1,10	-1,76	5260195
CCDC104	0,44	1,44E-04	-1,15	-1,76	990114
LOC399900	0,32	1,49E-04	-1,21	-1,76	4490594

TCEAL3	0,48	3,41E-03	-1,22	-1,77	4780072
NUCB2	0,60	5,31E-04	-1,12	-1,77	60427
CLEC2B	0,26	2,22E-03	-1,39	-1,77	2490161
TPP1	0,31	1,48E-03	-1,31	-1,77	670113
LOC391045	0,77	1,71E-02	-1,13	-1,77	430019
LOC729500	0,47	6,95E-03	-1,26	-1,78	6250537
CLYBL	0,35	3,02E-04	-1,22	-1,78	4610273
FAIM3	0,71	2,06E-02	-1,17	-1,78	5270520
BCL2	0,48	3,49E-03	-1,23	-1,78	4150201
LETMD1	0,36	4,16E-04	-1,23	-1,78	4150575
VWA5A	0,10	1,69E-04	-1,39	-1,78	5080592
SH3BGRL	0,54	1,59E-03	-1,17	-1,79	5890242
RAP1GAP	0,86	2,73E-02	1,09	-1,79	4890181
RNF19A	1,00	5,35E-03	1,00	-1,79	7160010
GZMM	0,27	5,64E-03	-1,46	-1,79	1710279
FAM113B	0,80	6,14E-03	-1,10	-1,79	4200541
KLF9	0,58	3,71E-04	-1,12	-1,79	3390292
PBX4	0,23	6,11E-04	-1,35	-1,79	2760544
HMGCL	0,47	5,22E-04	-1,17	-1,80	7380608
PLCH2	0,17	3,14E-03	-1,52	-1,80	650452
PTPRF	0,51	1,62E-02	-1,28	-1,80	3060398
FAM62B	0,32	8,22E-04	-1,28	-1,80	510762
ACSS2	0,29	6,11E-04	-1,30	-1,80	4670544
HSH2D	0,37	1,03E-03	-1,26	-1,80	6040647
SDCBP	0,63	4,67E-04	-1,12	-1,80	630167
PHF11	0,56	2,54E-03	-1,18	-1,80	6100521
GPSM1	0,77	2,22E-03	-1,10	-1,81	6280100
NFKBIZ	0,47	1,47E-02	-1,31	-1,81	2470348
LOC642989	0,63	5,85E-03	-1,17	-1,81	6280446
TSTD1	0,34	2,31E-04	-1,22	-1,81	7100471
FYB	0,55	1,83E-03	-1,18	-1,82	5890414
LOC389787	0,49	4,71E-04	-1,17	-1,82	160047
FAAH2	0,58	5,49E-04	-1,14	-1,82	130167
LOC392437	0,31	3,86E-04	-1,26	-1,82	2750685
HMGCS1	0,92	1,81E-03	1,04	-1,82	5270112
GNG4	0,66	1,83E-03	1,14	-1,83	4050671
CCDC28A	0,38	1,68E-04	-1,20	-1,83	2000504
DHX40	0,38	1,17E-04	-1,18	-1,84	5220433
AIF1	0,10	6,16E-04	-1,50	-1,84	3800047
IRF2BP2	0,51	9,05E-04	-1,18	-1,84	3290224

BTG2	0,38	2,25E-03	-1,30	-1,84	1010487
LOC730525	0,58	1,05E-02	-1,23	-1,84	730709
LOC100132291	0,40	1,74E-03	-1,27	-1,84	7150414
CST7	0,78	2,58E-03	-1,10	-1,84	4810341
LIMS1	0,38	2,27E-03	-1,30	-1,84	1090739
CCDC106	0,34	2,34E-03	-1,34	-1,84	3940471
MYLIP	0,51	5,49E-04	-1,17	-1,85	4830424
GYPC	0,20	1,64E-04	-1,31	-1,85	7210398
ABLIM1	0,36	5,20E-03	-1,37	-1,85	2570112
LOC401152	0,64	3,86E-04	-1,11	-1,85	1980369
IGBP1	0,20	1,29E-04	-1,30	-1,85	6270427
DNAJB2	0,71	9,06E-03	-1,15	-1,85	3830653
MT1F	0,41	2,35E-03	-1,27	-1,86	4220672
MST1	0,32	1,68E-03	-1,34	-1,86	3710202
ABCA1	0,18	1,12E-03	-1,46	-1,86	4060358
GK	0,62	6,78E-03	-1,19	-1,86	4150369
RHOC	0,29	5,09E-04	-1,31	-1,86	4250327
C6ORF105	0,36	1,16E-02	-1,43	-1,86	2650192
PGK1	0,32	1,58E-05	-1,17	-1,87	360735
TRPT1	0,42	1,96E-04	-1,18	-1,87	940669
SNORD3A	0,10	1,76E-03	-1,65	-1,87	2510164
PDCD4	0,82	7,54E-03	-1,10	-1,87	2570433
APBB3	0,31	4,80E-04	-1,29	-1,87	7320402
GNA15	0,96	2,70E-03	-1,02	-1,87	5670424
TGIF1	0,80	6,82E-04	-1,07	-1,87	4260189
VEGFB	0,35	4,62E-04	-1,26	-1,88	4060333
RPL9	0,36	5,49E-04	-1,26	-1,88	6420730
ASGR1	0,40	1,35E-02	-1,41	-1,88	2370064
ZCCHC12	0,35	3,86E-04	1,25	-1,88	2690279
PMM1	0,25	6,66E-05	-1,25	-1,88	4890408
SIDT2	0,28	7,61E-04	-1,34	-1,89	4890328
P4HA2	0,59	3,11E-03	-1,19	-1,89	4010064
PHGDH	0,76	2,51E-03	-1,11	-1,89	240086
FBLN7	0,13	2,03E-04	-1,41	-1,89	5670154
CA2	0,39	1,52E-02	-1,43	-1,89	2060674
ZFP90	0,28	3,93E-04	-1,31	-1,89	5900286
TMEM71	0,99	4,21E-03	-1,01	-1,89	1710541
NCKIPSD	0,47	1,25E-03	-1,22	-1,89	7320468
HS.560343	0,36	2,61E-04	-1,24	-1,90	6400564
STAT3	0,57	3,40E-03	-1,20	-1,90	2100484

CBS	0,66	4,68E-02	-1,27	-1,90	1230047
FES	0,40	1,18E-02	-1,40	-1,90	4120689
DUSP5	0,94	1,74E-02	1,04	-1,91	5390161
GIMAP5	0,02	8,12E-04	-1,80	-1,91	5360079
MTSS1	0,93	8,25E-03	-1,04	-1,91	3170300
C10ORF75	0,62	1,49E-03	-1,16	-1,91	7330730
NAMPT	0,85	3,65E-02	1,12	-1,92	3060523
FGF11	0,23	1,00E-03	-1,42	-1,92	5900025
ACAD11	0,43	5,02E-04	-1,22	-1,93	3370136
DDIT3	0,87	2,51E-02	-1,10	-1,93	830619
TMEM140	0,33	9,01E-04	-1,32	-1,94	4670414
ITGAX	0,59	7,92E-03	-1,23	-1,94	4490500
STC2	0,66	8,69E-03	-1,19	-1,94	1170170
FYN	0,39	1,49E-04	-1,20	-1,94	610164
NGFRAP1	0,48	2,52E-03	-1,25	-1,94	6860220
BCKDHA	0,51	6,21E-04	-1,19	-1,94	2810296
SIRPG	0,65	1,25E-02	-1,21	-1,95	4220152
CAPN12	0,35	1,35E-03	-1,33	-1,95	3710253
HIST2H2AA4	0,35	1,68E-03	-1,35	-1,95	4290148
FAM80A	0,53	1,26E-03	-1,20	-1,95	6840619
LOC644774	0,67	1,76E-04	-1,10	-1,95	6580544
SERPINE2	0,87	2,16E-02	-1,10	-1,96	5080192
SDCBP	0,44	1,07E-04	-1,17	-1,96	6040324
HIST2H2AA3	0,67	5,63E-03	-1,18	-1,97	610451
MYADM	0,37	1,67E-04	-1,23	-1,97	2970730
HBP1	0,63	4,18E-04	-1,13	-1,97	3780270
FAM116B	0,24	7,65E-04	-1,41	-1,97	6520241
ARID5B	0,33	1,49E-04	-1,25	-1,97	1410408
SLC29A4	0,30	1,42E-03	-1,39	-1,97	7650047
BEXL1	0,62	4,80E-03	-1,20	-1,97	4490180
CD96	0,63	7,85E-03	-1,21	-1,97	2710754
LOC100131905	0,27	3,86E-04	-1,35	-1,97	6650603
TSHZ2	0,44	6,00E-03	-1,34	-1,97	4890292
PHF11	0,43	1,66E-03	-1,28	-1,97	1510196
PIK3IP1	0,61	1,28E-02	-1,25	-1,98	5390730
LOC654194	0,32	1,66E-03	-1,37	-1,98	1260156
ZBTB25	0,57	9,85E-04	-1,18	-1,98	2030368
BHLHB2	0,58	7,55E-03	-1,24	-1,98	2640735
ZNF358	0,26	1,14E-03	-1,43	-1,98	6860026
FBLN5	0,77	8,34E-04	-1,10	-1,99	5690639

LOC729500	0,39	3,93E-03	-1,37	-1,99	4040307
SNORD3D	0,13	6,11E-04	-1,54	-1,99	380685
TIGA1	0,28	1,76E-04	-1,30	-1,99	150441
SBK1	0,81	1,69E-03	-1,09	-2,00	3850767
ATHL1	0,83	1,18E-03	-1,07	-2,00	4070239
SNORD13	0,80	1,35E-02	-1,13	-2,00	7210035
ANKRD37	0,66	2,55E-02	-1,25	-2,00	240682
NGLY1	0,41	2,53E-04	-1,22	-2,00	3780670
FAM119A	0,49	5,83E-04	-1,20	-2,00	1090646
WDR54	0,28	5,80E-05	-1,26	-2,00	2030148
RPL14	0,38	2,72E-03	-1,36	-2,01	2140753
GBE1	0,45	7,85E-04	-1,24	-2,01	6280176
PDE9A	0,27	1,49E-03	-1,45	-2,01	830563
IRF7	0,40	2,91E-02	-1,55	-2,02	6400176
FAM134B	0,31	4,78E-04	-1,33	-2,02	6420309
WSB1	0,53	3,55E-04	-1,17	-2,02	2230615
STAT3	0,40	5,98E-04	-1,27	-2,05	4250538
TMPRSS3	0,79	7,12E-03	-1,13	-2,05	6980470
AK3L1	0,41	6,39E-05	-1,19	-2,06	4610554
GBP5	0,02	1,77E-03	-2,15	-2,06	1510364
LOC154761	0,42	3,25E-04	-1,23	-2,06	3180360
PTRF	0,73	2,53E-02	-1,21	-2,06	4850301
SPRY1	0,55	4,07E-03	-1,25	-2,07	3310692
ZNF277	0,39	2,68E-04	-1,26	-2,08	5870180
CACNA1I	0,20	7,59E-04	-1,50	-2,08	6980546
NCRNA00219	0,22	2,10E-04	-1,38	-2,08	4070376
RNASET2	0,44	7,40E-05	-1,18	-2,09	2850100
METRNL	0,35	6,17E-03	-1,48	-2,09	4150689
HIST1H2BD	0,49	1,28E-03	-1,25	-2,09	290730
TM6SF1	0,39	3,07E-03	-1,38	-2,09	240653
AK3L1	0,38	7,94E-05	-1,22	-2,10	4290192
GIMAP1	0,07	1,63E-04	-1,55	-2,10	6420671
TXK	0,07	1,82E-04	-1,58	-2,10	1190138
APBB3	0,36	7,82E-04	-1,33	-2,11	4120279
CD96	0,54	5,59E-03	-1,28	-2,12	4560743
BEX2	0,28	4,67E-04	-1,39	-2,12	4830674
ALPK1	0,14	1,82E-04	-1,47	-2,12	540390
CLYBL	0,18	1,85E-05	-1,31	-2,13	2070044
HS.568741	0,57	1,40E-03	-1,21	-2,13	2450435
GNLY	0,51	3,60E-02	-1,45	-2,13	6580041

ICA1	0,50	7,50E-04	-1,23	-2,13	1710019
NAMPT	0,91	1,52E-02	1,08	-2,14	2230379
VLDLR	0,44	6,11E-04	-1,26	-2,14	5390661
FAM153B	0,42	3,52E-03	-1,36	-2,15	4780121
MCL1	0,29	6,21E-04	-1,41	-2,15	610750
RGL4	0,34	1,59E-03	-1,41	-2,15	7000465
C5ORF13	0,31	1,19E-04	-1,28	-2,15	940471
LOC143666	0,80	5,33E-03	-1,13	-2,15	2600136
NDRG1	0,43	1,03E-03	-1,29	-2,16	1230070
HS.296031	0,31	1,85E-05	-1,23	-2,16	4150102
DHX32	0,67	1,12E-03	-1,16	-2,16	1980164
RORA	0,28	2,14E-04	-1,35	-2,17	1110180
SERPINB1	0,15	6,65E-05	-1,41	-2,18	3190112
FAM57A	0,43	1,04E-04	-1,21	-2,19	5910600
TCEA2	0,25	1,44E-04	-1,36	-2,21	4880014
GSDMB	0,13	1,33E-04	-1,48	-2,21	6270615
YPEL3	0,29	3,86E-04	-1,39	-2,21	130750
IQCG	0,28	1,64E-02	-1,82	-2,23	70551
UPRT	0,90	1,19E-03	-1,06	-2,23	6100414
ASCL2	0,36	5,98E-04	-1,35	-2,23	7200435
DUSP3	0,25	2,11E-04	-1,40	-2,24	6560156
EPSTI1	0,31	7,45E-03	-1,63	-2,25	5700725
ENO2	0,38	2,55E-03	-1,43	-2,25	50402
ZFP36	0,63	1,81E-03	-1,20	-2,25	2900348
FAM117B	0,36	4,62E-04	-1,34	-2,26	3120292
LAG3	0,56	4,69E-02	-1,47	-2,26	2680189
GCHFR	0,26	4,26E-05	-1,31	-2,26	5670475
JAM3	0,21	1,18E-03	-1,60	-2,28	1400689
MGC33556	0,45	1,03E-03	-1,30	-2,29	1430634
GIMAP4	0,19	1,65E-03	-1,69	-2,30	4880626
DDIT4L	0,34	2,87E-02	-1,82	-2,30	380019
SELL	0,55	1,67E-03	-1,25	-2,30	6940358
CA2	0,40	8,91E-03	-1,53	-2,30	870630
LIMS1	0,24	4,26E-05	-1,33	-2,30	990358
MKNK2	0,27	1,44E-04	-1,38	-2,32	940152
TSC22D3	0,58	6,55E-04	-1,21	-2,34	6350446
IFNGR2	0,57	5,46E-03	1,30	-2,35	2570291
CBLB	0,70	1,10E-03	-1,16	-2,36	5270132
EGR1	0,43	3,51E-03	-1,41	-2,37	870338
IL8	0,78	3,76E-02	-1,24	-2,37	1570553

RPS29	0,56	1,09E-03	-1,24	-2,39	2760452
BTG1	0,45	1,24E-03	-1,33	-2,40	4730369
MIAT	0,31	6,11E-04	-1,44	-2,41	430438
SIRPG	0,40	9,79E-04	-1,37	-2,41	3940041
FBLN5	0,53	2,72E-04	-1,21	-2,41	4670441
P4HA1	0,31	1,05E-04	-1,33	-2,42	4220731
JUN	0,65	1,40E-02	-1,30	-2,43	6510367
CD69	0,64	6,42E-04	-1,18	-2,44	2710575
CXCR5	0,02	6,65E-05	-1,80	-2,44	3890400
GNLY	0,62	4,58E-02	-1,44	-2,44	5360064
BTBD11	0,10	5,40E-04	-1,81	-2,44	6510608
LRMP	0,53	1,57E-05	-1,14	-2,45	7150324
SGPP2	0,26	1,28E-05	-1,29	-2,46	2120612
PAM	0,45	3,88E-04	-1,29	-2,46	4210670
YPEL5	0,43	3,81E-04	-1,30	-2,48	2680097
SIRPG	0,44	8,85E-04	-1,34	-2,49	2680050
CCNG2	0,51	5,09E-04	-1,26	-2,49	5360672
STAT3	0,35	2,74E-04	-1,37	-2,52	5090619
PFKFB3	0,31	1,47E-04	-1,36	-2,52	4120053
FAM162A	0,24	9,99E-05	-1,42	-2,54	5310736
INSIG2	0,52	2,36E-03	-1,32	-2,57	2070039
ICA1	0,76	5,35E-04	-1,13	-2,57	4050121
RGS2	0,98	6,41E-05	-1,01	-2,58	3400019
PDE4D	0,41	2,63E-04	-1,32	-2,61	1770114
LY96	0,20	5,80E-05	-1,45	-2,61	70167
PNPLA7	0,38	1,34E-04	-1,32	-2,62	5050577
SPINT2	0,57	2,57E-03	-1,30	-2,62	1240730
SAT1	0,52	3,32E-03	-1,35	-2,63	5490431
RBKS	0,41	5,09E-04	-1,36	-2,63	4200209
PPFIA4	0,27	9,99E-05	-1,41	-2,66	7570095
P2RY11	0,44	5,80E-05	-1,24	-2,70	3930379
PASK	0,03	1,85E-05	-1,73	-2,70	4150100
SERPINB6	0,22	2,05E-04	-1,54	-2,70	4220504
RRAGD	0,41	6,74E-04	-1,39	-2,73	6480209
IFIT2	0,69	2,36E-02	-1,35	-2,74	2600747
BCAT1	0,84	2,17E-04	-1,08	-2,74	7650524
PASK	0,03	1,28E-05	-1,64	-2,76	2140382
IL18RAP	0,17	1,24E-03	-1,90	-2,79	6520180
TMPRSS6	0,44	9,02E-03	-1,59	-2,80	2000129
KLRB1	0,77	4,95E-03	-1,20	-2,80	6200019

SLC2A3	0,80	1,66E-03	-1,14	-2,82	3800168
FSCN1	0,27	3,43E-04	-1,56	-2,86	4560328
PITPNC1	0,00	1,78E-06	-1,84	-2,89	1230630
LOC202134	0,37	1,81E-03	-1,57	-2,90	1450471
IFITM2	0,48	2,88E-04	-1,30	-2,91	1230767
TXNIP	0,71	2,25E-03	-1,22	-2,93	1240440
HAVCR2	0,31	1,76E-04	-1,45	-2,93	5220093
TCEA3	0,07	1,53E-04	-1,92	-2,94	4050491
BNIP3L	0,82	8,89E-05	-1,09	-2,97	2640192
TSC22D3	0,40	6,65E-05	-1,31	-2,97	6350632
ISG20	0,76	1,83E-03	-1,19	-3,01	6330132
EFEMP2	0,28	3,36E-04	-1,58	-3,03	6100180
AK3L1	0,38	1,79E-05	-1,28	-3,06	160148
BCL6	0,47	1,05E-04	-1,27	-3,06	6280458
SPRY1	0,58	1,43E-03	-1,32	-3,08	6760669
TP53INP1	0,12	7,91E-06	-1,51	-3,10	5420538
SYTL3	0,72	3,14E-03	-1,24	-3,10	2600682
C20ORF100	0,40	8,84E-04	-1,49	-3,11	1400601
BEND5	0,32	2,20E-04	-1,49	-3,13	4540398
LOC653506	0,40	2,98E-03	-1,63	-3,16	2030132
CD27	0,21	1,69E-04	-1,65	-3,19	1240450
IFITM1	0,43	1,76E-04	-1,37	-3,32	5360156
SCD	0,86	3,85E-05	-1,07	-3,38	2140128
KISS1R	0,35	6,44E-04	-1,64	-3,54	4120131
CD7	0,23	8,80E-05	-1,63	-3,61	6330091
BNIP3	0,43	1,85E-05	-1,29	-3,67	6770608
IL8	0,90	2,54E-02	-1,15	-3,69	1980309
TP53INP1	0,23	4,26E-05	-1,61	-3,93	6660630
DPYSL4	0,26	1,49E-04	-1,70	-3,94	50309
DDIT4	0,51	2,04E-04	-1,35	-4,00	3190148
HS.10862	0,28	7,30E-06	-1,43	-4,12	1940563
ZNF395	0,35	3,85E-05	-1,50	-4,70	1980403
UPK1A	0,27	4,84E-05	-1,68	-4,79	2190408
SLC16A3	0,43	1,62E-05	-1,36	-5,00	110719
C7ORF68	0,78	3,62E-03	-1,30	-5,30	7320441
ADM	0,58	3,63E-03	-1,65	-5,93	5670465
PLAC8	0,01	1,28E-05	-3,05	-7,00	4830113
PLAC8	0,00	1,78E-06	-3,15	-8,07	2490372
MT3	0,11	1,85E-05	-2,57	-9,44	3060273
ALDOC	0,39	6,67E-06	-1,57	-10,78	7330544

IL17F	0,00	4,26E-05	-7,85	-12,77	5360682
PFKFB4	0,37	1,78E-06	-1,60	-12,90	7400653

A. MACS sorting

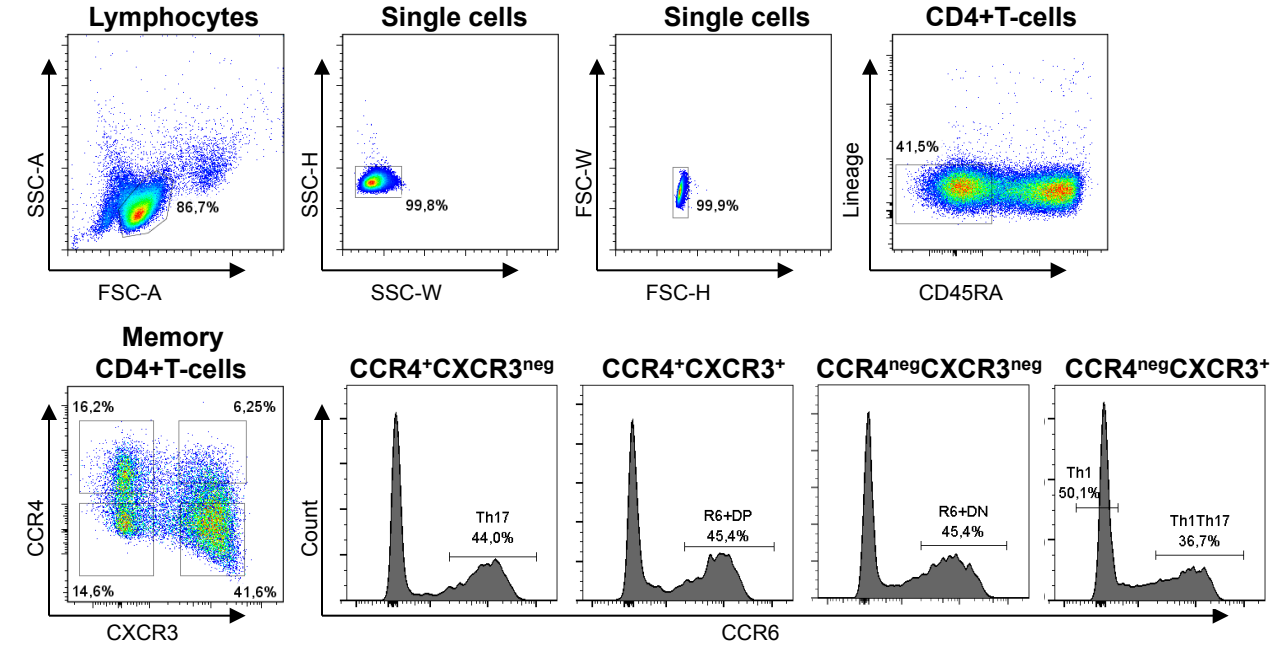

B. FACS sorting

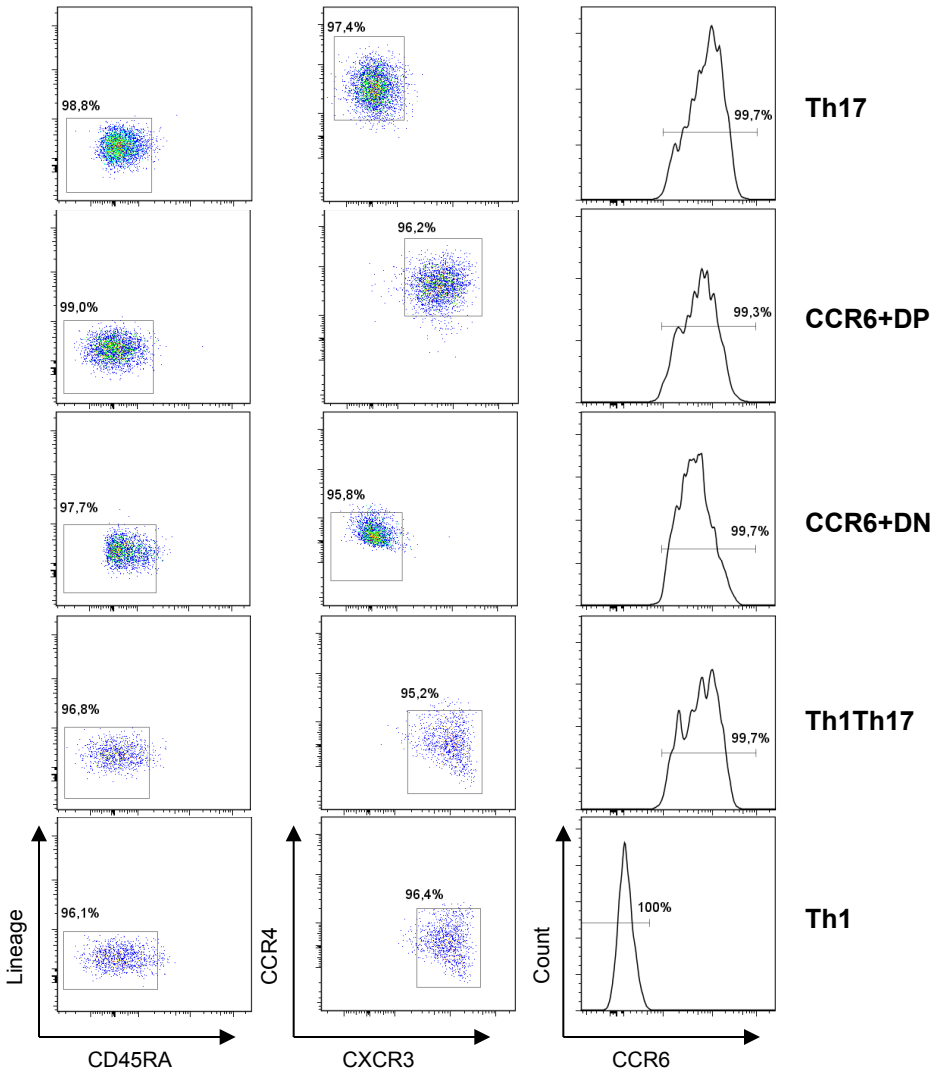

Wacleche et al., Suppl. Figure 1

A: Canonical Pathways (C2)

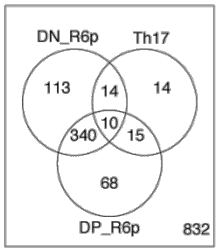

B: Biological Processes (C5)

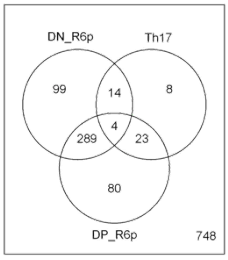

C: Cell migration

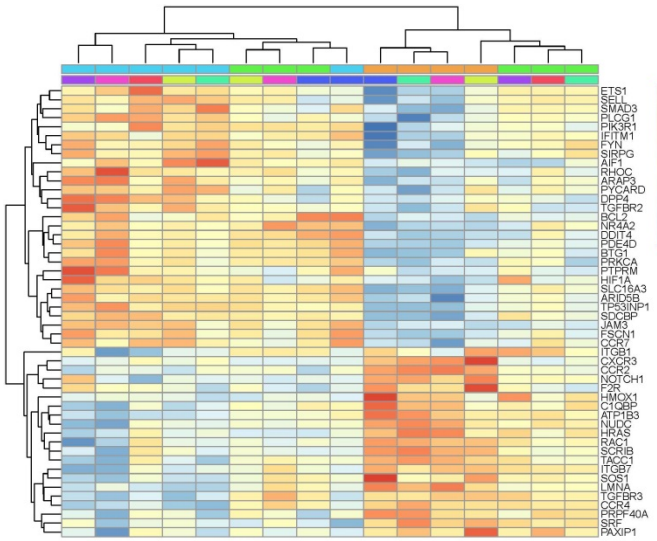

D: Chemotaxis

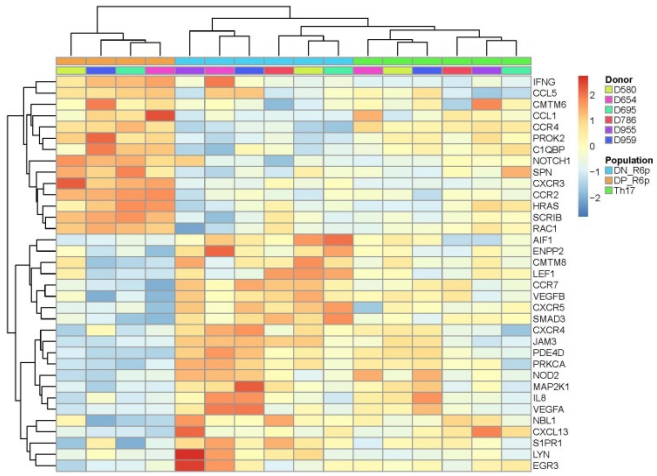

E: Cell differentiation

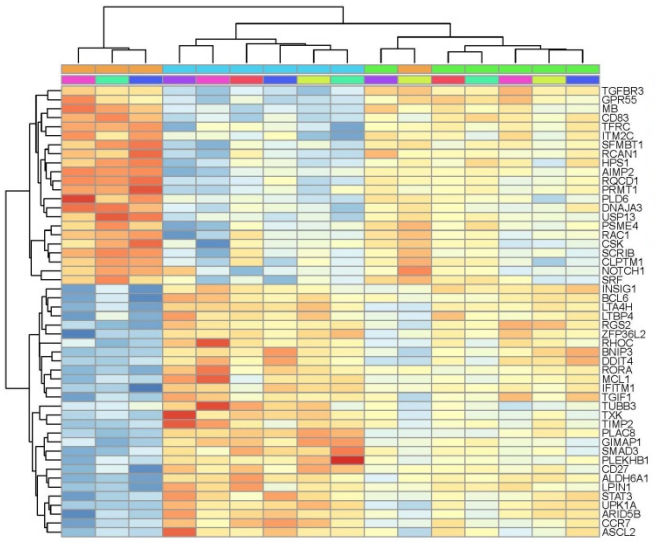

F: Transcription factors

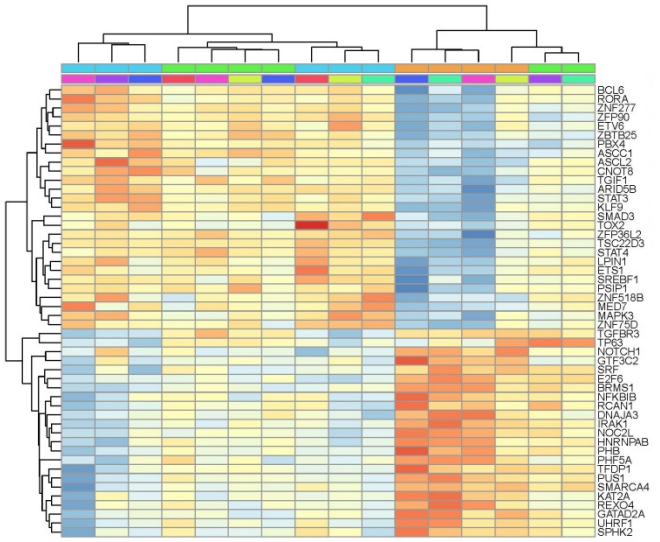

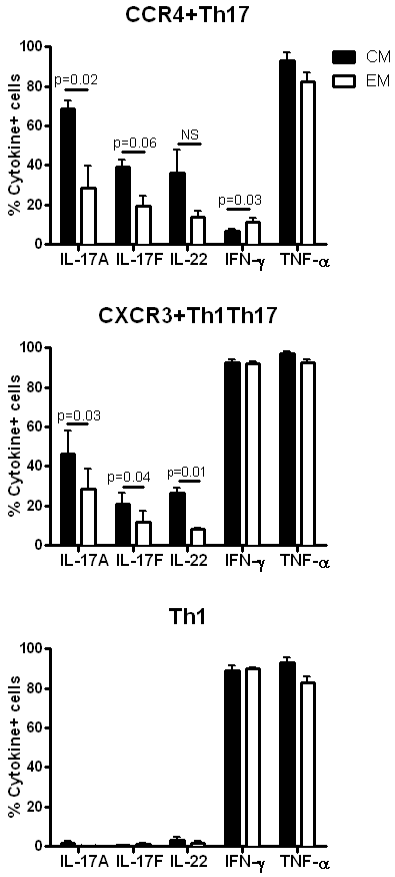

Wacleche et al., Suppl. Figure 3

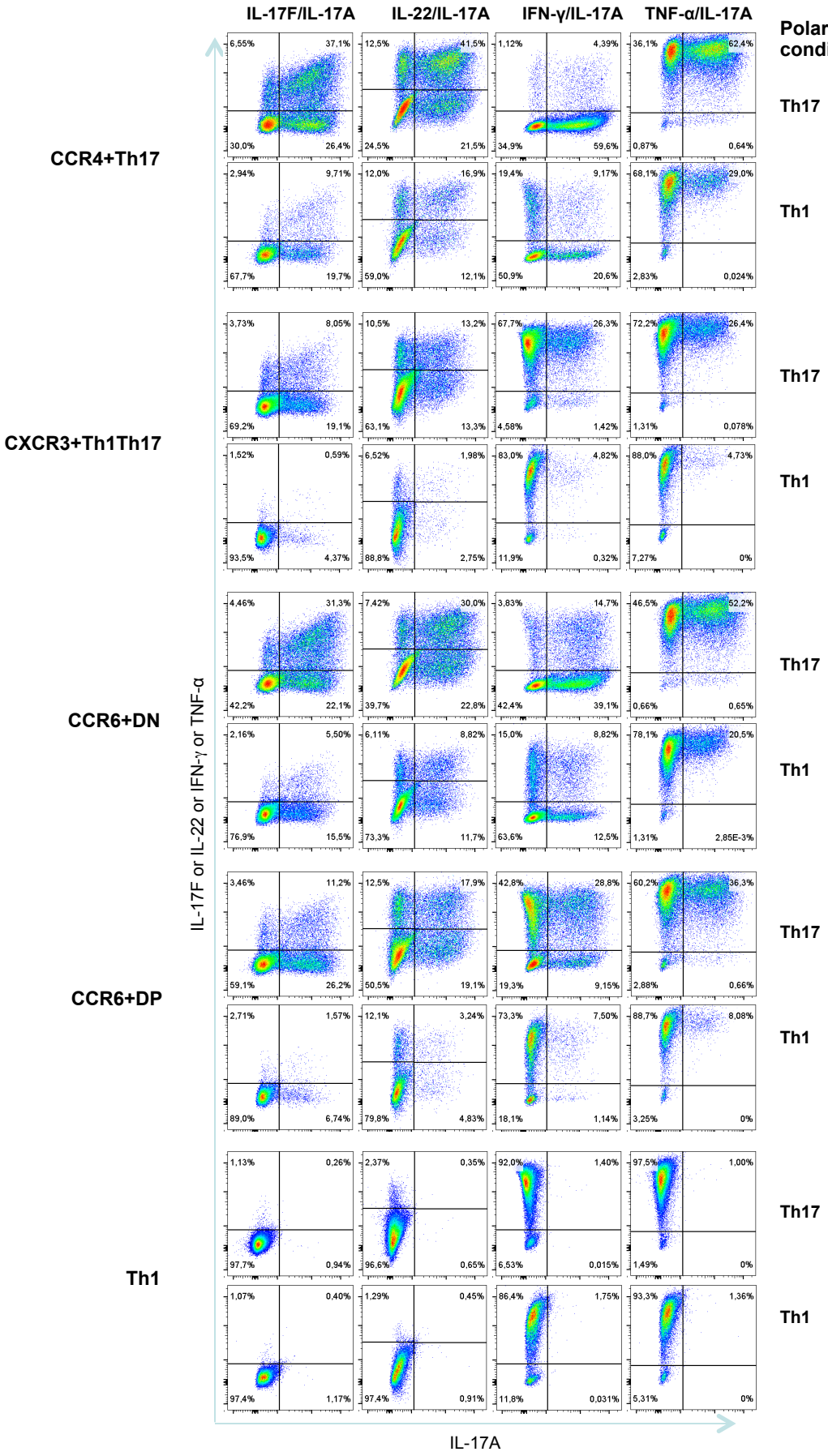

Wacleche et al. Supplemental Figure 4

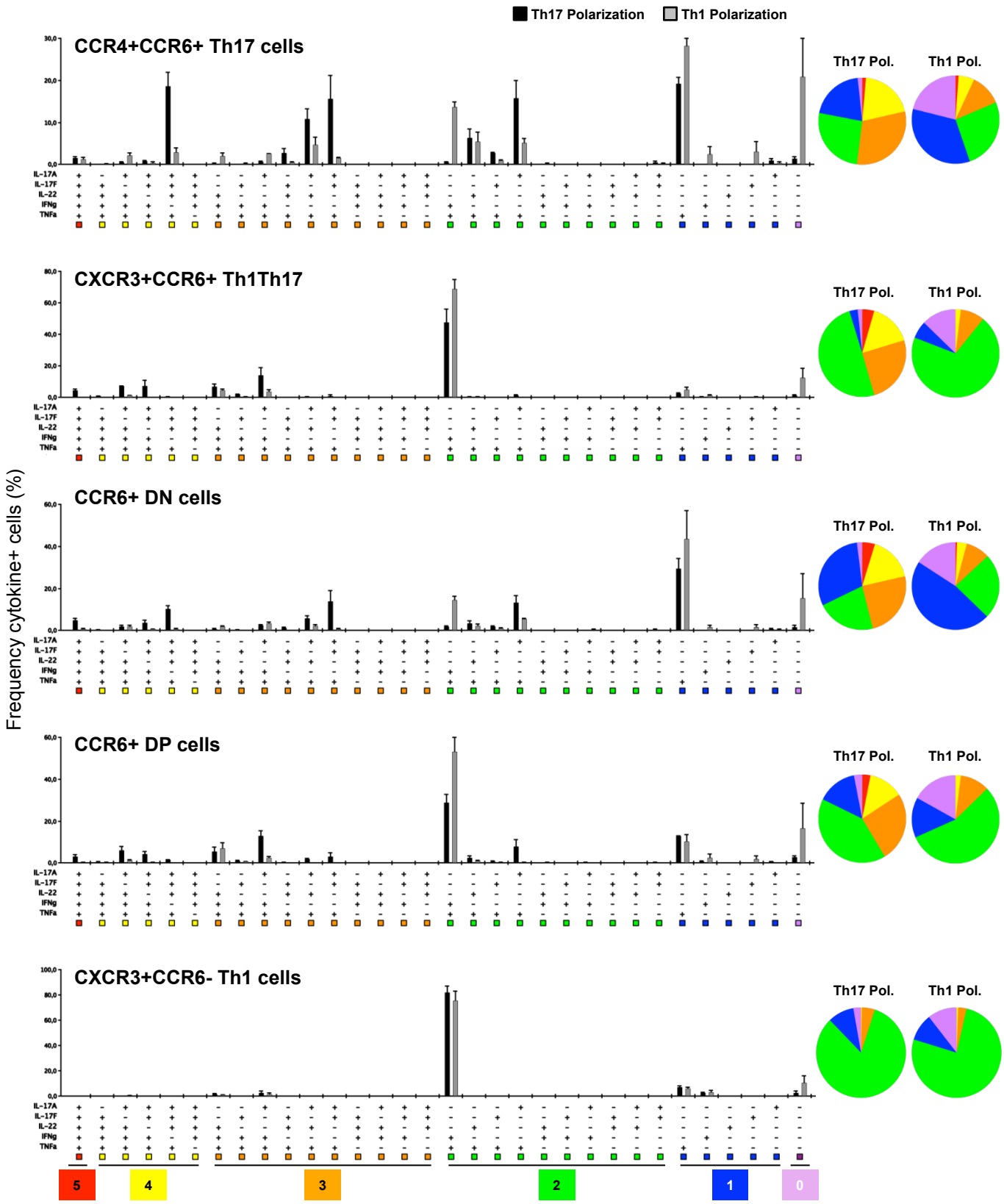

Wacleche *et al.*, Suppl. Figure 5

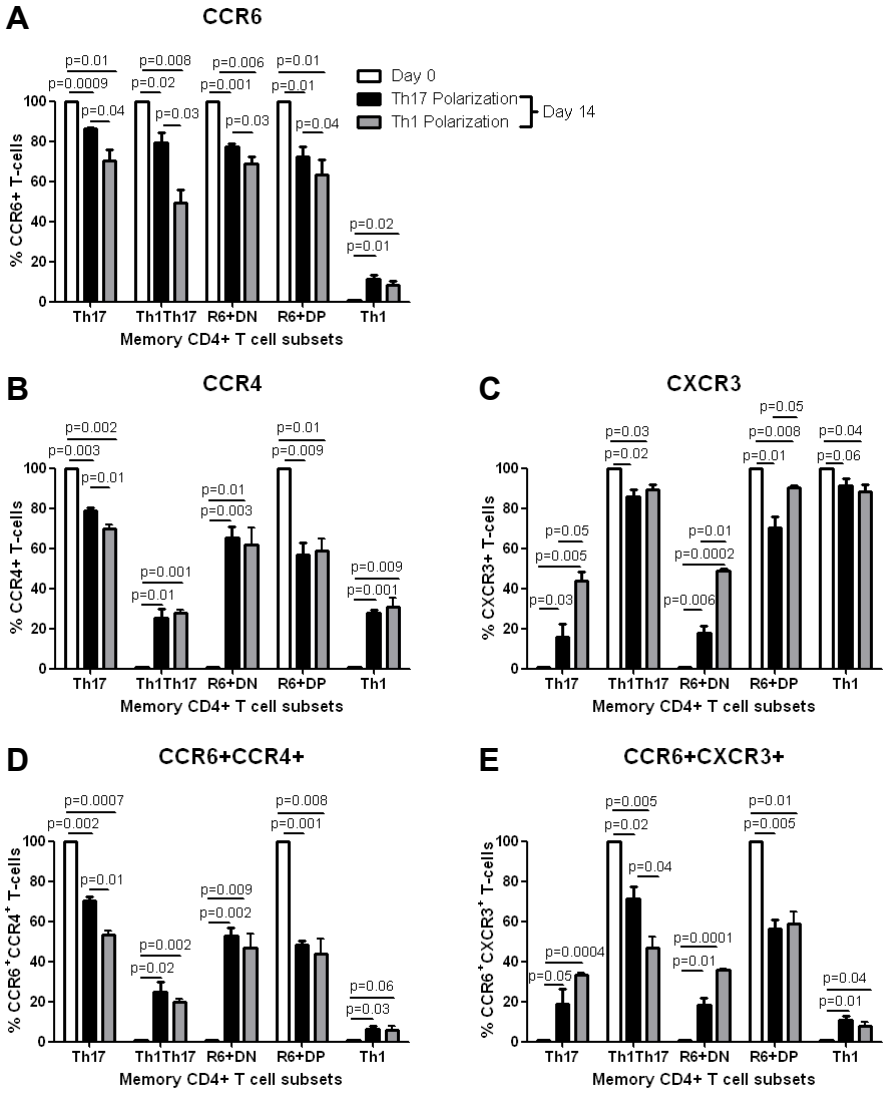
A
CCR6
Day 0
Th17 Polarization
Th1 Polarization
Day 14
% CCR6+ T-cells
Th17
Th1Th17
R6+DN
R6+DP
Th1
Memory CD4+ T cell subsets
B
CCR4
% CCR4+ T-cells
C
CXCR3
% CXCR3+ T-cells
D
CCR6+CCR4+
% CCR6+CCR4+ T-cells
E
CCR6+CXCR3+
% CCR6+CXCR3+ T-cells

A. Experimental flow chart

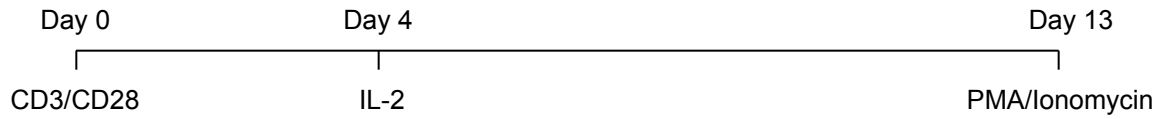

B. Intracellular cytokine expression – Day 13

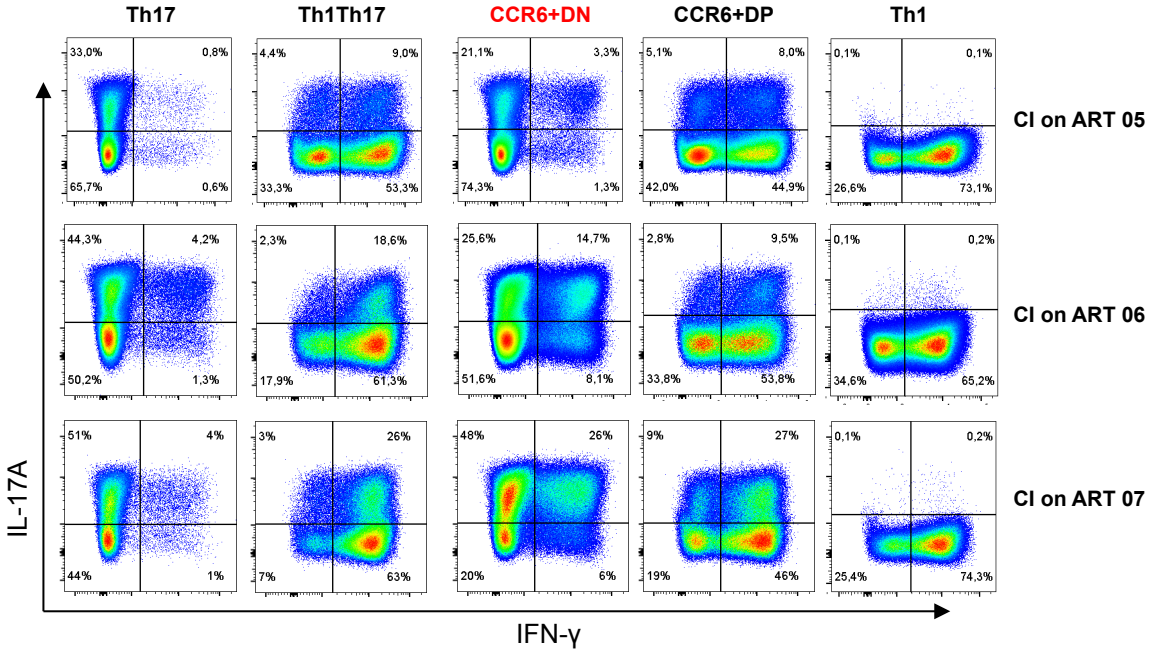

C

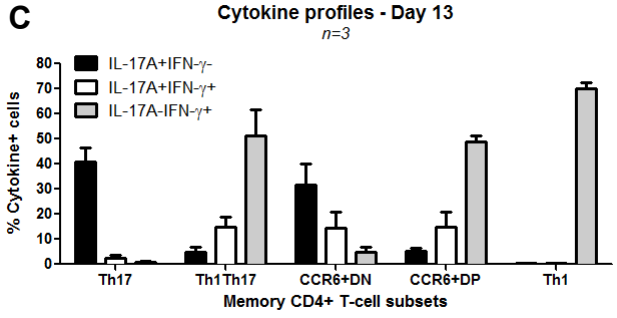

A. HIV+ viremics untreated

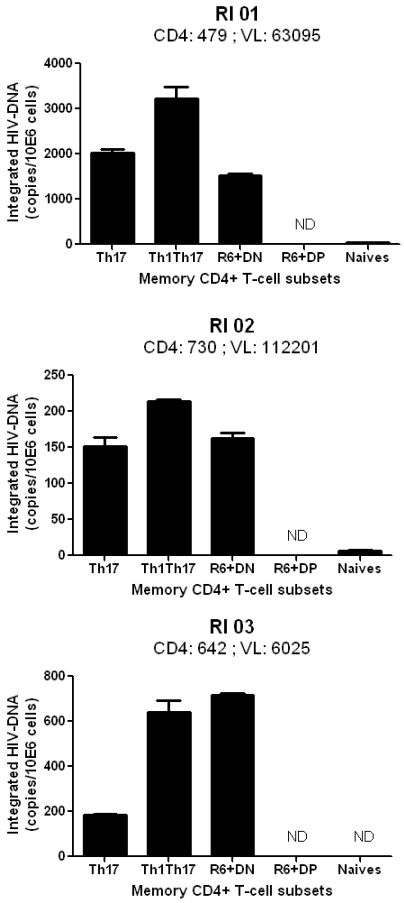

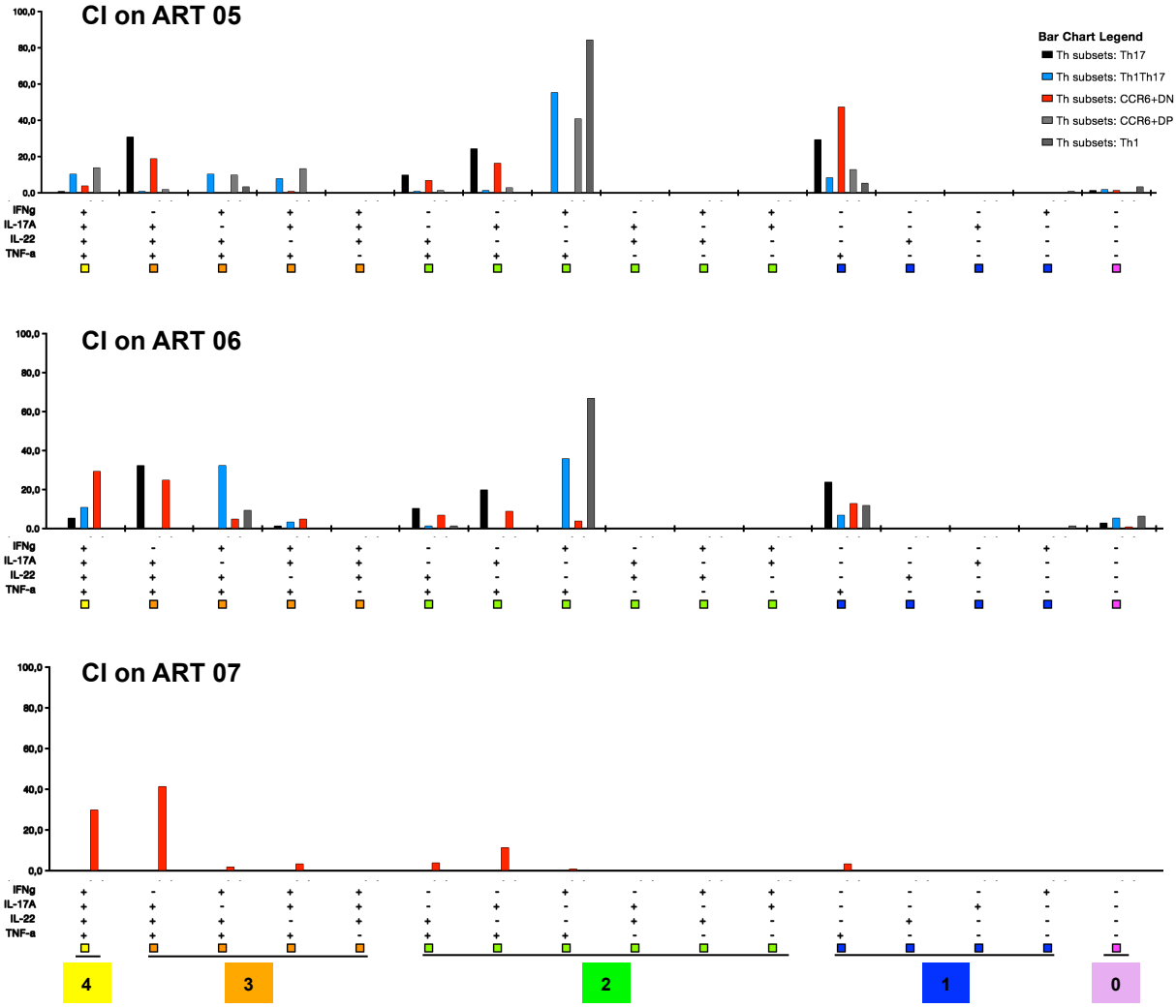

Wacleche *et al.*, Suppl. Figure 9

ONLINE SUPPLEMENTAL MATERIAL

AUTHORS' CONTRIBUTION

VSW performed research, analyzed data, and wrote the manuscript. JPG performed microarray analysis and generated figures. AG and PM performed experiments. HS contributed to research design and manuscript writing. RF performed experiments. MAJ, SGD, NC, and JPR ensured access to clinical samples/information and/or provided experimental protocols. PA designed research, analyzed data, and wrote the manuscript. All authors reviewed and accepted the manuscript.

SUPPLEMENTAL TABLES

Supplemental Table 1: Genome-wide transcriptional profiling of the newly identified $CCR6^{+}$DN and $CCR6^{+}$DP subsets relative to the previously characterized Th17/$CCR4^{+}CCR6^{+}$ cells. See attached document.

Supplemental Table 2: Clinical parameters of chronically HIV-infected subjects under long-term viral suppressive ART (CI on ART)

Subjects	CD4 counts[#]	CD8 counts[#]	Plasma viral load[&]	Time since infection*	ART	Time of aviremia[$]
RI 01	479	1,105	63,095	41	none	0
RI 02	730	520	112,201	8	none	0
RI 03	642	847	6,025	3	none	0
CI 01	498	531	<50	213	TMC114; RAL; ETR; RTV	52
CI 02	543	787	<50	214	TDF+FTC;RTV; TPV;RAL	66
CI 03	318	431	<50	148	DLV ; ABC+3TC	36
CI 04	847	944	<50	168	ATV; ABC+3TC	2
CI 05	581	1060	<50	96	EFV; TDF+FTC	N/D
CI 06	456	619	<50	52	FTC+RPV+TDF	80
CI 07	459	545	<50	215		N/D
CI 08	890	673	<50	57	AZT ; 3TC ; NEV	42
CI 09	463	757	<50	152	3TC; EFV; ABA	20
CI 10	602	767	<50	158	3TC; ABA ; SAQ	53
CI 11	563	613	<50	86	IND; 3TC ; AZT	71
CI 12	424	461	<50	84	3TC; D4T ; DLV	46
CI 13	731	413	<50	51	EFV; AZT ; 3TC	22
CI 14	834	527	<50	38	NEV; ATV ; TDF ; RTV	25
CI 15	552	715	<50	139	D4T; ATV	56
CI 16	671	1,120	<50	242	3TC; ABA ; LOP ; RTV	64
CI 17	510	765	<50	61	AZT; 3TC ; RTV	52
CI 18	799	1,727	<50	62	3TC; D4T; NEV	33
CI 19	501	278	<50	90	D4T; 3TC; IND	87
CI 20	344	642	<50	59	3TC; D4T; NEV	44
CI 21	604	1,281	<50	53	IND; AZT; 3TC	35
CI 22	443	322	<50	18	RTV; AZT; 3TC; KAL	12
CI 23	599	923	<50	86	AZT; 3TC; EFV	46
CI 24	688	1,273	<50	100	AZT; 3TC; EFV	59
CI 25	434	583	<50	165	3TC; EFV; ABA	34
CI 26	492	582	<50	170	RTV; ABC; 3TC; ATV	66
CI 27	529	690	<50	49	3TC; D4T; DLV	11
CI 28	776	478	<50	288	FTC+TDF+EFV	148
CI 29	277	909	<50	11	FTC+RPV+TDF	2
CI 30	616	330	<50	186	TDF+FTC + Viracept	14
CI 31	517	259	<50	82	ABC+3TC ; EFV	108
CI 32	886	579	<50	60	TDF+FTC; RAL	12
CI 33	569	462	<50	111	TMC114+RAL	13
CI 34	269	282	<50	96	EFV; TDF+FTC	ND
CI 35	391	620	<50	165	TMC114;ABC+3TC	4
CI 36	730	741	<50	312	TDF;NFV;TCV	173
CI 37	639	1317	<50	360	TDF+FTC, DTG	137
CI 38	873	886	<50	252	FTC+TDF+EFV	107
Median RI	**642**	**520**	**63,095**	**8**	**NA**	**NA**
Median CI	**557,5**	**582,5**	**<50**	**98**	**NA**	**NA**

[#], cells/µl; [&], HIV RNA copies per ml plasma; *, months; ART, antiretroviral therapy; [$], months

ART: 3TC, Lamivudine; ABA/ABC, Abacavir; ATV, Atazanavir; AZT, Zidovudine; D4T, Stavudine; DLV, Delavirdine; TMC114, Duranavir; EFV, Efavirenz; IND, Indinavir; ETR, Etravirine; KAL, Kaletra; ABC+3TC, Kivexa; LOP, Lopinavir; NA, not available; NEV, Nevirapine; RTV, Ritonavir; SAQ, Saquinavir; RAL, Raltegravir; TDF, Tenofovir; FTC, Emtricitabine; RPV, rilpivirine ; TDF+FTC, Truvada; FTC+TDF+EFV, Atripla ; FTC+RPV+TDF, complera ; ABC+3TC, Kivexa ; NA, not applicable ; ND, not determined.

Supplemental Table 3: Clinical parameters of the longitudinal cohort of HIV-infected subjects

Subjects	Visit #	CD4 counts[#]	Plasma viral load[&]	Time since infection*	Time since inclusion*	ART
HPI #1	V1	430	35,303	2.5	0	No
ETI <74 days	V2	520	2,301	3	0.5	No
ART at 8 months since infection	V3	450	24,845	3.5	1	No
	V4	350	38,395	4	1.5	No
	V8	310	681	8.5	6	Yes
	V9	690	40	12	9	Yes
	V11	690	40	18	15	Yes
	V12	-	40	21	18	Yes
	V13	650	40	24	21	Yes
HPI #2	V1	510	127,175	1.5	0	No
ETI <47 days	V6	380	51,426	5	3	No
ART at 12 months since infection	V7	510	19,884	6	4	No
	V8	420	196,433	7.5	6	No
	V9	510	75,053	10	8	No
	V10	500	286	12.5	11	Yes
HPI #3	V1	580	86,627	1.5	0	No
ETI <46 days	V2	540	37,335	2	1	No
ART at 11 months since infection	V4	740	27,348	3	1,5	No
	V5	730	20,076	3.5	2	No
	V7	670	11,127	5	4	No
	V8	530	26,574	7.5	6	No
	V9	460	85,718	10	9	No
	V10	380	664	13.5	12	Yes
	V11	660	113	17	16	Yes
	V12	640	40	20	18	Yes
	V13	780	40	22	21	Yes
HPI #4	V1	240	29,981,000	1	0	No
ETI <31	V3	700	129,717	2	1	No
ART at 4 months since infection	V4	340	76,626	2.5	2	No
	V7	650	712	5	4	Yes
	V11	670	40	16	15	Yes
	V12	870	40	20	18	Yes
	V13	830	40	23	21	Yes
HPI #5	V1	407	189,343	2.5	0	No
ETI <76	V2	430	173,044	3.5	1	No
ART at 9.5 months since infection	V3	403	59,181	4	2	No
	V7	396	81,037	6.5	4	No
	V9	467	74	11	9	Yes
	V10	496	50	13	11	Yes
	V11	516	50	17	14	Yes
	V12	567	50	20.5	18	Yes

[#], cells/µL; [&], HIV-RNA copies per mL plasma (log_{10}); *, months; ART, antiretroviral therapy; ETI: estimated time of infection

SUPPLEMENTAL FIGURE LEGENDS

Supplemental Figure 1: Purity of flow cytometry-sorted memory CD4$^+$ T-cell subsets. Total CD4$^+$ T-cells were isolated from PBMCs of healthy individuals by negative selection using magnetic beads (Miltenyi). Cells were stained with a cocktail of fluorochrome-conjugated Abs and analyzed by polychromatic flow cytometry (see Supplemental Experimental Procedure). Memory (CD45RA$^-$) cells lacking the lineage-specific markers CD8 (CD8$^+$ T-cells), CD19 (B cells), and CD56 (NK cells) and with differential expression of CCR6, CCR4, and CXCR3 were sorted by flow cytometry (BDAria II) as follows: CCR6$^+$CCR4$^+$CXCR3$^-$ (Th17), CCR6$^+$CCR4$^-$CXCR3$^-$ (CCR6$^+$DN), CCR6$^+$CCR4$^+$CXCR3$^+$ (CCR6$^+$DP), CCR6$^+$CCR4$^-$CXCR3$^+$ (Th1Th17) and CCR6$^-$CCR4$^-$CXCR3$^+$ (Th1). A viability staining was used to exclude dead cells. The positivity gates where defined based on fluorescence minus one (FMO) controls. Shown is **(A)** the gating strategy for the identification of different subsets on CD4$^+$ T-cells sorted by MACS and **(B)** purity upon FACS sorting of different memory T-cell subsets. The percentage of each subset is indicated on the figures. Results are from one donor representative of experiments performed with cells from >10 different donors. The positivity gates where defined based on fluorescence minus one (FMO) controls.

Supplemental Figure 2: GO classification of differentially expressed genes in 3 CCR6$^+$ subsets. (**A-B**) Shown are Venn diagram representation of GSVA-generated canonical pathways (**A**) and biological functions (**B**), illustrating the number of differentially expressed pathways common or unique between Th17, CCR6$^+$DN, and CCR6$^+$DP. (**C-F**) Further, differentially expressed genes between ($p < 0.05$, FC cut-off 1.3) were classified based on their biological functions using *Gene Ontology* (GO) as follows: (**C**) Cell migration, (**D**) Chemotaxis, (**E**) Cell differentiation, and (**F**) Transcription factors. The heatmaps were generated using the R programming language and the

heatmap and ggplot2 libraries (R Core Team). For each heat map, genes up and down regulated in different subsets are represented in red and blue, respectively.

Supplemental Figure 3: Superior Th17-lineage commitment of CM *versus* EM Th17 and Th1Th17-subsets. FACS-sorted Th17, Th1Th17 and Th1 subsets with CM ($CD45RA^-CCR7^+$) and EM ($CD45RA^-CCR7^-$) phenotype were cultured for 14 days under Th17-polarizing conditions, as in Figure 5. Shown are the statistical analyses of the intracellular expression of IL-17A, IL-17F, IL-22, IFN-γ and TNF-α by distinct Th17-polarized CM (black bars) *versus* EM (white bars) Th17, Th1Th17 and Th1 subsets. Results (mean±SEM) were generated with matched samples from n=3 different subjects. Paired t-test *p*-values are indicated in the figures (CM *versus* EM).

Supplemental Figure 4: Flow cytometry analysis of cytokine co-expression at single-cell level by CM subsets upon long-term culture under Th17 *vs.* Th1 polarizing conditions. Central memory (CM) Th17, Th1Th17, $CCR6^+$DN, $CCR6^+$DP, and Th1 subsets were sorted and cultured for 14 days under Th17 or Th1 polarizing conditions, as described in Figure 5. Shown are flow cytometry dot plots illustrating the co-expression of IL-17A with IL-17F, IL-22, IFN-γ or TNF-α for each Th17- or Th1-polarized subset. Results are from one donor representative of results generated with cells from three different donors. The positivity gates where defined based on fluorescence minus one (FMO) controls.

Supplemental Figure 5: Poly-functional profiles of CM $CCR6^+$ subsets upon long-term culture under Th17 *versus* Th1 polarizing conditions *in vitro*. FACS-sorted CM subsets were analyzed for the expression of lineage-specific cytokines upon Th17/Th1-polarization *in vitro* (Figure 5). Shown are bar graph representations generated with SPICE software for all possible combinations of one (blue), two (green), three (orange), four (yellow), and five (red) or no (purple) cytokines produced by T-cell

subsets upon culture *in vitro* (mean±SEM), together with pie charts summarizing the polyfunctional profiles (median relative contribution, n=3).

Supplemental Figure 6: The four CCR6$^+$ T-cell subsets isolated from HIV-infected subjects receiving ART preserve their Th17-polarizing profiles upon long term culture *in vitro*. (A) FACS-sorted Th17, Th1Th17 and Th1 subsets were stimulated with CD3/CD28 for four days then cultured in the presence of IL-2 (5ng/ml) for an additional 9 days. At day 13, cells were stimulated with PMA and Ionomycin in the presence of Brefeldin A for 6 hours. Intracellular staining was performed with cytokine-specific Abs. (**B**) Shown are flow cytometry dot plots illustrating the co-expression of IL-17A and IFNγ (n=3). (**C**) Shown is the frequency of cytokine-expressing T-cells cultured long-term *in vitro*. Results (mean±SEM) were generated with matches samples from n=3 different donors. Paired t-Test *p*-values are indicated on the figures.

Supplemental Figure 7: CCR6$^+$DN and CCR6$^+$DP subsets are permissive to HIV infection *in vitro*. (A) PBMCs from healthy individuals were stained with a cocktail of fluorochrome-conjugated CD3, CD4, CD45RA, CCR4, CXCR3, CCR6, and CCR5 or CXCR4 Abs. The gating strategy for the identification of distinct CCR6$^+$ and CCR6$^-$ T-cell subsets was designed as in Figure 1A. The frequency of cells expressing CCR5 (left panel) and CXCR4 (right panel) was analyzed within the Th17, Th1Th17, CCR6$^+$DN and CCR6$^+$DP subsets. Paired t-Test *p*-values are indicated on the figures. Horizontal bars indicate median values. (**B**) Memory CCR6$^+$ subsets from three HIV-uninfected subjects were sorted and stimulated *via* CD3/CD28 for 4 days, as in Figure 1E. Cells were exposed to a highly infectious R5 strain HIV-ADA8. Levels of HIV-p24 were quantified by ELISA in cell supernatants at day 3 posy-infection.

Supplemental Figure 8: All four CCR6$^+$ T-cell subsets carry integrated HIV-DNA in viremic untreated HIV-infected subjects. The four memory CCR6$^+$ subsets as well as naive cells from PBMCs of (**A**) HIV$^+$ recently infected untreated (RI) (n=3) and were sorted by FACS. Levels of integrated HIV-DNA were quantified by nested real-time PCR (mean±SD of triplicate wells).

Supplemental Figure 9: Poly-functional profiles of HIV-p24$^+$ CCR6$^+$ T-cell subsets of HIV-infected individuals receiving ART upon viral reactivation *in vitro*. HIV reservoir reactivation was performed as described in Suppl. Figure 6 legend. Briefly, at day 13, cells were stimulated with PMA/Ionomycin in the presence of Brefeldin A and intracellular staining was performed with cytokine (IFN-γ, IL-17A, IL-22, TNF-α) and HIV-p24 Abs. Shown are bar graph representations generated with SPICE software for all possible combinations of one (blue), two (green), three (orange), and four (yellow), or no (purple) cytokines produced by HIV-p24$^+$ Th17, Th1Th17, CCR6$^+$DN, CCR6$^+$DP and Th1 subsets (n=3 CI on ART subjects). In contrast to CI on ART 5 and 6, for donor CI on ART 07 HIV reactivation was observed only for CCR6$^+$DN (red).

ONLINE SUPPLEMENTAL MATERIAL

Antibodies and polychromatic flow cytometry analysis

Surface staining was performed with fluorochrome-conjugated Abs (Table below), as previously described (1). The viability dye LIVE/DEAD® Fixable Aqua Dead Cell Stain Kit (Invitrogen) was used to exclude dead cells. Cells were analyzed using a LSRII cytometer, Diva (BD Biosciences, San Jose, CA), and FlowJo (Tree Star, Inc). Positivity gates were placed using fluorescence minus one (FMO) (1, 2).

Antibodies used for flow cytometry

Antibodies	Fluorochrome	Clone	Vendor
CD3	Pacific blue	UCHT1	BD Pharmingen, San Diego, CA
CD4	Alexa Fluor 700	RPA-T4	
CD45RA	Allophycocyanin/Cy7	HI100	
CCR4	PE/Cy7	1G1	
CXCR3	PE/Cy5	1C6	
CCR6	PE	11A9	
CD161	PE/Cy5	DX12	
IFN-γ	Alexa700	B27	
CD27	BV650	L128	
CCR7	FITC	150503	R&D Systems, Minneapolis, MN
CXCR3	FITC	49801	
CD8	FITC	BW135/80	Miltenyi Biotec, Auburn, CA
CD19	FITC	LT19	
CD1c/BDCA-1	PE	AD5-8E7	
CD56	FITC	MEM188	eBioscience, San Diego, CA
IL-17A	PE	64DEC17	
IL-17F	Alexa647	SHLR17	
IL-22	PE/Cy7	22URTI	
TNF-α	Pacific Blue	MAB11	
HIV-p24	PE	KC57	Beckman Coulter, Brea, CA

SUPPLEMENTAL REFERENCES

1. Gosselin A, Monteiro P, Chomont N, Diaz-Griffero F, Said EA, Fonseca S, et al. Peripheral blood CCR4+CCR6+ and CXCR3+CCR6+CD4+ T cells are highly permissive to HIV-1 infection. Journal of immunology. 2010;184(3):1604-16.

2. Roederer M. Compensation in flow cytometry. Current protocols in cytometry / editorial board, J Paul Robinson, managing editor [et al]. 2002;Chapter 1:Unit 1 14.

CHAPTER 4:

MOLECULAR DETERMINANTS OF PATHOGENICITY IN DENDRITIC CELLS DERIVED FROM CD16^{+} MONOCYTES IN THE CONTEXT OF HIV-1 INFECTION (MANUSCRIPT #2)

&

HIV-1 IMPAIRS THE ABILITY OF MYELOID DENDRITIC CELLS TO PROMOTE CD4^{+} T-CELL RESPONSES AGAINST TH17-SPECIFIC PATHOGENS (MANUSCRIPT #3)

Authors Contribution: Manuscript entitled:
Molecular Determinants of Pathogenicity in Dendritic Cells Derived from CD16+ Monocytes in the Context of HIV-1 Infection

Vanessa Sue Wacleche performed research, analyzed data, and wrote the manuscript. Concerning the experimental approach, VSW performed the isolation and staining for cell sorting. She also performed all experiments involving cell stimulation, antigen presentation, trans-infection and HIV reactivation assays. Figures involved include Figure 1A-C, Figures 2-9 as well as supplemental 1 to 8.

Jean-Philippe Goulet performed microarray analysis and generated figures including Figure 2-9 as well as Figure supplemental 6.

Annie Gosselin performed experiments of staining shown in Supplemental Figure 4.

Marie-Claude Gaudreau performed trans-infection assay included in Figure 1D.

Aurélie Cleret-Buhot performed staining and microscopic analysis leading to the generation of Figure 1C.

Dominque Gauchat performed the cell sorting shown in Figures 1A-C, 2-8.

Yuwei Zhang help in manuscript writing.

Jean-Pierre Routy ensured access to clinical samples/information and/or provided experimental protocols figures 1-8 as well as all the supplemental figures.

Petronela Ancuta designed research, analyzed data, and wrote the manuscript. This includes all the figures, tables and supplemental figures.

Manuscript #2 in preparation for submission in the ***eBlood Journal***

Molecular Determinants of Pathogenicity in Dendritic Cells Derived from CD16+ Monocytes in the Context of HIV-1 Infection

Vanessa Sue Wacleche[1,2], Jean-Philippe Goulet[3], Annie Gosselin[2], Marie-Claude Gaudreau[1,2], Aurélie Cleret-Buhot[2], Dominique Gauchat[2], Yuwei Zhang[1,2], Jean-Pierre Routy[4,5,6], and Petronela Ancuta[1, 2,*]

[1]Université de Montréal, Faculté de Médecine, Département of microbiologie, infectiologie et immunologie, Montreal, QC, Canada.

[2]Centre de recherche du CHUM, Montreal, QC, Canada.

[3]Caprion, Montreal, QC, Canada.

[4]Department of Medicine, University of California San Francisco, San Francisco, CA, USA

[5]Chronic Viral Illness Service and Research Institute, McGill University Health Centre, Montreal, QC, Canada.

[6]Division of Hematology, McGill University Health Centre, Montreal, QC, Canada.

***, Corresponding author**

E-mail: petronela.ancuta@umontreal.ca

Running title: Pathogenicity of $CD16^+$ Monocyte-Derived Dendritic Cells

Abstract word count: 321
Text word count: 12,226 or 83,853 characters (spaces included)
Number of figures: 8
Number of supplemental figures: 6
Number of supplemental tables: 8
Number of references: 105

ABSTRACT

Background: The expansion of intermediate and non-classical $CD16^+$ monocytes to the detriment of classical $CD16^-$ monocytes occurs during multiple pathologic conditions. Here, we sought to identify unique features of $CD16^+$ and $CD16^-$ monocyte-derived DCs (MDDCs) with relevance for sepsis and HIV-1 pathogenesis.

Results: Despite a similar ability to express classical DC markers, $CD16^+$ differed from $CD16^-$ MDDC by a superior ability to transmit HIV infection to resting $CD4^+$ T-cells. Genome-wide transcriptional profiling revealed unique molecular signatures in $CD16^+$ *versus* $CD16^-$ MDDCs in terms of surface markers (CD16, CD86, CD97 and LY9 *versus* CD34, KIT and CCR6) as well as differences relative to the gene ontology terms transcription factors, cytokines, adhesion, chemotaxis, and cell projection. Gene set variation analysis identified canonical pathways and biological processes enriched in $CD16^+$ MDDCs (glutamate signaling, actin filament, positive regulation of T and B cell activation) and $CD16^-$ MDDCs (cell cycle, cell division, DNA replication, telomere maintenance). Transcripts enriched in $CD16^+$ *versus* $CD16^-$ MDDCs and listed in the NCBI HIV interactor data base included P2RX1, MDM2, ITGAL, IL-15, TCF7L2, ACTA2, PACS1, JAK1, and PPARG. LPS exposure up regulated numerous unique transcripts in $CD16^+$ (*i.e.,* CCL8, SIGLEC1, MIR4439, SCIN, IL-7R, PLTP, TNF, CFP, CLU, C2, MIR331, MAP3K8, SNX10, CXCL1, IL-18, P2RY8) and $CD16^-$ MDDCs (*i.e.,* MMP10, MMP1, TGM2, IL1A, TNFRSF11A, LAMP1, MMP8, ALDH1L2, TREM1, MALT1, ALCAM, PPARG, CXCL6, IL6ST, IL23A, S100A3). In contrast, HIV, consistent with the concept that DCs are limited in their ability to sense HIV, induced few transcriptional changes. Finally, gene set enrichment analysis demonstrated that canonical pathways linked to inflammation represent a unique feature of $CD16^+$ MDDCs under constitutive conditions as well as upon LPS or HIV exposure.

Conclusions: Altogether these results provide evidence that $CD16^+$ monocytes are precursors for unique DCs that play a pathogenic role during HIV disease progression. Finding ways to reduce the frequency and the pathogenic features of $CD16^+$ monocytes will be crucial for limiting HIV disease pathogenesis.

Key words: human, $CD16^+$ monocytes, dendritic cells, LPS, HIV-1, transcriptional profiling

Authors' contributions

VSW performed research, analyzed data, and wrote the manuscript. JPG performed microarray data analysis and generated figures. AG and PM performed experiments. HS contributed to research design and manuscript writing. RF performed experiments. MAJ, SV, SGD, NC, and JPR ensured access to clinical samples/information and/or provided experimental protocols. PA designed research, analyzed data, and wrote the manuscript. All authors reviewed and accepted the manuscript.

INTRODUCTION

Peripheral blood monocytes are derived from the bone marrow and represent key players in the immunity against viral, bacterial, fungal or parasitic infections [1,2]. Their functions include the killing of pathogens *via* phagocytosis, the production of reactive oxygen species (ROS), nitric oxide (NO), myeloidperoxydase (MPO), and inflammatory cytokines [2]. Human monocytes can be classified into three major subsets based on their differential expression of CD14 and CD16: classical $CD14^{++}CD16^{-}$, intermediate $CD14^{++}CD16^{+}$, and non-classical $CD14^{+}CD16^{++}$ monocytes [3]. Classical monocytes express high levels of CCR2, CD62L, CD11b and TLR-4 but low levels of the fractalkine/CX3CL1 receptor CX3CR1 [4,5]. Compared to intermediate and non-classical, classical monocytes exhibit superior phagocytic activity and myeloperoxidase expression and release higher levels of superoxide [6]. Following lipopolysaccharide (LPS) stimulation, classical monocytes produces high levels of IL-10 but lower levels of TNF-α and IL-1 [7]. Non-classical compared to classical monocytes are less granular, express high levels of CX3CR1, CXCR4, HLA-DR, and LFA1, but low to undetectable levels of CCR2 and CD11b [3,8,9]. In contrast to classical monocytes, non-classical monocytes produce massively TNF-α [10,11]. Non-classical monocytes appear to represent a mature version of monocytes as they show transcription program common to macrophage and DCs [12]. $CD14^{++}CD16^{+}$ cells were reported to have an intermediate phenotype between the classical and non-classical monocytes [3,13,14]. In fact, genome-wide transcriptional profiling demonstrated 90% of genes expressed highly in classical or non-classical monocytes were observed at intermediate levels on $CD14^{++}CD16^{+}$ cells [15]. Nevertheless, intermediate monocytes were shown to express higher levels of MHC-class II including HLA-DR and transmembrane receptor CD74, scavenger receptor CD163, the C-type lectin/C-type lectin-like domain member CLEC10A, Glial cell line-derived neurotrophic factor family receptor α 2 (GFRA2) [15-18]. All

together, these lines of evidence support the concept that classical, intermediate and non-classical monocytes represent distinct stages of differentiation with specific functional features. In line with this concept, studies by Cros *et al.* proposed a division of labor between monocytes subsets, with classical $CD16^-$ monocytes sensing bacterial pathogens via TLR2 and 4 and intermediate/non-classical CD16- monocytes developing responses against viruses via TLR7 and 8 [13,19].

Monocytes are renowned for their developmental plasticity reflected by their ability to differentiate into macrophages and DCs [20-22]. Although human $CD16^+$ monocytes were reported to preferentially acquire DC markers in a model of trans endothelial migration [23], both $CD16^-$ and $CD16^+$ monocytes differentiate into DC in the presence of GM-CSF and IL-4 *in vitro* [6,24]. Early studies demonstrated that $CD16^-$ and $CD16^+$ monocyte-derived dendritic cell (MDDC) subsets internalize soluble antigen and induce effector T-cells proliferation with similar efficacy [24]. In additions, these MDDC subsets express at cell surface CD11b, CD11c, MHC-II, Dendritic Cell-Specific Intercellular adhesion molecule-3-Grabbing Non-integrin (DC-SIGN), cell adhesion molecule CD24, SIRPα and macrophage markers CD107b and LAMP2 [6]. Compared to $CD16^+$ MDDCs, $CD16^-$ MDDCs primed with LPS expressed increased mRNA levels of IL-12p40 mRNA and produced higher secretion of IL-12 compared to $CD16^+$ MDDCs counterpart [24]. $CD16^-$ MDDCs also express higher levels of the DC maturation marker CD83 following ligation of TLR-2, TLR-3 and TLR-4 [25], suggesting possible differences in the activation of signal transduction molecules between the two subsets of MDDCs. Conversely, $CD16^+$ MDDCs express superior levels of CD86, CD11a and CD11c as well as lower levels of CD1a and B cell co-receptors CD32 [24]. Also, $CD16^+$ MDDCs express higher levels of TGF-β1. $CD16^+$ MDDCs were reported to represent migratory DCs that transiently traffic to lymphoid and non-lymphoid organ to perform immunosurveillance [23]. Furthermore, $CD16^+$ MDDCs

induce the production of IL-4 following stimulation with TLR-2 ligand peptidoglycan, TLR-3 ligand poly-IC and TLR-4 ligand LPS [25]. Together these lines of evidence support the concept that $CD16^-$ and $CD16^+$ monocytes differentiate into functionally distinct DC subsets.

HIV infection alters the phenotype and function of the innate immune cells, including peripheral blood monocytes. While the numbers of circulating classical monocytes remain unaltered during HIV infection [10,26],the pool of $CD16^+$ monocytes is significantly expanded within the monocytic population. This increase ranges from 30-50% in HIV-chronically infected and AIDS patients [10,27-30], as opposed to 5-10 % observed in healthy individuals. HIV induces a superior production of TNF-α by $CD16^+$ monocytes [26]. Of note, the frequency of $CD16^+$ monocytes is not normalized under antiretroviral therapy [27,29]. Whether $CD16^-$ *versus* $CD16^+$ MDDCs differ in their pathogenic potential during HIV infection remains unknown.

In this study, we investigated the ability of $CD16^-$ *versus* $CD16^+$ MDDCs to transmit HIV-1 infection to $CD4^+$ T-cells and used a systems biology approach to identify molecular mechanisms underlying functional differences between these subsets. Our results support model in which the expansion of $CD16^+$ monocytes significantly contribute to HIV disease progression by their ability to differentiate into DCs with a superior ability to disseminate HIV and increased pro-inflammatory profile. Our study support the need for novel therapeutic interventions aimed at reducing the frequency of $CD16^+$ monocytes and the pathogenicity of $CD16^+$ MDDCs during various pathological conditions including HIV-1 infection [31].

RESULTS

Peripheral blood CD16$^+$ and CD16$^-$ monocytes acquire typical dendritic cells features *in vitro*

The CD16$^+$ monocytes preferentially acquire dendritic cell (DCs) features in a *trans* endothelial migration model *in vitro* [23]. Whether CD16$^+$ *versus* CD16$^-$ monocytes differentiate into functionally distinct DC remains poorly documented[6,24]. Here we investigated phenotypic and morphologic features of immature and mature CD16$^+$ and CD16$^-$ monocyte-derived DCs (MDDCs). FACS-sorted monocyte subsets (Figure 1A; Supplemental Figure 1) were cultured in the presence of GM-CSF and IL-4 for 6 days. For FACS sorting, total monocytes were first purified by negative selection using magnetic beads were stained with CD16 Abs but not CD14 Abs in an effort to avoid deleterious consequences of CD14-mediated triggering on the ability to monocyte to undergo DC differentiation. To determine whether CD16 Abs impact on well-established functions of MDDCs as previously demonstrated for CD14 [32], total monocytes were stained or not with CD16 Abs, differentiated into DCs and their ability to induce antigen-specific CD4$^+$ T-cell proliferation as well as HIV dissemination were investigated. The CD16+ monocytes represent in average 5-10% of total monocytic population [3]. Exposure to CD16 Abs did not change significantly the ability of MDCCs loaded with staphylococcal enterotoxin B (SEB), *cytomegalovirus* (CMV), or *Staphylococcus aureus* (*S. aureus*) to induce antigen-specific proliferation of autologous CD4$^+$ T-cells (Supplemental Figure 2). Similarly, results in Supplemental Figure 3 demonstrated that CD16 Abs did not interfere with the ability of MDDCs to transmit HIV to autologous CD4$^+$ T-cells proliferating in response to SEB, CMV or *S. aureus*. Thus, our cell sorting strategy appears appropriate for the investigation of molecular and functional features of CD16$^+$ and CD16$^-$ MDDCs.

Results in Figure 1B demonstrate that both $CD16^+$ and $CD16^-$ monocytes differentiate into DC as reflected by the acquisition of high levels of CD1c and HLA-DR and the loss of CD14 expression. Of note, CD16 expression was conserved on a fraction of $CD16^+$ but not $CD16^-$ MDDCs (Figure 1B). Further, changes in the expression of immature (CD1a, CD1c, DC-SIGN) *versus* mature (CD83, CCR7) DC surface markers were assessed upon LPS-induced maturation. Both immature $CD16^+$ and $CD16^-$ MDDCs expressed similarly high levels of CD1a, CD1c, and DC-SIGN, while treatment with LPS resulted in the induction of CD83 and CCR7 expression at similarly high levels on the two MDDC subsets (Supplemental Figure 4A-B). Staining with CD1a Abs and phalloidin (which binds to actin filaments) followed by confocal microscopy visualization demonstrated that both $CD16^+$ and $CD16^-$ MDDCs acquired a typical veiled morphology, with a tendency for more protrusions/filopodia on the surface of $CD16^+$ MDDCs (Figure 1C). Thus, both $CD16^+$ and $CD16^-$ monocytes differentiate into DCs expressing classical immature and immature DC phenotypic markers and a typical veiled morphology.

$CD16^+$ MDDCs preferentially disseminate HIV-1

We previously demonstrated that $CD16^+$ monocytes activate resting $CD4^+$ T-cells for increased permissiveness to HIV infection *via* the production of CCR3 (CCL24) and CCR4 (CCL2, CCL22) binding chemokines [33]. Here we investigated the ability of $CD16^+$ *versus* $CD16^-$ MDDCs to transmit HIV-1 to autologous $CD4^+$ T-cells. To this aim, MDDCs subsets were exposed to a R5 HIV strain and then co-cultured with resting $CD4^+$ T-cells. Co-cultures were treated or not with E. coli LPS to induce MDDC maturation. The LPS treatment was also designed to mimic the situation in which bacterial products such as LPS are present in the circulation of HIV-infected subjects as a consequence of the process of microbial translocation [34]. Results in Figure 1D demonstrate HIV

replication in co-cultures of $CD16^+$ but not $CD16^-$ MDDCs with resting $CD4^+$ T-cells. These differences can be explained by a superior ability of $CD16^+$ compared to $CD16^-$ MDDCs to capture and transmit HIV and/or a higher efficacy of $CD16^+$ MDDCs in inducing T-cell activation. Indeed, it is well established that TCR triggering increases T-cell permissiveness to HIV infection [35] likely by the neutralization of intrinsic restriction factors such as SAMHD1 [36,37]. To distinguish between these possibilities, HIV integration in MDDC subsets, together with their ability to transmit HIV to autologous CD3/CD28-activated $CD4^+$ T-cells were quantified in four different donors (Figure 2A). Results in Figure 2B demonstrate that levels of HIV-DNA integration in $CD16^+$ *versus* $CD16^-$ MDDCs were similar in 3 of 4 subjects and significantly higher only one subject (Donor #2). Of note, a higher HIV *trans* infection by $CD16^+$ *versus* $CD16^-$ MDDCs upon co-culture with activated T-cells were observed only in one out of 4 donors, exactly Donor #2 where integrated HIV-DNA levels were higher in $CD16^+$ compared to $CD16^-$ MDDCs (Figure 2C). This suggests that $CD16^+$ and $CD16^-$ MDDCs differ mainly in their ability to render $CD4^+$ T-cells permissive to HIV-1 infection. To test this possibility, supernatants from immature MDDC subsets were used to quantify levels of CCL2, CCL22, and CCL24, since these chemokines were previously demonstrated to activate $CD4^+$ T-cells for increased HIV-1 permissiveness [33]. Results in Supplemental Figure 5 demonstrate that $CD16^+$ compared to $CD16^-$ MDDCs produce superior levels of CCL2, CCL22, and CCL24. Together, these results provide evidence that $CD16^+$ compared to $CD16^-$ MDDCs have a unique ability to disseminate HIV to $CD4^+$ T-cells *via* mechanisms that likely involve a superior ability to activate resting T-cells.

Distinct transcriptional profiles in CD16$^+$ and CD16$^-$ MDDCs

To explore molecular mechanisms by which CD16$^+$ compared to CD16$^-$ MDDCs are more efficient in HIV-1 transmission to resting CD4$^+$ T-cells, we employed the Affymetrix microarray technology for genome-wide transcriptional analysis of gene expression using total RNA extracted from matched immature MDDC subsets of five healthy HIV-uninfected CMV$^+$ subjects. Differentially expressed probe sets were identified based on p-values ($p < 0.05$) or adjusted p-values (adj. $p < 0.05$), and fold change (FC) expression ratios (cut-off 1.3). Among differentially expressed genes (p-value <0.05; FC cut-off 1.3), 447 and 692 probe sets were preferentially expressed in immature CD16$^+$ and CD16$^-$ MDDCs, respectively (data not shown). When adj. $p < 0.05$ and FC cut-off 1.3 limits were applied 159 and 288 probe sets were found preferentially expressed in immature CD16$^+$ and CD16$^-$ MDDCs, respectively (Supplemental Tables 1-2). Among the differentially expressed probe sets with the most significant adj. p-values (and FC cut-off 1.3), we identified transcripts that represent new molecular markers for CD16$^+$ MDDCs (TCF7L2, LOC200772, EPS8, CABP4, ABHD2, CHST15, DOCK3, CCL22, PALLD, LY9, SYT17, MLLT4, UCP2, AQP9, FA2F) and CD16$^-$ MDDCs (PAK7, CCR6, MYBL1, NUP107, RXFP1, EPCAM, CDH1, DUOXA1, SERPINF1, PTGER3, COLEC12, SIGLEC1, CRH, RBM22, DUOX1, GGT5, LOC101927780, HR, TOX, CST7, ABCC4, RCBTB2, CREB3L1, PROS1, HIF1A, IL17RB, STEAP4, FZD3, PRSS36, ADAM23, IGFBP7, DDIT3, PARPBP, CLEC4G) (Figure 3A) (Supplemental Tables1-2).

Gene Set Variation Analysis (GSVA) of differentially expressed genes ($p<0.05$; FC cut-off 1.3) identified canonical pathways and biological processes preferentially associated with CD16$^+$ or CD16$^-$ MDDCs. Canonical pathways such as nuclear receptors and T helper pathways as well as regulation of IFNA pathway were enriched in CD16$^+$ MDDCs, while pathways linked to DNA

replication, repair and telomere maintenance were enriched in CD16$^-$ MDDCs (Figure 3B). Biological processes enriched in CD16$^+$ MDDCs included pathways linked to actin filament, response to extracellular stimulus, interferon gamma production, positive regulation of MAPKKK cascade, lymphocyte differentiation, regulation of lymphocyte activation, positive regulation of T cell activation, B cell activation and lymphocyte activation (Figure 3C). In contrast, biological processes enriched in CD16$^-$ MDDCs included nuclease and endonuclease activity, cell cycle, DNA replication, chromatin, and microtubule motor activity (Figure 3C).

Consistent with the GSVA results (Figure 3B-C), *Gene Ontology* (GO) classification of differentially expressed genes in CD16$^+$ and CD16$^-$ MDDCs (p-value <0.05; FC cut-off 1.3) revealed transcripts related to different biological functions including: transcription factors, cytokines, adhesion molecules, chemotaxis and cell projections; top regulated transcripts are depicted in Figure 4. For the GO term "transcription factors", transcripts enriched in CD16$^+$ MDDCs included the myocyte enhancer factor 2 (MEF2), polycomb group ring finger 2 (PCGF2), peroxisome proliferator-activated receptor gamma (PPARG), transcription factor 7-like 2 (TCF7L2), basic helix-loop-helix family member e41 (BHLHE41), forkhead box O1 (FOXO1), homeodomain interacting protein kinase 2 (HIPK2), and activating transcription factor 3 (ATF3), while transcription factors enriched in CD16$^-$ MDDCs included E2F transcription factor 6 (E2F6) and the hypoxia inducible factor 1, alpha subunit (HIF1A) (Figure 4A). The heat map in Figure 4A also reveals over expression of transcripts for the stem-cell surface markers CD34 and c-kit (KIT) in CD16$^-$ *versus* CD16$^+$ MDDCs. For the GO term cytokines JAK1, CCL22, IL-21R, PTGER4, IL-15, TNFSF14, CD86, SERPINA1, and aldehyde dehydrogenase 1 family member A1 (ALDH1A1) transcripts were enriched in CD16$^+$ MDDCs, while IL1RL2, dual oxidase 1 (DUOX1), IFI16,

IL17RB, and CCL18 were enriched in CD16$^-$ MDDCs (Figure 4B). For the GO term "adhesion molecules", CD16$^+$ MDDCs were enriched in CD97, signaling lymphocytic activation molecule family 7 (SLAMF7), TNFRSF12A, ITGAL, paladin (PALLD), RAPH1, ALCAM, LY9 and ITGAE transcripts, while CLEC4M, ITGA9, SIGLEC1, CDH1, ADAM23, CDH2, EPCAM, SELL, KIT, CD34, and IFT74 transcripts were up regulated in CD16$^-$ MDDCs (Figure 4C). The search for the GO term "chemotaxis" further revealed preferential expression of CCR6 in CD16$^-$ MDDCs (Figure 4D). Finally, several transcripts associated with the GO term "cell projections" were differentially expressed in CD16$^+$ *versus* CD16$^-$ MDDCs (Figure 4E).

Together these results demonstrate that CD16$^+$ and CD16$^-$ monocytes are precursors for phenotypically distinct DC subsets with unique trafficking potential and immune functions under the control of specific transcriptional regulators.

The CD16$^+$ and CD16$^-$ MDDCs differentially respond to LPS and HIV exposure

CD16$^+$ and CD16$^-$ monocytes subsets differ in their expression of TLR and subsequently have a distinct ability to respond to bacterial *versus* viral pathogens[13,19]. To investigate whether this division of labor is maintained upon monocyte differentiation into DCs, transcriptional similarities/differences were investigated in CD16$^+$ and CD16$^-$ MDDCs upon exposure to LPS or HIV.

Both MDDC subsets strongly responded to LPS stimulation, with 2,554 and 2,868 probe sets up and down regulated, respectively, in CD16$^+$ MDDCs compared to 2,559 and 3,218 probe sets up and down regulated, respectively, in CD16$^-$ MDDCs (adj. $p<0.05$; FC cut-off 1.3) (Supplemental Figure

6). Consistent with results in Supplemental Figure 4, large numbers of transcripts were commonly up or down regulated by LPS exposure in both $CD16^+$ and $CD16^-$ MDDCs (Figure 5A-B). Nevertheless, the analysis of differentially expressed genes revealed unique transcriptional signatures induced by LPS in each MDDC subset. Specifically 261 and 221 transcripts were up and down regulated by LPS, respectively, in $CD16^+$ MDDC (Supplemental Tables 3-4); while 265 and 467 transcripts were up and down regulated by LPS, respectively, in $CD16^-$ MDDC (adj. $p<0.05$; FC cut-off 1.3) (Supplemental Tables 5-6 and Supplemental Figure 6). Among the transcripts specifically modulated by LPS in $CD16^+$ MDDCs, CCL8, SIGLEC1, MIR4439, SCIN, IL7R, PLTP, TNF, CFP (properdin, the positive regulator of the alternative pathway of complement activation [38,39]), clusterin (CLU), complement component 2 (C2), MIR331, TREM139, MAP3K8, CXCL1, IL-18, BCL11A, perforin 1 (PRF1), MIR4436, MIR299, and retinol dehydrogenase 11 (RDH11) transcripts were up regulated; and lipoprotein lipase (LPL), kelch-like family member 6 (KLHL6), CD109, TLR3, ITGAE, ABCA1, ITGAV, KLF10, and FCGR3A transcripts were down regulated (Supplemental Table 3-4). Among the transcripts specifically modulated by LPS in $CD16^-$ MDDCs, matrix metallopeptidase 10 (stromelysin 2, MMP10), MMP1, TNFRSF11A, IL-1A, lysosomal-associated membrane protein 1 (LAMP1), MMP8, fibrillin 1 (FBN), aldehyde dehydrogenase 1 family, member L2 (ALDH1L2), interleukin 1 receptor antagonist (IL-1RN), triggering receptor expressed on myeloid cells 1 (TREM1), and mucosa associated lymphoid tissue lymphoma translocation gene 1 (MALT1) transcripts were up regulated; and CD24, STEAP family member 4 (STEAP4), CD163 molecule-like 1(CD163L1), MIR146B, p21 protein (Cdc42/Rac)-activated kinase 7 (PAK7), CCL18, G protein-coupled receptor 34(GPR34), cell adhesion molecule 3 (CAM3), IL-17RB, CD207, CD180, legumain (LGMN), MIR3174, C-type lectin domain family 4,

member M (CLEC4M), CD69, CD163, IL-10, integrin, alpha 9 (ITGA9), and myeloperoxidase (MPO) transcripts were down regulated (Supplemental Table 5-6).

Using p-values <0.05 and FC cut-off of 13 as restriction criteria, we identified top modulated transcripts preferentially expressed for each MDDC subset upon exposure to medium or LPS that are illustrated in Figure 5C. Of note, mature $CD16^-$ but not $CD16^+$ MDDCs express IFNA1 transcripts. These results reveal new functional markers for immature and mature $CD16^+$ and $CD16^-$ MDDCs.

GO classification of differentially expressed genes in $CD16^+$ and $CD16^-$ MDDCs exposed to LPS (p-value <0.05; FC cut-off 1.3) revealed transcripts linked to cell migration and cytokines. For the GO term "chemotaxis", top regulated transcripts included OR1D2, TNFRSF11A, RALA, CXCR4 and CCL18 for $CD16^-$ MDDCs, and AMICA1, chemerin chemokine-like receptor 1 (CMKLR1), ITGAM, protein tyrosine phosphatase, receptor type, J (PTPRJ), CCL22, and proteolipid protein 2 (PLP2) for $CD16^+$ MDDCs (Figure 5D). For the GO term "cytokines", top regulated transcript enriched in $CD16^-$ MDDCs included FLT3, MALT1, NUP107, IGF1R, CXCR4, IL17RB, CCL18, EGR1, IL-7, IL-23R, IFNA1, and IL-1R1), while in $CD16^+$ MDDCs included IL-21R, LTB, IL-18, LTA, CCL22, TNF, MYD88, interferon alpha-inducible protein 6 (IFI6), CD86, and DUOX2 (Figure 5E). These results demonstrate that $CD16^+$ and $CD16^-$ MDDCs are both able to detect LPS but respond to stimulation in transcriptionally distinct manners thus suggesting the possibility that they fulfill distinct immunological functions likely in distinct anatomic sites. Of note, $CD16^+$ compared to $CD16^-$ MDDCs appear to have a superior pro-inflammatory profile as reflected by their up regulated expression of LTB, IL-18, LTA, CCL22, TNF, MYD88 and DUOX2 transcripts.

Consistent with the concept that DCs are limited in the ability to properly sense HIV [40-42], transcriptional changes observed in $CD16^+$ or $CD16^-$ MDDCs upon exposure to HIV were minimal. A number of 44 and 84 transcripts were specifically up and down regulated, respectively, in $CD16^+$ MDDCs (Supplemental Table 7). A number of 25 and 30 transcripts were specifically up and down regulated, respectively, in $CD16^-$ MDDCs ($p < 0.05$; FC cut-off 1.3) (Supplemental Table 8). Heat maps in Figure 6A-B illustrate top transcripts modulated by HIV in $CD16^+$ and $CD16^-$ MDDCs ($p<0.05$, FC cut-off 1.3). None of these changes in gene expression reached an adj. p-value <0.05. Of note, there was a tendency for HIV to regulate the expression of MIRs in both $CD16^+$ and $CD16^-$ MDDCs. Transcripts up regulated by HIV in $CD16^+$ MDDCs included the interferon alpha-inducible protein 6 (IFI6), MIR568, MIR4718, CD101 (a molecule potentially involved in the negative regulation of T cell activation [43]), MIR4717, SIGLEC1, MIR3692, MIR3188, MIR4441, Kruppel-like factor 10 (KLF10), MIR4672, MIR548S, CASP6, MIR583, and MIR4491; while down regulated transcript included the Rho-associated, coiled-coil containing protein kinase 1 pseudogene 1 (ROCK1P1), ubiquitin specific peptidase 17-like family member 5 (USP17L5), cytokine receptor-like factor 2 (CRLF2), MIR548I3, MIR509-3, interferon alpha 1 (IFNA1), fms-related tyrosine kinase 3 (FLT3), IL-2RA, mediator complex subunit 27 (MED27), activating transcription factor 3 (ATF3), interferon, alpha 16 (IFNA16), and CCR4 (Supplemental Table 7; Figure 6A-B). Transcripts up regulated by HIV in $CD16^-$ MDDCs included MIR1271, MIR516A2, MIR3911, MIR196A1, S100B, MIR320C1, MIR3665, MIR3201, and MIR523; while down regulated transcript included MIR4499, MIR3975, MIR4263, MIR545, MIR130B, and MIR4308 (Supplemental Table 8; Figure 6A-B).

The heat map in Figure 6C illustrates top differentially expressed transcripts in $CD16^+$ and $CD16^-$ MDDCs upon HIV exposure. Of note, HIV-exposed $CD16^-$ MDDCs cluster separately from HIV-exposed $CD16^+$ MDDCs and share transcripts with immature $CD16^+$ MDDCs (Figure 6C). When GO analysis was performed with data sets from MDDC subsets exposed to HIV, transcripts associated to exosomes appeared the most predominant and differentially expressed in $CD16^+$ *versus* $CD16^-$ MDDCs (Figure 6D). These results reveal minor but unique effects HIV exerts on the functionality of $CD16^+$ and $CD16^-$ MDDCs. Nevertheless, the increased expression of CD101 together with the decreased expression of IFNA1 in $CD16^+$ MDDCs *versus* $CD16^-$ MDDCs exposed to HIV suggest a potential decreased immunogenic potential and superior ability to transmit HIV infection for $CD16^+$ MDDCs.

Altogether, these results suggest that $CD16^+$ and $CD16^-$ MDDCs represent distinct DC subsets with different migratory profiles and ability to respond to bacterial and viral pathogens.

Meta-analysis in search of HIV interactors in $CD16^+$ and $CD16^-$ MDDCs

To further investigate mechanisms that regulate differential HIV-1 transmission by $CD16^+$ *versus* $CD16^-$ MDDCs, we performed a meta-analysis where genes differentially expressed in immature $CD16^+$ and $CD16^-$ MDDCs ($p<0.05$) were matched to known HIV interactors included in the NCBI database. Among human genes in the category "*HIV-1 protein interacts with*", MDM2, PACS1, ITGAL, and IL-15 were preferentially expressed in $CD16^+$ MDDCs; while RNASE1, TRIM15, SIGLEC1, and HIF1A were expressed in $CD16^-$ MDDCs (Figure 7A). In the category "*HIV-1 protein regulated by*", TCF7L2, ACTA2, MDM2, AKT3, PACS1, JAK1, PPARG, SNF8, LRP1, and MGAT1 were preferentially in $CD16^+$ MDDCs and MAP1A, DNM1, HSPA2, GRIN3B,

TOP2A, and EIF2AK2 were up regulated in CD16$^-$ MDDCs (Figure 7B). Thus, CD16$^+$ *versus* CD16$^-$ MDDCs appear enriched in several transcripts that are known to play a role in the positive or the negative regulation of HIV replication.

Unique molecular signatures expressed by CD16$^+$ and CD16$^-$ MDDCs

Monocytes are precursors for DCs but whether DCs derived from CD16$^+$ and CD16$^-$ monocytes preserve their unique features during homeostasis and pathological conditions such as sepsis and HIV infection remains unknown. To identify molecular signatures specific to CD16$^+$ and CD16$^-$ MDDCs expressed constitutively or upon pathogen exposure, gene set enrichment analysis (GSEA) for canonical pathways was performed on genes differentially expressed in MDDC subsets upon exposure to medium, LPS or HIV. Results in Figure 8A illustrate canonical pathways that were up and down regulated in CD16$^+$ *versus* CD16$^-$ MDDCs by both LPS and HIV stimulations; nevertheless a number of canonical pathways remained constantly enriched in CD16$^+$ *versus* CD16$^-$ MDDCs regardless of the stimulatory conditions: 20S proteasome, myeloid lineage, myeloid macrophages dendritic cell inflammatory interleukin, and inflammation II. Changes in canonical pathways were associated with changes in the expression of various MIRs, including the preferential expression in CD16$^+$ *versus* CD16$^-$ MDDCs of MIR1271 under constitutive conditions, MIR146b upon LPS stimulation, and MIR4499 upon HIV exposure (Figure 8B). Thus, CD16$^+$ monocytes are precursors for DCs that conserve a superior inflammatory profile compared to CD16$^-$ MDDCs and may act as pathogenic cells during sepsis and HIV infection. These functional differences appear under the regulation of complex molecular mechanisms including at least in part the microRNA machinery.

DISCUSSION

Classical, intermediate and non-classical monocytes subsets differ in their pro-inflammatory profiles and trafficking potential [3,22,44]. While classical $CD16^-$ monocytes traffic into the tissues *via* CCR2/CCL2 [45], non-classical $CD16^+$ monocytes patrol endothelial beds *via* the FKN/CX3CL1 receptor CX3CR1 and are immediate effector cells upon interaction with pathogen components [8,9,46]. Peripheral blood monocytes represent an important pool of DC precursors. Studies demonstrating that DCs derived from $CD16^+$ *versus* $CD16^-$ monocytes are functionally distinct [24,25] raise the possibility that alterations in the $CD16^-/CD16^+$ monocyte ratio during pathological conditions may significantly impact the quality if immune responses and the rate of disease progression. The well-documented expansion of $CD16^+$ monocytes during HIV-1 infection and the lack of normalization under antiretroviral therapy [27,29] prompted us to investigate similarities and differences between $CD16^+$ and $CD16^-$ monocyte-derived DCs (MDDCs) with relevance for HIV-1 infection where exposure to bacterial and viral components occur simultaneously [34].

In this manuscript, we observed that highly pure $CD16^+$ and $CD16^-$ monocytes differentiated immature $CD16^+$ and $CD16^-$ MDDCs with a typical veiled morphology and similar expression of classical DC markers such as CD1a, CD1c and DC-SIGN. Of note, the expression of CD16 was maintained in a fraction of total $CD16^+$ MDDCs population. Exposure to LPS induced the maturation of both $CD16^+$ and $CD16^-$ MDDCs as reflected by the up-regulation of the CCR7 and CD83 expression at cell surface. These results suggest that $CD16^+$ and $CD16^-$ monocytes may both represent important pools of DC precursors under specific conditions *in vivo*. In contrast to these similarities, we reveal here for the first time at our knowledge that $CD16^+$ but not $CD16^-$ MDDCs

promoted the R5 HIV-1 *trans* infection of resting $CD4^+$ T-cells. Our results suggest that $CD16^+$ compared to $CD16^-$ monocytes are progenitors for DCs that may contribute to HIV dissemination by their superior ability to transmit the virus to target cells. Thus, HIV likely takes advantage of the higher frequency of CD16+ monocytes [10,27-30] for its persistence. However, both $CD16^+$ and $CD16^-$ MDDCs shared similar capacity to transmit R5 HIV-1 to activated $CD4^+$ T-cells. This indicates that $CD16^+$ MDDCs have a higher capacity to activate resting $CD4^+$ T-cells for increased permissiveness to active viral replication. Indeed, HIV replication is restricted in resting $CD4^+$ T-cells at levels during reverse transcription and prior to HIV-DNA integration [47,48]. Activation *via* the TCR or other stimuli is required for HIV-DNA integration in $CD4^+$ T-cells and subsequent productive viral replication [35,49,50]. We previously demonstrated that $CD16^+$ monocyte/macrophages (MΦ) promote HIV replication in resting $CD4^+$ T-cells *via* the production of CCR3 and CCR4 ligands [33]. Similarly, $CD16^+$ compared to $CD16^-$ MDDCs produced constitutively higher levels of chemokines CCL2 and CCL22 and CCL24, suggesting that these chemokines may deliver co-stimulatory signals to resting $CD4^+$ T-cells thus contributing to their activation for HIV replication. Hence, our study demonstrated that the $CD16^+$ MDDCs share some features of their precursors (e.g., CCL2 and CCL22) together with their ability to efficiently transmit HIV replication to resting $CD4^+$T-cells. Our results also emphasize the similarities between DCs and MΦ derived from $CD16^+$ monocytes in their ability to promote T-cell activation. Our support the idea that that $CD16^+$ monocytes are imprinted with a transcriptional program and or epigenetic modifications that is preserved upon differentiation, consistent with a the novel concept of trained innate immunity [51,52]. Thus, the exacerbation of CD16+ monocyte differentiation during pathological conditions has an impact on the quality of immune responses mediated by DC derived from functionally distinct monocyte progenitors.

Our genome-wide transcriptional profiling led to a detailed characterization of these two MDDCs subsets. The unique biological features of $CD16^+$ *versus* $CD16^-$ MDDCs may explain their different ability to induce HIV replication in resting $CD4^+$ T-cells. Biological processes enriched in $CD16^+$ *versus* $CD16^-$ MDDCs included lymphocyte activation, positive regulation of T cell activation, B cell activation and lymphocyte activation. As a first validation of our transcriptional results, we observed that CD16 and CCL22 were up-regulated in $CD16^+$ *versus* $CD16^-$ MDDCs. Several markers of DC maturation and activation were enriched in $CD16^+$ MDDCs. Indeed, $CD16^+$ MDDC expressed transcripts involved in T-cell interaction and immunological synapse including activation molecule CD86 (B7-2) [53], CD97 (adhesion G protein-coupled receptor E5) [12] and LY9 [54], adhesion molecules ALCAM [55] and ITGAL/LFA-1 [56], as well as transcription factor FOXO1 [57]. Of note, CD97 was previously identified as an HIV permissiveness factor [58]. Subsequent events following the formation of the immunological synapse involves the up-regulation of FOXO1 in DC cytoplasm to promote cell survival [57]. Furthermore, in activated DCs, FOXO1 upregulates CCR7 and ICAM1 for complete DC maturation [59]. Other transcription factors such as the activating transcription factor 3 (ATF3) and transcription factor 7-like 2 (TCF7L2) were also preferentially expressed in $CD16^+$ *versus* $CD16^-$ MDDCs. Consistent with the role of ATF3 in decreasing IL-23 production and Th17 polarization [60], transcripts for IL-23 were down regulated in $CD16^+$ *versus* $CD16^-$ MDDCs upon LPS exposure. The transcription factor TCF7L2, a component of the Wnt pathway, regulates the glucose metabolism and cell survival; of note, polymorphism in this gene is associated with type 2 diabetes [61,62]. Moreover, the enriched expression in $CD16^+$ *versus* $CD16^-$ MDDCs of transcripts for the integrin alpha E (ITGAE/CD103), a gut-homing marker, suggest a potential superior ability of $CD16^+$ *versus* $CD16^-$ MDDCs to localize in the gut. CD103 identifies a specific subset of Th17-

polarizing DCs that are depleted during the course of SIV infection [63]. It remains unknown whether $CD16^+$ monocytes are precursors for $CD103^+$ DCs *in vivo*. Furthermore, $CD16^+$ *versus* $CD16^-$ MDDCs were also enriched in transcripts for the enzyme aldehyde dehydrogenase 1 family member A2 (ALDH1A2, or RALDH2) involved in the biosynthesis of the retinoic acid (RA) from vitamin A [64], a gut-homing elixir [65], thus suggesting their ability to imprint other immune cells with a gut-homing potential. Indeed, RA produced by DCs was reported to imprint gut homing specificity to $CD4^+$ T-cells during antigenic stimulation [66]. We previously demonstrated that RA treatment increases HIV permissiveness in Th17 cells [67] thus raising the possibility that $CD16^+$ MDDCs may preferentially contribute to the establishment of HIV replication at mucosal levels, a major site of HIV replication [68], *via* the RA production. This scenario is also supported by the fact that $CD16^+$ monocyte express high levels of CX3CR1 [8,46], a chemokine receptor that play a critical role for the migration into the gut [69]. The pathogenic potential of $CD16^+$ *versus* $CD16^-$ MDDCs in te context of HIV-1 infection may also be mediated by the production of the homeostatic cytokine IL-15, reported to increase SIV replication in T-cells [70,71]. Finally, the mRNA for the transcription factor PPARG (a regulator of inflammation [72] and HIV replication [73]) were found up regulated in $CD16^+$ *versus* $CD16^-$ MDDCs thus suggesting that therapeutic interventions against PPARG may restrain the pathogenic potential of $CD16^+$ MDDCs.

As opposed to $CD16^+$ MDDCs, transcriptional profiles in $CD16^-$ MDDCs indicated a less active cellular metabolism. $CD16^-$ *versus* $CD16^+$ MDDCs were enriched in transcripts for early hematopoietic precursors and stem cells such as CD34 [74], c-kit [75], and ITAG9 [76], the hypoxia factor 1A (HIF1A), cell migration markers (CCR6, SELL and EPCAM), cytoskeleton (PAK7), adhesion molecules (CDH1 and CDH2) and phagocytosis (SIGLEC1). $CD16^-$ compared to $CD16^+$ MDDCs

also expressed the myeloid marker six transmembrane epithelial antigen of prostate 1 (STEAP4). Following differentiation, $CD16^-$ MDDCs acquired the expression of gene transcript involved in anti-oxidation including MPO, DUOX1 and DUOAX1 allowing protection against oxidative stress [77]. Interestingly, $CD16^-$ MDDCs also express sensor for bacterial DNA IFI16 [78], which was reported to sense HIV in $CD4^+$ T-cells [79]. The biological processes enriched in $CD16^-$ *versus* $CD16^+$ MDDCs included biological terms such as cell cycle, DNA replication, chromatin, and microtubule motor activity. Hence, our results indicate that $CD16^-$ and $CD16^+$ monocytes differentiate into DCs that play distinct roles in host defense and therefore the alteration of the $CD16^+/CD16^-$ ratio likely has deleterious consequences during disease pathogenesis. Compared to $CD16^-$ MDDCs, $CD16^+$ MDDCs appear to act like inflammatory DCs ready to stimulate T-cells to induce fast immune responses. Conversely, $CD16^-$ MDDCs appear to have a minor inflammatory potential and role in the maintenance of immune homeostasis. The advanced stage of activation status displayed by $CD16^+$ MDDC likely predisposes them to interact and stimulate $CD4^+$ T-cells, even in the absence of exogenous antigens *in vitro*. We cannot however exclude the possibility that CD16+ monocytes captured antigens *in vivo* during the process of marginalization or recirculation [44]. Indeed, monocytes were reported to cross peripheral tissues where they uptake antigens and to return into the circulation with minimal phenotypic changes [80]. This raises the possibility that circulating $CD16^+$ monocytes represent a pool of monocytes that have already sampled antigens from tissues. This activation state may explain $CD16^+$ MDDCs ability to induce HIV replication in resting $CD4^+$ T-cells.

The LPS stimulation led to changes in the transcriptional programs of both $CD16^+$ and $CD16^-$ MDDCs. For instance, LPS decreased the expression of ITGAE/CD103 transcripts in $CD16^+$

MDDCs but increased retinol dehydrogenase 11 (RDH11), another enzyme involved in retinoic acid biosynthesis. As expected, LPS induced the expression of DC maturation markers such as CD86, CD80, and CCR7 in $CD16^+$ and $CD16^-$ MDDCs. Gene transcripts preferentially up regulated in $CD16^+$ MDDCs in response to LPS included inflammatory cytokines and chemokines (TNF, IL-18, CXCL1 and CCL18), molecules part of the complement system (C2, CFP), phagocytosis (Siglec1) and micro RNA (Mir-331, Mir-4439). Furthermore, LPS stimulation increased the expression of transcripts involved in the regulation of secretory vesicle (scinderin; SCIN [81]), of endocytosis (SNX10) [82], of lipid transport (PLTP), of T-cell homeostasis (IL-17R [83]) and in the induction of pro-inflammatory cytokines including TNF-α and IL-12 [84,85]. Of note, LPS also induced in $CD16^+$ MDDCs markers of follicular dendritic cells including molecular chaperone clusterin (CLU) [86] and G-protein coupled receptor P2RY8 [87], supporting the possibility that $CD16^+$ MDDCs are precursors for follicular DCs. Interestingly, LPS stimulation in $CD16^-$ MDDCs led to the up-regulation of a transcriptional profile distinct from the one observed in the $CD16^+$ MDDCs. The molecular signature induced by LPS in $CD16^-$ MDDCs included transcripts associated with the type-1 interferon response (IL1A, IFNA1), the inflammasome activation pathway (MALT1 [88,89]), with cell migration including the chemokine CXCL6 and metalloproteinases MMP1 [90], MMP8 [91] and MMP10 [92], with Th17 polarization (IL-23, IL-6ST), with T-DC interaction including adhesion molecule ALCAM and tumor necrosis factor receptor TNFRSF11 and with biosynthesis of retinoic acid (ALDH1L2). Furthermore, LPS induced up regulation of damage-associated molecular pattern (DAMP) and calcium-binding protein S100A3 [93], NK and $CD8^+$ T-cell degranulation marker and potentially a DC activation marker LAMP/CD107A [94], M2 macrophage marker transglutaminase 2 (TGM2) [95] and Ig receptor TREM1 implicated in the amplification of an induced immune response [96]. Thus, $CD16^+$ and $CD16^-$ MDDCs respond differently to LPS. The production of factors such as

IFN-1α, known to restrict HIV replication [97], may limit the ability of CD16$^-$ MDDCs to transmit HIV to CD4$^+$ T-cells.

In contrast to LPS, HIV exposure induced minimal changes in the transcriptional profiles of both CD16$^+$ and CD16$^-$ MDDCs, with no signs of DC maturation, consistent with our results included in different manuscript [98]. Indeed, the transcriptional profile of HIV-exposed MDDC subsets reassembled to one to immature MDDCs. Our results are in line with studies published by other groups demonstrating the incapacity of HIV-exposed MDDCs to reach a complete maturation state linked to their incapacity to sense HIV [99]. Nevertheless, HIV exposition to CD16$^+$ MDDCs led to the up-regulation of gene transcripts associated with micro-RNAS (MIR568, MIR4718, MIR4717), type 1 interferon response (IFI6), surface proteins involved in T-cell response CD101/V7 [43] and zinc finger proteins ZNF714 and ZNF429. In CD16-MDDCs, HIV exposition resulted in the upregulation of other micro-RNAs (MIR1271, MIR516A2, MIR196A1, MIR3911 and plakophilin 2 involved in cytoskeleton structure cell adhesion [100]. The role in immunity associated with the majority of these mentioned gene transcripts remains unknown. Interestingly, HIV induces in CD16$^-$ MDDCs a DC maturation marker the calcium-binding protein S100B. The loss of S100B in DCs was associated with SIV disease progression in primate animal models [101].

The GSEA revealed unique canonical pathways enriched in CD16$^+$ *versus* CD16$^-$ MDDCs constitutively, as well as upon exposure to LPS and HIV *in vitro*: 20S proteasome, myeloid lineage, myeloid macrophages dendritic cell inflammatory interleukin, and inflammation II. Previous studies on CD16$^+$ *versus* CD16$^-$ monocytes generated by our group demonstrated that CD16$^+$ monocytes display a MΦ/DC-like transcription program [12]. Of note, some transcripts preferentially expressed in

CD16$^+$ *versus* CD16$^-$ monocytes [12] such as LFA1/ITGAL, MTSS1 and MGLL, were also found enriched in CD16$^+$ *versus* CD16$^-$ MDDCs. Also, similar to monocytes CD16$^+$ monocytes, CD16$^+$ *versus* CD16$^-$ MDDCs were demonstrated to be the producers of TNF. These results indicate that despite the morphological and biological changes that monocytes undergo during differentiation toward the DC lineage and subsequent exposition to pathological conditions such as sepsis and HIV infection, their core pro-inflammatory properties are conserved. As described for the CD16$^+$ monocytes, the CD16$^+$ MDDCs appear to be inflammatory DCs. Of note, we observed changes in micro-RNAs (mir) expression upon exposure to LPS or HIV compared to immature MDDCs. Particularly, HIV exposure led to a decreased expression of mir1271 while promoting the up regulation of mir146B, mir4499, mir583 and mir3193 expression. The role of these micro-RNAs in controlling the pathogenic features of CD16$^+$ MDDCs during HIV infection remains to be investigated.

In conclusion, we provide here a detailed characterization on the differentiation fate of two peripheral blood monocyte subsets, CD16$^+$ and CD16$^-$, at homeostasis and upon exposure to LPS or HIV. We identified the CD16$^+$ MDDCs as major contributors to HIV dissemination, likely by an increased potential to activate resting CD4$^+$ T-cells. In line with these functional differences, we reveal a unique molecular signature (i.e., transcription factors, surface markers, trafficking molecules, cytokines and functional markers) expressed by immature CD16$^+$ *versus* CD16$^-$ MDDCs, as well as specific sets of transcripts differentially regulated by LPS and HIV in these two MDDC subsets (Figure 9). The pro-inflammatory features of CD16$^+$ compared to CD16-MDDCs may underlie their superior capacity to induce activation in resting CD4$^+$ T-cells and subsequent HIV replication. The present genome-wide transcriptional characterization of CD16$^+$ and CD16$^-$ MDDCs

offers a solid platform for future validations of the identified molecular determinants of pathogenicity with relevance for pathological conditions such as sepsis and HIV-1 infection.

MATERIAL AND METHODS

Study subjects

Healthy HIV-uninfected donors were recruited at the Montreal Chest Institute, McGill University Health Centre and Centre Hospitalier de l'Universite de Montreal (CHUM, Montreal, QC, Canada). Large quantities of PBMCs (10^9–10^{10} cells) were collected by leukapheresis as previously described [102]. Cytomegalovirus (CMV) infection was determined upon detection of CMV-specific Abs using chemiluminescent microparticle immunoassay (CMIA) [103].

Ethics statement

This study, using PBMC samples from healthy HIV-uninfected subjects, was conducted in compliance with the principles included in the Declaration of Helsinki. This study received approval from the Institutional Review Board of the McGill University Health Centre and the CHUM-Research Centre, Montreal, Quebec, Canada. All human subjects that donated biological samples for this study provided written informed consent for their participation to the study. All human subjects agreed with the publication of the subsequent results generated using the samples.

Magnetic (MACS) and fluorescence activated cell sorting (FACS)

Total monocytes (Mo) were isolated from PBMC of HIV-uninfected subjects by negative selection using magnetic beads (Miltenyi) [12] and further stained with a cocktail of CD16, CD3, CD6, CD56, and CD1c Abs for FACS sorting. Our choice of not using CD14 Abs was to avoid any potential stimulation *via* CD14. The $CD16^+$ (including mainly non-classical $CD14^+CD16^{++}$ monocytes) and $CD16^-$ monocytes, lacking expression of the lineage markers CD3, CD8, CD19, CD56, and CD1c

were sorted by FACS (BDAria II; BD Biosciences). Quality control analysis post-sort indicated an average purity >99% (S1 Figure).

Generation of monocyte-derived dendritic cells

Monocyte subsets were differentiated into immature dendritic cells (DC) (MDDC, monocyte-derived DC) by culture in the presence of GM-CSF and IL-4 (20 ng/ml (R&D Systems) in RPMI media with 2% FBS for six days. Media containing cytokines was refreshed every two days.

Confocal microscopy

The cell staining protocol for confocal microscopy visualization was performed as previously described [104]. Briefly, MDDCs were fixed with PFA on glass slides and stained on the surface with CD1a Abs. Cells were further permeabilized using the Cytofix/Cytoperm buffer (BD Biosciences) and stained for actin with Phalloidin. The nuclear dye DAPI was included in the mounting media. Cells were analyzed using an inverted spinning disc confocal fluorescent microscope with a 100X objective. Z-sections and a 3D reconstitution were performed.

Genome-wide transcriptional profiling

Matched $CD16^{high}$ and $CD16^{-}$ MDDCs were generated from 5 different donors and stimulated or not with 100 ng/ml LPS or 50 ng/ml HIV for 24 hours. Total RNA was isolated using RNeasy columns kit (Qiagen) according to the manufacturer's protocol. RNA quantity was determined by Pearl nanophotometer (Implen, Germany) (10^6 cells yielded 1-5 µg RNA). Genome-wide analysis of gene expression was performed on total RNA in collaboration with Génome Québec Innovation Centre (Montreal, Qc, Canada) using the Affymetrix ST 2.0 chips providing coverage for more then 46,000

transcripts and known splice variants across the human transcriptome. The expression of differentially expressed genes was identified as previously described [73]. The entire microarray dataset and technical information requested by Minimum Information About a Microarray Experiment (MIAME) are available at the Gene Expression Omnibus (GEO) database under accession number **GSEXXX**. Differentially expressed genes (cut-off 1.3-fold; $p < 0.05$) were classified through Gene Ontology using the NetAffx web-based application (Affymetrix), while differentially expressed pathways were identified using *Ingenuity Pathway Analysis* (IPA) and *Gene Set Variation Analysis* (GSVA). Corresponding heat maps for biological function categories were generated using programming language R [73].

Cytokine and chemokine quantification

Cytokine levels in cell culture supernatants were quantified by ELISA using commercial kits for CCL2, CCL22, CCL24 and TNF (R&D Systems).

Antigen presentation assay

$CD4^+$ T-cell proliferation was measured using the CFSE dilution assay [103] upon co-culture with autologous monocyte-derived dendritic cells (MDDC) exposed or not to HIV-1 infection and loaded with antigens. Briefly, $CD16^+$ and $CD16^-$ MDDC were exposed to the R5 HIV-1 strain NL4.3BAL (50 ng HIV-p24/per 10^6 cells in 300 µl) for 3 hours. Cell were extensively washed with RPMI 10% FBS to remove unbound virions. MDDCs were then loaded with SEB (25 ng/ml; Toxin Technologies), CMV-pp65 peptide pool (1 µg/ml; Miltenyi), or and lysates of *Candida albicans* hyphae LAM-1 [105] (25 µl protein lysate [103]) and *S. aureus* ($5x10^6$cells/assay). MDDC were further co-cultured with FACS-sorted CFSE-loaded $CD4^+$ T-cells (MDDC: T ration of 1:4) and incubated

for 5 days at 37 °C. Then, MDDC: T co-cultures were stained with CD3 (T-cell marker) and CD1c (DC marker) analyzed by FACS for the frequency of proliferating T-cells, identified as $CFSE^{low}CD3^{+}CD1c^{-}$. In parallel, MDDC: T co-cultures were stimulated with PMA and Ionomycin in the presence of brefeldin A for additional 16 hours. The cytokine expression in proliferating T-cells was quantified by FACS upon intracellular staining with specific anti-cytokine Abs, as previously described [103].

HIV *trans* infection by MDDC

Immature $CD16^{+}$ and $CD16^{-}$ MDDC were exposed to NL4.3BaL HIV-1 (10 ng HIV-p24 *per* 10^{6} cells per 300 µl) or 3h at 37°C. Cell were extensively washed with RPMI 10% FBS to remove unbound virions. MDDC subsets were then co-cultured with autologous memory $CD4^{+}$ T-cells previously activated for 3 days *via* CD3/CD28. Cell culture supernatants were harvested at day 3, 6 and 9 post-infection and HIV replication was measured by HIV-p24 ELISA using a homemade kit, as previously described [67,73,106,107] and detailed below. HIV-DNA integration in MDDC exposed to HIV and cultured alone for 2 days was quantified by nested real-time PCR as previously described [67,73,106-108] and detailed below. In other experiments, MDDCs were exposed to HIV and loaded with antigens as described above and then co-cultured with freshly isolated not stimulated autologous memory $CD4^{+}$ T-cells. Cells were harvested at day 5 post co-culture, stained with CD3, CD1c and HIV-p24 Abs and the frequency of $CD4^{+}$ T-cells productively infected with HIV ($CD3^{+}CD1c^{-}$HIV-$p24^{+}$) was determined by FACS.

HIV-p24 ELISA

The quantification of HIV-p24 levels in cell culture supernatants were performed using an in house designed assay, as previously described [67,106].

Real-time PCR quantification of integrated HIV-DNA

The quantification of integrated HIV-DNA was performed as we previously described [67,73,106-108]. Briefly, cells were digested in a proteinase K buffer (Invitrogen), and 10^5 cells/15 µl lysate were used *per* amplification. Integrated HIV-DNA was amplified first (12 cycles) using two outward-facing *Alu* primers and one HIV LTR primer tagged with a lambda sequence; the CD3 gene was amplified in the same reaction. The HIV and CD3 amplicons were then amplified in separate reactions (Light Cycler 480, Roche Diagnostics). The HIV-DNA was amplified using a lambda-specific primer and an inner LTR primer in the presence of two fluorescent probes specific for HIV LTR. The CD3 DNA was amplified using inner primers and two fluorescent probes specific for CD3. Amplification reactions were carried out with Light Cycler 480 Probe Master Mix (Roche) and Taq Polymerase (Invitrogen). The ACH2 cells carrying one copy of integrated HIV-DNA per cell (NIAIDS reagent program) were used as standard curve.

Statistics

Statistical analyses were performed using the GraphPad Prism 6. Details are included in Figure legends. Sample size calculations for microarray studies and all other investigations were based on preliminary results generated in the lab [12,67,73,106,107].

ACCESSION NUMBERS

The entire microarray dataset and technical information requested by Minimum Information About a Microarray Experiment (MIAME) are available at the Gene Expression Omnibus (GEO) database under accession number **GSEXXXX**.

ONLINE SUPPLEMENTAL MATERIAL

The supplemental information includes eight Tables and six Figures.

ACKNOWLEDGEMENTS

The authors thank the CHUM-Research Centre FACS Core Facility for expert technical support in FACS analysis and cell sorting, Mario Legault (HIV/AIDS and Infectious Diseases Network of the Fonds de Recherche Québec-Santé (FRQ-S)) for help with ethical approvals and informed consents, Dr. Louis de Repentigny and Mathieu Goupil for *Candida albicans* LAM-1 strain preparation, and Dr. Dana Gabuzda (Dana-Farber Cancer Institute, Boston, MA, USA) for the HIV molecular clones. We thank Josée Girouard and Angie Massicotte (McGill University Health Centre) for their involvement in human subject recruitment for leukapheresis collection. We finally acknowledge the major contribution to this work of all human donors *via* their gift of leukapheresis.

Footnote

This work was supported by grants to PA from the CIHR (HOP-120239). This study was also supported by The Canadian HIV Cure Enterprise Team Grant HIG-133050 (to PA) from the CIHR

in partnership with CANFAR and IAS. VSW received a CIHR Ph.D. Fellowships. JPR holds a Louis-Lowenstein Chair in Hematology and Oncology, McGill University.

REFERENCES

1 Serbina, N. V., Jia, T., Hohl, T. M. & Pamer, E. G. Monocyte-mediated defense against microbial pathogens. *Annual review of immunology* **26**, 421-452 (2008).

2 Saha, P. & Geissmann, F. Toward a functional characterization of blood monocytes. *Immunology and cell biology* **89**, 2-4, doi:10.1038/icb.2010.130 (2011).

3 Ziegler-Heitbrock, L. *et al.* Nomenclature of monocytes and dendritic cells in blood. *Blood* **116**, e74-80, doi:10.1182/blood-2010-02-258558 (2010).

4 Qu, X. *et al.* Comparison of the innate immune responses of porcine monocyte-derived dendritic cells and splenic dendritic cells stimulated with LPS. *Innate Immun* **21**, 242-254, doi:10.1177/1753425914526266 (2015).

5 Anbazhagan, K., Duroux-Richard, I., Jorgensen, C. & Apparailly, F. Transcriptomic network support distinct roles of classical and non-classical monocytes in human. *International reviews of immunology* **33**, 470-489, doi:10.3109/08830185.2014.902453 (2014).

6 Qu, C., Brinck-Jensen, N. S., Zang, M. & Chen, K. Monocyte-derived dendritic cells: targets as potent antigen-presenting cells for the design of vaccines against infectious diseases. *International journal of infectious diseases : IJID : official publication of the International Society for Infectious Diseases* **19**, 1-5, doi:10.1016/j.ijid.2013.09.023 (2014).

7 Frankenberger, M., Sternsdorf, T., Pechumer, H., Pforte, A. & Ziegler-Heitbrock, H. W. Differential cytokine expression in human blood monocyte subpopulations: a polymerase chain reaction analysis. *Blood* **87**, 373-377. (1996).

8 Ancuta, P. *et al.* Fractalkine preferentially mediates arrest and migration of CD16+ monocytes. *The Journal of experimental medicine* **197**, 1701-1707. (2003).

9 Auffray, C. *et al.* Monitoring of blood vessels and tissues by a population of monocytes with patrolling behavior. *Science* **317**, 666-670 (2007).

10 Thieblemont, N., Weiss, L., Sadeghi, H. M., Estcourt, C. & Haeffner-Cavaillon, N. CD14lowCD16high: a cytokine-producing monocyte subset which expands during human immunodeficiency virus infection. *European journal of immunology* **25**, 3418-3424. (1995).

11 Belge, K. U. *et al.* The Proinflammatory CD14(+)CD16(+)DR(++) Monocytes Are a Major Source of TNF. *Journal of immunology* **168**, 3536-3542. (2002).

12 Ancuta, P. *et al.* Transcriptional profiling reveals developmental relationship and distinct biological functions of CD16+ and CD16- monocyte subsets. *BMC Genomics* **10**, 403 (2009).

13 Cros, J. *et al.* Human CD14dim monocytes patrol and sense nucleic acids and viruses via TLR7 and TLR8 receptors. *Immunity* **33**, 375-386, doi:10.1016/j.immuni.2010.08.012 (2010).

14 Ziegler-Heitbrock, L. Blood Monocytes and Their Subsets: Established Features and Open Questions. *Frontiers in immunology* **6**, 423, doi:10.3389/fimmu.2015.00423 (2015).

15 Wong, K. L. *et al.* Gene expression profiling reveals the defining features of the classical, intermediate, and nonclassical human monocyte subsets. *Blood* **118**, e16-31, doi:10.1182/blood-2010-12-326355 (2011).

16 Buechler, C. *et al.* Regulation of scavenger receptor CD163 expression in human monocytes and macrophages by pro- and antiinflammatory stimuli. *Journal of leukocyte biology* **67**, 97-103 (2000).

17 Zawada, A. M. *et al.* SuperSAGE evidence for CD14++CD16+ monocytes as a third monocyte subset. *Blood* **118**, e50-61, doi:10.1182/blood-2011-01-326827 (2011).

18 Shantsila, E. & Lip, G. Y. Monocytes: possible mediators of benefits and harms from physical activity? *Thromb Haemost* **105**, 387-389, doi:10.1160/TH11-01-0009 (2011).

19 van de Veerdonk, F. L. & Netea, M. G. Diversity: a hallmark of monocyte society. *Immunity* **33**, 289-291, doi:10.1016/j.immuni.2010.09.007 (2010).

20 Randolph, G. J., Beaulieu, S., Lebecque, S., Steinman, R. M. & Muller, W. A. Differentiation of monocytes into dendritic cells in a model of transendothelial trafficking. *Science* **282**, 480-483. (1998).

21 Randolph, G. J., Inaba, K., Robbiani, D. F., Steinman, R. M. & Muller, W. A. Differentiation of phagocytic monocytes into lymph node dendritic cells in vivo. *Immunity* **11**, 753-761. (1999).

22 Auffray, C., Sieweke, M. H. & Geissmann, F. Blood Monocytes: Development, Heterogeneity, and Relationship with Dendritic Cells. *Annual review of immunology* (2009).

23 Randolph, G. J., Sanchez-Schmitz, G., Liebman, R. M. & Schakel, K. The CD16(+) (FcgammaRIII(+)) Subset of Human Monocytes Preferentially Becomes Migratory Dendritic Cells in a Model Tissue Setting. *The Journal of experimental medicine* **196**, 517-527. (2002).

24 Sanchez-Torres, C., Garcia-Romo, G. S., Cornejo-Cortes, M. A., Rivas-Carvalho, A. & Sanchez-Schmitz, G. CD16+ and CD16- human blood monocyte subsets differentiate in vitro to dendritic cells with different abilities to stimulate CD4+ T cells. *International immunology* **13**, 1571-1581. (2001).

25 Rivas-Carvalho, A. *et al.* CD16+ human monocyte-derived dendritic cells matured with different and unrelated stimuli promote similar allogeneic Th2 responses: regulation by pro- and anti-inflammatory cytokines. *International immunology* **16**, 1251-1263, doi:10.1093/intimm/dxh127 (2004).

26 Dutertre, C. A. *et al.* Pivotal role of M-DC8(+) monocytes from viremic HIV-infected patients in TNFalpha overproduction in response to microbial products. *Blood* **120**, 2259-2268, doi:10.1182/blood-2012-03-418681 (2012).

27 Amirayan-Chevillard, N. *et al.* Impact of highly active anti-retroviral therapy (HAART) on cytokine production and monocyte subsets in HIV-infected patients. *Clin Exp Immunol* **120**, 107-112. (2000).

28 Pulliam, L., Gascon, R., Stubblebine, M., McGuire, D. & McGrath, M. S. Unique monocyte subset in patients with AIDS dementia. *Lancet* **349**, 692-695. (1997).

29 Ancuta, P. *et al.* Microbial translocation is associated with increased monocyte activation and dementia in AIDS patients. *PloS one* **3**, e2516 (2008).

30 Allen, J. B., Wong, H. L., Guyre, P. M., Simon, G. L. & Wahl, S. M. Association of circulating receptor Fc gamma RIII-positive monocytes in AIDS patients with elevated levels of transforming growth factor-beta. *The Journal of clinical investigation* **87**, 1773-1779 (1991).

31 Moniuszko, M. *et al.* Glucocorticoid treatment at moderate doses of SIVmac251-infected rhesus macaques decreases the frequency of circulating CD14+CD16++ monocytes but does not alter the tissue virus reservoir. *AIDS Res Hum Retroviruses* **31**, 115-126, doi:10.1089/AID.2013.0220 (2015).

32 Kim, D. & Kim, J. Y. Anti-CD14 antibody reduces LPS responsiveness via TLR4 internalization in human monocytes. *Mol Immunol* **57**, 210-215, doi:10.1016/j.molimm.2013.09.009 (2014).

33 Ancuta, P. *et al.* CD16+ Monocyte-Derived Macrophages Activate Resting T Cells for HIV Infection by Producing CCR3 and CCR4 Ligands. *J Immunol.* **176**, 5760-5771. (2006).

34 Brenchley, J. M. & Douek, D. C. Microbial translocation across the GI tract. *Annual review of immunology* **30**, 149-173, doi:10.1146/annurev-immunol-020711-075001 (2012).

35 Oswald-Richter, K., Grill, S. M., Leelawong, M. & Unutmaz, D. HIV infection of primary human T cells is determined by tunable thresholds of T cell activation. *European journal of immunology* **34**, 1705-1714. (2004).

36 Yan, N. & Lieberman, J. SAMHD1 does it again, now in resting T cells. *Nature medicine* **18**, 1611-1612, doi:10.1038/nm.2980 (2012).

37 Ruffin, N. *et al.* Low SAMHD1 expression following T-cell activation and proliferation renders CD4+ T cells susceptible to HIV-1. *Aids* **29**, 519-530, doi:10.1097/QAD.0000000000000594 (2015).

38 Schwaeble, W. *et al.* Expression of properdin in human monocytes. *Eur J Biochem* **219**, 759-764 (1994).

39 Reis, E. S., Barbuto, J. A. & Isaac, L. Human monocyte-derived dendritic cells are a source of several complement proteins. *Inflamm Res* **55**, 179-184, doi:10.1007/s00011-006-0068-y (2006).

40 Manel, N. *et al.* A cryptic sensor for HIV-1 activates antiviral innate immunity in dendritic cells. *Nature* **467**, 214-217, doi:10.1038/nature09337 (2010).

41 Laguette, N. *et al.* SAMHD1 is the dendritic- and myeloid-cell-specific HIV-1 restriction factor counteracted by Vpx. *Nature* **474**, 654-657, doi:10.1038/nature10117 (2011).

42 Lahaye, X. *et al.* The capsids of HIV-1 and HIV-2 determine immune detection of the viral cDNA by the innate sensor cGAS in dendritic cells. *Immunity* **39**, 1132-1142, doi:10.1016/j.immuni.2013.11.002 (2013).

43 Rainbow, D. B. *et al.* Evidence that Cd101 is an autoimmune diabetes gene in nonobese diabetic mice. *Journal of immunology* **187**, 325-336, doi:10.4049/jimmunol.1003523 (2011).

44 Ancuta, P. A slan-based nomenclature for monocytes? *Blood* **126**, 2536-2538, doi:10.1182/blood-2015-10-675470 (2015).

45 Weber, C. *et al.* Differential chemokine receptor expression and function in human monocyte subpopulations. *Journal of leukocyte biology* **67**, 699-704. (2000).

46 Geissmann, F., Jung, S. & Littman, D. R. Blood monocytes consist of two principal subsets with distinct migratory properties. *Immunity* **19**, 71-82. (2003).

47 Zack, J. A. The role of the cell cycle in HIV-1 infection. *Adv Exp Med Biol* **374**, 27-31. (1995).

48 Zack, J. A. *et al.* HIV-1 entry into quiescent primary lymphocytes: molecular analysis reveals a labile, latent viral structure. *Cell* **61**, 213-222. (1990).

49 Cameron, P. U. *et al.* Establishment of HIV-1 latency in resting CD4+ T cells depends on chemokine-induced changes in the actin cytoskeleton. *Proceedings of the National Academy of Sciences of the United States of America* **107**, 16934-16939, doi:10.1073/pnas.1002894107 (2010).

50 Evans, V. A. *et al.* Myeloid dendritic cells induce HIV-1 latency in non-proliferating CD4+ T cells. *PLoS pathogens* **9**, e1003799, doi:10.1371/journal.ppat.1003799 (2013).

51 Crisan, T. O., Netea, M. G. & Joosten, L. A. Innate immune memory: Implications for host responses to damage-associated molecular patterns. *European journal of immunology* **46**, 817-828, doi:10.1002/eji.201545497 (2016).

52 van der Meer, J. W., Joosten, L. A., Riksen, N. & Netea, M. G. Trained immunity: A smart way to enhance innate immune defence. *Mol Immunol* **68**, 40-44, doi:10.1016/j.molimm.2015.06.019 (2015).

53 Pentcheva-Hoang, T., Egen, J. G., Wojnoonski, K. & Allison, J. P. B7-1 and B7-2 selectively recruit CTLA-4 and CD28 to the immunological synapse. *Immunity* **21**, 401-413. (2004).

54 Hagberg, N. *et al.* Systemic lupus erythematosus immune complexes increase the expression of SLAM family members CD319 (CRACC) and CD229 (LY-9) on plasmacytoid dendritic cells and CD319 on CD56(dim) NK cells. *Journal of immunology* **191**, 2989-2998, doi:10.4049/jimmunol.1301022 (2013).

55 Te Riet, J. *et al.* Dynamic coupling of ALCAM to the actin cortex strengthens cell adhesion to CD6. *Journal of cell science* **127**, 1595-1606, doi:10.1242/jcs.141077 (2014).

56 Sims, T. N. & Dustin, M. L. The immunological synapse: integrins take the stage. *Immunological reviews* **186**, 100-117 (2002).

57 Riol-Blanco, L. *et al.* Immunological synapse formation inhibits, via NF-kappaB and FOXO1, the apoptosis of dendritic cells. *Nature immunology* **10**, 753-760, doi:10.1038/ni.1750 (2009).

58 Zhou, H. *et al.* Genome-scale RNAi screen for host factors required for HIV replication. *Cell host & microbe* **4**, 495-504, doi:10.1016/j.chom.2008.10.004 (2008).

59 Dong, G. *et al.* FOXO1 regulates dendritic cell activity through ICAM-1 and CCR7. *Journal of immunology* **194**, 3745-3755, doi:10.4049/jimmunol.1401754 (2015).

60 Guenova, E. *et al.* IL-4 abrogates T(H)17 cell-mediated inflammation by selective silencing of IL-23 in antigen-presenting cells. *Proceedings of the National Academy of Sciences of the United States of America* **112**, 2163-2168, doi:10.1073/pnas.1416922112 (2015).

61 Welters, H. J. & Kulkarni, R. N. Wnt signaling: relevance to beta-cell biology and diabetes. *Trends Endocrinol Metab* **19**, 349-355, doi:10.1016/j.tem.2008.08.004 (2008).

62 Yao, D. D. *et al.* Geniposide promotes beta-cell regeneration and survival through regulating beta-catenin/TCF7L2 pathway. *Cell death & disease* **6**, e1746, doi:10.1038/cddis.2015.107 (2015).

63 Klatt, N. R. *et al.* Loss of mucosal CD103+ DCs and IL-17+ and IL-22+ lymphocytes is associated with mucosal damage in SIV infection. *Mucosal immunology* **5**, 646-657, doi:10.1038/mi.2012.38 (2012).

64 Denning, T. L., Wang, Y. C., Patel, S. R., Williams, I. R. & Pulendran, B. Lamina propria macrophages and dendritic cells differentially induce regulatory and interleukin 17-producing T cell responses. *Nature immunology* **8**, 1086-1094 (2007).

65 Mora, J. R. & von Andrian, U. H. Retinoic acid: an educational "vitamin elixir" for gut-seeking T cells. *Immunity* **21**, 458-460 (2004).

66 Iwata, M. *et al.* Retinoic acid imprints gut-homing specificity on T cells. *Immunity* **21**, 527-538 (2004).

67 Monteiro, P. *et al.* Memory CCR6+CD4+ T cells are preferential targets for productive HIV type 1 infection regardless of their expression of integrin beta7. *Journal of immunology* **186**, 4618-4630, doi:10.4049/jimmunol.1004151 (2011).

68 Veazey, R. S. & Lackner, A. A. Getting to the guts of HIV pathogenesis. *The Journal of experimental medicine* **200**, 697-700. (2004).

69 Niess, J. H. What are CX3CR1+ mononuclear cells in the intestinal mucosa? *Gut Microbes* **1**, 396-400, doi:10.4161/gmic.1.6.13939 (2010).

70 Lugli, E. *et al.* IL-15 delays suppression and fails to promote immune reconstitution in virally suppressed chronically SIV-infected macaques. *Blood* **118**, 2520-2529, doi:10.1182/blood-2011-05-351155 (2011).

71 Eberly, M. D. *et al.* Increased IL-15 production is associated with higher susceptibility of memory CD4 T cells to simian immunodeficiency virus during acute infection. *Journal of immunology* **182**, 1439-1448 (2009).

72 Ahmadian, M. *et al.* PPARgamma signaling and metabolism: the good, the bad and the future. *Nature medicine* **19**, 557-566, doi:10.1038/nm.3159 (2013).

73 Bernier, A. *et al.* Transcriptional profiling reveals molecular signatures associated with HIV permissiveness in Th1Th17 cells and identifies peroxisome proliferator-activated receptor gamma as an intrinsic negative regulator of viral replication. *Retrovirology* **10**, 160, doi:10.1186/1742-4690-10-160 (2013).

74 McNamara, L. A. & Collins, K. L. Hematopoietic stem/precursor cells as HIV reservoirs. *Current opinion in HIV and AIDS* **6**, 43-48, doi:10.1097/COH.0b013e32834086b3 (2011).

75 Fogg, D. K. *et al.* A clonogenic bone marrow progenitor specific for macrophages and dendritic cells. *Science.* **311**, 83-87. Epub 2005 Dec 2001. (2006).

76 Schreiber, T. D. *et al.* The integrin alpha9beta1 on hematopoietic stem and progenitor cells: involvement in cell adhesion, proliferation and differentiation. *Haematologica* **94**, 1493-1501, doi:10.3324/haematol.2009.006072 (2009).

77 Van Brussel, I. *et al.* Transcript and protein analysis reveals better survival skills of monocyte-derived dendritic cells compared to monocytes during oxidative stress. *PloS one* **7**, e43357, doi:10.1371/journal.pone.0043357 (2012).

78 Unterholzner, L. *et al.* IFI16 is an innate immune sensor for intracellular DNA. *Nature immunology* **11**, 997-1004, doi:10.1038/ni.1932 (2010).

79 Monroe, K. M. *et al.* IFI16 DNA sensor is required for death of lymphoid CD4 T cells abortively infected with HIV. *Science* **343**, 428-432, doi:10.1126/science.1243640 (2014).

80 Jakubzick, C. *et al.* Minimal differentiation of classical monocytes as they survey steady-state tissues and transport antigen to lymph nodes. *Immunity* **39**, 599-610, doi:10.1016/j.immuni.2013.08.007 (2013).

81 Trifaro, J. M., Rose, S. D. & Marcu, M. G. Scinderin, a Ca2+-dependent actin filament severing protein that controls cortical actin network dynamics during secretion. *Neurochemical research* **25**, 133-144 (2000).

82 Cullen, P. J. Endosomal sorting and signalling: an emerging role for sorting nexins. *Nature reviews. Molecular cell biology* **9**, 574-582, doi:10.1038/nrm2427 (2008).

83 Guimond, M. *et al.* Interleukin 7 signaling in dendritic cells regulates the homeostatic proliferation and niche size of CD4+ T cells. *Nature immunology* **10**, 149-157, doi:10.1038/ni.1695 (2009).

84 Dumitru, C. D. *et al.* TNF-alpha induction by LPS is regulated posttranscriptionally via a Tpl2/ERK-dependent pathway. *Cell* **103**, 1071-1083 (2000).

85 Sugimoto, K. *et al.* A serine/threonine kinase, Cot/Tpl2, modulates bacterial DNA-induced IL-12 production and Th cell differentiation. *The Journal of clinical investigation* **114**, 857-866, doi:10.1172/JCI20014 (2004).

86 Verbrugghe, P., Kujala, P., Waelput, W., Peters, P. J. & Cuvelier, C. A. Clusterin in human gut-associated lymphoid tissue, tonsils, and adenoids: localization to M cells and follicular dendritic cells. *Histochemistry and cell biology* **129**, 311-320, doi:10.1007/s00418-007-0369-4 (2008).

87 Muppidi, J. R., Lu, E. & Cyster, J. G. The G protein-coupled receptor P2RY8 and follicular dendritic cells promote germinal center confinement of B cells, whereas S1PR3 can contribute to their dissemination. *The Journal of experimental medicine*, doi:10.1084/jem.20151250 (2015).

88 Dupaul-Chicoine, J. & Saleh, M. A new path to IL-1beta production controlled by caspase-8. *Nature immunology* **13**, 211-212, doi:10.1038/ni.2241 (2012).

89 Yu, J. W. *et al.* MALT1 Protease Activity Is Required for Innate and Adaptive Immune Responses. *PloS one* **10**, e0127083, doi:10.1371/journal.pone.0127083 (2015).

90 Saalbach, A. *et al.* Fibroblasts support migration of monocyte-derived dendritic cells by secretion of PGE2 and MMP-1. *Experimental dermatology* **24**, 598-604, doi:10.1111/exd.12722 (2015).

91 Xiao, Q. *et al.* Functional role of matrix metalloproteinase-8 in stem/progenitor cell migration and their recruitment into atherosclerotic lesions. *Circulation research* **112**, 35-47, doi:10.1161/CIRCRESAHA.112.274019 (2013).

92 Murray, M. Y. *et al.* Macrophage migration and invasion is regulated by MMP10 expression. *PloS one* **8**, e63555, doi:10.1371/journal.pone.0063555 (2013).

93 Donato, R. *et al.* Functions of S100 proteins. *Current molecular medicine* **13**, 24-57 (2013).

94 Hennersdorf, F. *et al.* Identification of CD13, CD107a, and CD164 as novel basophil-activation markers and dissection of two response patterns in time kinetics of IgE-dependent upregulation. *Cell research* **15**, 325-335, doi:10.1038/sj.cr.7290301 (2005).

95 Martinez, P. *et al.* Macrophage polarization alters the expression and sulfation pattern of glycosaminoglycans. *Glycobiology* **25**, 502-513, doi:10.1093/glycob/cwu137 (2015).

96 Zanzinger, K., Schellack, C., Nausch, N. & Cerwenka, A. Regulation of triggering receptor expressed on myeloid cells 1 expression on mouse inflammatory monocytes. *Immunology* **128**, 185-195, doi:10.1111/j.1365-2567.2009.03091.x (2009).

97 Acchioni, C. *et al.* Type I IFN--a blunt spear in fighting HIV-1 infection. *Cytokine & growth factor reviews* **26**, 143-158, doi:10.1016/j.cytogfr.2014.10.004 (2015).

98 Wacleche, V. S. *et al.* HIV-1 Impairs the Ability of Myeloid Dendritic Cells to Promote CD4+ T-Cell Responses against Th17-Specific Pathogens. *Journal of immunology* (2015; in preparation).

99 Blanchet, F., Moris, A., Mitchell, J. P. & Piguet, V. A look at HIV journey: from dendritic cells to infection spread in CD4(+) T cells. *Current opinion in HIV and AIDS* **6**, 391-397, doi:10.1097/COH.0b013e328349b0a0 (2011).

100 Bass-Zubek, A. E., Godsel, L. M., Delmar, M. & Green, K. J. Plakophilins: multifunctional scaffolds for adhesion and signaling. *Current opinion in cell biology* **21**, 708-716, doi:10.1016/j.ceb.2009.07.002 (2009).

101 Soderlund, J. *et al.* Dichotomy between CD1a+ and CD83+ dendritic cells in lymph nodes during SIV infection of macaques. *Journal of medical primatology* **33**, 16-24, doi:10.1111/j.1600-0684.2003.00053.x (2004).

102 Boulassel, M. R. *et al.* Changes in immunological and virological parameters in HIV-1 infected subjects following leukapheresis. *J Clin Apher* **18**, 55-60 (2003).

103 Wacleche, V. S. *et al.* The colocalization potential of HIV-specific CD8+ and CD4+ T-cells is mediated by integrin beta7 but not CCR6 and regulated by retinoic acid. *PloS one* **7**, e32964, doi:10.1371/journal.pone.0032964 (2012).

104 Cleret-Buhot, A. *et al.* Identification of novel HIV-1 dependency factors in primary CCR4(+)CCR6(+)Th17 cells via a genome-wide transcriptional approach. *Retrovirology* **12**, 102, doi:10.1186/s12977-015-0226-9 (2015).

105 Goupil, M. *et al.* Macrophage-mediated responses to Candida albicans in mice expressing the human immunodeficiency virus type 1 transgene. *Infection and immunity* **77**, 4136-4149, doi:10.1128/IAI.00453-09 (2009).

106 Gosselin, A. *et al.* Peripheral blood CCR4+CCR6+ and CXCR3+CCR6+CD4+ T cells are highly permissive to HIV-1 infection. *Journal of immunology* **184**, 1604-1616, doi:10.4049/jimmunol.0903058 (2010).

107 DaFonseca, S. *et al.* Impaired Th17 polarization of phenotypically naive CD4(+) T-cells during chronic HIV-1 infection and potential restoration with early ART. *Retrovirology* **12**, 38, doi:10.1186/s12977-015-0164-6 (2015).

108 Chomont, N. *et al.* HIV reservoir size and persistence are driven by T cell survival and homeostatic proliferation. *Nature medicine* **15**, 893-900 (2009).

Figure Legends

Figure 1: $CD16^+$ and $CD16^-$ monocytes differentiate into dendritic cells with distinct transcriptional profiles. Total monocytes were isolated from PBMCs of healthy HIV-uninfected individuals by negative selection using magnetic beads. Highly pure $CD16^+$ and $CD16^-$ monocytes were sorted by FACS upon staining with CD16 Abs as well as a cocktail of FITC-conjugated non-monocyte lineage-specific Abs (CD3, CD8, CD19, and CD56). Immature monocyte-derived dendritic cells (MDDCs) were generated by culturing monocytes in the presence of GM-CSF and IL-4 for 6 days. **(A)** Shown are the expressions of CD14 and CD16 on total monocytes before sort and the purity of monocyte subsets after sort. **(B)** The expression of CD14, CD16, CD1c and HLA-DR was analyzed on $CD16^+$ and $CD16^-$ MDDCs. Results in **A-B** are from one donor representative of results generated with cells from >10 donors. **(C)** The morphology of $CD16^+$ and $CD16^-$ MDDCs was visualized by confocal microscopy upon staining with CD1a (a DC marker), phalloidin (an active stain) and DAPI (a nuclear dye). Results in **C** are from one donor representative of results generated with cells from three different donors. **(D)** MDDC subsets were exposed to the R5 NL4.3BaL HIV-1 strain (10 ng HIV-p24/106 MDDCs) for 3h, the unbound HIV was removed, and MDDCs were co-cultured with autologous resting $CD4^+$ T-cells (MDDC: T-cell ratio 1:4). Co-cultured were stimulated or not with *E. coli* LPS (100 ng/ml). Shown are HIV-p24 levels quantified by ELISA in cell culture supernatants collected at days 3-14 post-infections. Results in **D** are from one donor representative of results generated with cells from three different donors.

Figure 2: Both $CD16^+$ and $CD16^-$ MDDCs transmit HIV infection to activated $CD4^+$ T-cells. The experimental flow chart is illustrated in panel **A**. Briefly, the $CD16^+$ and $CD16^-$ MDDC subsets

were exposed to HIV for 3h as in Figure 1D and cultured alone for 3 days in the presence of GM-CSF and IL-4 or immediately co-cultured with autologous activated $CD4^+$ T-cells (MDDC: T-cell ratio 1:4). **(B)** Shown are levels of HIV-DNA integration in MDDCs measured by real-time nested PCR. In parallel, HIV-exposed MDDC subsets were co-cultured with autologous $CD4^+$ T-cells that were previously stimulated with CD3/CD28 Abs. **(C)** Shown are HIV-p24 levels measured by ELISA in cell culture supernatants harvested at days 3-15 post-infection. Results in B-C are generated with cells from four different donors.

Figure 3: Differential gene expression in immature $CD16^+$ and $CD16^-$ MDDCs. Total RNA was extracted from immature MDDC subsets and a genome-wide analysis of gene expression was performed using the Affymetrix technology. **(A)** Shown are top regulated genes in $CD16^+$ *versus* $CD16^-$ MDDCs based on a fold change cut-off of 1.3 and adjusted p-values (adj. p) <0.05. Top canonical pathways (C2) **(B)** and biological processes (C5) **(C)** differentially expressed in $CD16^+$ *versus* $CD16^-$ MDDCs identified based on Gene Set Variation Analysis (GSVA) are illustrated. Results in **A-C** were generated with cells from five different donors indicated with different color codes.

Figure 4: Gene Ontology classification of differentially expressed genes in immature $CD16^+$ and $CD16^-$ MDDCs. Differentially expressed genes in $CD16^+$ (blue) *versus* $CD16^-$ (green) MDDCs exposed to Media (immature) ($p<0.05$ and FC cut-off 1.3) were classified using Gene Ontology in **(A)** transcription factors, **(B)** cytokines, adhesion, **(D)** chemotaxis, and **(E)** cell projections. Results were generated with cells from five different donors. Each heat map column represents data from a distinct donor.

Figure 5: Differential gene expression in CD16$^+$ and CD16$^-$ MDDCs exposed to LPS. Total RNA was extracted from MDDC subsets exposed to LPS for 24h and a genome-wide analysis of gene expression was performed using the Affymetrix technology. **(A-B)** Shown are top transcripts up regulated by LPS in CD16$^+$ and CD16$^-$ MDDCs, identified based on a fold change cut-off of 1.3 and adjusted p-values (adj. p) <0.05. **(C)** Shown are top differentially regulated genes in immature (medium) and mature (LPS) CD16$^+$ and CD16$^-$ MDDCs. **(D-E)** Differentially expressed genes in CD16$^+$ (blue) *versus* CD16$^-$ (green) MDDC subsets exposed to LPS (mature) ($p<0.05$ and FC cut-off 1.3) linked to the Gene Ontology terms chemotaxis and cytokines are illustrated. Heatmap cells are scaled by the expression level z-scores for each probe individually. Results in were generated with cells from five different donors identified with different color codes.

Figure 6: Differential gene expression in CD16$^+$ and CD16$^-$ MDDCs exposed to HIV. Total RNA was extracted from MDDC subsets exposed to HIV for 24h and a genome-wide analysis of gene expression was performed using the Affymetrix technology. **(A-B)** Shown are top transcripts up regulated by HIV in CD16$^+$ and CD16$^-$ MDDCs, identified based on a fold change cut-off of 1.3 and adjusted p-values (adj. p) <0.05. **(C)** Shown are top differentially regulated genes in immature (medium) and HIV exposed CD16$^+$ and CD16$^-$ MDDCs. **(D)** Differentially expressed genes in CD16$^+$ (blue) *versus* CD16$^-$ (green) MDDC subsets exposed to HIV ($p<0.05$ and FC cut-off 1.3) linked to the Gene Ontology terms exosomes are illustrated. Heatmap cells are scaled by the expression level z-scores for each probe individually. Results in were generated with cells from five different donors identified with different color codes.

Figure 7: Meta-analysis using the NCBI HIV interaction database for the identification of HIV-1 interactors enriched in immature CD16$^+$ *versus* CD16$^-$ MDDCs. Differentially expressed genes between CD16$^+$ (blue) *versus* CD16$^-$ (green) MDDCs exposed to Media (immature) ($p<0.05$, FC cut-off 1.3) were matched to the NCBI HIV interaction database for the identification of human genes coding for molecules known to interact with HIV-1 proteins **(A)** and to regulate expression of HIV proteins **(B)**. Shown are significant probes with the smallest p-value for each overlapping gene. Heatmap cells are scaled by the expression level z-scores for each probe individually.

Figure 8: CD16$^+$ and CD16$^-$ MDDCs exposed to media, LPS or HIV exhibit unique molecular signatures. Genome-wide transcriptional profiles were generated as described in Figure 1 for MDDCs subsets that were exposed to Media, E. coli LPS, or R5 NBaL HIV-1 for 24 hours. **(A)** Gene Set Enrichment Analysis (GSEA) allowed the identification of top regulated canonical pathways (C2) common as well as differentially expressed between CD16$^+$ *versus* CD16$^-$ MDDCs exposed to Media, LPS or HIV-1. **(B)** Shown are top regulated micro-RNAs (MIR) differentially expressed between CD16$^+$ *versus* CD16$^-$ MDDCs exposed to Media, LPS or HIV-1. Results in **A-B** were generated with cells from five different donors.

Figure 9: The CD16$^+$ and CD16$^-$ monocytes are precursors for unique MDDCs subsets. Shown is a synthesis of top differentially expressed genes in immature CD16$^+$ *versus* CD16$^-$ MDDCs, transcript coding for transcriptional factors, trafficking molecules, cytokines and other functional

markers. Illustrated are also the most significant transcriptional changes in $CD16^+$ and $CD16^-$ MDDCs upon LPS or HIV exposure.

Supplemental Figure Legends

Supplemental Figure 1: Purity of FACS isolated monocyte subsets. Total monocytes were isolated by negative selection using magnetic beads (Miltenyi). Cells were stained with a cocktail of Abs against lineage markers (CD3, CD8, CD19, CD56) and CD16 Abs. A viability dye (Molecular Probes® LIVE/DEAD® Fixable Dead Cell Stain Kits, Invitrogen) was used to exclude dead cells. Viable lineage$^-$ CD16$^+$ and CD16$^-$ monocytes were isolated by flow cytometry under low sorting pressure. Shown are the expressions of CD16 on total monocytes before sort **(A)** and the purity of CD16$^+$ and CD16$^-$ monocytes after sorting **(B)**. Results are from one donor, representative of results obtained with cells from >5 different donors.

Supplemental Figure 2: CD16 Abs do not alter the immunogenic potential of MDDCs. Total monocytes were stained or not with CD16 Abs, differentiated into MDDC by culture in RPMI media containing FBS (2%), and GM-CSF and IL-4 (20 ng/ml) for six days. The generated MDDC subsets were exposed or not to HIV-1 NL4.3BaL (10 ng/10E6 cells) for 3h at 37 ºC, and subsequently co-cultured for 5 days with autologous CFSE-loaded CD4$^+$ T-cells at a MDDC: T ratio 1:4 in the presence or absence of antigens (SEB, CMV or *S. aureus*). (**A**) Shown is the gating strategy to determine the proliferative capacity of T-cells in response to an antigen (proliferating cells were identified as CFSE^{low}). **(B)** Shown is the frequency of T-cells proliferating in response to SEB, CMV and *S. aureus* at day 5 post co-culture for MDDCs generated from monocytes exposed or not to CD16. Results generated are on matched samples from five different donors.

Supplemental Figure 3: CD16 Abs do not alter the HIV *trans* infection potential of MDDCs. Total monocytes stained or not with CD16 Abs were differentiated into MDDC and exposed or not

to HIV-1 NL4.3BaL (10 ng/10E6 cells) for 3h at 37 ºC. MDDCs were subsequently co-cultured with autologous CFSE-loaded $CD4^+$ T-cells at a MDDC: T ratio 1:4 in the presence or absence of antigens (SEB, CMV or *S.aureus*) for 5 days. The ability to proliferate ($CFSE^{low}$) and express HIV-p24 was analyzed. (**A**) The expression of HIV-p24 was measured in cells proliferating to antigens. **(B)** Shown is the frequency of HIV p24-expressing T-cells proliferating in response to SEB, CMV and *S. aureus* day 5 post co-culture for MDDCs generated from monocytes exposed or not to CD16 Abs. Results generated are on matched samples from five different donors.

Supplemental Figure 4: Both $CD16^+$ and $CD16^-$ MDDCs express classical immature and mature DC markers. Peripheral blood $CD16^+$ and $CD16^-$ monocytes were differentiated into immature MDDCs and then mature MDDCs upon exposure to LPS for 48h. Shown is the expression of CD14, CD1a, CD1c, DC-SIGN, CD83 and CCR7 on immature MDDCs **(A)** and mature MDDCs **(B)**. Results are from one donor representative of results generated with cells from three different donors.

Supplemental Figure 5: Immature $CD16^+$ MDDCs are a major source of CCL2, CCL22 and CCL24. Levels of CCL2, CCL22, CCL24 and TNF-α were measured by ELISA in cell culture supernatants from immature $CD16^+$ and $CD16^-$ MDDCs collected at day 6 of differentiation. Results (mean±SD triplicate wells) are from one donor representative of results generated with cells from three different donors.

Supplemental Figure 6: Transcriptional differences between $CD16^+$ *versus* $CD16^-$ MDDCs. $CD16^+$ and $CD16^-$ MDDCs were exposed to media, LPS or HIV for 24h. RNA was extracted and a genome-wide transcriptional analysis was performed using the Affymetrix technology. Shown are the numbers of genes differentially expressed in $CD16^+$ *versus* $CD16^-$ MDDCs upon exposure to media, LPS or HIV identified based on p-values and Benjamini Hochberg (BH) p-values (or false discovery rate, FDR, adjusted p-values). Results are generated with matched $CD16^+$ and $CD16^-$ MDDCs from five different HIV-uninfected subjects.

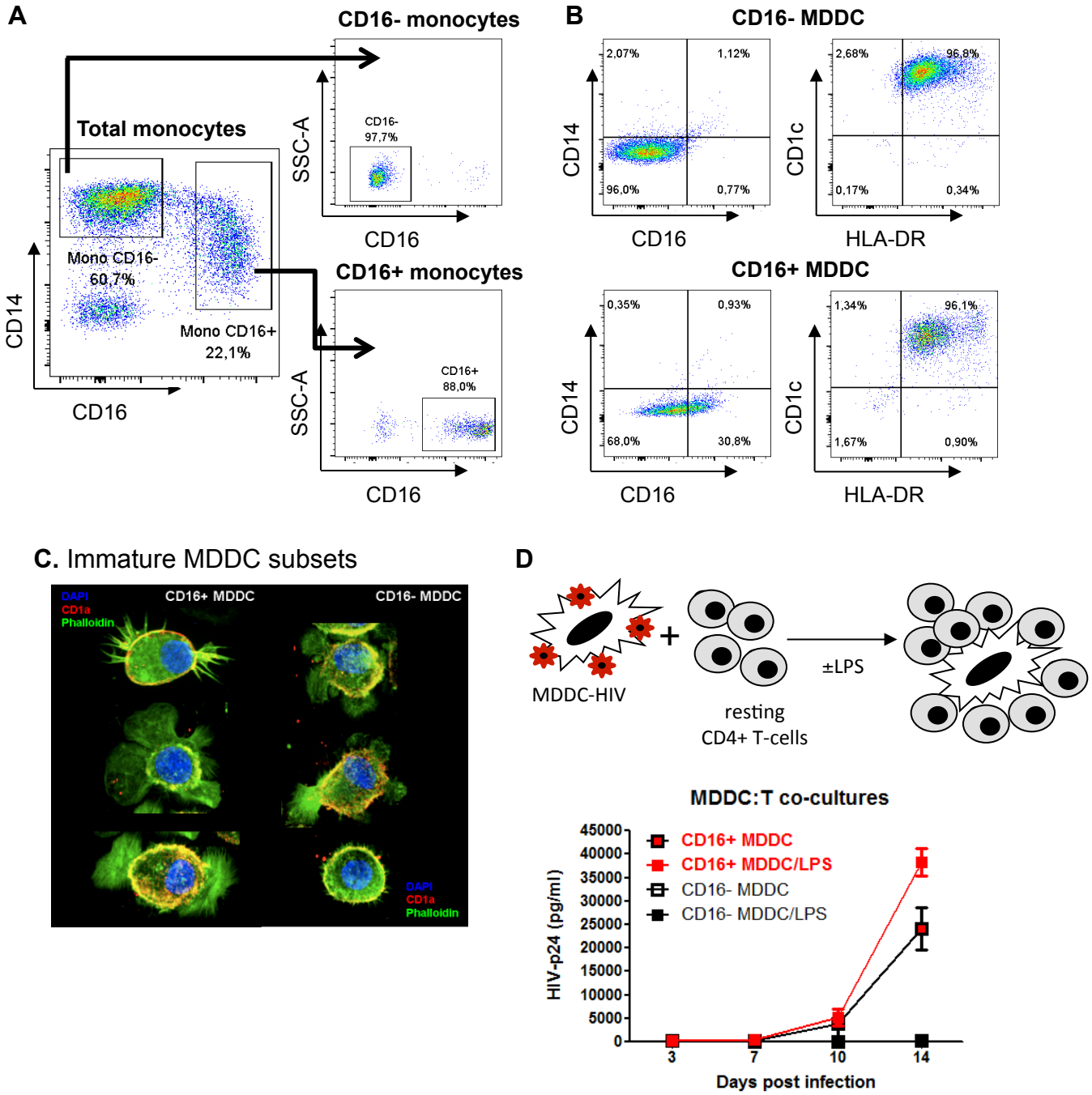

Wacleche *et al.* Figure 1

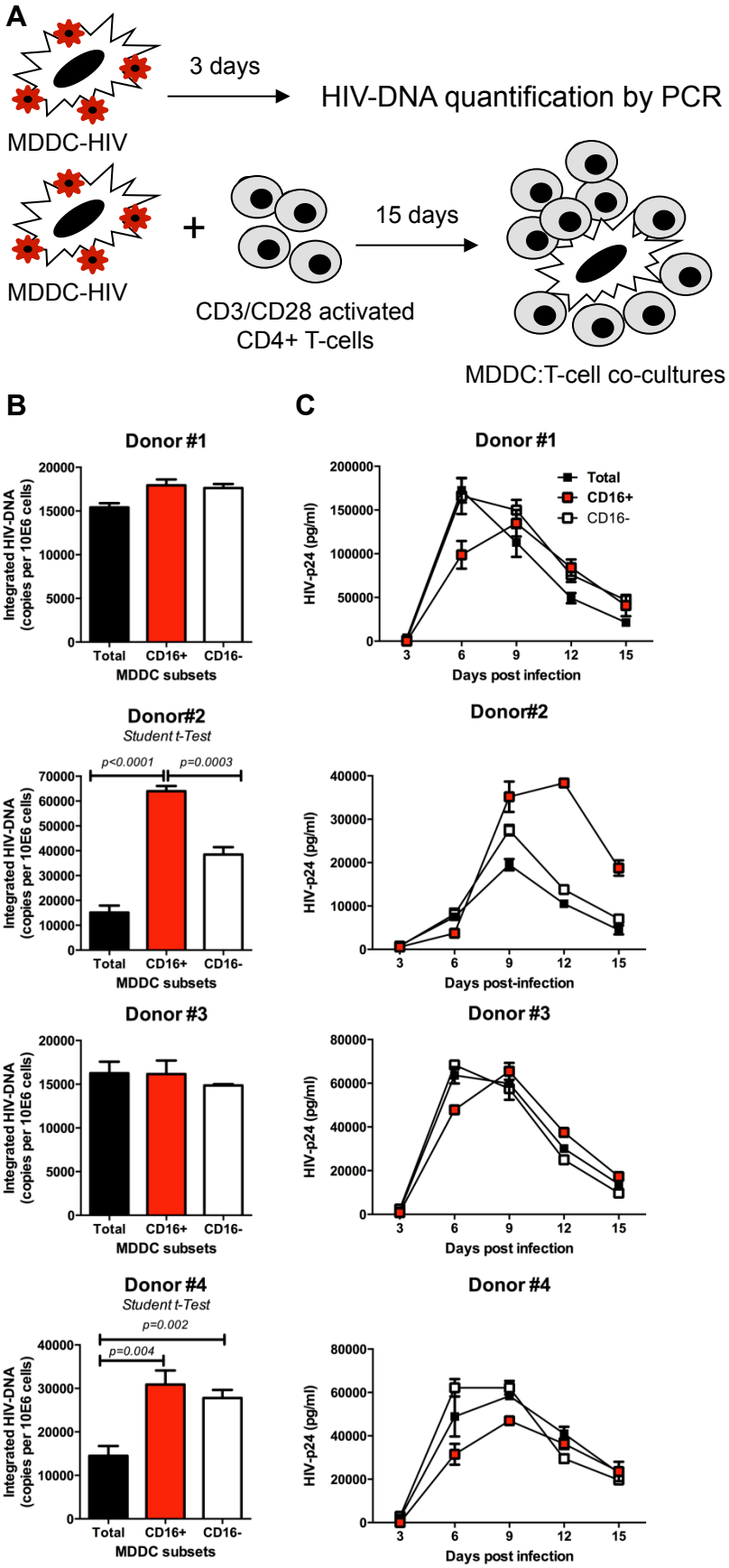

Wacleche *et al.* Figure 2

A. Top Modulated Genes

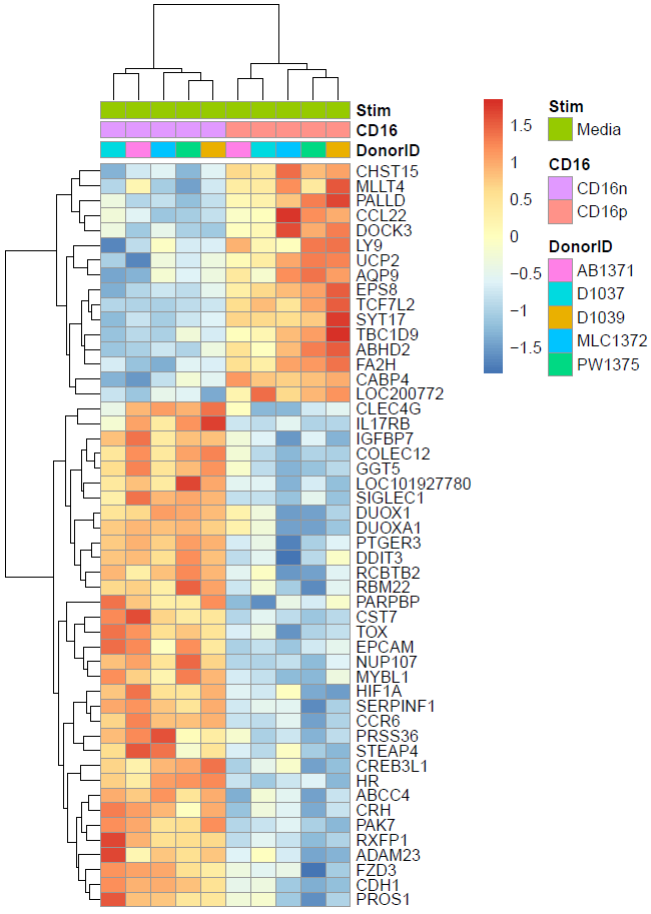

Wacleche *et al.* Figure 3

B. GSVA C2 Canonical pathways

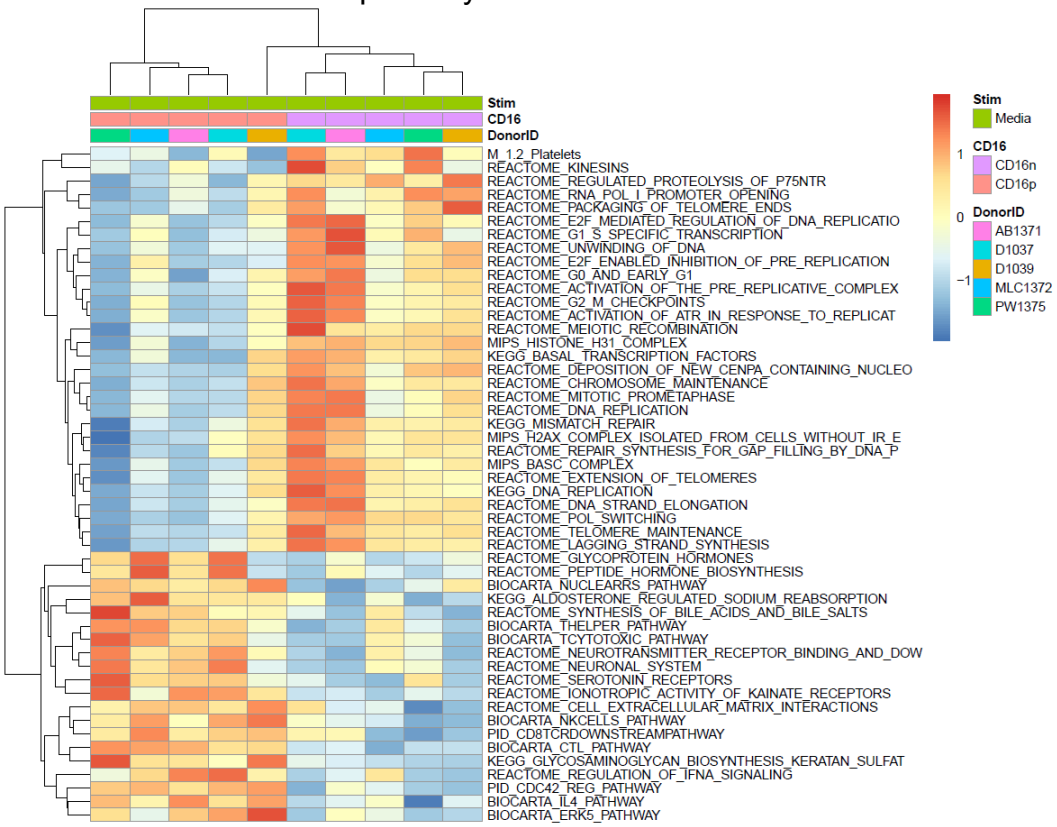

C. GSVA C5 Biological processes

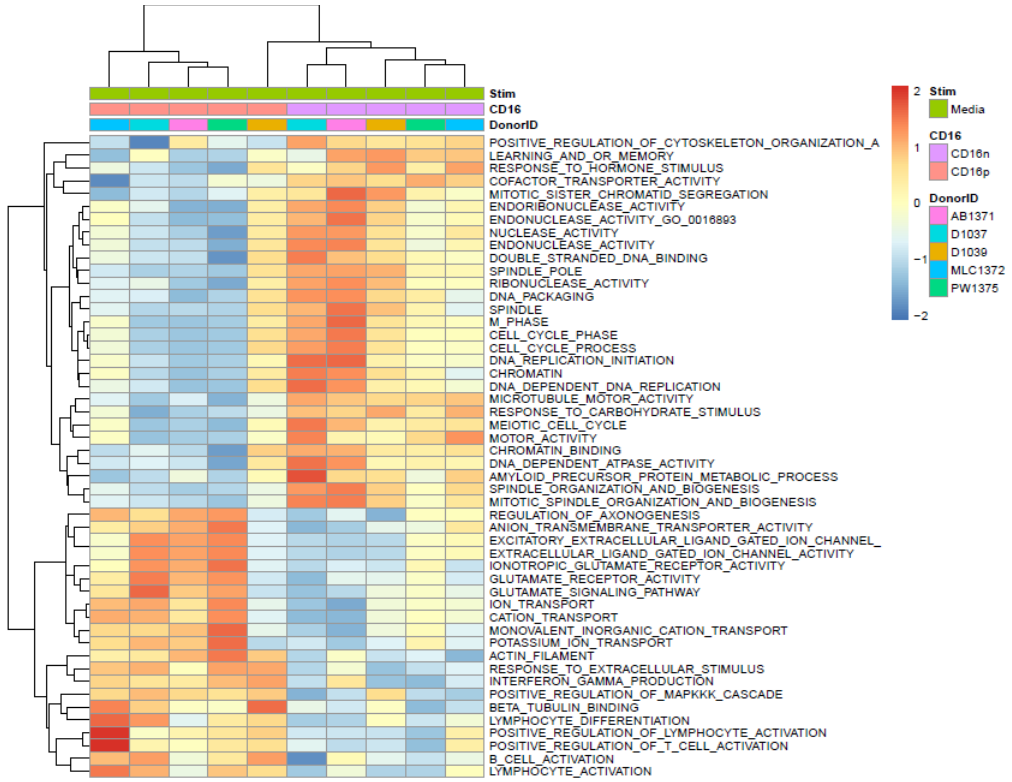

Wacleche *et al.* Figure 3 continued

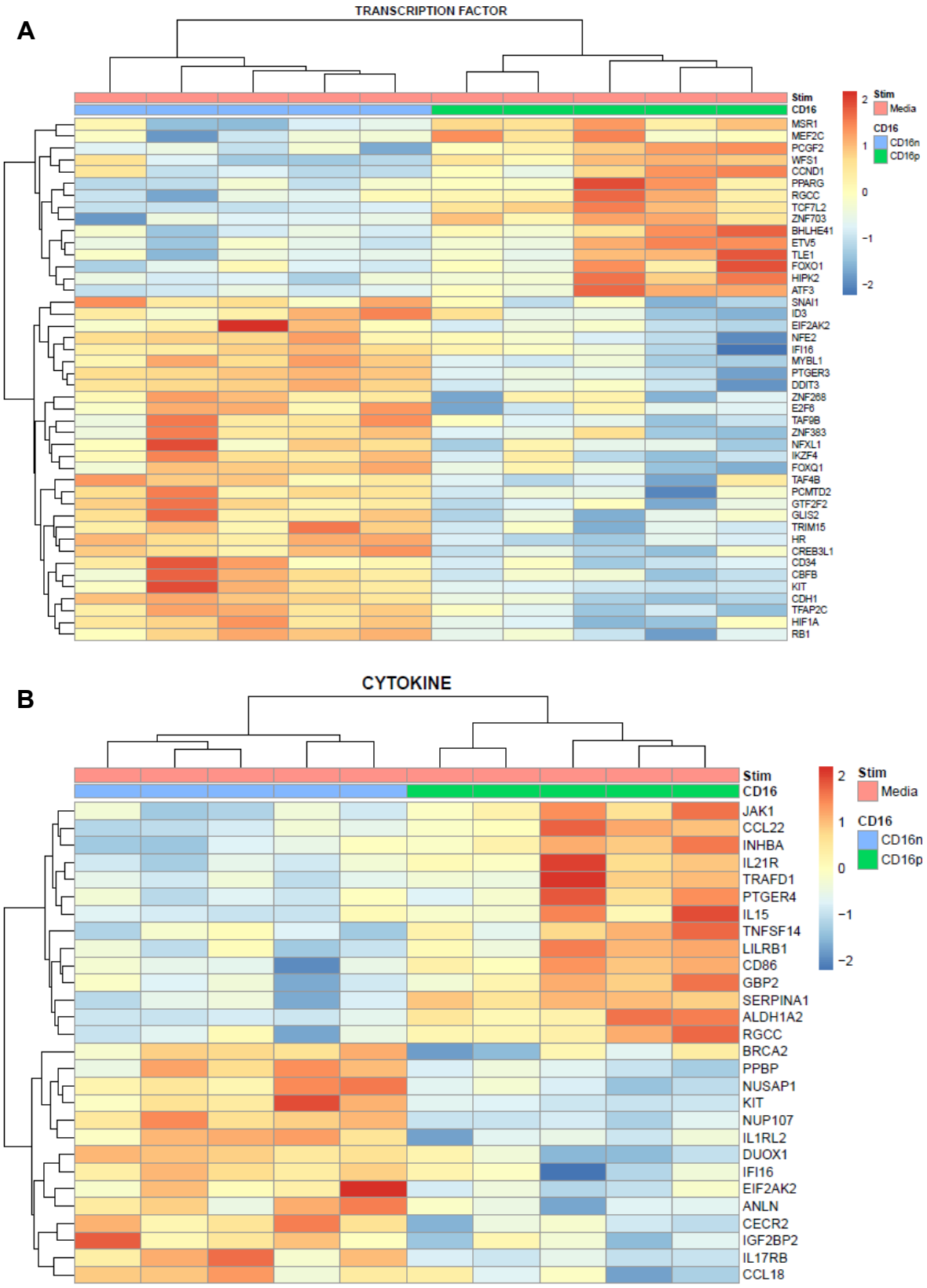

Wacleche *et al.* Figure 4

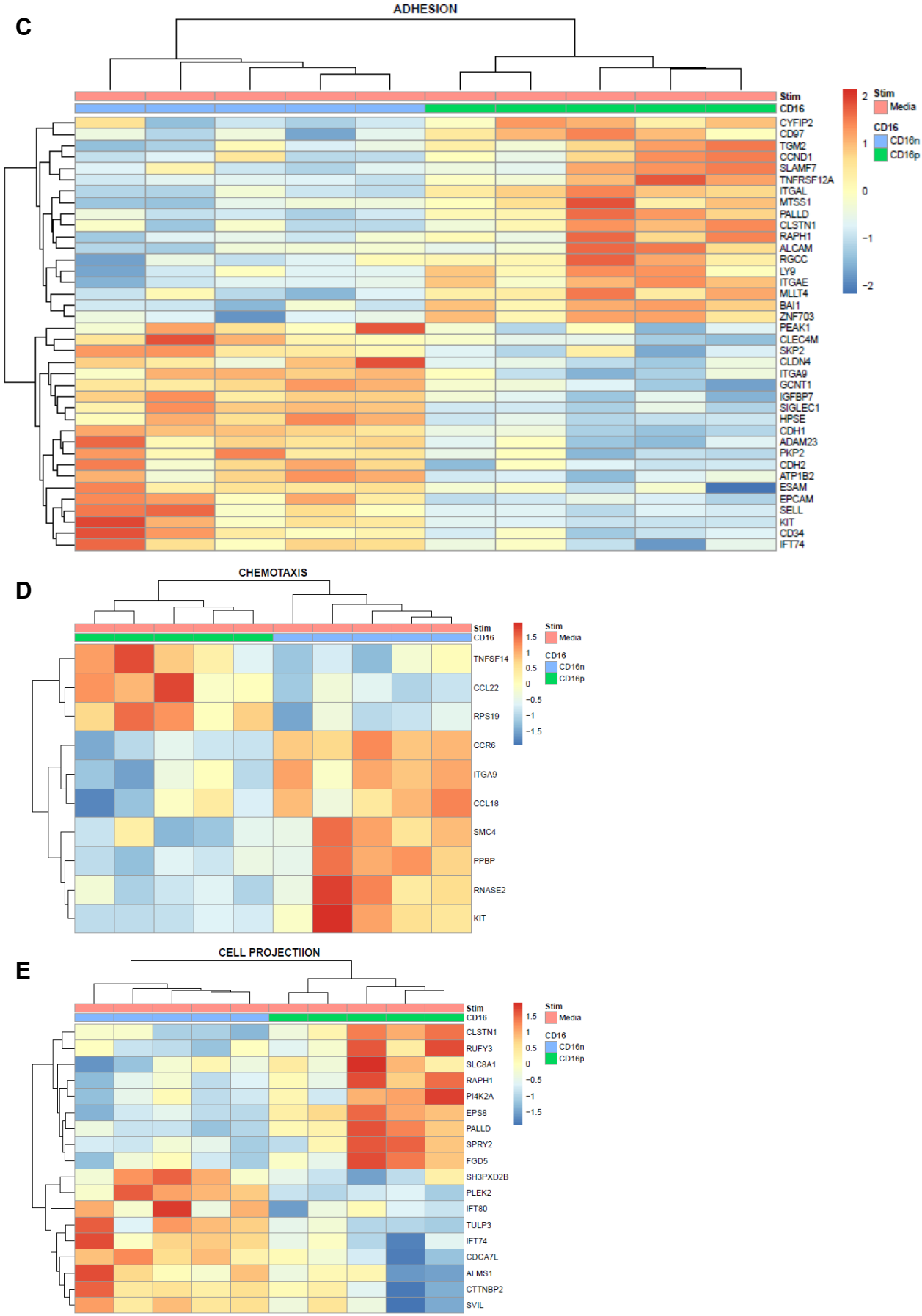

Wacleche *et al.* Figure 4 - continued

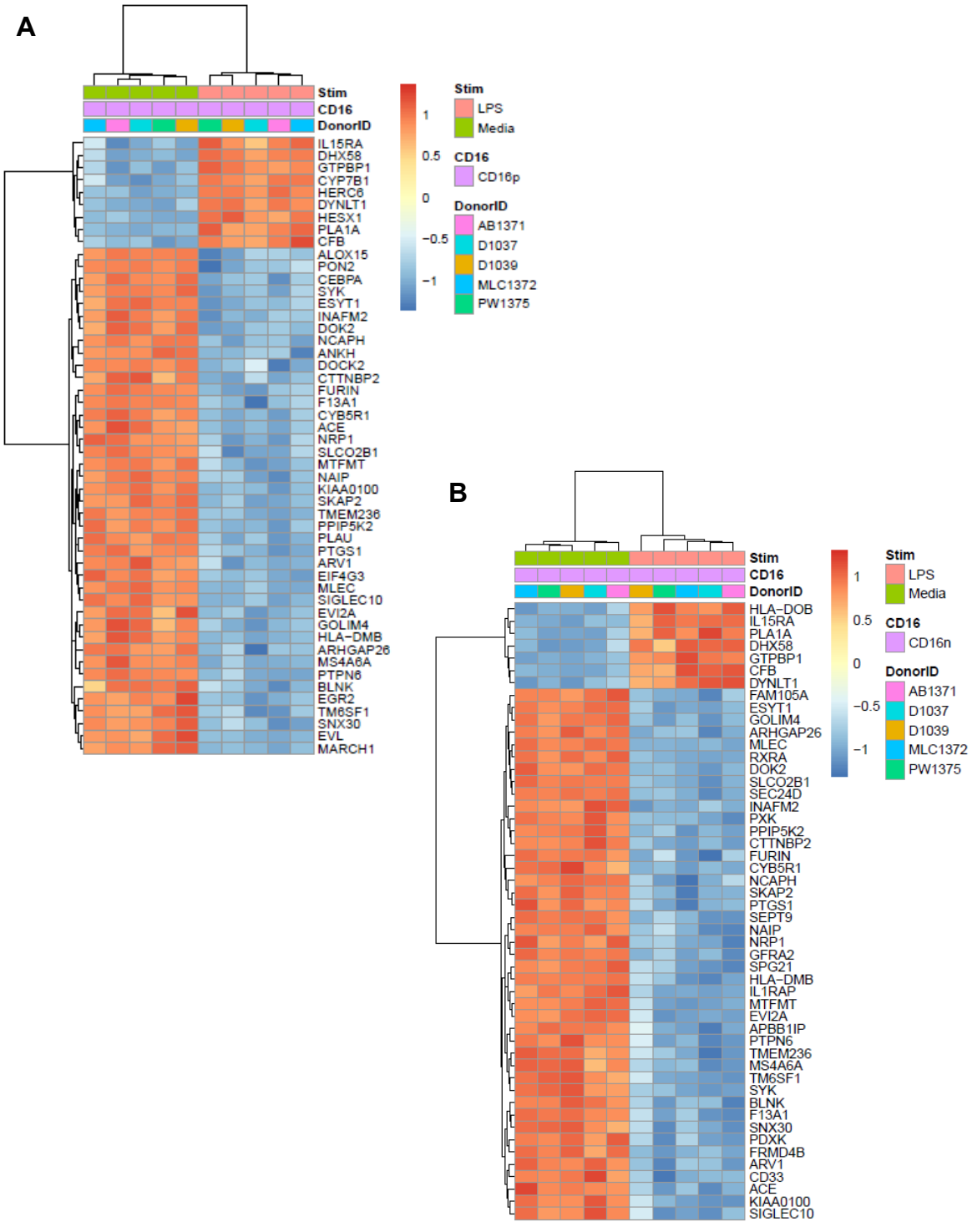

Wacleche *et al.* Figure 5

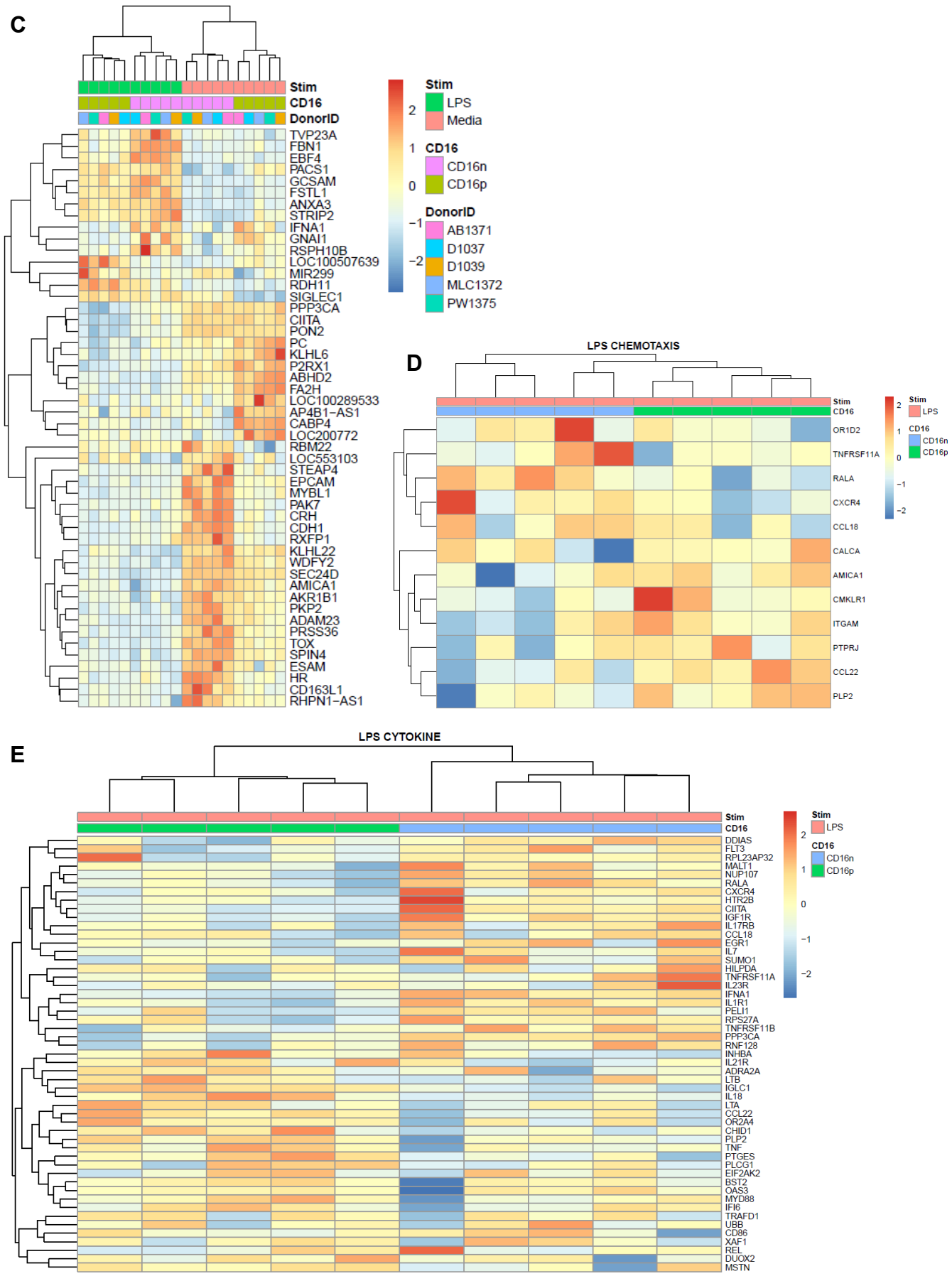

Wacleche *et al.* Figure 5 continued

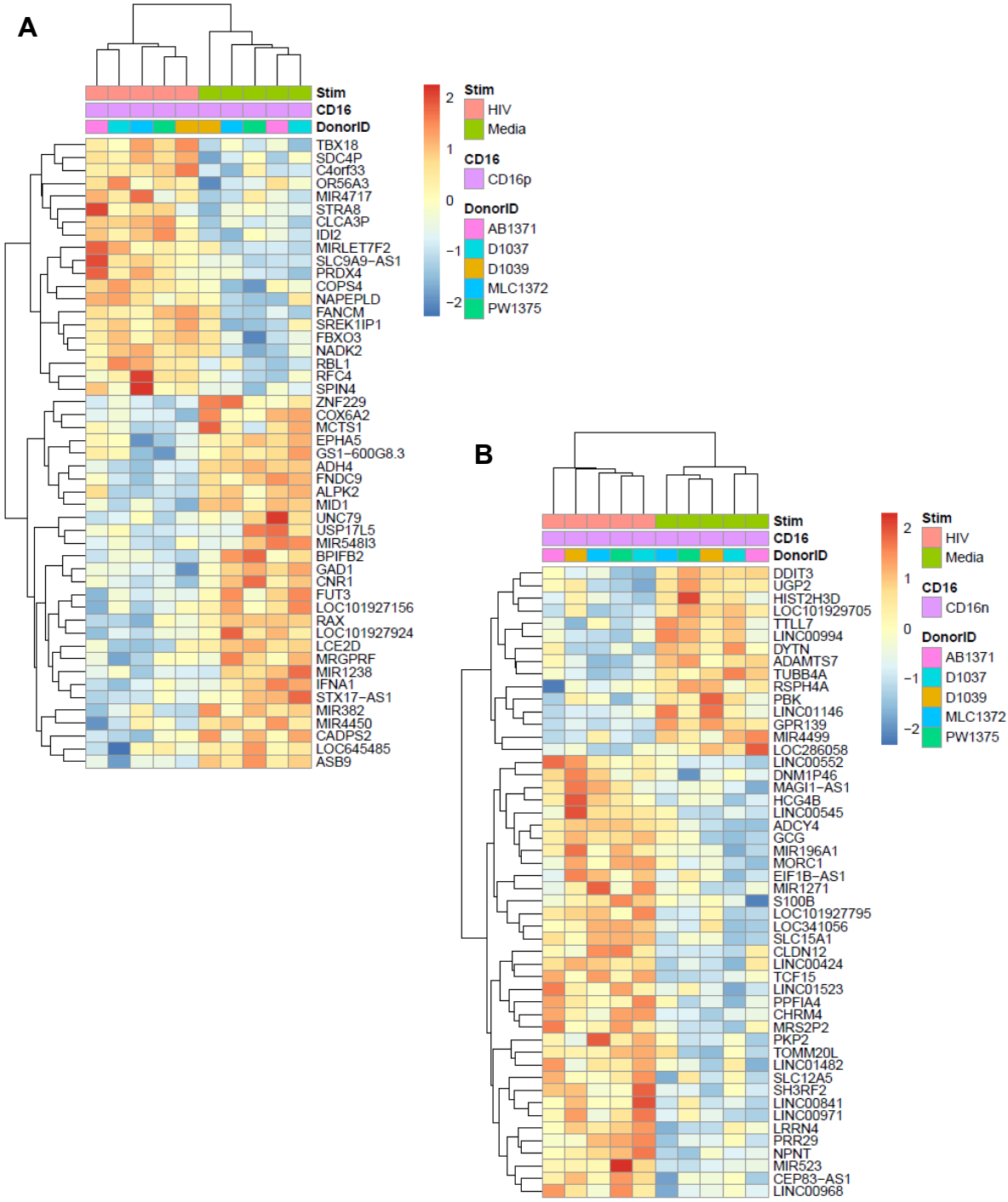

Wacleche *et al.* Figure 6

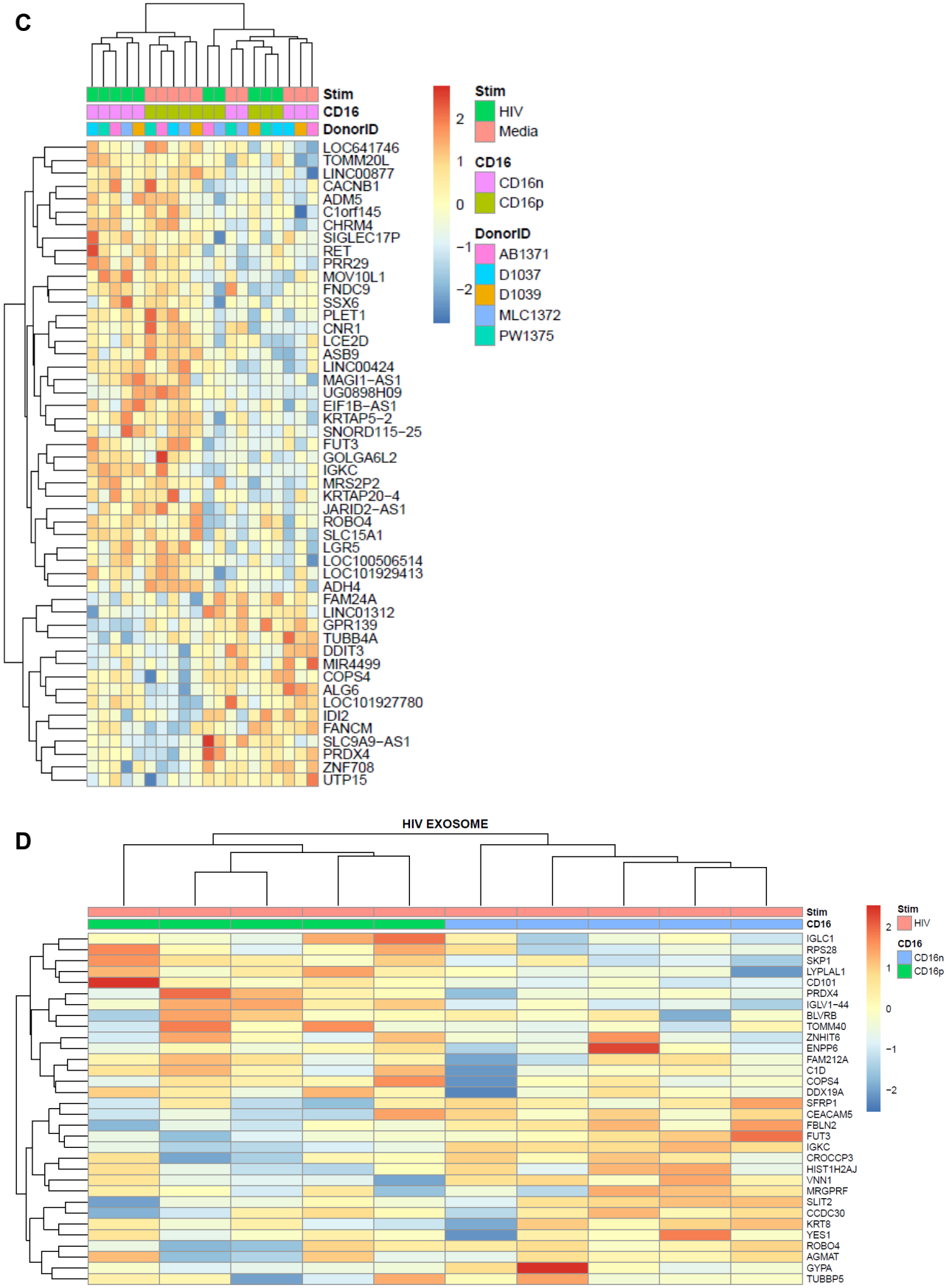

Wacleche *et al.* Figure 6, continued

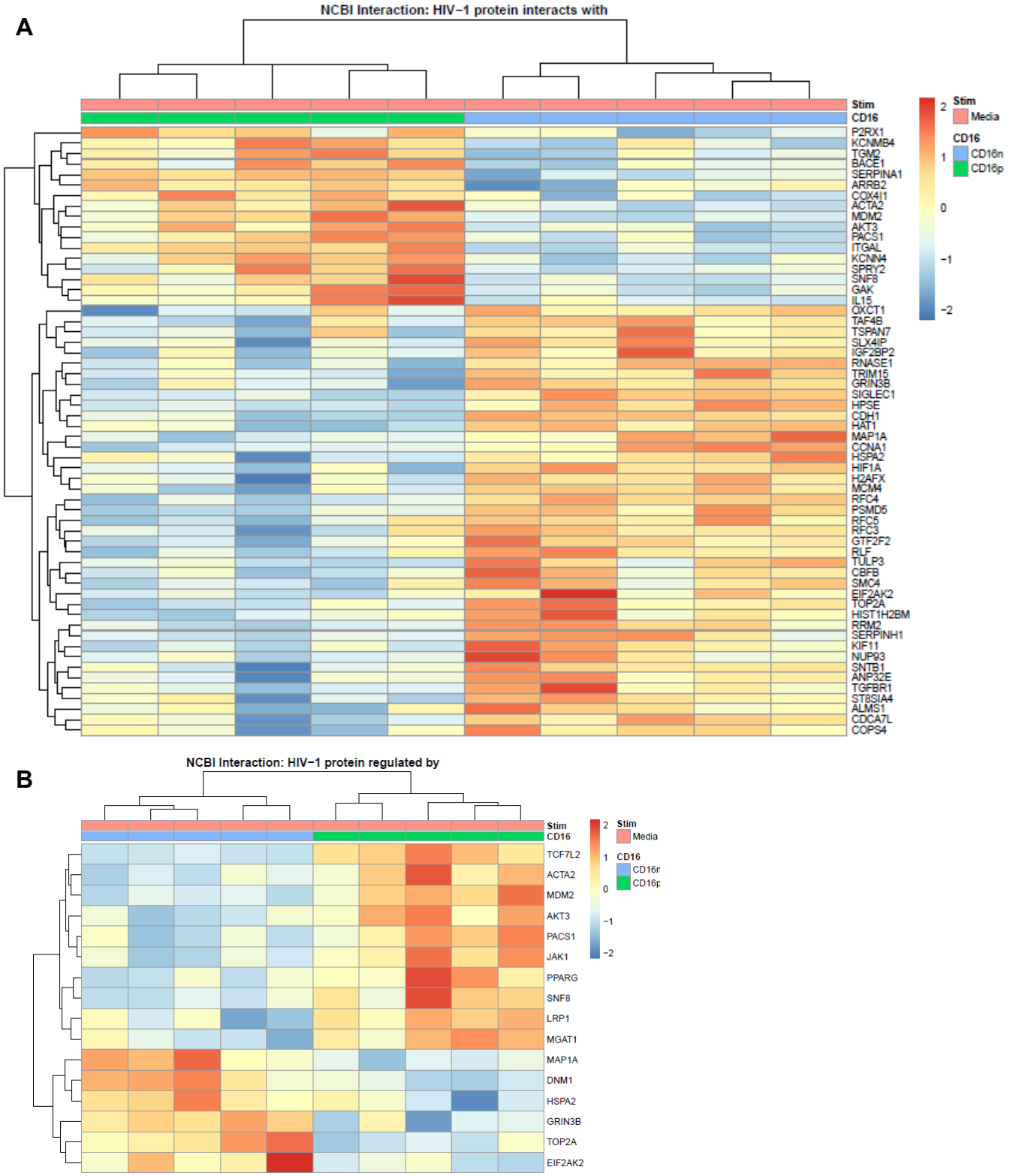

Wacleche *et al.* Figure 7

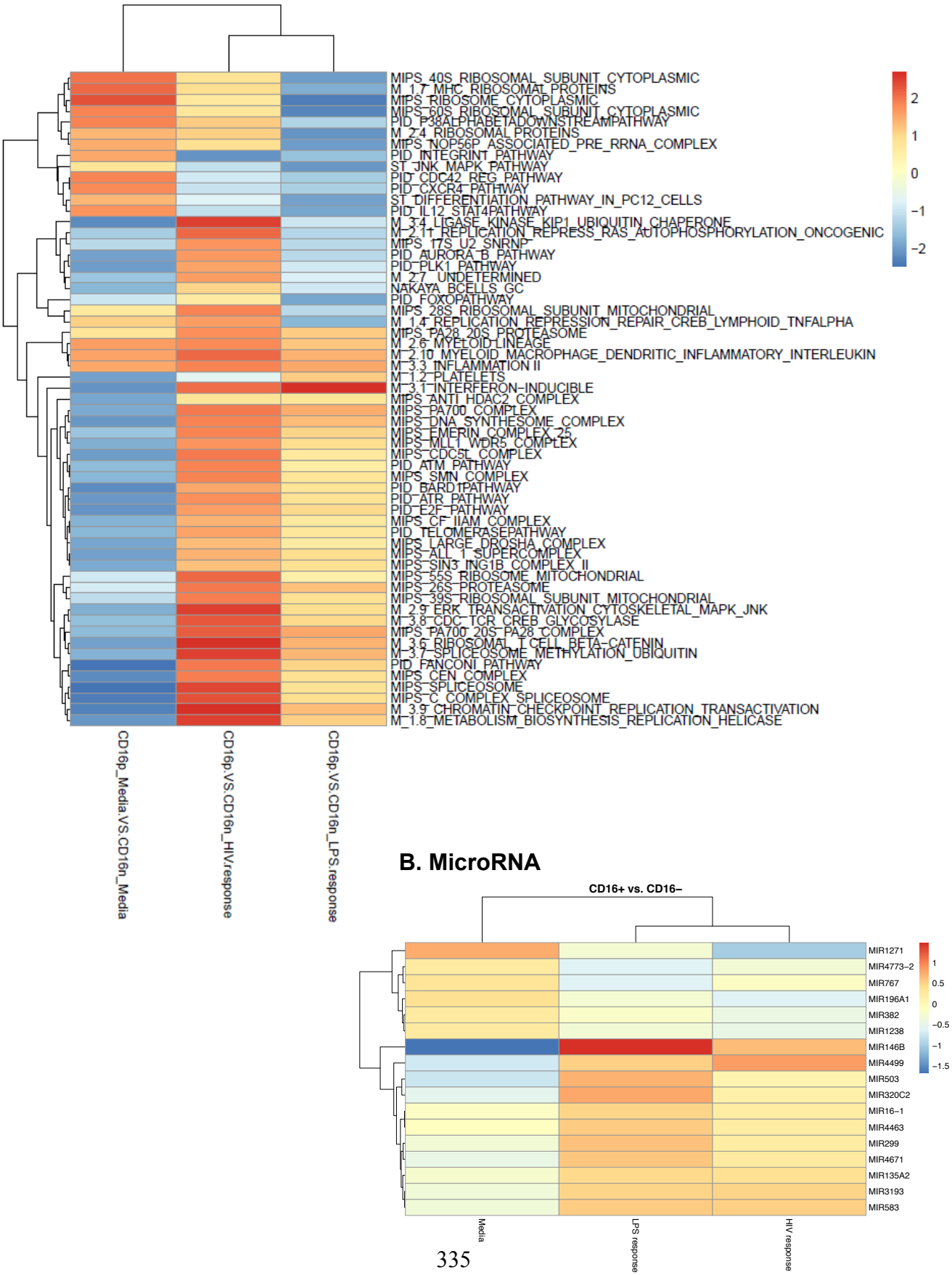

Wacleche *et al.* Figure 8

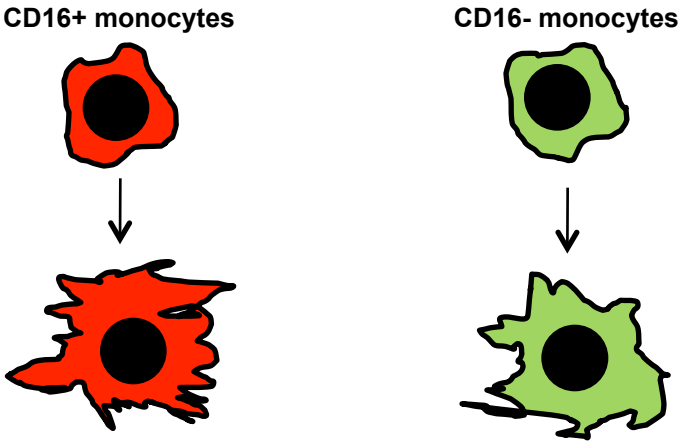

	CD16+ MDDC	CD16- MDDC
Transcription factors	TCF7L2, PPARG, FOXO1, ATF3	HIF1A
Surface markers	CD16, CD86, CD97, LY9,	CD34, c-kit, BRCA2
Adhesion molecules	ITGAL, ALCAM, ITGAE	CDH1, ITGA9, CDH2, SIGLEC1, EPCAM, SELL
Chemotaxis	CCL22	CCR6, CCL18, PPBP/CXCL7
Cytokines	IL-15	IL-7, IFNA1
Functional markers	ALDH1A2, JAK1, MGLL, FAH2, MTSS1, P2RX1	STEAP4, PAK7, TRIM15, TRIM10, IFI16, S100B, MPO, DUOX1, DUOXA1
HIV interactors	P2RX1, MDM2, ITGAL, IL-15, TCF7L2, ACTA2, PACS1, JAK1, and PPARG	TRIM15, SIGLEC1, CDH1, HIF1A, NUP93
LPS response	CCL8, SIGLEC1, MIR4439, SCIN, IL-7R, PLTP, TNF, CFP, CLU, C2, MIR331, MAP3K8, SNX10, CXCL1, IL-18, P2RY8	MMP10, MMP1, TGM2, IL1A, TNFRSF11A, LAMP1, MMP8, ALDH1L2, TREM1, MALT1, ALCAM, PPARG, CXCL6, IL6ST, IL23A, S100A3
HIV response	IFI6, MIR568, MIR4718, CD101, MIR4717, ZNF714, ZNF429	MIR1271, MIR516A2, MIR3911, PKP2, MIR196A1, S100B

Wacleche *et al.* Figure 9

A. Phenotype before FACS sort

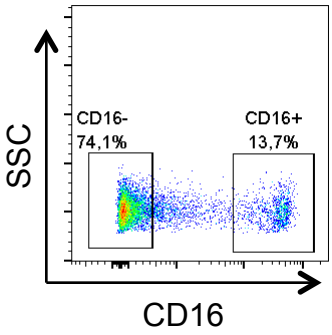

Total monocytes

B. Quality control after FACS sort

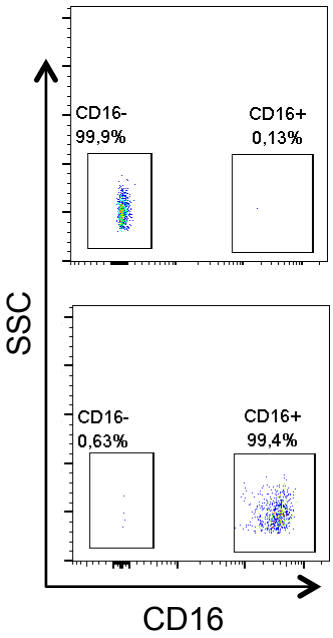

CD16- monocytes

CD16+ monocytes

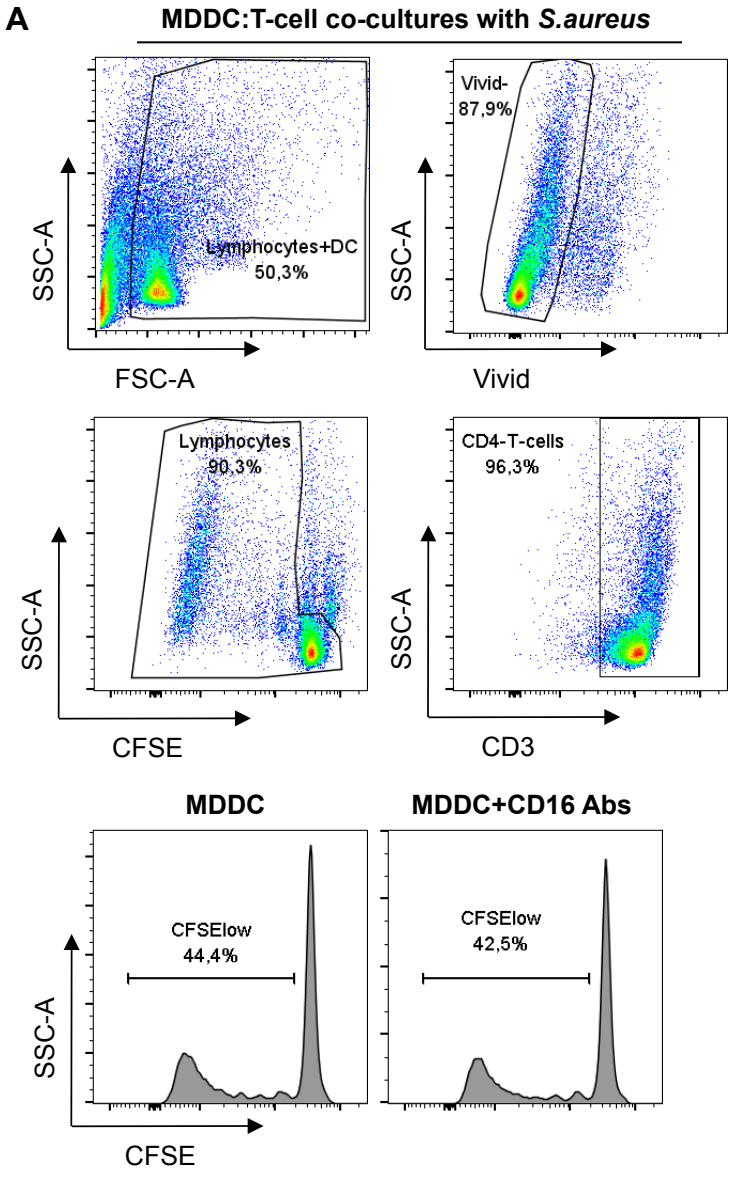

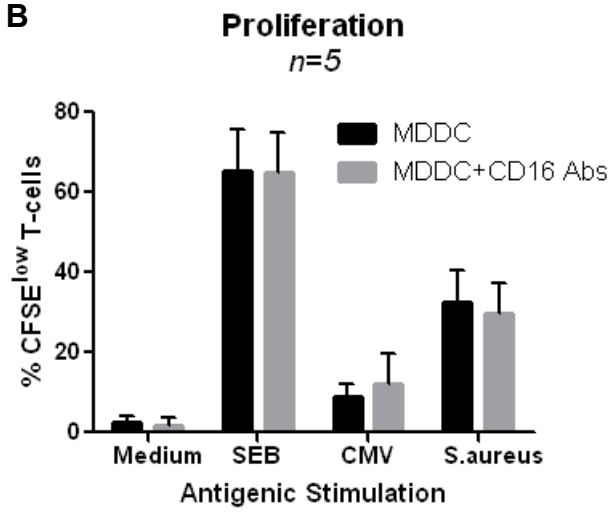

Wacleche *et al.* Supplemental Figure 2

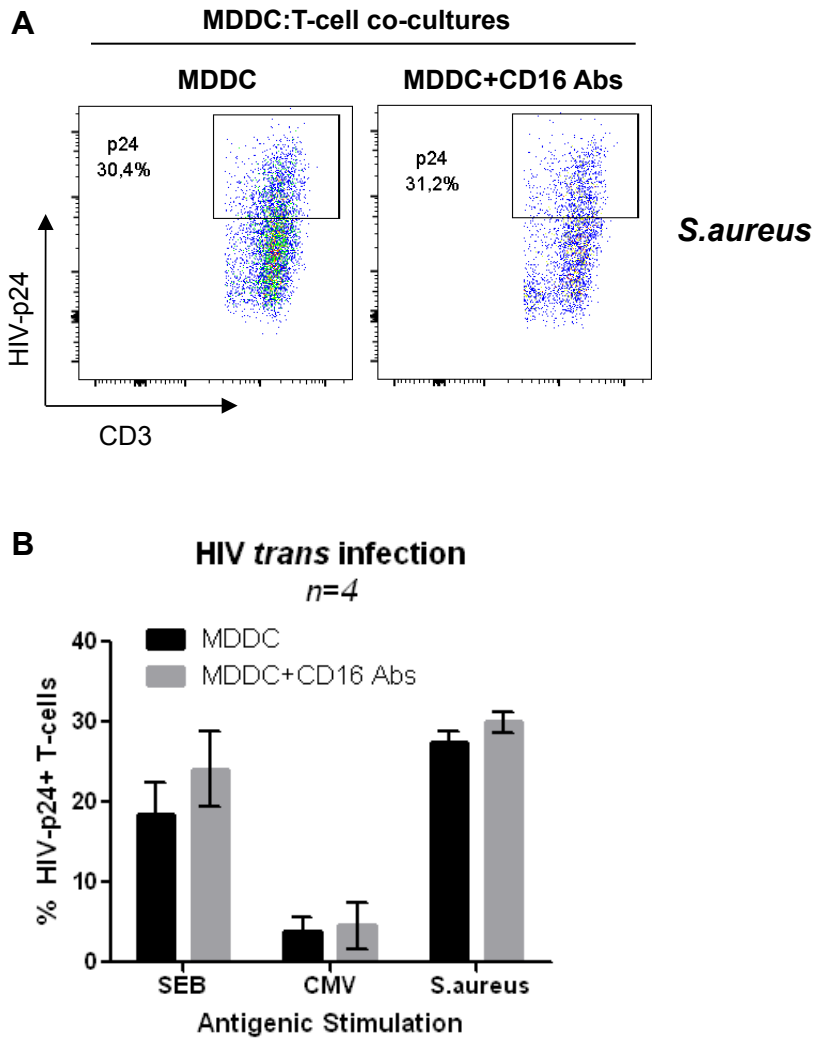

Wacleche *et al.* Supplemental Figure 3

A. Immature MDDC

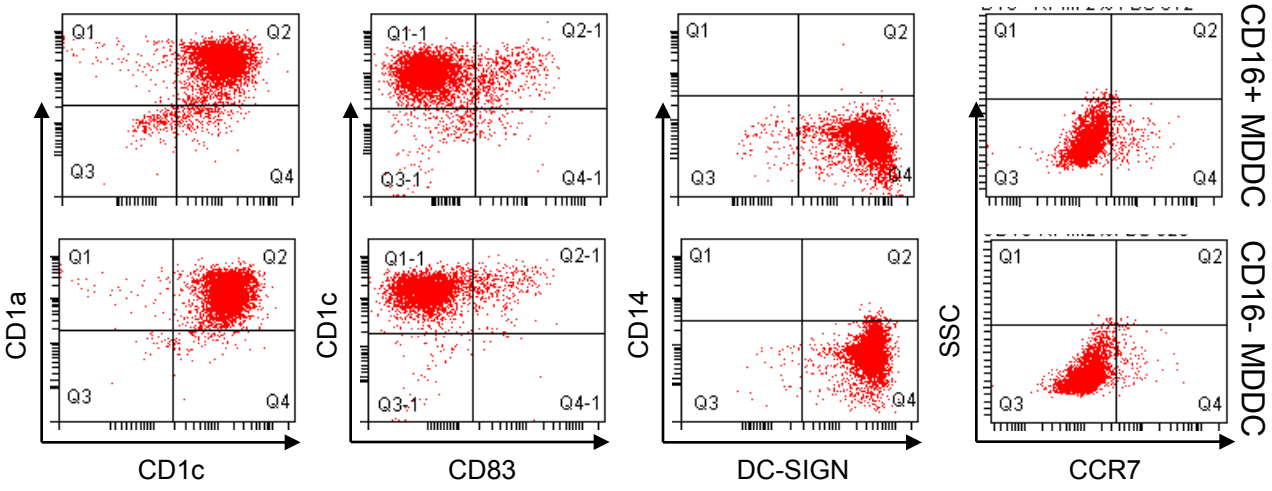

B. Mature MDDC

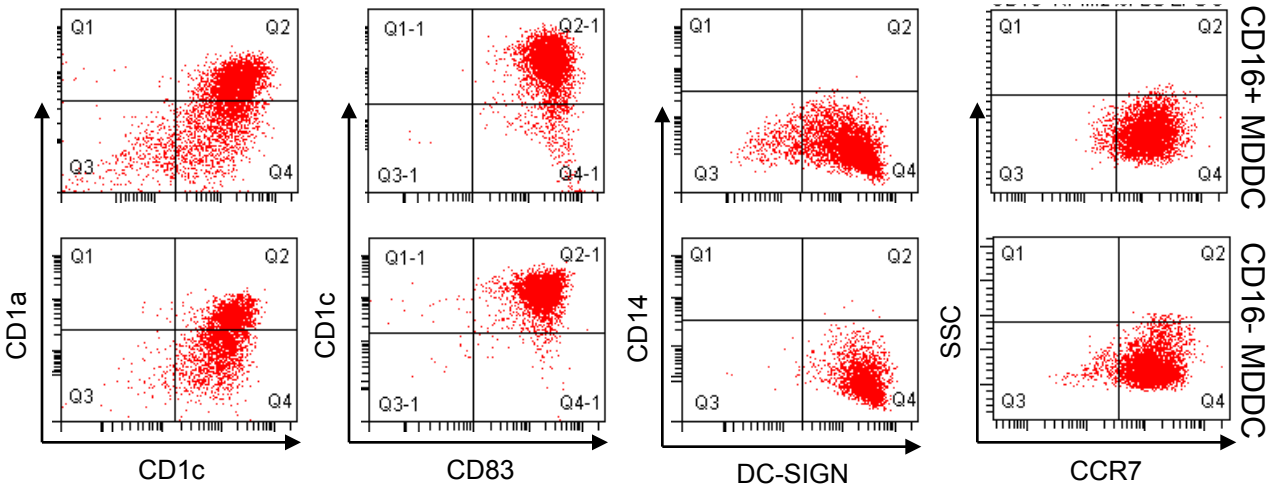

Wacleche *et al.* Suppl. Figure 4

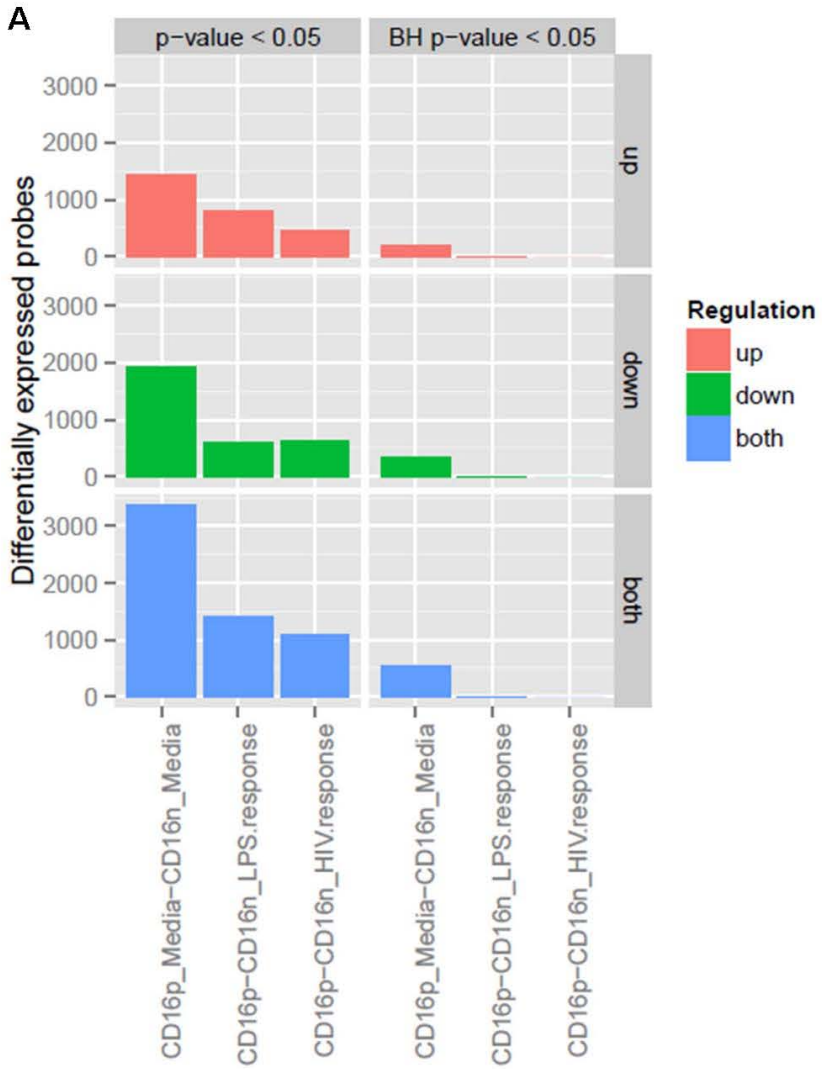

Wacleche *et al.* Suppl Figure 6

Suppl. Table 1: Up regulated genes in CD16+ *versus* CD16-MDDC

Symbol	adj. p	FC	description
AQP9	0,001345084	4,63	aquaporin 9
DCSTAMP	0,020286374	3,93	dendrocyte expressed seven transmembrane protein
TGM2	0,028211439	3,09	transglutaminase 2
CH25H	0,034619967	3,07	cholesterol 25-hydroxylase
TCF7L2	3,34E-07	3,05	transcription factor 7-like 2 (T-cell specific, HMG-box)
LILRB1	0,036864756	2,98	leukocyte immunoglobulin-like receptor, subfamily B (with TM and ITIM domains), member 1
RGCC	0,021578042	2,83	regulator of cell cycle
CHST15	0,000199888	2,75	carbohydrate (N-acetylgalactosamine 4-sulfate 6-O) sulfotransferase 15
ALDH1A2	0,004504132	2,70	aldehyde dehydrogenase 1 family, member A2
LRP1	0,00404557	2,57	low density lipoprotein receptor-related protein 1
GBP4	0,032916924	2,55	guanylate binding protein 4
GIMAP4	0,020906716	2,53	GTPase, IMAP family member 4
LPL	0,003332613	2,51	lipoprotein lipase
CCND2	0,021343315	2,50	cyclin D2
SLAMF7	0,032922542	2,46	SLAM family member 7
EPS8	9,94E-06	2,38	epidermal growth factor receptor pathway substrate 8
INHBA	0,005886239	2,34	inhibin, beta A
IL21R	0,003557576	2,32	interleukin 21 receptor
SCIMP	0,041179995	2,30	SLP adaptor and CSK interacting membrane protein
GPC4	0,009520189	2,27	glypican 4
TIMP3	0,014365449	2,24	TIMP metallopeptidase inhibitor 3
SASH1	0,006627678	2,24	SAM and SH3 domain containing 1
FAM20A	0,005999118	2,24	family with sequence similarity 20, member A
PIK3AP1	0,022387659	2,22	phosphoinositide-3-kinase adaptor protein 1
ITGAL	0,003432854	2,20	integrin, alpha L (antigen CD11A (p180), lymphocyte function-associated antigen 1; alpha polypeptide)
ABHD2	0,000179965	2,16	abhydrolase domain containing 2
SETBP1	0,006424162	2,15	SET binding protein 1

C1orf162	0,028319964	2,15	chromosome 1 open reading frame 162
DOCK3	0,000226732	2,09	dedicator of cytokinesis 3
LOC100507639	0,012768831	2,06	uncharacterized LOC100507639
SYT17	0,000981734	2,05	synaptotagmin XVII
SEL1L3	0,042374321	2,04	sel-1 suppressor of lin-12-like 3 (C. elegans)
PPARG	0,016111031	2,03	peroxisome proliferator-activated receptor gamma
FGD5	0,042374321	2,02	FYVE, RhoGEF and PH domain containing 5
MSR1	0,007283765	2,00	macrophage scavenger receptor 1
GALNT12	0,020574533	1,99	polypeptide N-acetylgalactosaminyltransferase 12
MLLT4	0,001235784	1,99	myeloid/lymphoid or mixed-lineage leukemia (trithorax homolog, Drosophila); translocated to, 4
LY9	0,000844131	1,98	lymphocyte antigen 9
IL15	0,040047509	1,98	interleukin 15
GCH1	0,004766439	1,97	GTP cyclohydrolase 1
TREM2	0,020299151	1,97	triggering receptor expressed on myeloid cells 2
OCSTAMP	0,014217266	1,94	osteoclast stimulatory transmembrane protein
SPRY2	0,019516901	1,91	sprouty homolog 2 (Drosophila)
CLEC19A	0,049290329	1,88	C-type lectin domain family 19, member A
LOC200772	4,46E-06	1,88	uncharacterized LOC200772
HEG1	0,022396076	1,87	heart development protein with EGF-like domains 1
FAR2	0,042362266	1,87	fatty acyl CoA reductase 2
ATF3	0,016735127	1,86	activating transcription factor 3
CCL22	0,000456819	1,86	chemokine (C-C motif) ligand 22
GBP2	0,005119835	1,84	guanylate binding protein 2, interferon-inducible
TBC1D9	0,001763953	1,83	TBC1 domain family, member 9 (with GRAM domain)
BCAT1	0,00929276	1,81	branched chain amino-acid transaminase 1, cytosolic
DHRS11	0,025314821	1,81	dehydrogenase/reductase (SDR family) member 11
DENND5A	0,003704764	1,80	DENN/MADD domain containing 5A
ETV5	0,022110824	1,80	ets variant 5
ITPKB	0,007283765	1,78	inositol-trisphosphate 3-kinase B

RAPH1	0,01446133	1,78	Ras association (RalGDS/AF-6) and pleckstrin homology domains 1
KCNN4	0,018925464	1,77	potassium intermediate/small conductance calcium-activated channel, subfamily N, member 4
PHLDA1	0,01544101	1,77	pleckstrin homology-like domain, family A, member 1
SLC8A1	0,042362266	1,76	solute carrier family 8 (sodium/calcium exchanger), member 1
ALCAM	0,049461456	1,75	activated leukocyte cell adhesion molecule
FA2H	0,001436212	1,75	fatty acid 2-hydroxylase
MGLL	0,046207314	1,74	monoglyceride lipase
MREG	0,013526454	1,73	melanoregulin
ROR1-AS1	0,041940432	1,71	ROR1 antisense RNA 1
BHLHE41	0,010636839	1,71	basic helix-loop-helix family, member e41
TLE1	0,032344918	1,71	transducin-like enhancer of split 1 (E(sp1) homolog, Drosophila)
PAG1	0,010636839	1,69	phosphoprotein membrane anchor with glycosphingolipid microdomains 1
SERPINA1	0,004504132	1,69	serpin peptidase inhibitor, clade A (alpha-1 antiproteinase, antitrypsin), member 1
CABP4	3,35E-05	1,68	calcium binding protein 4
MCOLN3	0,006424162	1,67	mucolipin 3
MEF2C	0,020299151	1,67	myocyte enhancer factor 2C
H6PD	0,00404557	1,65	hexose-6-phosphate dehydrogenase (glucose 1-dehydrogenase)
SLC7A7	0,02872293	1,64	solute carrier family 7 (amino acid transporter light chain, y+L system), member 7
CD86	0,00399585	1,62	CD86 molecule
NBEAL2	0,003432854	1,62	neurobeachin-like 2
ST3GAL1	0,014365449	1,60	ST3 beta-galactoside alpha-2,3-sialyltransferase 1
AKT3	0,00929276	1,58	v-akt murine thymoma viral oncogene homolog 3
SLC15A3	0,007899462	1,58	solute carrier family 15 (oligopeptide transporter), member 3
CHST11	0,010952307	1,58	carbohydrate (chondroitin 4) sulfotransferase 11
DOCK5	0,022477926	1,58	dedicator of cytokinesis 5
UCP2	0,001235784	1,58	uncoupling protein 2 (mitochondrial, proton carrier)
ACTA2	0,003743328	1,57	actin, alpha 2, smooth muscle, aorta
P2RX1	0,013526454	1,56	purinergic receptor P2X, ligand-gated ion channel, 1
EML4	0,028211439	1,55	echinoderm microtubule associated protein like 4

KIAA0513	0,034619967	1,55	KIAA0513
ITGAE	0,005886239	1,55	integrin, alpha E (antigen CD103, human mucosal lymphocyte antigen 1; alpha polypeptide)
ARAP2	0,002656371	1,54	ArfGAP with RhoGAP domain, ankyrin repeat and PH domain 2
UPP1	0,018925464	1,54	uridine phosphorylase 1
HIPK2	0,016111031	1,53	homeodomain interacting protein kinase 2
CYFIP2	0,032073993	1,53	cytoplasmic FMR1 interacting protein 2
TRAFD1	0,017252121	1,52	TRAF-type zinc finger domain containing 1
CD97	0,04029774	1,52	CD97 molecule
PTGER4	0,035188415	1,51	prostaglandin E receptor 4 (subtype EP4)
RUFY3	0,033109948	1,51	RUN and FYVE domain containing 3
DOCK8	0,003307121	1,50	dedicator of cytokinesis 8
LOC100289533	0,003619948	1,50	uncharacterized LOC100289533
GAL	0,036803238	1,49	galanin/GMAP prepropeptide
BAI1	0,010636839	1,49	brain-specific angiogenesis inhibitor 1
PALLD	0,00079014	1,49	palladin, cytoskeletal associated protein
LINC00847	0,018579295	1,48	long intergenic non-protein coding RNA 847
ZDHHC18	0,030339052	1,48	zinc finger, DHHC-type containing 18
PACS1	0,003212011	1,48	phosphofurin acidic cluster sorting protein 1
TBC1D1	0,013307413	1,47	TBC1 (tre-2/USP6, BUB2, cdc16) domain family, member 1
FMNL2	0,008924837	1,47	formin-like 2
FOXO1	0,028431173	1,46	forkhead box O1
DLGAP4	0,013670143	1,46	discs, large (Drosophila) homolog-associated protein 4
VWCE	0,004585029	1,45	von Willebrand factor C and EGF domains
ASB9	0,028211439	1,45	ankyrin repeat and SOCS box containing 9
PC	0,010636839	1,45	pyruvate carboxylase
GEM	0,013391517	1,44	GTP binding protein overexpressed in skeletal muscle
TRAV12-2	0,046736442	1,44	T cell receptor alpha variable 12-2
SLC22A23	0,035188415	1,44	solute carrier family 22, member 23
SPOCD1	0,026751204	1,43	SPOC domain containing 1

PRR5L	0,010088172	1,43	proline rich 5 like
PLA2G15	0,049290329	1,43	phospholipase A2, group XV
BACE1	0,029628827	1,43	beta-site APP-cleaving enzyme 1
ZNF732	0,042362266	1,43	zinc finger protein 732
WFS1	0,026394663	1,43	Wolfram syndrome 1 (wolframin)
KLHL6	0,012543702	1,42	kelch-like family member 6
TMC8	0,006424162	1,42	transmembrane channel-like 8
MTSS1	0,016087396	1,41	metastasis suppressor 1
LOC100506928	0,020506014	1,41	uncharacterized LOC100506928
MFSD12	0,013670143	1,40	major facilitator superfamily domain containing 12
PI4K2A	0,048825732	1,40	phosphatidylinositol 4-kinase type 2 alpha
C19orf60	0,007949832	1,39	chromosome 19 open reading frame 60
TMC6	0,047758353	1,39	transmembrane channel-like 6
CADPS2	0,004626759	1,39	Ca++-dependent secretion activator 2
PDE6G	0,013501033	1,38	phosphodiesterase 6G, cGMP-specific, rod, gamma
RASSF3	0,006424162	1,38	Ras association (RalGDS/AF-6) domain family member 3
RNF207	0,018925464	1,38	ring finger protein 207
CYP27A1	0,042374321	1,38	cytochrome P450, family 27, subfamily A, polypeptide 1
PGBD5	0,038626888	1,37	piggyBac transposable element derived 5
SLC28A3	0,012729886	1,37	solute carrier family 28 (concentrative nucleoside transporter), member 3
TNFRSF12A	0,039903772	1,36	tumor necrosis factor receptor superfamily, member 12A
CA14	0,005123585	1,36	carbonic anhydrase XIV
TCIRG1	0,024088086	1,35	T-cell, immune regulator 1, ATPase, H+ transporting, lysosomal V0 subunit A3
UG0898H09	0,029628827	1,35	uncharacterized LOC643763
PCGF2	0,009633151	1,34	polycomb group ring finger 2
NDST1	0,042362266	1,34	N-deacetylase/N-sulfotransferase (heparan glucosaminyl) 1
HCP5	0,030415845	1,34	HLA complex P5 (non-protein coding)
CLSTN1	0,032451965	1,34	calsyntenin 1
ZNF703	0,034828727	1,33	zinc finger protein 703

LONRF3	0,042362266	1,33	LON peptidase N-terminal domain and ring finger 3
LOC101927438	0,044282374	1,33	uncharacterized LOC101927438
AP4B1-AS1	0,022396076	1,33	AP4B1 antisense RNA 1
TNFSF14	0,034619967	1,33	tumor necrosis factor (ligand) superfamily, member 14
JAK1	0,004504132	1,33	Janus kinase 1
TMEM164	0,012516633	1,33	transmembrane protein 164
SNORD89	0,003815492	1,33	small nucleolar RNA, C/D box 89
CCND1	0,042058257	1,32	cyclin D1
SLC15A1	0,036921459	1,32	solute carrier family 15 (oligopeptide transporter), member 1
TBC1D30	0,047095338	1,32	TBC1 domain family, member 30
DOPEY2	0,036371377	1,31	dopey family member 2
LOC100506514	0,023532351	1,31	uncharacterized LOC100506514
LINC00877	0,04272916	1,31	long intergenic non-protein coding RNA 877
ZNF454	0,020906716	1,31	zinc finger protein 454
RPS19	0,006424162	1,30	ribosomal protein S19
KCNMB4	0,042362266	1,30	potassium large conductance calcium-activated channel, subfamily M, beta member 4

Suppl. Table 2: Down regulated genes in CD16+ *versus* CD16-MDDC

Symbol	adj. p	FC	description
CDH1	4,48E-05	-8,59	cadherin 1, type 1, E-cadherin (epithelial)
RXFP1	1,06E-05	-7,58	relaxin/insulin-like family peptide receptor 1
STEAP4	0,000967676	-6,78	STEAP family member 4
PAK7	2,68E-08	-5,16	p21 protein (Cdc42/Rac)-activated kinase 7
CCR6	1,74E-07	-3,91	chemokine (C-C motif) receptor 6
CD163L1	0,003432854	-3,86	CD163 molecule-like 1
RNASE2	0,00846588	-3,84	ribonuclease, RNase A family, 2 (liver, eosinophil-derived neurotoxin)
COLEC12	6,47E-05	-3,75	collectin sub-family member 12
PPBP	0,016735127	-3,74	pro-platelet basic protein (chemokine (C-X-C motif) ligand 7)
MPO	0,003743328	-3,59	myeloperoxidase
HRH4	0,008015255	-3,49	histamine receptor H4
GPR171	0,002428325	-3,44	G protein-coupled receptor 171
IL17RB	0,00079014	-3,39	interleukin 17 receptor B
PTGER3	5,65E-05	-3,31	prostaglandin E receptor 3 (subtype EP3)
SLC40A1	0,007700021	-3,29	solute carrier family 40 (iron-regulated transporter), member 1
ME1	0,00730176	-3,23	malic enzyme 1, NADP(+)-dependent, cytosolic
MIR146B	0,009004086	-3,20	microRNA 146b
DUOXA1	4,48E-05	-2,98	dual oxidase maturation factor 1
ITGA9	0,014365449	-2,96	integrin, alpha 9
DUOX1	0,000150649	-2,95	dual oxidase 1
TOX	0,000203362	-2,94	thymocyte selection-associated high mobility group box
CPA3	0,00330199	-2,93	carboxypeptidase A3 (mast cell)
HIST1H2AJ	0,005560076	-2,92	histone cluster 1, H2aj
CCL18	0,038436376	-2,83	chemokine (C-C motif) ligand 18 (pulmonary and activation-regulated)
ATP1B2	0,006424162	-2,73	ATPase, Na+/K+ transporting, beta 2 polypeptide
ALOX5AP	0,005886239	-2,69	arachidonate 5-lipoxygenase-activating protein
FZD3	0,000969723	-2,65	frizzled class receptor 3

PROS1	0,000699561	-2,64	protein S (alpha)
TMPRSS13	0,009206754	-2,56	transmembrane protease, serine 13
ZNF827	0,010067462	-2,53	zinc finger protein 827
SERPINF1	4,75E-05	-2,51	serpin peptidase inhibitor, clade F (alpha-2 antiplasmin, pigment epithelium derived factor), member 1
HIST1H2BM	0,020906716	-2,50	histone cluster 1, H2bm
GGT5	0,000199888	-2,49	gamma-glutamyltransferase 5
SCN9A	0,012516633	-2,48	sodium channel, voltage-gated, type IX, alpha subunit
IGJ	0,021343315	-2,43	immunoglobulin J polypeptide, linker protein for immunoglobulin alpha and mu polypeptides
NFXL1	0,015958926	-2,41	nuclear transcription factor, X-box binding-like 1
TSPAN15	0,00330199	-2,40	tetraspanin 15
CREB3L1	0,000687329	-2,38	cAMP responsive element binding protein 3-like 1
ADAM23	0,001345084	-2,38	ADAM metallopeptidase domain 23
CDH2	0,005938694	-2,34	cadherin 2, type 1, N-cadherin (neuronal)
SIGLEC1	6,47E-05	-2,31	sialic acid binding Ig-like lectin 1, sialoadhesin
MYBL1	7,85E-06	-2,31	v-myb avian myeloblastosis viral oncogene homolog-like 1
RAB27B	0,01514017	-2,30	RAB27B, member RAS oncogene family
EPCAM	2,27E-05	-2,27	epithelial cell adhesion molecule
LSR	0,033101676	-2,27	lipolysis stimulated lipoprotein receptor
CRH	9,36E-05	-2,26	corticotropin releasing hormone
TSPAN7	0,045708897	-2,24	tetraspanin 7
CLEC4G	0,001997598	-2,22	C-type lectin domain family 4, member G
CD34	0,008015255	-2,20	CD34 molecule
SMARCA1	0,005938694	-2,18	SWI/SNF related, matrix associated, actin dependent regulator of chromatin, subfamily a, member 1
NUP107	7,85E-06	-2,18	nucleoporin 107kDa
SNORD75	0,005952553	-2,14	small nucleolar RNA, C/D box 75
GIPC3	0,005119835	-2,11	GIPC PDZ domain containing family, member 3
TPX2	0,006615125	-2,10	TPX2, microtubule-associated
RALGPS2	0,002491484	-2,08	Ral GEF with PH domain and SH3 binding motif 2
LOC101927780	0,000199888	-2,05	uncharacterized LOC101927780

CST7	0,000398548	-2,04	cystatin F (leukocystatin)
FAM189A2	0,032829728	-2,04	family with sequence similarity 189, member A2
ZNF480	0,003432854	-2,04	zinc finger protein 480
SLC2A1	0,009101532	-2,03	solute carrier family 2 (facilitated glucose transporter), member 1
SH3PXD2B	0,015493578	-2,03	SH3 and PX domains 2B
PPAP2A	0,016111031	-2,00	phosphatidic acid phosphatase type 2A
TOP2A	0,012543702	-1,99	topoisomerase (DNA) II alpha 170kDa
DNM1	0,006424162	-1,99	dynamin 1
LOC101928161	0,014294496	-1,96	uncharacterized LOC101928161
MSI2	0,014365449	-1,96	musashi RNA-binding protein 2
GAPT	0,015493578	-1,94	GRB2-binding adaptor protein, transmembrane
CLEC4M	0,012516633	-1,93	C-type lectin domain family 4, member M
CRIM1	0,038436376	-1,93	cysteine rich transmembrane BMP regulator 1 (chordin-like)
FNBP1L	0,020722946	-1,93	formin binding protein 1-like
DNASE1L3	0,008149648	-1,91	deoxyribonuclease I-like 3
CCNA1	0,012768831	-1,91	cyclin A1
SGCB	0,036921459	-1,90	sarcoglycan, beta (43kDa dystrophin-associated glycoprotein)
SLC22A5	0,003743328	-1,89	solute carrier family 22 (organic cation/carnitine transporter), member 5
CECR2	0,008677393	-1,88	cat eye syndrome chromosome region, candidate 2
HSPA2	0,019422107	-1,87	heat shock 70kDa protein 2
SLC35F3	0,032670604	-1,86	solute carrier family 35, member F3
NCR3LG1	0,014348784	-1,85	natural killer cell cytotoxicity receptor 3 ligand 1
TULP3	0,004766439	-1,83	tubby like protein 3
ESCO2	0,005560076	-1,81	establishment of sister chromatid cohesion N-acetyltransferase 2
SKA3	0,010088172	-1,80	spindle and kinetochore associated complex subunit 3
RCBTB2	0,00061286	-1,80	regulator of chromosome condensation (RCC1) and BTB (POZ) domain containing protein 2
ID3	0,025521001	-1,80	inhibitor of DNA binding 3, dominant negative helix-loop-helix protein
KIF11	0,006434531	-1,78	kinesin family member 11
SNHG19	0,043947273	-1,78	small nucleolar RNA host gene 19 (non-protein coding)

SAMD9	0,005999118	-1,75	sterile alpha motif domain containing 9
FAM171B	0,048060436	-1,74	family with sequence similarity 171, member B
PLEK2	0,018398082	-1,74	pleckstrin 2
LONRF1	0,003432854	-1,74	LON peptidase N-terminal domain and ring finger 1
EIF2AK2	0,013526454	-1,73	eukaryotic translation initiation factor 2-alpha kinase 2
S100B	0,004155399	-1,72	S100 calcium binding protein B
HSPA4L	0,049536531	-1,71	heat shock 70kDa protein 4-like
ESAM	0,00330199	-1,71	endothelial cell adhesion molecule
DDIT3	0,001436212	-1,71	DNA-damage-inducible transcript 3
HR	0,000199888	-1,71	hair growth associated
ADHFE1	0,021154624	-1,70	alcohol dehydrogenase, iron containing, 1
PRSS36	0,000969723	-1,70	protease, serine, 36
TXLNB	0,013670143	-1,69	taxilin beta
GCNT1	0,032616994	-1,69	glucosaminyl (N-acetyl) transferase 1, core 2
MIR503	0,005502371	-1,69	microRNA 503
KBTBD7	0,010977951	-1,68	kelch repeat and BTB (POZ) domain containing 7
CDR2L	0,006927827	-1,68	cerebellar degeneration-related protein 2-like
HIST1H2BL	0,035886512	-1,68	histone cluster 1, H2bl
C9orf72	0,005886239	-1,67	chromosome 9 open reading frame 72
BUB1	0,017612594	-1,66	BUB1 mitotic checkpoint serine/threonine kinase
LINC00967	0,015493578	-1,66	long intergenic non-protein coding RNA 967
EZH2	0,016735127	-1,65	enhancer of zeste 2 polycomb repressive complex 2 subunit
TRIM15	0,003946823	-1,65	tripartite motif containing 15
ABCC4	0,000411135	-1,65	ATP-binding cassette, sub-family C (CFTR/MRP), member 4
MIR4499	0,024937371	-1,64	microRNA 4499
SELL	0,035023187	-1,64	selectin L
SYCP2	0,044034996	-1,63	synaptonemal complex protein 2
IL1RL2	0,005345224	-1,63	interleukin 1 receptor-like 2
RNF138P1	0,029646979	-1,63	ring finger protein 138, E3 ubiquitin protein ligase pseudogene 1

RNASE1	0,008598691	-1,62	ribonuclease, RNase A family, 1 (pancreatic)
IGFBP7	0,001355833	-1,62	insulin-like growth factor binding protein 7
SLC44A1	0,00399585	-1,62	solute carrier family 44 (choline transporter), member 1
PKP2	0,007283765	-1,62	plakophilin 2
ITM2C	0,01800465	-1,62	integral membrane protein 2C
MKI67	0,008015255	-1,61	marker of proliferation Ki-67
HCAR3	0,006250764	-1,61	hydroxycarboxylic acid receptor 3
TFAP2C	0,012205232	-1,61	transcription factor AP-2 gamma (activating enhancer binding protein 2 gamma)
AIG1	0,010636839	-1,60	androgen-induced 1
TRIM15	0,005938694	-1,59	tripartite motif containing 15
TRIM15	0,005938694	-1,59	tripartite motif containing 15
TRIM15	0,005938694	-1,59	tripartite motif containing 15
IKZF4	0,004504132	-1,59	IKAROS family zinc finger 4 (Eos)
TRIM15	0,005886239	-1,58	tripartite motif containing 15
TRIM15	0,005886239	-1,58	tripartite motif containing 15
TRIM15	0,005886239	-1,58	tripartite motif containing 15
C4orf32	0,018773627	-1,58	chromosome 4 open reading frame 32
NUSAP1	0,005938694	-1,58	nucleolar and spindle associated protein 1
NCKAP5	0,018150712	-1,58	NCK-associated protein 5
EDDM3A	0,046736442	-1,58	epididymal protein 3A
BANK1	0,003815492	-1,58	B-cell scaffold protein with ankyrin repeats 1
KIT	0,038436376	-1,58	v-kit Hardy-Zuckerman 4 feline sarcoma viral oncogene homolog
HSPA12B	0,013249297	-1,57	heat shock 70kD protein 12B
WDFY2	0,018599272	-1,56	WD repeat and FYVE domain containing 2
SLX4IP	0,00846588	-1,56	SLX4 interacting protein
ICA1	0,01294825	-1,55	islet cell autoantigen 1, 69kDa
SGOL1	0,048060436	-1,55	shugoshin-like 1 (S. pombe)
CRYM-AS1	0,01446133	-1,55	CRYM antisense RNA 1
RFC4	0,004504132	-1,55	replication factor C (activator 1) 4, 37kDa

FAM95B1	0,046173976	-1,55	family with sequence similarity 95, member B1
DEPDC1B	0,04501606	-1,54	DEP domain containing 1B
TRIM15	0,010411394	-1,54	tripartite motif containing 15
MVB12B	0,0148961	-1,54	multivesicular body subunit 12B
PDCD1LG2	0,005886239	-1,54	programmed cell death 1 ligand 2
CCNE2	0,017612594	-1,54	cyclin E2
KDELC2	0,012345555	-1,54	KDEL (Lys-Asp-Glu-Leu) containing 2
TIPIN	0,010407667	-1,53	TIMELESS interacting protein
SVIL	0,036921459	-1,53	supervillin
RNF24	0,00501938	-1,53	ring finger protein 24
CDCA7L	0,006424162	-1,52	cell division cycle associated 7-like
IGF2BP2	0,042362266	-1,52	insulin-like growth factor 2 mRNA binding protein 2
PCMTD2	0,003589583	-1,52	protein-L-isoaspartate (D-aspartate) O-methyltransferase domain containing 2
ZCCHC7	0,004905648	-1,52	zinc finger, CCHC domain containing 7
LOC100288814	0,020041698	-1,52	uncharacterized LOC100288814
PGAP1	0,048026791	-1,51	post-GPI attachment to proteins 1
GPSM2	0,023641524	-1,51	G-protein signaling modulator 2
FOXQ1	0,020286374	-1,51	forkhead box Q1
ST8SIA4	0,024937371	-1,51	ST8 alpha-N-acetyl-neuraminide alpha-2,8-sialyltransferase 4
B3GALNT1	0,005560076	-1,51	beta-1,3-N-acetylgalactosaminyltransferase 1 (globoside blood group)
PRIM1	0,013015434	-1,50	primase, DNA, polypeptide 1 (49kDa)
BRCA2	0,027977573	-1,50	breast cancer 2, early onset
TWSG1	0,046946294	-1,50	twisted gastrulation BMP signaling modulator 1
ZNF383	0,036803238	-1,50	zinc finger protein 383
TMEM255B	0,045104724	-1,49	transmembrane protein 255B
MBOAT2	0,006484723	-1,49	membrane bound O-acyltransferase domain containing 2
STX2	0,009413945	-1,49	syntaxin 2
SHCBP1	0,008175731	-1,49	SHC SH2-domain binding protein 1
RRS1-AS1	0,048059158	-1,49	RRS1 antisense RNA 1 (head to head)

RHPN1-AS1	0,012543702	-1,49	RHPN1 antisense RNA 1 (head to head)
MAP1A	0,012669679	-1,49	microtubule-associated protein 1A
ARL4A	0,008366345	-1,48	ADP-ribosylation factor-like 4A
NFE2	0,013391517	-1,48	nuclear factor, erythroid 2
KBTBD11	0,006424162	-1,48	kelch repeat and BTB (POZ) domain containing 11
CLDN4	0,026610987	-1,48	claudin 4
KIF20B	0,022458066	-1,48	kinesin family member 20B
KIF15	0,031101368	-1,48	kinesin family member 15
SNTB1	0,007853219	-1,48	syntrophin, beta 1 (dystrophin-associated protein A1, 59kDa, basic component 1)
LRRCC1	0,049536531	-1,47	leucine rich repeat and coiled-coil centrosomal protein 1
NCR3LG1	0,011384085	-1,47	natural killer cell cytotoxicity receptor 3 ligand 1
FLJ22447	0,016087396	-1,47	uncharacterized LOC400221
HIF1A	0,000716838	-1,47	hypoxia inducible factor 1, alpha subunit (basic helix-loop-helix transcription factor)
AKR1B1	0,048060436	-1,46	aldo-keto reductase family 1, member B1 (aldose reductase)
CWF19L1	0,022396076	-1,46	CWF19-like 1, cell cycle control (S. pombe)
STIL	0,035608235	-1,46	SCL/TAL1 interrupting locus
LYRM7	0,005350352	-1,46	LYR motif containing 7
TGFBR1	0,012926609	-1,45	transforming growth factor, beta receptor 1
ACAP1	0,039439794	-1,45	ArfGAP with coiled-coil, ankyrin repeat and PH domains 1
ZNF823	0,038551127	-1,45	zinc finger protein 823
STOX2	0,020299151	-1,45	storkhead box 2
RFC3	0,017185822	-1,45	replication factor C (activator 1) 3, 38kDa
SMAGP	0,048413261	-1,45	small cell adhesion glycoprotein
LINC01150	0,013249297	-1,44	long intergenic non-protein coding RNA 1150
TAF4B	0,044199813	-1,44	TAF4b RNA polymerase II, TATA box binding protein (TBP)-associated factor, 105kDa
RBM22	0,000147152	-1,44	RNA binding motif protein 22
RB1	0,005886239	-1,44	retinoblastoma 1
SPIN4	0,006250764	-1,44	spindlin family, member 4
SCN5A	0,039819189	-1,44	sodium channel, voltage-gated, type V, alpha subunit

CTTNBP2	0,027413904	-1,44	cortactin binding protein 2
PEAK1	0,048650506	-1,44	pseudopodium-enriched atypical kinase 1
AK2	0,006822062	-1,44	adenylate kinase 2
GLIS2	0,015229132	-1,44	GLIS family zinc finger 2
DSTNP2	0,028438957	-1,43	destrin (actin depolymerizing factor) pseudogene 2
IFT74	0,016139908	-1,43	intraflagellar transport 74
ANLN	0,033720643	-1,43	anillin, actin binding protein
PIBF1	0,00873694	-1,43	progesterone immunomodulatory binding factor 1
TRIM10	0,015958926	-1,43	tripartite motif containing 10
ALMS1	0,036921459	-1,42	Alstrom syndrome 1
CACNA2D4	0,030507412	-1,42	calcium channel, voltage-dependent, alpha 2/delta subunit 4
NSUN6	0,04501606	-1,42	NOP2/Sun domain family, member 6
ZDHHC2	0,023005619	-1,42	zinc finger, DHHC-type containing 2
CAPN2	0,035023187	-1,41	calpain 2, (m/II) large subunit
C6orf25	0,017706592	-1,41	chromosome 6 open reading frame 25
C6orf25	0,017706592	-1,41	chromosome 6 open reading frame 25
C6orf25	0,017706592	-1,41	chromosome 6 open reading frame 25
C6orf25	0,017706592	-1,41	chromosome 6 open reading frame 25
CBFB	0,010952307	-1,41	core-binding factor, beta subunit
CHDH	0,035188415	-1,40	choline dehydrogenase
GRIN3B	0,020227341	-1,40	glutamate receptor, ionotropic, N-methyl-D-aspartate 3B
MPP5	0,036921459	-1,40	membrane protein, palmitoylated 5 (MAGUK p55 subfamily member 5)
ALG6	0,008895971	-1,40	ALG6, alpha-1,3-glucosyltransferase
KIAA0825	0,048060436	-1,40	KIAA0825
POLD2	0,029376149	-1,40	polymerase (DNA directed), delta 2, accessory subunit
CENPI	0,032451965	-1,40	centromere protein I
CDKN2C	0,011349411	-1,39	cyclin-dependent kinase inhibitor 2C (p18, inhibits CDK4)
HPSE	0,008924837	-1,39	heparanase
LCLAT1	0,00822055	-1,39	lysocardiolipin acyltransferase 1

C6orf25	0,013526454	-1,39	chromosome 6 open reading frame 25
MCM8	0,010407667	-1,39	minichromosome maintenance complex component 8
PBLD	0,007853219	-1,39	phenazine biosynthesis-like protein domain containing
LYSMD3	0,039658199	-1,38	LysM, putative peptidoglycan-binding, domain containing 3
RNF168	0,036921459	-1,38	ring finger protein 168, E3 ubiquitin protein ligase
SLC37A1	0,048650506	-1,38	solute carrier family 37 (glucose-6-phosphate transporter), member 1
LNX2	0,026159721	-1,38	ligand of numb-protein X 2
SAMD9L	0,022941834	-1,38	sterile alpha motif domain containing 9-like
SNAI1	0,016958742	-1,38	snail family zinc finger 1
APMAP	0,013391517	-1,38	adipocyte plasma membrane associated protein
IFI16	0,035023187	-1,38	interferon, gamma-inducible protein 16
ATAD2	0,02593725	-1,37	ATPase family, AAA domain containing 2
OXCT1	0,046645784	-1,37	3-oxoacid CoA transferase 1
PHF10	0,043438334	-1,37	PHD finger protein 10
LTBP1	0,017706592	-1,37	latent transforming growth factor beta binding protein 1
CKS2	0,022134562	-1,37	CDC28 protein kinase regulatory subunit 2
MAFA	0,029628827	-1,37	v-maf avian musculoaponeurotic fibrosarcoma oncogene homolog A
MCUR1	0,041582811	-1,37	mitochondrial calcium uniporter regulator 1
WDR76	0,017612594	-1,36	WD repeat domain 76
ZNF268	0,026528057	-1,36	zinc finger protein 268
NRSN2	0,034619967	-1,36	neurensin 2
POLA2	0,01060777	-1,36	polymerase (DNA directed), alpha 2, accessory subunit
PIGM	0,041149605	-1,36	phosphatidylinositol glycan anchor biosynthesis, class M
LOC728323	0,038626888	-1,36	uncharacterized LOC728323
SMC4	0,013291554	-1,36	structural maintenance of chromosomes 4
ZNF280D	0,018064564	-1,35	zinc finger protein 280D
PARPBP	0,001614762	-1,35	PARP1 binding protein
GTF2F2	0,005312877	-1,35	general transcription factor IIF, polypeptide 2, 30kDa
LANCL1	0,006629956	-1,35	LanC lantibiotic synthetase component C-like 1 (bacterial)

FAM101B	0,036921459	-1,35	family with sequence similarity 101, member B
RRM2	0,042362266	-1,35	ribonucleotide reductase M2
TAF9B	0,025308058	-1,35	TAF9B RNA polymerase II, TATA box binding protein (TBP)-associated factor, 31kDa
WDR89	0,018287459	-1,35	WD repeat domain 89
SLC16A5	0,030379263	-1,35	solute carrier family 16 (monocarboxylate transporter), member 5
CHAF1B	0,005560076	-1,35	chromatin assembly factor 1, subunit B (p60)
THOC1	0,015493578	-1,34	THO complex 1
FANCD2	0,024359738	-1,34	Fanconi anemia, complementation group D2
ANP32E	0,035188415	-1,34	acidic (leucine-rich) nuclear phosphoprotein 32 family, member E
RABL3	0,025889635	-1,34	RAB, member of RAS oncogene family-like 3
WDR91	0,012768831	-1,34	WD repeat domain 91
C6orf25	0,038754116	-1,34	chromosome 6 open reading frame 25
IFT80	0,04272916	-1,34	intraflagellar transport 80
TMEM106B	0,03899335	-1,34	transmembrane protein 106B
TUBGCP4	0,011377838	-1,34	tubulin, gamma complex associated protein 4
MCM4	0,040576794	-1,34	minichromosome maintenance complex component 4
C12orf65	0,0148961	-1,34	chromosome 12 open reading frame 65
ANO10	0,035886512	-1,34	anoctamin 10
LOC286058	0,032451965	-1,33	uncharacterized LOC286058
RRP1B	0,034145192	-1,32	ribosomal RNA processing 1B
LOC284023	0,021343315	-1,32	uncharacterized LOC284023
ALG9	0,038436376	-1,32	ALG9, alpha-1,2-mannosyltransferase
SKP2	0,019437303	-1,32	S-phase kinase-associated protein 2, E3 ubiquitin protein ligase
CTPS2	0,049822679	-1,32	CTP synthase 2
C5orf42	0,022993709	-1,31	chromosome 5 open reading frame 42
MNS1	0,039439794	-1,31	meiosis-specific nuclear structural 1
ZNF766	0,030507412	-1,31	zinc finger protein 766
BPGM	0,032878606	-1,30	2,3-bisphosphoglycerate mutase
E2F6	0,049651938	-1,30	E2F transcription factor 6

Supplemental Table 3: LPS up regulated genes in CD16+ MDDCs

Symbol	adj. p	FC	description
CCL8	0,000677682	4,50308442	chemokine (C-C motif) ligand 8
LOC100507639	6,80E-07	3,21855039	uncharacterized LOC100507639
SIGLEC1	1,56E-09	3,13329865	sialic acid binding Ig-like lectin 1, sialoadhesin
MIR4439	0,002688544	3,05668516	microRNA 4439
SCIN	7,69E-06	2,84738199	scinderin
IL7R	0,012918023	2,27259981	interleukin 7 receptor
PLTP	0,000879659	2,26124204	phospholipid transfer protein
TNF	0,000348163	2,23862297	tumor necrosis factor
TNF	0,000348163	2,23862297	tumor necrosis factor
TNF	0,000348163	2,23862297	tumor necrosis factor
TNF	0,000348163	2,23862297	tumor necrosis factor
TNF	0,000348163	2,23862297	tumor necrosis factor
TNF	0,000348163	2,23862297	tumor necrosis factor
TNF	0,000348163	2,23862297	tumor necrosis factor
TNF	0,000518666	2,23486738	tumor necrosis factor
LOC644090	0,001087289	2,22539335	uncharacterized LOC644090
CFP	0,006639592	2,17943735	complement factor properdin
CLU	5,09E-05	2,16901214	clusterin
PAXIP1OS	2,21E-05	1,93972731	PAXIP1 opposite strand
ZNF876P	0,000922801	1,8900249	zinc finger protein 876, pseudogene
SNORD12C	0,000408488	1,83555893	small nucleolar RNA, C/D box 12C
C2	0,00010197	1,83236963	complement component 2
MIR331	0,004058197	1,81308173	microRNA 331
TMEM139	0,00026407	1,79657414	transmembrane protein 139
MAP3K8	0,003836354	1,79076549	mitogen-activated protein kinase kinase kinase 8
SNX10	0,000296299	1,76769641	sorting nexin 10
CXCL1	0,01039801	1,76015071	chemokine (C-X-C motif) ligand 1 (melanoma growth stimulating activity, alpha)

IL18	0,003128375	1,71234122	interleukin 18
MIR544A	0,003109696	1,69905612	microRNA 544a
ARID5B	0,011988904	1,69493231	AT rich interactive domain 5B (MRF1-like)
H2AFY2	0,008305814	1,67483419	H2A histone family, member Y2
BCL11A	0,00357192	1,67295544	B-cell CLL/lymphoma 11A (zinc finger protein)
CTD-2270F17.1	0,000338803	1,66315114	uncharacterized LOC101928033
EPT1	0,000298243	1,65170358	ethanolaminephosphotransferase 1 (CDP-ethanolamine-specific)
ELL3	0,001040794	1,60099507	elongation factor RNA polymerase II-like 3
IRG1	0,001967929	1,59844173	immunoresponsive 1 homolog (mouse)
ZG16B	0,012141797	1,59682062	zymogen granule protein 16B
NIPAL1	0,002075607	1,59392558	NIPA-like domain containing 1
PRF1	0,003910422	1,57527365	perforin 1 (pore forming protein)
ANKRD36	0,009295741	1,57043233	ankyrin repeat domain 36
HORMAD1	0,003621411	1,55476078	HORMA domain containing 1
DHCR24	0,001569093	1,55149432	24-dehydrocholesterol reductase
B4GALT6	0,029790009	1,55068917	UDP-Gal:betaGlcNAc beta 1,4- galactosyltransferase, polypeptide 6
CENPI	0,000126771	1,54620488	centromere protein I
NUPR1	0,007466001	1,53073022	nuclear protein, transcriptional regulator, 1
SLC2A1	0,033277853	1,52644641	solute carrier family 2 (facilitated glucose transporter), member 1
CLIC3	0,001082505	1,5258458	chloride intracellular channel 3
SCML1	0,0018776	1,52176284	sex comb on midleg-like 1 (Drosophila)
MIR4463	0,000876066	1,51657936	microRNA 4463
C17orf96	0,002950107	1,51016979	chromosome 17 open reading frame 96
CADM1	0,003132244	1,50309467	cell adhesion molecule 1
PGA3	0,006117016	1,49969587	pepsinogen 3, group I (pepsinogen A)
FAM205B	0,002474454	1,49819013	transmembrane protein C9orf144B pseudogene
GOLGA8H	0,004561425	1,49116001	golgin A8 family, member H
P2RY8	0,039308578	1,48832973	purinergic receptor P2Y, G-protein coupled, 8
LPIN1	0,000540284	1,48349351	lipin 1

STAG3	0,001748159	1,48341968	stromal antigen 3
ARHGAP5	0,001421964	1,4831615	Rho GTPase activating protein 5
LPAR3	0,00220545	1,48181635	lysophosphatidic acid receptor 3
RIMBP3B	0,026419097	1,47997201	RIMS binding protein 3B
ZFAND6	0,02269288	1,47916708	zinc finger, AN1-type domain 6
VEZT	0,000262009	1,47575738	vezatin, adherens junctions transmembrane protein
RABAC1	0,000751744	1,47440425	Rab acceptor 1 (prenylated)
MIR449C	0,004192427	1,47352356	microRNA 449c
LOC101929057	0,008999451	1,46521468	uncharacterized LOC101929057
SLC50A1	0,004462298	1,45932297	solute carrier family 50 (sugar efflux transporter), member 1
MIR4772	0,003133619	1,45871236	microRNA 4772
PAM	0,028199043	1,45662318	peptidylglycine alpha-amidating monooxygenase
C9orf72	0,005348477	1,45006613	chromosome 9 open reading frame 72
SLFN12	0,000325185	1,44762908	schlafen family member 12
MVB12A	1,52E-05	1,44297847	multivesicular body subunit 12A
NOLC1	0,000568328	1,4408301	nucleolar and coiled-body phosphoprotein 1
SERPINF1	0,021264137	1,44030529	serpin peptidase inhibitor, clade F (alpha-2 antiplasmin, pigment epithelium derived factor), member 1
CST7	0,010888214	1,43848121	cystatin F (leukocystatin)
PARP11	0,000857381	1,43458278	poly (ADP-ribose) polymerase family, member 11
KIAA1109	0,001424278	1,43422011	KIAA1109
ARIH2OS	7,51E-05	1,43275552	ariadne homolog 2 opposite strand
RNPS1	0,010445309	1,43168125	RNA binding protein S1, serine-rich domain
MPP5	0,001815788	1,43118765	membrane protein, palmitoylated 5 (MAGUK p55 subfamily member 5)
GK3P	0,017234296	1,43003179	glycerol kinase 3 pseudogene
ARHGAP25	0,000533648	1,42961735	Rho GTPase activating protein 25
OXER1	0,005464163	1,42709746	oxoeicosanoid (OXE) receptor 1
LOC100129781	0,003356043	1,42617815	uncharacterized LOC100129781
STARD5	0,046075743	1,42616515	StAR-related lipid transfer (START) domain containing 5
OR56B1	0,025072828	1,42394059	olfactory receptor, family 56, subfamily B, member 1

ADPRM	0,005416828	1,4230329	ADP-ribose/CDP-alcohol diphosphatase, manganese-dependent
RND3	0,022332021	1,42139362	Rho family GTPase 3
ZFYVE26	0,000166252	1,42123403	zinc finger, FYVE domain containing 26
NPPA	0,000467566	1,42033926	natriuretic peptide A
AIDA	0,000718288	1,41722541	axin interactor, dorsalization associated
CTPS2	0,000456172	1,41633478	CTP synthase 2
MIR3188	0,015275612	1,41481707	microRNA 3188
TPI1P2	0,028116217	1,41474728	triosephosphate isomerase 1 pseudogene 2
LOC100190986	0,049402386	1,4145766	uncharacterized LOC100190986
MIR4299	0,003415548	1,41432602	microRNA 4299
MIR3945	0,000809506	1,41399096	microRNA 3945
GRHL1	0,009316438	1,41370092	grainyhead-like 1 (Drosophila)
LILRA5	0,016874502	1,41294545	leukocyte immunoglobulin-like receptor, subfamily A (with TM domain), member 5
KCNMB3	0,009919811	1,41059707	potassium large conductance calcium-activated channel, subfamily M beta member 3
EXD2	0,000300349	1,41051348	exonuclease 3'-5' domain containing 2
BLZF1	0,007478875	1,40902083	basic leucine zipper nuclear factor 1
TLCD2	0,002293498	1,4081406	TLC domain containing 2
PCYT2	0,001057193	1,40752269	phosphate cytidylyltransferase 2, ethanolamine
TMCO5B	0,001484452	1,40344728	transmembrane and coiled-coil domains 5B, pseudogene
TMEM182	0,001355041	1,40297926	transmembrane protein 182
FBXO48	0,001822945	1,40281935	F-box protein 48
CASP10	0,006759615	1,40276064	caspase 10, apoptosis-related cysteine peptidase
ZC2HC1A	0,015727397	1,39928268	zinc finger, C2HC-type containing 1A
LOC399815	0,002365799	1,39918071	chromosome 10 open reading frame 88 pseudogene
LOC100506317	0,000243574	1,39625043	uncharacterized LOC100506317
FAM76B	0,000317673	1,39498332	family with sequence similarity 76, member B
MAGOH	0,024356316	1,39455538	mago-nashi homolog, proliferation-associated (Drosophila)
LOC100506606	0,024989857	1,39161976	uncharacterized LOC100506606
C9orf153	0,006308072	1,39140709	chromosome 9 open reading frame 153

SLC13A5	0,001938215	1,38995217	solute carrier family 13 (sodium-dependent citrate transporter), member 5
FAM63B	0,023515223	1,38783324	family with sequence similarity 63, member B
CNNM4	0,003724751	1,38560503	cyclin and CBS domain divalent metal cation transport mediator 4
AKT1S1	0,017440698	1,3849948	AKT1 substrate 1 (proline-rich)
PHLDB3	0,006056815	1,38142824	pleckstrin homology-like domain, family B, member 3
XRCC6BP1	0,007903342	1,37933298	XRCC6 binding protein 1
MIR135A2	0,001560857	1,37827315	microRNA 135a-2
LNX2	0,00204894	1,37824755	ligand of numb-protein X 2
ADAMTS4	0,022672526	1,37753998	ADAM metallopeptidase with thrombospondin type 1 motif, 4
NHLRC2	0,000303706	1,37607056	NHL repeat containing 2
CCDC71	0,000559841	1,37606713	coiled-coil domain containing 71
RHOB	0,016092785	1,3758662	ras homolog family member B
FLJ32255	0,019429315	1,37378364	uncharacterized LOC643977
GOLGA2P9	0,002644164	1,37363144	golgin A2 pseudogene 9
LOC100128751	0,025038245	1,37331492	INM04
CPLX3	0,002484241	1,37296903	complexin 3
MIRLET7D	0,017335194	1,37223456	microRNA let-7d
MIR329-2	0,013479932	1,37186494	microRNA 329-2
KRTAP5-3	0,040136833	1,37096191	keratin associated protein 5-3
RAB39B	0,000610317	1,37039579	RAB39B, member RAS oncogene family
MAATS1	4,26E-05	1,37027756	MYCBP-associated, testis expressed 1
YME1L1	0,006167815	1,36981296	YME1-like 1 ATPase
CXorf28	0,043616562	1,36866982	chromosome X open reading frame 28
MORC3	0,028263738	1,36671522	MORC family CW-type zinc finger 3
LOC100288842	0,005655877	1,3654556	UDP-GlcNAc:betaGal beta-1,3-N-acetylglucosaminyltransferase 5 pseudogene
CHI3L2	0,014971058	1,36467808	chitinase 3-like 2
LINC01191	0,041781767	1,36459141	long intergenic non-protein coding RNA 1191
ZNF462	0,011626437	1,36332504	zinc finger protein 462
ARMCX1	0,028160031	1,36248503	armadillo repeat containing, X-linked 1

FIGNL1	0,017637373	1,35959347	fidgetin-like 1
MIR4768	0,007391045	1,35843762	microRNA 4768
LINC01029	0,040338523	1,35759967	long intergenic non-protein coding RNA 1029
NIPSNAP3B	0,028271625	1,35747209	nipsnap homolog 3B (C. elegans)
SPDYE4	0,037563307	1,35551325	speedy/RINGO cell cycle regulator family member E4
TMEM222	0,000194021	1,35444662	transmembrane protein 222
CYP4F24P	0,038902246	1,3537105	cytochrome P450, family 4, subfamily F, polypeptide 24, pseudogene
C11orf57	0,027154449	1,35308729	chromosome 11 open reading frame 57
SLC6A9	0,009195176	1,35251984	solute carrier family 6 (neurotransmitter transporter, glycine), member 9
UHRF2	0,002758212	1,35117278	ubiquitin-like with PHD and ring finger domains 2, E3 ubiquitin protein ligase
CDADC1	0,002028727	1,35107715	cytidine and dCMP deaminase domain containing 1
ADA	0,00985111	1,35004476	adenosine deaminase
KIAA1407	0,005048555	1,35002583	KIAA1407
LINC00987	0,011978089	1,34977712	long intergenic non-protein coding RNA 987
CLDN17	0,001283796	1,34923821	claudin 17
TUBA1B	0,025814961	1,34760267	tubulin, alpha 1b
TNIP3	0,049660959	1,34752035	TNFAIP3 interacting protein 3
C1orf147	0,002394686	1,34704972	chromosome 1 open reading frame 147
ADPRHL2	0,005058735	1,34662944	ADP-ribosylhydrolase like 2
OR2T2	0,010281598	1,3463376	olfactory receptor, family 2, subfamily T, member 2
TBPL1	0,003175773	1,34566441	TBP-like 1
GNG11	0,016612336	1,34523783	guanine nucleotide binding protein (G protein), gamma 11
MC3R	0,001737901	1,34492426	melanocortin 3 receptor
OR7E156P	0,008572627	1,34432461	olfactory receptor, family 7, subfamily E, member 156 pseudogene
TM7SF2	0,006162234	1,34319153	transmembrane 7 superfamily member 2
DMTF1	0,011543145	1,34297338	cyclin D binding myb-like transcription factor 1
LINC00334	0,007700963	1,34272733	long intergenic non-protein coding RNA 334
MPV17L	0,004158699	1,34254481	MPV17 mitochondrial membrane protein-like
LOC339622	0,002104478	1,34241337	uncharacterized LOC339622

LOC100129138	0,048619287	1,34185469	THAP domain containing, apoptosis associated protein 3 pseudogene
GINS1	0,01308078	1,34169483	GINS complex subunit 1 (Psf1 homolog)
SASS6	0,01314431	1,34047361	spindle assembly 6 homolog (C. elegans)
POLN	0,001576956	1,34016431	polymerase (DNA directed) nu
MIR299	0,001016493	1,33984359	microRNA 299
TMEM139	0,001674462	1,33932864	transmembrane protein 139
TBK1	0,00030199	1,338563	TANK-binding kinase 1
FAM212A	0,003342161	1,33841149	family with sequence similarity 212, member A
LOC101927056	0,03498659	1,33835442	uncharacterized LOC101927056
HLA-F-AS1	0,041469515	1,33788095	HLA-F antisense RNA 1
FRK	0,012979768	1,33787199	fyn-related Src family tyrosine kinase
LOC727896	0,006903022	1,33637582	cysteine and histidine-rich domain (CHORD) containing 1 pseudogene
C6orf132	0,003459234	1,33624557	chromosome 6 open reading frame 132
JMJD1C-AS1	0,005226981	1,33477065	JMJD1C antisense RNA 1
LMAN2L	0,002676439	1,33396407	lectin, mannose-binding 2-like
TIMM8B	0,002643197	1,33293887	translocase of inner mitochondrial membrane 8 homolog B (yeast)
RNF144B	0,016834267	1,33255835	ring finger protein 144B
MTBP	0,022923592	1,33009826	MDM2 binding protein
KDM4D	0,012734482	1,32979186	lysine (K)-specific demethylase 4D
FAM127A	0,002008726	1,32922401	family with sequence similarity 127, member A
MACF1	0,020785437	1,32846746	microtubule-actin crosslinking factor 1
TPBG	0,023742368	1,32821424	trophoblast glycoprotein
CEP192	0,015570205	1,32785986	centrosomal protein 192kDa
SCPEP1	0,008903403	1,32734799	serine carboxypeptidase 1
RPARP-AS1	0,02356728	1,32712918	RPARP antisense RNA 1
MAB21L2	0,003172586	1,32700495	mab-21-like 2 (C. elegans)
ARL4A	0,009127043	1,32593625	ADP-ribosylation factor-like 4A
C8orf31	0,015657447	1,32586317	chromosome 8 open reading frame 31
PERP	0,005289507	1,32492006	PERP, TP53 apoptosis effector

TRIM49	0,023104814	1,32390769	tripartite motif containing 49
UBTFL1	0,043912478	1,32311609	upstream binding transcription factor, RNA polymerase I-like 1
PDCD5	0,007825866	1,32275029	programmed cell death 5
HEXDC	0,002103952	1,3226796	hexosaminidase (glycosyl hydrolase family 20, catalytic domain) containing
OXCT1	0,011888616	1,32214786	3-oxoacid CoA transferase 1
KATNAL1	0,019026725	1,32157834	katanin p60 subunit A-like 1
LOC100128988	0,017471506	1,31872921	uncharacterized LOC100128988
MIR1295A	0,010084622	1,31843057	microRNA 1295a
RNU6-76P	0,034336522	1,31807904	RNA, U6 small nuclear 76, pseudogene
C21orf91-OT1	0,034047669	1,31804959	C21orf91 overlapping transcript 1
RPGRIP1	0,031354751	1,31790352	retinitis pigmentosa GTPase regulator interacting protein 1
C14orf28	0,009288773	1,31690027	chromosome 14 open reading frame 28
RUSC1	0,002348714	1,31619763	RUN and SH3 domain containing 1
SLC25A2	0,004876591	1,31563187	solute carrier family 25 (mitochondrial carrier; ornithine transporter) member 2
SLC35B3	0,000240629	1,31529539	solute carrier family 35 (adenosine 3'-phospho 5'-phosphosulfate transporter), member B3
UBB	0,016154501	1,31432922	ubiquitin B
LCN10	0,006097507	1,31431496	lipocalin 10
C19orf54	0,016752829	1,31355315	chromosome 19 open reading frame 54
LINC00607	0,030921136	1,31248497	long intergenic non-protein coding RNA 607
C20orf85	0,007591554	1,31205354	chromosome 20 open reading frame 85
CHAF1B	0,000478723	1,31063724	chromatin assembly factor 1, subunit B (p60)
TCF7	0,002886223	1,31035715	transcription factor 7 (T-cell specific, HMG-box)
ORAI1	0,001321413	1,30976869	ORAI calcium release-activated calcium modulator 1
PRRT2	0,025165098	1,30975896	proline-rich transmembrane protein 2
SLC14A2	0,000214028	1,30909061	solute carrier family 14 (urea transporter), member 2
SVIP	0,007984599	1,30889229	small VCP/p97-interacting protein
DND1	0,002291722	1,30886431	DND microRNA-mediated repression inhibitor 1
DND1	0,002291722	1,30886431	DND microRNA-mediated repression inhibitor 1
VDR	0,011707214	1,30876577	vitamin D (1,25- dihydroxyvitamin D3) receptor

SLA2	0,039026675	1,30874877	Src-like-adaptor 2
METTL3	0,002766495	1,3086095	methyltransferase like 3
LINC01133	0,010802345	1,30858583	long intergenic non-protein coding RNA 1133
HCG27	0,011228806	1,30815236	HLA complex group 27 (non-protein coding)
RAB9B	0,015459022	1,30811121	RAB9B, member RAS oncogene family
SLC7A11-AS1	0,02808087	1,30708568	SLC7A11 antisense RNA 1
LINC00605	0,000397355	1,30634243	long intergenic non-protein coding RNA 605
KRTAP4-5	0,024699045	1,30621681	keratin associated protein 4-5
PSMB9	0,000970699	1,3061081	proteasome (prosome, macropain) subunit, beta type, 9
PSMB9	0,000970699	1,3061081	proteasome (prosome, macropain) subunit, beta type, 9
PSMB9	0,000970699	1,3061081	proteasome (prosome, macropain) subunit, beta type, 9
FAM163A	0,002479577	1,30594872	family with sequence similarity 163, member A
KRTAP27-1	0,006785645	1,30518504	keratin associated protein 27-1
MTUS2-AS1	0,004660295	1,3048128	MTUS2 antisense RNA 1
LOC285740	0,003100162	1,30463468	uncharacterized LOC285740
CCDC115	0,028745079	1,30435386	coiled-coil domain containing 115
METTL6	0,038974863	1,30375592	methyltransferase like 6
TRIM35	0,005609546	1,30347307	tripartite motif containing 35
CDRT15	0,005867779	1,30344852	CMT1A duplicated region transcript 15
ADM	0,004850017	1,30343521	adrenomedullin
TMED1	0,002420481	1,30322357	transmembrane emp24 protein transport domain containing 1
SLCO3A1	0,001152535	1,30318418	solute carrier organic anion transporter family, member 3A1
NANOS1	0,004439153	1,30317821	nanos homolog 1 (Drosophila)
OTOL1	0,043359125	1,30308559	otolin 1
POU3F4	0,001604928	1,30292297	POU class 3 homeobox 4
TRPA1	0,004939931	1,30261283	transient receptor potential cation channel, subfamily A, member 1
GFAP	0,003350966	1,30217121	glial fibrillary acidic protein
MIR4534	0,047311812	1,30205225	microRNA 4534
TRIM46	0,000598968	1,3016715	tripartite motif containing 46

B3GALT6	0,001121245	1,30166005	UDP-Gal:betaGal beta 1,3-galactosyltransferase polypeptide 6
RNASEH2A	0,000540036	1,30020596	ribonuclease H2, subunit A

Supplemental Table 4: LPS down regulated genes in CD16+ MDDCs

Symbol	adj. p	FC	description
LPL	1,45E-05	-2,767835456	lipoprotein lipase
OCSTAMP	6,23E-06	-2,589996962	osteoclast stimulatory transmembrane protein
SPP1	0,03095551	-2,541131005	secreted phosphoprotein 1
ETV5	1,89E-05	-2,304477335	ets variant 5
ROCK1P1	0,04485881	-2,173537359	Rho-associated, coiled-coil containing protein kinase 1 pseudogene 1
GPC4	0,00091243	-2,149332855	glypican 4
CLEC19A	0,00085757	-2,127651351	C-type lectin domain family 19, member A
MERTK	2,99E-05	-2,09909593	MER proto-oncogene, tyrosine kinase
USP17L15	0,00909561	-2,003262907	ubiquitin specific peptidase 17-like family member 15
PTGFRN	0,01085785	-1,947670803	prostaglandin F2 receptor inhibitor
ERRFI1	0,00969738	-1,900857411	ERBB receptor feedback inhibitor 1
CHST15	0,001047	-1,889141366	carbohydrate (N-acetylgalactosamine 4-sulfate 6-O) sulfotransferase 15
PHLDA1	0,00024822	-1,88760527	pleckstrin homology-like domain, family A, member 1
ZNF93	0,00035721	-1,839240326	zinc finger protein 93
MYO1E	1,83E-06	-1,82935744	myosin IE
MIR548I3	0,00643356	-1,827073321	microRNA 548i-3
ACPP	0,00616781	-1,805166416	acid phosphatase, prostate
PITPNC1	2,87E-05	-1,789625705	phosphatidylinositol transfer protein, cytoplasmic 1
TNC	0,00998483	-1,773834789	tenascin C
DOCK3	0,00010218	-1,773193428	dedicator of cytokinesis 3
KLHL6	7,16E-07	-1,766955699	kelch-like family member 6
SORL1	0,0008654	-1,756984151	sortilin-related receptor, L(DLR class) A repeats containing
CD109	0,0078581	-1,726730047	CD109 molecule
SLC7A7	0,00077657	-1,724754487	solute carrier family 7 (amino acid transporter light chain, y+L system), member 7
KBTBD8	0,00115357	-1,718505267	kelch repeat and BTB (POZ) domain containing 8
CASS4	0,02783237	-1,710842942	Cas scaffolding protein family member 4
PDGFC	0,03393946	-1,71076994	platelet derived growth factor C

USP41	0,01172528	-1,703178767	ubiquitin specific peptidase 41
OR6C75	0,00858284	-1,698684981	olfactory receptor, family 6, subfamily C, member 75
SLC4A7	0,00054004	-1,685318218	solute carrier family 4, sodium bicarbonate cotransporter, member 7
TLR3	0,04515105	-1,670996061	toll-like receptor 3
ITGAE	2,41E-05	-1,663857212	integrin, alpha E (antigen CD103, human mucosal lymphocyte antigen 1; alpha polypeptide)
CA2	0,01680938	-1,651272024	carbonic anhydrase II
MCOLN3	0,0003328	-1,647066127	mucolipin 3
TMC8	1,98E-06	-1,632243452	transmembrane channel-like 8
DDIAS	0,00026019	-1,629439188	DNA damage-induced apoptosis suppressor
LOC286437	0,00074699	-1,617238243	uncharacterized LOC286437
TRPM2	0,00014847	-1,615868901	transient receptor potential cation channel, subfamily M, member 2
CAPNS2	0,00592599	-1,612717079	calpain, small subunit 2
GNGT2	0,00047569	-1,611779083	guanine nucleotide binding protein (G protein), gamma transducing activity polypeptide 2
MSR1	0,01074165	-1,610011423	macrophage scavenger receptor 1
CIART	0,00054115	-1,60893289	circadian associated repressor of transcription
STRBP	5,62E-05	-1,60296165	spermatid perinuclear RNA binding protein
LOC200772	3,69E-06	-1,582275525	uncharacterized LOC200772
MCTS2P	0,0288248	-1,572756407	malignant T cell amplified sequence 2, pseudogene
GPBAR1	0,00043258	-1,567043102	G protein-coupled bile acid receptor 1
CABP4	2,28E-06	-1,564294382	calcium binding protein 4
ABCA1	0,00068874	-1,559372546	ATP-binding cassette, sub-family A (ABC1), member 1
ITGAV	0,03318706	-1,558348388	integrin, alpha V
CC2D2B	0,00777518	-1,552823387	coiled-coil and C2 domain containing 2B
MIR767	0,00085787	-1,551370604	microRNA 767
NT5DC3	0,02564173	-1,544419855	5'-nucleotidase domain containing 3
RFPL4AL1	0,01593782	-1,542855399	ret finger protein-like 4A-like 1
BEST1	8,88E-05	-1,542374843	bestrophin 1
DTNB	0,0009947	-1,53845844	dystrobrevin, beta
TMEM2	0,01766924	-1,5382591	transmembrane protein 2

SAMD4A	0,00211276	-1,534009515	sterile alpha motif domain containing 4A
ZNF506	0,0064358	-1,532600974	zinc finger protein 506
PDLIM7	7,31E-05	-1,530595215	PDZ and LIM domain 7 (enigma)
LOC100289533	4,17E-05	-1,528812729	uncharacterized LOC100289533
KLF10	0,01241298	-1,524333691	Kruppel-like factor 10
RPL13AP20	7,53E-05	-1,518787654	ribosomal protein L13a pseudogene 20
CYYR1	0,03635987	-1,515970499	cysteine/tyrosine-rich 1
TMEM14A	0,01700151	-1,514465328	transmembrane protein 14A
HIST2H2AB	0,01257951	-1,513294705	histone cluster 2, H2ab
LSM6	0,00185826	-1,509069372	LSM6 homolog, U6 small nuclear RNA associated (S. cerevisiae)
ZMAT3	0,00046352	-1,501822135	zinc finger, matrin-type 3
MIR378E	0,01054676	-1,499222371	microRNA 378e
SIPA1L3	0,00078799	-1,495177211	signal-induced proliferation-associated 1 like 3
TMEM26	0,00303843	-1,494919543	transmembrane protein 26
FCGR3A	0,02131883	-1,491852254	Fc fragment of IgG, low affinity IIIa, receptor (CD16a)
ZNF573	0,00485774	-1,491576442	zinc finger protein 573
GPR174	0,03696092	-1,491536513	G protein-coupled receptor 174
MBP	0,00019967	-1,488236815	myelin basic protein
ABCC1	0,00112125	-1,486476205	ATP-binding cassette, sub-family C (CFTR/MRP), member 1
APP	0,00624143	-1,486164835	amyloid beta (A4) precursor protein
ZNF486	0,00654548	-1,483094724	zinc finger protein 486
RPL23AP53	0,00240467	-1,474397589	ribosomal protein L23a pseudogene 53
C10orf54	0,00305245	-1,473892197	chromosome 10 open reading frame 54
PMEPA1	0,01446822	-1,471361271	prostate transmembrane protein, androgen induced 1
MIR4727	0,02675053	-1,471169142	microRNA 4727
POLR2J	0,00321913	-1,466780823	polymerase (RNA) II (DNA directed) polypeptide J, 13.3kDa
BCAT1	0,02112882	-1,465779343	branched chain amino-acid transaminase 1, cytosolic
EPS8	0,00432769	-1,46432336	epidermal growth factor receptor pathway substrate 8
LINC00965	0,01038609	-1,463692782	long intergenic non-protein coding RNA 965

CATSPER1	0,00177752	-1,463457721	cation channel, sperm associated 1
TMEM51	0,02809101	-1,453360029	transmembrane protein 51
ETS1	0,02398809	-1,453231844	v-ets avian erythroblastosis virus E26 oncogene homolog 1
MOSPD2	9,35E-05	-1,437653439	motile sperm domain containing 2
RPS18	0,00242988	-1,436886276	ribosomal protein S18
ZNF563	0,0378406	-1,43532342	zinc finger protein 563
CCDC102B	0,01578904	-1,434745931	coiled-coil domain containing 102B
FMNL2	0,00076394	-1,433413614	formin-like 2
STIP1	2,41E-06	-1,426678087	stress-induced phosphoprotein 1
DEPTOR	0,01941812	-1,423095889	DEP domain containing MTOR-interacting protein
LPP-AS2	0,01203021	-1,420107746	LPP antisense RNA 2
C20orf27	0,00081695	-1,419306135	chromosome 20 open reading frame 27
PPM1H	0,00044484	-1,419017954	protein phosphatase, Mg2+/Mn2+ dependent, 1H
TGFB2	0,00768879	-1,4187548	transforming growth factor, beta 2
EIF1B	0,0051165	-1,417848776	eukaryotic translation initiation factor 1B
ZNF554	0,03620556	-1,416067229	zinc finger protein 554
TTC3P1	0,00263791	-1,414525558	tetratricopeptide repeat domain 3 pseudogene 1
RPS6KA2	0,00017091	-1,413966335	ribosomal protein S6 kinase, 90kDa, polypeptide 2
C11orf24	0,00573984	-1,412918295	chromosome 11 open reading frame 24
LOC100128668	0,0023815	-1,410917733	uncharacterized LOC100128668
FLJ43681	0,0086524	-1,41013873	ribosomal protein L23a pseudogene
RAB40B	0,00458733	-1,409409354	RAB40B, member RAS oncogene family
LOC115110	7,44E-05	-1,406740333	uncharacterized LOC115110
DNMT3A	0,00161184	-1,406347556	DNA (cytosine-5-)-methyltransferase 3 alpha
ZNF630	0,0288199	-1,406129781	zinc finger protein 630
SNORD116-15	0,03638432	-1,40342283	small nucleolar RNA, C/D box 116-15
PRR34	0,00013951	-1,402597457	proline rich 34
HIST1H1C	0,00771831	-1,401399629	histone cluster 1, H1c
ZNF714	0,04123948	-1,400777069	zinc finger protein 714

HEBP1	0,03454867	-1,400247992	heme binding protein 1
GOLM1	0,03261581	-1,399902144	golgi membrane protein 1
SLC28A3	0,00027346	-1,399095708	solute carrier family 28 (concentrative nucleoside transporter), member 3
ZRSR2	0,01110222	-1,398382568	zinc finger (CCCH type), RNA-binding motif and serine/arginine rich 2
LOC151475	0,02239145	-1,397677071	uncharacterized LOC151475
UBAC2	0,00060294	-1,397438285	UBA domain containing 2
POLA1	0,00236315	-1,391149023	polymerase (DNA directed), alpha 1, catalytic subunit
IGF2BP2	0,02436553	-1,387772643	insulin-like growth factor 2 mRNA binding protein 2
LOC100132352	0,01969596	-1,385635903	FSHD region gene 1 pseudogene
RASAL2	0,00426038	-1,383971719	RAS protein activator like 2
LOC100128508	0,01344749	-1,383728703	PP12100
RASSF1	0,00378103	-1,381014636	Ras association (RalGDS/AF-6) domain family member 1
LINC01422	0,01353779	-1,380835836	long intergenic non-protein coding RNA 1422
PLCXD1	4,42E-05	-1,378882889	phosphatidylinositol-specific phospholipase C, X domain containing 1
LGALSL	0,0171219	-1,377399382	lectin, galactoside-binding-like
ZNF329	0,00048835	-1,377347153	zinc finger protein 329
MCM6	0,00104519	-1,375834802	minichromosome maintenance complex component 6
MEF2D	3,02E-05	-1,374959944	myocyte enhancer factor 2D
PSG5	0,0462449	-1,373082339	pregnancy specific beta-1-glycoprotein 5
CD81	3,12E-05	-1,373079554	CD81 molecule
FKBP7	0,00111184	-1,373066382	FK506 binding protein 7
LINC00977	0,00824352	-1,372922145	long intergenic non-protein coding RNA 977
PGBD5	0,00307163	-1,37249649	piggyBac transposable element derived 5
CAMKK1	0,00120633	-1,372258221	calcium/calmodulin-dependent protein kinase kinase 1, alpha
RNF122	0,00013911	-1,371486106	ring finger protein 122
METTL7B	0,04378063	-1,370175082	methyltransferase like 7B
CD28	0,0038606	-1,365171351	CD28 molecule
MIR548J	0,04888486	-1,362195555	microRNA 548j
C10orf131	0,02128807	-1,361643004	chromosome 10 open reading frame 131

LOC100505909	0,00339507	-1,361634687	uncharacterized LOC100505909
ZNF100	0,00830115	-1,360626918	zinc finger protein 100
OR10J1	0,00249264	-1,360158162	olfactory receptor, family 10, subfamily J, member 1
FERMT1	0,01263924	-1,359807928	fermitin family member 1
AP4B1-AS1	0,00068333	-1,359724489	AP4B1 antisense RNA 1
GPRC5D	0,03970039	-1,359361543	G protein-coupled receptor, class C, group 5, member D
RPL22L1	0,00760461	-1,359054019	ribosomal protein L22-like 1
ZMYND11	0,0031097	-1,357443834	zinc finger, MYND-type containing 11
TULP4	0,01633409	-1,356576944	tubby like protein 4
CPB2	0,00982924	-1,356481751	carboxypeptidase B2 (plasma)
SLC35G6	0,04003482	-1,355437873	solute carrier family 35, member G6
MEP1A	0,01824132	-1,355247772	meprin A, alpha (PABA peptide hydrolase)
EXOC5	0,03780551	-1,354600455	exocyst complex component 5
LOC283440	0,0044623	-1,354477928	uncharacterized LOC283440
MAP1LC3C	0,01127859	-1,354420087	microtubule-associated protein 1 light chain 3 gamma
TSPAN4	0,00092616	-1,353699233	tetraspanin 4
DUXA	0,00184294	-1,353565153	double homeobox A
MIR181B1	0,04930392	-1,352451053	microRNA 181b-1
ZNF697	0,00032597	-1,351048858	zinc finger protein 697
ABHD12	0,00166172	-1,347679169	abhydrolase domain containing 12
XPNPEP3	0,00185256	-1,347571653	X-prolyl aminopeptidase (aminopeptidase P) 3, putative
SNORD66	0,00666451	-1,346771503	small nucleolar RNA, C/D box 66
RNF128	0,0114907	-1,346559681	ring finger protein 128, E3 ubiquitin protein ligase
FLNA	0,00152707	-1,344468361	filamin A, alpha
PLD4	0,01339988	-1,343660235	phospholipase D family, member 4
CALCR	0,0068943	-1,341941617	calcitonin receptor
NMD3	0,00563024	-1,341767396	NMD3 ribosome export adaptor
ELF5	0,00080689	-1,3415979	E74-like factor 5 (ets domain transcription factor)
ZNF112	0,02563608	-1,340069657	zinc finger protein 112

GAS6	0,00134589	-1,339358488	growth arrest-specific 6
SORBS1	0,01340506	-1,339207738	sorbin and SH3 domain containing 1
C19orf10	0,00041505	-1,338863543	chromosome 19 open reading frame 10
HCG8	0,0462445	-1,338584813	HLA complex group 8
TPTEP1	0,03562986	-1,335602498	transmembrane phosphatase with tensin homology pseudogene 1
LOC400541	0,0357821	-1,334685096	uncharacterized LOC400541
ZNF274	0,00022858	-1,334329973	zinc finger protein 274
LRRC3C	0,04349534	-1,333973274	leucine rich repeat containing 3C
TMEM130	0,00678185	-1,333570174	transmembrane protein 130
PICALM	0,00037943	-1,332819122	phosphatidylinositol binding clathrin assembly protein
LOC101927924	0,00014644	-1,332772041	uncharacterized LOC101927924
LONRF3	0,00356496	-1,332120969	LON peptidase N-terminal domain and ring finger 3
RPL39	0,00341134	-1,331457406	ribosomal protein L39
LOC641746	0,03747659	-1,331260748	glycine cleavage system protein H (aminomethyl carrier) pseudogene
BZW2	0,02523498	-1,331232804	basic leucine zipper and W2 domains 2
USP13	0,01053687	-1,329461897	ubiquitin specific peptidase 13 (isopeptidase T-3)
ZNF551	0,01817184	-1,329188449	zinc finger protein 551
FAM138C	0,01594365	-1,328263023	family with sequence similarity 138, member C
MTMR12	0,00166582	-1,32682117	myotubularin related protein 12
ALG10	0,01068316	-1,326211804	ALG10, alpha-1,2-glucosyltransferase
TXNRD1	0,03299491	-1,325874472	thioredoxin reductase 1
HOOK3	0,00171357	-1,325187718	hook microtubule-tethering protein 3
NBR2	0,00101717	-1,323845166	neighbor of BRCA1 gene 2 (non-protein coding)
LDOC1L	0,00319076	-1,323777071	leucine zipper, down-regulated in cancer 1-like
SUN2	0,04761981	-1,322769191	Sad1 and UNC84 domain containing 2
MAPKAPK5	0,0005277	-1,321248357	mitogen-activated protein kinase-activated protein kinase 5
PLEKHA6	0,00720102	-1,320395827	pleckstrin homology domain containing, family A member 6
LRIG1	0,00752621	-1,320199183	leucine-rich repeats and immunoglobulin-like domains 1
PIAS2	0,02730918	-1,316146378	protein inhibitor of activated STAT, 2

AGO2	0,00794925	-1,315537084	argonaute RISC catalytic component 2
STK39	0,00537462	-1,314907934	serine threonine kinase 39
HDAC9	0,00323155	-1,314334705	histone deacetylase 9
ATR	0,00833876	-1,313374595	ATR serine/threonine kinase
MIG7	0,04731482	-1,313212354	mig-7
ADAM1A	0,03478149	-1,312780711	ADAM metallopeptidase domain 1A, pseudogene
MIEF1	0,0035842	-1,310305086	mitochondrial elongation factor 1
RPL22	0,00096707	-1,307874834	ribosomal protein L22
CCDC28A	0,00040235	-1,307743974	coiled-coil domain containing 28A
RPTOR	0,00024114	-1,307634484	regulatory associated protein of MTOR, complex 1
HECA	0,00427652	-1,307162743	headcase homolog (Drosophila)
CBX3	0,01233404	-1,307154722	chromobox homolog 3
LOC729987	0,02242553	-1,305303565	uncharacterized LOC729987
C1orf180	0,01935646	-1,304697746	chromosome 1 open reading frame 180
IL1RL2	0,03583293	-1,304657408	interleukin 1 receptor-like 2
LOC100507316	0,01761792	-1,302911727	uncharacterized LOC100507316
ZNF677	0,01139516	-1,302631674	zinc finger protein 677
LINC00470	0,00433167	-1,302597005	long intergenic non-protein coding RNA 470
ESF1	0,02052807	-1,301846584	ESF1, nucleolar pre-rRNA processing protein, homolog (S. cerevisiae)
GCSHP3	0,01642234	-1,300148285	glycine cleavage system protein H (aminomethyl carrier) pseudogene 3

Supplemental Table 5: LPS up regulated genes in CD16- MDDCs

Symbol	adj. p	FC	description
MMP10	0,00010874	9,84407272	matrix metallopeptidase 10 (stromelysin 2)
MMP1	0,00121759	6,53092248	matrix metallopeptidase 1 (interstitial collagenase)
TGM2	0,00050368	3,6065825	transglutaminase 2
NCCRP1	5,67E-05	3,45171634	non-specific cytotoxic cell receptor protein 1 homolog (zebrafish)
TNFRSF11A	0,00020385	2,7021087	tumor necrosis factor receptor superfamily, member 11a, NFKB activator
IL1A	0,03703324	2,44590278	interleukin 1, alpha
DCLK2	0,00037846	2,36559735	doublecortin-like kinase 2
TMEM176B	0,03647502	2,31916068	transmembrane protein 176B
LAMC2	0,00181119	2,20642343	laminin, gamma 2
FAM13A	4,55E-06	2,15766995	family with sequence similarity 13, member A
ROBO1	0,02104274	2,08560438	roundabout, axon guidance receptor, homolog 1 (Drosophila)
ZNF608	5,36E-07	2,07076125	zinc finger protein 608
TBC1D9	3,54E-06	1,99345149	TBC1 domain family, member 9 (with GRAM domain)
HSD52	4,03E-05	1,96331694	uncharacterized LOC729467
LAMP1	0,00508357	1,94399198	lysosomal-associated membrane protein 1
GBP6	0,00628319	1,94096415	guanylate binding protein family, member 6
MMP8	0,01799375	1,91456843	matrix metallopeptidase 8 (neutrophil collagenase)
CSRP2	1,25E-05	1,8870485	cysteine and glycine-rich protein 2
DSC2	0,00019583	1,87071869	desmocollin 2
DLGAP1-AS2	0,00023045	1,83974752	DLGAP1 antisense RNA 2
CHD7	7,45E-07	1,82730927	chromodomain helicase DNA binding protein 7
RGS2	0,00133739	1,81602648	regulator of G-protein signaling 2
SULT1C4	0,00123928	1,81321328	sulfotransferase family, cytosolic, 1C, member 4
FBN1	1,00E-10	1,81276053	fibrillin 1
SLC16A9	0,01563733	1,80138643	solute carrier family 16, member 9
ALDH1L2	0,00041277	1,79277009	aldehyde dehydrogenase 1 family, member L2
CEP70	9,61E-05	1,79005838	centrosomal protein 70kDa

IL1RN	0,00553958	1,78359072	interleukin 1 receptor antagonist
FOXD4	0,03462564	1,74482951	forkhead box D4
TREM1	0,03212097	1,72862125	triggering receptor expressed on myeloid cells 1
SNORA70C	0,00669115	1,72008043	small nucleolar RNA, H/ACA box 70C
LUM	0,00056495	1,71889576	lumican
TLE1	0,00218665	1,71686285	transducin-like enhancer of split 1 (E(sp1) homolog, Drosophila)
URAD	2,52E-05	1,70391898	ureidoimidazoline (2-oxo-4-hydroxy-4-carboxy-5-) decarboxylase
IL31RA	0,00119256	1,70227019	interleukin 31 receptor A
SEL1L3	0,03400768	1,69089625	sel-1 suppressor of lin-12-like 3 (C. elegans)
PTPRG	0,00261407	1,6894293	protein tyrosine phosphatase, receptor type, G
YBX3P1	0,0005595	1,68715273	Y box binding protein 3 pseudogene 1
AMOT	0,00553184	1,67132484	angiomotin
MALT1	0,00218712	1,66513949	mucosa associated lymphoid tissue lymphoma translocation gene 1
RNU6-55P	0,0065015	1,66329444	RNA, U6 small nuclear 55, pseudogene
NBEAL2	3,01E-05	1,65731248	neurobeachin-like 2
TUBAL3	0,00056838	1,65468545	tubulin, alpha-like 3
ZFP69B	3,00E-07	1,65207388	ZFP69 zinc finger protein B
LYPD1	0,00081913	1,64928888	LY6/PLAUR domain containing 1
LOC100130476	0,00033461	1,643935	uncharacterized LOC100130476
RET	1,58E-05	1,64011425	ret proto-oncogene
BAALC	0,00051687	1,63865504	brain and acute leukemia, cytoplasmic
ENPP6	0,00030621	1,6375102	ectonucleotide pyrophosphatase/phosphodiesterase 6
OSBPL3	0,00153562	1,63565664	oxysterol binding protein-like 3
ALCAM	0,01302005	1,63489501	activated leukocyte cell adhesion molecule
BHLHA15	2,55E-05	1,63310778	basic helix-loop-helix family, member a15
PTP4A3	0,00474589	1,6296168	protein tyrosine phosphatase type IVA, member 3
PPARG	0,02326198	1,61789582	peroxisome proliferator-activated receptor gamma
METTL1	0,00222099	1,60564404	methyltransferase like 1
RAPGEF5	0,00034274	1,60397062	Rap guanine nucleotide exchange factor (GEF) 5

KLHL42	0,00221448	1,60335415	kelch-like family member 42
LOC154761	0,0056715	1,59804231	family with sequence similarity 115, member C pseudogene
UBE2R2	2,55E-07	1,59580564	ubiquitin-conjugating enzyme E2R 2
MIR139	6,67E-06	1,59031841	microRNA 139
GPR55	0,00047136	1,57999724	G protein-coupled receptor 55
PROB1	0,0005829	1,56871517	proline-rich basic protein 1
LANCL2	0,00014411	1,5665287	LanC lantibiotic synthetase component C-like 2 (bacterial)
APOD	0,00257231	1,56335639	apolipoprotein D
HCG27	0,01322876	1,56225611	HLA complex group 27 (non-protein coding)
ZXDA	5,63E-05	1,5583292	zinc finger, X-linked, duplicated A
SMCO4	0,00123748	1,55131649	single-pass membrane protein with coiled-coil domains 4
RNF150	0,0371703	1,55113827	ring finger protein 150
STEAP1B	0,00141887	1,54927896	STEAP family member 1B
LDHAL6B	0,00075682	1,54810039	lactate dehydrogenase A-like 6B
IL2RG	0,00100744	1,54245025	interleukin 2 receptor, gamma
MIR3685	0,01553237	1,53328738	microRNA 3685
SFMBT2	0,0014358	1,5328886	Scm-like with four mbt domains 2
MEX3C	0,00120115	1,52966529	mex-3 RNA binding family member C
MXRA5	5,42E-05	1,52860501	matrix-remodelling associated 5
DENND5B	0,00010815	1,52798282	DENN/MADD domain containing 5B
PRKCA	0,01786917	1,52512252	protein kinase C, alpha
MIR1183	0,00932307	1,51660195	microRNA 1183
LINC00467	0,0044964	1,51415048	long intergenic non-protein coding RNA 467
ENO3	0,0006588	1,51358243	enolase 3 (beta, muscle)
STX17-AS1	0,00052805	1,50973665	STX17 antisense RNA 1
PXDC1	0,00032209	1,50812138	PX domain containing 1
GEMIN8P4	0,00423541	1,50661887	gem (nuclear organelle) associated protein 8 pseudogene 4
RGS6	0,00037009	1,50482214	regulator of G-protein signaling 6
ULK4P3	0,01574078	1,50387441	ULK4 pseudogene 3

MIR196A2	0,00209078	1,50194427	microRNA 196a-2
NCAPG	0,01888124	1,49591556	non-SMC condensin I complex, subunit G
MIR4529	0,00360645	1,4923092	microRNA 4529
SGOL1	0,00982665	1,48777803	shugoshin-like 1 (S. pombe)
KRT6B	0,00942411	1,48515873	keratin 6B
DAPL1	0,00888402	1,48494793	death associated protein-like 1
HTR2B	0,00011349	1,48443539	5-hydroxytryptamine (serotonin) receptor 2B, G protein-coupled
ARHGAP22	0,03134851	1,48039582	Rho GTPase activating protein 22
LINC00540	0,00103639	1,48014961	long intergenic non-protein coding RNA 540
C6orf226	0,00117497	1,47610627	chromosome 6 open reading frame 226
CXorf65	0,00254515	1,4732676	chromosome X open reading frame 65
OR6P1	0,01352039	1,47318569	olfactory receptor, family 6, subfamily P, member 1
PACSIN2	0,03136255	1,47107583	protein kinase C and casein kinase substrate in neurons 2
CXCL6	0,00930794	1,46769959	chemokine (C-X-C motif) ligand 6
IL1R1	0,02477091	1,46731032	interleukin 1 receptor, type I
C6orf106	3,74E-06	1,46698461	chromosome 6 open reading frame 106
DLL4	0,01437969	1,46557737	delta-like 4 (Drosophila)
ACOT4	0,00188839	1,46506219	acyl-CoA thioesterase 4
FCHSD2	0,00102854	1,46373356	FCH and double SH3 domains 2
USP27X	0,03486878	1,46196775	ubiquitin specific peptidase 27, X-linked
PPP1R2	3,17E-05	1,46163676	protein phosphatase 1, regulatory (inhibitor) subunit 2
CAPN6	8,30E-05	1,46080386	calpain 6
ENOX1	0,00119875	1,45984509	ecto-NOX disulfide-thiol exchanger 1
LOC401312	0,02160285	1,45765615	uncharacterized LOC401312
PRB4	0,00471365	1,45723028	proline-rich protein BstNI subfamily 4
RSPH10B	0,00010562	1,45680468	radial spoke head 10 homolog B (Chlamydomonas)
HGF	0,0046325	1,45370753	hepatocyte growth factor (hepapoietin A; scatter factor)
ZNF581	0,00063743	1,45286845	zinc finger protein 581
SPECC1	0,00051929	1,44710918	sperm antigen with calponin homology and coiled-coil domains 1

SNORD11B	0,0318753	1,44469489	small nucleolar RNA, C/D box 11B
ATP11A	0,01015482	1,44405273	ATPase, class VI, type 11A
ABCD1	2,84E-05	1,44402406	ATP-binding cassette, sub-family D (ALD), member 1
TAC3	0,00131159	1,4434761	tachykinin 3
IFT57	0,00827512	1,44104695	intraflagellar transport 57
CCDC30	0,00847249	1,44078357	coiled-coil domain containing 30
TRIB1	0,01394086	1,44007418	tribbles pseudokinase 1
ROR1	0,01054616	1,43880754	receptor tyrosine kinase-like orphan receptor 1
AP1S3	0,02730301	1,43566508	adaptor-related protein complex 1, sigma 3 subunit
OVOL2	0,00081475	1,4353668	ovo-like zinc finger 2
IL6ST	0,00831284	1,43444991	interleukin 6 signal transducer
KRTAP19-8	0,01650805	1,43317239	keratin associated protein 19-8
IL23A	0,00425683	1,43269329	interleukin 23, alpha subunit p19
MIR4660	0,01544226	1,42795642	microRNA 4660
ITPR1	0,03116663	1,42632538	inositol 1,4,5-trisphosphate receptor, type 1
RAPH1	0,04005715	1,42392107	Ras association (RalGDS/AF-6) and pleckstrin homology domains 1
CELSR1	0,00500063	1,42327308	cadherin, EGF LAG seven-pass G-type receptor 1
LOX	0,00266988	1,42296415	lysyl oxidase
ACTA2	0,00130778	1,42295786	actin, alpha 2, smooth muscle, aorta
LINC01359	0,00795274	1,42257521	long intergenic non-protein coding RNA 1359
LINC01000	0,01031066	1,42181922	long intergenic non-protein coding RNA 1000
ELMSAN1	0,00184753	1,42079212	ELM2 and Myb/SANT-like domain containing 1
COCH	0,01842659	1,42047763	cochlin
KRTAP9-8	0,00237863	1,41891868	keratin associated protein 9-8
LOC93432	0,03518739	1,41809172	maltase-glucoamylase (alpha-glucosidase)
LOC100652931	0,00685452	1,41691712	RNA binding motif protein, Y-linked, family 1, member A1 pseudogene
SNORD13P2	0,01306252	1,41604555	small nucleolar RNA, C/D box 13 pseudogene 2
RAD51	0,00711707	1,41481313	RAD51 recombinase
MKNK2	0,00081924	1,41440286	MAP kinase interacting serine/threonine kinase 2

FLJ45248	0,00954192	1,41358928	FLJ45248 protein
EGOT	0,00245647	1,41285667	eosinophil granule ontogeny transcript (non-protein coding)
CYP2J2	0,0026036	1,41274795	cytochrome P450, family 2, subfamily J, polypeptide 2
TBC1D1	0,00219963	1,41142462	TBC1 (tre-2/USP6, BUB2, cdc16) domain family, member 1
RPS27A	0,0024681	1,40790602	ribosomal protein S27a
S100A3	0,01328032	1,40771728	S100 calcium binding protein A3
YME1L1	0,02456638	1,40492576	YME1-like 1 ATPase
AES	0,01600998	1,40276491	amino-terminal enhancer of split
SNORA77	0,04166989	1,40241387	small nucleolar RNA, H/ACA box 77
RNF17	0,00059201	1,40158172	ring finger protein 17
HTR1D	0,00112043	1,40076279	5-hydroxytryptamine (serotonin) receptor 1D, G protein-coupled
ASH1L-AS1	0,00060153	1,39714523	ASH1L antisense RNA 1
DRD4	0,01605167	1,39576584	dopamine receptor D4
BAALCOS	0,01247766	1,39562286	BAALC opposite strand
MGAT3	0,00011293	1,39252214	mannosyl (beta-1,4-)-glycoprotein beta-1,4-N-acetylglucosaminyltransferase
LINC01391	0,00752353	1,39201298	long intergenic non-protein coding RNA 1391
SLC36A4	0,00625696	1,3917917	solute carrier family 36 (proton/amino acid symporter), member 4
ENDOU	0,00880484	1,39157632	endonuclease, polyU-specific
TNKS1BP1	0,00040895	1,39108887	tankyrase 1 binding protein 1, 182kDa
STRN3	0,01786917	1,38928344	striatin, calmodulin binding protein 3
FAM117A	4,16E-06	1,38883488	family with sequence similarity 117, member A
GABARAPL2	0,00447648	1,38867166	GABA(A) receptor-associated protein-like 2
NDC80	0,00179936	1,38854244	NDC80 kinetochore complex component
TGFA	0,0448859	1,3884865	transforming growth factor, alpha
MIR665	0,03660083	1,38845172	microRNA 665
FANCI	0,02297811	1,386688	Fanconi anemia, complementation group I
OR6C4	0,02915088	1,38473674	olfactory receptor, family 6, subfamily C, member 4
LOC643085	0,00031463	1,38457791	uncharacterized LOC643085
STAG3L4	0,00233665	1,38396832	stromal antigen 3-like 4 (pseudogene)

ARRB2	2,78E-05	1,3827333	arrestin, beta 2
TOR4A	0,01855731	1,38152471	torsin family 4, member A
MIR3189	0,02312562	1,38123283	microRNA 3189
LOC389607	0,01452049	1,376713	uncharacterized LOC389607
ARHGEF3	0,02567796	1,37580606	Rho guanine nucleotide exchange factor (GEF) 3
CUTC	0,00297318	1,37569816	cutC copper transporter
DEXI	0,0016965	1,37518346	Dexi homolog (mouse)
CLSTN1	0,00088831	1,37472969	calsyntenin 1
CST2	0,0203123	1,37046626	cystatin SA
MYOZ1	0,00848976	1,37043232	myozenin 1
LOC723805	0,0273346	1,37020169	interleukin-like
EDIL3	0,02298555	1,36916241	EGF-like repeats and discoidin I-like domains 3
ERVK13-1	0,03203536	1,3680835	endogenous retrovirus group K13, member 1
GTF2IRD2B	0,0435421	1,36670142	GTF2I repeat domain containing 2B
TAL2	0,00633731	1,36570417	T-cell acute lymphocytic leukemia 2
APOA1	0,00105014	1,36525984	apolipoprotein A-I
OAF	0,00172334	1,36506981	OAF homolog (Drosophila)
FAHD2CP	0,04042811	1,36386175	fumarylacetoacetate hydrolase domain containing 2C, pseudogene
TMEM72-AS1	0,01395915	1,36365019	TMEM72 antisense RNA 1
CDCA4	0,00109383	1,361577	cell division cycle associated 4
CHRNA10	0,01224152	1,36145245	cholinergic receptor, nicotinic, alpha 10 (neuronal)
FGFR1OP	0,00050546	1,36079769	FGFR1 oncogene partner
LAMB1	0,04265295	1,35936966	laminin, beta 1
PTCD2	0,02509316	1,35860582	pentatricopeptide repeat domain 2
CHIAP2	0,04695095	1,3576481	chitinase, acidic pseudogene 2
ARL13B	0,01509087	1,35542273	ADP-ribosylation factor-like 13B
MIRLET7A1	0,01689638	1,35437064	microRNA let-7a-1
PTGS2	0,02323166	1,3529559	prostaglandin-endoperoxide synthase 2 (prostaglandin G/H synthase and cyclooxygenase)
FABP5	0,02478833	1,35157664	fatty acid binding protein 5 (psoriasis-associated)

SERPINB3	0,02009834	1,35148534	serpin peptidase inhibitor, clade B (ovalbumin), member 3
GFPT2	0,00098748	1,35115151	glutamine-fructose-6-phosphate transaminase 2
TECTA	0,0046488	1,3510723	tectorin alpha
FAM71B	0,00894823	1,34707329	family with sequence similarity 71, member B
THAP9	0,02234681	1,3465939	THAP domain containing 9
ZNF600	0,03617649	1,34658659	zinc finger protein 600
SPTSSB	0,00032345	1,34651278	serine palmitoyltransferase, small subunit B
CEACAM22P	0,00851193	1,3463478	carcinoembryonic antigen-related cell adhesion molecule 2, pseudogene
ASMTL	0,02557718	1,34546095	acetylserotonin O-methyltransferase-like
LOC100507564	0,00577303	1,34487766	uncharacterized LOC100507564
MYH7	0,01049147	1,34355082	myosin, heavy chain 7, cardiac muscle, beta
OR3A3	0,02295028	1,34209189	olfactory receptor, family 3, subfamily A, member 3
EHD1	0,01972088	1,34072972	EH-domain containing 1
FNIP2	0,02569521	1,33881817	folliculin interacting protein 2
TMTC2	0,00192777	1,33874333	transmembrane and tetratricopeptide repeat containing 2
DUSP16	0,02777451	1,33773927	dual specificity phosphatase 16
DEFB108B	0,03285613	1,33747565	defensin, beta 108B
SLC35D1	0,00809797	1,33661353	solute carrier family 35 (UDP-GlcA/UDP-GalNAc transporter), member D1
LINC01482	0,01816117	1,33568994	long intergenic non-protein coding RNA 1482
AXIN2	0,0074874	1,33565995	axin 2
LINC01101	0,00890403	1,33505614	long intergenic non-protein coding RNA 1101
FIZ1	0,00825088	1,33320874	FLT3-interacting zinc finger 1
POM121L10P	0,02022838	1,33315072	POM121 transmembrane nucleoporin-like 10, pseudogene
SYNJ2	0,01935401	1,3316833	synaptojanin 2
MIR500A	0,00121283	1,33110893	microRNA 500a
LINC00173	0,02367898	1,33075497	long intergenic non-protein coding RNA 173
MRGPRX1	0,02104274	1,32989957	MAS-related GPR, member X1
OR1L6	0,0463079	1,32932522	olfactory receptor, family 1, subfamily L, member 6
SRP19	0,00352481	1,32903366	signal recognition particle 19kDa

GCKR	0,00160376	1,32865899	glucokinase (hexokinase 4) regulator
ZNF260	0,02206843	1,3286024	zinc finger protein 260
DLGAP4-AS1	0,00306129	1,32856673	DLGAP4 antisense RNA 1
CAMTA1	0,00019902	1,32747457	calmodulin binding transcription activator 1
NUDT15	0,02190818	1,32514332	nudix (nucleoside diphosphate linked moiety X)-type motif 15
LOC440982	0,00557025	1,32444386	uncharacterized LOC440982
PIGX	0,00587423	1,32405698	phosphatidylinositol glycan anchor biosynthesis, class X
TARP	0,02005161	1,32105843	TCR gamma alternate reading frame protein
PALLD	0,00094364	1,31978867	palladin, cytoskeletal associated protein
FAM83G	0,02127246	1,31968213	family with sequence similarity 83, member G
RABGAP1	0,00050115	1,31935638	RAB GTPase activating protein 1
CCDC90B	0,00755509	1,31791839	coiled-coil domain containing 90B
RRM2	0,00739034	1,31656357	ribonucleotide reductase M2
NRXN2	0,02782997	1,31639368	neurexin 2
OR1F2P	0,00779448	1,31617419	olfactory receptor, family 1, subfamily F, member 2
C2CD4A	0,01108996	1,31576446	C2 calcium-dependent domain containing 4A
RRN3P3	0,0059694	1,315292	RNA polymerase I transcription factor homolog (S. cerevisiae) pseudogene 3
THNSL2	0,00226623	1,3140497	threonine synthase-like 2 (S. cerevisiae)
MIR4804	0,02782986	1,31211361	microRNA 4804
STK11	0,00194406	1,31209095	serine/threonine kinase 11
ANGPTL4	0,00583191	1,31169177	angiopoietin-like 4
RAPGEF1	0,00347238	1,31063594	Rap guanine nucleotide exchange factor (GEF) 1
PSG10P	0,03251818	1,30971374	pregnancy specific beta-1-glycoprotein 10, pseudogene
LOC728989	0,04094152	1,30934792	phosphodiesterase 4D interacting protein pseudogene
ANKRD20A9P	0,03004043	1,30715513	ankyrin repeat domain 20 family, member A9, pseudogene
FAM78B	0,01667191	1,30511785	family with sequence similarity 78, member B
TBC1D19	0,01712013	1,30471176	TBC1 domain family, member 19
RASA1	0,02839614	1,30355847	RAS p21 protein activator (GTPase activating protein) 1
CASC4	0,00151231	1,30335462	cancer susceptibility candidate 4

ZBTB21	0,00109899	1,30319679	zinc finger and BTB domain containing 21
CEP89	0,00086334	1,30302137	centrosomal protein 89kDa
C7orf66	0,02366215	1,30231678	chromosome 7 open reading frame 66
MIRLET7I	0,02160285	1,30202918	microRNA let-7i
RGS20	0,02079368	1,30170476	regulator of G-protein signaling 20
AP4M1	0,00177067	1,30126013	adaptor-related protein complex 4, mu 1 subunit

Supplemental Table 6: LPS down regulated genes in CD16- MDDCs

Symbol	adj. p	FC	description
CD24	0,000499533	-20,001668	CD24 molecule
STEAP4	1,75E-06	-8,6502205	STEAP family member 4
SLC40A1	1,60E-06	-5,4747125	solute carrier family 40 (iron-regulated transporter), member 1
CD163L1	2,21E-06	-5,379027	CD163 molecule-like 1
RXFP1	1,60E-06	-5,2782444	relaxin/insulin-like family peptide receptor 1
MIR146B	3,43E-06	-5,068615	microRNA 146b
PAK7	6,72E-11	-4,9638446	p21 protein (Cdc42/Rac)-activated kinase 7
CCL18	5,12E-05	-4,4359942	chemokine (C-C motif) ligand 18 (pulmonary and activation-regulated)
GPR34	0,002101415	-3,2156477	G protein-coupled receptor 34
CADM3	0,000123844	-3,178473	cell adhesion molecule 3
IL17RB	2,36E-05	-3,1411647	interleukin 17 receptor B
CD207	0,03974339	-3,1022789	CD207 molecule, langerin
CD180	0,002048505	-3,0789129	CD180 molecule
FOLR2	2,61E-05	-3,0046642	folate receptor 2 (fetal)
SH3PXD2B	3,34E-06	-2,9031087	SH3 and PX domains 2B
COL14A1	1,54E-05	-2,9022029	collagen, type XIV, alpha 1
SNORD75	2,20E-06	-2,7974126	small nucleolar RNA, C/D box 75
LGMN	0,001107383	-2,7157909	legumain
SLC25A23	0,000364522	-2,6188486	solute carrier family 25 (mitochondrial carrier; phosphate carrier), member 23
MS4A7	0,005428892	-2,5804042	membrane-spanning 4-domains, subfamily A, member 7
MIR3174	0,00063092	-2,4401554	microRNA 3174
CRH	1,92E-07	-2,4097644	corticotropin releasing hormone
CLEC4M	1,64E-05	-2,3682708	C-type lectin domain family 4, member M
ME1	0,006232556	-2,3560572	malic enzyme 1, NADP(+)-dependent, cytosolic
TSPAN15	8,08E-05	-2,3304277	tetraspanin 15
SNORD104	0,017892754	-2,3245559	small nucleolar RNA, C/D box 104
CACNA1D	0,001428839	-2,3058106	calcium channel, voltage-dependent, L type, alpha 1D subunit

TIMP1	0,001177993	-2,2935295	TIMP metallopeptidase inhibitor 1
CD69	0,04220658	-2,275088	CD69 molecule
CD163	0,011676421	-2,2310124	CD163 molecule
SMARCA1	0,000179892	-2,1800704	SWI/SNF related, matrix associated, actin dependent regulator of chromatin, subfamily a, member 1
IL10	0,003749465	-2,1780732	interleukin 10
ESAM	1,40E-07	-2,1705069	endothelial cell adhesion molecule
MIR4520-1	0,006763103	-2,1425697	microRNA 4520-1
NOV	1,63E-05	-2,1013819	nephroblastoma overexpressed
HIST1H2AJ	0,007629355	-2,0730082	histone cluster 1, H2aj
TREML2	0,005753383	-2,0454538	triggering receptor expressed on myeloid cells-like 2
ITGA9	0,030961006	-1,9982146	integrin, alpha 9
NCR3LG1	0,000208661	-1,9827211	natural killer cell cytotoxicity receptor 3 ligand 1
SERPINI1	0,008100131	-1,9818424	serpin peptidase inhibitor, clade I (neuroserpin), member 1
HSPA2	0,000597491	-1,942542	heat shock 70kDa protein 2
HSD17B14	0,001339216	-1,9394908	hydroxysteroid (17-beta) dehydrogenase 14
MPO	0,034448903	-1,9368248	myeloperoxidase
RHPN1-AS1	3,38E-07	-1,9340079	RHPN1 antisense RNA 1 (head to head)
FAM95B1	4,07E-05	-1,9212645	family with sequence similarity 95, member B1
SNHG8	9,46E-05	-1,916005	small nucleolar RNA host gene 8 (non-protein coding)
ATP13A2	0,000107102	-1,910537	ATPase type 13A2
LINC00967	4,34E-05	-1,8992503	long intergenic non-protein coding RNA 967
LAIR1	0,002790157	-1,8978046	leukocyte-associated immunoglobulin-like receptor 1
SLC35F3	0,001753925	-1,8952076	solute carrier family 35, member F3
SEPP1	0,000225915	-1,8902953	selenoprotein P, plasma, 1
ANTXR1	0,000452928	-1,8700233	anthrax toxin receptor 1
EDDM3A	0,000148935	-1,867113	epididymal protein 3A
MOCOS	0,002877427	-1,8656038	molybdenum cofactor sulfurase
COLEC12	0,006844418	-1,8653507	collectin sub-family member 12
ID1	0,000478973	-1,8539048	inhibitor of DNA binding 1, dominant negative helix-loop-helix protein

GATSL2	0,000109505	-1,8408549	GATS protein-like 2
ADRB2	0,003802233	-1,8407055	adrenoceptor beta 2, surface
RNF138P1	0,000188216	-1,8363838	ring finger protein 138, E3 ubiquitin protein ligase pseudogene 1
ATP6V0D2	0,013742496	-1,8348259	ATPase, H+ transporting, lysosomal 38kDa, V0 subunit d2
HR	2,05E-07	-1,8287868	hair growth associated
SLC11A2	0,000294502	-1,8234123	solute carrier family 11 (proton-coupled divalent metal ion transporter), member 2
RHO	0,000100989	-1,8210092	rhodopsin
BCRP3	0,044028168	-1,8106542	breakpoint cluster region pseudogene 3
MIR3143	0,001857726	-1,7952666	microRNA 3143
ZFP14	0,005515905	-1,7946576	ZFP14 zinc finger protein
SLC16A10	0,000386458	-1,7807195	solute carrier family 16 (aromatic amino acid transporter), member 10
LINC00264	0,0056115	-1,7805193	long intergenic non-protein coding RNA 264
CD99P1	0,003101948	-1,7701808	CD99 molecule pseudogene 1
RASD1	0,00067543	-1,761895	RAS, dexamethasone-induced 1
MIR425	0,002063472	-1,7586574	microRNA 425
CD34	0,008222423	-1,7584199	CD34 molecule
SHROOM2	5,04E-06	-1,7530949	shroom family member 2
GPX3	1,37E-05	-1,7425819	glutathione peroxidase 3 (plasma)
CRYM-AS1	4,76E-05	-1,7255143	CRYM antisense RNA 1
DNASE2	0,028941828	-1,7220985	deoxyribonuclease II, lysosomal
TMEM37	0,00014734	-1,7169021	transmembrane protein 37
ESCO2	0,000463582	-1,7137675	establishment of sister chromatid cohesion N-acetyltransferase 2
ACKR1	0,001235875	-1,7063119	atypical chemokine receptor 1 (Duffy blood group)
SNORA26	0,001260323	-1,7021998	small nucleolar RNA, H/ACA box 26
IQCK	0,000141109	-1,7015971	IQ motif containing K
HCAR1	0,00017281	-1,7000946	hydroxycarboxylic acid receptor 1
RCAN1	0,000268924	-1,6852945	regulator of calcineurin 1
IFT88	2,62E-05	-1,6845418	intraflagellar transport 88
SMAGP	0,000121436	-1,6784331	small cell adhesion glycoprotein

RRS1-AS1	0,000273802	-1,677287	RRS1 antisense RNA 1 (head to head)
MIR938	0,000604885	-1,6772719	microRNA 938
HHLA2	0,029556541	-1,6696313	HERV-H LTR-associating 2
LINC01150	8,65E-06	-1,6628515	long intergenic non-protein coding RNA 1150
LOC100288814	0,000116889	-1,6622281	uncharacterized LOC100288814
NDUFA6-AS1	0,000286547	-1,6533974	NDUFA6 antisense RNA 1 (head to head)
BMPR1A	0,028101578	-1,6531444	bone morphogenetic protein receptor, type IA
RTN4IP1	3,07E-06	-1,6491016	reticulon 4 interacting protein 1
AKR7A3	0,000454975	-1,643009	aldo-keto reductase family 7, member A3 (aflatoxin aldehyde reductase)
CTSD	0,002812954	-1,6428395	cathepsin D
ZNF724P	0,025678991	-1,6416131	zinc finger protein 724, pseudogene
LOC648987	0,00026769	-1,6310908	uncharacterized LOC648987
PPFIBP2	6,66E-05	-1,6306711	PTPRF interacting protein, binding protein 2 (liprin beta 2)
COLGALT2	0,000617804	-1,6257704	collagen beta(1-O)galactosyltransferase 2
NFE2	4,70E-05	-1,6253116	nuclear factor, erythroid 2
HSPA4L	0,010513341	-1,6247748	heat shock 70kDa protein 4-like
LOC389641	1,88E-06	-1,6174877	uncharacterized LOC389641
MAGED2	0,008411199	-1,613271	melanoma antigen family D, 2
B3GNTL1	0,000116605	-1,6131269	UDP-GlcNAc:betaGal beta-1,3-N-acetylglucosaminyltransferase-like 1
ICA1	0,000231873	-1,6116932	islet cell autoantigen 1, 69kDa
IBA57-AS1	5,91E-05	-1,60445	IBA57 antisense RNA 1 (head to head)
FAM95B1	0,004920554	-1,6030774	family with sequence similarity 95, member B1
MAFA	1,44E-05	-1,6003577	v-maf avian musculoaponeurotic fibrosarcoma oncogene homolog A
ZNF17	0,002692983	-1,6002171	zinc finger protein 17
DNAJC5B	0,002217369	-1,5972639	DnaJ (Hsp40) homolog, subfamily C, member 5 beta
ZNF567	0,000437961	-1,5963279	zinc finger protein 567
ZNF763	0,021909973	-1,5920757	zinc finger protein 763
PMFBP1	3,19E-05	-1,5906457	polyamine modulated factor 1 binding protein 1
TRIM15	0,000221752	-1,5878638	tripartite motif containing 15

TFAP2C	0,000709137	-1,5873363	transcription factor AP-2 gamma (activating enhancer binding protein 2 gamma)
HS3ST2	0,011996668	-1,5832958	heparan sulfate (glucosamine) 3-O-sulfotransferase 2
MTMR9LP	1,33E-05	-1,5797289	myotubularin related protein 9-like, pseudogene
GPR135	0,000295619	-1,5752243	G protein-coupled receptor 135
PKD1L3	8,06E-05	-1,5711118	polycystic kidney disease 1-like 3
PLEKHG3	0,004280724	-1,5645901	pleckstrin homology domain containing, family G (with RhoGef domain) member 3
RAB3IL1	0,000405219	-1,5645282	RAB3A interacting protein (rabin3)-like 1
LINC01132	9,88E-05	-1,563179	long intergenic non-protein coding RNA 1132
ARMCX3	3,27E-06	-1,5627845	armadillo repeat containing, X-linked 3
CHDH	0,000148298	-1,5559747	choline dehydrogenase
TMEM150B	0,003484912	-1,5527812	transmembrane protein 150B
ROR2	0,002354816	-1,5507566	receptor tyrosine kinase-like orphan receptor 2
PTENP1	0,02171795	-1,5500667	phosphatase and tensin homolog pseudogene 1 (functional)
B3GNT6	0,000559733	-1,5499351	UDP-GlcNAc:betaGal beta-1,3-N-acetylglucosaminyltransferase 6 (core 3 synthase)
CLDN4	0,000583168	-1,5484976	claudin 4
SIDT2	0,001539311	-1,5479397	SID1 transmembrane family, member 2
TNFRSF10A	0,000309141	-1,5444218	tumor necrosis factor receptor superfamily, member 10a
TRAM1	0,030510727	-1,5409062	translocation associated membrane protein 1
LTB	0,00172893	-1,5358124	lymphotoxin beta (TNF superfamily, member 3)
PLEKHA8P1	2,47E-06	-1,5349961	pleckstrin homology domain containing, family A member 8 pseudogene 1
WLS	0,00362655	-1,5328912	wntless Wnt ligand secretion mediator
NDUFV2	0,00099165	-1,5312554	NADH dehydrogenase (ubiquinone) flavoprotein 2, 24kDa
MIR4671	0,000496438	-1,5300675	microRNA 4671
TRIM15	0,000415028	-1,5298216	tripartite motif containing 15
TRIM15	0,000415028	-1,5298216	tripartite motif containing 15
TRIM15	0,000415028	-1,5298216	tripartite motif containing 15
RDH13	0,000872749	-1,5298191	retinol dehydrogenase 13 (all-trans/9-cis)
FRAT1	8,38E-05	-1,5296878	frequently rearranged in advanced T-cell lymphomas 1
CACNA2D4	0,00030621	-1,5276534	calcium channel, voltage-dependent, alpha 2/delta subunit 4

SNORD116-11	0,015127534	-1,5272132	small nucleolar RNA, C/D box 116-11
TRIM15	0,000555952	-1,5233475	tripartite motif containing 15
TRIM15	0,000555952	-1,5233475	tripartite motif containing 15
TRIM15	0,000555952	-1,5233475	tripartite motif containing 15
TTC9	0,0172245	-1,5222683	tetratricopeptide repeat domain 9
C1orf115	0,00100919	-1,5214047	chromosome 1 open reading frame 115
FKTN	0,000829689	-1,5195164	fukutin
GSTM3	0,037404423	-1,518168	glutathione S-transferase mu 3 (brain)
TRIM15	0,000671306	-1,517382	tripartite motif containing 15
TRIQK	9,20E-06	-1,5166249	triple QxxK/R motif containing
PEAK1	0,001264474	-1,5163937	pseudopodium-enriched atypical kinase 1
ZNF814	0,000263179	-1,5157512	zinc finger protein 814
MRRF	0,005814283	-1,5151306	mitochondrial ribosome recycling factor
STOX2	0,000366418	-1,5149426	storkhead box 2
MIR4499	0,007930989	-1,5146017	microRNA 4499
MYO1B	0,010095522	-1,5108576	myosin IB
NTPCR	0,000362556	-1,5108409	nucleoside-triphosphatase, cancer-related
APCDD1	0,011900934	-1,51045	adenomatosis polyposis coli down-regulated 1
PUS7L	0,00036193	-1,5086352	pseudouridylate synthase 7 homolog (S. cerevisiae)-like
CD99	0,002986311	-1,5079482	CD99 molecule
CTSS	9,26E-05	-1,5070188	cathepsin S
LPP	0,007003942	-1,5059348	LIM domain containing preferred translocation partner in lipoma
LOC284023	1,05E-05	-1,5036375	uncharacterized LOC284023
CES3	0,000693926	-1,5019248	carboxylesterase 3
MOB3B	0,026926317	-1,5014536	MOB kinase activator 3B
TRIM10	0,000194463	-1,5003544	tripartite motif containing 10
GAB1	0,000736781	-1,4991865	GRB2-associated binding protein 1
C3orf33	7,37E-05	-1,4975384	chromosome 3 open reading frame 33
GRK4	0,002078272	-1,4969547	G protein-coupled receptor kinase 4

C15orf65	0,001641063	-1,4944593	chromosome 15 open reading frame 65
SMPDL3A	0,030446028	-1,4938267	sphingomyelin phosphodiesterase, acid-like 3A
ZNF774	0,000509808	-1,4913138	zinc finger protein 774
TAF1L	0,013555116	-1,4906843	TAF1 RNA polymerase II, TATA box binding protein (TBP)-associated factor, 210kDa-like
TJP2	0,02949097	-1,4892559	tight junction protein 2
MIR3198-1	0,001884935	-1,488524	microRNA 3198-1
CST6	0,002477082	-1,4877758	cystatin E/M
PAPSS2	0,007001729	-1,4877048	3'-phosphoadenosine 5'-phosphosulfate synthase 2
TPI1	0,000118396	-1,4872695	triosephosphate isomerase 1
DMXL2	0,027197238	-1,4852174	Dmx-like 2
LOC339874	0,001840173	-1,4846588	uncharacterized LOC339874
TRAM2-AS1	0,004248964	-1,4810875	TRAM2 antisense RNA 1 (head to head)
ZNF790-AS1	0,001530823	-1,4788879	ZNF790 antisense RNA 1
ZNF493	0,031789466	-1,4754588	zinc finger protein 493
ZNF571	0,001052739	-1,4739368	zinc finger protein 571
SRGAP1	0,004897989	-1,4720222	SLIT-ROBO Rho GTPase activating protein 1
IFI16	0,000366236	-1,4701312	interferon, gamma-inducible protein 16
TRIM51EP	0,031100444	-1,46964	tripartite motif-containing 51E, pseudogene
TMEM44	0,000170953	-1,4693214	transmembrane protein 44
LOC643339	0,000571161	-1,4678041	uncharacterized LOC643339
PRSS21	0,027710696	-1,4658206	protease, serine, 21 (testisin)
PTAR1	1,51E-05	-1,4652626	protein prenyltransferase alpha subunit repeat containing 1
GSTM2	0,015041291	-1,4640603	glutathione S-transferase mu 2 (muscle)
RCN3	0,003048702	-1,4630873	reticulocalbin 3, EF-hand calcium binding domain
PFKFB2	0,001201665	-1,4623959	6-phosphofructo-2-kinase/fructose-2,6-biphosphatase 2
GIMAP8	0,016886437	-1,4622552	GTPase, IMAP family member 8
ADD3	0,008795926	-1,4607276	adducin 3 (gamma)
RRM2B	0,000194599	-1,4606587	ribonucleotide reductase M2 B (TP53 inducible)
HAMP	0,024250068	-1,4599418	hepcidin antimicrobial peptide

CYP1B1-AS1	0,001465045	-1,4589009	CYP1B1 antisense RNA 1
GIMAP2	0,001342809	-1,4579091	GTPase, IMAP family member 2
HKR1	2,16E-05	-1,4579002	HKR1, GLI-Kruppel zinc finger family member
PPIP5K1	0,015041291	-1,4569024	diphosphoinositol pentakisphosphate kinase 1
CHST13	0,000489157	-1,4566426	carbohydrate (chondroitin 4) sulfotransferase 13
LOC113230	0,005571695	-1,4556958	uncharacterized protein LOC113230
DCAF13P3	0,011533051	-1,4545063	DDB1 and CUL4 associated factor 13 pseudogene 3
CD44	0,000575287	-1,4511236	CD44 molecule (Indian blood group)
MAP7	0,007597033	-1,4505506	microtubule-associated protein 7
PGM2L1	0,000562372	-1,4498554	phosphoglucomutase 2-like 1
MSL3P1	0,014358136	-1,4473552	male-specific lethal 3 homolog (Drosophila) pseudogene 1
POM121L8P	0,001130682	-1,445684	POM121 transmembrane nucleoporin-like 8 pseudogene
SEMA4A	0,016484092	-1,4451056	semaphorin 4A
OR2L1P	0,005749868	-1,4449099	olfactory receptor, family 2, subfamily L, member 1 pseudogene
ITPKB	0,018114213	-1,4429284	inositol-trisphosphate 3-kinase B
RMI1	0,004622491	-1,4421338	RecQ mediated genome instability 1
MIR543	0,008227333	-1,4380608	microRNA 543
DIP2A-IT1	0,027274203	-1,4365062	DIP2A intronic transcript 1 (non-protein coding)
FAM13A-AS1	0,011244971	-1,4358684	FAM13A antisense RNA 1
REXO2	0,000128416	-1,4327103	RNA exonuclease 2
LINC01114	0,029251052	-1,4322814	long intergenic non-protein coding RNA 1114
NBEAL1	0,002737261	-1,4309839	neurobeachin-like 1
CWF19L1	0,00250501	-1,4296623	CWF19-like 1, cell cycle control (S. pombe)
LRRCC1	0,008741457	-1,4288482	leucine rich repeat and coiled-coil centrosomal protein 1
FOSB	0,008169809	-1,4281672	FBJ murine osteosarcoma viral oncogene homolog B
GPR162	0,002636471	-1,4256495	G protein-coupled receptor 162
ACO1	0,027849739	-1,4252253	aconitase 1, soluble
GNB4	0,015260386	-1,4250966	guanine nucleotide binding protein (G protein), beta polypeptide 4
GATAD1	0,000312825	-1,4250777	GATA zinc finger domain containing 1

ZNF823	0,004907445	-1,4250128	zinc finger protein 823
ZNF699	0,014307858	-1,4239135	zinc finger protein 699
PMS2	0,005438942	-1,4223821	PMS2 postmeiotic segregation increased 2 (S. cerevisiae)
TTC30A	0,037354248	-1,4222317	tetratricopeptide repeat domain 30A
LINC01137	0,008072514	-1,4219179	long intergenic non-protein coding RNA 1137
USPL1	0,002545148	-1,4213205	ubiquitin specific peptidase like 1
ZNF484	0,000153788	-1,4210163	zinc finger protein 484
ERO1LB	0,000412017	-1,4197643	ERO1-like beta (S. cerevisiae)
NOP16	0,000215659	-1,4194031	NOP16 nucleolar protein
RBM41	0,000419817	-1,419083	RNA binding motif protein 41
LOC731157	0,026933689	-1,4168306	uncharacterized LOC731157
ATP6V1B1	0,012882297	-1,4140243	ATPase, H+ transporting, lysosomal 56/58kDa, V1 subunit B1
PLCG1	0,000700287	-1,4136578	phospholipase C, gamma 1
COL24A1	0,000341179	-1,4133049	collagen, type XXIV, alpha 1
LIMD1-AS1	0,001020484	-1,4121847	LIMD1 antisense RNA 1
SPAG5-AS1	0,001344877	-1,4104449	SPAG5 antisense RNA 1
TCTN1	1,47E-05	-1,4099007	tectonic family member 1
FAM210B	0,00590983	-1,4085436	family with sequence similarity 210, member B
RCBTB1	0,007091952	-1,4076109	regulator of chromosome condensation (RCC1) and BTB (POZ) domain containing protein 1
DEPDC1B	0,025076335	-1,4048836	DEP domain containing 1B
ZMIZ1	0,001595712	-1,4046333	zinc finger, MIZ-type containing 1
GUSBP4	0,008930638	-1,4044534	glucuronidase, beta pseudogene 4
DCTPP1	0,000731143	-1,4029193	dCTP pyrophosphatase 1
FAM195A	0,007890011	-1,4021874	family with sequence similarity 195, member A
NMT2	2,83E-05	-1,4012554	N-myristoyltransferase 2
ACSS1	0,000246014	-1,3996559	acyl-CoA synthetase short-chain family member 1
HSPA6	0,010783394	-1,3983845	heat shock 70kDa protein 6 (HSP70B')
COA6	0,001461722	-1,3981544	cytochrome c oxidase assembly factor 6 homolog (S. cerevisiae)
MAGED1	8,89E-05	-1,3981024	melanoma antigen family D, 1

EPHB6	0,000239825	-1,3975778	EPH receptor B6
COPS4	7,68E-05	-1,3968423	COP9 signalosome subunit 4
TRIM5	0,019701874	-1,3967297	tripartite motif containing 5
LOC286058	0,000510816	-1,3966374	uncharacterized LOC286058
CLIP4	0,009199265	-1,3964564	CAP-GLY domain containing linker protein family, member 4
LOC100129940	0,017086302	-1,3960118	uncharacterized LOC100129940
G6PC3	0,000533704	-1,3958501	glucose 6 phosphatase, catalytic, 3
CYP4A11	0,013330556	-1,3958163	cytochrome P450, family 4, subfamily A, polypeptide 11
MTURN	0,004350172	-1,3950918	maturin, neural progenitor differentiation regulator homolog (Xenopus)
BMP1	0,002666463	-1,3948265	bone morphogenetic protein 1
MAT2A	0,008543603	-1,394354	methionine adenosyltransferase II, alpha
KLHL25	0,000248875	-1,3942661	kelch-like family member 25
LRP5L	0,001395625	-1,392415	low density lipoprotein receptor-related protein 5-like
FAM160A1	0,002576123	-1,3918841	family with sequence similarity 160, member A1
EIF2B3	0,003552378	-1,3916595	eukaryotic translation initiation factor 2B, subunit 3 gamma, 58kDa
SLC16A7	0,001600712	-1,3916315	solute carrier family 16 (monocarboxylate transporter), member 7
C11orf54	7,68E-05	-1,3906022	chromosome 11 open reading frame 54
ALG6	0,000454618	-1,3897371	ALG6, alpha-1,3-glucosyltransferase
GPR146	0,026442512	-1,387915	G protein-coupled receptor 146
MIR486-1	0,000146293	-1,387846	microRNA 486-1
C8orf37-AS1	7,19E-05	-1,3878237	C8orf37 antisense RNA 1
KIAA1462	0,008033162	-1,3875029	KIAA1462
USP51	0,002304744	-1,3872944	ubiquitin specific peptidase 51
BDKRB2	0,012532432	-1,3853948	bradykinin receptor B2
ZNF850	0,021356228	-1,3850618	zinc finger protein 850
FLJ22447	0,004390116	-1,3838559	uncharacterized LOC400221
FAM35A	0,000551568	-1,3827439	family with sequence similarity 35, member A
HIST1H2BO	0,02324354	-1,3825361	histone cluster 1, H2bo
CLN3	0,001840487	-1,3806518	ceroid-lipofuscinosis, neuronal 3

SELENBP1	0,010788641	-1,3800147	selenium binding protein 1
LOC100129033	0,000919935	-1,3789632	QIQN5815
NEGR1	0,012730827	-1,3787719	neuronal growth regulator 1
DUOX2	0,003807377	-1,3782909	dual oxidase 2
LOC100507306	0,007899283	-1,3777919	uncharacterized LOC100507306
GNS	0,002327632	-1,3777885	glucosamine (N-acetyl)-6-sulfatase
OSCAR	0,004820499	-1,3776465	osteoclast associated, immunoglobulin-like receptor
MIR4720	0,044411823	-1,3763442	microRNA 4720
ARRDC5	1,62E-05	-1,3760884	arrestin domain containing 5
CMC1	0,019217283	-1,3759334	C-x(9)-C motif containing 1
WDR35	0,001915369	-1,3750625	WD repeat domain 35
TCEAL3	0,004473901	-1,3747298	transcription elongation factor A (SII)-like 3
CETN2	0,000700287	-1,3738461	centrin, EF-hand protein, 2
ITPKB-IT1	0,012106388	-1,3735976	ITPKB intronic transcript 1 (non-protein coding)
SLC35C2	0,00051025	-1,3730373	solute carrier family 35 (GDP-fucose transporter), member C2
GAS2L1	0,001011416	-1,3705783	growth arrest-specific 2 like 1
HCG11	0,02181167	-1,370411	HLA complex group 11 (non-protein coding)
LINC00630	0,002000047	-1,3699071	long intergenic non-protein coding RNA 630
LINC00294	0,018321511	-1,3698779	long intergenic non-protein coding RNA 294
PIK3IP1	0,022959076	-1,368881	phosphoinositide-3-kinase interacting protein 1
ARHGEF15	0,000293167	-1,3686806	Rho guanine nucleotide exchange factor (GEF) 15
USP6NL	0,030510727	-1,3685442	USP6 N-terminal like
TRG-AS1	0,025805716	-1,3673025	T cell receptor gamma locus antisense RNA 1
LOC100131510	0,022716831	-1,365628	uncharacterized LOC100131510
TRMT12	0,012209822	-1,3649663	tRNA methyltransferase 12 homolog (S. cerevisiae)
PTPRJ	0,00347278	-1,364882	protein tyrosine phosphatase, receptor type, J
MIR4440	0,003561277	-1,3647104	microRNA 4440
LOC100506804	0,002257275	-1,364249	uncharacterized LOC100506804
ZNF286A	0,005081192	-1,364218	zinc finger protein 286A

PHYHD1	7,40E-05	-1,3630876	phytanoyl-CoA dioxygenase domain containing 1
VSIG10L	0,003818406	-1,3630407	V-set and immunoglobulin domain containing 10 like
EDDM3B	0,01853872	-1,3628867	epididymal protein 3B
PEX11A	0,004012746	-1,3602833	peroxisomal biogenesis factor 11 alpha
PACRGL	0,002585619	-1,3600652	PARK2 co-regulated-like
LINC01125	0,000644448	-1,3598387	long intergenic non-protein coding RNA 1125
MYOM1	0,003733369	-1,3591299	myomesin 1
SLC39A14	0,010670794	-1,3586849	solute carrier family 39 (zinc transporter), member 14
SH3YL1	0,000323352	-1,3580948	SH3 and SYLF domain containing 1
HDHD1	0,007039279	-1,3579963	haloacid dehalogenase-like hydrolase domain containing 1
HSD17B8	0,000165203	-1,3575603	hydroxysteroid (17-beta) dehydrogenase 8
HSD17B8	0,000165203	-1,3575603	hydroxysteroid (17-beta) dehydrogenase 8
HSD17B8	0,000165203	-1,3575603	hydroxysteroid (17-beta) dehydrogenase 8
HSD17B8	0,000165203	-1,3575603	hydroxysteroid (17-beta) dehydrogenase 8
HSD17B8	0,000165203	-1,3575603	hydroxysteroid (17-beta) dehydrogenase 8
HSD17B8	0,000165203	-1,3575603	hydroxysteroid (17-beta) dehydrogenase 8
LINC00032	0,009199726	-1,3569656	long intergenic non-protein coding RNA 32
DUOXA2	0,014471117	-1,3557451	dual oxidase maturation factor 2
LOC553103	0,000253998	-1,3554473	uncharacterized LOC553103
TAS2R4	0,029790983	-1,3551161	taste receptor, type 2, member 4
PKIA	0,006591557	-1,3550631	protein kinase (cAMP-dependent, catalytic) inhibitor alpha
SLC17A7	0,000712759	-1,3534706	solute carrier family 17 (vesicular glutamate transporter), member 7
DOLK	0,002060571	-1,3531737	dolichol kinase
ACAP2	0,001868308	-1,352932	ArfGAP with coiled-coil, ankyrin repeat and PH domains 2
SLC11A1	0,03493697	-1,3528685	solute carrier family 11 (proton-coupled divalent metal ion transporter), member 1
SLC25A30	0,022852452	-1,3527998	solute carrier family 25, member 30
POLR3F	0,000790869	-1,3524854	polymerase (RNA) III (DNA directed) polypeptide F, 39 kDa
NDST2	0,001935974	-1,3523293	N-deacetylase/N-sulfotransferase (heparan glucosaminyl) 2
UBXN8	0,01616741	-1,3521127	UBX domain protein 8

KBTBD11	0,003571968	-1,351386	kelch repeat and BTB (POZ) domain containing 11
C3orf79	0,004526856	-1,3508558	chromosome 3 open reading frame 79
MIR3118-4	0,011692439	-1,3499107	microRNA 3118-4
MIR3118-4	0,011692439	-1,3499107	microRNA 3118-4
DCAF17	0,000123673	-1,3477949	DDB1 and CUL4 associated factor 17
OSBPL10	0,002313495	-1,3475067	oxysterol binding protein-like 10
CYTH3	7,75E-05	-1,3460582	cytohesin 3
ADI1	0,00316008	-1,3455353	acireductone dioxygenase 1
RABL3	0,001555548	-1,3454712	RAB, member of RAS oncogene family-like 3
LOC284513	0,001112	-1,3450594	uncharacterized LOC284513
ADAL	0,026450724	-1,3446248	adenosine deaminase-like
PRMT6	0,002350785	-1,3445433	protein arginine methyltransferase 6
HSPA12B	0,024053678	-1,3443937	heat shock 70kD protein 12B
CAPN2	0,009711111	-1,3443498	calpain 2, (m/II) large subunit
COL4A3BP	0,006874022	-1,3430889	collagen, type IV, alpha 3 (Goodpasture antigen) binding protein
LIPA	0,004520748	-1,342897	lipase A, lysosomal acid, cholesterol esterase
ZSCAN26	0,000181306	-1,3427562	zinc finger and SCAN domain containing 26
ZNF568	0,000268535	-1,3427371	zinc finger protein 568
SOX8	0,046507243	-1,3426507	SRY (sex determining region Y)-box 8
SNX25	0,011340685	-1,3426066	sorting nexin 25
LOC100129473	0,011533051	-1,3425911	uncharacterized LOC100129473
ZNF583	0,001696945	-1,3422278	zinc finger protein 583
GPR85	0,002304744	-1,3421533	G protein-coupled receptor 85
TOMM40	0,037903094	-1,3410932	translocase of outer mitochondrial membrane 40 homolog (yeast)
PPP1R12B	0,002220758	-1,3398506	protein phosphatase 1, regulatory subunit 12B
CETN3	0,028881835	-1,3385272	centrin, EF-hand protein, 3
SPG7	0,004733672	-1,3364935	spastic paraplegia 7 (pure and complicated autosomal recessive)
ZNF529	0,000253678	-1,3355919	zinc finger protein 529
DHODH	0,001392747	-1,3350546	dihydroorotate dehydrogenase (quinone)

SCN5A	0,020801651	-1,3346584	sodium channel, voltage-gated, type V, alpha subunit
ANO8	0,000505613	-1,3342568	anoctamin 8
PICK1	0,007532039	-1,3341758	protein interacting with PRKCA 1
MAP4K2	0,004338812	-1,333747	mitogen-activated protein kinase kinase kinase kinase 2
LOC100505501	0,046389098	-1,3331681	uncharacterized LOC100505501
GLCCI1	0,00359157	-1,3330513	glucocorticoid induced transcript 1
TIGD7	0,000586222	-1,3330274	tigger transposable element derived 7
WWP1	0,012321611	-1,3321218	WW domain containing E3 ubiquitin protein ligase 1
PRTN3	0,026518809	-1,3316916	proteinase 3
BTN2A3P	0,041430329	-1,3316115	butyrophilin, subfamily 2, member A3, pseudogene
LEPROTL1	0,00052555	-1,3314097	leptin receptor overlapping transcript-like 1
PAFAH2	0,001088906	-1,3300401	platelet-activating factor acetylhydrolase 2, 40kDa
IGF2R	0,016478017	-1,3296409	insulin-like growth factor 2 receptor
ZNF597	0,000411582	-1,3295353	zinc finger protein 597
POP5	0,002283477	-1,3273461	processing of precursor 5, ribonuclease P/MRP subunit (S. cerevisiae)
CTGLF12P	0,004819567	-1,327185	centaurin, gamma-like family, member 12 pseudogene
WDHD1	0,010795352	-1,3270463	WD repeat and HMG-box DNA binding protein 1
SCGB1D2	0,021003823	-1,3267899	secretoglobin, family 1D, member 2
SLC24A1	0,001967434	-1,3257515	solute carrier family 24 (sodium/potassium/calcium exchanger), member 1
FCF1	0,000893052	-1,3253516	FCF1 rRNA-processing protein
FUZ	0,001702425	-1,3252056	fuzzy planar cell polarity protein
SLC22A18	0,007251161	-1,324906	solute carrier family 22, member 18
ATP5G2	0,000709645	-1,3248081	ATP synthase, H+ transporting, mitochondrial Fo complex, subunit C2 (subunit 9)
RORA	0,006631345	-1,3234951	RAR-related orphan receptor A
EMC3	0,008169809	-1,3229588	ER membrane protein complex subunit 3
SLC48A1	0,039669834	-1,3222461	solute carrier family 48 (heme transporter), member 1
FAM114A2	0,00708291	-1,3216804	family with sequence similarity 114, member A2
SH3BP1	0,011792514	-1,321656	SH3-domain binding protein 1
TSHZ1	0,014596959	-1,3211625	teashirt zinc finger homeobox 1

C12orf66	0,000203941	-1,3210868	chromosome 12 open reading frame 66
ELMOD3	0,020024314	-1,3208707	ELMO/CED-12 domain containing 3
ZFAND4	0,012688677	-1,3197611	zinc finger, AN1-type domain 4
ZNF552	0,016306817	-1,3193199	zinc finger protein 552
AAMDC	0,001439407	-1,3189167	adipogenesis associated, Mth938 domain containing
CCDC80	0,012785421	-1,3176459	coiled-coil domain containing 80
01-mars	0,002144075	-1,3170426	mitochondrial amidoxime reducing component 1
COPZ2	0,00446735	-1,3168432	coatomer protein complex, subunit zeta 2
FGFR1OP2	0,044780384	-1,3166358	FGFR1 oncogene partner 2
FAM188A	0,003648237	-1,3165661	family with sequence similarity 188, member A
LOC100129831	0,011641242	-1,3164446	EPWW6493
NAT2	0,002680263	-1,316322	N-acetyltransferase 2 (arylamine N-acetyltransferase)
GTF2E1	0,001884065	-1,3161585	general transcription factor IIE, polypeptide 1, alpha 56kDa
DSTYK	0,007108797	-1,3157935	dual serine/threonine and tyrosine protein kinase
SIPA1L2	0,047313325	-1,3148525	signal-induced proliferation-associated 1 like 2
LOC284926	0,024090944	-1,3145791	uncharacterized LOC284926
KMT2C	0,009645868	-1,3144941	lysine (K)-specific methyltransferase 2C
BOD1	0,002680423	-1,3138467	biorientation of chromosomes in cell division 1
KLK7	0,022303523	-1,3136588	kallikrein-related peptidase 7
AASS	0,006582401	-1,3135639	aminoadipate-semialdehyde synthase
C6orf89	0,000611295	-1,3133824	chromosome 6 open reading frame 89
SNORA24	0,035296152	-1,3131291	small nucleolar RNA, H/ACA box 24
ZNF181	0,001880708	-1,3129778	zinc finger protein 181
FAM114A1	0,018195681	-1,312034	family with sequence similarity 114, member A1
NRARP	0,020693483	-1,311789	NOTCH-regulated ankyrin repeat protein
MSTN	0,022254945	-1,3117369	myostatin
PBLD	0,002076173	-1,3116632	phenazine biosynthesis-like protein domain containing
LINC01220	0,00316008	-1,3104798	long intergenic non-protein coding RNA 1220
WASH3P	0,045402003	-1,3096695	WAS protein family homolog 3 pseudogene

LINC00888	0,032781303	-1,3096368	long intergenic non-protein coding RNA 888
UGP2	0,000421148	-1,3094742	UDP-glucose pyrophosphorylase 2
HIBCH	0,018276002	-1,3092099	3-hydroxyisobutyryl-CoA hydrolase
ZRANB2-AS1	0,001225605	-1,3089163	ZRANB2 antisense RNA 1
LOC100507642	0,0089658	-1,3085335	uncharacterized LOC100507642
NARS2	0,008072514	-1,308363	asparaginyl-tRNA synthetase 2, mitochondrial (putative)
COQ7	0,001663171	-1,3082361	coenzyme Q7 homolog, ubiquinone (yeast)
ABCC4	0,006899952	-1,3080828	ATP-binding cassette, sub-family C (CFTR/MRP), member 4
UNC50	0,00045447	-1,3077205	unc-50 homolog (C. elegans)
LIN54	0,000115584	-1,307675	lin-54 DREAM MuvB core complex component
ECRP	0,049460309	-1,3075926	ribonuclease, RNase A family, 2 (liver, eosinophil-derived neurotoxin) pseudogene
SMIM8	0,009451373	-1,3075159	small integral membrane protein 8
FRMD6	0,006988321	-1,3071283	FERM domain containing 6
SNAI1	0,005358947	-1,3070879	snail family zinc finger 1
SLC25A37	0,012638396	-1,3068283	solute carrier family 25 (mitochondrial iron transporter), member 37
STK16	0,004456323	-1,3063921	serine/threonine kinase 16
APAF1	0,016727863	-1,3056144	apoptotic peptidase activating factor 1
FBN2	0,001555372	-1,3052843	fibrillin 2
PTPDC1	0,001937868	-1,3043393	protein tyrosine phosphatase domain containing 1
SNTB1	0,011261414	-1,3039621	syntrophin, beta 1 (dystrophin-associated protein A1, 59kDa, basic component 1)
HERC2P10	0,002247642	-1,3038698	hect domain and RLD 2 pseudogene 10
NME7	0,010830808	-1,303706	NME/NM23 family member 7
UBE2H	0,003404064	-1,3035155	ubiquitin-conjugating enzyme E2H
EFR3B	0,009063648	-1,3033233	EFR3 homolog B (S. cerevisiae)
FAM111A	0,005440964	-1,3029492	family with sequence similarity 111, member A
RNU6ATAC	0,028072235	-1,3028096	RNA, U6atac small nuclear (U12-dependent splicing)
UGGT2	0,045455808	-1,3026241	UDP-glucose glycoprotein glucosyltransferase 2
ARHGEF17	0,020246587	-1,3025311	Rho guanine nucleotide exchange factor (GEF) 17
GOLGA8I	0,002905279	-1,3022005	golgin A8 family, member I

OTUD1	0,026590855	-1,3021712	OTU deubiquitinase 1
NUDT1	0,001214281	-1,301479	nudix (nucleoside diphosphate linked moiety X)-type motif 1
PROX2	0,004981875	-1,3014476	prospero homeobox 2
MED20	0,000759746	-1,301134	mediator complex subunit 20
C1RL	0,026241998	-1,3001489	complement component 1, r subcomponent-like

Supplemental Table 7: HIV modulated genes in CD16+ MDDCs

Symbol	p-value	FC	description
IFI6	0,010221956	1,968091	interferon, alpha-inducible protein 6
OR56A3	0,002357016	1,66518148	olfactory receptor, family 56, subfamily A, member 3
MIR568	0,040890114	1,56560746	microRNA 568
MIR4718	0,024762177	1,54548873	microRNA 4718
SNORA5A	0,003895082	1,53541148	small nucleolar RNA, H/ACA box 5A
SNORA30	0,007230177	1,52762718	small nucleolar RNA, H/ACA box 30
KRTAP6-3	0,00694776	1,45609	keratin associated protein 6-3
FANCM	0,000270071	1,45062457	Fanconi anemia, complementation group M
CD101	0,008782713	1,44986461	CD101 molecule
MIR4717	0,001891888	1,44467935	microRNA 4717
ZNF714	0,007858588	1,43397999	zinc finger protein 714
LINC00864	0,019410526	1,41647605	long intergenic non-protein coding RNA 864
ZNF429	0,045714769	1,41191091	zinc finger protein 429
LOC101927780	0,003900453	1,3959715	uncharacterized LOC101927780
LOC645513	0,025011597	1,39384275	uncharacterized LOC645513
KBTBD7	0,007735633	1,38795765	kelch repeat and BTB (POZ) domain containing 7
SKP1	0,027506979	1,38561761	S-phase kinase-associated protein 1
SIGLEC1	0,008329708	1,38177798	sialic acid binding Ig-like lectin 1, sialoadhesin
MIR3692	0,021478142	1,38015051	microRNA 3692
OR1F1	0,0097904	1,37583921	olfactory receptor, family 1, subfamily F, member 1
ZNHIT6	0,002811787	1,37084049	zinc finger, HIT-type containing 6
CCDC122	0,033813873	1,36929275	coiled-coil domain containing 122
MIR3188	0,008186345	1,36920461	microRNA 3188
MIR4441	0,036939034	1,35856016	microRNA 4441
TAF1	0,003414014	1,35846164	TAF1 RNA polymerase II, TATA box binding protein (TBP)-associated factor, 250kDa
YTHDC1	0,018870484	1,35066555	YTH domain containing 1
OSTCP1	0,013699726	1,34066132	oligosaccharyltransferase complex subunit pseudogene 1

SCARNA1	0,039900606	1,34036652	small Cajal body-specific RNA 1
KLF10	0,037547325	1,32951119	Kruppel-like factor 10
MIR4672	0,029647765	1,32760385	microRNA 4672
MIR548S	0,018225471	1,32654998	microRNA 548s
RFC4	0,002375303	1,32432101	replication factor C (activator 1) 4, 37kDa
RBM5-AS1	0,005270973	1,3221625	RBM5 antisense RNA 1
ZNF461	0,022592554	1,31688106	zinc finger protein 461
EIF2AK2	0,03560488	1,316649	eukaryotic translation initiation factor 2-alpha kinase 2
DSTNP2	0,004970196	1,31626219	destrin (actin depolymerizing factor) pseudogene 2
SLC9A9-AS1	0,000229358	1,31484914	SLC9A9 antisense RNA 1
KRTAP19-3	0,014239561	1,31475759	keratin associated protein 19-3
CASP6	0,013581768	1,31155655	caspase 6, apoptosis-related cysteine peptidase
ZNF671	0,026552925	1,31064429	zinc finger protein 671
DDIAS	0,013119191	1,30711789	DNA damage-induced apoptosis suppressor
MIR583	0,004009033	1,30573938	microRNA 583
ZNF502	0,007326323	1,30490537	zinc finger protein 502
MIR4491	0,047645655	1,30048258	microRNA 4491
CACHD1	0,022633845	-1,3003855	cache domain containing 1
LINC01227	0,011920412	-1,3017127	long intergenic non-protein coding RNA 1227
LOC101927048	0,031657254	-1,302562	uncharacterized LOC101927048
IGHG1	0,023429579	-1,3025629	immunoglobulin heavy constant gamma 1 (G1m marker)
MIR668	0,006754652	-1,3038167	microRNA 668
CPB2	0,006969596	-1,304655	carboxypeptidase B2 (plasma)
OR4Q3	0,038772054	-1,3046751	olfactory receptor, family 4, subfamily Q, member 3
PTGIR	0,045493925	-1,3053578	prostaglandin I2 (prostacyclin) receptor (IP)
YME1L1	0,006586036	-1,3080892	YME1-like 1 ATPase
FUT3	0,000930999	-1,309466	fucosyltransferase 3 (galactoside 3(4)-L-fucosyltransferase, Lewis blood group)
MIR4535	0,009038383	-1,3128914	microRNA 4535
LOC100507600	0,042026527	-1,3149904	uncharacterized LOC100507600

SCUBE2	0,00467118	-1,3186049	signal peptide, CUB domain, EGF-like 2
MIR4660	0,022351703	-1,3188539	microRNA 4660
GPR157	0,02667323	-1,319101	G protein-coupled receptor 157
KRT33A	0,011441411	-1,3200227	keratin 33A
CEACAM3	0,039753348	-1,3201396	carcinoembryonic antigen-related cell adhesion molecule 3
OR4C15	0,012683765	-1,320524	olfactory receptor, family 4, subfamily C, member 15
ADH4	9,07E-06	-1,3256659	alcohol dehydrogenase 4 (class II), pi polypeptide
PRDM8	0,032879378	-1,3264211	PR domain containing 8
DPPA2P3	0,027837763	-1,3276574	developmental pluripotency associated 2 pseudogene 3
ACTR3BP2	0,012585715	-1,3289025	ACTR3B pseudogene 2
FNDC9	5,53E-05	-1,3315931	fibronectin type III domain containing 9
IGKC	0,004790646	-1,3326149	immunoglobulin kappa constant
OR4C46	0,002924049	-1,3339919	olfactory receptor, family 4, subfamily C, member 46
ROR1	0,013954291	-1,3372708	receptor tyrosine kinase-like orphan receptor 1
GTF2IRD2B	0,019655188	-1,3418047	GTF2I repeat domain containing 2B
CNR1	0,000118855	-1,3454607	cannabinoid receptor 1 (brain)
LCE2D	0,000220042	-1,3482892	late cornified envelope 2D
PSG5	0,019579212	-1,3495535	pregnancy specific beta-1-glycoprotein 5
MIR3138	0,004340243	-1,3513563	microRNA 3138
MIR4450	0,001278039	-1,3535304	microRNA 4450
COX6A2	0,001239072	-1,3550833	cytochrome c oxidase subunit VIa polypeptide 2
OR8G2	0,035758808	-1,3575106	olfactory receptor, family 8, subfamily G, member 2
LINC01005	0,003473389	-1,3579652	long intergenic non-protein coding RNA 1005
CCR4	0,033393456	-1,3595554	chemokine (C-C motif) receptor 4
IFNA16	0,003641616	-1,3612035	interferon, alpha 16
OR1D2	0,034194074	-1,3623369	olfactory receptor, family 1, subfamily D, member 2
LOC101927123	0,035194429	-1,3632814	uncharacterized LOC101927123
XKRX	0,004620171	-1,36333	XK, Kell blood group complex subunit-related, X-linked
ATF3	0,040012329	-1,3641792	activating transcription factor 3

STX17-AS1	0,002002675	-1,3642297	STX17 antisense RNA 1
LOC641746	0,005818948	-1,3681907	glycine cleavage system protein H (aminomethyl carrier) pseudogene
OR2T27	0,018329986	-1,3693531	olfactory receptor, family 2, subfamily T, member 27
MED27	0,038605833	-1,3719773	mediator complex subunit 27
MYO1G	0,027554106	-1,3745789	myosin IG
DPCR1	0,005393344	-1,3751977	diffuse panbronchiolitis critical region 1
CCDC30	0,005556183	-1,3834838	coiled-coil domain containing 30
SNORD114-2	0,005264758	-1,385326	small nucleolar RNA, C/D box 114-2
MRGPRF	0,00155234	-1,385951	MAS-related GPR, member F
OR7E91P	0,046244484	-1,3869837	olfactory receptor, family 7, subfamily E, member 91 pseudogene
ARHGDIG	0,01742141	-1,3878794	Rho GDP dissociation inhibitor (GDI) gamma
LGALS17A	0,007934522	-1,3967619	Charcot-Leyden crystal protein pseudogene
OR1E2	0,010562849	-1,4033784	olfactory receptor, family 1, subfamily E, member 2
PIM1	0,016264855	-1,4034802	Pim-1 proto-oncogene, serine/threonine kinase
TM4SF1	0,015272953	-1,4125108	transmembrane 4 L six family member 1
SYNPO2	0,045636933	-1,4232858	synaptopodin 2
TNC	0,044861797	-1,4357688	tenascin C
GPRC5D	0,003437914	-1,4386597	G protein-coupled receptor, class C, group 5, member D
GADD45B	0,006868853	-1,4394911	growth arrest and DNA-damage-inducible, beta
ANXA3	0,047021491	-1,4436867	annexin A3
KRTAP5-2	0,006475139	-1,4493416	keratin associated protein 5-2
LRRC32	0,004734083	-1,469846	leucine rich repeat containing 32
CYP7B1	0,014564978	-1,4711518	cytochrome P450, family 7, subfamily B, polypeptide 1
VAT1L	0,044666471	-1,4713233	vesicle amine transport 1-like
SSX6	0,002804592	-1,4730097	synovial sarcoma, X breakpoint 6 (pseudogene)
RNU6-71P	0,011547322	-1,4780684	RNA, U6 small nuclear 71, pseudogene
OR5L2	0,03045223	-1,4870442	olfactory receptor, family 5, subfamily L, member 2
JADE3	0,006203094	-1,4982212	jade family PHD finger 3
OR10K2	0,008998587	-1,5110778	olfactory receptor, family 10, subfamily K, member 2

ASB9	0,000103973	-1,5211856	ankyrin repeat and SOCS box containing 9
OR2J3	0,004540337	-1,5242646	olfactory receptor, family 2, subfamily J, member 3
OR6C75	0,010914591	-1,5303631	olfactory receptor, family 6, subfamily C, member 75
USP17L15	0,04663262	-1,536454	ubiquitin specific peptidase 17-like family member 15
IL2RA	0,049518186	-1,5714987	interleukin 2 receptor, alpha
FLT3	0,041744562	-1,6068745	fms-related tyrosine kinase 3
TMEM176A	0,019301509	-1,6180501	transmembrane protein 176A
MFI2	0,013617843	-1,6447771	antigen p97 (melanoma associated) identified by monoclonal antibodies 133.2 and 96.5
IFNA1	9,19E-05	-1,6458915	interferon, alpha 1
MIR509-3	0,006282835	-1,7023894	microRNA 509-3
MIR548I3	0,002205234	-1,7798673	microRNA 548i-3
CRLF2	0,037775954	-1,8259217	cytokine receptor-like factor 2
USP17L5	0,002405697	-1,8370337	ubiquitin specific peptidase 17-like family member 5
ROCK1P1	0,03887543	-1,8946092	Rho-associated, coiled-coil containing protein kinase 1 pseudogene 1

Supplemental Table 8: HIV modulated genes in CD16- MDDCs

Symbol	p-value	FC	description
MIR1271	0,00320353	1,68465532	microRNA 1271
MIR516A2	0,0066327	1,55339607	microRNA 516a-2
MIR3911	0,01464117	1,43881251	microRNA 3911
PKP2	0,00132011	1,42950038	plakophilin 2
PNRC2	0,01478631	1,40814485	proline-rich nuclear receptor coactivator 2
LINC01482	0,00158313	1,39425015	long intergenic non-protein coding RNA 1482
MIR196A1	0,00107515	1,38737478	microRNA 196a-1
S100B	0,00379993	1,38731961	S100 calcium binding protein B
OR14J1	0,02526722	1,38335967	olfactory receptor, family 14, subfamily J, member 1
DAPL1	0,01117891	1,37696886	death associated protein-like 1
LINC00424	0,00353778	1,36513011	long intergenic non-protein coding RNA 424
MIR320C1	0,03420108	1,35681946	microRNA 320c-1
CFHR4	0,0225081	1,35064297	complement factor H-related 4
LINC00971	0,00194834	1,34401165	long intergenic non-protein coding RNA 971
MIR3665	0,03484974	1,33711721	microRNA 3665
MRGPRX1	0,00567116	1,33233456	MAS-related GPR, member X1
SLC15A1	0,00046748	1,33209542	solute carrier family 15 (oligopeptide transporter), member 1
LOC100132781	0,03086186	1,3245989	cyclin Y-like 1 pseudogene
MIR3201	0,03550733	1,32251538	microRNA 3201
NOV	0,03681012	1,31873791	nephroblastoma overexpressed
MYH8	0,02901191	1,31650693	myosin, heavy chain 8, skeletal muscle, perinatal
MIR523	0,00261917	1,31519087	microRNA 523
LINC00841	0,00286886	1,3108561	long intergenic non-protein coding RNA 841
TOMM20L	0,0003556	1,3093606	translocase of outer mitochondrial membrane 20 homolog (yeast)-like
PRR29	0,00310369	1,30516836	proline rich 29
HAVCR1P1	0,04764594	-1,3022709	hepatitis A virus cellular receptor 1 pseudogene 1
BUB1	0,03401889	-1,305262	BUB1 mitotic checkpoint serine/threonine kinase

POLR3G	0,00724593	-1,3077108	polymerase (RNA) III (DNA directed) polypeptide G (32kD)
GSTA3	0,01108908	-1,3169463	glutathione S-transferase alpha 3
OR52B4	0,01880424	-1,3226039	olfactory receptor, family 52, subfamily B, member 4
MIR4308	0,00721187	-1,3301939	microRNA 4308
CCNE2	0,00687041	-1,3430922	cyclin E2
ADAMTS7	0,00170555	-1,3459929	ADAM metallopeptidase with thrombospondin type 1 motif, 7
LINC01146	0,00077437	-1,3516697	long intergenic non-protein coding RNA 1146
TNKS	0,04313061	-1,3523867	tankyrase, TRF1-interacting ankyrin-related ADP-ribose polymerase
MIR130B	0,0498077	-1,3524797	microRNA 130b
SNORD12C	0,02671416	-1,357668	small nucleolar RNA, C/D box 12C
TAPT1-AS1	0,01481401	-1,3628192	TAPT1 antisense RNA 1 (head to head)
GPR139	2,12E-05	-1,3763213	G protein-coupled receptor 139
OR2M1P	0,01444679	-1,3834148	olfactory receptor, family 2, subfamily M, member 1 pseudogene
CD99P1	0,03658546	-1,391496	CD99 molecule pseudogene 1
ANTXR1	0,02106583	-1,3973597	anthrax toxin receptor 1
MIR545	0,04325518	-1,3975958	microRNA 545
SNORD75	0,03014721	-1,4204792	small nucleolar RNA, C/D box 75
HIST2H3D	0,00490891	-1,4336476	histone cluster 2, H3d
TUBB4A	2,59E-05	-1,434088	tubulin, beta 4A class IVa
SNORA70B	0,02683601	-1,4438313	small nucleolar RNA, H/ACA box 70B
DDIT3	0,00026278	-1,4683294	DNA-damage-inducible transcript 3
HIST1H2BL	0,00704575	-1,4787993	histone cluster 1, H2bl
MIR4263	0,0234331	-1,4971114	microRNA 4263
TACC1	0,04009342	-1,562148	transforming, acidic coiled-coil containing protein 1
MIR3975	0,01988061	-1,5686144	microRNA 3975
MIR4499	0,00078196	-1,5810924	microRNA 4499
SNORD99	0,01060176	-1,6034008	small nucleolar RNA, C/D box 99
HIST1H2AJ	0,00672921	-1,8646805	histone cluster 1, H2aj

Authors Contribution: Manuscript entitled:
HIV-1 Impairs the Ability of Myeloid Dendritic Cells to Promote CD4+ T-Cell Responses against Th17-Specific Pathogens

Vanessa Sue Wacleche performed research, analyzed data, and wrote the manuscript. Concerning the experimental approach, VSW performed the isolation and staining for cell sorting. She also performed all experiments involving cell stimulation, antigen presentation, trans-infection and HIV reactivation assays. Figures involved include Figure 2-5.

Tevy-Suzy Tep performed staining experiment shown in Figure 1.

Annie Gosselin performed leukapheresis of patients included concerning all the figures.

Dominque Gauchat performed the cell sorting shown in Figures 3-5.

Jean-Pierre Routy ensured access to clinical samples/information and/or provided experimental protocols figures 1-8 as well as all the supplemental figures.

Petronela Ancuta designed research, analyzed data, and wrote the manuscript. This includes all the figures, tables and supplemental figures.

Manuscript #3 in preparation for submission to ***The Journal of Immunology***

HIV-1 Impairs the Ability of Myeloid Dendritic Cells to Promote CD4+ T-Cell Responses against Th17-Specific Pathogens

Vanessa Sue Wacleche[1,2], Tevy-Suzy Tep[1,2], Annie Gosselin[2], Dominique Gauchat[2], Jean-Pierre Routy[3,4,5], and Petronela Ancuta[1, 2,*]

[1]Université de Montréal, Faculté de Médecine, Département of microbiologie, infectiologie et immunologie, Montreal, QC, Canada.

[2]Centre de recherche du CHUM, Montreal, QC, Canada.

[3]Department of Medicine, University of California San Francisco, San Francisco, CA, USA

[4]Chronic Viral Illness Service and Research Institute, McGill University Health Centre, Montreal, QC, Canada.

[5]Division of Hematology, McGill University Health Centre, Montreal, QC, Canada.

***, Corresponding author e-mail**: petronela.ancuta@umontreal.ca

Running title: HIV-1 *trans* infection impairs dendritic cell immunogenicity

Abstract word count: 245
Text word count: 8, 015 words; 52,633 characters (spaces included)
Number of Figures: 5
Number of References: 81

ABSTRACT

HIV-1 infection is associated with the depletion of Th17 cells and impaired Th17-mediated immunity against mucosal pathogens such as *Candida albicans and Staphylococcus aureus*. Dendritic cells (DCs) are major players in the initiation of adaptive immune responses. The process of antigen presentation is exploited by HIV-1 for its own dissemination advantage. Here we investigated the impact of HIV exposure on the ability of monocyte-derived DCs (MDDCs) to mount antigen-specific $CD4^+$ T-cell responses. Exposure to HIV *in vitro* dramatically impaired the ability of antigen-loaded MDDC to induce proliferation of autologous $CD4^+$ T-cells in response to *Staphylococcus aureus,* and at lower extent *cytomegalovirus* (CMV, Th1-mediated response). In contrast, MDDC-mediated T-cell proliferation in response to the superantigen *Staphylococcal enterotoxin B* (SEB) was not diminished by HIV. The extent of HIV-induced immune alterations was negatively correlated with the efficacy of HIV *trans* infection, as measured by the frequency of HIV-$p24^+$ T-cells in the MDDC: T-cell co-cultures. Consistently, $CD16^-$ compared to $CD16^+$ MDDCs exhibited a superior immunogenic potential but a decreased ability to promote HIV *trans* infection. Of note, HIV exposure reduced the immunogenic potential in both $CD16^-$ and $CD16^+$ MDDCs. These results demonstrate that HIV impairs the ability of DCs to promote Th17 responses and reveal a negative correlation between immunogenicity and HIV *trans* infection by MDDC subsets. Finding ways to limit the expansion of $CD16^+$ monocytes in HIV-infected subjects is required for the restoration of Th17-mediated immune responses, together with the prevention of HIV dissemination.

Key words: human, $CD16^+$ monocytes, dendritic cells, LPS, HIV-1, transcriptional profiling

Authors' contribution:

WSW designed and performed experiments, analyzed the results, prepared the figures, and wrote the manuscript. TST performed experiments in Figure 1. AGO contributed to leukapheresis preparation. JPR allowed access to leukapheresis and clinical information from human individuals and contributed to manuscript writing. PA designed the study, analyzed results, designed the figures, and wrote the manuscript. All authors read and approved the manuscript.

Introduction

Myeloid dendritic cells (DCs) are professional antigen presenting cells (1-3). The interaction between DCs and $CD4^+$ T-cells is a key event in the initiation of adaptive immunity against pathogens (4, 5). Circulating monocytes represent a major pool of DC precursors (6, 7). Human monocytes represent a heterogeneous population of circulating cells composed of different stages of monocyte differentiation (7-9). The differential expression of CD14 and CD16 allows the identification of at least three distinct subsets: classical $CD14^{++}CD16^-$, intermediate $CD14^{++}CD16^+$, and non-classical $CD14^+CD16^{++}$ monocytes (10). Most recent studies demonstrated that the expression of slan/M-DC8 allows a better identification of non-classical monocytes (11). Several pathological conditions including HIV-1 infection are associated with an expansion in the frequency of $CD16^+$ monocytes (12-15). $CD16^+$ monocytes represent a more advanced stage of monocyte differentiation (16) with pro-inflammatory potential (12, 17) and ability to migrate into tissues *via* the CX3CR1/CX3CL1 axis (18-20). Compared to $CD16^-$ monocytes, $CD16^+$ monocytes were reported to be more permissive to HIV infection as they preferentially harbored HIV-DNA (21, 22). Furthermore, $CD16^+$ monocytes were reported to render $CD4^+$ T-cells highly permissive to HIV infection via the production of CCR3 and CCR4 binding chemokines (23, 24). Of note, both human $CD16^-$ and $CD16^+$ monocytes can differentiate into dendritic cells (DCs) (25, 26). The distinct relative contribution of $CD16^-$ *versus* $CD16^+$ monocyte-derived DCs (MDDCs) to HIV-1 pathogenesis remains to be investigated.

The interaction between DCs and $CD4^+$ T-cells during the process of antigen presentation is efficiently exploited by HIV-1 to ensure its dissemination (27-30). HIV virions captured by DCs are efficiently transmitted to $CD4^+$ T-cells at the level of the immunological/infectious synapse (31-33).

The loss of CD4 counts is the hallmark of HIV infection (34-36). The immune deficiency observed in HIV-infected subjects coincides with the preferential infection of $CD4^+$ T-cells specific for HIV itself (37) and other opportunistic pathogens such as *Mycobacterium tuberculosis* (MT) (38, 39). In contrast, cytomegalovirus (CMV)-specific $CD4^+$ T-cells were reported to be relatively resistant to infection due to the autocrine production of CCR5 binding chemokines (40). Nevertheless, alterations in the quality of CMV-specific immune responses exist in HIV-infected subjects (39). Despite the fact that DCs are limited in their ability to support HIV replication in *cis* (41-44) and to sense HIV RNA/DNA (45, 46), HIV has a deleterious impact on the functional properties of DCs (47). Indeed, the antigen presenting capacity of DCs is impaired upon HIV exposure *via* mechanisms involving at least in part the inhibition of the autophagy process (48, 49). Responses to several pathogens are impaired in HIV-infected subjects, especially at mucosal surfaces, where the persistent depletion of antigen-specific $CD4^+$ T-cells, mainly Th17 cells, promotes microbial translocation, chronic immune activation and disease progression (36, 50). Th17 cells are major players in the immunity against pathogens at mucosal surfaces (51-53). Th17 cells promote immunity against *C. albicans* (54) and *S. aureus* (55) a process dependent on the production of IL-23 by DCs (56). Th17 cells are highly permissive to HIV infection and therefore depleted in HIV-infected subjects (57, 58). This depletion may explain why *C. albicans* and *S. aureus* are two opportunistic pathogens during HIV infection (59). Whether HIV specifically interferes with the ability of DCs to promote Th17 polarization in response to specific pathogens remains unclear.

In this study, we investigated the impact of HIV-1 on the capacity of DCs derived from total as well as $CD16^+$ and $CD16^-$ monocytes to promote $CD4^+$ T-cell proliferation and cytokine production in

response to Th1- (CMV) and Th17-specific (*S. aureus*) antigens, as well as super antigens (*Staphylococcal enterotoxin B*, SEB), and explored these alterations in relationship with the efficacy of HIV dissemination by monocyte-derived DC (MDDC) subsets.

RESULTS

HIV-1 fails to induce maturation of monocyte-derived DCs (MDDCs). The lack of efficient immune responses against HIV was linked to the poor ability of DCs to be productively infected and sense HIV RNA/DNA (46, 60). Alternatively, HIV can impair the immunogenic potential of DCs *via* an effect on autophagy, a process essential for antigen presentation (48, 61). Here, we investigated the ability of HIV to induce the monocyte-derived DCs (MDDC) maturation, a process essential for immunogenicity. For this, monocytes were isolated by negative selection using magnetic beads and differentiated into DCs by culture in the presence of GM-CSF and IL-4 for 6 days. MDDC were cultured in the presence or absence of R5 HIV (NL4.3BaL) or E. coli LPS for 48h and their phenotype was evaluated by flow cytometry. Immature MDDCs (medium) expressed CD1c (or blood dendritic cell antigen 1. BDCA-1) and low/undetectable levels of the monocyte/macrophage marker and LPS co-receptor CD14 (Figure 1A). As expected, LPS exposure resulted in the significant up regulation of HLA-DR, CD83 and CCR7 expression in terms of frequency of positive cells (%) and mean fluorescence intensity (MFI) (Figure 1A-B), indicative of MDDC maturation. Interestingly, the percentage of HLA-DRhi *versus* HLA-DRmed is 81% *versus* 13% and for CD83hi versus CD83med is 45% *versus* 24% (data not shown). Of note, HIV induced minor changes in the expression of HLA-DR, CD83 and CCR7 (Figure 1A-B). Consistently, HIV-1 replication in MDDCs was low to undetectable (data not shown). Thus, MDDC maturation does not occur upon HIV-1 exposure, likely due to an inefficient process of viral sensing.

Exposure to HIV-1 alters the immunogenic potential of MDDC. HIV infection is associated with an impaired ability to control opportunistic infections (39). Indeed, HIV-1 impairs the immunogenic potential of DCs while promoting its dissemination (49, 62). Here, we investigated the impact of

HIV exposure on the ability of MDDCs to promote $CD4^+$ T-cell proliferation in response to Th1-specific (CMV) and Th17-specific (*S. aureus*) antigens, as well as the super antigen SEB. For this, MDDCs were generated as in Figure 1. In parallel, autologous $CD4^+$ T-cells were isolated negative selection using magnetic beads. MDDCs were exposed or not to the R5 HIV strain NL4.3BaL (low doses: 10 ng HIV-p24 per 10^6 cells), loaded with antigens and cultured with autologous CFSE-loaded $CD4^+$ T-cells for 5 days (MDDC: T-cell ratio 1:4) (Figure 2A). Results generated with cells from five different donors demonstrate that HIV exposure dramatically reduces the frequency of proliferating $CD4^+$ T-cells in response to *S. aureus* ($p=0.0001$) and at a lower extent in response to CMV ($p=0.02$); while the proliferation in response to SEB was not significantly reduced (Figure 2B). The HIV *trans* infection efficacy, measured as the frequency of HIV-$p24^+$ $CD4^+$ T-cells in MDDC: T-cell co-cultures, was the highest when MDDCs were loaded with *S.aureus* compared to CMV or SEB (Figure 2C). Of note, there was an inverse correlation between the magnitude of T-cell proliferation impairment induced by HIV exposure and the HIV *trans* infection efficacy (Figure 2D). These results demonstrate that HIV impairs the immunogenic potential of MDDCs in an antigen-specific manner, and reveal a dichotomy between the HIV *trans* infection efficacy and the immunogenic potential.

$CD16^-$ *versus* $CD16^+$ MDDCs exhibit a superior immunogenic potential and a lower ability to disseminate HIV. Peripheral blood monocytes represent are highly heterogeneous population and include classical $CD16^-$ and intermediate/non-classical $CD16^+$ monocytes that give rise to DCs with specific immunologic features (26). Here we investigated differences between $CD16^-$ and $CD16^+$ MDDCs loaded with CMV, *C. albicans*, *S. aureus*, or SEB in their ability to promote antigen-specific proliferation of autologous $CD4^+$ T-cells and explored the impact of HIV exposure on these

processes. Highly pure $CD16^-$ and $CD16^+$ were isolated by FACS and cultured in the presence of GM-CSF and IL-4 for 6 days. In a first series of experiments, $CD16^-$ and $CD16^+$ MDDCs were loaded with antigens and co-cultured with autologous $CD4^+$ T-cells ((MDDC: T-cell ratio 1:4)) to evaluate differences in their ability to promote antigen-specific T-cell proliferation. The intracellular expression of IL-17A, IL-17F and IFN-γ was measured in proliferating ($CFSE^{low}$) cells by FACS upon stimulation with PMA and Ionomycin. Of note, we previously demonstrated that PMA and Ionomycin stimulation did not impact on the frequency of proliferating T-cells (63). Results in Figure 3A-B, illustrate for all four antigenic stimulations the highest frequencies of $CD4^+$ T-cell proliferation in the presence of antigen-loaded $CD16^-$ MDDC compared to $CD16^+$ MDDC. Regarding the frequency of cells expressing IL-17A, IL-17F, and/or IFN-γ within proliferating cells differences were observed between $CD16^-$ MDDC: T and $CD16^+$ MDDC: T co-cultures in response to *C. albicans* but not *S. aureus* (Figure 3D); nevertheless the total number of T-cells proliferating and producing cytokines remained significantly higher in $CD16^-$ MDDC: T *versus* $CD16^+$ MDDC: T co-cultures (data not shown). Consistent with results in Figure 2D, the superior immunogenic potential coincided with a lower ability of $CD16^-$ MDDC compared to $CD16^+$ MDDC to *trans* infect $CD4^+$ T-cells, mainly for S. aureus-specific T-cells (Figure 4). Of note, HIV-p24 expression was observed only in proliferating $CFSE^{low}$ but not in $CFSE^{high}$ T-cells (data not shown). These results reveal that $CD16^-$ *versus* $CD16^+$ MDDCs have a superior capacity to induce antigen-specific $CD4^+$ T-cell responses and a reduced ability to promote HIV *trans* infection.

HIV-1 exposure alters the immunogenic potential of both $CD16^-$ and $CD16^+$ MDDC. Results in Figure 2 demonstrate that HIV impairs the ability of MDDCs to present antigens, in line with previous reports (48, 49). In this context, we investigated the effect of HIV exposure on the

immunogenic potential of $CD16^-$ and $CD16^+$ MDDCs. To this aim, both MDDC subsets were exposed to high doses of the R5 HIV strain NL4.3BaL (50 ng HIV-p24 *per* 10^6 cells), loaded with antigens (SEB, CMV, *C. albicans* and *S.aureus*), and then co-cultured with autologous $CD4^+$ T-cells for five days (MDDC: T-cell ratio 1:4). Exposure of $CD16^-$ MDDCs to HIV caused a dramatic reduction in the frequency of $CD4^+$ T-cells proliferating in response to all four antigens (Figure 5A). Similar changes were also observed when $CD16^+$ MDDCs were exposed to HIV for SEB- and S. aureus-specific T-cell responses, and at a lower extend for CMV- and *C. albicans*-specific T-cells (Figure 5B). The exposition of $CD16^-$ MDDC to HIV did not reduce the frequency of $IL\text{-}17A^+$ and $IL\text{-}17F^+$ T-cells proliferating in response to *S. aureus;* surprisingly, $CD16^+$ MDDC exposure to HIV led to a slight increase in the frequency of $IL\text{-}17A^+$ and $IL\text{-}17F^+$ T-cells proliferating in response to *S. aureus* (Figure 5C). Nevertheless, HIV-exposed $CD16^-$ and $CD16^+$ MDDC were both less efficient in the generation of *S.aureus*-specific T-cells expressing IFN-γ (Figure 5C). In conclusion, these results demonstrate that HIV exposure alters the antigen-specific proliferation of $CD4^+$ T-cells induced by both $CD16^-$ and $CD16^+$ MDDCs. Noteworthy, even in the presence of HIV, the immunogenic potential of $CD16^-$ *versus* $CD16^+$ MDDCs remains higher.

DISCUSSION

The HIV-1 infection is associated with the increased occurrence of opportunistic infections (39). An impaired immunity against pathogens, especially at mucosal surfaces, leads to microbial translocation, immune activation and HIV disease progression (36, 50). The functional properties of DCs are hijacked by HIV for its own dissemination advantage (30). Indeed, DCs have the unique capacity to render small quantities of viruses infectious (27, 29). Molecules expressed by DCs such as DC-SIGN (41) and DCIR (64) have the capacity to bind HIV virions. DC-SIGN mediated the internalization of HIV virions thus preserving virulence and insuring efficient transmission to $CD4^+$ T-cells (65). DCs are specialized in pathogen uptake, degradation and processing (2, 5). In order to preserve HIV virulence, DCs internalize virions in specific compartments (65). Also, HIV evolved mechanisms to interfere with the autophagy process in DCs to the detriment of the antigen presentation to $CD4^+$ T-cells (49). Additionally, HIV preferentially infects and subsequently depletes $CD4^+$ T-cells with specific antigenic specificities such as HIV and *Mycobacterium tuberculosis* (MT) (39). Thus, an optimal dissemination of HIV from DCs to $CD4^+$ T-cells coincides with alterations in the quality of immune responses against HIV itself and other opportunistic pathogens in HIV-infected subjects.

In this study, we performed a characterization of $CD16^-$ and $CD16^+$ MDDCs in terms of their capacity to induce antigen-specific $CD4^+$ T-cells. We also evaluated the impact of HIV on the quality of immune responses using cells from two donors. We acknowledge the fact that the inclusion of up to 7 donors is needed in the future for a solid conclusion. Our preliminary findings revealed that $CD16^-$ MDDCs display a superior ability to generate CMV, *C.albicans* and *S.aureus*-specific $CD4^+$ T-cells. Furthermore, $CD16^-$ MDDCs induced higher levels of IL-17A and IL-17F in

cells proliferating in response to *C.albicans* but not *S.aureus*. We also found that HIV infection lead to a decrease in the generation of antigen-specific lymphocytes induced either by total, $CD16^-$ or $CD16^+$ MDDCs. In fact, T-cell proliferation was inversely correlated with viral *trans* infection. Also, *S. aureus*-specific $CD4^+$ T-cells cultured with total MDDCs were susceptible to HIV infection compared to cells proliferating in response to CMV. $CD16^+$ *versus* $CD16^-$ MDDCs had a higher capacity of transmitting HIV to proliferating cells.

Few studies focused in the description of $CD16^-$ and $CD16^+$ MDDCs (26, 66-68). Previous findings originally indicated that both DC subsets induce similarly effector T-cells proliferation from autologous or allogeneic cultures (26). In our study, we found that $CD16^-$ compared to $CD16^+$ MDDCs had higher capacity to induce the proliferation of $CD4^+$ T-cells in response to CMV and *S. aureus*. CMV was shown to induce a Th1 polarization (69) whereas *C. albicans* and *S. aureus* were demonstrated to promote Th17 responses (55). At the opposite, another group reported that $CD16^+$ but not $CD16^-$ MDDCs led to stronger T-cell proliferation in response to antigens from *M. tuberculosis* and *Tetanus toxoid* (68). Whether these discrepancies are due to the different techniques used to generate $CD16^-$ and $CD16^+$ MDDCs remains to be determined. Nevertheless, we cannot exclude the possibility that $CD16^-$ and $CD16^+$ MDDCs may present different antigens at optimal levels. This property may be dependent on the antigen that the DC subset encounters. Indeed studies by the group of Geissmann demonstrated a division of labor between $CD16^-$ and $CD16^+$ monocytes in terms of TLR expression and ability to sense different bacterial and viral pathogens (70). Therefore, whether *M. tuberculosis* but not *S.aureus* is better sensed and processed for antigen presentation by $CD16^+$ MDDC to induce higher T-lymphocyte proliferation remains to be tested. This concept is also in line with our results that $CD16^-$ MDDCs drive higher frequency of

Th17-specific cytokines following encounter with *C. albicans* but not *S. aureus* antigens. Although *C. albicans* and *S. aureus* both generate Th17 responses, the cytokine profile induce by identical APCs are distinct as previously reported (55). *S. aureus* but not *C. albicans* induced IL-10 production, in addition to IL-17A (55). Our studies re-emphasized the appreciation that each antigens encountered has a unique way to shape host defense.

We have demonstrated that HIV exposure decreases the antigenic-specific T-cell proliferation induced by MDDCs despite the fact that HIV does not promote DC maturation. Our results are consistent with previous finding reporting that HIV-exposed MDDCs do not fully mature and are poorly activated (71). MDDCs exposed to HIV are thus unable to stimulate lymphocyte proliferation. Interestingly, the decrease observed in the proliferation of T-cells in response to SEB upon HIV infection was only observed in $CD16^-$ and $CD16^+$ MDDCs but not in total MDDCs. This may be explained by the viral quantity used in these two separate series of experiments. Total MDDCs were exposed to 10 ng of HIV-p24, whereas $CD16^-$ and $CD16^+$ MDDCs were infected with 50 ng of virus. Therefore, future experiments should test whether HIV affects the immunogenic potential of DCs in a dose response manner. $CD4^+$ T-cells proliferating to *S. aureus* were more susceptible to HIV infection compared to CMV-specific T-cells. This is consistent to previous finding demonstrating that the CMV-specific $CD4^+$ T-cells are resistant to HIV infection due to their autocrine production of CCR5 binding chemokines that limit the CCR5-mediated HIV entry (40). Furthermore, CMV-specific $CD4^+$ T-cells mainly exhibit a Th1 profile (54, 69) and our group previously demonstrated that Th1 compared to Th17 cells are more resistant to HIV infection *in vitro* (57). As demonstrated in this study, stimulation with *S. aureus* antigens leads to Th17 immune response. Studies by our group and others demonstrated that Th17 cells are highly permissive to

HIV infection (57, 58, 72). Therefore, the susceptibility of *S. aureus*-specific cells to HIV infection is likely to be linked to their polarization profile. One of the reasons explaining the lack of HIV-p24 in cells proliferating to *C.albicans* is their low frequency. In fact, in our experimental settings, HIV drastically decreased the frequency of *C. albicans*-specific T-cells induced by the $CD16^-$ MDDCs. $CD16^+$ MDDCs generate low to undetectable levels of proliferating cells. Thus, it appears that HIV has a superior capacity to decrease C. albicans compared to S. aureus antigen presentation by MDDCs. This is consistent with findings in a Nef transgenic mouse model, where an impaired frequency of Th17 responses and oropharyngeal candidiasis was reported (73, 74).

As demonstrated for the $CD16^+$ monocyte-derived macrophages (MDM) (23, 24), we report here that $CD16^+$ compared to $CD16^-$ MDDCs exhibit a higher ability to transmit HIV to $CD4^+$ T-cells in the context of antigen presentation. This indicates that $CD16^+$ MDMs and $CD16^+$ MDDCs share features that allow an efficient HIV dissemination. Similar to $CD16^+$ MDM (23, 24), $CD16^+$ MDDCs may induce higher activation of $CD4^+$ T-cells leading to their susceptibility to HIV infection. Ancuta *et al.* reported that $CD16^+$ MDM produce chemokines including CCL22 and CCL24, chemokines that activate resting $CD4^+$ T-cells for increased HIV permissiveness (23). The ability of $CD16^+$ MDDCs to produce these chemokines was demonstrated and results are included in a manuscript in preparation (75). Other unidentified factors expressed by $CD16^+$APCs may also favor HIV replication in target cells (75).

In conclusion, we demonstrate that HIV dramatically impairs the ability of MDDCs to promote antigen-specific immune responses and reveal a positive correlation between the efficacy of HIV dissemination by MDDCs and the magnitude of the HIV-mediated immunological alterations. We

further describe a division of labor between $CD16^-$ and $CD16^+$ MDDCs, with $CD16^-$ MDDCs having a superior immunogenic potential and $CD16^+$ MDDCs contributing more efficiently to HIV dissemination. This work provides a new original understanding of the functional heterogeneity of MDDCs subsets and highlights the pathogenic potential of $CD16^+$ MDDCs in the context of HIV-1 infection. Therefore, the expansion of $CD16^+$ monocytes in HIV-infected subjects should be used as biomarker to evaluate disease progression and response to treatment. Future studies should identify molecular determinants mediating HIV *trans* infection in $CD16^+$ MDDCs for the design of new intelligent cell-targeted therapeutic strategies aimed at HIV cure.

MATERIAL AND METHODS

Study subjects

Healthy HIV-uninfected donors were recruited at the Montreal Chest Institute, McGill University Health Centre and Centre Hospitalier de l'Université de Montreal (CHUM, Montreal, QC, Canada). Large quantities of PBMCs (10^9–10^{10} cells) were collected by leukapheresis as previously described (76). Cytomegalovirus (CMV) infection was determined upon detection of CMV-specific Abs using chemiluminescent microparticle immunoassay (CMIA) (63).

Ethics statement

This study, using PBMC samples from healthy HIV-uninfected subjects, was conducted in compliance with the principles included in the Declaration of Helsinki. This study received approval from the Institutional Review Board of the McGill University Health Centre and the CHUM-Research Centre, Montreal, Quebec, Canada. All human subjects that donated biological samples for this study provided written informed consent for their participation to the study. All human subjects agreed with the publication of the subsequent results generated using the samples.

Magnetic (MACS) and fluorescence activated cell sorting (FACS)

Total monocytes (Mo) were isolated from PBMC of HIV-uninfected subjects by negative selection using magnetic beads (Miltenyi) (16) and further stained with a cocktail of CD16, CD3, CD6, CD56, and CD1c Abs for FACS sorting. Our choice of not using CD14 Abs was to avoid any potential stimulation *via* CD14. The $CD16^+$ (including mainly non-classical $CD14^+CD16^{++}$ monocytes) and $CD16^-$ monocytes, lacking expression of the lineage markers CD3, CD8, CD19,

CD56, and CD1c were sorted by FACS (BDAria II; BD Biosciences). Quality control analysis post-sort indicated an average purity >95%.

Generation of monocyte-derived dendritic cells

Monocytes monocyte-derived DCs (MDDCs) were obtained by culturing monocytes in the presence of GM-CSF and IL-4 (20 ng/ml (R&D Systems) and RPMI 2% FBS media for six days. Media containing cytokines was refreshed every two days. The acquisition of an immature DC phenotype was assessed using a cocktail of CD14, CD1a, HLA-DR, CD83, and CCR7 Abs, as previously described (77).

Intracellular cytokine staining

Intracellular expression of cytokines was measured by FACS using the BD Cytofix/Cytoperm kit (BD Biosciences) and specific Abs, as previously described (63).

Antigen presentation assay

Cell proliferation was measured using the carboxyfluoroscein succinimidyl ester (CFSE) dilution assay (63), following co-culture with antigen-loaded autologous monocyte-derived dendritic cells (MDDC). Briefly, monocytes isolated from PBMCs by negative selection using magnetic beads (Miltenyi Biotec) (23) were differentiated into MDDC in the presence of GM-CSF and IL-4 (20 ng/ml; R&D Systems). MDDCs were loaded with SEB (25 ng/ml; Toxin Technologies), CMV-pp65 peptide pool (1 µg/ml; Miltenyi), *Candida albicans* hyphae LAM-1 (78) (25 µl protein lysate (63)) or heat-inactivated *S.aureus* (50µl of suspension) for one hour at 37°C and co-cultured with FACS-sorted CFSE-loaded T-cell subsets. MDDC:T-cell co-cultures (1:4 ratio) were maintained for 5 days

at 37 °C. MDDC:T-cell co-cultures were stained with CD3 (T-cell marker) and CD1c (DC marker). Proliferating T-cells were identified as cells with a $CFSE^{low}CD3^{+}CD1c^{-}$ phenotype. In parallel, MDDC:T-cell co-cultures were stimulated with PMA (50 ng/ml) and Ionomycin (1 μg/ml) in the presence of brefeldin A (2 μg/ml) and the expression of cytokines in proliferating T-cell subsets was quantified by FACS upon intracellular staining with specific IL-17A, IL-17F and IFN-γ Abs. Intracellular expression of cytokines was quantified by FACS (63).

HIV *trans* infection assay

Immature MDDC derived from total or $CD16^{+}$ and $CD16^{-}$ monocytes were exposed to the R5 NL4.3BaL HIV-1 strain (10 or 50 ng HIV-p24 *per* 10^{6} cells per 300 μl) or 3h at 37°C. Cells were extensively washed with RPMI 10% FBS to remove unbound virions. MDDCs were loaded in antigens as described above and then co-cultured with autologous memory $CD4^{+}$ T-cells. Cells were harvested at day 5 post co-culture, stained with CD3, CD1c and HIV-p24 Abs and the frequency of $CD4^{+}$ T-cells productively infected with HIV ($CD3^{+}CD1c^{-}$HIV-$p24^{+}$) was determined by FACS.

Statistics

Statistical analyses were performed using the GraphPad Prism 6. Details are included in Figure legends. Sample size calculations for microarray studies and all other investigations were based on preliminary results generated in the lab (16, 57, 79-81).

ACKNOWLEDGEMENTS

The authors thank the CHUM-Research Centre FACS Core Facility for expert technical support in FACS analysis and cell sorting, Mario Legault (HIV/AIDS and Infectious Diseases Network of the Fonds de Recherche Québec-Santé (FRQ-S)) for help with ethical approvals and informed consents, Dr. Louis de Repentigny and Mathieu Goupil for *Candida albicans* LAM-1 strain preparation, Dr. Dana Gabuzda (Dana-Farber Cancer Institute, Boston, MA, USA) for the HIV molecular clones. We thank Josée Girouard and Angie Massicotte (McGill University Health Centre) for their involvement in human subject recruitment for leukapheresis collection. We finally acknowledge the major contribution to this work of all human donors *via* their gift of leukapheresis.

Footnote

This work was supported by grants to PA from the CIHR (HOP-120239). This study was also supported by The Canadian HIV Cure Enterprise Team Grant HIG-133050 (to PA) from the CIHR in partnership with CANFAR and IAS. VSW received a CIHR Ph.D. Fellowships. JPR holds a Louis-Lowenstein Chair in Hematology and Oncology, McGill University.

REFERENCES

1. Mellman, I., and R. M. Steinman. 2001. Dendritic cells: specialized and regulated antigen processing machines. *Cell* 106: 255-258.
2. Savina, A., and S. Amigorena. 2007. Phagocytosis and antigen presentation in dendritic cells. *Immunol Rev* 219: 143-156.
3. Merad, M., P. Sathe, J. Helft, J. Miller, and A. Mortha. 2013. The dendritic cell lineage: ontogeny and function of dendritic cells and their subsets in the steady state and the inflamed setting. *Annu Rev Immunol* 31: 563-604.
4. Steinman, R. M. 2012. Decisions about dendritic cells: past, present, and future. *Annu Rev Immunol* 30: 1-22.
5. Guermonprez, P., J. Valladeau, L. Zitvogel, C. Thery, and S. Amigorena. 2002. Antigen presentation and T cell stimulation by dendritic cells. *Annu Rev Immunol* 20: 621-667.
6. Geissmann, F., M. G. Manz, S. Jung, M. H. Sieweke, M. Merad, and K. Ley. 2010. Development of monocytes, macrophages, and dendritic cells. *Science* 327: 656-661.
7. Ziegler-Heitbrock, L. 2015. Blood Monocytes and Their Subsets: Established Features and Open Questions. *Front Immunol* 6: 423.
8. Gordon, S., and P. R. Taylor. 2005. Monocyte and macrophage heterogeneity. *Nat Rev Immunol.* 5: 953-964.
9. Auffray, C., M. H. Sieweke, and F. Geissmann. 2009. Blood monocytes: development, heterogeneity, and relationship with dendritic cells. *Annu Rev Immunol* 27: 669-692.
10. Ziegler-Heitbrock, L., P. Ancuta, S. Crowe, M. Dalod, V. Grau, D. N. Hart, P. J. Leenen, Y. J. Liu, G. MacPherson, G. J. Randolph, J. Scherberich, J. Schmitz, K. Shortman, S. Sozzani,

H. Strobl, M. Zembala, J. M. Austyn, and M. B. Lutz. 2010. Nomenclature of monocytes and dendritic cells in blood. *Blood* 116: e74-80.

11. Hofer, T. P., A. M. Zawada, M. Frankenberger, K. Skokann, A. A. Satzl, W. Gesierich, M. Schuberth, J. Levin, A. Danek, B. Rotter, G. H. Heine, and L. Ziegler-Heitbrock. 2015. Characterization of subsets of the CD16-positive monocytes: impact of granulomatous inflammation and M-CSF-receptor mutation. *Blood*.

12. Thieblemont, N., L. Weiss, H. M. Sadeghi, C. Estcourt, and N. Haeffner-Cavaillon. 1995. CD14lowCD16high: a cytokine-producing monocyte subset which expands during human immunodeficiency virus infection. *Eur J Immunol* 25: 3418-3424.

13. Amirayan-Chevillard, N., H. Tissot-Dupont, C. Capo, C. Brunet, F. Dignat-George, Y. Obadia, H. Gallais, and J. L. Mege. 2000. Impact of highly active anti-retroviral therapy (HAART) on cytokine production and monocyte subsets in HIV-infected patients. *Clin Exp Immunol* 120: 107-112.

14. Pulliam, L., R. Gascon, M. Stubblebine, D. McGuire, and M. S. McGrath. 1997. Unique monocyte subset in patients with AIDS dementia. *Lancet* 349: 692-695.

15. Ancuta, P., A. Kamat, K. J. Kunstman, E. Y. Kim, P. Autissier, A. Wurcel, T. Zaman, D. Stone, M. Mefford, S. Morgello, E. J. Singer, S. M. Wolinsky, and D. Gabuzda. 2008. Microbial translocation is associated with increased monocyte activation and dementia in AIDS patients. *PLoS ONE* 3: e2516.

16. Ancuta, P., K. Y. Liu, V. Misra, V. S. Wacleche, A. Gosselin, X. Zhou, and D. Gabuzda. 2009. Transcriptional profiling reveals developmental relationship and distinct biological functions of CD16+ and CD16- monocyte subsets. *BMC Genomics* 10: 403.

17. Dutertre, C. A., S. Amraoui, A. DeRosa, J. P. Jourdain, L. Vimeux, M. Goguet, S. Degrelle, V. Feuillet, A. S. Liovat, M. Muller-Trutwin, N. Decroix, C. Deveau, L. Meyer, C. Goujard, P. Loulergue, O. Launay, Y. Richard, and A. Hosmalin. 2012. Pivotal role of M-DC8(+) monocytes from viremic HIV-infected patients in TNFalpha overproduction in response to microbial products. *Blood* 120: 2259-2268.

18. Ancuta, P., R. Rao, A. Moses, A. Mehle, S. K. Shaw, F. W. Luscinskas, and D. Gabuzda. 2003. Fractalkine preferentially mediates arrest and migration of CD16+ monocytes. *J Exp Med* 197: 1701-1707.

19. Geissmann, F., S. Jung, and D. R. Littman. 2003. Blood monocytes consist of two principal subsets with distinct migratory properties. *Immunity* 19: 71-82.

20. Auffray, C., D. Fogg, M. Garfa, G. Elain, O. Join-Lambert, S. Kayal, S. Sarnacki, A. Cumano, G. Lauvau, and F. Geissmann. 2007. Monitoring of blood vessels and tissues by a population of monocytes with patrolling behavior. *Science* 317: 666-670.

21. Jaworowski, A., D. D. Kamwendo, P. Ellery, S. Sonza, V. Mwapasa, E. Tadesse, M. E. Molyneux, S. J. Rogerson, S. R. Meshnick, and S. M. Crowe. 2007. CD16+ monocyte subset preferentially harbors HIV-1 and is expanded in pregnant malawian women with plasmodium falciparum malaria and HIV-1 infection. *J Infect Dis* 196: 38-42.

22. Ellery, P. J., E. Tippett, Y. L. Chiu, G. Paukovics, P. U. Cameron, A. Solomon, S. R. Lewin, P. R. Gorry, A. Jaworowski, W. C. Greene, S. Sonza, and S. M. Crowe. 2007. The CD16+ monocyte subset is more permissive to infection and preferentially harbors HIV-1 in vivo. *J Immunol* 178: 6581-6589.

23. Ancuta, P., P. Autissier, A. Wurcel, T. Zaman, D. Stone, and D. Gabuzda. 2006. CD16+ Monocyte-Derived Macrophages Activate Resting T Cells for HIV Infection by Producing CCR3 and CCR4 Ligands. *J Immunol.* 176: 5760-5771.

24. Ancuta, P., K. J. Kunstman, P. Autissier, T. Zaman, D. Stone, S. M. Wolinsky, and D. Gabuzda. 2006. CD16+ monocytes exposed to HIV promote highly efficient viral replication upon differentiation into macrophages and interaction with T cells. *Virology.* 344: 267-276. .

25. Qu, C., N. S. Brinck-Jensen, M. Zang, and K. Chen. 2014. Monocyte-derived dendritic cells: targets as potent antigen-presenting cells for the design of vaccines against infectious diseases. *International journal of infectious diseases : IJID : official publication of the International Society for Infectious Diseases* 19: 1-5.

26. Sanchez-Torres, C., G. S. Garcia-Romo, M. A. Cornejo-Cortes, A. Rivas-Carvalho, and G. Sanchez-Schmitz. 2001. CD16+ and CD16- human blood monocyte subsets differentiate in vitro to dendritic cells with different abilities to stimulate CD4+ T cells. *Int Immunol* 13: 1571-1581.

27. Cameron, P. U., P. S. Freudenthal, J. M. Barker, S. Gezelter, K. Inaba, and R. M. Steinman. 1992. Dendritic cells exposed to human immunodeficiency virus type-1 transmit a vigorous cytopathic infection to CD4+ T cells. *Science* 257: 383-387.

28. Granelli-Piperno, A., B. Moser, M. Pope, D. Chen, Y. Wei, F. Isdell, U. O'Doherty, W. Paxton, R. Koup, S. Mojsov, N. Bhardwaj, I. Clark-Lewis, M. Baggiolini, and R. M. Steinman. 1996. Efficient interaction of HIV-1 with purified dendritic cells via multiple chemokine coreceptors. *J Exp Med* 184: 2433-2438.

29. Pope, M., M. G. Betjes, N. Romani, H. Hirmand, P. U. Cameron, L. Hoffman, S. Gezelter, G. Schuler, and R. M. Steinman. 1994. Conjugates of dendritic cells and memory T lymphocytes from skin facilitate productive infection with HIV-1. *Cell* 78: 389-398.

30. Steinman, R. M. 2000. DC-SIGN: a guide to some mysteries of dendritic cells. *Cell* 100: 491-494.

31. McDonald, D., L. Wu, S. M. Bohks, V. N. KewalRamani, D. Unutmaz, and T. J. Hope. 2003. Recruitment of HIV and its receptors to dendritic cell-T cell junctions. *Science* 300: 1295-1297. Epub 2003 May 1291.

32. Piguet, V., and R. M. Steinman. 2007. The interaction of HIV with dendritic cells: outcomes and pathways. *Trends Immunol* 28: 503-510.

33. Jolly, C., K. Kashefi, M. Hollinshead, and Q. J. Sattentau. 2004. HIV-1 cell to cell transfer across an Env-induced, actin-dependent synapse. *J Exp Med* 199: 283-293.

34. Lane, H. C., and A. S. Fauci. 1985. Immunologic abnormalities in the acquired immunodeficiency syndrome. *Annu Rev Immunol.* 3: 477-500.

35. Haase, A. T. 2011. Early events in sexual transmission of HIV and SIV and opportunities for interventions. *Annu Rev Med* 62: 127-139.

36. Brenchley, J. M., and D. C. Douek. 2012. Microbial translocation across the GI tract. *Annu Rev Immunol* 30: 149-173.

37. Douek, D. C., J. M. Brenchley, M. R. Betts, D. R. Ambrozak, B. J. Hill, Y. Okamoto, J. P. Casazza, J. Kuruppu, K. Kunstman, S. Wolinsky, Z. Grossman, M. Dybul, A. Oxenius, D. A. Price, M. Connors, and R. A. Koup. 2002. HIV preferentially infects HIV-specific CD4+ T cells. *Nature* 417: 95-98.

38. Geldmacher, C., N. Ngwenyama, A. Schuetz, C. Petrovas, K. Reither, E. J. Heeregrave, J. P. Casazza, D. R. Ambrozak, M. Louder, W. Ampofo, G. Pollakis, B. Hill, E. Sanga, E. Saathoff, L. Maboko, M. Roederer, W. A. Paxton, M. Hoelscher, and R. A. Koup. 2010. Preferential infection and depletion of Mycobacterium tuberculosis-specific CD4 T cells after HIV-1 infection. *J Exp Med* 207: 2869-2881.

39. Saharia, K. K., and R. A. Koup. 2013. T cell susceptibility to HIV influences outcome of opportunistic infections. *Cell* 155: 505-514.

40. Casazza, J. P., J. M. Brenchley, B. J. Hill, R. Ayana, D. Ambrozak, M. Roederer, D. C. Douek, M. R. Betts, and R. A. Koup. 2009. Autocrine production of beta-chemokines protects CMV-Specific CD4 T cells from HIV infection. *PLoS Pathog* 5: e1000646.

41. Geijtenbeek, T. B., D. S. Kwon, R. Torensma, S. J. van Vliet, G. C. van Duijnhoven, J. Middel, I. L. Cornelissen, H. S. Nottet, V. N. KewalRamani, D. R. Littman, C. G. Figdor, and Y. van Kooyk. 2000. DC-SIGN, a dendritic cell-specific HIV-1-binding protein that enhances trans-infection of T cells. *Cell* 100: 587-597.

42. Bakri, Y., C. Schiffer, V. Zennou, P. Charneau, E. Kahn, A. Benjouad, J. C. Gluckman, and B. Canque. 2001. The maturation of dendritic cells results in postintegration inhibition of HIV-1 replication. *J Immunol* 166: 3780-3788.

43. Nobile, C., C. Petit, A. Moris, K. Skrabal, J. P. Abastado, F. Mammano, and O. Schwartz. 2005. Covert human immunodeficiency virus replication in dendritic cells and in DC-SIGN-expressing cells promotes long-term transmission to lymphocytes. *J Virol* 79: 5386-5399.

44. Laguette, N., B. Sobhian, N. Casartelli, M. Ringeard, C. Chable-Bessia, E. Segeral, A. Yatim, S. Emiliani, O. Schwartz, and M. Benkirane. 2011. SAMHD1 is the dendritic- and myeloid-cell-specific HIV-1 restriction factor counteracted by Vpx. *Nature* 474: 654-657.

45. Manel, N., B. Hogstad, Y. Wang, D. E. Levy, D. Unutmaz, and D. R. Littman. 2010. A cryptic sensor for HIV-1 activates antiviral innate immunity in dendritic cells. *Nature* 467: 214-217.

46. Silvin, A., and N. Manel. 2015. Innate immune sensing of HIV infection. *Curr Opin Immunol* 32: 54-60.

47. Miller, E., and N. Bhardwaj. 2013. Dendritic cell dysregulation during HIV-1 infection. *Immunol Rev* 254: 170-189.

48. Blanchet, F., A. Moris, J. P. Mitchell, and V. Piguet. 2011. A look at HIV journey: from dendritic cells to infection spread in CD4(+) T cells. *Curr Opin HIV AIDS* 6: 391-397.

49. Blanchet, F. P., A. Moris, D. S. Nikolic, M. Lehmann, S. Cardinaud, R. Stalder, E. Garcia, C. Dinkins, F. Leuba, L. Wu, O. Schwartz, V. Deretic, and V. Piguet. 2010. Human immunodeficiency virus-1 inhibition of immunoamphisomes in dendritic cells impairs early innate and adaptive immune responses. *Immunity* 32: 654-669.

50. Sandler, N. G., and D. C. Douek. 2012. Microbial translocation in HIV infection: causes, consequences and treatment opportunities. *Nat Rev Microbiol* 10: 655-666.

51. Dong, C. 2008. TH17 cells in development: an updated view of their molecular identity and genetic programming. *Nat Rev Immunol* 8: 337-348.

52. Weaver, C. T., C. O. Elson, L. A. Fouser, and J. K. Kolls. 2013. The Th17 pathway and inflammatory diseases of the intestines, lungs, and skin. *Annu Rev Pathol* 8: 477-512.

53. Gaffen, S. L., R. Jain, A. V. Garg, and D. J. Cua. 2014. The IL-23-IL-17 immune axis: from mechanisms to therapeutic testing. *Nat Rev Immunol* 14: 585-600.

54. Acosta-Rodriguez, E. V., L. Rivino, J. Geginat, D. Jarrossay, M. Gattorno, A. Lanzavecchia, F. Sallusto, and G. Napolitani. 2007. Surface phenotype and antigenic specificity of human interleukin 17-producing T helper memory cells. *Nat Immunol* 8: 639-646.

55. Zielinski, C. E., F. Mele, D. Aschenbrenner, D. Jarrossay, F. Ronchi, M. Gattorno, S. Monticelli, A. Lanzavecchia, and F. Sallusto. 2012. Pathogen-induced human TH17 cells produce IFN-gamma or IL-10 and are regulated by IL-1beta. *Nature* 484: 514-518.

56. Acosta-Rodriguez, E. V., G. Napolitani, A. Lanzavecchia, and F. Sallusto. 2007. Interleukins 1beta and 6 but not transforming growth factor-beta are essential for the differentiation of interleukin 17-producing human T helper cells. *Nat Immunol* 8: 942-949.

57. Gosselin, A., P. Monteiro, N. Chomont, F. Diaz-Griffero, E. A. Said, S. Fonseca, V. Wacleche, M. El-Far, M. R. Boulassel, J. P. Routy, R. P. Sekaly, and P. Ancuta. 2010. Peripheral blood CCR4+ CCR6+ and CXCR3+ CCR6+ CD4+ T cells are highly permissive to HIV-1 infection. *J Immunol* 184: 1604-1616.

58. El Hed, A., A. Khaitan, L. Kozhaya, N. Manel, D. Daskalakis, W. Borkowsky, F. Valentine, D. R. Littman, and D. Unutmaz. 2010. Susceptibility of human Th17 cells to human immunodeficiency virus and their perturbation during infection. *J Infect Dis* 201: 843-854.

59. Milner, J. D., N. G. Sandler, and D. C. Douek. 2010. Th17 cells, Job's syndrome and HIV: opportunities for bacterial and fungal infections. *Curr Opin HIV AIDS* 5: 179-183.

60. Lahaye, X., and N. Manel. 2015. Viral and cellular mechanisms of the innate immune sensing of HIV. *Curr Opin Virol* 11: 55-62.

61. Arrighi, J. F., M. Pion, M. Wiznerowicz, T. B. Geijtenbeek, E. Garcia, S. Abraham, F. Leuba, V. Dutoit, O. Ducrey-Rundquist, Y. van Kooyk, D. Trono, and V. Piguet. 2004. Lentivirus-mediated RNA interference of DC-SIGN expression inhibits human

immunodeficiency virus transmission from dendritic cells to T cells. *J Virol* 78: 10848-10855.

62. Che, K. F., R. L. Sabado, E. M. Shankar, V. Tjomsland, D. Messmer, N. Bhardwaj, J. D. Lifson, and M. Larsson. 2010. HIV-1 impairs in vitro priming of naive T cells and gives rise to contact-dependent suppressor T cells. *Eur J Immunol* 40: 2248-2258.

63. Wacleche, V. S., N. Chomont, A. Gosselin, P. Monteiro, M. Goupil, H. Kared, C. Tremblay, N. Bernard, M. R. Boulassel, J. P. Routy, and P. Ancuta. 2012. The colocalization potential of HIV-specific CD8+ and CD4+ T-cells is mediated by integrin beta7 but not CCR6 and regulated by retinoic acid. *PLoS One* 7: e32964.

64. Lambert, A. A., C. Gilbert, M. Richard, A. D. Beaulieu, and M. J. Tremblay. 2008. The C-type lectin surface receptor DCIR acts as a new attachment factor for HIV-1 in dendritic cells and contributes to trans- and cis-infection pathways. *Blood* 112: 1299-1307.

65. Kwon, D. S., G. Gregorio, N. Bitton, W. A. Hendrickson, and D. R. Littman. 2002. DC-SIGN-mediated internalization of HIV is required for trans-enhancement of T cell infection. *Immunity* 16: 135-144.

66. Randolph, G. J., G. Sanchez-Schmitz, R. M. Liebman, and K. Schakel. 2002. The CD16(+) (FcgammaRIII(+)) Subset of Human Monocytes Preferentially Becomes Migratory Dendritic Cells in a Model Tissue Setting. *J Exp Med* 196: 517-527.

67. Rivas-Carvalho, A., M. A. Meraz-Rios, L. Santos-Argumedo, S. Bajana, G. Soldevila, M. E. Moreno-Garcia, and C. Sanchez-Torres. 2004. CD16+ human monocyte-derived dendritic cells matured with different and unrelated stimuli promote similar allogeneic Th2 responses: regulation by pro- and anti-inflammatory cytokines. *Int Immunol* 16: 1251-1263.

68. Bajana, S., N. Herrera-Gonzalez, J. Narvaez, H. Torres-Aguilar, A. Rivas-Carvalho, S. R. Aguilar, and C. Sanchez-Torres. 2007. Differential CD4(+) T-cell memory responses induced by two subsets of human monocyte-derived dendritic cells. *Immunology* 122: 381-393.

69. Rivino, L., M. Messi, D. Jarrossay, A. Lanzavecchia, F. Sallusto, and J. Geginat. 2004. Chemokine receptor expression identifies Pre-T helper (Th)1, Pre-Th2, and nonpolarized cells among human CD4+ central memory T cells. *J Exp Med* 200: 725-735.

70. Cros, J., N. Cagnard, K. Woollard, N. Patey, S. Y. Zhang, B. Senechal, A. Puel, S. K. Biswas, D. Moshous, C. Picard, J. P. Jais, D. D'Cruz, J. L. Casanova, C. Trouillet, and F. Geissmann. 2010. Human CD14dim monocytes patrol and sense nucleic acids and viruses via TLR7 and TLR8 receptors. *Immunity* 33: 375-386.

71. Manches, O., D. Frleta, and N. Bhardwaj. 2014. Dendritic cells in progression and pathology of HIV infection. *Trends Immunol* 35: 114-122.

72. Alvarez, Y., M. Tuen, G. Shen, F. Nawaz, J. Arthos, M. J. Wolff, M. A. Poles, and C. E. Hioe. 2013. Preferential HIV Infection of CCR6+ Th17 Cells Is Associated with Higher Levels of Virus Receptor Expression and Lack of CCR5 Ligands. *J Virol* 87: 10843-10854.

73. Goupil, M., V. Cousineau-Cote, F. Aumont, S. Senechal, L. Gaboury, Z. Hanna, P. Jolicoeur, and L. de Repentigny. 2014. Defective IL-17- and IL-22-dependent mucosal host response to Candida albicans determines susceptibility to oral candidiasis in mice expressing the HIV-1 transgene. *BMC immunology* 15: 49.

74. de Repentigny, L., M. Goupil, and P. Jolicoeur. 2015. Oropharyngeal Candidiasis in HIV Infection: Analysis of Impaired Mucosal Immune Response to Candida albicans in Mice Expressing the HIV-1 Transgene. *Pathogens* 4: 406-421.

75. Wacleche, V. S., J. P. Goulet, A. Gosselin, M. C. Gaudreau, A. Cleret-Buhot, D. Gauchat, Y. Zhang, J. P. Routy, and P. Ancuta. 2015. Molecular Determinants of Pathogenicity in Dendritic Cells Derived from CD16+ Monocytes in the Context of HIV-1 Infection. *Journal of Immunology* in preparation for submission.

76. Boulassel, M. R., G. Spurll, D. Rouleau, C. Tremblay, M. Edwardes, R. P. Sekaly, R. Lalonde, and J. P. Routy. 2003. Changes in immunological and virological parameters in HIV-1 infected subjects following leukapheresis. *J Clin Apher* 18: 55-60.

77. Ancuta, P., L. Weiss, and N. Haeffner-Cavaillon. 2000. CD14+CD16++ cells derived in vitro from peripheral blood monocytes exhibit phenotypic and functional dendritic cell-like characteristics. *Eur J Immunol* 30: 1872-1883.

78. Goupil, M., E. B. Trudelle, V. Dugas, C. Racicot-Bergeron, F. Aumont, S. Senechal, Z. Hanna, P. Jolicoeur, and L. de Repentigny. 2009. Macrophage-mediated responses to Candida albicans in mice expressing the human immunodeficiency virus type 1 transgene. *Infect Immun* 77: 4136-4149.

79. Monteiro, P., A. Gosselin, V. S. Wacleche, M. El-Far, E. A. Said, H. Kared, N. Grandvaux, M. R. Boulassel, J. P. Routy, and P. Ancuta. 2011. Memory CCR6+CD4+ T cells are preferential targets for productive HIV type 1 infection regardless of their expression of integrin beta7. *J Immunol* 186: 4618-4630.

80. Bernier, A., A. Cleret-Buhot, Y. Zhang, J. P. Goulet, P. Monteiro, A. Gosselin, S. Dafonseca, V. S. Wacleche, M. A. Jenabian, J. P. Routy, C. Tremblay, and P. Ancuta. 2013. Transcriptional profiling reveals molecular signatures associated with HIV permissiveness in Th1Th17 cells and identifies Peroxisome Proliferator-Activated Receptor Gamma as an intrinsic negative regulator of viral replication. *Retrovirology* 10: 160.

81. DaFonseca, S., J. Niessl, S. Pouvreau, V. S. Wacleche, A. Gosselin, A. Cleret-Buhot, N. Bernard, C. Tremblay, M. A. Jenabian, J. P. Routy, and P. Ancuta. 2015. Impaired Th17 polarization of phenotypically naive CD4(+) T-cells during chronic HIV-1 infection and potential restoration with early ART. *Retrovirology* 12: 38.

Figure Legends

Figure 1: HIV-1 fails to promote dendritic cell (DC) maturation. Peripheral blood monocytes were isolated by negative selection using magnetic beads (Miltenyi) and cultured in presence of GM-CSF and IL-4 (20 ng/mL) for 6 days. Monocyte-derived DCs (MDDC) were exposed to the R5 NL4.3BaL HIV strain (100 ng HIV-p24/10^6 cells) and cultured for additional 45h. In parallel, MDDCs were stimulated or not with *E. coli* LPS (1 μg/mL) for 48h. MDDC were then stained with CD14, CD1c, HLA-DR, CD83 and CCR7 Abs and analyzed by FACS. **(A)** Shown is the phenotype of immature (Media), mature (LPS) and HIV exposed MDDCs. Results are from one donor representative of results generated with cells from six different donors (n=6). **(B)** Shown are the statistical analyses for the frequency and the MFI of HLA-DR, CD83 and CCR7 expression in MDDCs from six different donors. Kruskal-Wallis p-values are indicated on the graphs.

Figure 2: HIV impairs the immunogenic potential of MDDCs. (A) Shown is the flowchart of the experimental approach. Briefly, MDDC generated as in Figure 1 were incubated in the presence or absence of R5 NL4.3BaL HIV (10 ng HIV-p24/10^6 cells) during 3h and the unbound virus was removed by extensive washing. MDDCs were subsequently loaded with *Staphylococcal enterotoxin B* (SEB; 1μg/ml), *Cytomegalovirus* (CMV) pp65 recombinant protein (1 μg/ml), or *Staphylococcus aureus* (*S. aureus*) ($5x10^6$cells/assay). Then, MDDC were co-cultured with $CD4^+$ T-cells loaded with CFSE (0.5 μM) (MDDC:T-cell ratio 1:4) for 5 days at 37ºC. Proliferating cells were identified by FACS analysis as $CFSE^{low}$ cells. **(B)** Shown here is the statistical analysis of $CD4^+$ T-cell proliferation in response to SEB, CMV and S. aureus in five different donors. Paired t-Test p-values are presented on the graphs. **(C)** Intracellular staining with HIV-p24 Abs was performed and the expression of HIV-p24 was analyzed by FACS in $CFSE^{low}$ cells. Shown are statistical analyses of

the frequency of HIV-p24^{+}CFSE^{low} T-cells in five different donors. **(D)** Shown is a correlation calculated between the relative proliferation of antigen-specific T-cells when MDDC were exposed or not to HIV (indicative of the immunogenic impairment in the presence of HIV) and the frequency of HIV-p24^{+}CFSE^{low} T-cells (indicative of the magnitude of HIV *trans* infection) in five different donors for all three antigenic specificities. Spearman correlation (p and r values) and linear regression calculations (p and r^2 values) are indicated on the graph.

Figure 3: Differences in the ability of CD16^{+} and CD16^{-} MDDCs to promote antigen-specific CD4^{+} T-cell proliferation. Sorted CD16^{+} and CD16^{-} monocytes were differentiated into immature MDDC as described in Figure 1. The MDDC subsets were loaded with antigens (SEB, CMV, or *S.aureus*) and co-cultured with autologous CFSE-loaded CD4^{+} T-cells (MDDC:T-cell ratio 1:4) for 5 days. Co-cultures were stimulated with PMA and Ionomycin in the presence of Brefeldin A for 16h. Surface staining was performed with CD3 Abs to identify T cells in MDDC:T-cell co-cultures. Intracellular staining was performed with IL-17A, IL-17F and IFN-γ Abs. (**A**) Shown is the FACS gating strategy for the identification of proliferating CD4^{+} T-cells (CD3^{+}CFSE^{low}). (**B**) Shown is the frequency of T-cells proliferating in response to SEB, CMV, or *S.aureus* in CD16^{+} and CD16^{-} MDDC:T-cell co-cultures. (**C-D**) Antigen-specific T-cells were further analyzed for the co-expression of IL-17A, IL-17F or TNF-α. (**C**) Shown is the FACS gating strategy for the intracellular expression of cytokines by CD3^{+} T-cells. (**D**) Shown is the frequency of cytokine-expressing T-cells proliferating in response to *S.aureus* within each subset. (**B**, **D**) Shown are results on matched samples from one donor representative of results obtained with cells from three different donors.

Figure 4: Differences in the ability of $CD16^+$ and $CD16^-$ MDDCs to promote HIV *trans* infection in antigen-specific $CD4^+$ T-cells. $CD16^+$ and $CD16^-$ MDDC subsets were generated as in Figure 3. Cells were exposed or not to R5 NL4.3BaL HIV (50 ng/10E6 cells) for 3h and unbound virions were removed by extensive washing. MDDCs were loaded in antigens and co-cultured with autologous CFSE-loaded $CD4^+$ T-cells (MDDC:T-cell ratio 1:4) for 5 days. Surface staining was performed with CD3 Abs to identify T cells in MDDC:T-cell co-cultures. Intracellular staining was performed with HIV-p24 Abs. Shown is the expression of HIV-p24 in $CD3^+CFSE^{low}$ T-cells specific to SEB, CMV, and *S. aureus*. Shown are results on matched samples from one donor representative of results obtained with cells from two different donors.

Figure 5: Effects of HIV exposure on the immunogenic potential of $CD16^+$ and $CD16^-$ MDDCs. MDDC subsets were generated, exposed to HIV, loaded in antigens and co-cultured with $CD4^+$ T-cells for five days as in Figure 4. MDDC:T-cell co-cultures were stimulated with PMA and Ionomycin in the presence of Brefeldin A for 16h. Surface staining was performed with CD3 Abs to identify T cells in MDDC:T-cell co-cultures. Intracellular staining was performed with IL-17A, IL-17F and IFN-γ Abs. **(A-B)** The % of $CD3^+CFSE^{low}$ T-cells was compared in $CD16^+$ and $CD16^-$ MDDC:T-cell co-cultures exposed or not to HIV. **(C)** The % of cells expressing IL-17A, IL-17F and IFN-γ was analyzed within $CD3^+CFSE^{low}$ T-cells from $CD16^+$ and $CD16^-$ MDDC: T-cell co-cultures. Shown are results on matched samples from one donor representative of results obtained with cells from two different donors.

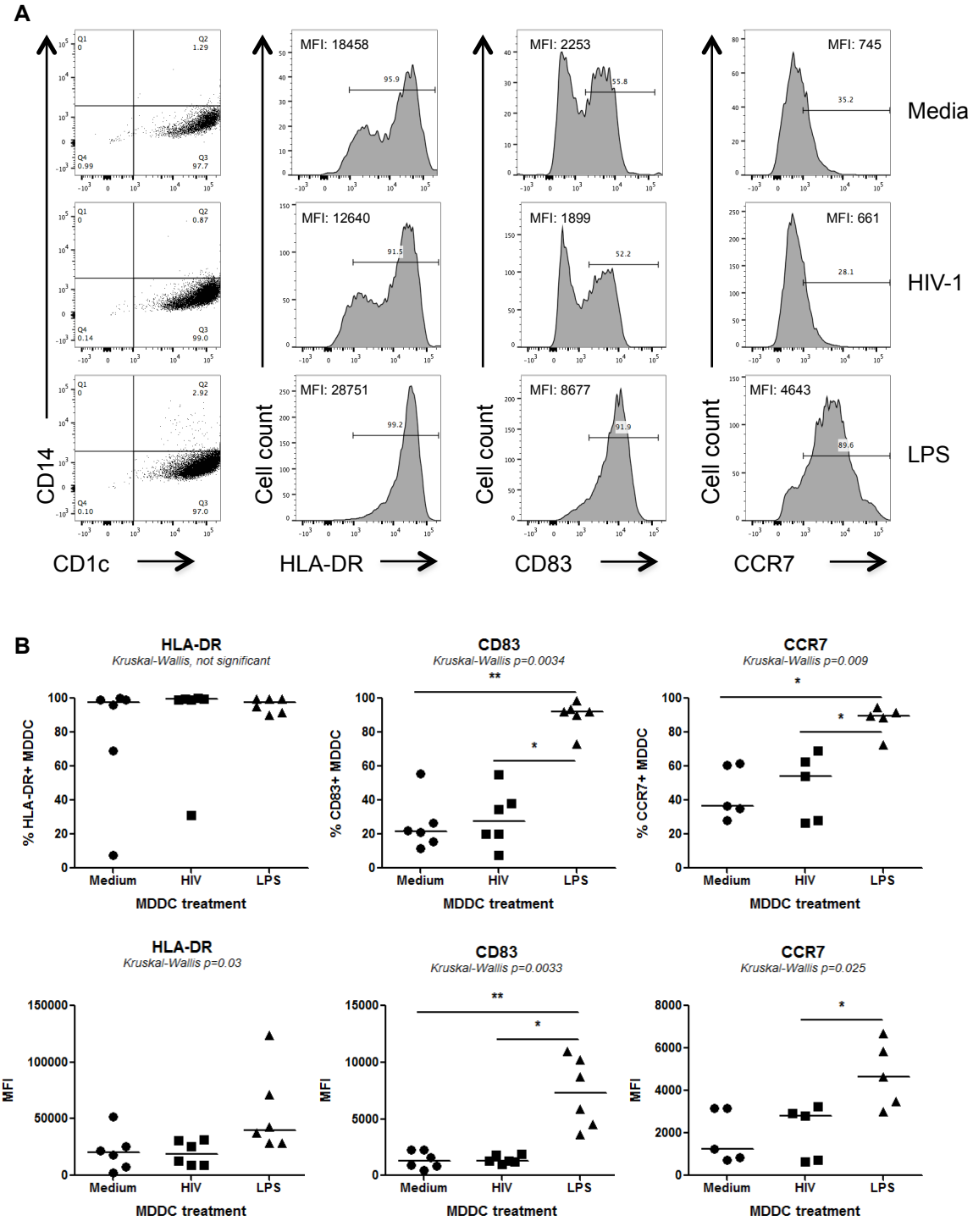

Wacleche *et al.* Figure 1

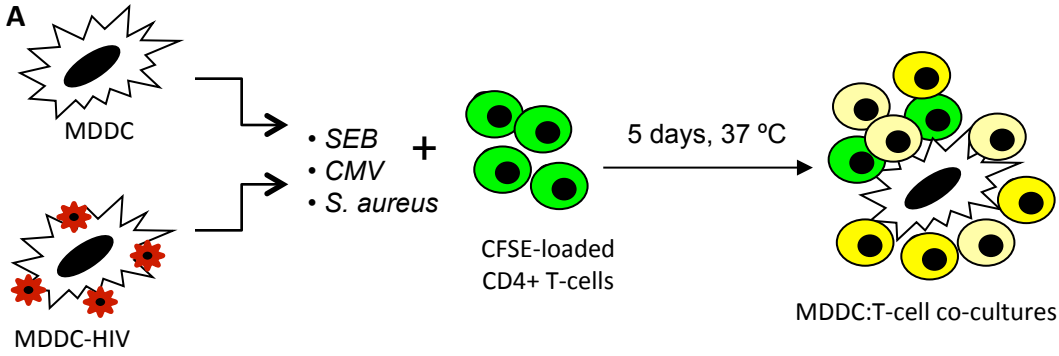

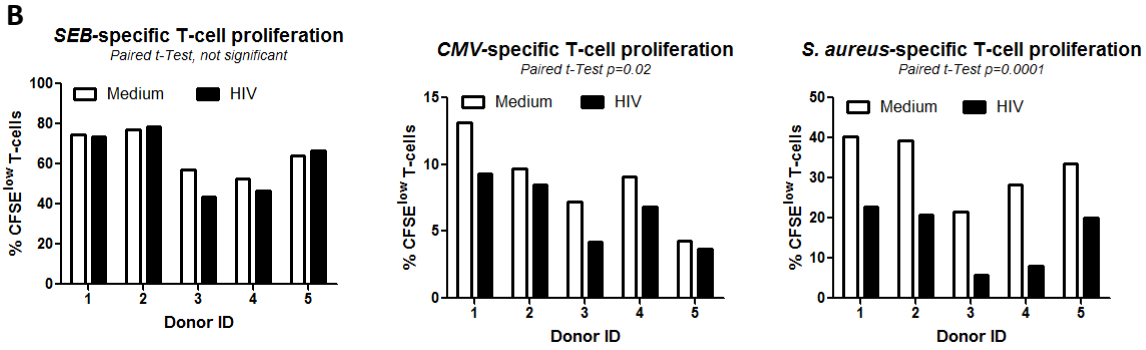

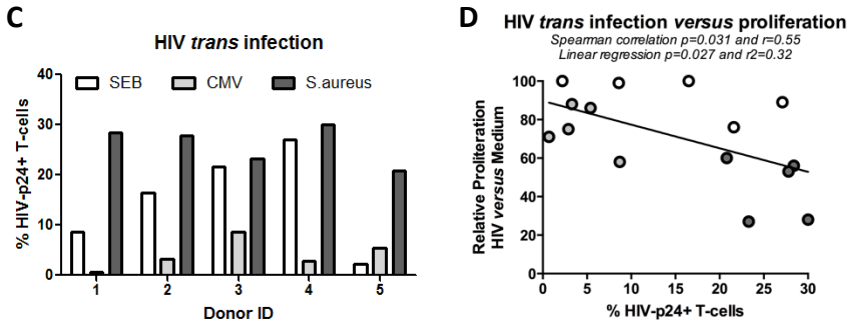

Wacleche *et al.* Figure 2

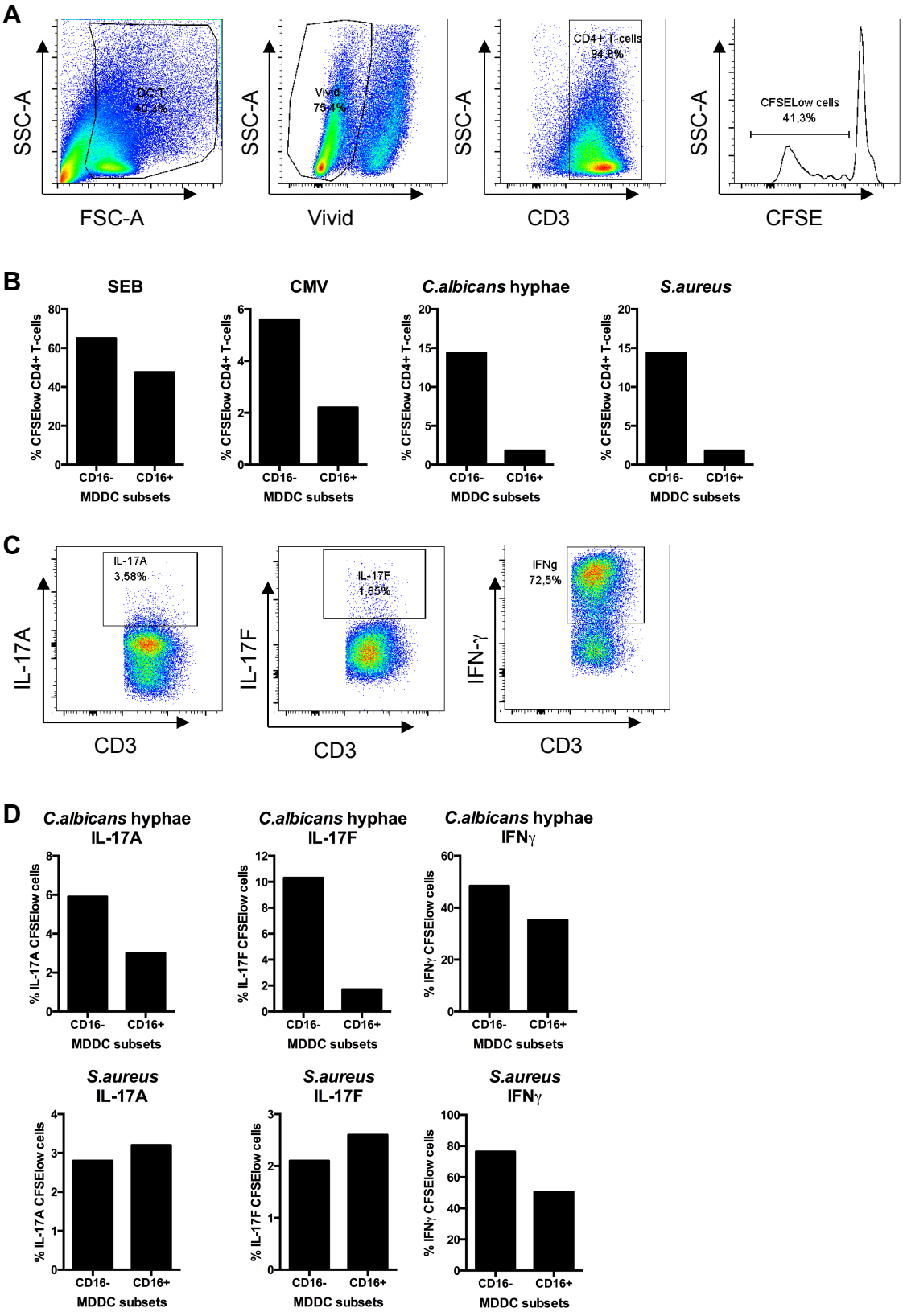

Wacleche *et al.* Figure 3

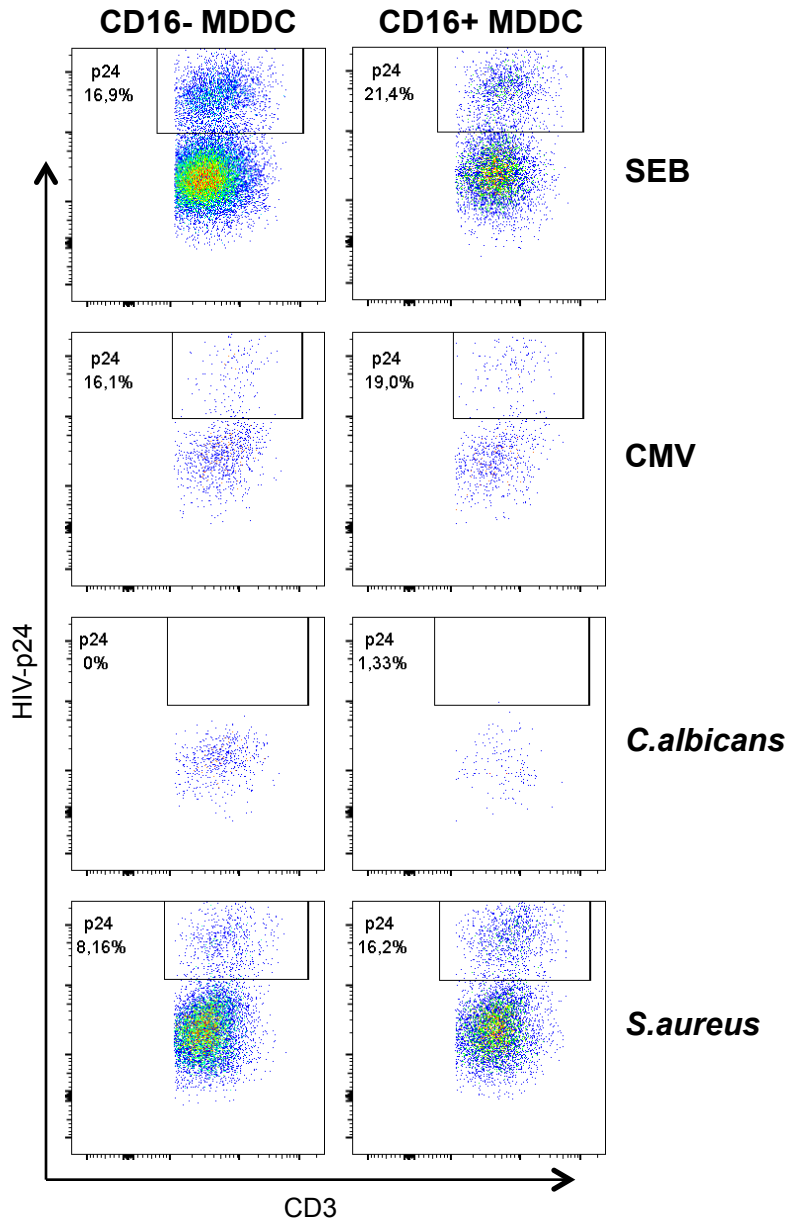

Wacleche *et al.* Figure 4

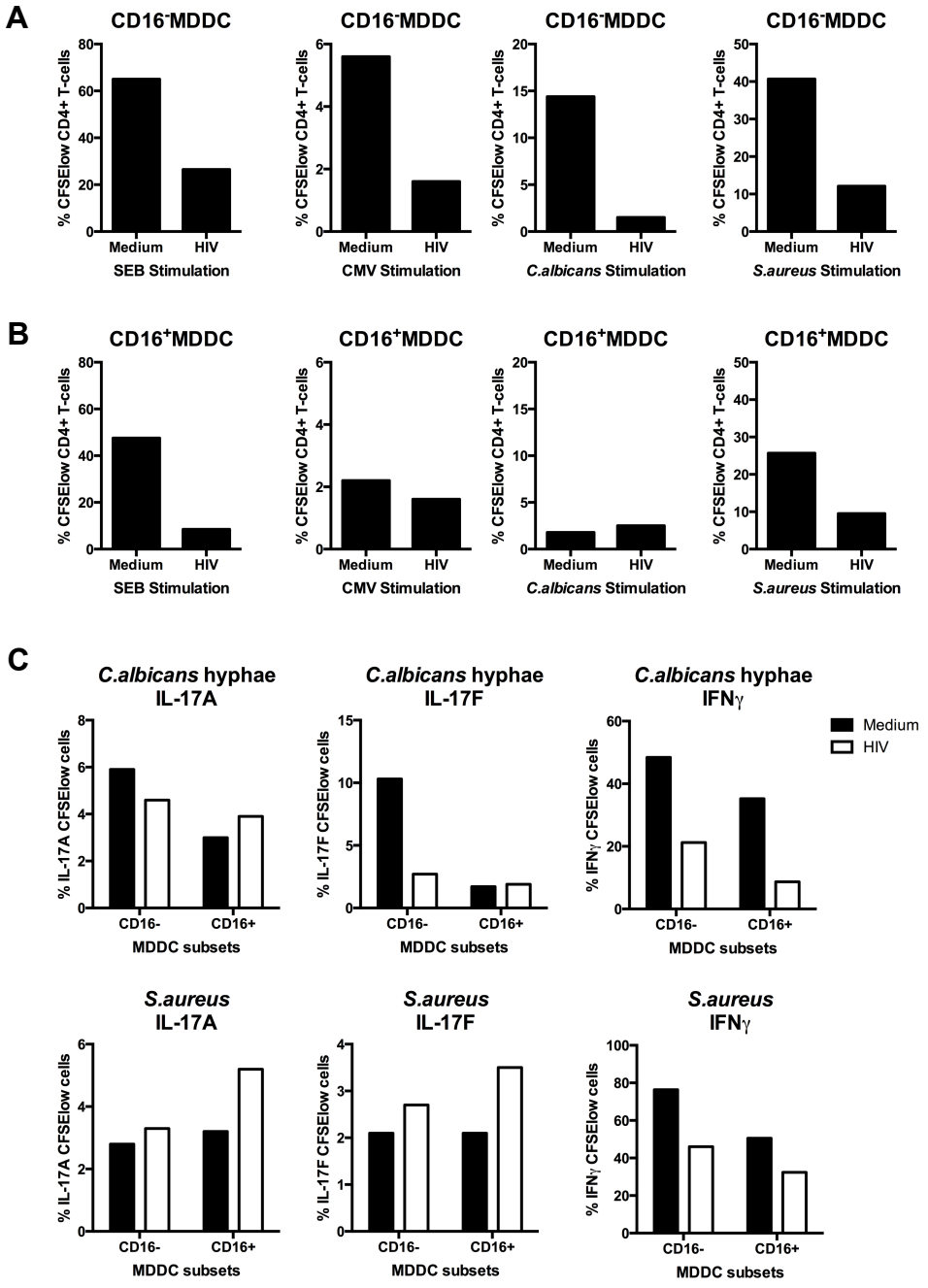

Wacleche *et al.* Figure 5

CHAPTER 5:
DISCUSSION AND CONCLUSION

The goal of this thesis was to improve our fundamental and translational knowledge on the contribution of Th17 cells and $CD16^+$ monocyte-derived DCs (MDDCs) to HIV-1 pathogenesis.

In the first part of this thesis (Manuscript #1), our goal was to study the lineage commitment and susceptibility to HIV in two new previously uncharacterized memory $CCR6^+CD4^+$ T-cell subsets with differential expression of CCR4 and CXCR3, referred to as the $CCR6^+$DN and $CCR6^+$DP cells. The preliminary results that stimulated this research project showed that $CCR6^+$DN and $CCR6^+$DP expressed the main Th17-specific transcription factor RORC; this supported the possibility that $CCR6^+$DN and $CCR6^+$DP subsets are part of the Th17 development program. Considering the phenotypic heterogeneity within the $CCR6^+$ population (Figures 13-14), the previous surface characterization of Th17 ($CCR4^+CCR6^+$) and Th1Th17 ($CXCR3^+CCR6^+$) may not reflect the whole complexity of the Th17 lineage during homeostasis and inflammatory conditions. Furthermore, the existence of pathogenic and non-pathogenic Th17 cells in autoimmunity (355, 356, 359) prompted us to further define this concept in the context of Th17 contribution to HIV persistence.

In the second part of this thesis, we performed an in-depth characterization of two distinct DC subsets *(i.e.,* $CD16^+$ and $CD16^-$ MDDCs) derived from monocytic precursors with differential expression of the FcγRIII/CD16: classical $CD16^-$ monocytes and non-classical and intermediate $CD16^+$ monocytes. Our goal was to further understand the functional diversity of DC subsets in the induction of an immune response (Manuscript #2 and Manuscript #3). Also, the fact that HIV infection is associated with the expansion of $CD16^+$ monocytes (63, 499, 521, 524, 525) prompted us to investigate the contribution of each MDDC subset to viral dissemination and to identify molecular mechanism of HIV permissiveness *versus* resistance in the two DC subsets. We have generated preliminary results demonstrating a superior capacity of $CD16^+$ MDDCs to induce HIV replication in autologous $CD4^+$ T-cells (Figure 15). This study provides additional understanding of the mechanisms by which HIV exploits the innate immune system for its own dissemination advantage.

5.1 THE HETEROGENEITY OF TH17 CELLS AND ROLE IN HIV-1 INFECTION (MANUSCRIPT #1)

5.1.1 IDENTIFICATION OF TWO NEW TRANSCRIPTIONALLY DISTINCT TH17 SUBSETS WITH DIFFERENTIAL EXPRESSION OF CCR4 AND CXCR3

One of the purposes of this study was to investigate the lineage commitment of two new previously uncharacterized $CCR6^+$ subsets with differential expression of CCR4 and CXCR3. In 2007, CCR6 was identified as a marker expressed on the surface of Th17 cells (297). In 2007, the group of Sallusto functionally characterized two populations of CD4+ T-cells expressing CCR6 as follows: Th17-polarized cells with a $CCR4^+CXCR3^-$ phenotype and Th1Th17-polarized cells with a $CCR4^-CXCR3^+$ phenotype (298). The $CCR4^+$Th17 population was originally characterized as being enriched in cells producing homogenously IL-17A, whereas the $CCR4^-CXCR3^+$Th1Th17 cells were found to comprise a major fraction of Th1 cell producing IFN-γ along with minor population of cells expressing both IL-17A and IFN-γ. Several groups including ours subsequently published an in-depth characterization of these subsets (276, 302, 304, 344, 436). Of note, Th1Th17 cells are also referred in some studies as Th1* cells (276, 304).

Based on the differential expression of CCR4 and CXCR3, we identified the $CCR6^+$DN and $CCR6^+$DP subsets as two new populations of the Th17 lineage. Following TCR triggering, we found that the $CCR6^+$DN cells produced IL-17A at levels similar to those observed in the $CCR4^+CXCR3^-$Th17 cells (referred to as Th17 cells), whereas the $CCR6^+$DP cells expressed lower levels of IL-17A comparable to those detected in the Th1Th17 cells (Figure 1, Manuscript #1). These results are in line with our hypothesis and are consistent with preliminary findings in which both $CCR6^+$DN and $CCR6^+$DP subsets expressed RORC (Figure 14). As opposed to Th17, $CCR6^+$DN and $CCR6^+$DP subsets produced IFN-γ but at levels lower compared to those of $CCR4^-CXCR3^+$Th1Th17 cells (referred to as Th1Th17 cells). These results indicate that similar to Th1Th17 cells, $CCR6^+$DN and $CCR6^+$DP represent heterogeneous population of the Th17 lineage. All four $CCR6^+$ subsets produced low to undetectable levels of the Th2-specific cytokine, IL-5 (data not shown). Among total memory cells, the frequency of $CCR6^+$DN is similar to that observed in Th17 and Th1Th17 cells. The frequency of $CCR6^+$DP is slightly inferior. Moreover, genome-wide transcriptional analysis demonstrated that $CCR6^+$DN and

CCR6$^+$DP share similar expression of Th17-associated markers, including RORC, IL-17F, RORA, IL-23R, CCL20, IL-22, and IL-26 (Figure 1, Manuscript #1). Our results indicated that the human Th17 lineage is not restricted only to cells strictly co-expressing CCR6/CCR4 and CCR6/CXCR3 as originally thought (298). This current surface phenotype characterization of the human Th17 subsets may underestimate the diversity of the entire lineage. Interestingly, our findings are supported by recent studies of the group of Sallusto in which a population resembling to the CCR6$^+$DP is described (304). Therefore, immune monitoring studies should take into consideration changes in the frequency and function of four Th17 subsets identified based on the differential expression of CCR6, CCR4, and CXCR3.

Despite the expression of common of Th17-specific markers, CCR6$^+$DN and CCR6$^+$DP cells represented distinct populations as reflected by differences in their transcriptional profiles. The number of differentially expressed genes (DEG) between the CCR6$^+$DN and Th17 was inferior to the number of DEG observed between the Th17 and CCR6$^+$DP cells (p-value <0.05; FC cut-off 1.3) (Figure 2, Manuscript #1). In fact, when considering the adjusted p-values (adj. p<0.05), the number DEG was even lower for the contrast between CCR6$^+$DN and Th17 cells with 13 up-regulated and 13 down-regulated probe sets, (Table S1). The most striking differences in the number of DEG were observed for the contrast between CCR6$^+$DN and CCR6$^+$DP cells. These results indicate that the transcriptome of CCR6$^+$DN is similar to that of Th17 but distinct from that of the CCR6$^+$DP.

Further analysis allowed us to understand the significance of the transcriptional dissimilarities displayed by these three CCR6$^+$ subsets in terms of immunological functions (Figure 2, Supplemental Figure 2). We observed that the CCR6$^+$DN had a different tissue homing potential compared to Th17 and CCR6$^+$DP cells. Transcripts for molecules associated with migration into lymph nodes, including CCR7, CXCR5 and its ligand CXCL13, SELL, SIRP1, JAM3, and AIF1, were preferentially confined to the CCR6$^+$DN subsets. Markers for homing into peripheral tissues, such as integrin β7 (gut), integrin β1 (cervix), CXCR3 (inflammatory sites), CCR2, and CCR4 (skin), were differently up-regulated in the Th17 and CCR6$^+$DP subsets (Supplemental Figure 2). These results introduce a concept in which the existence of several Th17 subsets with distinct trafficking potentials allow the adaptive immune system to efficiently coordinate host

defenses in different anatomic sites while maintaining a pool of IL-17A^{+} T-cells, represented by the CCR6^{+}DN, that will mainly traffic into lymph nodes to ensure effective protection.

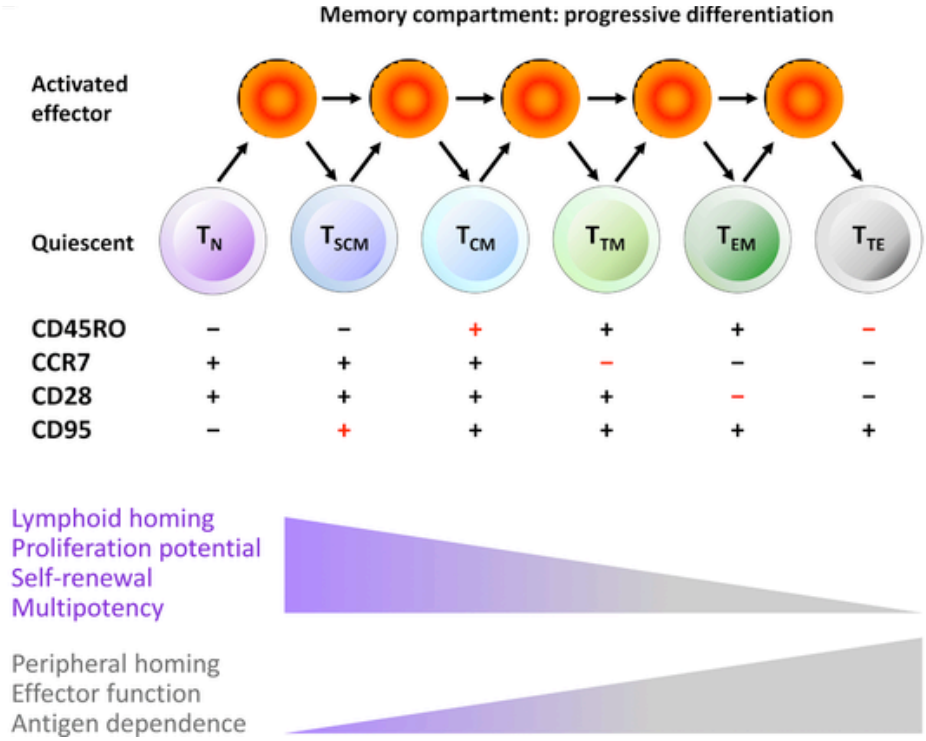

Figure 16: Different differential stages adopted by a cell during biological life. Shown is the model of progressive differentiation of T cell subsets from a naive to a terminal effector stage. Reproduced with the permission of European Journal of Immunology (742), author copyrights 2013.

The CCR6^{+}DN cells were also found to express at high levels markers of the Th17 differentiation program including: IL-17F, STAT3, RORA (255), IL-23R (311), SOSC3 (743), TIM3 (744) as well as CD26/DPP4 (307). Of note, IL-17F was included among the top up-regulated transcripts in CCR6^{+}DN cells compared to the Th17 and CCR6^{+}DP subsets. Previous studies demonstrated that during the Th17 lymphocyte differentiation from naive T-cells, cells first acquired the expression of IL-17F homodimer and IL-17A/F heterodimer (372, 373) suggesting that IL-17F is an early marker of Th17 cell differentiation. Similarly, STAT3 is one of the first transcription factors to be up-regulated within the first few hours following Th17 differentiation of naive CD4^{+} T-cells (258). Interestingly, CCR6^{+}DN were further found to express a typical stem cell-molecular signature, including RORA, STAT3, LEF1 (a transcription factor of the wnt pathway

(745)), MYC (transcription factor of the wnt pathway (746)), and TERC (a telomerase component (747)). The Th17 cells expressing the self-renewal markers LEF1 and MYC were previously characterized in mice and humans (423, 424). In addition, signal transduction pathways involved in the maintenance of stem cells (NANOG (748)) and lymphopoiesis (IL-3 (749)) were up-regulated in CCR6$^+$DN vs. CCR6$^+$DP and down-regulated in CCR6$^+$DP *versus* Th17. Therefore, our results provide evidence that CCR6$^+$DN cells share features with the previously described long-lived Th17 cells (423, 424). In contrast to CCR6$^+$DN, CCR6$^+$DP cells preferentially express transcripts for Lamine A (LMNA), a marker of senescence in human cells (750). A theory of a hierarchical system of memory cells was proposed in which naive cells can differentiate and acquire distinct memory phenotypes and functions during their life span (Figure 16) (742). According to this theory, a naive cell is believed to first differentiate into a T_{SCM}, which will subsequently give rise to T_{CM}, T_{TM} and T_{EM}. At the very end of their biological life cycle, the T-cells most likely acquire markers of senescence, decrease their functional capacities, and adopt a phenotype of terminal effector cells (T_{TE}). This theory relies on the idea that as cells transition into an older stage of differentiation, they gradually acquire receptors for homing into peripheral tissue while progressively losing expression of lymph node homing markers as well as self-renewal and proliferation ability (742, 751). In that sense, our results suggest the existence of a hierarchical system among the Th17 lineage with the CCR6$^+$DN cells representing an early stage of Th17 differentiation, while Th17 and CCR6$^+$DP subsets appear to represent later stages of Th17 development program.

Furthermore, we observed that CCR6$^+$DN cells preferentially express transcripts associated with the Tfh lineage. Indeed, CCR6$^+$DN cells highly express transcripts for the Tfh-specific transcription factors Bcl-6 and ASCL2 as well as the surface marker CXCR5 (336, 752). These results indicate that at least a fraction of CCR6$^+$DN cells may exhibit Tfh functions that include the ability to support B-cell differentiation leading to immunoglobulin production. The Tfh development pathway is still not clear, and one of the proposed models involve the concept that a naive CD4$^+$ T-cell initially undergoes a Th1, Th2, or Th17 differentiation program before becoming a Tfh lymphocyte (335). Recent studies imply there is a fine line between the Th17 and Tfh developmental program (753). The Tfh cells express markers of the Th17 differentiation program that are also expressed preferentially in CCR6$^+$DN cells (*e.g.,* Stat3, c-Maf, RORα). In

addition to Bcl-6 and ASCL2, Stat3, Stat4, and MAF (also known as c-Maf) are required for Tfh differentiation (336, 753). The Stat4 was found to be highly expressed in CCR6^{+}DN compared to CCR6^{+}DP (Table S1). In addition, LEF1, another transcript highly expressed in CCR6^{+}DN, was also reported to promote Tfh differentiation (754). The NFAT signaling transduction pathway, involved in IL-17A production (755) and expressed in CCR6^{+}DN *versus* CCR6^{+}DP, was also reported to promote Tfh function (756). CXCR4 as well as its signaling transduction pathway, which is preferentially expressed in CCD6^{+}DN cells, was also described to be expressed in Tfh (336). Further evidence supports our results indicating that a Th17 subset can have Tfh properties. A fraction of human CXCR5^{+}Tfh cells was identified to co-express Blc-6 and Rorγt (753). Also, the *in vitro* induction of the human Tfh development program in the presence of TGFβ, IL-23 and/or IL-12 showed co-expression of Blc-6 and RORγt as well as production of IL-17A (753), indicating that a cell exhibiting properties associated with different lineages can have several functions. The same study showed a positive correlation between the expression of BCL-6 and Th17-specific transcription factors including RORγt, RORα and AHR (Section 1.2.2). Of note, RORα was shown to be expressed in murine Tfh cells, and its expression was dependent on RORγt (757). Interestingly, *Morita et al.* showed that CXCR5^{+}CXCR3^{-}CCR6^{+} memory T-cells in human peripheral blood, which include the CCR6^{+}DN population we describe in this thesis, induce immunoglobulin production in B-cells (758).

Overall, our results demonstrate that CCR6^{+}DN and CCR6^{+}DP are two previously uncharacterized Th17-polaized subsets with distinct transcriptional programs. The transcriptional profile of CCR6^{+}DN indicates that these cells may represent an early stage of Th17 differentiation. Also, genome-wide transcriptional analysis demonstrated that CCR6^{+}DN cells include cells with Tfh features, indicating that a particular Th17 subset may be heterogeneous by displaying multiple immunological functions.

5.1.2 TH17-SPECIFIC EFFECTOR CYTOKINES PRODUCED BY CCR6^{+}DN AND CCR6^{+}DP SUBSETS

The finding that CCR6^{+}DN and CCR6^{+}DP are two Th17 subsets with distinct transcriptional profiles prompted us to further explore their production of Th17-specific effector cytokines as compared to the previously characterized Th17 and Th1Th17 subsets. In line with the genome-

wide transcriptional analysis, we found that CCR6$^+$DN cells stimulated *via* the TCR were major producers of IL-17F (Figure 3, Manuscript #1). Also, CCR6$^+$DN cells were a major source of IL-21 and IL-8/CXCL8. Similar to Th1Th17 cells, CCR6$^+$DN cells produced high levels of IL-22 and CCL20.

IL-17F was originally discovered in bronchoalveolar lavage cells from asthmatic individuals upon allergen stimulation (759). Despite overlapping biological function with IL-17A (760, 761), IL-17F was reported to have an important regulatory role in restricting allergic asthma development (762). IL-17F, but not IL-17A-deficient mice, showed an increased frequency of eosinophil infiltration and higher levels of IL-4, IL-5, and IL-13 in the lung-draining lymph nodes following induction of chronic asthma. Since the CCR6/CCL20 axis participates in lung mucosal immunity (763, 764), it is likely that the recruitment of CCR6$^+$DN cells to the site of inflammation may serve as a source of IL-17F to neutralize or reduce Th2 responses and asthma.

One of the many roles of the Th17 lineage throughout an immune response involves the secretion of chemokines to induce leukocytes trafficking into inflammatory sites (210, 366). The fact that CCR6$^+$DN cells produce the highest levels of IL-8, when compared to the other CCR6$^+$ subsets producing IL-17A, indicates their superior ability to attract neutrophils. Similarly, CCR6$^+$DN and Th1Th17 cells when compared to Th17 and CCR6$^+$DP subsets produce higher levels of CCL20; this supports their superior potential to attract cells of the innate and adaptive immunity expressing CCR6. Of note, CCL20 was previously reported to exhibit antiviral properties and to limit HIV replication in CD4$^+$ T-cells *via* the induction of the HIV restriction factor APOBEC3G (765).

The finding that CCR6+DN cells mainly produce IL-21 is in agreement with our transcriptional analysis revealing that this subset shares Tfh markers. Consistent with the preferential production of IL-21 by CCR6$^+$DN, CCR6$^+$DN *versus* Th17 and CCR6$^+$DP expressed superior levels of the BCL-6 mRNA, a transcription factor documented to increase IL-21 production (766). The CXCR5$^+$CXCR3$^-$CCR6$^+$ lymphocytes described by *Morita et al.* (758) essentially make up the CCR6$^+$DN and Th17 subsets (Figure 1, Manuscript #1). Similar to the CCR6$^+$ subsets we described in this thesis, CXCR5$^+$CXCR3$^-$CCR6$^+$ Tfh produce IL-17A and IL-22 (758) (Figure 3,

Manuscript #1). Nevertheless, the fact that CCR6$^+$DN cells highly produce IL-21 in addition to their expression of key Tfh markers suggests that this subset is more likely to represent the described CXCR5$^+$CXCR3$^-$CCR6$^+$ T-cells. Considering that IL-21 is a major survival factor for Th17 cells (332), the autocrine production of IL-21 by CCR6$^+$DN cells supports the possibility that CCR6$^+$DN when compared to Th17 and CCR6$^+$DP cells exhibit a superior capacity to expand and survive *in vivo*. Except for Th1Th17 cells, CCR6$^+$ subsets produce low levels of IL-2 and thus rely on other cytokines such as IL-21 to promote their survival. These results are in line with previous studies demonstrating the incapacity of Th17 cells to produce high levels of IL-2 (333, 436).

In contrast to CCR6$^+$DN cells, the CCR6$^+$DP subsets produced low to undetectable levels of IL-17F, IL-8, CCL20, IL-21, and IL-22 following TCR-triggering (Figure 3, Manuscript #1). In line with the genome-wide transcriptional analysis, these results suggest that the CCR6$^+$DP cells represent a later stage of Th17 differentiation with decreased functional capacities. Overall, our results persist in suggesting the existence of two new Th17 subsets with distinct functional roles in immunity. In addition, these findings emphasize the poly-functionalities of the CCR6$^+$DN cells during the course of an immune response.

5.1.3 THE POTENTIAL PATHOGENIC *VERSUS* NON-PATHOGENIC FEATURES OF TH17 SUBSETS IN THE CONEXT OF AUTOIMMUNITY

Pathogenic and non-pathogenic Th17 cells originally described in the context of autoimmunity surface markers for Th17 cells, including CD161 and CD26, were previously shown to be expressed in pathogenic Th17 cells (307, 333, 396, 767, 768). CD161$^+$ cells were shown to include both Th17 and Th1Th17 subsets (308, 344). Also, the high expression of CD26 was previously reported to be detected on CD161$^+$ cells producing IL-17A (307). We demonstrated that the CCR6$^+$DN and the CCR6$^+$DP cells expressed CD161 at levels superior to those detected on the Th17 cells and similar to those expressed by Th1Th17 cells (Figure 1, Manuscript #1). In addition, the expression of CD26 mRNA transcript was enriched in CCR6$^+$DN compared to Th17 and CCR6$^+$DP cells (Table S1) as mentioned in Section 5.1.1. These results suggest CCR6$^+$DN may include pathogenic Th17 cells. Interestingly, among pathogenic Th17 markers previously reported in mice (355, 356) and humans (344), CCL5, CCL4L2, CSF2/GM-CSF, IL-3, and

CXCR3 were enriched in CCR6^{+}DP *versus* Th17 or CCR6^{+}DN. These findings suggest a superior pathogenic profile for CCR6^{+}DP cells compared to Th17 and CCR6+DN subsets. The identity of the pathogenic Th17 cells is still unclear because they are not fully characterized and may be highly heterogeneous; this may include cells with CCR6^{+}DN and CCR6^{+}DP phenotypes. The actual definition of pathogenic Th17 cells in mice and humans may underestimate the number and variety of deleterious subsets responsible for the destructive tissue inflammation observed in autoimmune disorders.

One of the key features distinguishing pathogenic from non-pathogenic Th17 cells is the ability to produce pro-inflammatory cytokines, including TNF-α (239). Non-pathogenic Th17 cells produce anti-inflammatory cytokine IL-10 and exhibit immune-suppressive properties limiting tissue inflammation (355-360). We looked at the pro- *versus* anti-inflammatory profile of the four CCR6^{+} subsets (Figure 3, Manuscript #1). As in previous results (436), Th1Th17 cells were a major source of TNF-α. Indeed, Th1Th17 cells were described as the pathogenic Th17 cells in the context of autoimmunity (344, 769). We also observed that CCR6^{+}DN cells produced TNF-α at superior levels compared to Th17 and CCR6^{+}DP cells, but at lower levels compared to Th1Th17 subsets. The capacity to produce substantially TNF- α, in addition to highly expressing CD161 and CD26, may predispose the CCR6^{+}DN, as opposed to the Th17, to act as deleterious cells in disease pathogenesis. In contrast to CCR6^{+}DN cells, Th17 and Th1Th17 were major sources of IL-10. The result that Th17 cells produce low levels of TNF-α while producing strongly IL-10 suggests that these cells may represent the non-pathogenic Th17 cells in humans. Because Th1Th17 produces high levels of IL-10, our results suggest that this subset may itself be heterogeneous and include non-pathogenic Th17 cells. Furthermore, we found that IL-13 production was the highest in Th17 and Th1Th17 cells. Although IL-13 was reported to play a dominant role in fibrosis related to autoimmunity (770, 771), this cytokine could still exert anti-inflammatory effects when acting on the T-cell compartment (772). Non-pathogenic Th17 cells were discovered in mice. To our knowledge, non-pathogenic memory Th17 cells in humans have not yet been identified although one study showed successful *in vitro* generation of memory Th17 cells with immuno-regulatory functions (773). Therefore, our results support the idea suggesting the existence of human Th17 subsets with anti-inflammatory properties.

5.1.4 ANTIGENIC SPECIFICITY OF CCR6$^+$DN SUBSETS

The group of Sallusto previously described the Th17 subsets as the main population of the adaptive immune system responding against *C. albicans* hyphae (298). Furthermore, this group originally reported that the Th1Th17 and Th1 cells had poor or no proliferative response to *C. albicans*. We demonstrated that CCR6$^+$DN cells proliferated in response to the hyphal form of this fungus at level similar to that of Th17 cells, indicating the ability of the CCR6$^+$DN cells to provide an immune defense against a Th17-specific pathogen. We found that the Th1Th17 cells, similar to the Th17 and CCR6$^+$DN cells, proliferated abundantly in response to *C. albicans,* whereas the Th1 cells exhibited lower proliferative capacity in response to this pathogen. These results are consistent with the latest study by the group of Sallusto demonstrating the existence of substantial *C. albicans*-specific Th17, Th1Th17, and Th1 cells exhibiting clonotype sharing (304). *C. albicans*-specific CCR6$^+$DN proliferating cells produced IL-17A at similar levels compared to the Th17 proliferating in response to the same antigens. Moreover, CCR6$^+$DN immune response against *C. albicans* included single-producing cells for IL-17A or IFN-γ as well as IL-17A and IFN-γ double-producing cells. Therefore, the effector cytokine profile of the CCR6$^+$DN cells can be considered intermediate between the profiles exhibited by the Th17 and Th1Th17 cells. As in the study of *Becattini et al.* (304), our results suggest that the host immune system engenders heterogeneous populations of memory lymphocytes that can belong to the same Th lineage; this allows for effective, complete protection against a specific pathogen. Of note, we showed that Th1Th17 and Th1 cells, but not CCR6$^+$DN and Th17 cells, proliferate in response to CMV. These results are consistent with earlier work demonstrating that CMV-specific responses are restricted to the CXCR3$^+$ T-subsets (296). These results confirm once again the appurtenance of CCR6$^+$DN subsets to the Th17 lineage.

5.1.5 DIFFERENTIATION RELATIONSHIP BETWEEN THE FOUR CCR6+ SUBSETS

Th17 cells are remarkably plastic in their developmental programming compared to Th1 cells (339). Th17 cells integrate signals from the environment to conserve their lineage-commitment (*e.g.,* RORC, IL-17A/F) or *trans*-differentiate into Th1 (*e.g.,* T-bet, IFN-γ) (297, 346) *via* flexible/stable epigenetic modifications (337). We examined lineage stability and plasticity of CCR6$^+$DN and CCR6$^+$DP subsets, relative to Th17 and Th1Th17 when cultured under Th17

versus Th1-polarizing conditions. We focused on Th17 subsets with T_{CM} phenotype because T_{CM} maintain long-term immunological memory against pathogens (137, 295, 774) and also because Th17 subsets with a T_{CM} phenotype were predominant among the four Th17-subsets (Figure 1, Manuscript #1) and produced higher levels of Th17-specific cytokine compared to T_{TM}/T_{EM} (Supplemental Figure 3, Manuscript #1). For all four Th17 subsets, IL-17A, IL-17F, and IL-22 expression was dramatically increased upon long-term exposure to Th17-polarizing signals (Day 4 *versus* Day 14; Figure 5; Manuscript #1). The up-regulation of Th17-specific effector functions paralleled the loss of the CM marker CCR7 (data not shown); this is consistent with the linear model of T-cell differentiation where CM differentiates into EM upon antigenic re-encountering (742, 774) (Figure 16). Notably, $CCR6^+$DN and Th17 cells were distinguished from $CCR6^+$DP and Th1Th17 subsets by their superior IL-17A/IL-17F and inferior IFN-γ expression (Figure 5; Manuscript #1). Consistent with the concept of Th17 plasticity (209), all Th17-subsets diminished expression of Th17-cytokines and enhanced IFN-γ in response to Th1-polarizing signals including IL-12 (Figure 5; Supplemental Figure 4 & 5, Manuscript #1). The *trans*-differentiation of Th17 into Th1 is consistent with studies in mice and humans demonstrating the down-regulation of RORγt/RORC, as well as IL-17A, IL-17F, and IL-22 expression upon IL-12 exposure (297, 340-343). In contrast to the plasticity of Th17-subsets, our results confirm the stability of the Th1 transcriptional program (339).

Interestingly, we observed similarities in the cytokine profile among the $CCR6^+$ subsets upon long-term culture, especially when using the SPICE analysis program (Figure 5, Supplemental Figure 5, Manuscript #1). Th17 and $CCR6^+$DN cells shared similar cytokine profile, regardless of the polarization condition. Also, Th1Th17 and $CCR6^+$DP cells had similar cytokine profiles (Supplemental Figure 4 and 5, Manuscript #1). Including these results, there are many indications throughout the study that point to a differentiation relationship between the Th17 and $CCR6^+$DN cells as well as between the Th1Th17 and $CCR6^+$DP cells. In addition to producing comparable levels of IL-17A, the Th17 and the $CCR6^+$DN cells share similar population distribution in terms of T_{CM}, $T_{TM,}$ and T_{EM} (Figure 1, Manuscript #1). The Th17 and the $CCR6^+$DN cell subsets share transcriptional signatures as mentioned in Section 5.1.1. Also, $CCR6^+$DN and Th17 cells proliferate in response to *C.albicans* but not CMV. In contrast, Th1Th17 and $CCR6^+$DP subsets produce comparable low levels of IL-17A and exhibit similar frequencies of T_{CM}, T_{TM} and T_{EM} (Figure 1, Manuscript #1). The possibility that Th1Th17 cells share a differential relationship

with CCR6$^+$DP cells is supported by studies by *Becattini et al*. who described a population of Th17 cells with a CCR6$^+$DP phenotype, named CXCR3$^+$CCR4$^+$ T-cells, that display clonotype sharing with *M.tuberculosis*-specific Th1Th17 cells (304). Similar to CCR6$^+$DP cells characterized by our group in Manuscript #1 included in this thesis, the CXCR3$^+$CCR4$^+$ T-cells described by *Becattini et al*. produced high levels of IFN-γ and low levels of IL-17A (304); this indicates that the two subsets are overlapping. Globally, our results demonstrate that the Th17 and CCR6$^+$DN cells are different from the Th1Th17 and CCR6$^+$DP cells.

Of note, the cytokine profile of CCR6$^+$DP cells after TCR triggering *ex vivo* was distinct compared to the one observed when cells were cultured under Th17- or Th1-polarizing cytokines *in vitro*. Indeed, we first reported that the CCR6$^+$DN and CCR6$^+$DP cells produced similarly low but detectable levels of IFN-γ following TCR-triggering stimulation (Figure 1, Manuscript #1). Interestingly, the CCR6$^+$DP subsets produced higher levels of IFN-γ compared to CCR6$^+$DN cells upon short-term and long-term culture, regardless of the polarization conditions (Figure 5, Manuscript #1). Furthermore, we observed that CCR6$^+$DP subsets produced low to undetectable levels of IL-17F, IL-22 and TNF-α upon TCR-triggering *ex vivo* (Figure 3, Manuscript #1). Nonetheless, they exhibited a cytokine profile similar to that of Th1Th17 cells in terms of IL-17F, IL-22, and TNF-α after 14 days of culture under Th17-polarizing conditions. These findings support the possibility that CCR6$^+$DP cells represent an advanced stage of Th17 differentiation with effector functions that can be restored under appropriate Th17 polarizing conditions. CCR6$^+$DP cells may need additional signals with the TCR stimulation to produce considerable levels of pro-inflammatory cytokines. Elderly cells were reported to have an altered T-cell signaling leading to a distinct production of inflammatory cytokines (775). Overall, our results demonstrate the existence of four CCR6$^+$ population associated with the Th17 lineage having distinct characteristics and indicating a potential differential relationships among these four subsets.

5.1.6 THE PERMISSIVENESS OF TH17 SUBSETS TO HIV INFECTION

Previous studies by our group and others demonstrated the ability of Th17 and Th1Th17 cells to support HIV-1 replication *in vitro* (435, 436, 440). To determine whether CCR6$^+$DN and

CCR6$^+$DP subsets are HIV-1 targets, we first determined the expression of HIV co-receptor at their surface. We found that CCR6$^+$DN and CCR6$^+$DP expressed CCR5 and CXCR4 at levels similar to Th17 and Th1Th17, respectively (Supplemental Figure 6, Manuscript #1). These results reiterate the similarities that we already described between the CCR6$^+$DN and Th17 as well as between the CCR6$^+$DP and Th1Th17 cells. Furthermore, we demonstrated that the CCR6$^+$DN and CCR6$^+$DP cells, similar to Th17 and Th1Th17 subsets, were permissive to HIV infection *in vitro* (Supplemental Figure 6, Manuscript #1). Investigations in HIV-infected individuals recently infected (RI) untreated and/or in chronically infected on ART (CI on ART) allowed us to demonstrate that all four CCR6$^+$ subsets carry HIV-DNA *in vivo*. To the best of our knowledge, this is the first study that shows levels of integrated HIV-DNA in four different Th17 subsets of HIV-infected individuals. These results support previous findings by our group and others that CCR6 expression is linked to HIV-1 susceptibility in CD4$^+$ T-cells (435, 436, 440, 441). Our results are consistent with recent studies of *Sun et al.* that also observed persistence of HIV-DNA in Th17 and Th1/Th17 cells from HIV-infected subjects receiving ART (776). CCR6 expression may direct Th17 subsets into anatomical sites of replication including the gut and brain thus contributing to HIV dissemination and the establishment of viral reservoir. Therefore, permissiveness to HIV infection might represent a key feature of the Th17 lineage. The idea that the Th17 transcriptional program is favorable to HIV replication challenges our search for strategies to limit HIV replication in these cells without interfering with their role in mucosal immunity.

5.1.7 THE ROLE THE TH17 SUBSETS IN HIV-1 PERSISTENCE

HIV-disease progression is associated with Th17 depletion (49, 121, 777). Indeed, we previously reported that the frequency and counts of Th17 and Th1Th17, as well as total CCR6$^+$ cells, are significantly diminished in the peripheral blood of CI on ART compared to uninfected controls (436). Similar to Th17 and Th1Th17 cells, results included in Manuscript #1 demonstrated that the frequency and counts of CCR6$^+$DP cells is decreased in CI on ART compared to uninfected controls. Interestingly, the frequency and counts of CCD6$^+$DN subsets were preserved in CI on ART. Furthermore, longitudinal studies following five HIV-infected subsets during their first

years of infection demonstrated that CCR6$^+$DN cells were the most preponderant subset of CCR6$^+$ cells before and after ART initiation (Figure 7, Manuscript #1).

The depletion of Th17, Th1Th17, and CCR6$^+$DP cells may be linked to their permissiveness to HIV infection. These results are in agreement with previous findings reporting the decrease of peripheral blood CCR6$^+$ T-cells from HIV-infected individuals as HIV disease progressed and subsequent cell death by apoptosis following trafficking into the spleen (778). The depletion of these CCR6$^+$ subsets may explain the impaired immunity against pathogens including *M. tuberculosis* and *C. albican*s in HIV-infected subjects (779, 780). A very recent study by the group of Lichterfeld demonstrated that the HIV-DNA measured in the Th17 and Th1Th17 cells remained present for a long period (more than 50 months) (776), indicating the important contribution of these subsets in HIV persistence. Furthermore, Th1Th17 cells were found by the same study to have the highest contribution to HIV reservoir among the memory T-cell population, including the Th17, Th1 and Th2 cells. Our results support the conclusion that CCR6$^+$DP cells, similar to Th17 and Th1Th17 cells, can be considered pathogenic Th17 cells due to their depletion in peripheral blood that may be explained at least in part by their permissiveness to HIV replication.

In contrast, the CCR6$^+$DN cells seem to contribute to HIV pathogenesis in a different manner. In addition to being preponderant in the peripheral blood, CCR6$^+$DN subsets were found at high frequency in the lymph nodes of CI on ART (Supplemental Figure 7, Manuscript #1). CCR6$^+$DN as well as the CCR6$^+$DP cells represent stable population in terms of their surface phenotype as they can migrate in lymphoid organs without losing or acquiring CCR4 and/or CXCR3. There are many mechanisms that may explain the preservation of the CCR6$^+$DN in CI on ART. At homeostasis and following cellular activation, the CCR6$^+$DN cells display a T_{CM} phenotype (Figure 1, Supplemental Figure 2 and Figure 7, Manuscript #1). Compared to T_{EM}, T_{CM} are known to have a superior survival capacity as they are more resistant to apoptosis (137) and have a higher ability to self-renew (781). Furthermore, our genome-wide transcriptional analysis revealed that CCR6$^+$DN cells express transcripts for several markers of self-renewal previously reported to be expressed in T_{SCM} (Section 5.1.1). The expression of these markers may promote survival of the CCR6$^+$DN subsets during HIV infection and avoid the viral cytopathic effect.

Moreover, CCR6^{+}DN cells express low levels of integrin α4β7 and may not traffic into the gut, the main anatomical site of viral replication (42, 49). The facts that CCR6^{+}DN cells are the main producer of IL-17F (Figure 3, Manuscript #1), that IL-17F is expressed in lungs of asthmatic individuals (759), and that IL-17F is induced in CD4^{+} T-cells following allergen stimulation (759) suggest the possibility that CCR6^{+}DN may be recruited into the lungs. Of note, *Brenchley et al*. previously reported that Th17 cells are depleted from the gut but not the lungs of HIV-infected individuals (735). Therefore, CCR6^{+}DN subsets may represent the Th17 population located in the lung tissues and resistant to depletion for mechanisms that remain to be examined. The preservation of DN CCR6^{+}DN cells in the peripheral blood of HIV-infected subjects may also explain reports by other groups that IL-17-producing cells are not depleted from peripheral blood during HIV infection (434).

The T_{CM} were identified as the main reservoir for latent HIV (55). Our current results demonstrating that CCR6^{+}DN cells display a T_{CM} phenotype, harbor HIV-integrated DNA, and are not depleted during chronic HIV-infection under ART strongly support the possibility that these cells represent an important cellular reservoir for HIV. CCR6^{+}DN potentially carry replication competent HIV-DNA promoting viral replication and persistence following the trigger of cellular activation. That CCR6^{+}DN display Tfh and T_{SCM} features further indicates their role as a cellular reservoir for HIV infection. Indeed, CCR6^{+}DN cells were found present at high frequencies in lymph nodes from two different ART-treated HIV-infected subjects, a site where a substantial frequency of Tfh are located (782). Similar to CCR6^{+}DN cells, Tfh were found to harbor HIV/SIV DNA (135, 783). In addition, Tfh were reported to exhibit long-lived memory ability by down-regulating their expression of signature markers such as Bcl-6, CXCR5, and PD-1 (784). Once activated by TCR triggering, Tfh cells re-acquire their markers and produce high levels of IL-21. Our result suggesting that a fraction of CCR6^{+}DN are Tfh is in line with a recent study demonstrating the restoration under ART of a CCR6^{+} subset expressing a Tfh signature (CCR7^{high}CXCR5^{high}PD-1^{high}) and that is able to support B-cell maturation (785). Furthermore, HIV was reported to exploit T_{SCM} properties for its own survival (786). T_{SCM} were shown to harbor HIV-DNA that persists for more than 50 months of ART. The accumulated evidence points to the possibility that CCD6^{+}DN are important contributors to HIV cellular reservoir.

Overall, compared to the Th17, Th1Th17, and CCR6^{+}DP subsets, our results indicate that the CCR6^{+}DN have an important role in HIV persistence.

In conclusion, our results support a model in which CCR6^{+}DN represent long-lived Th17 cells that are pathogenic in the context of HIV-1 infection through their ability to harbor replication competent HIV reservoirs and to avoid the cytopathic effect of viral infection (Figure 8, Manuscript #1).

5.2 THE IMMUNOLOGICAL FUNCTIONS OF CD16$^+$ AND CD16$^-$ MDDCS AT HOMEOSTASIS AND DURING HIV PATHOGENESIS (MANUSCRIPTS #2 AND #3)

5.2.1 FATE OF CD16$^+$ AND CD16$^-$ MONOCYTES DIFFERENTIATION INTO DENDRITIC CELLS

Classical CD16$^-$ and CD16$^+$ monocytes were identified as two major monocytic subsets with distinct phenotypes and immunological functions. These subsets share a large set of transcriptional markers suggesting they originate from common myeloid precursors (477, 495). However, CD16$^+$ *versus* CD16$^-$ monocytes express several macrophage and DCs markers and therefore are considered a more advanced stage of differentiation (495). Indeed, many groups including our own generated results that support the concept of a developmental relationship between classical and non-classical monocytes (495, 505, 507, 518, 519). In this thesis, we first investigated the fate of CD16$^+$ and CD16$^-$ monocyte differentiation into dendritic cells. As previously reported by several groups (483, 595, 606), we confirm that CD16$^+$ and CD16$^-$ monocytes are both capable of differentiating into DCs with typical veiled morphology as well as similar levels of CD1a, CD1c and DC-SIGN expression (Figure 1, Supplemental Figure 4; Manuscript 2). Also, we demonstrated that immature DCs differentiated from CD16$^+$ and CD16$^-$ monocytes acquire at similar levels the expression of the maturation markers CD83 and CCR7 in response to LPS stimulation. Despite the common expression of typical immature and mature DC markers, our genome-wide transcriptional analysis demonstrated that CD16$^+$ and CD16$^-$ MDDCs also express unique transcriptional features, similar to transcriptional differences observed between CD16$^+$ and CD16- monocytes (478, 495, 501). Interestingly, we observed that CD16$^+$ and CD16- MDDCs lose certain original features that were expressed by their monocyte precursors. For instance, CD16$^+$ MDDCs were not found to preferentially express the CD16$^+$ monocyte marker CX3CR1. Similarly, CD16$^-$ MDDCs did not retain preferential expression of CCR2, a marker expressed on CD16$^-$ monocytes. Nevertheless, both CD16$^+$ and CD16$^-$ MDDCs maintained preferential expression of certain gene transcripts up-regulated in their respective precursors. Indeed, the expression of the FcγRIII/CD16 (Figure 1; Manuscript #2), the co-stimulatory molecule CD86, the receptor for complement decay accelerating factor CD97, the adhesion molecule LFA-1, the negative regulator of cell cycle MTSS1, the monoglyceride lipase

MGLL involved in lipid metabolism, and the transcription factor TCF7L2 were all found to be preferentially expressed in $CD16^+$ MDDCs similar to $CD16^+$ monocytes (495, 606) (Supplemental Tables 1 and 2; Manuscript #2). Of note, CD86 expression was also reported by other groups to be preferentially expressed in $CD16^+$ *versus* $CD16^-$ MDDCs under homeostatic conditions (606). As well, similar to $CD16^-$ monocytes, $CD16^-$ MDDCs maintained preferential expression of CD14, the adhesion molecule SELL/CD62L, the calcium-binding protein S100A9, and the transcription factor HIF1 (549). However, we observed that gene transcripts preferentially expressed in $CD16^-$ monocytes, including the water-selective membrane channels AQP9 involved in immune response ((787)), and the marker of myeloid lineage MNDA (myeloid cell nuclear differentiation antigen) were up-regulated in the $CD16^+$ MDDCs; this emphasizes that generated MDDC subsets are also distinct from their precursors.

Our transcriptional analysis results suggest that $CD16^+$ and $CD16^-$ MDDCs display distinct immunological roles. Precisely, Gene Set Variation Analysis (GSVA) and Gene Set Enrichment Analysis (GSEA) of differentially expressed genes revealed that $CD16^+$ MDDCs as opposed to $CD16^-$ MDDCs express canonical pathways involved in inflammation and biological processes linked to lymphocyte differentiation and the positive regulation of T-cell activation (Figure 3; Manuscript #2). Indeed, $CD16^+$ MDDCs were found to preferentially express gene transcripts involved in the induction of T-cell immune response such as the T-lymphocyte surface antigen LY9, the adhesion molecules ALCAM, the transcription factors FOXO1 and ATF3 in addition to CD86 and CD97 (Figure 4; Manuscript #2). Of interest, $CD16^+$ MDDCs expressed transcripts for the gut lamina propria marker ITGAE/CD103 and genes related to retinoic acid biosynthesis (the transcription factor PPARγ and the enzyme ALDH1A2) (788-790). These results indicate that the $CD16^+$ MDDCs are prone to be located in the intestinal tract where they have the potential to imprint T-cells with gut-homing tropism, upon immune activation, through the production of retinoic acid as previously suggested (791). $CD16^-$ MDDCs preferentially express the phagocytosis marker SIGLEC1, the chemokine receptor CCR6, the stem cell markers CD34, C-KIT, and ITGA9 as well as the langerin, the myeloid signature gene STEAP4, the anti-oxidant enzymes MPO, DUOX1, DUOAX1, and the bacterial DNA sensor IFI16 (Figure 4;Supplemental Table 1-2; Manuscript #2). The preferential expression of SIGLEC1 and MPO suggests that similar to $CD16^-$ monocytes and in contrast to $CD16^+$ MDDCs, $CD16^-$ MDDCs exhibit superior

phagocytic and microbicidal activities. Although CCR6 is known as a gut-homing marker towards the Peyer's patches, the expression of this chemokine receptor was also found to be important for cell migration into the lungs and the brain, indicating the potential anatomical location in which the $CD16^-$ MDDCs may traffic. DCs expressing CD34 and langerin were reported to be located in the skin (792). Of interest, the expression of STEP4, langerin, and CD34 suggests that CD16- MDDCs may have a role in mediating immune tolerance. Indeed, the expression of STEAP4 was shown to be involved in anti-inflammatory responses (793) while DCs expressing CD34 and langerin were demonstrated to express the enzyme indoleamine-pyrrole 2,3-dioxygenase 1 (IDO-1), an enzyme involved in the catabolism of tryptophan and the generation of T-regs (794).

Overall, our results indicate that during the differentiation of $CD16^+$ and $CD16^-$ monocytes into DCs, certain core features are maintained thus allowing the generation of functionally distinct DC subsets. Similar to $CD16^+$ monocytes, $CD16^+$ when compared to $CD16^-$ MDDCs appear to display a more advanced stage of maturation as reflected by the expression of co-stimulatory molecules involved in the immunological synapse formation (*i.e.,* CD86, ALCAM, CD97). As demonstrated for $CD16^+$ monocytes (498, 499, 613), $CD16^+$ MDDCs can be considered inflammatory cells. Similar to $CD16^-$ monocytes, $CD16^-$ MDDCs can be perceived as phagocytic cells of the innate immune system. Studies from the group of Geissmann (613) have divided the $CD16^-$ and the $CD16^+$ monocytes into two categories: the phagocytic $CD16^-$ monocytes specialized in immunity against extracellular pathogen such as bacteria and fungi and the inflammatory $CD16^+$ monocytes specialized in viral immune response *via* expression of TLR7 and TLR8. Although the bacterial DNA sensor IFI16 expression was enriched in $CD16^-$ MDDCs, our results cannot reach a similar conclusion because a differential expression of TLR7/8 was not detected in our transcriptional analysis. Nevertheless, the existence of false positive and negative calls is accepted for high throughput transcriptional screens, and therefore, validations by RT-PCR should be performed to come to a solid conclusion.

5.2.2 THE IMMUNIGENIC POTENTIAL OF CD16$^+$ AND CD16$^-$ MDDCS

Limited information exists in the literature relative to the quality of immune response induced by CD16$^+$ and CD16$^-$ MDDCs (609, 795). Following monocyte differentiation into DCs, we assessed the capacity of each immature MDDC subset to acquire maturation and to mount an immune response after antigen recognition. Upon LPS stimulation, both CD16$^+$ and CD16$^-$ MDDCs up-regulated the expression of the DC maturation markers CD83 and CCR7 (Supplemental Figure 4; Manuscript #2). The maturation induced by LPS led to important changes in the transcriptome of both CD16$^+$ and CD16$^-$ MDDCs. Upon encounter with an antigen, DCs acquire new effector functions that are important for antigen presentation, the attraction and the activation of T-cells at the level of the immunological synapse (796). Accordingly, LPS stimulation resulted in the down-regulation of ITGAE/CD103 and the up-regulation of the phagocytic marker SIGLEC1 in CD16$^+$ MDDCs. The maturation of CD16$^-$ MDDCs in response to LPS led to a repression of MPO, STEP4, and ITAG9 gene expression and the acquisition of ALCAM and PPARγ expression. Therefore, these results reveal the ability of CD16$^+$ MDDCs to acquire features of CD16-MDDCs and *vice versa* upon maturation. Globally, LPS triggered the expression of TNF-α, lymphotoxin alpha (LTA), lymphotoxin beta (LTB), IL-18, CXCL1, CCL18 as well as members of the complement system C2 and CFP in CD16$^+$ MDDCs, re-emphasizing their identity as inflammatory DCs (Figure 5, Supplemental Table 3-4; Manuscript #2). Also, CD16$^+$ MDDCs acquired higher levels of CD86 and CCL22 upon LPS stimulation. Of interest, we noticed that LPS stimulation led to the expression of chaperone protein clusterin (CLU) and G-protein coupled receptor P2RY8 gene transcripts, both markers of follicular DCs (FDCs) (797, 798) that are responsible for B-cell maturation (799). Of note, TNF-α and LTB were shown to be important for FDC development and maintenance (800). These results evoke the possibility that the interaction with an antigen can induce major transformation in DCs that will adopt new specialized functions. In contrast to CD16$^+$ MDDCs, upon LPS interaction, CD16$^-$ MDDCs acquired the expression of distinct gene transcripts involved in inflammation including IFN-α, IL-1α, CXCL6, IL-23, IL-23R, IL-6ST, and TREM (Supplemental Table 5, Figure 5; Manuscript #2). These results demonstrate that CD16$^+$ and CD16$^-$ MDDCs respond to LPS stimulation in transcriptionally distinct manners, thus providing evidence that CD16$^+$ and CD16$^-$ MDDCs exert distinct functional roles in immunity.

To further characterize $CD16^+$ and $CD16^-$ MDDC-mediated immune response, we sought to determine the capacity of each MDDCs subset to induce T-cell proliferation and polarization following stimulation by CMV, *C. albicans,* and *S. aureus* (Figure 3; Manuscript #3). Although both MDDCs expressed at homeostasis similar levels of DC-SIGN (Supplemental Figure 4; Manuscript #2), reported for the uptake of *C. albicans* in DCs (801), $CD16^-$MDDCs induced higher levels of *C. albicans*-specific $CD4^+$ T-cell proliferation (Figure 3; Manuscript #3). In fact, $CD16^-$ MDDCs displayed a superior ability to induce T-cell proliferation in response to CMV peptide and *S. aureus* as well as in response to SEB, used as a polyclonal control; this suggests their superior immunogenic potential compared to $CD16^+$ MDDCs. Interestingly, $CD16^-$ *versus* $CD16^+$ MDDCs induced higher expression of Th17-associated cytokines (IL-17A and IL-17F) in T-cells specific to *C. albicans* but not *S. aureus*. Altogether, these findings are in agreement with previous studies demonstrating differential expression of PRRs in $CD16^+$ and $CD16^-$ monocytes (613). These two MDDC subsets may also have a distinct ability to modulate signaling transduction pathways leading to different incidences of cytokine production and cell proliferation, all for an efficient adaptation in response to specific types of pathogens.

Overall, these results indicate that $CD16^+$ and $CD16^-$ MDDCs mount different immune responses against identical antigens. Of interest, our genome-wide transcriptional analysis demonstrated that upon LPS stimulation, $CD16^+$ and $CD16^-$ MDDCs will each acquire new features distinct from the homeostatic conditions. $CD16^+$ MDDCs will acquire the expression of gene transcripts related to phagocytosis (*i.e.,* SIGLEC, C2, CFP), whereas $CD16^-$ MDDCs will gain the capacity to produce pro-inflammatory cytokines (*i.e.,* IFN-1α, IL-1α, and CCL18).

5.2.3 THE EFFECT OF HIV INFECTION ON DENTRITIC CELL IMMUNE RESPONSES

Dendritic cells were previously reported to display a limited ability to sense HIV RNA/DNA thus explaining the poor induction of antiviral immunity (697, 699). We sought to determine similarities and differences in the effect of HIV exposure on the ability of $CD16^+$ and $CD16^-$ MDDCs to mount an immune response. HIV-exposed $CD16^+$ or $CD16^-$ MDDCs did not express DC maturation markers at transcriptional levels (Supplemental Tables 7 and 8; Manuscript #2). This was also reflected by our results on total MDDCs where HIV exposure failed to up-regulate

CD83 and CCR7 expression (Figure 1; Manuscript #3); this is consistent with previous findings reported by other groups ((47)). Nevertheless, DC activation marker S100B (802) was up-regulated by HIV in $CD16^-$ MDDCs, indicating their superior ability compared to $CD16^+$MDDCs to reach a certain level of activation. A short list of gene transcripts, including principally micro-RNAs, was up-regulated in both $CD16^+$ and $CD16^-$MDDCs exposed to HIV (Supplemental Tables 7 and 8; Manuscript #2). Despite minor transcriptional changes in MDDCs, the HIV exposure led to a decrease in the MDDC-mediated T-cell proliferation in response to SEB, CMV, *C. albicans,* and *S. aureus* (Figure 2; Manuscript #3). This decrease in the generation of antigenic-specific cells affected mostly the $CD16^-$ MDDCs. We found an inverse correlation between DC-induced T-cell proliferation and HIV replication. Our results are consistent with studies from other groups demonstrating the inability of DCs to stimulate T-cell proliferation upon HIV infection (803, 804). HIV also had a negative effect on the Th17-associated cytokine production by *C. albicans*-specific T-cells. DC maturation not only involves the up-regulation of co-stimulatory molecules but also involves the ability of DC to process and present antigens at cell surface *via* the expression of MHC-II. Previous studies demonstrated that HIV-Nef down-regulated the expression of MHC-II in APCs (805). HIV-gp120 was also shown to be a component involved in the negative effect of HIV on host defense. Indeed, the binding of HIV-gp20 initiated a signaling cascade that induced exhaustion of the autophagy system in DCs, leading to an altered immune response (701). Autophagy is an important biological process involved in antigenic presentation as inhibition with drug treatment impairs MHC-II presentation of both non-self and self-antigens (806). Components of the autophagy machinery were found to enhance antigen stability and to prolong MHC presentation in DCs. Furthermore, HIV-gp120 was reported to alter the ability of DCs to produce cytokine following antigenic recognition (807, 808) and to mediate inhibition of T-cell signaling and proliferation (809-811). Taken as a whole, these lines of evidence may explain the decreased capacity of $CD16^+$ and $CD16^-$ MDDCs to mount immune responses in the presence of HIV.

5.2.4 CONTRIBUTION OF MDDC SUBSETS TO HIV PERSISTENCE

Regardless of their limited ability to mount adequate immune response during HIV infection, DCs were found to efficiently transmit virions to $CD4^+$ T-cell (661-664, 669, 739). Previous

studies demonstrated that only a fraction of myeloid DCs are responsible for viral transmission (740). DCs can capture HIV *via* the expression of cell surface receptors including the C-lectin receptors DC-SIGN and DCIR (663, 668, 674). Despite a similar expression of DC-SIGN at the surface of $CD16^+$ and $CD16^-$ MDDCs, we identified the $CD16^+$ MDDCs as the APCs with the highest ability to promote HIV replication in resting $CD4^+$ T-cells; of note, such differences were not observed when HIV-loaded MDDCs were co-cultured with activated $CD4^+$ T-cells (Figure 1; Manuscript #2 and Figure 4; Manuscript #3). These results indicated that the $CD16^+$ MDDCs display a higher ability to induce the activation of resting $CD4^+$ T-cells for increased HIV permissiveness. Therefore, we tried to determine the molecular mechanisms favoring HIV replication with the analysis of $CD16^+$ and $CD16^-$ MDDC transcriptional profiles (Manuscript #2).

First, we observed that immature $CD16^+$ *versus* $CD16^-$ MDDCs had a superior state of activation as reflected by their inflammatory profile. The preferential expression of gene transcripts involved in cell activation and in the formation of the immunological synapse (*i.e.,* CD86, CD97, ALCAM, LY9, and LFA-1) predisposes the $CD16^+$ MDDCs to interact with $CD4^+$ T-cells and deliver activator signals even in the absence of antigens. Also, $CD16^+$ MDDCs, similar to $CD16^+$ monocytes-derived macrophages, produced chemokine such as CCL22, which led to active replication in resting $CD4^+$ T-cells (549). In addition to their role in mediating cell migration, chemokines were suggested to act as immunotransmitters, providing co-stimulatory signals to T-cell *via* their interaction with specific chemokine receptors and this upon the engagement of the TCR by specific antigens (812, 813). Therefore, $CD16^+$ MDDCs express and produce molecules possibly involved in lowering the threshold for T-cell activation that is normally mediated by TCR-triggering; this opens the door for active replication in target cells. Another mechanism by which $CD16^+$ MDDCs may favor HIV replication is their anatomical location. Our transcriptional analysis suggests that $CD16^+$ MDDCs are potentially intestinal DCs with the capacity to imprint T-cells with gut tropism. This implies the presence of $CD16^+$ MDDCs in the gut prior and during initial HIV infection. Therefore, it is reasonable to assume that when HIV reaches the intestine, the presence of $CD16^+$ MDDCs with their associated high activation state facilitates viral dissemination to surrounding T-cells.

As a consequence of microbial translocation, bacterial products including LPS are released from

the intestine luminal region and can be detected in the circulation of HIV-infected subjects (49). LPS enhanced the activation level of $CD16^+$ MDDCs and induced higher expression of CCL22 resulting in a superior ability of $CD16^+$ MDDCs to induce active viral replication in target resting $CD4^+$ T-cells. Furthermore, LPS-stimulated $CD16^+$ MDDCs expressed markers of follicular DCs; this evokes the possibility that $CD16^+$ MDDCs are precursors of a subset of follicular DCs. Interestingly, follicular DCs were shown to contribute to viral persistence by providing shelter to HIV (814) and by promoting replication in adjacent infected monocytic cells (815). In contrast to $CD16^+$ MDDCs, $CD16^-$MDDCs had a lower capacity to induce replication in resting $CD4^+$ T-cells at homeostasis and upon antigenic recognition; this indicates their ability to produce factors limiting HIV replication. In that sense, LPS-stimulated $CD16^-$ MDDCs were enriched in transcripts for IFN-1α, which are reported to restrict HIV infection (816).

As mentioned earlier (Section 5.2.3), HIV exposure led to very few changes in the transcriptome of $CD16^+$ and $CD16^-$ MDDCs (Figure 9; Manuscript #2). HIV modulated mostly the expression of micro-RNAs in both MDDC subsets. The function of these detected micro-RNAs had been poorly characterized. Interestingly, mIR-1271 was up-regulated by HIV in $CD16^-$ MDDCs. mIR-1271 was reported to increase cell proliferation *via* the down-regulation of the transcription factor HOXA5 (817) HOXA5 is known to down-regulate the phosphatase PTEN (818). HIV-Tat was reported to induce $CD4^+$ T-cell death *via* PTEN-dependent mechanisms (819). The function of all detected mIRs differentially regulated by HIV in $CD16^+$ *versus* $CD16^-$ MDDC subsets remains to be examined.

5.3 CONCLUSIONS

Immunity is defined as a balanced state with the goal of providing effective protection against fungal, bacterial, and viral infection while maintaining proper tolerance to self to avoid inflammatory conditions including asthma and autoimmune diseases. Immunity is made up of two arcs: the adaptive and innate immune response. HIV impairs the functional properties of both arcs and exploits certain components of immunity to ensure its survival. In this thesis, we first explored the diversity of the Th17 lineage, which is preferentially targeted by HIV, and provided a deeper understanding of the Th17 cell biology. We also shed light on the concept of pathogenic Th17 cells in HIV pathogenesis thus acknowledging the contribution to viral persistence of each of the four Th17 subsets identified. Furthermore, we turned our attention to the biology of DCs responsible for shaping the adaptive immune response. Precisely, we provided a thorough characterization of two subsets of DCs derived from two distinct monocytic populations in terms of their immunological functions. We demonstrated the negative effect of HIV infection in preventing DCs from stimulating an adequate $CD4^+$ T-cells immune response. We also revealed the identity of DC subsets that promote HIV dissemination. Overall, we characterized further different components of the immune system and provided additional understanding on the immunological consequences caused by HIV infection.

5.3.1 TH17 HETEROGENEITY AND CONTRIBUTION TO HIV PATHOGENESIS

Immunological memory is an important aspect of the adaptive immune system that allows rapid recognition of a re-encountered antigen leading to a stronger and faster protective response. The expression of chemokine receptor at the cell surface allowed the description of specific memory subsets that migrate into lymph nodes (e.g. T_{CM}) versus those that preferentially traffic in non-lymphoid organs (e.g. T_{EM}) (295). Further studies identified chemokine receptors as surface markers for memory $CD4^+$ T-cells, including the Th1, Th2, and Th17 cells, with distinct immunological roles and polarization profiles (296, 298). We focused our study on dissecting Th17 heterogeneity. One major conclusion from our findings is the existence of four Th17 subsets with differential expression of CCR4 and CXCR3 as opposed to two or three Th17 subsets previously documented by the group of Sallusto (298, 304). These subsets are the Th17,

Th1Th17, CCR6$^+$DN, and CCR6$^+$DP cells. To our knowledge, the Th17 in contrast to the Th1 and Th2 lineages represents the population among the CD4$^+$ memory T-lymphocytes with the most described diversity of transcriptional and functional characteristics. The four subsets have distinct capacities to produce Th17-associated cytokines as demonstrated. Based on the quantitative production of Th17-specific signature cytokine IL-17A, the Th17 subsets can be divided in two groups. The first group includes cells that produce the highest level of IL-17A: Th17 and CCR6$^+$DN cells. The second group includes cells producing low levels of IL-17A: Th1Th17 and CCR6$^+$DP cells. Also, the four subsets have different capacities to produce IFN-γ, a Th1 cytokine. Indeed, Th17 cells produce low to undetectable levels of IFN-γ compared to CCR6$^+$DN cells, which secrete IFN-γ but at levels inferior to those in CCR6$^+$DP and Th1Th17 cells.

Of note, CCR6$^+$DN cells were found to produce the highest levels of Th17 associated cytokines including IL-17F, IL-8, IL-21, IL-22, and CCL20. Interestingly, CCR6$^+$DN cells were demonstrated to exhibit multiple features; this indicates their ability to display various immunological roles. Our genome-wide transcriptional profiling revealed that the CCR6$^+$DN have a T_{CM} signature, suggesting that they migrate mainly into the lymph node. Of interest, we detected the presence of CCR6$^+$DN cells in the lymph nodes of two HIV-infected subjects (Figure Supplemental 7). T_{CM} are known for their extensive proliferative characteristics and ability to produce high levels of IL-2, a cytokine essential for T-cell survival (295). It is well established that Th17 cells lack the ability to produce IL-2 and that IL-21, a cytokine mainly produced by Tfh cells (336) that is essential for their survival (332). Although CCR6$^+$DN produce low levels of IL-2, they can sustain their expansion as T_{CM} by the autocrine production of IL-21. Also, our results suggest that CCR6$^+$DN hold Tfh characteristics enabling them to induce B-cell maturation. Furthermore, the finding that CCR6$^+$DN express markers associated to early Th17 commitment (e.g. IL-17F, STAT3) combined with the enrichment of T_{SCM} features (e.g. LEF1, TERC, RORA, MYC, STAT3) strongly indicates that the CCR6$^+$DN cells represent an earlier stage of Th17 differentiation. Globally, we have demonstrated that a single Th17 subset can present poly-functional profiles.

The diversity of Th17 lineage is therefore more complex than what was originally documented (298). Because of their many features that we have identified, especially concerning the $CCR6^+$DN cells, we think that the four described Th17 subsets include within them heterogeneous population with distinct function and migratory properties. In that sense, only a fraction of $CCR6^+$DN cells would represent the Th17 cells with Tfh features. Also, the fraction of $CCR6^+$DN expressing IL-17F could represent the population that is targeted to traffic into the lungs. This conclusion is supported by previous findings identifying a fraction of $CCR7^-$Th1Th17 subsets expressing MDR-1 as pathogenic Th17 cells in the context of autoimmunity (344). Our results show that Th1Th17 cells are major sources of TNF-α and IL-10; this indicates that this subset includes not only pathogenic but also non-pathogenic Th17 population. Our transcriptional analysis and functional assays also point to the possibility that both $CCR6^+$DN and $CCR6^+$DP cells include fractions of pathogenic Th17 cells. In contrast, Th17 cells may include non-pathogenic Th17 with their ability to produce strongly IL-10 while expressing low to undetectable levels of TNF-α. Furthermore, we demonstrated that Th17, Th1Th17, $CCR6^+$DN and $CCR6^+$DP cells include the T_{CM}, T_{TM} and T_{EM} population, emphasizing once again the heterogeneity observed within these four subsets.

Results from this thesis and findings from other groups suggest that different Th17 subsets can induce an immune response against common pathogens (304, 305) while displaying a specific cytokine profile in terms of IL-17A and IFN-γ (304). We demonstrated that $CCR6^+$DN cells along with Th17 and Th1Th17 cells proliferate in response to *C. albicans*. The three subsets exhibit different distribution of IL-17A and IFN-γ expression following antigenic stimulation. Therefore, an antigen can drive the adaptive immune system to generate different memory populations belonging to a particular Th lineage that are intrinsically programmed to produce various levels of common cytokines (*e.g.,* IL-17A and IFN-γ) to allow a thorough protection. By displaying differential expression of chemokine receptors, these memory populations are destined to traffic into distinct anatomical site to ensure proper immunosurveillance. Upon re-stimulation, a fraction of them will be directed toward the lymph nodes where subsequent expansion will follow whereas the other portion will home to peripheral tissues to eliminate the pathogen.

Lineage plasticity is a key feature of the Th17 lymphocytes as confirmed by our findings. Indeed, all of the four Th17 subsets were subjected to flexibility in their cytokine profile upon Th1 polarization. Cells with a Th1Th17 polarization were reported to derive from highly pure Th17 cells, as a consequence of their acquisition of Th1 characteristics under inflammatory conditions (339, 346, 820), thus establishing a differential relationship between these two populations. The similar transcriptome, antigenic specificity, and cytokine profile after long-term culture shared by the $CCR6^+$DN and Th17 cells indicate the existence of a differential relationship between these two cells. Evidence provided in this thesis and by other groups (304) also suggests a differentiation relationship between the Th1Th17 and $CCR6^+$DP cells. Our findings leave us to question whether the four Th17 subsets are derived from a common clone of naive T-cells adopting a modified surface phenotype upon encounter with a specific pathogen or a change of environmental cytokine or whether these four Th17 subsets are derived from different naive T-cell clones.

Our results revealed that the concept of pathogenic Th17 cells in the context of HIV pathogenesis is less simple then initially thought. HIV targets Th17 cells for viral replication and induces their depletion in the peripheral blood and intestinal tissues (49, 431, 777). The permissiveness of Th17 cells to HIV infection and subsequent loss leading to chronic immune activation and microbial translocation initially characterized the pathogenicity of Th17 cells. As previously shown (436, 776), our results confirm the initial pathogenic Th17 characteristics of Th17 and Th1Th17 cells. Both subsets harbor HIV-DNA and are depleted in HIV CI on ART. The same result was found in the $CCR6^+$DP cells, adding this subset to the list of HIV-pathogenic Th17 cells. In contrast to Th17, Th1Th17, and $CCR6^+$DP cells, the frequency and counts of the $CCR6^+$DN cells were preserved in CI on ART. Similar to Th17, Th1Th17, and $CCR6^+$DP, $CCR6^+$DN cells express integrated HIV-DNA. All $CCR6^+$ subsets were able to support HIV replication *in vitro*. Therefore, we have demonstrated that HIV permissiveness is a key feature of the Th17 lineage. This feature is not exclusive to Th17 cells since HIV also targets other $CD4^+$ T-lymphocytes with distinct lineage commitment, including the Tfh cells (135). The preservation of the $CCR6^+$DN cells in CI on ART leads to us to think that $CCR6^+$DN cells are protected from the cytopathic effect of HIV due to unidentified mechanisms/factors. The T_{CM} and/or T_{SCM} feature displayed by $CCR6^+$DN may favor their survival. Of note, T_{CM} and T_{SCM} were shown to act as a

cellular reservoir promoting long-term HIV persistence (55, 786). Therefore, the T_{CM}, T_{SCM}, and Tfh characteristics of $CCR6^+$DN cells may also promote their susceptibility to HIV infection. We conclude that $CCR6^+$DN cells are pathogenic Th17 cells different from the Th17, Th1Th17, and $CCR6^+$DP cells. HIV uses the $CCR6^+$DN subset survival capacity for its dissemination and persistence. Thus, the concept of pathogenic Th17 cells during HIV infection includes cells that are permissive to infection and depleted but also HIV-infected cells that are long-lived and contribute to HIV reservoir persistence under ART. The preservation of $CCR6^+$DN cells may provide a certain immune protection against opportunistic infections but appears to be insufficient to compensate for the absence of the other three $CCR6^+$ subsets as HIV disease progresses. As previously mentioned the Th17 lineage is highly heterogeneous. Not all Th17 cells are permissive to HIV infection. Unfortunately, this thesis has not identified a non-pathogenic Th17 population resistant to HIV infection but acknowledged their existence based on the work of other groups (435, 440). Non-pathogenic Th17 cells may be included within the $CCR6^+$DN population. Further studies need to focus on the identification of non-pathogenic Th17 cells; this can lead to the development of new therapeutic strategies to eradicate HIV infection.

Overall, we have further defined Th17 heterogeneity and the concept of Th17 pathogenicity during HIV infection. Future studies need to be pursued to provide a better understanding of Th17 biology during HIV infection.

5.3.2 CHARACTERIZATION OF $CD16^+$ AND $CD16^-$ MDDCS AT HOMEOSTASIS AND DURING HIV INFECTION

Cells of the innate immune system, such as the monocytes and DCs, provide the first line of defense against common microorganisms. Features of DCs allow the early response against a particular antigen to be translated into memory response with the activation of the adaptive immune system. DCs and monocytes originate from specific hematopoietic lineages in the bone marrow (477). When homeostasis is perturbed, monocytes will differentiate *in situ* at the site of inflammation to give rise to distinct subsets of DCs that will be able to rapidly stimulate effector T-lymphocytes. These cells are termed inflammatory-DCs (inf-DCs) and have been described during bacterial, viral, and fungal infection (821). Although inf-DCs have been characterized phenotypically, distinguishing them from conventional DCs and macrophages remains a challenge. Two human monocytic populations have been characterized based on the differential expression of CD16: the $CD16^-$ (classical monocytes) and $CD16^+$ (intermediate and non-classical) monocytes that exhibit different roles in immunity. We focused on dissecting the heterogeneity between two MDDCs subsets derived from $CD16^-$ and $CD16^+$ monocytes.

We confirmed the similar ability of both $CD16^+$ and $CD16^-$ monocytes to undergo differentiation and to acquire typical immature and mature DC markers at their cellular surface. One conclusion from our findings is that $CD16^+$ and $CD16^-$ MDDCs represent transcriptionally unique populations that are distinct from their related precursors. For example, they do not maintain preferential expression of the trafficking receptors CX3CR1 and CCR2 that phenotypically defined the $CD16^+$ and $CD16^-$ monocytes, respectively (491, 492). Nevertheless, $CD16^+$ and $CD16^-$ MDDCs retain the core identity attributed to their respective precursors. As demonstrated for the $CD16^+$ monocytes (495), the $CD16^+$ MDDCs display an advanced stage of maturation as reflected by their superior state of cellular activation. Upon antigenic recognition, these cells are equipped to rapidly acquire maturation, which leads to a faster initiation of T-cell mediated immune responses. The mechanism explaining the acquisition of an advanced maturation stage remains unknown and requires further investigation. Also, similar to $CD16^+$ monocytes, $CD16^+$ MDDCs display pro-inflammatory features. Conversely, $CD16^-$ monocytes and $CD16^-$ MDDCs present minor pro-inflammatory features but exhibit superior phagocytic properties. $CD16^-$ as opposed to $CD16^+$ MDDCs appear to be involved in maintenance of immunological homeostasis.

We can conclude that despite morphological changes due to differentiation, MDDCs carry their immunological specificities acquired as monocytes circulating in peripheral tissues. In line with the concept of a developmental relationship between classical and non-classical monocytes (495, 505, 507, 518, 519), $CD16^-$ monocytes recruited in the peripheral tissues can upon encounter with various stimuli differentiate into $CD16^+$ monocytes with the acquisition of a new transcriptional profile linked to inflammatory properties. Changes in the cytokine milieu can force these converted $CD16^+$ monocytes to undergo differentiation towards the DC lineage with the maintenance of their core properties. Alternatively, $CD16^-$ monocytes can directly differentiate into MDDCs with a similar outcome in maintaining their fundamental properties.

Upon LPS antigen recognition, we found that significant changes occur in the transcriptome of $CD16^+$ MDDCs and $CD16^-$ MDDCs. Nevertheless, LPS-stimulated $CD16^+$ MDDCs remain inflammatory cells as reflected by their ability to express TNF-α, LTA, LTB, and other pro-inflammatory cytokines. Also, $CD16^+$ MDDCs exposed to LPS acquire phagocytic features as reflected by the expression of SIGLEC1 and members of the complement system C2 and CFP. Furthermore, LPS induced expression of transcripts that are markers of follicular DCs, suggesting that $CD16^+$ MDDCs have the ability to acquire new immunological functions. Interestingly, LPS-stimulated $CD16^-$ MDDCs will acquire pro-inflammatory features as reflected by their ability to produce IFN-α, IL-1α, CXCL6, and IL-23. These results indicate that $CD16^-$ MDDCs are also Inf-DCs. Our results suggest the concept that the innate immune system engenders different types of Inf-DCs to induce distinct responses against identical pathogens to ensure efficient protection. Consistent with results obtained from LPS stimulation, $CD16^+$ and $CD16^-$ MDDCs displayed distinct capacities to mount a response against CMV, *C. albicans,* and *S. aureus.* Indeed, $CD16^-$ compared to $CD16^+$ MDDCs induced higher T-cell proliferation in response to these pathogens. Although $CD16^-$ MDDCs induced superior levels of Th17-associated cytokines in response to *C. albicans*, both MDDCs had similar effects on the induction of Th17-specific response following encounters with *S. aureus*. These results emphasize that each antigen has a unique ability to promote immune responses.

We confirmed the negative effect of HIV on the immunogenic potential of DCs, as previously demonstrated by other groups (803, 804). We reveal for the first time to our knowledge the

existence of a negative correlation between the ability of DCs to initiate immune responses in the presence of HIV and the magnitude of HIV dissemination. We also reveal a division of labor between $CD16^+$ and $CD16^-$ MDDCs with $CD16^+$ MDDCs more able to transmit HIV infection and $CD16^-$ MDDCs exhibiting a superior immunogenic potential. HIV acts on both $CD16^+$ and $CD16^-$ MDDCs and impairs their capacity to stimulate T-cell proliferation and polarization. Also, HIV exploits the intrinsic characteristics of $CD16^+$ MDDCs, including their high activation state, to promote viral dissemination. Furthermore, HIV may benefit from the anatomical location of $CD16^+$ MDDCs, which according to our transcription analysis is the gut, to ensure its pathogenesis. This represents a serious issue for the control and eradication of HIV infection. Therefore, we propose that future therapeutic strategies should be developed with the aim of targeting the T-cell reservoir (*i.e.,* $CCR6^+$DN cells) for destruction and blocking the capacity of APCs (*i.e.,* $CD16^+$ MDDCs) to transmit the virus. As opposed to $CD16^+$ MDDCs, $CD16^-$ MDDCs had less capacity to induce HIV replication in resting T-cells. This evidence indicates the ability of $CD16^-$ MDDCs to produce antiviral factors blocking HIV replication and supports previous findings suggesting that only a fraction of myeloid DCs transmit HIV (740).

Overall, our study led to the conclusion that $CD16^+$ and $CD16^-$ monocytes give rise to two transcriptionally different MDDCs with distinct immunological features and anatomical locations. We identified the $CD16^+$ MDDCs as the DC subsets that promote HIV dissemination. The innate immune system generates inf-DCs for a specific purpose. Once the inflammation is resolved, inf-DCs are cleared from the immune system. This mechanism is critical for the return to and maintenance of homeostasis.

CHAPTER 6: PERSPECTIVE

In this thesis, we provided a detailed characterization of Th17 cell and DC biology. The continuation of this work should be focused on: 1) further dissecting the heterogeneity displayed by the Th17 lineage in terms of their immunological function, and 2) examining the extensive differences in the capacity of the $CD16^-$ and $CD16^+$ MDDCs to mount an immune response. This will provide a better understanding of host defense during homeostasis and under chronic inflammatory conditions including HIV infection.

6.1 UNDERSTANDING THE EXTENSIVE IMMUNOLOGICAL ROLE OF TH17 CELLS AT HOMEOSTASIS AND UNDER INFLAMMATORY CONDITIONS

Several gaps related to the complete immunological function of the Th17 lineage remain to be explained. Precisely, the role of CCR6$^+$DN cells as Tfh cells helping B-cell produce immunoglobulin must be investigated. The differentiation relationship among the four Th17 subsets should be explored to understand the origin of each Th17 subsets. Also, the biological function of IL-17F distinct from the one attributed to IL-17A must be investigated to provide a better grasp of the role of CCR6$^+$DN cells in host defense. In the context of autoimmunity, the complete characterization of human pathogenic and non-pathogenic Th17 cells must be studied for a better understanding of this concept. In the context of HIV pathogenesis, the molecular mechanism /factors allowing for the survival of CCR6$^+$DN cells in CI on ART must be also investigated. Furthermore, the contribution of CCR6$^+$DN cells to HIV persistence, as a cellular reservoir must be determined. Finally, the identification of non-pathogenic cells and molecular factors inhibiting HIV replication is necessary for the discovery of a therapeutic strategy for the eradication of HIV infection.

6.1.1 DETERMINING THE OVERLAP BETWEEN CCR6$^+$DN AND TFH CELLS

Accumulating evidence from this thesis combined with findings from the literature (753, 754, 758, 784, 785) support the hypothesis that CCR6$^+$DN cells are Th17 cells with Tfh functions (see Section 5.1.1 and 5.1.2). CCR6$^+$DN cells may represent the circulating Tfh cells that down-regulate the expression of Tfh markers (*e.g.,* Bcl6, CXCR5, and PD-1) and adopt a phenotype of long-lived memory cells to promote survival (784). Once activated by TCR triggering, these cells reacquire the expression of Tfh markers and produce high levels of IL-21. Of note, our results showing that CCR6$^+$DN with Tfh features were from experiments where sorted CCR6$^+$ subsets were stimulated with CD3/CD28 Abs. Therefore, a characterization identifying CCR6$^+$DN as Tfh cells must be performed *ex vivo*. We have already validated our transcriptional analysis concerning the preferential expression of Bcl6 mRNA in CCR6$^+$DN cells. The expression of Tfh surface markers CXCR5 along with ICOS and PD-1 at the cell surface on CCR6$^+$DN cells

compared to Th17 subsets will have to be examined. Next, the capacity of CCR6$^+$DN cells to induce maturation in naive B-cells, including the up-regulation expression of activation molecule CD38 on B cells, will have to be determined. Furthermore, and most importantly, the ability of CCR6$^+$DN *versus* Th17 cells to stimulate B-cells to produce immunoglobulin such as IgM, IgG, and IgG will have to be investigated. One interesting point to investigate is whether the T_{CM} feature of CCR6$^+$DN cells is linked to the displayed Tfh characteristics. Although Tfh cells were reported to express low levels of CCR7 while expressing highly CXCR5 (336), recent studies demonstrated that functional Tfh cells can co-express CCR7 and CXCR5 (785, 822). HIV infection was demonstrated to impair the function of Tfh in shaping B-cell immunity (823), as demonstrated in this thesis, HIV does not alter CCR6$^+$DN frequency/count in CI on ART but may impair their functional role. The effect of HIV on the immunological role of CCR6$^+$DN cell in CI on ART must be investigated.

6.1.2 DETERMINING THE DIFFERENTIATION RELATIONSHIP BETWEEN THE FOUR TH17 SUBSETS

Future studies should be focused on identifying the origin of each of the four memory CCR6$^+$ subsets. Accumulating findings indicate that highly pure Th17 cells producing homogeneously IL-17A acquire Th1 features, including the capacity to produce IFN-γ (306, 339, 346). Other studies suggest that a fraction of Th1Th17 cells can originate directly from naive precursors without any transition through an initial Th17 stage (304). Evidence from this thesis suggests the existence of a differentiation relationship between the CCR6$^+$DN and Th17 subsets as well as between the Th1Th17 and CCR6$^+$DP cells. Results from our genome-wide transcriptional analysis demonstrated that CCR6$^+$DN cells represent an early stage of Th17 differentiation. Conversely, results from transcriptional characterization and functional assay lead us to think CCR6$^+$DP cells represent advanced stage Th17 differentiation. Therefore, the hierarchal position of each CCR6$^+$ subset in the Th17 development program will need to be addressed. In that sense, the measure of telomere shortening and telomerase activity, both indicators of cellular aging, must be performed. The expression of senescence marker pro-lamin A in each CCR6$^+$ subsets must be evaluated using western blot techniques. Of note, CCR6$^+$DP cells express the highest level of pro-lamin associated gene LMNA as demonstrated in this thesis.

We have evidence suggesting that CCR6$^+$DN cells are precursors of Th17 subsets. CCR6$^+$DN were shown to adopt a CCR6$^+$CCR4$^+$CXCR3$^-$ phenotype in long-term cultures under Th17 or Th1 polarizing condition (Supplemental Figure 6; Manuscript #1). The acquisition of CCR4 appears to be associated to polyclonal TCR-triggering. Whether CCR6$^+$DN acquire a Th17 phenotype following antigenic stimulation remains to be investigated. Previous studies reported that as Th17 cells differentiation progresses, IL-17F expression decreases to favor the expression of IL-17A (372). This phenomenon is thought to be mediated by IL-23. Preliminary results from one donor showed the effect of IL-23 on the production of Th17-associated cytokines on CCR6$^+$ subsets (Figure 1, Appendix). IL-23 had no effect on the production of IL-17A by CCR6$^+$DN cells. However, IL-23 drastically diminished the production of IL-17F in CCR6$^+$DN; this provides an explanation for the similar cytokine profile observed between the CCR6$^+$DN and Th17 cells after short-term and long-term culture (Supplemental Figure 5; Manuscript #1). Further donors must be used to confirm this conclusion. To determine the existence of a differential relationship between Th1Th17 and CCR6$^+$DP cells, it is necessary to analyze their transcriptome for similarities. The antigenic specificity of the CCR6$^+$DP cells must be determined as well. Also, the TCRβ sequencing of cells specific to one pathogen (e.g., *C. albicans versus S. aureus*) from each of the four CCR6$^+$ subsets must be performed to determine whether these cells share clonotypes. In the case pathogen-specific CCR6$^+$ subsets share TCR clonotypes, this would further indicate that the differentiation of functionally distinct Th17 cells originates from one single clone. Overall, this study will allow a better understanding of the life cycle of a particular T-cell lineage in response to specific pathogens.

6.1.3 DETERMINING THE BIOLOGICAL FUNCTION OF IL-17F

Our transcriptional analysis and functional assay revealed that IL-17F expression is confined within the CCR6$^+$DN subset. Other than being a marker of early Th17 differentiation, there must be a reason explaining the high expression of IL-17F on a single CCR6$^+$ memory subset. The significance of IL-17F expression on CCR6$^+$DN cells may be directly linked to a specific immunological role displayed by this particular Th17 subset. Previous studies from animal models suggest that IL-17F attenuates the Th2 immune response characterized by the decrease of IL-4, IL-5, and IL-13 production and eosinophil recruitment upon chronic asthma (762).

Evidence supporting this possible function of IL-17F in humans comes from studies performed in HIES patients who exhibit a defect in IL-17A and IL-17F expression due to mutations in STAT3 (section 1.1.2) while expressing elevated levels of Th2-specific cytokine and IgE (259, 260, 824). One of the roles of Th2 immunity is to help B-cells induce IgE. The hypothesis that the production of IL-17F by $CCR6^+$DN cells lead to the neutralization of Th2 immune response resulting in a decrease of IgE production will have to be explored.

6.1.4 IDENTIFYING FURTHER THE HUMAN PATHOGENIC AND NON PATHOGENIC TH17 CELLS IN THE CONTEXT OF AUTOIMMUNITY

Effector memory Th1Th17 subset expressing MDR-1 were identified as pathogenic Th17 cells in humans (344). We have generated evidence indicating that $CCR6^+$DN and $CCR6^+$DP cells include pathogenic Th17 cells. Therefore, a detailed characterization of these subsets expressing pathogenic markers will have to be performed. In that sense, the expression of MDR-1, GM-CSF, ligands of CCR5, as well as the recently described molecules GRP65, TOSO, and PLZP (825), will have to be determined on $CCR6^+$DN and $CCR6^+$DP cells. Since Th17 and Th1Th17 were shown as major sources of IL-10 in this thesis, the identification of non-pathogenic Th17 cells within the Th17 and the Th1Th17 subsets must be investigated. Non-pathogenic Th17 cells were described as including an immunosuppressive function linked with the expression of IL-10 (355); therefore, the immunosuppressive function of Th17 and Th1Th17 cells remains to be evaluated. Expression of other non-pathogenic markers including the recently described CD5L/AIM (826) will have to be explored. Interestingly, the group of Sallusto demonstrated that stimulation with *C. albicans* and *S. aureus* leads to the different immune responses displayed by the Th17 subsets (302). *S. aureus* induces IL-17A combined with IL-10 in Th17 cells. In contrast, *C. albicans* induces IL-17A with IFN-γ. The ability of these two pathogens to induce pathogenic *versus* non-pathogenic Th17 cells within the Th17 and Th1Th17 subsets will have to be determined. In the case that *S. aureus* induces non-pathogenic Th17 cells as hypothesized here and suggested by others (354), the molecular epitope responsible for this phenomenon must be identified. Furthermore, the use of animal models will be crucial in determining the role and the degree of involvement of the four Th17 subsets in autoimmunity. The four $CCR6^+$ subsets were also identified in mice (unpublished results from Dr. De Repentigny's laboratory). Also, techniques

such as adoptive cell transfer and induction of autoimmunity (e.g. MOG immunization to induce EAE) will have to be used.

6.1.5 DETERMINING THE FACTOR/MECHANISM INVOLVED IN THE PRESERVATION OF CCR6$^+$DN CELLS DURING CHRONIC HIV INFECTION

The mechanisms allowing the CCR6$^+$DN cells to resist the cytopathic effect of HIV infection must be explored. T_{CM} and T_{SCM} were shown to express factors promoting cell survival (137, 425). Precisely, the activity level of FOXO3a, the transcription factor permitting survival of T_{CM} versus T_{EM} (137), will have to be determined in CCR6$^+$DN cells. The common γ chain-using IL-7 was shown to be important for the survival of memory CD4$^+$ T-cells at homeostasis ((827, 828)). The ability of CCR6$^+$DN cells from CI on ART to express CD127 (IL-7R) and respond to IL-7 will have to be examined. The expression of TSCM markers (MYC, LEF1, TERC, STAT3, RORA) as demonstrated in CCR6$^+$DN cells from HIV-uninfected individuals will have to be evaluated in CCR6$^+$DN cells from CI on ART. It would be interesting to determine whether HIV blocks the expression of T_{SCM} features in CCR6$^+$DN cells. Other unidentified factors promoting T-cell expansion may also explain the preservation of CCR6$^+$DN cells during HIV infection. Although not discussed in this thesis, our genome-wide transcriptional analysis revealed that CCR6$^+$DN cell preferentially expressed oncogenic molecules including PLAC8 (829), TP63 (830)), and PFKFB4 (831) (Supplemental Table 1; Manuscript #1). The preferential expression of these molecules in CCR6$^+$DN cells *versus* the Th17, Th1Th17, and CCR6$^+$DP cells from CI on ART will have to be evaluated. Furthermore, the anatomical location of the CCR6$^+$DN cells will have to be determined using primate animal models or human biopsies. Although we have detected CCR6$^+$DN cells in lymph nodes in two CI on ART patients, their location in the lung, particularly in the bronchus-associated lymphoid tissue *versus* the gut, the principal site of viral replication, remains to be investigated.

6.1.6 FURTHER DEFINING THE CHARACTERISTICS OF PATHOGENIC AND NON-PATHOGENIC TH17 CELLS IN HIV PATHOGENESIS

We demonstrated that similar to Th17, Th1Th17, and CCR6$^+$DP cells, the CCR6$^+$DN cells harbor HIV-DNA. The PCR technique used determined that 300/10^6 of resting CD4$^+$ T-cells on average

contain replication-competent virus (832). However, other sophisticated experimental methods demonstrated that only $1/10^6$ memory resting $CD4^+$ T-cells carry replication-competent virus (833). Consequently, the cellular reservoir represents less than one percent of the total $CD4^+$ T-lymphocyte memory population. Because the PCR technique detects intact and defective proviruses, our generated results using this technology do not confirm the presence of replication-competent virus in $CCR6^+$ subsets from CI on ART. Therefore, we tried to address this question in experiments using an adapted viral outgrowth assay similar to that proposed by *Siliciano et al.* (833). Following TCR-triggering, the highest level of viral-RNA was detected between the Th17 and $CCR6^+$DN subsets (Figure 8; Manuacript#1). Furthermore, results from HIV reactivation experiments performed in the four $CCR6^+$ subsets from four distinct CI on ART subjects demonstrated that $CCR6^+$DN cells harbor replication-competent integrated HIV-DNA (Figure 8; Manuacript#1). Interestingly, in one CI on ART patient, $CCR6^+$DN cells were the only $CCR6^+$ subset capable of expressing intracellular HIV-p24 upon reactivation *in vitro* (Figure 8; Manuacript#1). These results must be performed on at least seven CI on ART donors to make final conclusions. As demonstrated in this thesis, the results from our HIV reactivation assay showed that IL-17A was detected in only a fraction of each $CCR6^+$ subsets (Figure Supplementary 6; Manuacript#1). Among the total population expressing IL-17A within the $CCR6^+$ subsets, only a fraction co-expressed HIV-p24, indicating the existence of $IL\text{-}17^+$ T-cells that are resistant to HIV infection. These results again confirm the presence of non-pathogenic Th17 cells in HIV infection as previously shown in autoimmunity (355, 359, 435, 440). Experience will have to be repeated in a larger cohort of at least n=10 for concise conclusions. Using a cytokine capture assay (Miltenyi technology), $IL\text{-}17A^+$ cells expressing or not HIV-p24 from the $CCR6^+$ subsets will have to be sorted for the characterization of genome-wide transcriptional signatures associated with HIV permissiveness *versus* resistance. Together, these future directions in research will increase our knowledge of the molecular determinants of Th17 pathogenicity during HIV infection and will orient new therapeutic strategies for the restoration of Th17 functions.

6.2. FURTHER CHARACTERIZING THE IMMUNOLOGICAL ROLE OF CD16+ AND CD16- MDDCS AT HOMEOSTASIS AND IN HIV PATHOGENESIS

Despite the exciting results obtained in this study as described in Manuscripts #2 and #3, several points require clarification in order to further understand the immunobiology of each MDDC and their contribution to HIV infection. Precisely, validations of our results from the transcriptional and functional assays will need to be performed. Additional characterizations of the mechanisms by which HIV exploits the process of autophagy for its own dissemination advantage will have to be explored. The different transcriptional profile observed in $CD16^+$ and $CD16^-$ indicates a distinct modulation of endogenous biological process within each subset. Also, description of the fate of $CD16^+$ monocytes differentiating in MDDCS from chronically HIV-infected patients must be examined to acknowledge the consequences of the expansion of this monocytic subset during HIV pathogenesis.

6.2.1 VALIDATION OF OUR RESULTS FROM THE TRANSCRIPTIONAL ANALYSIS AND FUNCTIONAL ASSAY

Our genome-wide transcriptional analysis provided a detailed description of the $CD16^+$ and $CD16^-$ MDDCs in terms of their respective immunological functions. Nevertheless, considering the existence of false positive and negative calls in high throughput transcriptional screens, validation by the RT-PCR and functional assays should be performed to confirm our conclusions. Regarding the homeostatic conditions, which characterized the immature MDDCs, validation of gene transcripts includes ITGAE, CD86, ALCAM, LFA-1, and FOXO1 that were preferentially expressed in $CD16^+$ MDDCs as well as CCR6, CD34, ITAG9, IFI16, and HIF1A that were found to be preferentially up-regulated in $CD16^-$ MDDCs. Concerning the stimulation with LPS where we characterized the mature MDDCs, gene transcripts selected for validation are C2, CFP, SIGLEC1, CLU, and P2RY8 that were found to be preferentially up-regulated in LPS-stimulated $CD16^+$ MDDCs as well as TREM1 and IFN-1α which were highly expressed in LPS-stimulated $CD16^-$ MDDCs. Of note, the possibility that $CD16^+$ monocytes are precursors for follicular DCs requires detailed investigations. In that sense, the expression of follicular DCs markers CD23, CD21, and CD35 (834) as well as their capacity to induce the maturation of naive B-cells should be investigated. All transcripts for cytokines detected constitutively and upon LPS stimulation should be validated at the protein level with the use of ELISA kits. These cytokines include IL-

15, CCL22, TNF-α, IL-1α, IL-1β, LTA, LTB, CXCL1, CXCL6, IL-18, CCL18, and IL-23. All functional validations should be performed with cells from at least seven different HIV-uninfected donors. Of interest, the expression of PRRs, such as TLR7 and TLR8, will have to be measured in immature $CD16^+$ and $CD16^-$ MDDCs to further characterize their differential ability to mount immune responses against bacterial/fungal *versus* viral pathogens as described for the $CD16^-$ and $CD16^+$ monocytes (613).

A detailed description of mIRs, especially mIR-1271 that was found up-regulated in the $CD16^-$ MDDCs, as well as their involvement in HIV pathogenesis should be investigated. The role of IFN-1α as a mechanism used by $CD16^-$ MDDCs to restrict HIV replication in resting T-cells must be also determined. Although not discussed, we found that $CD16^+$ compared to $CD16^-$ MDDCs expressed several genes related to cell protrusion, and we observed under a microscope that these subsets had a different physical morphology including filopodia projections. We will need to confirm these observations with further microscopic confocal studies as cell protrusion formation have been shown to be involved in the HIV *trans* infection (835) and can be another mechanism used by HIV to promote its dissemination.

In addition, the assays involving DC: T-cell co-culture for HIV *trans* infection and antigenic presentation, as shown in Manuscript #2 and Manuscript #3, were performed using a small number of donors and should be repeated at least three to four more times to come to a final conclusion.

6.2.2 DETAILED CHARACTERIZATION OF MOLECULAR MECHANISMS FAVORING HIV TRANS-INFECTION: STUDY OF THE AUTOPHAGY SYSTEM

Elegant studies from the group of Vincent Piguet demonstrated that HIV shuts down the autophagy system in DCs by inducing the activation of mTOR and in this manner insures its efficient *trans* infection of $CD4^+$ T-cells across the virological synapse (701). It would be important to determine how the autophagy system of each MDDCs subset is affected upon HIV infection and whether this mechanism is preferentially used in $CD16^+$ *versus* $CD16^-$ MDDCs with the purpose of further explaining the superior ability of $CD16^+$ MDDCs to promote HIV replication in resting T-cells. The first goal would be to determine the autophagy potential of

each MDDC from HIV-uninfected individuals. To do so, the expression of mTOR, an inhibitor of autophagy, as well as molecules involved in the positive regulation of autophagy (*i.e.,* LC3-I and LC3-II) must be measured by RT-PCR and western blot techniques. These experiments must be performed in immature and mature MDDCs before and after HIV exposure. Furthermore, the ability each MDDCs subset to promote HIV replication in $CD4^+$ T-cells in the presence or absence of a drug that inhibits (*i.e.,* bafilomycin A) or stimulates (*i.e.,* rapamycin) autophagy must be examined. This is particularly important in the actual context where autophagy modulators such as metformin are used successfully for cancer treatment (836) and are currently being tested for their ability to improve immune competence in HIV-infected subjects.

6.2.3 EVALUATING THE CONSEQUENCE OF $CD16^+$ AND $CD16^-$ MONOCYTE DIFFERENTIATION INTO DCS IN HIV-INFECTED SUBJECTS

Although our *in vitro* assay did not show any differences in the levels of HIV-DNA integration in HIV-exposed $CD16^+$ *versus* $CD16^-$ MDDCs (3 of 4 subjects), previous studies including those from the group of Suzanne Crowe demonstrated that $CD16^+$ monocytes are more permissive to HIV infection and harbored preferentially HIV-DNA compared to $CD14^{++}CD16^-$ monocytes, even in subjects successfully treated with HAART (530, 540, 541). Our study presented in this thesis suggests that $CD16^+$ and $CD16^-$ MDDCs are imprinted with a specific transcriptional landscape acquired from their respective precursors. Consistently, $CD16^+$ MDDCs highly likely carry virions and/or integrated HIV-DNA. Therefore, it would be of interest to determine the fate of these MDDCs to promote adaptive immunity and HIV *trans* infection in CI on ART subsets. Chronic inflammation induced by HIV may result in the differentiation of monocytes into DCs Unfortunately, due to the difficulty of discriminating the MDDCs from macrophages and cDCs as mentioned earlier, it would be impossible to obtain them from biopsies of HIV patients. To conduct this study, we will first isolate $CD16^+$ and $CD16^-$ monocytes, as described in Manuscript #2 and Manuscript #3, then proceed to the measure of *ex vivo* integrated HIV-DNA to confirm results from other groups. The $CD16^+$ and $CD16^-$ monocytes will then be differentiated into MDDCs. Genome-wide transcriptional analysis would have to be performed for the characterization of their transcriptome. The transcriptome of $CD16^+$ and $CD16^-$ MDDCs from CI on ART subjects should be compared to that of MDDCs subsets from HIV-uninfected individuals to determine the effect on HIV infection on DC biology. Also, their capacity to induce an

immune response against opportunistic pathogens including CMV, *S. aureus,* and *C. albicans* as well as their ability to induce Th17 polarization in antigen-specific T-cells will have to be explored. Lastly, $CD16^+$ and $CD16^-$ MDDCs generated from monocytes of CI on ART subjects should be investigated for their capacity to transmit virus to $CD4^+$ T-cells from HIV-uninfected individuals.

CHAPTER 7: APPENDIX

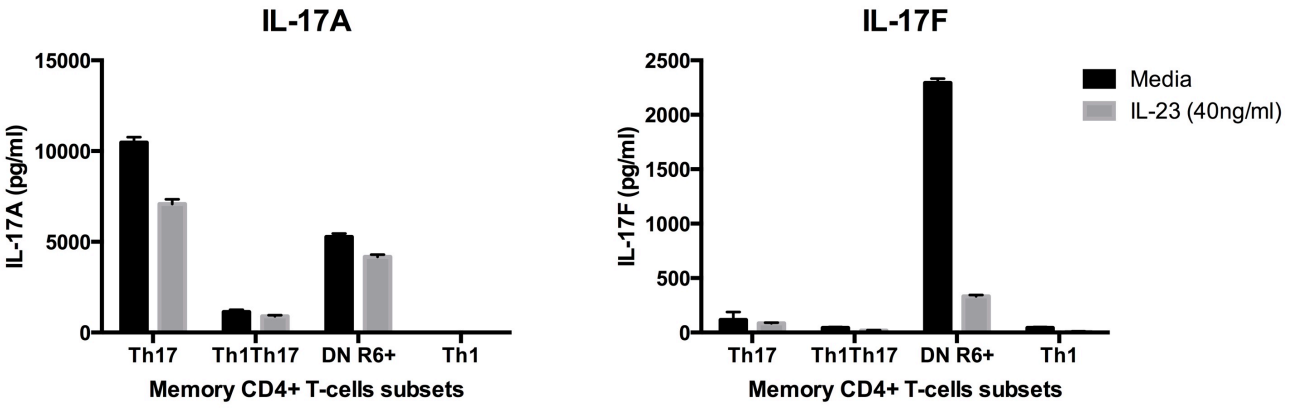

Figure 1. IL-23 decreases the production of IL-17F in CCR6^{+}DN. FACS-sorted memory subsets were stimulated *via* CD3/CD28 for 4 days. The production of the Th17 lineage-specific cytokines IL-17A and IL-17F in the presence or absence of IL-23 (40ng/ml) was quantified by ELISA.

BIBLIOGRAPHY

1. Schaechter M, Lederberg J. 2009. *Desk encyclopedia of microbiology*. Boston, MA: Elsevier
2. Barre-Sinoussi F, Chermann JC, Rey F, Nugeyre MT, Chamaret S, Gruest J, Dauguet C, Axler-Blin C, Vezinet-Brun F, Rouzioux C, Rozenbaum W, Montagnier L. 1983. Isolation of a T-lymphotropic retrovirus from a patient at risk for acquired immune deficiency syndrome (AIDS). *Science.* 220: 868-71.
3. Coffin J, Haase A, Levy JA, Montagnier L, Oroszlan S, Teich N, Temin H, Toyoshima K, Varmus H, Vogt P, et al. 1986. Human immunodeficiency viruses. *Science* 232: 697
4. WHO. 2014. MDG 6: combat HIV/AIDS, malaria and other diseases. WHO
5. PHAC. 2012. ARCHIVED - Summary: Estimates of HIV Prevalence and Incidence in Canada, 2011. Canada: Her Majesty the Queen in Right of Canada
6. Friedman H, Specter S, Bendinelli M. 2006. *In vivo models of HIV disease and control*. New York, NY: Springer. xviii, 436 p. pp.
7. Sharp PM, Hahn BH. 2010. The evolution of HIV-1 and the origin of AIDS. *Philos Trans R Soc Lond B Biol Sci* 365: 2487-94
8. Charneau P, Borman AM, Quillent C, Guetard D, Chamaret S, Cohen J, Remy G, Montagnier L, Clavel F. 1994. Isolation and envelope sequence of a highly divergent HIV-1 isolate: definition of a new HIV-1 group. *Virology* 205: 247-53
9. Wainberg MA. 2004. HIV-1 subtype distribution and the problem of drug resistance. *AIDS* 18 Suppl 3: S63-8
10. Plantier JC, Leoz M, Dickerson JE, De Oliveira F, Cordonnier F, Lemee V, Damond F, Robertson DL, Simon F. 2009. A new human immunodeficiency virus derived from gorillas. *Nat Med* 15: 871-2
11. Murray PR, Rosenthal KS, Pfaller M. 2009. *Medical Microbiology*. Philadelphia: Elsevier. 960 pp.
12. Karlsson Hedestam GB, Fouchier RA, Phogat S, Burton DR, Sodroski J, Wyatt RT. 2008. The challenges of eliciting neutralizing antibodies to HIV-1 and to influenza virus. *Nat Rev Microbiol* 6: 143-55
13. Greene WC, Peterlin BM. 2002. Charting HIV's remarkable voyage through the cell: Basic science as a passport to future therapy. *Nat Med* 8: 673-80
14. Ayinde D, Maudet C, Transy C, Margottin-Goguet F. 2010. Limelight on two HIV/SIV accessory proteins in macrophage infection: is Vpx overshadowing Vpr? *Retrovirology* 7: 35
15. Hallenberger S, Bosch V, Angliker H, Shaw E, Klenk HD, Garten W. 1992. Inhibition of furin-mediated cleavage activation of HIV-1 glycoprotein gp160. *Nature* 360: 358-61
16. Morikawa Y, Barsov E, Jones I. 1993. Legitimate and illegitimate cleavage of human immunodeficiency virus glycoproteins by furin. *J Virol* 67: 3601-4
17. Gabuzda DH, Lawrence K, Langhoff E, Terwilliger E, Dorfman T, Haseltine WA, Sodroski J. 1992. Role of vif in replication of human immunodeficiency virus type 1 in CD4+ T lymphocytes. *J Virol* 66: 6489-95
18. Romani B, Engelbrecht S. 2009. Human immunodeficiency virus type 1 Vpr: functions and molecular interactions. *J Gen Virol* 90: 1795-805

19. Fisher AG, Feinberg MB, Josephs SF, Harper ME, Marselle LM, Reyes G, Gonda MA, Aldovini A, Debouk C, Gallo RC, et al. 1986. The trans-activator gene of HTLV-III is essential for virus replication. *Nature* 320: 367-71
20. Berkhout B, Silverman RH, Jeang KT. 1989. Tat trans-activates the human immunodeficiency virus through a nascent RNA target. *Cell* 59: 273-82
21. Malim MH, Hauber J, Fenrick R, Cullen BR. 1988. Immunodeficiency virus rev trans-activator modulates the expression of the viral regulatory genes. *Nature* 335: 181-3
22. Malim MH, Hauber J, Le SY, Maizel JV, Cullen BR. 1989. The HIV-1 rev trans-activator acts through a structured target sequence to activate nuclear export of unspliced viral mRNA. *Nature* 338: 254-7
23. Foster JL, Garcia JV. 2008. HIV-1 Nef: at the crossroads. *Retrovirology* 5: 84
24. Nomaguchi M, Fujita M, Adachi A. 2008. Role of HIV-1 Vpu protein for virus spread and pathogenesis. *Microbes Infect* 10: 960-7
25. Stevenson M. 2003. HIV-1 pathogenesis. *Nat Med* 9: 853-60.
26. Paul WE. 2013. *Fundamental immunology*. Philadelphia: Wolters Kluwer Health/Lippincott Williams & Wilkins. xviii, 1283 p. pp.
27. Klatzmann D, Champagne E, Chamaret S, Gruest J, Guetard D, Hercend T, Gluckman JC, Montagnier L. 1984. T-lymphocyte T4 molecule behaves as the receptor for human retrovirus LAV. *Nature* 312: 767-8.
28. Janeway CA, Travers P, Mark W, Mark S. 2001. *Immunobiology*. New York and London: Garland Science. 732 pp.
29. Clapham PR, McKnight A. 2001. HIV-1 receptors and cell tropism. *Br Med Bull* 58: 43-59
30. Alkhatib G, Combadiere C, Broder CC, Feng Y, Kennedy PE, Murphy PM, Berger EA. 1996. CC CKR5: a RANTES, MIP-1alpha, MIP-1beta receptor as a fusion cofactor for macrophage-tropic HIV-1. *Science* 272: 1955-8.
31. Bleul CC, Farzan M, Choe H, Parolin C, Clark-Lewis I, Sodroski J, Springer TA. 1996. The lymphocyte chemoattractant SDF-1 is a ligand for LESTR/fusin and blocks HIV-1 entry. *Nature* 382: 829-33.
32. Deng H, Liu R, Ellmeier W, Choe S, Unutmaz D, Burkhart M, Di Marzio P, Marmon S, Sutton RE, Hill CM, Davis CB, Peiper SC, Schall TJ, Littman DR, Landau NR. 1996. Identification of a major co-receptor for primary isolates of HIV-1. *Nature* 381: 661-6.
33. Choe H, Farzan M, Sun Y, Sullivan N, Rollins B, Ponath PD, Wu L, Mackay CR, LaRosa G, Newman W, Gerard N, Gerard C, Sodroski J. 1996. The beta-chemokine receptors CCR3 and CCR5 facilitate infection by primary HIV-1 isolates. *Cell* 85: 1135-48.
34. Feng Y, Broder CC, Kennedy PE, Berger EA. 1996. HIV-1 entry cofactor: functional cDNA cloning of a seven-transmembrane, G protein-coupled receptor. *Science* 272: 872-7.
35. Doranz BJ, Rucker J, Yi Y, Smyth RJ, Samson M, Peiper SC, Parmentier M, Collman RG, Doms RW. 1996. A dual-tropic primary HIV-1 isolate that uses fusin and the beta-chemokine receptors CKR-5, CKR-3, and CKR-2b as fusion cofactors. *Cell* 85: 1149-58
36. Dragic T, Litwin V, Allaway GP, Martin SR, Huang Y, Nagashima KA, Cayanan C, Maddon PJ, Koup RA, Moore JP, Paxton WA. 1996. HIV-1 entry into CD4+ cells is mediated by the chemokine receptor CC-CKR-5. *Nature* 381: 667-73.
37. Berger EA, Doms RW, Fenyo EM, Korber BT, Littman DR, Moore JP, Sattentau QJ, Schuitemaker H, Sodroski J, Weiss RA. 1998. A new classification for HIV-1. *Nature* 391: 240.

38. Abbas W, Herbein G. 2012. Molecular Understanding of HIV-1 Latency. *Adv Virol* 2012: 574967
39. Tozser J. 2003. Stages of HIV replication and targets for therapeutic intervention. *Curr Top Med Chem* 3: 1447-57
40. Goff SP. 2007. Host factors exploited by retroviruses. *Nat Rev Microbiol* 5: 253-63
41. Barre-Sinoussi F, Ross AL, Delfraissy JF. 2013. Past, present and future: 30 years of HIV research. *Nat Rev Microbiol* 11: 877-83
42. Douek DC, Picker LJ, Koup RA. 2003. T cell dynamics in HIV-1 infection. *Annu Rev Immunol* 21: 265-304. Epub 2001 Dec 19.
43. Grossman Z, Meier-Schellersheim M, Paul WE, Picker LJ. 2006. Pathogenesis of HIV infection: what the virus spares is as important as what it destroys. *Nat Med.* 12: 289-95.
44. Doms RW. 2001. Chemokine receptors and HIV entry. *AIDS* 15 Suppl 1: S34-5
45. Scarlatti G, Tresoldi E, Bjorndal A, Fredriksson R, Colognesi C, Deng HK, Malnati MS, Plebani A, Siccardi AG, Littman DR, Fenyo EM, Lusso P. 1997. In vivo evolution of HIV-1 co-receptor usage and sensitivity to chemokine-mediated suppression. *Nat Med* 3: 1259-65.
46. Connor RI, Sheridan KE, Ceradini D, Choe S, Landau NR. 1997. Change in coreceptor use correlates with disease progression in HIV-1--infected individuals. *J Exp Med* 185: 621-8
47. Miller E, Bhardwaj N. 2013. Dendritic cell dysregulation during HIV-1 infection. *Immunol Rev* 254: 170-89
48. Marchetti G, Tincati C, Silvestri G. 2013. Microbial translocation in the pathogenesis of HIV infection and AIDS. *Clin Microbiol Rev* 26: 2-18
49. Sandler NG, Douek DC. 2012. Microbial translocation in HIV infection: causes, consequences and treatment opportunities. *Nat Rev Microbiol* 10: 655-66
50. Lamana A, Martin P, de la Fuente H, Martinez-Munoz L, Cruz-Adalia A, Ramirez-Huesca M, Escribano C, Gollmer K, Mellado M, Stein JV, Rodriguez-Fernandez JL, Sanchez-Madrid F, del Hoyo GM. 2011. CD69 modulates sphingosine-1-phosphate-induced migration of skin dendritic cells. *J Invest Dermatol* 131: 1503-12
51. Teijaro JR, Turner D, Pham Q, Wherry EJ, Lefrancois L, Farber DL. 2011. Cutting edge: Tissue-retentive lung memory CD4 T cells mediate optimal protection to respiratory virus infection. *J Immunol* 187: 5510-4
52. Veazey RS, Mansfield KG, Tham IC, Carville AC, Shvetz DE, Forand AE, Lackner AA. 2000. Dynamics of CCR5 expression by CD4(+) T cells in lymphoid tissues during simian immunodeficiency virus infection. *J Virol* 74: 11001-7
53. Kunkel EJ, Boisvert J, Murphy K, Vierra MA, Genovese MC, Wardlaw AJ, Greenberg HB, Hodge MR, Wu L, Butcher EC, Campbell JJ. 2002. Expression of the Chemokine Receptors CCR4, CCR5, and CXCR3 by Human Tissue-Infiltrating Lymphocytes. *Am J Pathol* 160: 347-55.
54. Biancotto A, Iglehart SJ, Vanpouille C, Condack CE, Lisco A, Ruecker E, Hirsch I, Margolis LB, Grivel JC. 2008. HIV-1 induced activation of CD4+ T cells creates new targets for HIV-1 infection in human lymphoid tissue ex vivo. *Blood* 111: 699-704
55. Chomont N, El-Far M, Ancuta P, Trautmann L, Procopio FA, Yassine-Diab B, Boucher G, Boulassel MR, Ghattas G, Brenchley JM, Schacker TW, Hill BJ, Douek DC, Routy JP, Haddad EK, Sekaly RP. 2009. HIV reservoir size and persistence are driven by T cell survival and homeostatic proliferation. *Nat Med* 15: 893-900

56. Douek DC, Roederer M, Koup RA. 2009. Emerging concepts in the immunopathogenesis of AIDS. *Annu Rev Med* 60: 471-84
57. Doitsh G, Cavrois M, Lassen KG, Zepeda O, Yang Z, Santiago ML, Hebbeler AM, Greene WC. 2010. Abortive HIV infection mediates CD4 T cell depletion and inflammation in human lymphoid tissue. *Cell* 143: 789-801
58. Cooper A, Garcia M, Petrovas C, Yamamoto T, Koup RA, Nabel GJ. 2013. HIV-1 causes CD4 cell death through DNA-dependent protein kinase during viral integration. *Nature* 498: 376-9
59. DaFonseca S, Niessl J, Pouvreau S, Wacleche VS, Gosselin A, Cleret-Buhot A, Bernard N, Tremblay C, Jenabian MA, Routy JP, Ancuta P. 2015. Impaired Th17 polarization of phenotypically naive CD4(+) T-cells during chronic HIV-1 infection and potential restoration with early ART. *Retrovirology* 12: 38
60. Brenchley JM, Silvestri G, Douek DC. 2010. Nonprogressive and progressive primate immunodeficiency lentivirus infections. *Immunity* 32: 737-42
61. Brenchley JM, Vinton C, Tabb B, Hao XP, Connick E, Paiardini M, Lifson JD, Silvestri G, Estes JD. 2012. Differential infection patterns of CD4+ T cells and lymphoid tissue viral burden distinguish progressive and nonprogressive lentiviral infections. *Blood* 120: 4172-81
62. Chahroudi A, Bosinger SE, Vanderford TH, Paiardini M, Silvestri G. 2012. Natural SIV hosts: showing AIDS the door. *Science* 335: 1188-93
63. Ancuta P, Kamat A, Kunstman KJ, Kim EY, Autissier P, Wurcel A, Zaman T, Stone D, Mefford M, Morgello S, Singer EJ, Wolinsky SM, Gabuzda D. 2008. Microbial translocation is associated with increased monocyte activation and dementia in AIDS patients. *PLoS ONE* 3: e2516
64. Ye P, Kirschner DE, Kourtis AP. 2004. The thymus during HIV disease: role in pathogenesis and in immune recovery. *Curr HIV Res* 2: 177-83
65. Dion ML, Poulin JF, Bordi R, Sylvestre M, Corsini R, Kettaf N, Dalloul A, Boulassel MR, Debre P, Routy JP, Grossman Z, Sekaly RP, Cheynier R. 2004. HIV infection rapidly induces and maintains a substantial suppression of thymocyte proliferation. *Immunity*. 21: 757-68.
66. Schacker TW, Nguyen PL, Beilman GJ, Wolinsky S, Larson M, Reilly C, Haase AT. 2002. Collagen deposition in HIV-1 infected lymphatic tissues and T cell homeostasis. *J Clin Invest* 110: 1133-9
67. van Grevenynghe J, Halwani R, Chomont N, Ancuta P, Peretz Y, Tanel A, Procopio FA, shi Y, Said EA, Haddad EK, Sekaly RP. 2008. Lymph node architecture collapse and consequent modulation of FOXO3a pathway on memory T- and B-cells during HIV infection. *Semin Immunol* 20: 196-203
68. Haase AT. 1999. Population biology of HIV-1 infection: viral and CD4+ T cell demographics and dynamics in lymphatic tissues. *Annu Rev Immunol* 17: 625-56
69. Lu W, Mehraj V, Vyboh K, Cao W, Li T, Routy JP. 2015. CD4:CD8 ratio as a frontier marker for clinical outcome, immune dysfunction and viral reservoir size in virologically suppressed HIV-positive patients. *J Int AIDS Soc* 18: 20052
70. Joseph SB, Swanstrom R, Kashuba AD, Cohen MS. 2015. Bottlenecks in HIV-1 transmission: insights from the study of founder viruses. *Nat Rev Microbiol* 13: 414-25
71. Chohan B, Lang D, Sagar M, Korber B, Lavreys L, Richardson B, Overbaugh J. 2005. Selection for human immunodeficiency virus type 1 envelope glycosylation variants with

shorter V1-V2 loop sequences occurs during transmission of certain genetic subtypes and may impact viral RNA levels. *J Virol* 79: 6528-31

72. Sagar M, Laeyendecker O, Lee S, Gamiel J, Wawer MJ, Gray RH, Serwadda D, Sewankambo NK, Shepherd JC, Toma J, Huang W, Quinn TC. 2009. Selection of HIV variants with signature genotypic characteristics during heterosexual transmission. *J Infect Dis* 199: 580-9
73. Ping LH, Joseph SB, Anderson JA, Abrahams MR, Salazar-Gonzalez JF, Kincer LP, Treurnicht FK, Arney L, Ojeda S, Zhang M, Keys J, Potter EL, Chu H, Moore P, Salazar MG, Iyer S, Jabara C, Kirchherr J, Mapanje C, Ngandu N, Seoighe C, Hoffman I, Gao F, Tang Y, Labranche C, Lee B, Saville A, Vermeulen M, Fiscus S, Morris L, Karim SA, Haynes BF, Shaw GM, Korber BT, Hahn BH, Cohen MS, Montefiori D, Williamson C, Swanstrom R, Study CAI, the Center for HIVAVIC. 2013. Comparison of viral Env proteins from acute and chronic infections with subtype C human immunodeficiency virus type 1 identifies differences in glycosylation and CCR5 utilization and suggests a new strategy for immunogen design. *J Virol* 87: 7218-33
74. Parrish NF, Gao F, Li H, Giorgi EE, Barbian HJ, Parrish EH, Zajic L, Iyer SS, Decker JM, Kumar A, Hora B, Berg A, Cai F, Hopper J, Denny TN, Ding H, Ochsenbauer C, Kappes JC, Galimidi RP, West AP, Jr., Bjorkman PJ, Wilen CB, Doms RW, O'Brien M, Bhardwaj N, Borrow P, Haynes BF, Muldoon M, Theiler JP, Korber B, Shaw GM, Hahn BH. 2013. Phenotypic properties of transmitted founder HIV-1. *Proc Natl Acad Sci U S A* 110: 6626-33
75. Malim MH, Bieniasz PD. 2012. HIV Restriction Factors and Mechanisms of Evasion. *Cold Spring Harb Perspect Med* 2: a006940
76. Simon V, Bloch N, Landau NR. 2015. Intrinsic host restrictions to HIV-1 and mechanisms of viral escape. *Nat Immunol* 16: 546-53
77. Sheehy AM, Gaddis NC, Choi JD, Malim MH. 2002. Isolation of a human gene that inhibits HIV-1 infection and is suppressed by the viral Vif protein. *Nature* 418: 646-50
78. Stremlau M, Owens CM, Perron MJ, Kiessling M, Autissier P, Sodroski J. 2004. The cytoplasmic body component TRIM5alpha restricts HIV-1 infection in Old World monkeys. *Nature* 427: 848-53
79. Van Damme N, Goff D, Katsura C, Jorgenson RL, Mitchell R, Johnson MC, Stephens EB, Guatelli J. 2008. The interferon-induced protein BST-2 restricts HIV-1 release and is downregulated from the cell surface by the viral Vpu protein. *Cell Host Microbe* 3: 245-52
80. Neil SJ, Zang T, Bieniasz PD. 2008. Tetherin inhibits retrovirus release and is antagonized by HIV-1 Vpu. *Nature* 451: 425-30
81. Laguette N, Sobhian B, Casartelli N, Ringeard M, Chable-Bessia C, Segeral E, Yatim A, Emiliani S, Schwartz O, Benkirane M. 2011. SAMHD1 is the dendritic- and myeloid-cell-specific HIV-1 restriction factor counteracted by Vpx. *Nature* 474: 654-7
82. Hrecka K, Hao C, Gierszewska M, Swanson SK, Kesik-Brodacka M, Srivastava S, Florens L, Washburn MP, Skowronski J. 2011. Vpx relieves inhibition of HIV-1 infection of macrophages mediated by the SAMHD1 protein. *Nature* 474: 658-61
83. Rosa A, Chande A, Ziglio S, De Sanctis V, Bertorelli R, Goh SL, McCauley SM, Nowosielska A, Antonarakis SE, Luban J, Santoni FA, Pizzato M. 2015. HIV-1 Nef promotes infection by excluding SERINC5 from virion incorporation. *Nature* 526: 212-7
84. Usami Y, Wu Y, Gottlinger HG. 2015. SERINC3 and SERINC5 restrict HIV-1 infectivity and are counteracted by Nef. *Nature* 526: 218-23

85. Jia X, Zhao Q, Xiong Y. 2015. HIV suppression by host restriction factors and viral immune evasion. *Curr Opin Struct Biol* 31: 106-14
86. Santa-Marta M, de Brito PM, Godinho-Santos A, Goncalves J. 2013. Host Factors and HIV-1 Replication: Clinical Evidence and Potential Therapeutic Approaches. *Front Immunol* 4: 343
87. Strebel K. 2013. HIV accessory proteins versus host restriction factors. *Curr Opin Virol* 3: 692-9
88. Newman EN, Holmes RK, Craig HM, Klein KC, Lingappa JR, Malim MH, Sheehy AM. 2005. Antiviral function of APOBEC3G can be dissociated from cytidine deaminase activity. *Curr Biol* 15: 166-70
89. Shindo K, Takaori-Kondo A, Kobayashi M, Abudu A, Fukunaga K, Uchiyama T. 2003. The enzymatic activity of CEM15/Apobec-3G is essential for the regulation of the infectivity of HIV-1 virion but not a sole determinant of its antiviral activity. *J Biol Chem* 278: 44412-6
90. Goila-Gaur R, Khan MA, Miyagi E, Strebel K. 2009. Differential sensitivity of "old" versus "new" APOBEC3G to human immunodeficiency virus type 1 vif. *J Virol* 83: 1156-60
91. Sayah DM, Sokolskaja E, Berthoux L, Luban J. 2004. Cyclophilin A retrotransposition into TRIM5 explains owl monkey resistance to HIV-1. *Nature* 430: 569-73
92. Pertel T, Hausmann S, Morger D, Zuger S, Guerra J, Lascano J, Reinhard C, Santoni FA, Uchil PD, Chatel L, Bisiaux A, Albert ML, Strambio-De-Castillia C, Mothes W, Pizzato M, Grutter MG, Luban J. 2011. TRIM5 is an innate immune sensor for the retrovirus capsid lattice. *Nature* 472: 361-5
93. Nisole S, Stoye JP, Saib A. 2005. TRIM family proteins: retroviral restriction and antiviral defence. *Nat Rev Microbiol* 3: 799-808
94. Uchil PD, Pawliczek T, Reynolds TD, Ding S, Hinz A, Munro JB, Huang F, Floyd RW, Yang H, Hamilton WL, Bewersdorf J, Xiong Y, Calderwood DA, Mothes W. 2014. TRIM15 is a focal adhesion protein that regulates focal adhesion disassembly. *J Cell Sci* 127: 3928-42
95. Miyakawa K, Ryo A, Murakami T, Ohba K, Yamaoka S, Fukuda M, Guatelli J, Yamamoto N. 2009. BCA2/Rabring7 promotes tetherin-dependent HIV-1 restriction. *PLoS Pathog* 5: e1000700
96. Galao RP, Le Tortorec A, Pickering S, Kueck T, Neil SJ. 2012. Innate sensing of HIV-1 assembly by Tetherin induces NFkappaB-dependent proinflammatory responses. *Cell Host Microbe* 12: 633-44
97. Tokarev A, Suarez M, Kwan W, Fitzpatrick K, Singh R, Guatelli J. 2013. Stimulation of NF-kappaB activity by the HIV restriction factor BST2. *J Virol* 87: 2046-57
98. Douglas JL, Viswanathan K, McCarroll MN, Gustin JK, Fruh K, Moses AV. 2009. Vpu directs the degradation of the human immunodeficiency virus restriction factor BST-2/Tetherin via a {beta}TrCP-dependent mechanism. *J Virol* 83: 7931-47
99. Dube M, Roy BB, Guiot-Guillain P, Binette J, Mercier J, Chiasson A, Cohen EA. 2010. Antagonism of tetherin restriction of HIV-1 release by Vpu involves binding and sequestration of the restriction factor in a perinuclear compartment. *PLoS Pathog* 6: e1000856
100. Goffinet C, Allespach I, Homann S, Tervo HM, Habermann A, Rupp D, Oberbremer L, Kern C, Tibroni N, Welsch S, Krijnse-Locker J, Banting G, Krausslich HG, Fackler OT,

Keppler OT. 2009. HIV-1 antagonism of CD317 is species specific and involves Vpu-mediated proteasomal degradation of the restriction factor. *Cell Host Microbe* 5: 285-97
101. Iwabu Y, Fujita H, Kinomoto M, Kaneko K, Ishizaka Y, Tanaka Y, Sata T, Tokunaga K. 2009. HIV-1 accessory protein Vpu internalizes cell-surface BST-2/tetherin through transmembrane interactions leading to lysosomes. *J Biol Chem* 284: 35060-72
102. Mitchell RS, Katsura C, Skasko MA, Fitzpatrick K, Lau D, Ruiz A, Stephens EB, Margottin-Goguet F, Benarous R, Guatelli JC. 2009. Vpu antagonizes BST-2-mediated restriction of HIV-1 release via beta-TrCP and endo-lysosomal trafficking. *PLoS Pathog* 5: e1000450
103. Skasko M, Wang Y, Tian Y, Tokarev A, Munguia J, Ruiz A, Stephens EB, Opella SJ, Guatelli J. 2012. HIV-1 Vpu protein antagonizes innate restriction factor BST-2 via lipid-embedded helix-helix interactions. *J Biol Chem* 287: 58-67
104. Hofmann H, Logue EC, Bloch N, Daddacha W, Polsky SB, Schultz ML, Kim B, Landau NR. 2012. The Vpx lentiviral accessory protein targets SAMHD1 for degradation in the nucleus. *J Virol* 86: 12552-60
105. Baldauf HM, Pan X, Erikson E, Schmidt S, Daddacha W, Burggraf M, Schenkova K, Ambiel I, Wabnitz G, Gramberg T, Panitz S, Flory E, Landau NR, Sertel S, Rutsch F, Lasitschka F, Kim B, Konig R, Fackler OT, Keppler OT. 2012. SAMHD1 restricts HIV-1 infection in resting CD4(+) T cells. *Nat Med* 18: 1682-7
106. Kyei GB, Cheng X, Ramani R, Ratner L. 2015. Cyclin L2 is a critical HIV dependency factor in macrophages that controls SAMHD1 abundance. *Cell Host Microbe* 17: 98-106
107. Ruffin N, Brezar V, Ayinde D, Lefebvre C, Schulze Zur Wiesch J, van Lunzen J, Bockhorn M, Schwartz O, Hocini H, Lelievre JD, Banchereau J, Levy Y, Seddiki N. 2015. Low SAMHD1 expression following T-cell activation and proliferation renders CD4+ T cells susceptible to HIV-1. *AIDS* 29: 519-30
108. Goff SP. 2008. Knockdown screens to knockout HIV-1. *Cell* 135: 417-20
109. Brass AL, Dykxhoorn DM, Benita Y, Yan N, Engelman A, Xavier RJ, Lieberman J, Elledge SJ. 2008. Identification of host proteins required for HIV infection through a functional genomic screen. *Science* 319: 921-6
110. Hug P, Lin HM, Korte T, Xiao X, Dimitrov DS, Wang JM, Puri A, Blumenthal R. 2000. Glycosphingolipids promote entry of a broad range of human immunodeficiency virus type 1 isolates into cell lines expressing CD4, CXCR4, and/or CCR5. *J Virol* 74: 6377-85
111. Puri A, Rawat SS, Lin HM, Finnegan CM, Mikovits J, Ruscetti FW, Blumenthal R. 2004. An inhibitor of glycosphingolipid metabolism blocks HIV-1 infection of primary T-cells. *AIDS* 18: 849-58
112. Nehete PN, Vela EM, Hossain MM, Sarkar AK, Yahi N, Fantini J, Sastry KJ. 2002. A post-CD4-binding step involving interaction of the V3 region of viral gp120 with host cell surface glycosphingolipids is common to entry and infection by diverse HIV-1 strains. *Antiviral Res* 56: 233-51
113. Konig R, Zhou Y, Elleder D, Diamond TL, Bonamy GM, Irelan JT, Chiang CY, Tu BP, De Jesus PD, Lilley CE, Seidel S, Opaluch AM, Caldwell JS, Weitzman MD, Kuhen KL, Bandyopadhyay S, Ideker T, Orth AP, Miraglia LJ, Bushman FD, Young JA, Chanda SK. 2008. Global analysis of host-pathogen interactions that regulate early-stage HIV-1 replication. *Cell* 135: 49-60
114. Sobhian B, Laguette N, Yatim A, Nakamura M, Levy Y, Kiernan R, Benkirane M. 2010. HIV-1 Tat assembles a multifunctional transcription elongation complex and stably associates with the 7SK snRNP. *Mol Cell* 38: 439-51

115. Morita E, Sundquist WI. 2004. Retrovirus budding. *Annu Rev Cell Dev Biol* 20: 395-425
116. Murray JL, Mavrakis M, McDonald NJ, Yilla M, Sheng J, Bellini WJ, Zhao L, Le Doux JM, Shaw MW, Luo CC, Lippincott-Schwartz J, Sanchez A, Rubin DH, Hodge TW. 2005. Rab9 GTPase is required for replication of human immunodeficiency virus type 1, filoviruses, and measles virus. *J Virol* 79: 11742-51
117. Archin NM, Sung JM, Garrido C, Soriano-Sarabia N, Margolis DM. 2014. Eradicating HIV-1 infection: seeking to clear a persistent pathogen. *Nat Rev Microbiol* 12: 750-64
118. Chun TW, Engel D, Berrey MM, Shea T, Corey L, Fauci AS. 1998. Early establishment of a pool of latently infected, resting CD4(+) T cells during primary HIV-1 infection. *Proc Natl Acad Sci U S A* 95: 8869-73.
119. Thompson KA, Varrone JJ, Jankovic-Karasoulos T, Wesselingh SL, McLean CA. 2009. Cell-specific temporal infection of the brain in a simian immunodeficiency virus model of human immunodeficiency virus encephalitis. *J Neurovirol* 15: 300-11
120. International ASSWGoHIVC, Deeks SG, Autran B, Berkhout B, Benkirane M, Cairns S, Chomont N, Chun TW, Churchill M, Di Mascio M, Katlama C, Lafeuillade A, Landay A, Lederman M, Lewin SR, Maldarelli F, Margolis D, Markowitz M, Martinez-Picado J, Mullins JI, Mellors J, Moreno S, O'Doherty U, Palmer S, Penicaud MC, Peterlin M, Poli G, Routy JP, Rouzioux C, Silvestri G, Stevenson M, Telenti A, Van Lint C, Verdin E, Woolfrey A, Zaia J, Barre-Sinoussi F. 2012. Towards an HIV cure: a global scientific strategy. *Nat Rev Immunol* 12: 607-14
121. Klatt NR, Chomont N, Douek DC, Deeks SG. 2013. Immune activation and HIV persistence: implications for curative approaches to HIV infection. *Immunol Rev* 254: 326-42
122. Chun TW, Nickle DC, Justement JS, Large D, Semerjian A, Curlin ME, O'Shea MA, Hallahan CW, Daucher M, Ward DJ, Moir S, Mullins JI, Kovacs C, Fauci AS. 2005. HIV-infected individuals receiving effective antiviral therapy for extended periods of time continually replenish their viral reservoir. *J Clin Invest* 115: 3250-5
123. Douek DC, Brenchley JM, Betts MR, Ambrozak DR, Hill BJ, Okamoto Y, Casazza JP, Kuruppu J, Kunstman K, Wolinsky S, Grossman Z, Dybul M, Oxenius A, Price DA, Connors M, Koup RA. 2002. HIV preferentially infects HIV-specific CD4+ T cells. *Nature* 417: 95-8.
124. Naeger DM, Martin JN, Sinclair E, Hunt PW, Bangsberg DR, Hecht F, Hsue P, McCune JM, Deeks SG. 2010. Cytomegalovirus-specific T cells persist at very high levels during long-term antiretroviral treatment of HIV disease. *PLoS One* 5: e8886
125. Casazza JP, Brenchley JM, Hill BJ, Ayana R, Ambrozak D, Roederer M, Douek DC, Betts MR, Koup RA. 2009. Autocrine production of beta-chemokines protects CMV-Specific CD4 T cells from HIV infection. *PLoS Pathog* 5: e1000646
126. Gianella S, Anderson CM, Vargas MV, Richman DD, Little SJ, Morris SR, Smith DM. 2013. Cytomegalovirus DNA in semen and blood is associated with higher levels of proviral HIV DNA. *J Infect Dis* 207: 898-902
127. Chun TW, Engel D, Mizell SB, Ehler LA, Fauci AS. 1998. Induction of HIV-1 replication in latently infected CD4+ T cells using a combination of cytokines. *J Exp Med* 188: 83-91.
128. Saleh S, Wightman F, Ramanayake S, Alexander M, Kumar N, Khoury G, Pereira C, Purcell D, Cameron PU, Lewin SR. 2011. Expression and reactivation of HIV in a chemokine induced model of HIV latency in primary resting CD4+ T cells. *Retrovirology* 8: 80

129. Iannello A, Boulassel MR, Samarani S, Tremblay C, Toma E, Routy JP, Ahmad A. 2010. HIV-1 causes an imbalance in the production of interleukin-18 and its natural antagonist in HIV-infected individuals: implications for enhanced viral replication. *J Infect Dis* 201: 608-17
130. Cameron PU, Saleh S, Sallmann G, Solomon A, Wightman F, Evans VA, Boucher G, Haddad EK, Sekaly RP, Harman AN, Anderson JL, Jones KL, Mak J, Cunningham AL, Jaworowski A, Lewin SR. 2010. Establishment of HIV-1 latency in resting CD4+ T cells depends on chemokine-induced changes in the actin cytoskeleton. *Proc Natl Acad Sci U S A* 107: 16934-9
131. Saleh S, Solomon A, Wightman F, Xhilaga M, Cameron PU, Lewin SR. 2007. CCR7 ligands CCL19 and CCL21 increase permissiveness of resting memory CD4+ T cells to HIV-1 infection: a novel model of HIV-1 latency. *Blood* 110: 4161-4
132. Vandergeeten C, Fromentin R, Chomont N. 2012. The role of cytokines in the establishment, persistence and eradication of the HIV reservoir. *Cytokine Growth Factor Rev* 23: 143-9
133. Hatano H, Jain V, Hunt PW, Lee TH, Sinclair E, Do TD, Hoh R, Martin JN, McCune JM, Hecht F, Busch MP, Deeks SG. 2013. Cell-based measures of viral persistence are associated with immune activation and programmed cell death protein 1 (PD-1)-expressing CD4+ T cells. *J Infect Dis* 208: 50-6
134. Petrovas C, Yamamoto T, Gerner MY, Boswell KL, Wloka K, Smith EC, Ambrozak DR, Sandler NG, Timmer KJ, Sun X, Pan L, Poholek A, Rao SS, Brenchley JM, Alam SM, Tomaras GD, Roederer M, Douek DC, Seder RA, Germain RN, Haddad EK, Koup RA. 2012. CD4 T follicular helper cell dynamics during SIV infection. *J Clin Invest* 122: 3281-94
135. Perreau M, Savoye AL, De Crignis E, Corpataux JM, Cubas R, Haddad EK, De Leval L, Graziosi C, Pantaleo G. 2013. Follicular helper T cells serve as the major CD4 T cell compartment for HIV-1 infection, replication, and production. *J Exp Med* 210: 143-56
136. Banga R, Procopio FA, Noto A, Pollakis G, Cavassini M, Ohmiti K, Corpataux JM, de Leval L, Pantaleo G, Perreau M. 2016. PD-1+ and follicular helper T cells are responsible for persistent HIV-1 transcription in treated aviremic individuals. *Nat Med*
137. Riou C, Yassine-Diab B, Van grevenynghe J, Somogyi R, Greller LD, Gagnon D, Gimmig S, Wilkinson P, Shi Y, Cameron MJ, Campos-Gonzalez R, Balderas RS, Kelvin D, Sekaly RP, Haddad EK. 2007. Convergence of TCR and cytokine signaling leads to FOXO3a phosphorylation and drives the survival of CD4+ central memory T cells. *J Exp Med* 204: 79-91
138. Shan L, Siliciano RF. 2013. From reactivation of latent HIV-1 to elimination of the latent reservoir: the presence of multiple barriers to viral eradication. *Bioessays* 35: 544-52
139. Stevenson M. 2015. Role of myeloid cells in HIV-1-host interplay. *J Neurovirol* 21: 242-8
140. Crowe SM. 2006. Macrophages and residual HIV infection. *Curr Opin HIV AIDS* 1: 129-33
141. Tan J, Sattentau QJ. 2013. The HIV-1-containing macrophage compartment: a perfect cellular niche? *Trends Microbiol* 21: 405-12
142. Elion GB. 1989. The purine path to chemotherapy. *Science* 244: 41-7
143. Whitley RJ, Gnann JW, Jr. 1992. Acyclovir: a decade later. *N Engl J Med* 327: 782-9
144. Mitsuya H, Weinhold KJ, Furman PA, St Clair MH, Lehrman SN, Gallo RC, Bolognesi D, Barry DW, Broder S. 1985. 3'-Azido-3'-deoxythymidine (BW A509U): an antiviral

agent that inhibits the infectivity and cytopathic effect of human T-lymphotropic virus type III/lymphadenopathy-associated virus in vitro. *Proc Natl Acad Sci U S A* 82: 7096-100

145. Mitsuya H, Broder S. 1986. Inhibition of the in vitro infectivity and cytopathic effect of human T-lymphotrophic virus type III/lymphadenopathy-associated virus (HTLV-III/LAV) by 2',3'-dideoxynucleosides. *Proc Natl Acad Sci U S A* 83: 1911-5
146. Horwitz JP, Chua J, Noel M. 1964. The Monomesylates of 1-(2'-Deoxy-β-D-lyxofuranosyl)thymine. *J. Org. Chem.* 29: 2076–8
147. Broder S. 2010. The development of antiretroviral therapy and its impact on the HIV-1/AIDS pandemic. *Antiviral Res* 85: 1-18
148. Lange JM, Ananworanich J. 2014. The discovery and development of antiretroviral agents. *Antivir Ther* 19 Suppl 3: 5-14
149. Larder BA, Darby G, Richman DD. 1989. HIV with reduced sensitivity to zidovudine (AZT) isolated during prolonged therapy. *Science* 243: 1731-4
150. Dolin R, Masur H, Saag MS. 2003. *AIDS therapy*. New York: Churchill Livingstone. xx, 1024 p. pp.
151. Hammer SM, Squires KE, Hughes MD, Grimes JM, Demeter LM, Currier JS, Eron JJ, Jr., Feinberg JE, Balfour HH, Jr., Deyton LR, Chodakewitz JA, Fischl MA. 1997. A controlled trial of two nucleoside analogues plus indinavir in persons with human immunodeficiency virus infection and CD4 cell counts of 200 per cubic millimeter or less. AIDS Clinical Trials Group 320 Study Team. *N Engl J Med* 337: 725-33
152. Montaner JS, Reiss P, Cooper D, Vella S, Harris M, Conway B, Wainberg MA, Smith D, Robinson P, Hall D, Myers M, Lange JM. 1998. A randomized, double-blind trial comparing combinations of nevirapine, didanosine, and zidovudine for HIV-infected patients: the INCAS Trial. Italy, The Netherlands, Canada and Australia Study. *JAMA* 279: 930-7
153. Perelson AS, Neumann AU, Markowitz M, Leonard JM, Ho DD. 1996. HIV-1 dynamics in vivo: virion clearance rate, infected cell life-span, and viral generation time. *Science* 271: 1582-6
154. Palella FJ, Jr., Delaney KM, Moorman AC, Loveless MO, Fuhrer J, Satten GA, Aschman DJ, Holmberg SD. 1998. Declining morbidity and mortality among patients with advanced human immunodeficiency virus infection. HIV Outpatient Study Investigators. *N Engl J Med.* 338: 853-60.
155. Ho DD, Neumann AU, Perelson AS, Chen W, Leonard JM, Markowitz M. 1995. Rapid turnover of plasma virions and CD4 lymphocytes in HIV-1 infection. *Nature* 373: 123-6
156. Lalezari JP, Henry K, O'Hearn M, Montaner JS, Piliero PJ, Trottier B, Walmsley S, Cohen C, Kuritzkes DR, Eron JJ, Jr., Chung J, DeMasi R, Donatacci L, Drobnes C, Delehanty J, Salgo M, Group TS. 2003. Enfuvirtide, an HIV-1 fusion inhibitor, for drug-resistant HIV infection in North and South America. *N Engl J Med* 348: 2175-85
157. Lazzarin A, Clotet B, Cooper D, Reynes J, Arasteh K, Nelson M, Katlama C, Stellbrink HJ, Delfraissy JF, Lange J, Huson L, DeMasi R, Wat C, Delehanty J, Drobnes C, Salgo M, Group TS. 2003. Efficacy of enfuvirtide in patients infected with drug-resistant HIV-1 in Europe and Australia. *N Engl J Med* 348: 2186-95
158. Gulick RM, Lalezari J, Goodrich J, Clumeck N, DeJesus E, Horban A, Nadler J, Clotet B, Karlsson A, Wohlfeiler M, Montana JB, McHale M, Sullivan J, Ridgway C, Felstead S, Dunne MW, van der Ryst E, Mayer H, Teams MS. 2008. Maraviroc for previously treated patients with R5 HIV-1 infection. *N Engl J Med* 359: 1429-41

159. Fatkenheuer G, Nelson M, Lazzarin A, Konourina I, Hoepelman AI, Lampiris H, Hirschel B, Tebas P, Raffi F, Trottier B, Bellos N, Saag M, Cooper DA, Westby M, Tawadrous M, Sullivan JF, Ridgway C, Dunne MW, Felstead S, Mayer H, van der Ryst E, Motivate, Teams MS. 2008. Subgroup analyses of maraviroc in previously treated R5 HIV-1 infection. *N Engl J Med* 359: 1442-55
160. Steigbigel RT, Cooper DA, Kumar PN, Eron JE, Schechter M, Markowitz M, Loutfy MR, Lennox JL, Gatell JM, Rockstroh JK, Katlama C, Yeni P, Lazzarin A, Clotet B, Zhao J, Chen J, Ryan DM, Rhodes RR, Killar JA, Gilde LR, Strohmaier KM, Meibohm AR, Miller MD, Hazuda DJ, Nessly ML, DiNubile MJ, Isaacs RD, Nguyen BY, Teppler H, Teams BS. 2008. Raltegravir with optimized background therapy for resistant HIV-1 infection. *N Engl J Med* 359: 339-54
161. Cooper DA, Steigbigel RT, Gatell JM, Rockstroh JK, Katlama C, Yeni P, Lazzarin A, Clotet B, Kumar PN, Eron JE, Schechter M, Markowitz M, Loutfy MR, Lennox JL, Zhao J, Chen J, Ryan DM, Rhodes RR, Killar JA, Gilde LR, Strohmaier KM, Meibohm AR, Miller MD, Hazuda DJ, Nessly ML, DiNubile MJ, Isaacs RD, Teppler H, Nguyen BY, Teams BS. 2008. Subgroup and resistance analyses of raltegravir for resistant HIV-1 infection. *N Engl J Med* 359: 355-65
162. Cahn P, Pozniak AL, Mingrone H, Shuldyakov A, Brites C, Andrade-Villanueva JF, Richmond G, Buendia CB, Fourie J, Ramgopal M, Hagins D, Felizarta F, Madruga J, Reuter T, Newman T, Small CB, Lombaard J, Grinsztejn B, Dorey D, Underwood M, Griffith S, Min S, extended SST. 2013. Dolutegravir versus raltegravir in antiretroviral-experienced, integrase-inhibitor-naive adults with HIV: week 48 results from the randomised, double-blind, non-inferiority SAILING study. *Lancet* 382: 700-8
163. Raffi F, Jaeger H, Quiros-Roldan E, Albrecht H, Belonosova E, Gatell JM, Baril JG, Domingo P, Brennan C, Almond S, Min S, extended S-SG. 2013. Once-daily dolutegravir versus twice-daily raltegravir in antiretroviral-naive adults with HIV-1 infection (SPRING-2 study): 96 week results from a randomised, double-blind, non-inferiority trial. *Lancet Infect Dis* 13: 927-35
164. Maartens G, Celum C, Lewin SR. 2014. HIV infection: epidemiology, pathogenesis, treatment, and prevention. *Lancet* 384: 258-71
165. Wainberg MA, Albert J. 2010. Can the further clinical development of bevirimat be justified? *AIDS* 24: 773-4
166. Gallant JE, Koenig E, Andrade-Villanueva J, Chetchotisakd P, DeJesus E, Antunes F, Arasteh K, Moyle G, Rizzardini G, Fehr J, Liu Y, Zhong L, Callebaut C, Szwarcberg J, Rhee MS, Cheng AK. 2013. Cobicistat versus ritonavir as a pharmacoenhancer of atazanavir plus emtricitabine/tenofovir disoproxil fumarate in treatment-naive HIV type 1-infected patients: week 48 results. *J Infect Dis* 208: 32-9
167. Baeten JM, Grant R. 2013. Use of antiretrovirals for HIV prevention: what do we know and what don't we know? *Curr HIV/AIDS Rep* 10: 142-51
168. Price RW, Brew B, Sidtis J, Rosenblum M, Scheck AC, Cleary P. 1988. The brain in AIDS: central nervous system HIV-1 infection and AIDS dementia complex. *Science* 239: 586-92
169. Gorry PR, Howard JL, Churchill MJ, Anderson JL, Cunningham A, Adrian D, McPhee DA, Purcell DF. 1999. Diminished production of human immunodeficiency virus type 1 in astrocytes results from inefficient translation of gag, env, and nef mRNAs despite efficient expression of Tat and Rev. *J Virol* 73: 352-61

170. Ene L, Duiculescu D, Ruta SM. 2011. How much do antiretroviral drugs penetrate into the central nervous system? *J Med Life* 4: 432-9
171. Phillips AN, Neaton J, Lundgren JD. 2008. The role of HIV in serious diseases other than AIDS. *AIDS* 22: 2409-18
172. Zagury D, Leonard R, Fouchard M, Reveil B, Bernard J, Ittele D, Cattan A, Zirimwabagabo L, Kalumbu M, Justin W, et al. 1987. Immunization against AIDS in humans. *Nature* 326: 249-50
173. IAVI. 2014. Clinical trials database.
174. Wang HB, Mo QH, Yang Z. 2015. HIV vaccine research: the challenge and the way forward. *J Immunol Res* 2015: 503978
175. Miedema F. 2008. A brief history of HIV vaccine research: stepping back to the drawing board? *AIDS* 22: 1699-703
176. Gilbert PB, Ackers ML, Berman PW, Francis DP, Popovic V, Hu DJ, Heyward WL, Sinangil F, Shepherd BE, Gurwith M. 2005. HIV-1 virologic and immunologic progression and initiation of antiretroviral therapy among HIV-1-infected subjects in a trial of the efficacy of recombinant glycoprotein 120 vaccine. *J Infect Dis* 192: 974-83
177. Pitisuttithum P, Gilbert P, Gurwith M, Heyward W, Martin M, van Griensven F, Hu D, Tappero JW, Choopanya K, Bangkok Vaccine Evaluation G. 2006. Randomized, double-blind, placebo-controlled efficacy trial of a bivalent recombinant glycoprotein 120 HIV-1 vaccine among injection drug users in Bangkok, Thailand. *J Infect Dis* 194: 1661-71
178. Hirsch VM, Goldstein S, Hynes NA, Elkins WR, London WT, Zack PM, Montefiori D, Johnson PR. 1994. Prolonged clinical latency and survival of macaques given a whole inactivated simian immunodeficiency virus vaccine. *J Infect Dis* 170: 51-9
179. Shiver JW, Fu TM, Chen L, Casimiro DR, Davies ME, Evans RK, Zhang ZQ, Simon AJ, Trigona WL, Dubey SA, Huang L, Harris VA, Long RS, Liang X, Handt L, Schleif WA, Zhu L, Freed DC, Persaud NV, Guan L, Punt KS, Tang A, Chen M, Wilson KA, Collins KB, Heidecker GJ, Fernandez VR, Perry HC, Joyce JG, Grimm KM, Cook JC, Keller PM, Kresock DS, Mach H, Troutman RD, Isopi LA, Williams DM, Xu Z, Bohannon KE, Volkin DB, Montefiori DC, Miura A, Krivulka GR, Lifton MA, Kuroda MJ, Schmitz JE, Letvin NL, Caulfield MJ, Bett AJ, Youil R, Kaslow DC, Emini EA. 2002. Replication-incompetent adenoviral vaccine vector elicits effective anti-immunodeficiency-virus immunity. *Nature* 415: 331-5
180. Ensoli B, Cafaro A, Monini P, Marcotullio S, Ensoli F. 2014. Challenges in HIV Vaccine Research for Treatment and Prevention. *Front Immunol* 5: 417
181. Casimiro DR, Wang F, Schleif WA, Liang X, Zhang ZQ, Tobery TW, Davies ME, McDermott AB, O'Connor DH, Fridman A, Bagchi A, Tussey LG, Bett AJ, Finnefrock AC, Fu TM, Tang A, Wilson KA, Chen M, Perry HC, Heidecker GJ, Freed DC, Carella A, Punt KS, Sykes KJ, Huang L, Ausensi VI, Bachinsky M, Sadasivan-Nair U, Watkins DI, Emini EA, Shiver JW. 2005. Attenuation of simian immunodeficiency virus SIVmac239 infection by prophylactic immunization with dna and recombinant adenoviral vaccine vectors expressing Gag. *J Virol* 79: 15547-55
182. Shiver JW, Emini EA. 2004. Recent advances in the development of HIV-1 vaccines using replication-incompetent adenovirus vectors. *Annu Rev Med* 55: 355-72
183. Fauci AS. 2007. The Release of New Data from the HVTN 502 (STEP) HIV Vaccine Study.
184. Sekaly RP. 2008. The failed HIV Merck vaccine study: a step back or a launching point for future vaccine development? *J Exp Med* 205: 7-12

185. Excler JL, Robb ML, Kim JH. 2014. HIV-1 vaccines: challenges and new perspectives. *Hum Vaccin Immunother* 10: 1734-46
186. Johnson DC, McFarland EJ, Muresan P, Fenton T, McNamara J, Read JS, Hawkins E, Bouquin PL, Estep SG, Tomaras GD, Vincent CA, Rathore M, Melvin AJ, Gurunathan S, Lambert J. 2005. Safety and immunogenicity of an HIV-1 recombinant canarypox vaccine in newborns and infants of HIV-1-infected women. *J Infect Dis* 192: 2129-33
187. Rerks-Ngarm S, Pitisuttithum P, Nitayaphan S, Kaewkungwal J, Chiu J, Paris R, Premsri N, Namwat C, de Souza M, Adams E, Benenson M, Gurunathan S, Tartaglia J, McNeil JG, Francis DP, Stablein D, Birx DL, Chunsuttiwat S, Khamboonruang C, Thongcharoen P, Robb ML, Michael NL, Kunasol P, Kim JH, Investigators M-T. 2009. Vaccination with ALVAC and AIDSVAX to prevent HIV-1 infection in Thailand. *N Engl J Med* 361: 2209-20
188. Haynes BF, Gilbert PB, McElrath MJ, Zolla-Pazner S, Tomaras GD, Alam SM, Evans DT, Montefiori DC, Karnasuta C, Sutthent R, Liao HX, DeVico AL, Lewis GK, Williams C, Pinter A, Fong Y, Janes H, DeCamp A, Huang Y, Rao M, Billings E, Karasavvas N, Robb ML, Ngauy V, de Souza MS, Paris R, Ferrari G, Bailer RT, Soderberg KA, Andrews C, Berman PW, Frahm N, De Rosa SC, Alpert MD, Yates NL, Shen X, Koup RA, Pitisuttithum P, Kaewkungwal J, Nitayaphan S, Rerks-Ngarm S, Michael NL, Kim JH. 2012. Immune-correlates analysis of an HIV-1 vaccine efficacy trial. *N Engl J Med* 366: 1275-86
189. Gaschen B, Taylor J, Yusim K, Foley B, Gao F, Lang D, Novitsky V, Haynes B, Hahn BH, Bhattacharya T, Korber B. 2002. Diversity considerations in HIV-1 vaccine selection. *Science* 296: 2354-60
190. Walker BD, Korber BT. 2001. Immune control of HIV: the obstacles of HLA and viral diversity. *Nat Immunol* 2: 473-5
191. Kwong PD, Wyatt R, Robinson J, Sweet RW, Sodroski J, Hendrickson WA. 1998. Structure of an HIV gp120 envelope glycoprotein in complex with the CD4 receptor and a neutralizing human antibody. *Nature* 393: 648-59
192. Wyatt R, Kwong PD, Desjardins E, Sweet RW, Robinson J, Hendrickson WA, Sodroski JG. 1998. The antigenic structure of the HIV gp120 envelope glycoprotein. *Nature* 393: 705-11
193. Wei X, Decker JM, Wang S, Hui H, Kappes JC, Wu X, Salazar-Gonzalez JF, Salazar MG, Kilby JM, Saag MS, Komarova NL, Nowak MA, Hahn BH, Kwong PD, Shaw GM. 2003. Antibody neutralization and escape by HIV-1. *Nature* 422: 307-12
194. Hutter G, Nowak D, Mossner M, Ganepola S, Mussig A, Allers K, Schneider T, Hofmann J, Kucherer C, Blau O, Blau IW, Hofmann WK, Thiel E. 2009. Long-term control of HIV by CCR5 Delta32/Delta32 stem-cell transplantation. *N Engl J Med* 360: 692-8
195. Liu R, Paxton WA, Choe S, Ceradini D, Martin SR, Horuk R, MacDonald ME, Stuhlmann H, Koup RA, Landau NR. 1996. Homozygous defect in HIV-1 coreceptor accounts for resistance of some multiply-exposed individuals to HIV-1 infection. *Cell* 86: 367-77.
196. Hayden EC. 2013. Hopes of HIV cure in 'Boston patients' dashed. In *Nature*: Nature Publishing Group
197. Varela-Rohena A, Molloy PE, Dunn SM, Li Y, Suhoski MM, Carroll RG, Milicic A, Mahon T, Sutton DH, Laugel B, Moysey R, Cameron BJ, Vuidepot A, Purbhoo MA, Cole DK, Phillips RE, June CH, Jakobsen BK, Sewell AK, Riley JL. 2008. Control of HIV-1 immune escape by CD8 T cells expressing enhanced T-cell receptor. *Nat Med* 14: 1390-5

198. Archin NM, Margolis DM. 2014. Emerging strategies to deplete the HIV reservoir. *Curr Opin Infect Dis* 27: 29-35
199. Shan L, Deng K, Shroff NS, Durand CM, Rabi SA, Yang HC, Zhang H, Margolick JB, Blankson JN, Siliciano RF. 2012. Stimulation of HIV-1-specific cytolytic T lymphocytes facilitates elimination of latent viral reservoir after virus reactivation. *Immunity* 36: 491-501
200. Archin NM, Liberty AL, Kashuba AD, Choudhary SK, Kuruc JD, Crooks AM, Parker DC, Anderson EM, Kearney MF, Strain MC, Richman DD, Hudgens MG, Bosch RJ, Coffin JM, Eron JJ, Hazuda DJ, Margolis DM. 2012. Administration of vorinostat disrupts HIV-1 latency in patients on antiretroviral therapy. *Nature* 487: 482-5
201. Boehm D, Conrad RJ, Ott M. 2013. Bromodomain proteins in HIV infection. *Viruses* 5: 1571-86
202. Bartholomeeusen K, Xiang Y, Fujinaga K, Peterlin BM. 2012. Bromodomain and extra-terminal (BET) bromodomain inhibition activate transcription via transient release of positive transcription elongation factor b (P-TEFb) from 7SK small nuclear ribonucleoprotein. *J Biol Chem* 287: 36609-16
203. Boehm D, Calvanese V, Dar RD, Xing S, Schroeder S, Martins L, Aull K, Li PC, Planelles V, Bradner JE, Zhou MM, Siliciano RF, Weinberger L, Verdin E, Ott M. 2013. BET bromodomain-targeting compounds reactivate HIV from latency via a Tat-independent mechanism. *Cell Cycle* 12: 452-62
204. Zhu J, Gaiha GD, John SP, Pertel T, Chin CR, Gao G, Qu H, Walker BD, Elledge SJ, Brass AL. 2012. Reactivation of latent HIV-1 by inhibition of BRD4. *Cell Rep* 2: 807-16
205. Li Z, Guo J, Wu Y, Zhou Q. 2013. The BET bromodomain inhibitor JQ1 activates HIV latency through antagonizing Brd4 inhibition of Tat-transactivation. *Nucleic Acids Res* 41: 277-87
206. McKernan LN, Momjian D, Kulkosky J. 2012. Protein Kinase C: One Pathway towards the Eradication of Latent HIV-1 Reservoirs. *Adv Virol* 2012: 805347
207. Mousseau G, Kessing CF, Fromentin R, Trautmann L, Chomont N, Valente ST. 2015. The Tat Inhibitor Didehydro-Cortistatin A Prevents HIV-1 Reactivation from Latency. *MBio* 6: e00465
208. van der Meer JW, Netea MG. 2013. A salty taste to autoimmunity. *N Engl J Med* 368: 2520-1
209. Basu R, Hatton RD, Weaver CT. 2013. The Th17 family: flexibility follows function. *Immunol Rev* 252: 89-103
210. Gaffen SL, Jain R, Garg AV, Cua DJ. 2014. The IL-23-IL-17 immune axis: from mechanisms to therapeutic testing. *Nat Rev Immunol* 14: 585-600
211. Basso AS, Cheroutre H, Mucida D. 2009. More stories on Th17 cells. *Cell Res* 19: 399-411
212. Parish CR. 1971. Immune response to chemically modified flagellin. I. Induction of antibody tolerance to flagellin by acetoacetylated derivatives of the protein. *J Exp Med* 134: 1-20
213. Parish CR. 1971. Immune response to chemically modified flagellin. II. Evidence for a fundamental relationship between humoral and cell-mediated immunity. *J Exp Med* 134: 21-47
214. Steinman L. 2007. A brief history of T(H)17, the first major revision in the T(H)1/T(H)2 hypothesis of T cell-mediated tissue damage. *Nat Med* 13: 139-45

215. Parish CR. 1996. Immune deviation: a historical perspective. *Immunol Cell Biol* 74: 449-56
216. Mosmann TR, Cherwinski H, Bond MW, Giedlin MA, Coffman RL. 1986. Two types of murine helper T cell clone. I. Definition according to profiles of lymphokine activities and secreted proteins. *J Immunol* 136: 2348-57
217. Coffman RL, Carty J. 1986. A T cell activity that enhances polyclonal IgE production and its inhibition by interferon-gamma. *J Immunol* 136: 949-54
218. Hu-Li J, Shevach EM, Mizuguchi J, Ohara J, Mosmann T, Paul WE. 1987. B cell stimulatory factor 1 (interleukin 4) is a potent costimulant for normal resting T lymphocytes. *J Exp Med* 165: 157-72
219. Cher DJ, Mosmann TR. 1987. Two types of murine helper T cell clone. II. Delayed-type hypersensitivity is mediated by TH1 clones. *J Immunol* 138: 3688-94
220. Mosmann TR, Coffman RL. 1989. TH1 and TH2 cells: different patterns of lymphokine secretion lead to different functional properties. *Annu Rev Immunol* 7: 145-73
221. Rengarajan J, Szabo SJ, Glimcher LH. 2000. Transcriptional regulation of Th1/Th2 polarization. *Immunol Today* 21: 479-83
222. Murphy KM, Reiner SL. 2002. The lineage decisions of helper T cells. *Nat Rev Immunol* 2: 933-44.
223. Szabo SJ, Kim ST, Costa GL, Zhang X, Fathman CG, Glimcher LH. 2000. A novel transcription factor, T-bet, directs Th1 lineage commitment. *Cell* 100: 655-69
224. Moller G. 1988. Do suppressor T cells exist? *Scand J Immunol* 27: 247-50
225. Reiner SL, Locksley RM. 1995. The regulation of immunity to Leishmania major. *Annu Rev Immunol* 13: 151-77
226. Voorthuis JA, Uitdehaag BM, De Groot CJ, Goede PH, van der Meide PH, Dijkstra CD. 1990. Suppression of experimental allergic encephalomyelitis by intraventricular administration of interferon-gamma in Lewis rats. *Clin Exp Immunol* 81: 183-8
227. Billiau A, Heremans H, Vandekerckhove F, Dijkmans R, Sobis H, Meulepas E, Carton H. 1988. Enhancement of experimental allergic encephalomyelitis in mice by antibodies against IFN-gamma. *J Immunol* 140: 1506-10
228. Duong TT, Finkelman FD, Singh B, Strejan GH. 1994. Effect of anti-interferon-gamma monoclonal antibody treatment on the development of experimental allergic encephalomyelitis in resistant mouse strains. *J Neuroimmunol* 53: 101-7
229. Krakowski M, Owens T. 1996. Interferon-gamma confers resistance to experimental allergic encephalomyelitis. *Eur J Immunol* 26: 1641-6
230. Bettelli E, Sullivan B, Szabo SJ, Sobel RA, Glimcher LH, Kuchroo VK. 2004. Loss of T-bet, but not STAT1, prevents the development of experimental autoimmune encephalomyelitis. *J Exp Med* 200: 79-87
231. Zhang GX, Gran B, Yu S, Li J, Siglienti I, Chen X, Kamoun M, Rostami A. 2003. Induction of experimental autoimmune encephalomyelitis in IL-12 receptor-beta 2-deficient mice: IL-12 responsiveness is not required in the pathogenesis of inflammatory demyelination in the central nervous system. *J Immunol* 170: 2153-60
232. Leonard JP, Waldburger KE, Goldman SJ. 1995. Prevention of experimental autoimmune encephalomyelitis by antibodies against interleukin 12. *J Exp Med* 181: 381-6
233. Segal BM, Dwyer BK, Shevach EM. 1998. An interleukin (IL)-10/IL-12 immunoregulatory circuit controls susceptibility to autoimmune disease. *J Exp Med* 187: 537-46

234. Oppmann B, Lesley R, Blom B, Timans JC, Xu Y, Hunte B, Vega F, Yu N, Wang J, Singh K, Zonin F, Vaisberg E, Churakova T, Liu M, Gorman D, Wagner J, Zurawski S, Liu Y, Abrams JS, Moore KW, Rennick D, de Waal-Malefyt R, Hannum C, Bazan JF, Kastelein RA. 2000. Novel p19 protein engages IL-12p40 to form a cytokine, IL-23, with biological activities similar as well as distinct from IL-12. *Immunity* 13: 715-25
235. Schnurr M, Toy T, Shin A, Wagner M, Cebon J, Maraskovsky E. 2005. Extracellular nucleotide signaling by P2 receptors inhibits IL-12 and enhances IL-23 expression in human dendritic cells: a novel role for the cAMP pathway. *Blood* 105: 1582-9
236. Sheibanie AF, Tadmori I, Jing H, Vassiliou E, Ganea D. 2004. Prostaglandin E2 induces IL-23 production in bone marrow-derived dendritic cells. *FASEB J* 18: 1318-20
237. Aggarwal S, Ghilardi N, Xie MH, de Sauvage FJ, Gurney AL. 2003. Interleukin-23 promotes a distinct CD4 T cell activation state characterized by the production of interleukin-17. *J Biol Chem* 278: 1910-4
238. Cua DJ, Sherlock J, Chen Y, Murphy CA, Joyce B, Seymour B, Lucian L, To W, Kwan S, Churakova T, Zurawski S, Wiekowski M, Lira SA, Gorman D, Kastelein RA, Sedgwick JD. 2003. Interleukin-23 rather than interleukin-12 is the critical cytokine for autoimmune inflammation of the brain. *Nature* 421: 744-8
239. Langrish CL, Chen Y, Blumenschein WM, Mattson J, Basham B, Sedgwick JD, McClanahan T, Kastelein RA, Cua DJ. 2005. IL-23 drives a pathogenic T cell population that induces autoimmune inflammation. *J Exp Med* 201: 233-40
240. Murphy CA, Langrish CL, Chen Y, Blumenschein W, McClanahan T, Kastelein RA, Sedgwick JD, Cua DJ. 2003. Divergent pro- and antiinflammatory roles for IL-23 and IL-12 in joint autoimmune inflammation. *J Exp Med* 198: 1951-7
241. Happel KI, Dubin PJ, Zheng M, Ghilardi N, Lockhart C, Quinton LJ, Odden AR, Shellito JE, Bagby GJ, Nelson S, Kolls JK. 2005. Divergent roles of IL-23 and IL-12 in host defense against Klebsiella pneumoniae. *J Exp Med* 202: 761-9
242. Park H, Li Z, Yang XO, Chang SH, Nurieva R, Wang YH, Wang Y, Hood L, Zhu Z, Tian Q, Dong C. 2005. A distinct lineage of CD4 T cells regulates tissue inflammation by producing interleukin 17. *Nat Immunol* 6: 1133-41
243. Harrington LE, Hatton RD, Mangan PR, Turner H, Murphy TL, Murphy KM, Weaver CT. 2005. Interleukin 17-producing CD4+ effector T cells develop via a lineage distinct from the T helper type 1 and 2 lineages. *Nat Immunol* 6: 1123-32
244. Zheng Y, Rudensky AY. 2007. Foxp3 in control of the regulatory T cell lineage. *Nat Immunol* 8: 457-62
245. Wong MT, Ye JJ, Alonso MN, Landrigan A, Cheung RK, Engleman E, Utz PJ. 2010. Regulation of human Th9 differentiation by type I interferons and IL-21. *Immunol Cell Biol* 88: 624-31
246. Eyerich S, Eyerich K, Pennino D, Carbone T, Nasorri F, Pallotta S, Cianfarani F, Odorisio T, Traidl-Hoffmann C, Behrendt H, Durham SR, Schmidt-Weber CB, Cavani A. 2009. Th22 cells represent a distinct human T cell subset involved in epidermal immunity and remodeling. *J Clin Invest* 119: 3573-85
247. Wilson NJ, Boniface K, Chan JR, McKenzie BS, Blumenschein WM, Mattson JD, Basham B, Smith K, Chen T, Morel F, Lecron JC, Kastelein RA, Cua DJ, McClanahan TK, Bowman EP, de Waal Malefyt R. 2007. Development, cytokine profile and function of human interleukin 17-producing helper T cells. *Nat Immunol* 8: 950-7

248. Ivanov, II, McKenzie BS, Zhou L, Tadokoro CE, Lepelley A, Lafaille JJ, Cua DJ, Littman DR. 2006. The orphan nuclear receptor RORgammat directs the differentiation program of proinflammatory IL-17+ T helper cells. *Cell* 126: 1121-33
249. Unutmaz D. 2009. RORC2: the master of human Th17 cell programming. *Eur J Immunol* 39: 1452-5
250. Yang XO, Panopoulos AD, Nurieva R, Chang SH, Wang D, Watowich SS, Dong C. 2007. STAT3 regulates cytokine-mediated generation of inflammatory helper T cells. *J Biol Chem* 282: 9358-63
251. Schraml BU, Hildner K, Ise W, Lee WL, Smith WA, Solomon B, Sahota G, Sim J, Mukasa R, Cemerski S, Hatton RD, Stormo GD, Weaver CT, Russell JH, Murphy TL, Murphy KM. 2009. The AP-1 transcription factor Batf controls T(H)17 differentiation. *Nature* 460: 405-9
252. Brustle A, Heink S, Huber M, Rosenplanter C, Stadelmann C, Yu P, Arpaia E, Mak TW, Kamradt T, Lohoff M. 2007. The development of inflammatory T(H)-17 cells requires interferon-regulatory factor 4. *Nat Immunol* 8: 958-66
253. Quintana FJ, Basso AS, Iglesias AH, Korn T, Farez MF, Bettelli E, Caccamo M, Oukka M, Weiner HL. 2008. Control of T(reg) and T(H)17 cell differentiation by the aryl hydrocarbon receptor. *Nature*
254. Veldhoen M, Hirota K, Westendorf AM, Buer J, Dumoutier L, Renauld JC, Stockinger B. 2008. The aryl hydrocarbon receptor links T(H)17-cell-mediated autoimmunity to environmental toxins. *Nature*
255. Yang XO, Pappu BP, Nurieva R, Akimzhanov A, Kang HS, Chung Y, Ma L, Shah B, Panopoulos AD, Schluns KS, Watowich SS, Tian Q, Jetten AM, Dong C. 2008. T helper 17 lineage differentiation is programmed by orphan nuclear receptors ROR alpha and ROR gamma. *Immunity* 28: 29-39
256. Singh RP, Hasan S, Sharma S, Nagra S, Yamaguchi DT, Wong DT, Hahn BH, Hossain A. 2014. Th17 cells in inflammation and autoimmunity. *Autoimmun Rev* 13: 1174-81
257. Durant L, Watford WT, Ramos HL, Laurence A, Vahedi G, Wei L, Takahashi H, Sun HW, Kanno Y, Powrie F, O'Shea JJ. 2010. Diverse targets of the transcription factor STAT3 contribute to T cell pathogenicity and homeostasis. *Immunity* 32: 605-15
258. Yosef N, Shalek AK, Gaublomme JT, Jin H, Lee Y, Awasthi A, Wu C, Karwacz K, Xiao S, Jorgolli M, Gennert D, Satija R, Shakya A, Lu DY, Trombetta JJ, Pillai MR, Ratcliffe PJ, Coleman ML, Bix M, Tantin D, Park H, Kuchroo VK, Regev A. 2013. Dynamic regulatory network controlling TH17 cell differentiation. *Nature* 496: 461-8
259. Ma CS, Chew GY, Simpson N, Priyadarshi A, Wong M, Grimbacher B, Fulcher DA, Tangye SG, Cook MC. 2008. Deficiency of Th17 cells in hyper IgE syndrome due to mutations in STAT3. *J Exp Med* 205: 1551-7
260. Milner JD, Brenchley JM, Laurence A, Freeman AF, Hill BJ, Elias KM, Kanno Y, Spalding C, Elloumi HZ, Paulson ML, Davis J, Hsu A, Asher AI, O'Shea J, Holland SM, Paul WE, Douek DC. 2008. Impaired T(H)17 cell differentiation in subjects with autosomal dominant hyper-IgE syndrome. *Nature* 452: 773-6
261. Ciofani M, Madar A, Galan C, Sellars M, Mace K, Pauli F, Agarwal A, Huang W, Parkurst CN, Muratet M, Newberry KM, Meadows S, Greenfield A, Yang Y, Jain P, Kirigin FK, Birchmeier C, Wagner EF, Murphy KM, Myers RM, Bonneau R, Littman DR. 2012. A validated regulatory network for Th17 cell specification. *Cell* 151: 289-303
262. Oestreich KJ, Weinmann AS. 2012. Master regulators or lineage-specifying? Changing views on CD4+ T cell transcription factors. *Nat Rev Immunol* 12: 799-804

263. Tanaka S, Suto A, Iwamoto T, Kashiwakuma D, Kagami S, Suzuki K, Takatori H, Tamachi T, Hirose K, Onodera A, Suzuki J, Ohara O, Yamashita M, Nakayama T, Nakajima H. 2014. Sox5 and c-Maf cooperatively induce Th17 cell differentiation via RORgammat induction as downstream targets of Stat3. *J Exp Med* 211: 1857-74
264. Tripathi SK, Lahesmaa R. 2014. Transcriptional and epigenetic regulation of T-helper lineage specification. *Immunol Rev* 261: 62-83
265. Singh SP, Zhang HH, Tsang H, Gardina PJ, Myers TG, Nagarajan V, Lee CH, Farber JM. 2015. PLZF regulates CCR6 and is critical for the acquisition and maintenance of the Th17 phenotype in human cells. *J Immunol* 194: 4350-61
266. Hiramatsu Y, Suto A, Kashiwakuma D, Kanari H, Kagami S, Ikeda K, Hirose K, Watanabe N, Grusby MJ, Iwamoto I, Nakajima H. 2010. c-Maf activates the promoter and enhancer of the IL-21 gene, and TGF-beta inhibits c-Maf-induced IL-21 production in CD4+ T cells. *J Leukoc Biol* 87: 703-12
267. Bauquet AT, Jin H, Paterson AM, Mitsdoerffer M, Ho IC, Sharpe AH, Kuchroo VK. 2009. The costimulatory molecule ICOS regulates the expression of c-Maf and IL-21 in the development of follicular T helper cells and TH-17 cells. *Nat Immunol* 10: 167-75
268. Quintana FJ, Jin H, Burns EJ, Nadeau M, Yeste A, Kumar D, Rangachari M, Zhu C, Xiao S, Seavitt J, Georgopoulos K, Kuchroo VK. 2012. Aiolos promotes TH17 differentiation by directly silencing Il2 expression. *Nat Immunol* 13: 770-7
269. Laurence A, Tato CM, Davidson TS, Kanno Y, Chen Z, Yao Z, Blank RB, Meylan F, Siegel R, Hennighausen L, Shevach EM, O'Shea J J. 2007. Interleukin-2 signaling via STAT5 constrains T helper 17 cell generation. *Immunity* 26: 371-81
270. Yang XP, Ghoreschi K, Steward-Tharp SM, Rodriguez-Canales J, Zhu J, Grainger JR, Hirahara K, Sun HW, Wei L, Vahedi G, Kanno Y, O'Shea JJ, Laurence A. 2011. Opposing regulation of the locus encoding IL-17 through direct, reciprocal actions of STAT3 and STAT5. *Nat Immunol* 12: 247-54
271. Wong LY, Hatfield JK, Brown MA. 2013. Ikaros sets the potential for Th17 lineage gene expression through effects on chromatin state in early T cell development. *J Biol Chem* 288: 35170-9
272. Okamoto K, Iwai Y, Oh-Hora M, Yamamoto M, Morio T, Aoki K, Ohya K, Jetten AM, Akira S, Muta T, Takayanagi H. 2010. IkappaBzeta regulates T(H)17 development by cooperating with ROR nuclear receptors. *Nature* 464: 1381-5
273. Li L, Ruan Q, Hilliard B, Devirgiliis J, Karin M, Chen YH. 2011. Transcriptional regulation of the Th17 immune response by IKK(alpha). *J Exp Med* 208: 787-96
274. Zhang F, Meng G, Strober W. 2008. Interactions among the transcription factors Runx1, RORgammat and Foxp3 regulate the differentiation of interleukin 17-producing T cells. *Nat Immunol* 9: 1297-306
275. Dang EV, Barbi J, Yang HY, Jinasena D, Yu H, Zheng Y, Bordman Z, Fu J, Kim Y, Yen HR, Luo W, Zeller K, Shimoda L, Topalian SL, Semenza GL, Dang CV, Pardoll DM, Pan F. 2011. Control of T(H)17/T(reg) balance by hypoxia-inducible factor 1. *Cell* 146: 772-84
276. Okada S, Markle JG, Deenick EK, Mele F, Averbuch D, Lagos M, Alzahrani M, Al-Muhsen S, Halwani R, Ma CS, Wong N, Soudais C, Henderson LA, Marzouqa H, Shamma J, Gonzalez M, Martinez-Barricarte R, Okada C, Avery DT, Latorre D, Deswarte C, Jabot-Hanin F, Torrado E, Fountain J, Belkadi A, Itan Y, Boisson B, Migaud M, Arlehamn CS, Sette A, Breton S, McCluskey J, Rossjohn J, de Villartay JP, Moshous D, Hambleton S, Latour S, Arkwright PD, Picard C, Lantz O, Engelhard D, Kobayashi M,

Abel L, Cooper AM, Notarangelo LD, Boisson-Dupuis S, Puel A, Sallusto F, Bustamante J, Tangye SG, Casanova JL. 2015. IMMUNODEFICIENCIES. Impairment of immunity to Candida and Mycobacterium in humans with bi-allelic RORC mutations. *Science* 349: 606-13

277. Wan Q, Kozhaya L, ElHed A, Ramesh R, Carlson TJ, Djuretic IM, Sundrud MS, Unutmaz D. 2011. Cytokine signals through PI-3 kinase pathway modulate Th17 cytokine production by CCR6+ human memory T cells. *J Exp Med* 208: 1875-87
278. Gokmen MR, Dong R, Kanhere A, Powell N, Perucha E, Jackson I, Howard JK, Hernandez-Fuentes M, Jenner RG, Lord GM. 2013. Genome-wide regulatory analysis reveals that T-bet controls Th17 lineage differentiation through direct suppression of IRF4. *J Immunol* 191: 5925-32
279. Lazarevic V, Chen X, Shim JH, Hwang ES, Jang E, Bolm AN, Oukka M, Kuchroo VK, Glimcher LH. 2011. T-bet represses T(H)17 differentiation by preventing Runx1-mediated activation of the gene encoding RORgammat. *Nat Immunol* 12: 96-104
280. Zhou L, Lopes JE, Chong MM, Ivanov, II, Min R, Victora GD, Shen Y, Du J, Rubtsov YP, Rudensky AY, Ziegler SF, Littman DR. 2008. TGF-beta-induced Foxp3 inhibits T(H)17 cell differentiation by antagonizing RORgammat function. *Nature* 453: 236-40
281. Yu Q, Sharma A, Ghosh A, Sen JM. 2011. T cell factor-1 negatively regulates expression of IL-17 family of cytokines and protects mice from experimental autoimmune encephalomyelitis. *J Immunol* 186: 3946-52
282. Zhu J, Davidson TS, Wei G, Jankovic D, Cui K, Schones DE, Guo L, Zhao K, Shevach EM, Paul WE. 2009. Down-regulation of Gfi-1 expression by TGF-beta is important for differentiation of Th17 and CD103+ inducible regulatory T cells. *J Exp Med* 206: 329-41
283. Ouyang X, Zhang R, Yang J, Li Q, Qin L, Zhu C, Liu J, Ning H, Shin MS, Gupta M, Qi CF, He JC, Lira SA, Morse HC, 3rd, Ozato K, Mayer L, Xiong H. 2011. Transcription factor IRF8 directs a silencing programme for TH17 cell differentiation. *Nat Commun* 2: 314
284. Pham D, Walline CC, Hollister K, Dent AL, Blum JS, Firulli AB, Kaplan MH. 2013. The transcription factor Twist1 limits T helper 17 and T follicular helper cell development by repressing the gene encoding the interleukin-6 receptor alpha chain. *J Biol Chem* 288: 27423-33
285. Klotz L, Burgdorf S, Dani I, Saijo K, Flossdorf J, Hucke S, Alferink J, Nowak N, Beyer M, Mayer G, Langhans B, Klockgether T, Waisman A, Eberl G, Schultze J, Famulok M, Kolanus W, Glass C, Kurts C, Knolle PA. 2009. The nuclear receptor PPAR gamma selectively inhibits Th17 differentiation in a T cell-intrinsic fashion and suppresses CNS autoimmunity. *J Exp Med* 206: 2079-89
286. Moisan J, Grenningloh R, Bettelli E, Oukka M, Ho IC. 2007. Ets-1 is a negative regulator of Th17 differentiation. *J Exp Med* 204: 2825-35
287. Lee PH, Puppi M, Schluns KS, Yu-Lee LY, Dong C, Lacorazza HD. 2014. The transcription factor E74-like factor 4 suppresses differentiation of proliferating CD4+ T cells to the Th17 lineage. *J Immunol* 192: 178-88
288. Maruyama T, Li J, Vaque JP, Konkel JE, Wang W, Zhang B, Zhang P, Zamarron BF, Yu D, Wu Y, Zhuang Y, Gutkind JS, Chen W. 2011. Control of the differentiation of regulatory T cells and T(H)17 cells by the DNA-binding inhibitor Id3. *Nat Immunol* 12: 86-95

289. Miao T, Raymond M, Bhullar P, Ghaffari E, Symonds AL, Meier UC, Giovannoni G, Li S, Wang P. 2013. Early growth response gene-2 controls IL-17 expression and Th17 differentiation by negatively regulating Batf. *J Immunol* 190: 58-65
290. Mudter J, Yu J, Zufferey C, Brustle A, Wirtz S, Weigmann B, Hoffman A, Schenk M, Galle PR, Lehr HA, Mueller C, Lohoff M, Neurath MF. 2011. IRF4 regulates IL-17A promoter activity and controls RORgammat-dependent Th17 colitis in vivo. *Inflamm Bowel Dis* 17: 1343-58
291. Veldhoen M, Hirota K, Christensen J, O'Garra A, Stockinger B. 2009. Natural agonists for aryl hydrocarbon receptor in culture medium are essential for optimal differentiation of Th17 T cells. *J Exp Med* 206: 43-9
292. Sallusto F, Mackay CR, Lanzavecchia A. 1997. Selective expression of the eotaxin receptor CCR3 by human T helper 2 cells. *Science* 277: 2005-7.
293. Campbell JJ, Butcher EC. 2000. Chemokines in tissue-specific and microenvironment-specific lymphocyte homing. *Curr Opin Immunol* 12: 336-41
294. Altin JG, Sloan EK. 1997. The role of CD45 and CD45-associated molecules in T cell activation. *Immunol Cell Biol* 75: 430-45
295. Sallusto F, Lenig D, Forster R, Lipp M, Lanzavecchia A. 1999. Two subsets of memory T lymphocytes with distinct homing potentials and effector functions. *Nature* 401: 708-12.
296. Rivino L, Messi M, Jarrossay D, Lanzavecchia A, Sallusto F, Geginat J. 2004. Chemokine receptor expression identifies Pre-T helper (Th)1, Pre-Th2, and nonpolarized cells among human CD4+ central memory T cells. *J Exp Med* 200: 725-35.
297. Annunziato F, Cosmi L, Santarlasci V, Maggi L, Liotta F, Mazzinghi B, Parente E, Fili L, Ferri S, Frosali F, Giudici F, Romagnani P, Parronchi P, Tonelli F, Maggi E, Romagnani S. 2007. Phenotypic and functional features of human Th17 cells. *J Exp Med* 204: 1849-61
298. Acosta-Rodriguez EV, Rivino L, Geginat J, Jarrossay D, Gattorno M, Lanzavecchia A, Sallusto F, Napolitani G. 2007. Surface phenotype and antigenic specificity of human interleukin 17-producing T helper memory cells. *Nat Immunol* 8: 639-46
299. Singh SP, Zhang HH, Foley JF, Hedrick MN, Farber JM. 2008. Human T cells that are able to produce IL-17 express the chemokine receptor CCR6. *J Immunol* 180: 214-21
300. Hirota K, Yoshitomi H, Hashimoto M, Maeda S, Teradaira S, Sugimoto N, Yamaguchi T, Nomura T, Ito H, Nakamura T, Sakaguchi N, Sakaguchi S. 2007. Preferential recruitment of CCR6-expressing Th17 cells to inflamed joints via CCL20 in rheumatoid arthritis and its animal model. *J Exp Med* 204: 2803-12
301. Wang C, Kang SG, Lee J, Sun Z, Kim CH. 2009. The roles of CCR6 in migration of Th17 cells and regulation of effector T-cell balance in the gut. *Mucosal Immunol* 2: 173-83
302. Zielinski CE, Mele F, Aschenbrenner D, Jarrossay D, Ronchi F, Gattorno M, Monticelli S, Lanzavecchia A, Sallusto F. 2012. Pathogen-induced human TH17 cells produce IFN-gamma or IL-10 and are regulated by IL-1beta. *Nature* 484: 514-8
303. Cosmi L, Maggi L, Santarlasci V, Liotta F, Annunziato F. 2014. T helper cells plasticity in inflammation. *Cytometry A* 85: 36-42
304. Becattini S, Latorre D, Mele F, Foglierini M, De Gregorio C, Cassotta A, Fernandez B, Kelderman S, Schumacher TN, Corti D, Lanzavecchia A, Sallusto F. 2015. T cell immunity. Functional heterogeneity of human memory CD4(+) T cell clones primed by pathogens or vaccines. *Science* 347: 400-6

305. Duhen T, Campbell DJ. 2014. IL-1beta promotes the differentiation of polyfunctional human CCR6+CXCR3+ Th1/17 cells that are specific for pathogenic and commensal microbes. *J Immunol* 193: 120-9
306. Annunziato F, Cosmi L, Liotta F, Maggi E, Romagnani S. 2012. Defining the human T helper 17 cell phenotype. *Trends Immunol*
307. Bengsch B, Seigel B, Flecken T, Wolanski J, Blum HE, Thimme R. 2012. Human Th17 cells express high levels of enzymatically active dipeptidylpeptidase IV (CD26). *J Immunol* 188: 5438-47
308. Cosmi L, De Palma R, Santarlasci V, Maggi L, Capone M, Frosali F, Rodolico G, Querci V, Abbate G, Angeli R, Berrino L, Fambrini M, Caproni M, Tonelli F, Lazzeri E, Parronchi P, Liotta F, Maggi E, Romagnani S, Annunziato F. 2008. Human interleukin 17-producing cells originate from a CD161+CD4+ T cell precursor. *J Exp Med* 205: 1903-16
309. Stritesky GL, Yeh N, Kaplan MH. 2008. IL-23 promotes maintenance but not commitment to the Th17 lineage. *J Immunol* 181: 5948-55
310. Veldhoen M, Hocking RJ, Atkins CJ, Locksley RM, Stockinger B. 2006. TGFbeta in the context of an inflammatory cytokine milieu supports de novo differentiation of IL-17-producing T cells. *Immunity* 24: 179-89
311. Zhou L, Ivanov, II, Spolski R, Min R, Shenderov K, Egawa T, Levy DE, Leonard WJ, Littman DR. 2007. IL-6 programs T(H)-17 cell differentiation by promoting sequential engagement of the IL-21 and IL-23 pathways. *Nat Immunol* 8: 967-74
312. Bettelli E, Carrier Y, Gao W, Korn T, Strom TB, Oukka M, Weiner HL, Kuchroo VK. 2006. Reciprocal developmental pathways for the generation of pathogenic effector TH17 and regulatory T cells. *Nature* 441: 235-8
313. Mangan PR, Harrington LE, O'Quinn DB, Helms WS, Bullard DC, Elson CO, Hatton RD, Wahl SM, Schoeb TR, Weaver CT. 2006. Transforming growth factor-beta induces development of the T(H)17 lineage. *Nature* 441: 231-4
314. Veldhoen M, Hocking RJ, Flavell RA, Stockinger B. 2006. Signals mediated by transforming growth factor-beta initiate autoimmune encephalomyelitis, but chronic inflammation is needed to sustain disease. *Nat Immunol* 7: 1151-6
315. Li MO, Wan YY, Flavell RA. 2007. T cell-produced transforming growth factor-beta1 controls T cell tolerance and regulates Th1- and Th17-cell differentiation. *Immunity* 26: 579-91
316. Gutcher I, Donkor MK, Ma Q, Rudensky AY, Flavell RA, Li MO. 2011. Autocrine transforming growth factor-beta1 promotes in vivo Th17 cell differentiation. *Immunity* 34: 396-408
317. Das J, Ren G, Zhang L, Roberts AI, Zhao X, Bothwell AL, Van Kaer L, Shi Y, Das G. 2009. Transforming growth factor beta is dispensable for the molecular orchestration of Th17 cell differentiation. *J Exp Med* 206: 2407-16
318. Laurence A, O'Shea JJ. 2007. T(H)-17 differentiation: of mice and men. *Nat Immunol* 8: 903-5
319. Cosmi L, Santarlasci V, Maggi L, Liotta F, Annunziato F. 2014. Th17 plasticity: pathophysiology and treatment of chronic inflammatory disorders. *Curr Opin Pharmacol* 17C: 12-6
320. Acosta-Rodriguez EV, Napolitani G, Lanzavecchia A, Sallusto F. 2007. Interleukins 1beta and 6 but not transforming growth factor-beta are essential for the differentiation of interleukin 17-producing human T helper cells. *Nat Immunol* 8: 942-9

321. Ghoreschi K, Laurence A, Yang XP, Tato CM, McGeachy MJ, Konkel JE, Ramos HL, Wei L, Davidson TS, Bouladoux N, Grainger JR, Chen Q, Kanno Y, Watford WT, Sun HW, Eberl G, Shevach EM, Belkaid Y, Cua DJ, Chen W, O'Shea JJ. 2010. Generation of pathogenic T(H)17 cells in the absence of TGF-beta signalling. *Nature* 467: 967-71
322. Manel N, Unutmaz D, Littman DR. 2008. The differentiation of human T(H)-17 cells requires transforming growth factor-beta and induction of the nuclear receptor RORgammat. *Nat Immunol* 9: 641-9
323. Volpe E, Servant N, Zollinger R, Bogiatzi SI, Hupe P, Barillot E, Soumelis V. 2008. A critical function for transforming growth factor-beta, interleukin 23 and proinflammatory cytokines in driving and modulating human T(H)-17 responses. *Nat Immunol* 9: 650-7
324. Yang L, Anderson DE, Baecher-Allan C, Hastings WD, Bettelli E, Oukka M, Kuchroo VK, Hafler DA. 2008. IL-21 and TGF-beta are required for differentiation of human T(H)17 cells. *Nature* 454: 350-2
325. Chen Z, Tato CM, Muul L, Laurence A, O'Shea JJ. 2007. Distinct regulation of interleukin-17 in human T helper lymphocytes. *Arthritis Rheum* 56: 2936-46
326. Schmitt EG, Williams CB. 2013. Generation and function of induced regulatory T cells. *Front Immunol* 4: 152
327. McGeachy MJ, Chen Y, Tato CM, Laurence A, Joyce-Shaikh B, Blumenschein WM, McClanahan TK, O'Shea JJ, Cua DJ. 2009. The interleukin 23 receptor is essential for the terminal differentiation of interleukin 17-producing effector T helper cells in vivo. *Nat Immunol* 10: 314-24
328. Haines CJ, Chen Y, Blumenschein WM, Jain R, Chang C, Joyce-Shaikh B, Porth K, Boniface K, Mattson J, Basham B, Anderton SM, McClanahan TK, Sadekova S, Cua DJ, McGeachy MJ. 2013. Autoimmune memory T helper 17 cell function and expansion are dependent on interleukin-23. *Cell Rep* 3: 1378-88
329. Sutton C, Brereton C, Keogh B, Mills KH, Lavelle EC. 2006. A crucial role for interleukin (IL)-1 in the induction of IL-17-producing T cells that mediate autoimmune encephalomyelitis. *J Exp Med* 203: 1685-91
330. Chung Y, Chang SH, Martinez GJ, Yang XO, Nurieva R, Kang HS, Ma L, Watowich SS, Jetten AM, Tian Q, Dong C. 2009. Critical regulation of early Th17 cell differentiation by interleukin-1 signaling. *Immunity* 30: 576-87
331. Gulen MF, Kang Z, Bulek K, Youzhong W, Kim TW, Chen Y, Altuntas CZ, Sass Bak-Jensen K, McGeachy MJ, Do JS, Xiao H, Delgoffe GM, Min B, Powell JD, Tuohy VK, Cua DJ, Li X. 2010. The receptor SIGIRR suppresses Th17 cell proliferation via inhibition of the interleukin-1 receptor pathway and mTOR kinase activation. *Immunity* 32: 54-66
332. Micci L, Cervasi B, Ende ZS, Iriele RI, Reyes-Aviles E, Vinton C, Else J, Silvestri G, Ansari AA, Villinger F, Pahwa S, Estes JD, Brenchley JM, Paiardini M. 2012. Paucity of IL-21-producing CD4(+) T cells is associated with Th17 cell depletion in SIV infection of rhesus macaques. *Blood* 120: 3925-35
333. Santarlasci V, Maggi L, Capone M, Querci V, Beltrame L, Cavalieri D, D'Aiuto E, Cimaz R, Nebbioso A, Liotta F, De Palma R, Maggi E, Cosmi L, Romagnani S, Annunziato F. 2012. Rarity of human T helper 17 cells is due to retinoic acid orphan receptor-dependent mechanisms that limit their expansion. *Immunity* 36: 201-14
334. Pallikkuth S, Micci L, Ende ZS, Iriele RI, Cervasi B, Lawson B, McGary CS, Rogers KA, Else JG, Silvestri G, Easley K, Estes JD, Villinger F, Pahwa S, Paiardini M. 2013.

Maintenance of intestinal Th17 cells and reduced microbial translocation in SIV-infected rhesus macaques treated with interleukin (IL)-21. *PLoS Pathog* 9: e1003471
335. Crotty S. 2011. Follicular helper CD4 T cells (TFH). *Annu Rev Immunol* 29: 621-63
336. Crotty S. 2014. T follicular helper cell differentiation, function, and roles in disease. *Immunity* 41: 529-42
337. O'Shea JJ, Paul WE. 2010. Mechanisms underlying lineage commitment and plasticity of helper CD4+ T cells. *Science* 327: 1098-102
338. Wei G, Wei L, Zhu J, Zang C, Hu-Li J, Yao Z, Cui K, Kanno Y, Roh TY, Watford WT, Schones DE, Peng W, Sun HW, Paul WE, O'Shea JJ, Zhao K. 2009. Global mapping of H3K4me3 and H3K27me3 reveals specificity and plasticity in lineage fate determination of differentiating CD4+ T cells. *Immunity* 30: 155-67
339. Muranski P, Restifo NP. 2013. Essentials of Th17 cell commitment and plasticity. *Blood* 121: 2402-14
340. Shi G, Cox CA, Vistica BP, Tan C, Wawrousek EF, Gery I. 2008. Phenotype switching by inflammation-inducing polarized Th17 cells, but not by Th1 cells. *J Immunol* 181: 7205-13
341. Abromson-Leeman S, Bronson RT, Dorf ME. 2009. Encephalitogenic T cells that stably express both T-bet and ROR gamma t consistently produce IFNgamma but have a spectrum of IL-17 profiles. *J Neuroimmunol* 215: 10-24
342. Bending D, Newland S, Krejci A, Phillips JM, Bray S, Cooke A. 2011. Epigenetic changes at Il12rb2 and Tbx21 in relation to plasticity behavior of Th17 cells. *J Immunol* 186: 3373-82
343. Boniface K, Blumenschein WM, Brovont-Porth K, McGeachy MJ, Basham B, Desai B, Pierce R, McClanahan TK, Sadekova S, de Waal Malefyt R. 2010. Human Th17 cells comprise heterogeneous subsets including IFN-gamma-producing cells with distinct properties from the Th1 lineage. *J Immunol* 185: 679-87
344. Ramesh R, Kozhaya L, McKevitt K, Djuretic IM, Carlson TJ, Quintero MA, McCauley JL, Abreu MT, Unutmaz D, Sundrud MS. 2014. Pro-inflammatory human Th17 cells selectively express P-glycoprotein and are refractory to glucocorticoids. *J Exp Med* 211: 89-104
345. Sundrud MS, Trivigno C. 2013. Identity crisis of Th17 cells: many forms, many functions, many questions. *Semin Immunol* 25: 263-72
346. Hirota K, Duarte JH, Veldhoen M, Hornsby E, Li Y, Cua DJ, Ahlfors H, Wilhelm C, Tolaini M, Menzel U, Garefalaki A, Potocnik AJ, Stockinger B. 2011. Fate mapping of IL-17-producing T cells in inflammatory responses. *Nat Immunol* 12: 255-63
347. Mazzoni A, Santarlasci V, Maggi L, Capone M, Rossi MC, Querci V, De Palma R, Chang HD, Thiel A, Cimaz R, Liotta F, Cosmi L, Maggi E, Radbruch A, Romagnani S, Dong J, Annunziato F. 2015. Demethylation of the RORC2 and IL17A in human CD4+ T lymphocytes defines Th17 origin of nonclassic Th1 cells. *J Immunol* 194: 3116-26
348. Maggi L, Cimaz R, Capone M, Santarlasci V, Querci V, Simonini G, Nencini F, Liotta F, Romagnani S, Maggi E, Annunziato F, Cosmi L. 2014. Brief report: etanercept inhibits the tumor necrosis factor alpha-driven shift of Th17 lymphocytes toward a nonclassic Th1 phenotype in juvenile idiopathic arthritis. *Arthritis Rheumatol* 66: 1372-7
349. Cosmi L, Maggi L, Santarlasci V, Capone M, Cardilicchia E, Frosali F, Querci V, Angeli R, Matucci A, Fambrini M, Liotta F, Parronchi P, Maggi E, Romagnani S, Annunziato F. 2010. Identification of a novel subset of human circulating memory CD4(+) T cells that produce both IL-17A and IL-4. *J Allergy Clin Immunol* 125: 222-30 e1-4

350. Hirota K, Turner JE, Villa M, Duarte JH, Demengeot J, Steinmetz OM, Stockinger B. 2013. Plasticity of Th17 cells in Peyer's patches is responsible for the induction of T cell-dependent IgA responses. *Nat Immunol* 14: 372-9
351. Hoechst B, Gamrekelashvili J, Manns MP, Greten TF, Korangy F. 2011. Plasticity of human Th17 cells and iTregs is orchestrated by different subsets of myeloid cells. *Blood* 117: 6532-41
352. Yang XO, Nurieva R, Martinez GJ, Kang HS, Chung Y, Pappu BP, Shah B, Chang SH, Schluns KS, Watowich SS, Feng XH, Jetten AM, Dong C. 2008. Molecular antagonism and plasticity of regulatory and inflammatory T cell programs. *Immunity* 29: 44-56
353. Koenen HJ, Smeets RL, Vink PM, van Rijssen E, Boots AM, Joosten I. 2008. Human CD25highFoxp3pos regulatory T cells differentiate into IL-17-producing cells. *Blood* 112: 2340-52
354. Gagliani N, Vesely MC, Iseppon A, Brockmann L, Xu H, Palm NW, de Zoete MR, Licona-Limon P, Paiva RS, Ching T, Weaver C, Zi X, Pan X, Fan R, Garmire LX, Cotton MJ, Drier Y, Bernstein B, Geginat J, Stockinger B, Esplugues E, Huber S, Flavell RA. 2015. Th17 cells transdifferentiate into regulatory T cells during resolution of inflammation. *Nature* 523: 221-5
355. Esplugues E, Huber S, Gagliani N, Hauser AE, Town T, Wan YY, O'Connor W, Jr., Rongvaux A, Van Rooijen N, Haberman AM, Iwakura Y, Kuchroo VK, Kolls JK, Bluestone JA, Herold KC, Flavell RA. 2011. Control of TH17 cells occurs in the small intestine. *Nature* 475: 514-8
356. Lee Y, Awasthi A, Yosef N, Quintana FJ, Xiao S, Peters A, Wu C, Kleinewietfeld M, Kunder S, Hafler DA, Sobel RA, Regev A, Kuchroo VK. 2012. Induction and molecular signature of pathogenic TH17 cells. *Nat Immunol* 13: 991-9
357. Lochner M, Peduto L, Cherrier M, Sawa S, Langa F, Varona R, Riethmacher D, Si-Tahar M, Di Santo JP, Eberl G. 2008. In vivo equilibrium of proinflammatory IL-17+ and regulatory IL-10+ Foxp3+ RORgamma t+ T cells. *J Exp Med* 205: 1381-93
358. Nikoopour E, Schwartz JA, Huszarik K, Sandrock C, Krougly O, Lee-Chan E, Singh B. 2010. Th17 polarized cells from nonobese diabetic mice following mycobacterial adjuvant immunotherapy delay type 1 diabetes. *J Immunol* 184: 4779-88
359. McGeachy MJ, Bak-Jensen KS, Chen Y, Tato CM, Blumenschein W, McClanahan T, Cua DJ. 2007. TGF-beta and IL-6 drive the production of IL-17 and IL-10 by T cells and restrain T(H)-17 cell-mediated pathology. *Nat Immunol* 8: 1390-7
360. Yang Y, Weiner J, Liu Y, Smith AJ, Huss DJ, Winger R, Peng H, Cravens PD, Racke MK, Lovett-Racke AE. 2009. T-bet is essential for encephalitogenicity of both Th1 and Th17 cells. *J Exp Med* 206: 1549-64
361. Ivanov, II, Atarashi K, Manel N, Brodie EL, Shima T, Karaoz U, Wei D, Goldfarb KC, Santee CA, Lynch SV, Tanoue T, Imaoka A, Itoh K, Takeda K, Umesaki Y, Honda K, Littman DR. 2009. Induction of intestinal Th17 cells by segmented filamentous bacteria. *Cell* 139: 485-98
362. Gaboriau-Routhiau V, Rakotobe S, Lecuyer E, Mulder I, Lan A, Bridonneau C, Rochet V, Pisi A, De Paepe M, Brandi G, Eberl G, Snel J, Kelly D, Cerf-Bensussan N. 2009. The key role of segmented filamentous bacteria in the coordinated maturation of gut helper T cell responses. *Immunity* 31: 677-89
363. Lecuyer E, Rakotobe S, Lengline-Garnier H, Lebreton C, Picard M, Juste C, Fritzen R, Eberl G, McCoy KD, Macpherson AJ, Reynaud CA, Cerf-Bensussan N, Gaboriau-Routhiau V. 2014. Segmented filamentous bacterium uses secondary and tertiary

lymphoid tissues to induce gut IgA and specific T helper 17 cell responses. *Immunity* 40: 608-20
364. Atarashi K, Nishimura J, Shima T, Umesaki Y, Yamamoto M, Onoue M, Yagita H, Ishii N, Evans R, Honda K, Takeda K. 2008. ATP drives lamina propria T(H)17 cell differentiation. *Nature* 455: 808-12
365. Sano T, Huang W, Hall JA, Yang Y, Chen A, Gavzy SJ, Lee JY, Ziel JW, Miraldi ER, Domingos AI, Bonneau R, Littman DR. 2015. An IL-23R/IL-22 Circuit Regulates Epithelial Serum Amyloid A to Promote Local Effector Th17 Responses. *Cell* 163: 381-93
366. Pelletier M, Maggi L, Micheletti A, Lazzeri E, Tamassia N, Costantini C, Cosmi L, Lunardi C, Annunziato F, Romagnani S, Cassatella MA. 2009. Evidence for a cross-talk between human neutrophils and Th17 cells. *Blood*
367. Onishi RM, Gaffen SL. 2010. Interleukin-17 and its target genes: mechanisms of interleukin-17 function in disease. *Immunology* 129: 311-21
368. Hartupee J, Liu C, Novotny M, Li X, Hamilton T. 2007. IL-17 enhances chemokine gene expression through mRNA stabilization. *J Immunol* 179: 4135-41
369. Minegishi Y, Saito M, Nagasawa M, Takada H, Hara T, Tsuchiya S, Agematsu K, Yamada M, Kawamura N, Ariga T, Tsuge I, Karasuyama H. 2009. Molecular explanation for the contradiction between systemic Th17 defect and localized bacterial infection in hyper-IgE syndrome. *J Exp Med* 206: 1291-301
370. Kumar P, Chen K, Kolls JK. 2013. Th17 cell based vaccines in mucosal immunity. *Curr Opin Immunol* 25: 373-80
371. Hymowitz SG, Filvaroff EH, Yin JP, Lee J, Cai L, Risser P, Maruoka M, Mao W, Foster J, Kelley RF, Pan G, Gurney AL, de Vos AM, Starovasnik MA. 2001. IL-17s adopt a cystine knot fold: structure and activity of a novel cytokine, IL-17F, and implications for receptor binding. *EMBO J* 20: 5332-41
372. Lee YK, Turner H, Maynard CL, Oliver JR, Chen D, Elson CO, Weaver CT. 2009. Late developmental plasticity in the T helper 17 lineage. *Immunity* 30: 92-107
373. Liang SC, Long AJ, Bennett F, Whitters MJ, Karim R, Collins M, Goldman SJ, Dunussi-Joannopoulos K, Williams CM, Wright JF, Fouser LA. 2007. An IL-17F/A heterodimer protein is produced by mouse Th17 cells and induces airway neutrophil recruitment. *J Immunol* 179: 7791-9
374. Huber S, Gagliani N, Flavell RA. 2012. Life, death, and miracles: Th17 cells in the intestine. *Eur J Immunol* 42: 2238-45
375. Sanjabi S, Zenewicz LA, Kamanaka M, Flavell RA. 2009. Anti-inflammatory and pro-inflammatory roles of TGF-beta, IL-10, and IL-22 in immunity and autoimmunity. *Curr Opin Pharmacol* 9: 447-53
376. Boniface K, Bernard FX, Garcia M, Gurney AL, Lecron JC, Morel F. 2005. IL-22 inhibits epidermal differentiation and induces proinflammatory gene expression and migration of human keratinocytes. *J Immunol* 174: 3695-702
377. Zenewicz LA, Yancopoulos GD, Valenzuela DM, Murphy AJ, Stevens S, Flavell RA. 2008. Innate and adaptive interleukin-22 protects mice from inflammatory bowel disease. *Immunity* 29: 947-57
378. Sugimoto K, Ogawa A, Mizoguchi E, Shimomura Y, Andoh A, Bhan AK, Blumberg RS, Xavier RJ, Mizoguchi A. 2008. IL-22 ameliorates intestinal inflammation in a mouse model of ulcerative colitis. *J Clin Invest* 118: 534-44

379. Zenewicz LA, Yancopoulos GD, Valenzuela DM, Murphy AJ, Karow M, Flavell RA. 2007. Interleukin-22 but not interleukin-17 provides protection to hepatocytes during acute liver inflammation. *Immunity* 27: 647-59
380. Meller S, Di Domizio J, Voo KS, Friedrich HC, Chamilos G, Ganguly D, Conrad C, Gregorio J, Le Roy D, Roger T, Ladbury JE, Homey B, Watowich S, Modlin RL, Kontoyiannis DP, Liu YJ, Arold ST, Gilliet M. 2015. TH17 cells promote microbial killing and innate immune sensing of DNA via interleukin 26. *Nat Immunol* 16: 970-9
381. Khader SA, Bell GK, Pearl JE, Fountain JJ, Rangel-Moreno J, Cilley GE, Shen F, Eaton SM, Gaffen SL, Swain SL, Locksley RM, Haynes L, Randall TD, Cooper AM. 2007. IL-23 and IL-17 in the establishment of protective pulmonary CD4+ T cell responses after vaccination and during Mycobacterium tuberculosis challenge. *Nat Immunol* 8: 369-77
382. O'Connor W, Jr., Zenewicz LA, Flavell RA. 2010. The dual nature of T(H)17 cells: shifting the focus to function. *Nat Immunol* 11: 471-6
383. Apetoh L, Quintana FJ, Pot C, Joller N, Xiao S, Kumar D, Burns EJ, Sherr DH, Weiner HL, Kuchroo VK. 2010. The aryl hydrocarbon receptor interacts with c-Maf to promote the differentiation of type 1 regulatory T cells induced by IL-27. *Nat Immunol* 11: 854-61
384. Diveu C, McGeachy MJ, Boniface K, Stumhofer JS, Sathe M, Joyce-Shaikh B, Chen Y, Tato CM, McClanahan TK, de Waal Malefyt R, Hunter CA, Cua DJ, Kastelein RA. 2009. IL-27 blocks RORc expression to inhibit lineage commitment of Th17 cells. *J Immunol* 182: 5748-56
385. Marks BR, Nowyhed HN, Choi JY, Poholek AC, Odegard JM, Flavell RA, Craft J. 2009. Thymic self-reactivity selects natural interleukin 17-producing T cells that can regulate peripheral inflammation. *Nat Immunol* 10: 1125-32
386. Zuniga LA, Jain R, Haines C, Cua DJ. 2013. Th17 cell development: from the cradle to the grave. *Immunol Rev* 252: 78-88
387. Conti HR, Peterson AC, Brane L, Huppler AR, Hernandez-Santos N, Whibley N, Garg AV, Simpson-Abelson MR, Gibson GA, Mamo AJ, Osborne LC, Bishu S, Ghilardi N, Siebenlist U, Watkins SC, Artis D, McGeachy MJ, Gaffen SL. 2014. Oral-resident natural Th17 cells and gammadelta T cells control opportunistic Candida albicans infections. *J Exp Med* 211: 2075-84
388. Massot B, Michel ML, Diem S, Ohnmacht C, Latour S, Dy M, Eberl G, Leite-de-Moraes MC. 2014. TLR-induced cytokines promote effective proinflammatory natural Th17 cell responses. *J Immunol* 192: 5635-42
389. Hou MS, Huang ST, Tsai MH, Yen CC, Lai YG, Liou YH, Lin CK, Liao NS. 2015. The interleukin-15 system suppresses T cell-mediated autoimmunity by regulating negative selection and nT(H)17 cell homeostasis in the thymus. *J Autoimmun* 56: 118-29
390. Sherlock JP, Joyce-Shaikh B, Turner SP, Chao CC, Sathe M, Grein J, Gorman DM, Bowman EP, McClanahan TK, Yearley JH, Eberl G, Buckley CD, Kastelein RA, Pierce RH, Laface DM, Cua DJ. 2012. IL-23 induces spondyloarthropathy by acting on ROR-gammat+ CD3+CD4-CD8- entheseal resident T cells. *Nat Med* 18: 1069-76
391. Novelli L, Chimenti MS, Chiricozzi A, Perricone R. 2014. The new era for the treatment of psoriasis and psoriatic arthritis: perspectives and validated strategies. *Autoimmun Rev* 13: 64-9
392. Broome AM, Ryan D, Eckert RL. 2003. S100 protein subcellular localization during epidermal differentiation and psoriasis. *J Histochem Cytochem* 51: 675-85
393. Zhang Z, Zheng M, Bindas J, Schwarzenberger P, Kolls JK. 2006. Critical role of IL-17 receptor signaling in acute TNBS-induced colitis. *Inflamm Bowel Dis* 12: 382-8

394. Ogawa A, Andoh A, Araki Y, Bamba T, Fujiyama Y. 2004. Neutralization of interleukin-17 aggravates dextran sulfate sodium-induced colitis in mice. *Clin Immunol* 110: 55-62
395. Isaacs KL, Lewis JD, Sandborn WJ, Sands BE, Targan SR. 2005. State of the art: IBD therapy and clinical trials in IBD. *Inflamm Bowel Dis* 11 Suppl 1: S3-12
396. Kleinschek MA, Boniface K, Sadekova S, Grein J, Murphy EE, Turner SP, Raskin L, Desai B, Faubion WA, de Waal Malefyt R, Pierce RH, McClanahan T, Kastelein RA. 2009. Circulating and gut-resident human Th17 cells express CD161 and promote intestinal inflammation. *J Exp Med* 206: 525-34
397. Harbour SN, Maynard CL, Zindl CL, Schoeb TR, Weaver CT. 2015. Th17 cells give rise to Th1 cells that are required for the pathogenesis of colitis. *Proc Natl Acad Sci U S A* 112: 7061-6
398. Gottesman MM, Fojo T, Bates SE. 2002. Multidrug resistance in cancer: role of ATP-dependent transporters. *Nat Rev Cancer* 2: 48-58
399. El-Behi M, Ciric B, Dai H, Yan Y, Cullimore M, Safavi F, Zhang GX, Dittel BN, Rostami A. 2011. The encephalitogenicity of T(H)17 cells is dependent on IL-1- and IL-23-induced production of the cytokine GM-CSF. *Nat Immunol* 12: 568-75
400. Codarri L, Gyulveszi G, Tosevski V, Hesske L, Fontana A, Magnenat L, Suter T, Becher B. 2011. RORgammat drives production of the cytokine GM-CSF in helper T cells, which is essential for the effector phase of autoimmune neuroinflammation. *Nat Immunol* 12: 560-7
401. Kebir H, Kreymborg K, Ifergan I, Dodelet-Devillers A, Cayrol R, Bernard M, Giuliani F, Arbour N, Becher B, Prat A. 2007. Human TH17 lymphocytes promote blood-brain barrier disruption and central nervous system inflammation. *Nat Med* 13: 1173-5
402. Tzartos JS, Friese MA, Craner MJ, Palace J, Newcombe J, Esiri MM, Fugger L. 2008. Interleukin-17 production in central nervous system-infiltrating T cells and glial cells is associated with active disease in multiple sclerosis. *Am J Pathol* 172: 146-55
403. Kebir H, Ifergan I, Alvarez JI, Bernard M, Poirier J, Arbour N, Duquette P, Prat A. 2009. Preferential recruitment of interferon-gamma-expressing TH17 cells in multiple sclerosis. *Ann Neurol* 66: 390-402
404. Niu Q, Cai B, Huang ZC, Shi YY, Wang LL. 2012. Disturbed Th17/Treg balance in patients with rheumatoid arthritis. *Rheumatol Int* 32: 2731-6
405. Lubberts E. 2008. IL-17/Th17 targeting: on the road to prevent chronic destructive arthritis? *Cytokine* 41: 84-91
406. Shah K, Lee WW, Lee SH, Kim SH, Kang SW, Craft J, Kang I. 2010. Dysregulated balance of Th17 and Th1 cells in systemic lupus erythematosus. *Arthritis Res Ther* 12: R53
407. Yang J, Chu Y, Yang X, Gao D, Zhu L, Yang X, Wan L, Li M. 2009. Th17 and natural Treg cell population dynamics in systemic lupus erythematosus. *Arthritis Rheum* 60: 1472-83
408. Qin WZ, Chen LL, Pan HF, Leng RX, Zhai ZM, Wang C, Li RJ, Wang S, Wang HP, Ye DQ. 2011. Expressions of IL-22 in circulating CD4+/CD8+ T cells and their correlation with disease activity in SLE patients. *Clin Exp Med* 11: 245-50
409. Doreau A, Belot A, Bastid J, Riche B, Trescol-Biemont MC, Ranchin B, Fabien N, Cochat P, Pouteil-Noble C, Trolliet P, Durieu I, Tebib J, Kassai B, Ansieau S, Puisieux A, Eliaou JF, Bonnefoy-Berard N. 2009. Interleukin 17 acts in synergy with B cell-activating factor to influence B cell biology and the pathophysiology of systemic lupus erythematosus. *Nat Immunol* 10: 778-85

410. Lee JS, Tato CM, Joyce-Shaikh B, Gulan F, Cayatte C, Chen Y, Blumenschein WM, Judo M, Ayanoglu G, McClanahan TK, Li X, Cua DJ. 2015. Interleukin-23-Independent IL-17 Production Regulates Intestinal Epithelial Permeability. *Immunity*
411. Maxwell JR, Zhang Y, Brown WA, Smith CL, Byrne FR, Fiorino M, Stevens E, Bigler J, Davis JA, Rottman JB, Budelsky AL, Symons A, Towne JE. 2015. Differential Roles for Interleukin-23 and Interleukin-17 in Intestinal Immunoregulation. *Immunity*
412. Teng MW, Bowman EP, McElwee JJ, Smyth MJ, Casanova JL, Cooper AM, Cua DJ. 2015. IL-12 and IL-23 cytokines: from discovery to targeted therapies for immune-mediated inflammatory diseases. *Nat Med* 21: 719-29
413. Zhao F, Hoechst B, Gamrekelashvili J, Ormandy LA, Voigtlander T, Wedemeyer H, Ylaya K, Wang XW, Hewitt SM, Manns MP, Korangy F, Greten TF. 2012. Human CCR4+ CCR6+ Th17 cells suppress autologous CD8+ T cell responses. *J Immunol* 188: 6055-62
414. Yamada Y, Saito H, Ikeguchi M. 2012. Prevalence and clinical relevance of Th17 cells in patients with gastric cancer. *J Surg Res* 178: 685-91
415. Miyahara Y, Odunsi K, Chen W, Peng G, Matsuzaki J, Wang RF. 2008. Generation and regulation of human CD4+ IL-17-producing T cells in ovarian cancer. *Proc Natl Acad Sci U S A* 105: 15505-10
416. Maruyama T, Kono K, Mizukami Y, Kawaguchi Y, Mimura K, Watanabe M, Izawa S, Fujii H. 2010. Distribution of Th17 cells and FoxP3(+) regulatory T cells in tumor-infiltrating lymphocytes, tumor-draining lymph nodes and peripheral blood lymphocytes in patients with gastric cancer. *Cancer Sci* 101: 1947-54
417. Tosolini M, Kirilovsky A, Mlecnik B, Fredriksen T, Mauger S, Bindea G, Berger A, Bruneval P, Fridman WH, Pages F, Galon J. 2011. Clinical impact of different classes of infiltrating T cytotoxic and helper cells (Th1, th2, treg, th17) in patients with colorectal cancer. *Cancer Res* 71: 1263-71
418. Su X, Ye J, Hsueh EC, Zhang Y, Hoft DF, Peng G. 2010. Tumor microenvironments direct the recruitment and expansion of human Th17 cells. *J Immunol* 184: 1630-41
419. He S, Fei M, Wu Y, Zheng D, Wan D, Wang L, Li D. 2011. Distribution and clinical significance of Th17 cells in the tumor microenvironment and peripheral blood of pancreatic cancer patients. *Int J Mol Sci* 12: 7424-37
420. Martin-Orozco N, Muranski P, Chung Y, Yang XO, Yamazaki T, Lu S, Hwu P, Restifo NP, Overwijk WW, Dong C. 2009. T helper 17 cells promote cytotoxic T cell activation in tumor immunity. *Immunity* 31: 787-98
421. Muranski P, Boni A, Antony PA, Cassard L, Irvine KR, Kaiser A, Paulos CM, Palmer DC, Touloukian CE, Ptak K, Gattinoni L, Wrzesinski C, Hinrichs CS, Kerstann KW, Feigenbaum L, Chan CC, Restifo NP. 2008. Tumor-specific Th17-polarized cells eradicate large established melanoma. *Blood* 112: 362-73
422. Kryczek I, Banerjee M, Cheng P, Vatan L, Szeliga W, Wei S, Huang E, Finlayson E, Simeone D, Welling TH, Chang A, Coukos G, Liu R, Zou W. 2009. Phenotype, distribution, generation, and functional and clinical relevance of Th17 cells in the human tumor environments. *Blood* 114: 1141-9
423. Kryczek I, Zhao E, Liu Y, Wang Y, Vatan L, Szeliga W, Moyer J, Klimczak A, Lange A, Zou W. 2011. Human TH17 cells are long-lived effector memory cells. *Sci Transl Med* 3: 104ra0
424. Muranski P, Borman ZA, Kerkar SP, Klebanoff CA, Ji Y, Sanchez-Perez L, Sukumar M, Reger RN, Yu Z, Kern SJ, Roychoudhuri R, Ferreyra GA, Shen W, Durum SK,

Feigenbaum L, Palmer DC, Antony PA, Chan CC, Laurence A, Danner RL, Gattinoni L, Restifo NP. 2011. Th17 cells are long lived and retain a stem cell-like molecular signature. *Immunity* 35: 972-85

425. Gattinoni L, Lugli E, Ji Y, Pos Z, Paulos CM, Quigley MF, Almeida JR, Gostick E, Yu Z, Carpenito C, Wang E, Douek DC, Price DA, June CH, Marincola FM, Roederer M, Restifo NP. 2011. A human memory T cell subset with stem cell-like properties. *Nat Med* 17: 1290-7
426. Zhang Y, Joe G, Hexner E, Zhu J, Emerson SG. 2005. Host-reactive CD8+ memory stem cells in graft-versus-host disease. *Nat Med* 11: 1299-305
427. Gattinoni L, Zhong XS, Palmer DC, Ji Y, Hinrichs CS, Yu Z, Wrzesinski C, Boni A, Cassard L, Garvin LM, Paulos CM, Muranski P, Restifo NP. 2009. Wnt signaling arrests effector T cell differentiation and generates CD8+ memory stem cells. *Nat Med* 15: 808-13
428. Turtle CJ, Swanson HM, Fujii N, Estey EH, Riddell SR. 2009. A distinct subset of self-renewing human memory CD8+ T cells survives cytotoxic chemotherapy. *Immunity* 31: 834-44
429. Luckey CJ, Weaver CT. 2012. Stem-cell-like qualities of immune memory; CD4+ T cells join the party. *Cell Stem Cell* 10: 107-8
430. Gattinoni L, Ji Y, Restifo NP. 2010. Wnt/beta-catenin signaling in T-cell immunity and cancer immunotherapy. *Clin Cancer Res* 16: 4695-701
431. Bixler SL, Mattapallil JJ. 2013. Loss and dysregulation of Th17 cells during HIV infection. *Clin Dev Immunol* 2013: 852418
432. Cecchinato V, Trindade CJ, Laurence A, Heraud JM, Brenchley JM, Ferrari MG, Zaffiri L, Tryniszewska E, Tsai WP, Vaccari M, Parks RW, Venzon D, Douek DC, O'Shea JJ, Franchini G. 2008. Altered balance between Th17 and Th1 cells at mucosal sites predicts AIDS progression in simian immunodeficiency virus-infected macaques. *Mucosal Immunol* 1: 279-88
433. Raffatellu M, Santos RL, Verhoeven DE, George MD, Wilson RP, Winter SE, Godinez I, Sankaran S, Paixao TA, Gordon MA, Kolls JK, Dandekar S, Baumler AJ. 2008. Simian immunodeficiency virus-induced mucosal interleukin-17 deficiency promotes Salmonella dissemination from the gut. *Nat Med* 14: 421-8
434. Brenchley JM, Paiardini M, Knox KS, Asher AI, Cervasi B, Asher TE, Scheinberg P, Price DA, Hage CA, Kholi LM, Khoruts A, Frank I, Else J, Schacker T, Silvestri G, Douek DC. 2008. Differential Th17 CD4 T-cell depletion in pathogenic and nonpathogenic lentiviral infections. *Blood* 112: 2826-35
435. El Hed A, Khaitan A, Kozhaya L, Manel N, Daskalakis D, Borkowsky W, Valentine F, Littman DR, Unutmaz D. 2010. Susceptibility of human Th17 cells to human immunodeficiency virus and their perturbation during infection. *J Infect Dis* 201: 843-54
436. Gosselin A, Monteiro P, Chomont N, Diaz-Griffero F, Said EA, Fonseca S, Wacleche V, El-Far M, Boulassel MR, Routy JP, Sekaly RP, Ancuta P. 2010. Peripheral blood CCR4+CCR6+ and CXCR3+CCR6+CD4+ T cells are highly permissive to HIV-1 infection. *J Immunol* 184: 1604-16
437. Ndhlovu LC, Chapman JM, Jha AR, Snyder-Cappione JE, Pagan M, Leal FE, Boland BS, Norris PJ, Rosenberg MG, Nixon DF. 2008. Suppression of HIV-1 plasma viral load below detection preserves IL-17 producing T cells in HIV-1 infection. *Aids* 22: 990-2

438. Prendergast A, Prado JG, Kang YH, Chen F, Riddell LA, Luzzi G, Goulder P, Klenerman P. 2010. HIV-1 infection is characterized by profound depletion of CD161+ Th17 cells and gradual decline in regulatory T cells. *AIDS* 24: 491-502
439. Ciccone EJ, Greenwald JH, Lee PI, Biancotto A, Read SW, Yao MA, Hodge JN, Thompson WL, Kovacs SB, Chairez CL, Migueles SA, Kovacs JA, Margolis LB, Sereti I. 2011. CD4+ T cells, including Th17 and cycling subsets, are intact in the gut mucosa of HIV-1-infected long-term nonprogressors. *J Virol* 85: 5880-8
440. Alvarez Y, Tuen M, Shen G, Nawaz F, Arthos J, Wolff MJ, Poles MA, Hioe CE. 2013. Preferential HIV infection of CCR6+ Th17 cells is associated with higher levels of virus receptor expression and lack of CCR5 ligands. *J Virol* 87: 10843-54
441. Monteiro P, Gosselin A, Wacleche VS, El-Far M, Said EA, Kared H, Grandvaux N, Boulassel MR, Routy JP, Ancuta P. 2011. Memory CCR6+CD4+ T cells are preferential targets for productive HIV type 1 infection regardless of their expression of integrin beta7. *J Immunol* 186: 4618-30
442. Kader M, Wang X, Piatak M, Lifson J, Roederer M, Veazey R, Mattapallil JJ. 2009. Alpha4(+)beta7(hi)CD4(+) memory T cells harbor most Th-17 cells and are preferentially infected during acute SIV infection. *Mucosal Immunol* 2: 439-49
443. Rodriguez-Garcia M, Barr FD, Crist SG, Fahey JV, Wira CR. 2014. Phenotype and susceptibility to HIV infection of CD4+ Th17 cells in the human female reproductive tract. *Mucosal Immunol* 7: 1375-85
444. Ortiz AM, Klase ZA, DiNapoli SR, Vujkovic-Cvijin I, Carmack K, Perkins MR, Calantone N, Vinton CL, Riddick NE, Gallagher J, Klatt NR, McCune JM, Estes JD, Paiardini M, Brenchley JM. 2015. IL-21 and probiotic therapy improve Th17 frequencies, microbial translocation, and microbiome in ARV-treated, SIV-infected macaques. *Mucosal Immunol*
445. Mavigner M, Cazabat M, Dubois M, L'Faqihi FE, Requena M, Pasquier C, Klopp P, Amar J, Alric L, Barange K, Vinel JP, Marchou B, Massip P, Izopet J, Delobel P. 2012. Altered CD4+ T cell homing to the gut impairs mucosal immune reconstitution in treated HIV-infected individuals. *J Clin Invest* 122: 62-9
446. Favre D, Lederer S, Kanwar B, Ma ZM, Proll S, Kasakow Z, Mold J, Swainson L, Barbour JD, Baskin CR, Palermo R, Pandrea I, Miller CJ, Katze MG, McCune JM. 2009. Critical loss of the balance between Th17 and T regulatory cell populations in pathogenic SIV infection. *PLoS Pathog* 5: e1000295
447. Loiseau C, Requena M, Mavigner M, Cazabat M, Carrere N, Suc B, Barange K, Alric L, Marchou B, Massip P, Izopet J, Delobel P. 2016. CCR6- regulatory T cells blunt the restoration of gut Th17 cells along the CCR6-CCL20 axis in treated HIV-1-infected individuals. *Mucosal Immunol*
448. Kanwar B, Favre D, McCune JM. 2010. Th17 and regulatory T cells: implications for AIDS pathogenesis. *Curr Opin HIV AIDS* 5: 151-7
449. De Luca A, Montagnoli C, Zelante T, Bonifazi P, Bozza S, Moretti S, D'Angelo C, Vacca C, Boon L, Bistoni F, Puccetti P, Fallarino F, Romani L. 2007. Functional yet balanced reactivity to Candida albicans requires TRIF, MyD88, and IDO-dependent inhibition of Rorc. *J Immunol* 179: 5999-6008
450. Romani L, Fallarino F, De Luca A, Montagnoli C, D'Angelo C, Zelante T, Vacca C, Bistoni F, Fioretti MC, Grohmann U, Segal BH, Puccetti P. 2008. Defective tryptophan catabolism underlies inflammation in mouse chronic granulomatous disease. *Nature* 451: 211-5

451. Favre D, Mold J, Hunt PW, Kanwar B, Loke P, Seu L, Barbour JD, Lowe MM, Jayawardene A, Aweeka F, Huang Y, Douek DC, Brenchley JM, Martin JN, Hecht FM, Deeks SG, McCune JM. 2010. Tryptophan catabolism by indoleamine 2,3-dioxygenase 1 alters the balance of TH17 to regulatory T cells in HIV disease. *Sci Transl Med* 2: 32ra6
452. Brandt L, Benfield T, Mens H, Clausen LN, Katzenstein TL, Fomsgaard A, Karlsson I. 2011. Low level of regulatory T cells and maintenance of balance between regulatory T cells and TH17 cells in HIV-1-infected elite controllers. *J Acquir Immune Defic Syndr* 57: 101-8
453. Moutsopoulos NM, Vazquez N, Greenwell-Wild T, Ecevit I, Horn J, Orenstein J, Wahl SM. 2006. Regulation of the tonsil cytokine milieu favors HIV susceptibility. *J Leukoc Biol* 80: 1145-55
454. Bixler SL, Sandler NG, Douek DC, Mattapallil JJ. 2013. Suppressed Th17 levels correlate with elevated PIAS3, SHP2, and SOCS3 expression in CD4 T cells during acute simian immunodeficiency virus infection. *J Virol* 87: 7093-101
455. Kim CJ, McKinnon LR, Kovacs C, Kandel G, Huibner S, Chege D, Shahabi K, Benko E, Loutfy M, Ostrowski M, Kaul R. 2013. Mucosal Th17 cell function is altered during HIV infection and is an independent predictor of systemic immune activation. *J Immunol* 191: 2164-73
456. Chege D, Sheth PM, Kain T, Kim CJ, Kovacs C, Loutfy M, Halpenny R, Kandel G, Chun TW, Ostrowski M, Kaul R, Toronto Mucosal Immunology G. 2011. Sigmoid Th17 populations, the HIV latent reservoir, and microbial translocation in men on long-term antiretroviral therapy. *AIDS* 25: 741-9
457. Gaardbo JC, Hartling HJ, Gerstoft J, Nielsen SD. 2012. Incomplete immune recovery in HIV infection: mechanisms, relevance for clinical care, and possible solutions. *Clin Dev Immunol* 2012: 670957
458. He Y, Li J, Zheng Y, Luo Y, Zhou H, Yao Y, Chen X, Chen Z, He M. 2012. A randomized case-control study of dynamic changes in peripheral blood Th17/Treg cell balance and interleukin-17 levels in highly active antiretroviral-treated HIV type 1/AIDS patients. *AIDS Res Hum Retroviruses* 28: 339-45
459. Macal M, Sankaran S, Chun TW, Reay E, Flamm J, Prindiville TJ, Dandekar S. 2008. Effective CD4+ T-cell restoration in gut-associated lymphoid tissue of HIV-infected patients is associated with enhanced Th17 cells and polyfunctional HIV-specific T-cell responses. *Mucosal Immunol* 1: 475-88
460. Schuetz A, Deleage C, Sereti I, Rerknimitr R, Phanuphak N, Phuang-Ngern Y, Estes JD, Sandler NG, Sukhumvittaya S, Marovich M, Jongrakthaitae S, Akapirat S, Fletscher JL, Kroon E, Dewar R, Trichavaroj R, Chomchey N, Douek DC, RJ OC, Ngauy V, Robb ML, Phanuphak P, Michael NL, Excler JL, Kim JH, de Souza MS, Ananworanich J, Rv254/Search, Groups RSS. 2014. Initiation of ART during early acute HIV infection preserves mucosal Th17 function and reverses HIV-related immune activation. *PLoS Pathog* 10: e1004543
461. Klatt NR, Funderburg NT, Brenchley JM. 2013. Microbial translocation, immune activation, and HIV disease. *Trends Microbiol* 21: 6-13
462. Gonzalez-Hernandez LA, Jave-Suarez LF, Fafutis-Morris M, Montes-Salcedo KE, Valle-Gutierrez LG, Campos-Loza AE, Enciso-Gomez LF, Andrade-Villanueva JF. 2012. Synbiotic therapy decreases microbial translocation and inflammation and improves immunological status in HIV-infected patients: a double-blind randomized controlled pilot trial. *Nutr J* 11: 90

463. Klatt NR, Estes JD, Sun X, Ortiz AM, Barber JS, Harris LD, Cervasi B, Yokomizo LK, Pan L, Vinton CL, Tabb B, Canary LA, Dang Q, Hirsch VM, Alter G, Belkaid Y, Lifson JD, Silvestri G, Milner JD, Paiardini M, Haddad EK, Brenchley JM. 2012. Loss of mucosal CD103+ DCs and IL-17+ and IL-22+ lymphocytes is associated with mucosal damage in SIV infection. *Mucosal Immunol* 5: 646-57
464. Mercer F, Khaitan A, Kozhaya L, Aberg JA, Unutmaz D. 2014. Differentiation of IL-17-producing effector and regulatory human T cells from lineage-committed naive precursors. *J Immunol* 193: 1047-54
465. Patel DD, Kuchroo VK. 2015. Th17 Cell Pathway in Human Immunity: Lessons from Genetics and Therapeutic Interventions. *Immunity* 43: 1040-51
466. de Repentigny L, Goupil M, Jolicoeur P. 2015. Oropharyngeal Candidiasis in HIV Infection: Analysis of Impaired Mucosal Immune Response to Candida albicans in Mice Expressing the HIV-1 Transgene. *Pathogens* 4: 406-21
467. Gosselin A, Wiche Salinas TR, Planas D, Wacleche VS, Zhang Y, Fromentin R, Chomont N, Cohen EA, Shacklett B, Mehraj V, Ghali MP, Routy JP, Ancuta P. 2016. HIV persists in CCR6+CD4+ T-cells from colon and blood during antiretroviral therapy. *AIDS*
468. Cianfriglia M, Dupuis ML, Molinari A, Verdoliva A, Costi R, Galluzzo CM, Andreotti M, Cara A, Di Santo R, Palmisano L. 2007. HIV-1 integrase inhibitors are substrates for the multidrug transporter MDR1-P-glycoprotein. *Retrovirology* 4: 17
469. Srinivas RV, Middlemas D, Flynn P, Fridland A. 1998. Human immunodeficiency virus protease inhibitors serve as substrates for multidrug transporter proteins MDR1 and MRP1 but retain antiviral efficacy in cell lines expressing these transporters. *Antimicrob Agents Chemother* 42: 3157-62
470. Wacleche VS, Goulet JP, Gosselin A, Monteiro P, Soudeyns H, Fromentin R, Jenabian MA, Vartanian S, Deeks SG, Chomont N, Routy JP, Ancuta P. 2016. New insights into the heterogeneity of Th17 subsets contributing to HIV-1 persistence during antiretroviral therapy. *Retrovirology* 13: 59
471. Ziegler-Heitbrock L. 2014. Reprint of: Monocyte subsets in man and other species. *Cell Immunol* 291: 11-5
472. Ginhoux F, Jung S. 2014. Monocytes and macrophages: developmental pathways and tissue homeostasis. *Nat Rev Immunol* 14: 392-404
473. Williams MJ. 2007. Drosophila hemopoiesis and cellular immunity. *J Immunol* 178: 4711-6
474. Serbina NV, Jia T, Hohl TM, Pamer EG. 2008. Monocyte-mediated defense against microbial pathogens. *Annu Rev Immunol* 26: 421-52
475. Saha P, Geissmann F. 2011. Toward a functional characterization of blood monocytes. *Immunol Cell Biol* 89: 2-4
476. Nahrendorf M, Swirski FK, Aikawa E, Stangenberg L, Wurdinger T, Figueiredo JL, Libby P, Weissleder R, Pittet MJ. 2007. The healing myocardium sequentially mobilizes two monocyte subsets with divergent and complementary functions. *J Exp Med* 204: 3037-47
477. Geissmann F, Manz MG, Jung S, Sieweke MH, Merad M, Ley K. 2010. Development of monocytes, macrophages, and dendritic cells. *Science* 327: 656-61
478. Anbazhagan K, Duroux-Richard I, Jorgensen C, Apparailly F. 2014. Transcriptomic network support distinct roles of classical and non-classical monocytes in human. *Int Rev Immunol* 33: 470-89

479. Auffray C, Sieweke MH, Geissmann F. 2009. Blood Monocytes: Development, Heterogeneity, and Relationship with Dendritic Cells. *Annu Rev Immunol*
480. Mildner A, Schmidt H, Nitsche M, Merkler D, Hanisch UK, Mack M, Heikenwalder M, Bruck W, Priller J, Prinz M. 2007. Microglia in the adult brain arise from Ly-6ChiCCR2+ monocytes only under defined host conditions. *Nat Neurosci* 10: 1544-53
481. Epelman S, Lavine KJ, Beaudin AE, Sojka DK, Carrero JA, Calderon B, Brija T, Gautier EL, Ivanov S, Satpathy AT, Schilling JD, Schwendener R, Sergin I, Razani B, Forsberg EC, Yokoyama WM, Unanue ER, Colonna M, Randolph GJ, Mann DL. 2014. Embryonic and adult-derived resident cardiac macrophages are maintained through distinct mechanisms at steady state and during inflammation. *Immunity* 40: 91-104
482. Jakubzick C, Gautier EL, Gibbings SL, Sojka DK, Schlitzer A, Johnson TE, Ivanov S, Duan Q, Bala S, Condon T, van Rooijen N, Grainger JR, Belkaid Y, Ma'ayan A, Riches DW, Yokoyama WM, Ginhoux F, Henson PM, Randolph GJ. 2013. Minimal differentiation of classical monocytes as they survey steady-state tissues and transport antigen to lymph nodes. *Immunity* 39: 599-610
483. Qu C, Brinck-Jensen NS, Zang M, Chen K. 2014. Monocyte-derived dendritic cells: targets as potent antigen-presenting cells for the design of vaccines against infectious diseases. *Int J Infect Dis* 19: 1-5
484. Passlick B, Flieger D, Ziegler-Heitbrock HW. 1989. Identification and characterization of a novel monocyte subpopulation in human peripheral blood. *Blood* 74: 2527-34.
485. Ziegler-Heitbrock L, Ancuta P, Crowe S, Dalod M, Grau V, Hart DN, Leenen PJ, Liu YJ, MacPherson G, Randolph GJ, Scherberich J, Schmitz J, Shortman K, Sozzani S, Strobl H, Zembala M, Austyn JM, Lutz MB. 2010. Nomenclature of monocytes and dendritic cells in blood. *Blood* 116: e74-80
486. Lauvau G, Chorro L, Spaulding E, Soudja SM. 2014. Inflammatory monocyte effector mechanisms. *Cell Immunol* 291: 32-40
487. Murphy K, Travers P, Walport M, Janeway C. 2012. *Janeway's immunobiology*. New York: Garland Science. xix, 868 p. pp.
488. Mandelboim O, Malik P, Davis DM, Jo CH, Boyson JE, Strominger JL. 1999. Human CD16 as a lysis receptor mediating direct natural killer cell cytotoxicity. *Proc Natl Acad Sci U S A* 96: 5640-4
489. Ziegler-Heitbrock L, Hofer TP. 2013. Toward a refined definition of monocyte subsets. *Front Immunol* 4: 23
490. Weber C, Belge KU, von Hundelshausen P, Draude G, Steppich B, Mack M, Frankenberger M, Weber KS, Ziegler-Heitbrock HW. 2000. Differential chemokine receptor expression and function in human monocyte subpopulations. *J Leukoc Biol* 67: 699-704.
491. Ancuta P, Rao R, Moses A, Mehle A, Shaw SK, Luscinskas FW, Gabuzda D. 2003. Fractalkine preferentially mediates arrest and migration of CD16+ monocytes. *J Exp Med* 197: 1701-7.
492. Geissmann F, Jung S, Littman DR. 2003. Blood monocytes consist of two principal subsets with distinct migratory properties. *Immunity* 19: 71-82.
493. Ancuta P, Moses A, Gabuzda D. 2004. Transendothelial migration of CD16+ monocytes in response to fractalkine under constitutive and inflammatory conditions. *Immunobiology* 209: 11-20

494. Ancuta P, Kunstman KJ, Autissier P, Zaman T, Stone D, Wolinsky SM, Gabuzda D. 2006. CD16+ monocytes exposed to HIV promote highly efficient viral replication upon differentiation into macrophages and interaction with T cells. *Virology.* 344: 267-76.
495. Ancuta P, Liu KY, Misra V, Wacleche VS, Gosselin A, Zhou X, Gabuzda D. 2009. Transcriptional profiling reveals developmental relationship and distinct biological functions of CD16+ and CD16- monocyte subsets. *BMC Genomics* 10: 403
496. Gordon S, Taylor PR. 2005. Monocyte and macrophage heterogeneity. *Nat Rev Immunol.* 5: 953-64.
497. Auffray C, Fogg D, Garfa M, Elain G, Join-Lambert O, Kayal S, Sarnacki S, Cumano A, Lauvau G, Geissmann F. 2007. Monitoring of blood vessels and tissues by a population of monocytes with patrolling behavior. *Science* 317: 666-70
498. Belge KU, Dayyani F, Horelt A, Siedlar M, Frankenberger M, Frankenberger B, Espevik T, Ziegler-Heitbrock L. 2002. The Proinflammatory CD14(+)CD16(+)DR(++) Monocytes Are a Major Source of TNF. *J Immunol* 168: 3536-42.
499. Thieblemont N, Weiss L, Sadeghi HM, Estcourt C, Haeffner-Cavaillon N. 1995. CD14lowCD16high: a cytokine-producing monocyte subset which expands during human immunodeficiency virus infection. *Eur J Immunol* 25: 3418-24.
500. Shalova IN, Kajiji T, Lim JY, Gomez-Pina V, Fernandez-Ruiz I, Arnalich F, Iau PT, Lopez-Collazo E, Wong SC, Biswas SK. 2012. CD16 regulates TRIF-dependent TLR4 response in human monocytes and their subsets. *J Immunol* 188: 3584-93
501. Hofer TP, Zawada AM, Frankenberger M, Skokann K, Satzl AA, Gesierich W, Schuberth M, Levin J, Danek A, Rotter B, Heine GH, Ziegler-Heitbrock L. 2015. Characterization of subsets of the CD16-positive monocytes: impact of granulomatous inflammation and M-CSF-receptor mutation. *Blood*
502. Siedlar M, Frankenberger M, Ziegler-Heitbrock LH, Belge KU. 2000. The M-DC8-positive leukocytes are a subpopulation of the CD14+ CD16+ monocytes. *Immunobiology* 202: 11-7.
503. Schakel K, Kannagi R, Kniep B, Goto Y, Mitsuoka C, Zwirner J, Soruri A, von Kietzell M, Rieber E. 2002. 6-Sulfo LacNAc, a novel carbohydrate modification of PSGL-1, defines an inflammatory type of human dendritic cells. *Immunity* 17: 289-301.
504. Johansson MW. 2014. Activation states of blood eosinophils in asthma. *Clin Exp Allergy* 44: 482-98
505. Dutertre CA, Amraoui S, DeRosa A, Jourdain JP, Vimeux L, Goguet M, Degrelle S, Feuillet V, Liovat AS, Muller-Trutwin M, Decroix N, Deveau C, Meyer L, Goujard C, Loulergue P, Launay O, Richard Y, Hosmalin A. 2012. Pivotal role of M-DC8(+) monocytes from viremic HIV-infected patients in TNFalpha overproduction in response to microbial products. *Blood* 120: 2259-68
506. Steppich B, Dayyani F, Gruber R, Lorenz R, Mack M, Ziegler-Heitbrock HW. 2000. Selective mobilization of CD14(+)CD16(+) monocytes by exercise. *Am J Physiol Cell Physiol* 279: C578-86.
507. Wong KL, Tai JJ, Wong WC, Han H, Sem X, Yeap WH, Kourilsky P, Wong SC. 2011. Gene expression profiling reveals the defining features of the classical, intermediate, and nonclassical human monocyte subsets. *Blood* 118: e16-31
508. Zawada AM, Rogacev KS, Rotter B, Winter P, Marell RR, Fliser D, Heine GH. 2011. SuperSAGE evidence for CD14++CD16+ monocytes as a third monocyte subset. *Blood* 118: e50-61

509. Shantsila E, Wrigley B, Tapp L, Apostolakis S, Montoro-Garcia S, Drayson MT, Lip GY. 2011. Immunophenotypic characterization of human monocyte subsets: possible implications for cardiovascular disease pathophysiology. *J Thromb Haemost* 9: 1056-66
510. Buechler C, Ritter M, Orso E, Langmann T, Klucken J, Schmitz G. 2000. Regulation of scavenger receptor CD163 expression in human monocytes and macrophages by pro- and antiinflammatory stimuli. *J Leukoc Biol* 67: 97-103
511. Murdoch C, Tazzyman S, Webster S, Lewis CE. 2007. Expression of Tie-2 by human monocytes and their responses to angiopoietin-2. *J Immunol* 178: 7405-11
512. Coffelt SB, Tal AO, Scholz A, De Palma M, Patel S, Urbich C, Biswas SK, Murdoch C, Plate KH, Reiss Y, Lewis CE. 2010. Angiopoietin-2 regulates gene expression in TIE2-expressing monocytes and augments their inherent proangiogenic functions. *Cancer Res* 70: 5270-80
513. Skrzeczynska-Moncznik J, Bzowska M, Loseke S, Grage-Griebenow E, Zembala M, Pryjma J. 2008. Peripheral blood CD14high CD16+ monocytes are main producers of IL-10. *Scand J Immunol* 67: 152-9
514. Schakel K, von Kietzell M, Hansel A, Ebling A, Schulze L, Haase M, Semmler C, Sarfati M, Barclay AN, Randolph GJ, Meurer M, Rieber EP. 2006. Human 6-sulfo LacNAc-expressing dendritic cells are principal producers of early interleukin-12 and are controlled by erythrocytes. *Immunity* 24: 767-77
515. Geissmann F, Revy P, Brousse N, Lepelletier Y, Folli C, Durandy A, Chambon P, Dy M. 2003. Retinoids regulate survival and antigen presentation by immature dendritic cells. *J Exp Med* 198: 623-34.
516. Carlin LM, Stamatiades EG, Auffray C, Hanna RN, Glover L, Vizcay-Barrena G, Hedrick CC, Cook HT, Diebold S, Geissmann F. 2013. Nr4a1-dependent Ly6C(low) monocytes monitor endothelial cells and orchestrate their disposal. *Cell* 153: 362-75
517. Nguyen KD, Fentress SJ, Qiu Y, Yun K, Cox JS, Chawla A. 2013. Circadian gene Bmal1 regulates diurnal oscillations of Ly6C(hi) inflammatory monocytes. *Science* 341: 1483-8
518. Weiner LM, Li W, Holmes M, Catalano RB, Dovnarsky M, Padavic K, Alpaugh RK. 1994. Phase I trial of recombinant macrophage colony-stimulating factor and recombinant gamma-interferon: toxicity, monocytosis, and clinical effects. *Cancer Res* 54: 4084-90
519. Sunderkotter C, Nikolic T, Dillon MJ, Van Rooijen N, Stehling M, Drevets DA, Leenen PJ. 2004. Subpopulations of mouse blood monocytes differ in maturation stage and inflammatory response. *J Immunol* 172: 4410-7
520. Gama L, Shirk EN, Russell JN, Carvalho KI, Li M, Queen SE, Kalil J, Zink MC, Clements JE, Kallas EG. 2012. Expansion of a subset of CD14highCD16negCCR2low/neg monocytes functionally similar to myeloid-derived suppressor cells during SIV and HIV infection. *J Leukoc Biol* 91: 803-16
521. Allen JB, Wong HL, Guyre PM, Simon GL, Wahl SM. 1991. Association of circulating receptor Fc gamma RIII-positive monocytes in AIDS patients with elevated levels of transforming growth factor-beta. *J Clin Invest* 87: 1773-9
522. Dunne J, Feighery C, Whelan A. 1996. Beta-2-microglobulin, neopterin and monocyte Fc gamma receptors in opportunistic infections of HIV-positive patients. *Br J Biomed Sci* 53: 263-9
523. Vehmas A, Lieu J, Pardo CA, McArthur JC, Gartner S. 2004. Amyloid precursor protein expression in circulating monocytes and brain macrophages from patients with HIV-associated cognitive impairment. *J Neuroimmunol* 157: 99-110

524. Amirayan-Chevillard N, Tissot-Dupont H, Capo C, Brunet C, Dignat-George F, Obadia Y, Gallais H, Mege JL. 2000. Impact of highly active anti-retroviral therapy (HAART) on cytokine production and monocyte subsets in HIV-infected patients. *Clin Exp Immunol* 120: 107-12.
525. Pulliam L, Gascon R, Stubblebine M, McGuire D, McGrath MS. 1997. Unique monocyte subset in patients with AIDS dementia. *Lancet* 349: 692-5.
526. Buckner CM, Calderon TM, Willams DW, Belbin TJ, Berman JW. 2011. Characterization of monocyte maturation/differentiation that facilitates their transmigration across the blood-brain barrier and infection by HIV: implications for NeuroAIDS. *Cell Immunol* 267: 109-23
527. Williams DW, Eugenin EA, Calderon TM, Berman JW. 2012. Monocyte maturation, HIV susceptibility, and transmigration across the blood brain barrier are critical in HIV neuropathogenesis. *J Leukoc Biol* 91: 401-15
528. Hearps AC, Maisa A, Cheng WJ, Angelovich TA, Lichtfuss GF, Palmer CS, Landay AL, Jaworowski A, Crowe SM. 2012. HIV infection induces age-related changes to monocytes and innate immune activation in young men that persist despite combination antiretroviral therapy. *AIDS* 26: 843-53
529. Jaworowski A, Ellery P, Maslin CL, Naim E, Heinlein AC, Ryan CE, Paukovics G, Hocking J, Sonza S, Crowe SM. 2006. Normal CD16 expression and phagocytosis of Mycobacterium avium complex by monocytes from a current cohort of HIV-1-infected patients. *J Infect Dis* 193: 693-7
530. Jaworowski A, Kamwendo DD, Ellery P, Sonza S, Mwapasa V, Tadesse E, Molyneux ME, Rogerson SJ, Meshnick SR, Crowe SM. 2007. CD16+ monocyte subset preferentially harbors HIV-1 and is expanded in pregnant malawian women with plasmodium falciparum malaria and HIV-1 infection. *J Infect Dis* 196: 38-42
531. Moniuszko M, Liyanage NP, Doster MN, Parks RW, Grubczak K, Lipinska D, McKinnon K, Brown C, Hirsch V, Vaccari M, Gordon S, Pegu P, Fenizia C, Flisiak R, Grzeszczuk A, Dabrowska M, Robert-Guroff M, Silvestri G, Stevenson M, McCune J, Franchini G. 2015. Glucocorticoid treatment at moderate doses of SIVmac251-infected rhesus macaques decreases the frequency of circulating CD14+CD16++ monocytes but does not alter the tissue virus reservoir. *AIDS Res Hum Retroviruses* 31: 115-26
532. Ansari AW, Meyer-Olson D, Schmidt RE. 2013. Selective expansion of pro-inflammatory chemokine CCL2-loaded CD14+CD16+ monocytes subset in HIV-infected therapy naive individuals. *J Clin Immunol* 33: 302-6
533. Williams DW, Byrd D, Rubin LH, Anastos K, Morgello S, Berman JW. 2014. CCR2 on CD14(+)CD16(+) monocytes is a biomarker of HIV-associated neurocognitive disorders. *Neurol Neuroimmunol Neuroinflamm* 1: e36
534. Williams DW, Calderon TM, Lopez L, Carvallo-Torres L, Gaskill PJ, Eugenin EA, Morgello S, Berman JW. 2013. Mechanisms of HIV entry into the CNS: increased sensitivity of HIV infected CD14+CD16+ monocytes to CCL2 and key roles of CCR2, JAM-A, and ALCAM in diapedesis. *PLoS One* 8: e69270
535. Fischer-Smith T, Tedaldi EM, Rappaport J. 2008. CD163/CD16 coexpression by circulating monocytes/macrophages in HIV: potential biomarkers for HIV infection and AIDS progression. *AIDS Res Hum Retroviruses* 24: 417-21
536. Wilson EM, Singh A, Hullsiek KH, Gibson D, Henry WK, Lichtenstein K, Onen NF, Kojic E, Patel P, Brooks JT, Sereti I, Baker JV, Study to Understand the Natural History

of HIVAitEoETI. 2014. Monocyte-activation phenotypes are associated with biomarkers of inflammation and coagulation in chronic HIV infection. *J Infect Dis* 210: 1396-406
537. Kim WK, Sun Y, Do H, Autissier P, Halpern EF, Piatak M, Jr., Lifson JD, Burdo TH, McGrath MS, Williams K. 2010. Monocyte heterogeneity underlying phenotypic changes in monocytes according to SIV disease stage. *J Leukoc Biol* 87: 557-67
538. Ndhlovu LC, Umaki T, Chew GM, Chow DC, Agsalda M, Kallianpur KJ, Paul R, Zhang G, Ho E, Hanks N, Nakamoto B, Shiramizu BT, Shikuma CM. 2014. Treatment intensification with maraviroc (CCR5 antagonist) leads to declines in CD16-expressing monocytes in cART-suppressed chronic HIV-infected subjects and is associated with improvements in neurocognitive test performance: implications for HIV-associated neurocognitive disease (HAND). *J Neurovirol* 20: 571-82
539. Manuzak JA, Dillon SM, Lee EJ, Dong ZM, Hecht DK, Wilson CC. 2013. Increased Escherichia coli-induced interleukin-23 production by CD16+ monocytes correlates with systemic immune activation in untreated HIV-1-infected individuals. *J Virol* 87: 13252-62
540. Munsaka SM, Agsalda M, Troelstrup D, Hu N, Yu Q, Shiramizu B. 2009. Characteristics of Activated Monocyte Phenotype Support R5-Tropic Human Immunodeficiency Virus. *Immunol Immunogenet Insights* 1: 15-20
541. Ellery PJ, Tippett E, Chiu YL, Paukovics G, Cameron PU, Solomon A, Lewin SR, Gorry PR, Jaworowski A, Greene WC, Sonza S, Crowe SM. 2007. The CD16+ monocyte subset is more permissive to infection and preferentially harbors HIV-1 in vivo. *J Immunol* 178: 6581-9
542. McElrath MJ, Pruett JE, Cohn ZA. 1989. Mononuclear phagocytes of blood and bone marrow: comparative roles as viral reservoirs in human immunodeficiency virus type 1 infections. *Proc Natl Acad Sci U S A* 86: 675-9.
543. Triques K, Stevenson M. 2004. Characterization of restrictions to human immunodeficiency virus type 1 infection of monocytes. *J Virol* 78: 5523-7.
544. Arfi V, Riviere L, Jarrosson-Wuilleme L, Goujon C, Rigal D, Darlix JL, Cimarelli A. 2008. Characterization of the early steps of infection of primary blood monocytes by human immunodeficiency virus type 1. *J Virol* 82: 6557-65
545. Coleman CM, Wu L. 2009. HIV interactions with monocytes and dendritic cells: viral latency and reservoirs. *Retrovirology* 6: 51
546. Sonza S, Maerz A, Deacon N, Meanger J, Mills J, Crowe S. 1996. Human immunodeficiency virus type 1 replication is blocked prior to reverse transcription and integration in freshly isolated peripheral blood monocytes. *J Virol* 70: 3863-9.
547. Naif HM, Li S, Alali M, Sloane A, Wu L, Kelly M, Lynch G, Lloyd A, Cunningham AL. 1998. CCR5 expression correlates with susceptibility of maturing monocytes to human immunodeficiency virus type 1 infection. *J Virol* 72: 830-6
548. Tuttle DL, Harrison JK, Anders C, Sleasman JW, Goodenow MM. 1998. Expression of CCR5 increases during monocyte differentiation and directly mediates macrophage susceptibility to infection by human immunodeficiency virus type 1. *J Virol* 72: 4962-9
549. Ancuta P, Autissier P, Wurcel A, Zaman T, Stone D, Gabuzda D. 2006. CD16+ Monocyte-Derived Macrophages Activate Resting T Cells for HIV Infection by Producing CCR3 and CCR4 Ligands. *J Immunol.* 176: 5760-71.
550. Saphire AC, Bobardt MD, Zhang Z, David G, Gallay PA. 2001. Syndecans serve as attachment receptors for human immunodeficiency virus type 1 on macrophages. *J Virol* 75: 9187-200.

551. Bozzini S, Falcone V, Conaldi PG, Visai L, Biancone L, Dolei A, Toniolo A, Speziale P. 1998. Heparin-binding domain of human fibronectin binds HIV-1 gp120/160 and reduces virus infectivity. *J Med Virol* 54: 44-53
552. Williams DW, Veenstra M, Gaskill PJ, Morgello S, Calderon TM, Berman JW. 2014. Monocytes mediate HIV neuropathogenesis: mechanisms that contribute to HIV associated neurocognitive disorders. *Curr HIV Res* 12: 85-96
553. Gartner S. 2000. HIV infection and dementia. *Science* 287: 602-4.
554. Ances BM, Ellis RJ. 2007. Dementia and neurocognitive disorders due to HIV-1 infection. *Semin Neurol* 27: 86-92
555. Davis LE, Hjelle BL, Miller VE, Palmer DL, Llewellyn AL, Merlin TL, Young SA, Mills RG, Wachsman W, Wiley CA. 1992. Early viral brain invasion in iatrogenic human immunodeficiency virus infection. *Neurology* 42: 1736-9
556. Valcour VG, Shiramizu BT, Shikuma CM. 2010. HIV DNA in circulating monocytes as a mechanism to dementia and other HIV complications. *J Leukoc Biol* 87: 621-6
557. Pereira CF, Middel J, Jansen G, Verhoef J, Nottet HS. 2001. Enhanced expression of fractalkine in HIV-1 associated dementia. *J Neuroimmunol* 115: 168-75.
558. Fischer-Smith T, Croul S, Sverstiuk AE, Capini C, L'Heureux D, Regulier EG, Richardson MW, Amini S, Morgello S, Khalili K, Rappaport J. 2001. CNS invasion by CD14+/CD16+ peripheral blood-derived monocytes in HIV dementia: perivascular accumulation and reservoir of HIV infection. *J Neurovirol* 7: 528-41.
559. Fischer-Smith T, Croul S, Adeniyi A, Rybicka K, Morgello S, Khalili K, Rappaport J. 2004. Macrophage/microglial accumulation and proliferating cell nuclear antigen expression in the central nervous system in human immunodeficiency virus encephalopathy. *Am J Pathol.* 164: 2089-99.
560. Kumar A, Abbas W, Herbein G. 2014. HIV-1 latency in monocytes/macrophages. *Viruses* 6: 1837-60
561. Spudich S, Gonzalez-Scarano F. 2012. HIV-1-related central nervous system disease: current issues in pathogenesis, diagnosis, and treatment. *Cold Spring Harb Perspect Med* 2: a007120
562. Yadav A, Collman RG. 2009. CNS inflammation and macrophage/microglial biology associated with HIV-1 infection. *J Neuroimmune Pharmacol* 4: 430-47
563. Way KJ, Dinh H, Keene MR, White KE, Clanchy FI, Lusby P, Roiniotis J, Cook AD, Cassady AI, Curtis DJ, Hamilton JA. 2009. The generation and properties of human macrophage populations from hemopoietic stem cells. *J Leukoc Biol* 85: 766-78
564. Wang KX, Denhardt DT. 2008. Osteopontin: role in immune regulation and stress responses. *Cytokine Growth Factor Rev* 19: 333-45
565. Burdo TH, Ellis RJ, Fox HS. 2008. Osteopontin is increased in HIV-associated dementia. *J Infect Dis* 198: 715-22
566. Burdo TH, Wood MR, Fox HS. 2007. Osteopontin prevents monocyte recirculation and apoptosis. *J Leukoc Biol* 81: 1504-11
567. Burdo TH, Soulas C, Orzechowski K, Button J, Krishnan A, Sugimoto C, Alvarez X, Kuroda MJ, Williams KC. 2010. Increased monocyte turnover from bone marrow correlates with severity of SIV encephalitis and CD163 levels in plasma. *PLoS Pathog* 6: e1000842
568. Rowley DA, Fitch FW. 2012. The road to the discovery of dendritic cells, a tribute to Ralph Steinman. *Cell Immunol* 273: 95-8

569. Mishell RI, Dutton RW. 1967. Immunization of dissociated spleen cell cultures from normal mice. *J Exp Med* 126: 423-42
570. Steinman RM, Witmer MD. 1978. Lymphoid dendritic cells are potent stimulators of the primary mixed leukocyte reaction in mice. *Proc Natl Acad Sci U S A* 75: 5132-6
571. Steinman RM. 2007. Dendritic cells: understanding immunogenicity. *Eur J Immunol* 37 Suppl 1: S53-60
572. Banchereau J, Cohn F, Inaba K, Muller B, Mellman I, Nathan C, Nussenzweig M, O'Garra A, Seder B, Schuler G, Sher A. 2011. Remembering Ralph Steinman. *J Exp Med* 208: 2343-7
573. Mellman I, Nussenzweig M. 2011. Retrospective. Ralph M. Steinman (1943-2011). *Science* 334: 466
574. Galicia G, Gommerman JL. 2014. Plasmacytoid dendritic cells and autoimmune inflammation. *Biol Chem* 395: 335-46
575. Crozat K, Guiton R, Guilliams M, Henri S, Baranek T, Schwartz-Cornil I, Malissen B, Dalod M. 2010. Comparative genomics as a tool to reveal functional equivalences between human and mouse dendritic cell subsets. *Immunol Rev* 234: 177-98
576. Dalod M, Chelbi R, Malissen B, Lawrence T. 2014. Dendritic cell maturation: functional specialization through signaling specificity and transcriptional programming. *EMBO J* 33: 1104-16
577. Merad M, Sathe P, Helft J, Miller J, Mortha A. 2013. The dendritic cell lineage: ontogeny and function of dendritic cells and their subsets in the steady state and the inflamed setting. *Annu Rev Immunol* 31: 563-604
578. Di Pucchio T, Chatterjee B, Smed-Sorensen A, Clayton S, Palazzo A, Montes M, Xue Y, Mellman I, Banchereau J, Connolly JE. 2008. Direct proteasome-independent cross-presentation of viral antigen by plasmacytoid dendritic cells on major histocompatibility complex class I. *Nat Immunol* 9: 551-7
579. Yu CF, Peng WM, Oldenburg J, Hoch J, Bieber T, Limmer A, Hartmann G, Barchet W, Eis-Hubinger AM, Novak N. 2010. Human plasmacytoid dendritic cells support Th17 cell effector function in response to TLR7 ligation. *J Immunol* 184: 1159-67
580. Liu K, Victora GD, Schwickert TA, Guermonprez P, Meredith MM, Yao K, Chu FF, Randolph GJ, Rudensky AY, Nussenzweig M. 2009. In vivo analysis of dendritic cell development and homeostasis. *Science* 324: 392-7
581. Waskow C, Liu K, Darrasse-Jeze G, Guermonprez P, Ginhoux F, Merad M, Shengelia T, Yao K, Nussenzweig M. 2008. The receptor tyrosine kinase Flt3 is required for dendritic cell development in peripheral lymphoid tissues. *Nat Immunol* 9: 676-83
582. Schlitzer A, McGovern N, Ginhoux F. 2015. Dendritic cells and monocyte-derived cells: Two complementary and integrated functional systems. *Semin Cell Dev Biol* 41: 9-22
583. Crozat K, Guiton R, Contreras V, Feuillet V, Dutertre CA, Ventre E, Vu Manh TP, Baranek T, Storset AK, Marvel J, Boudinot P, Hosmalin A, Schwartz-Cornil I, Dalod M. 2010. The XC chemokine receptor 1 is a conserved selective marker of mammalian cells homologous to mouse CD8alpha+ dendritic cells. *J Exp Med* 207: 1283-92
584. Haniffa M, Shin A, Bigley V, McGovern N, Teo P, See P, Wasan PS, Wang XN, Malinarich F, Malleret B, Larbi A, Tan P, Zhao H, Poidinger M, Pagan S, Cookson S, Dickinson R, Dimmick I, Jarrett RF, Renia L, Tam J, Song C, Connolly J, Chan JK, Gehring A, Bertoletti A, Collin M, Ginhoux F. 2012. Human tissues contain CD141hi cross-presenting dendritic cells with functional homology to mouse CD103+ nonlymphoid dendritic cells. *Immunity* 37: 60-73

585. Guilliams M, Henri S, Tamoutounour S, Ardouin L, Schwartz-Cornil I, Dalod M, Malissen B. 2010. From skin dendritic cells to a simplified classification of human and mouse dendritic cell subsets. *Eur J Immunol* 40: 2089-94
586. Ohnuma K, Dang NH, Morimoto C. 2008. Revisiting an old acquaintance: CD26 and its molecular mechanisms in T cell function. *Trends Immunol* 29: 295-301
587. Matteucci E, Giampietro O. 2009. Dipeptidyl peptidase-4 (CD26): knowing the function before inhibiting the enzyme. *Curr Med Chem* 16: 2943-51
588. Watchmaker PB, Lahl K, Lee M, Baumjohann D, Morton J, Kim SJ, Zeng R, Dent A, Ansel KM, Diamond B, Hadeiba H, Butcher EC. 2014. Comparative transcriptional and functional profiling defines conserved programs of intestinal DC differentiation in humans and mice. *Nat Immunol* 15: 98-108
589. Bigley V, McGovern N, Milne P, Dickinson R, Pagan S, Cookson S, Haniffa M, Collin M. 2015. Langerin-expressing dendritic cells in human tissues are related to CD1c+ dendritic cells and distinct from Langerhans cells and CD141high XCR1+ dendritic cells. *J Leukoc Biol* 97: 627-34
590. Reynolds G, Haniffa M. 2015. Human and Mouse Mononuclear Phagocyte Networks: A Tale of Two Species? *Front Immunol* 6: 330
591. Schlitzer A, McGovern N, Teo P, Zelante T, Atarashi K, Low D, Ho AW, See P, Shin A, Wasan PS, Hoeffel G, Malleret B, Heiseke A, Chew S, Jardine L, Purvis HA, Hilkens CM, Tam J, Poidinger M, Stanley ER, Krug AB, Renia L, Sivasankar B, Ng LG, Collin M, Ricciardi-Castagnoli P, Honda K, Haniffa M, Ginhoux F. 2013. IRF4 transcription factor-dependent CD11b+ dendritic cells in human and mouse control mucosal IL-17 cytokine responses. *Immunity* 38: 970-83
592. Plantinga M, Guilliams M, Vanheerswynghels M, Deswarte K, Branco-Madeira F, Toussaint W, Vanhoutte L, Neyt K, Killeen N, Malissen B, Hammad H, Lambrecht BN. 2013. Conventional and monocyte-derived CD11b(+) dendritic cells initiate and maintain T helper 2 cell-mediated immunity to house dust mite allergen. *Immunity* 38: 322-35
593. Morelli AE, Rubin JP, Erdos G, Tkacheva OA, Mathers AR, Zahorchak AF, Thomson AW, Falo LD, Jr., Larregina AT. 2005. CD4+ T cell responses elicited by different subsets of human skin migratory dendritic cells. *J Immunol* 175: 7905-15
594. Persson EK, Uronen-Hansson H, Semmrich M, Rivollier A, Hagerbrand K, Marsal J, Gudjonsson S, Hakansson U, Reizis B, Kotarsky K, Agace WW. 2013. IRF4 transcription-factor-dependent CD103(+)CD11b(+) dendritic cells drive mucosal T helper 17 cell differentiation. *Immunity* 38: 958-69
595. Sallusto F, Lanzavecchia A. 1994. Efficient presentation of soluble antigen by cultured human dendritic cells is maintained by granulocyte/macrophage colony-stimulating factor plus interleukin 4 and downregulated by tumor necrosis factor alpha. *J Exp Med* 179: 1109-18.
596. Romani N, Gruner S, Brang D, Kampgen E, Lenz A, Trockenbacher B, Konwalinka G, Fritsch PO, Steinman RM, Schuler G. 1994. Proliferating dendritic cell progenitors in human blood. *J Exp Med* 180: 83-93.
597. Caux C, Dezutter-Dambuyant C, Schmitt D, Banchereau J. 1992. GM-CSF and TNF-alpha cooperate in the generation of dendritic Langerhans cells. *Nature* 360: 258-61
598. Segura E, Touzot M, Bohineust A, Cappuccio A, Chiocchia G, Hosmalin A, Dalod M, Soumelis V, Amigorena S. 2013. Human inflammatory dendritic cells induce Th17 cell differentiation. *Immunity* 38: 336-48

599. Coombes JL, Powrie F. 2008. Dendritic cells in intestinal immune regulation. *Nat Rev Immunol* 8: 435-46
600. Le Borgne M, Etchart N, Goubier A, Lira SA, Sirard JC, van Rooijen N, Caux C, Ait-Yahia S, Vicari A, Kaiserlian D, Dubois B. 2006. Dendritic cells rapidly recruited into epithelial tissues via CCR6/CCL20 are responsible for CD8+ T cell crosspriming in vivo. *Immunity* 24: 191-201
601. Wakim LM, Waithman J, van Rooijen N, Heath WR, Carbone FR. 2008. Dendritic cell-induced memory T cell activation in nonlymphoid tissues. *Science* 319: 198-202
602. Nakano H, Lin KL, Yanagita M, Charbonneau C, Cook DN, Kakiuchi T, Gunn MD. 2009. Blood-derived inflammatory dendritic cells in lymph nodes stimulate acute T helper type 1 immune responses. *Nat Immunol* 10: 394-402
603. Mochizuki K, Xie F, He S, Tong Q, Liu Y, Mochizuki I, Guo Y, Kato K, Yagita H, Mineishi S, Zhang Y. 2013. Delta-like ligand 4 identifies a previously uncharacterized population of inflammatory dendritic cells that plays important roles in eliciting allogeneic T cell responses in mice. *J Immunol* 190: 3772-82
604. Geissmann F, Auffray C, Palframan R, Wirrig C, Ciocca A, Campisi L, Narni-Mancinelli E, Lauvau G. 2008. Blood monocytes: distinct subsets, how they relate to dendritic cells, and their possible roles in the regulation of T-cell responses. *Immunol Cell Biol* 86: 398-408
605. Schlitzer A, Ginhoux F. 2014. Organization of the mouse and human DC network. *Curr Opin Immunol* 26: 90-9
606. Sanchez-Torres C, Garcia-Romo GS, Cornejo-Cortes MA, Rivas-Carvalho A, Sanchez-Schmitz G. 2001. CD16+ and CD16- human blood monocyte subsets differentiate in vitro to dendritic cells with different abilities to stimulate CD4+ T cells. *Int Immunol* 13: 1571-81.
607. Cheong C, Matos I, Choi JH, Dandamudi DB, Shrestha E, Longhi MP, Jeffrey KL, Anthony RM, Kluger C, Nchinda G, Koh H, Rodriguez A, Idoyaga J, Pack M, Velinzon K, Park CG, Steinman RM. 2010. Microbial stimulation fully differentiates monocytes to DC-SIGN/CD209(+) dendritic cells for immune T cell areas. *Cell* 143: 416-29
608. Randolph GJ, Sanchez-Schmitz G, Liebman RM, Schakel K. 2002. The CD16(+) (FcgammaRIII(+)) Subset of Human Monocytes Preferentially Becomes Migratory Dendritic Cells in a Model Tissue Setting. *J Exp Med* 196: 517-27.
609. Rivas-Carvalho A, Meraz-Rios MA, Santos-Argumedo L, Bajana S, Soldevila G, Moreno-Garcia ME, Sanchez-Torres C. 2004. CD16+ human monocyte-derived dendritic cells matured with different and unrelated stimuli promote similar allogeneic Th2 responses: regulation by pro- and anti-inflammatory cytokines. *Int Immunol* 16: 1251-63
610. Hansel A, Gunther C, Baran W, Bidier M, Lorenz HM, Schmitz M, Bachmann M, Dobel T, Enk AH, Schakel K. 2013. Human 6-sulfo LacNAc (slan) dendritic cells have molecular and functional features of an important pro-inflammatory cell type in lupus erythematosus. *J Autoimmun* 40: 1-8
611. Hansel A, Gunther C, Ingwersen J, Starke J, Schmitz M, Bachmann M, Meurer M, Rieber EP, Schakel K. 2011. Human slan (6-sulfo LacNAc) dendritic cells are inflammatory dermal dendritic cells in psoriasis and drive strong TH17/TH1 T-cell responses. *J Allergy Clin Immunol* 127: 787-94 e1-9
612. Robbins SH, Walzer T, Dembele D, Thibault C, Defays A, Bessou G, Xu H, Vivier E, Sellars M, Pierre P, Sharp FR, Chan S, Kastner P, Dalod M. 2008. Novel insights into the

relationships between dendritic cell subsets in human and mouse revealed by genome-wide expression profiling. *Genome Biol* 9: R17

613. Cros J, Cagnard N, Woollard K, Patey N, Zhang SY, Senechal B, Puel A, Biswas SK, Moshous D, Picard C, Jais JP, D'Cruz D, Casanova JL, Trouillet C, Geissmann F. 2010. Human CD14dim monocytes patrol and sense nucleic acids and viruses via TLR7 and TLR8 receptors. *Immunity* 33: 375-86
614. Qu C, Nguyen VA, Merad M, Randolph GJ. 2009. MHC class I/peptide transfer between dendritic cells overcomes poor cross-presentation by monocyte-derived APCs that engulf dying cells. *J Immunol* 182: 3650-9
615. Hoeffel G, Wang Y, Greter M, See P, Teo P, Malleret B, Leboeuf M, Low D, Oller G, Almeida F, Choy SH, Grisotto M, Renia L, Conway SJ, Stanley ER, Chan JK, Ng LG, Samokhvalov IM, Merad M, Ginhoux F. 2012. Adult Langerhans cells derive predominantly from embryonic fetal liver monocytes with a minor contribution of yolk sac-derived macrophages. *J Exp Med* 209: 1167-81
616. Onai N, Obata-Onai A, Schmid MA, Ohteki T, Jarrossay D, Manz MG. 2007. Identification of clonogenic common Flt3+M-CSFR+ plasmacytoid and conventional dendritic cell progenitors in mouse bone marrow. *Nat Immunol* 8: 1207-16
617. Naik SH, Sathe P, Park HY, Metcalf D, Proietto AI, Dakic A, Carotta S, O'Keeffe M, Bahlo M, Papenfuss A, Kwak JY, Wu L, Shortman K. 2007. Development of plasmacytoid and conventional dendritic cell subtypes from single precursor cells derived in vitro and in vivo. *Nat Immunol* 8: 1217-26
618. Onai N, Kurabayashi K, Hosoi-Amaike M, Toyama-Sorimachi N, Matsushima K, Inaba K, Ohteki T. 2013. A clonogenic progenitor with prominent plasmacytoid dendritic cell developmental potential. *Immunity* 38: 943-57
619. Schlitzer A, Sivakamasundari V, Chen J, Sumatoh HR, Schreuder J, Lum J, Malleret B, Zhang S, Larbi A, Zolezzi F, Renia L, Poidinger M, Naik S, Newell EW, Robson P, Ginhoux F. 2015. Identification of cDC1- and cDC2-committed DC progenitors reveals early lineage priming at the common DC progenitor stage in the bone marrow. *Nat Immunol* 16: 718-28
620. Cisse B, Caton ML, Lehner M, Maeda T, Scheu S, Locksley R, Holmberg D, Zweier C, den Hollander NS, Kant SG, Holter W, Rauch A, Zhuang Y, Reizis B. 2008. Transcription factor E2-2 is an essential and specific regulator of plasmacytoid dendritic cell development. *Cell* 135: 37-48
621. Moore AJ, Anderson MK. 2013. Dendritic cell development: a choose-your-own-adventure story. *Adv Hematol* 2013: 949513
622. Huang G, Wang Y, Chi H. 2012. Regulation of TH17 cell differentiation by innate immune signals. *Cell Mol Immunol* 9: 287-95
623. Matzinger P. 2002. The danger model: a renewed sense of self. *Science* 296: 301-5
624. Medzhitov R, Preston-Hurlburt P, Janeway CA, Jr. 1997. A human homologue of the Drosophila Toll protein signals activation of adaptive immunity. *Nature* 388: 394-7
625. Poltorak A, He X, Smirnova I, Liu MY, Van Huffel C, Du X, Birdwell D, Alejos E, Silva M, Galanos C, Freudenberg M, Ricciardi-Castagnoli P, Layton B, Beutler B. 1998. Defective LPS signaling in C3H/HeJ and C57BL/10ScCr mice: mutations in Tlr4 gene. *Science* 282: 2085-8
626. Lemaitre B, Nicolas E, Michaut L, Reichhart JM, Hoffmann JA. 1996. The dorsoventral regulatory gene cassette spatzle/Toll/cactus controls the potent antifungal response in Drosophila adults. *Cell* 86: 973-83

627. Dieu MC, Vanbervliet B, Vicari A, Bridon JM, Oldham E, Ait-Yahia S, Briere F, Zlotnik A, Lebecque S, Caux C. 1998. Selective recruitment of immature and mature dendritic cells by distinct chemokines expressed in different anatomic sites. *J Exp Med* 188: 373-86.
628. Iezzi G, Sonderegger I, Ampenberger F, Schmitz N, Marsland BJ, Kopf M. 2009. CD40-CD40L cross-talk integrates strong antigenic signals and microbial stimuli to induce development of IL-17-producing CD4+ T cells. *Proc Natl Acad Sci U S A* 106: 876-81
629. Purvis HA, Stoop JN, Mann J, Woods S, Kozijn AE, Hambleton S, Robinson JH, Isaacs JD, Anderson AE, Hilkens CM. 2010. Low-strength T-cell activation promotes Th17 responses. *Blood* 116: 4829-37
630. Kastirr I, Crosti M, Maglie S, Paroni M, Steckel B, Moro M, Pagani M, Abrignani S, Geginat J. 2015. Signal Strength and Metabolic Requirements Control Cytokine-Induced Th17 Differentiation of Uncommitted Human T Cells. *J Immunol* 195: 3617-27
631. Mele F, Basso C, Leoni C, Aschenbrenner D, Becattini S, Latorre D, Lanzavecchia A, Sallusto F, Monticelli S. 2015. ERK phosphorylation and miR-181a expression modulate activation of human memory TH17 cells. *Nat Commun* 6: 6431
632. Odobasic D, Leech MT, Xue JR, Holdsworth SR. 2008. Distinct in vivo roles of CD80 and CD86 in the effector T-cell responses inducing antigen-induced arthritis. *Immunology* 124: 503-13
633. Huang G, Wang Y, Vogel P, Kanneganti TD, Otsu K, Chi H. 2012. Signaling via the kinase p38alpha programs dendritic cells to drive TH17 differentiation and autoimmune inflammation. *Nat Immunol* 13: 152-61
634. Paulos CM, Carpenito C, Plesa G, Suhoski MM, Varela-Rohena A, Golovina TN, Carroll RG, Riley JL, June CH. 2010. The inducible costimulator (ICOS) is critical for the development of human T(H)17 cells. *Sci Transl Med* 2: 55ra78
635. Pot C, Apetoh L, Awasthi A, Kuchroo VK. 2011. Induction of regulatory Tr1 cells and inhibition of T(H)17 cells by IL-27. *Semin Immunol* 23: 438-45
636. Wilke CM, Wang L, Wei S, Kryczek I, Huang E, Kao J, Lin Y, Fang J, Zou W. 2011. Endogenous interleukin-10 constrains Th17 cells in patients with inflammatory bowel disease. *J Transl Med* 9: 217
637. Goto Y, Panea C, Nakato G, Cebula A, Lee C, Diez MG, Laufer TM, Ignatowicz L, Ivanov, II. 2014. Segmented filamentous bacteria antigens presented by intestinal dendritic cells drive mucosal Th17 cell differentiation. *Immunity* 40: 594-607
638. Atarashi K, Tanoue T, Honda K. 2010. Induction of lamina propria Th17 cells by intestinal commensal bacteria. *Vaccine* 28: 8036-8
639. van de Veerdonk FL, Marijnissen RJ, Kullberg BJ, Koenen HJ, Cheng SC, Joosten I, van den Berg WB, Williams DL, van der Meer JW, Joosten LA, Netea MG. 2009. The macrophage mannose receptor induces IL-17 in response to Candida albicans. *Cell Host Microbe* 5: 329-40
640. LeibundGut-Landmann S, Gross O, Robinson MJ, Osorio F, Slack EC, Tsoni SV, Schweighoffer E, Tybulewicz V, Brown GD, Ruland J, Reis e Sousa C. 2007. Syk- and CARD9-dependent coupling of innate immunity to the induction of T helper cells that produce interleukin 17. *Nat Immunol* 8: 630-8
641. Robinson MJ, Osorio F, Rosas M, Freitas RP, Schweighoffer E, Gross O, Verbeek JS, Ruland J, Tybulewicz V, Brown GD, Moita LF, Taylor PR, Reis e Sousa C. 2009. Dectin-2 is a Syk-coupled pattern recognition receptor crucial for Th17 responses to fungal infection. *J Exp Med* 206: 2037-51

642. Saijo S, Ikeda S, Yamabe K, Kakuta S, Ishigame H, Akitsu A, Fujikado N, Kusaka T, Kubo S, Chung SH, Komatsu R, Miura N, Adachi Y, Ohno N, Shibuya K, Yamamoto N, Kawakami K, Yamasaki S, Saito T, Akira S, Iwakura Y. 2010. Dectin-2 recognition of alpha-mannans and induction of Th17 cell differentiation is essential for host defense against Candida albicans. *Immunity* 32: 681-91
643. van Beelen AJ, Zelinkova Z, Taanman-Kueter EW, Muller FJ, Hommes DW, Zaat SA, Kapsenberg ML, de Jong EC. 2007. Stimulation of the intracellular bacterial sensor NOD2 programs dendritic cells to promote interleukin-17 production in human memory T cells. *Immunity* 27: 660-9
644. Manicassamy S, Ravindran R, Deng J, Oluoch H, Denning TL, Kasturi SP, Rosenthal KM, Evavold BD, Pulendran B. 2009. Toll-like receptor 2-dependent induction of vitamin A-metabolizing enzymes in dendritic cells promotes T regulatory responses and inhibits autoimmunity. *Nat Med* 15: 401-9
645. Gerosa F, Baldani-Guerra B, Lyakh LA, Batoni G, Esin S, Winkler-Pickett RT, Consolaro MR, De Marchi M, Giachino D, Robbiano A, Astegiano M, Sambataro A, Kastelein RA, Carra G, Trinchieri G. 2008. Differential regulation of interleukin 12 and interleukin 23 production in human dendritic cells. *J Exp Med* 205: 1447-61
646. Conforti-Andreoni C, Spreafico R, Qian HL, Riteau N, Ryffel B, Ricciardi-Castagnoli P, Mortellaro A. 2011. Uric acid-driven Th17 differentiation requires inflammasome-derived IL-1 and IL-18. *J Immunol* 187: 5842-50
647. Zaba LC, Cardinale I, Gilleaudeau P, Sullivan-Whalen M, Suarez-Farinas M, Fuentes-Duculan J, Novitskaya I, Khatcherian A, Bluth MJ, Lowes MA, Krueger JG. 2007. Amelioration of epidermal hyperplasia by TNF inhibition is associated with reduced Th17 responses. *J Exp Med* 204: 3183-94
648. Kuwabara T, Ishikawa F, Yasuda T, Aritomi K, Nakano H, Tanaka Y, Okada Y, Lipp M, Kakiuchi T. 2009. CCR7 ligands are required for development of experimental autoimmune encephalomyelitis through generating IL-23-dependent Th17 cells. *J Immunol* 183: 2513-21
649. Rao DA, Pober JS. 2008. Endothelial injury, alarmins, and allograft rejection. *Crit Rev Immunol* 28: 229-48
650. Wilson JM, Kurtz CC, Black SG, Ross WG, Alam MS, Linden J, Ernst PB. 2011. The A2B adenosine receptor promotes Th17 differentiation via stimulation of dendritic cell IL-6. *J Immunol* 186: 6746-52
651. Sheibanie AF, Yen JH, Khayrullina T, Emig F, Zhang M, Tuma R, Ganea D. 2007. The proinflammatory effect of prostaglandin E2 in experimental inflammatory bowel disease is mediated through the IL-23-->IL-17 axis. *J Immunol* 178: 8138-47
652. Murugaiyan G, Mittal A, Weiner HL. 2010. Identification of an IL-27/osteopontin axis in dendritic cells and its modulation by IFN-gamma limits IL-17-mediated autoimmune inflammation. *Proc Natl Acad Sci U S A* 107: 11495-500
653. Wu SY, Yu JS, Liu FT, Miaw SC, Wu-Hsieh BA. 2013. Galectin-3 negatively regulates dendritic cell production of IL-23/IL-17-axis cytokines in infection by Histoplasma capsulatum. *J Immunol* 190: 3427-37
654. Ahmed Z, Kawamura T, Shimada S, Piguet V. 2015. The role of human dendritic cells in HIV-1 infection. *J Invest Dermatol* 135: 1225-33
655. Haase AT. 2010. Targeting early infection to prevent HIV-1 mucosal transmission. *Nature* 464: 217-23

656. Li Q, Estes JD, Schlievert PM, Duan L, Brosnahan AJ, Southern PJ, Reilly CS, Peterson ML, Schultz-Darken N, Brunner KG, Nephew KR, Pambuccian S, Lifson JD, Carlis JV, Haase AT. 2009. Glycerol monolaurate prevents mucosal SIV transmission. *Nature* 458: 1034-8
657. Fontenot D, He H, Hanabuchi S, Nehete PN, Zhang M, Chang M, Nehete B, Wang YH, Wang YH, Ma ZM, Lee HC, Ziegler SF, Courtney AN, Miller CJ, Sun SC, Liu YJ, Sastry KJ. 2009. TSLP production by epithelial cells exposed to immunodeficiency virus triggers DC-mediated mucosal infection of CD4+ T cells. *Proc Natl Acad Sci U S A* 106: 16776-81
658. Smed-Sorensen A, Lore K, Vasudevan J, Louder MK, Andersson J, Mascola JR, Spetz AL, Koup RA. 2005. Differential susceptibility to human immunodeficiency virus type 1 infection of myeloid and plasmacytoid dendritic cells. *J Virol* 79: 8861-9
659. Zhang ZQ, Wietgrefe SW, Li Q, Shore MD, Duan L, Reilly C, Lifson JD, Haase AT. 2004. Roles of substrate availability and infection of resting and activated CD4+ T cells in transmission and acute simian immunodeficiency virus infection. *Proc Natl Acad Sci U S A* 101: 5640-5
660. Miller CJ, Li Q, Abel K, Kim EY, Ma ZM, Wietgrefe S, La Franco-Scheuch L, Compton L, Duan L, Shore MD, Zupancic M, Busch M, Carlis J, Wolinsky S, Haase AT. 2005. Propagation and dissemination of infection after vaginal transmission of simian immunodeficiency virus. *J Virol* 79: 9217-27
661. Cameron PU, Freudenthal PS, Barker JM, Gezelter S, Inaba K, Steinman RM. 1992. Dendritic cells exposed to human immunodeficiency virus type-1 transmit a vigorous cytopathic infection to CD4+ T cells. *Science* 257: 383-7.
662. Pope M, Betjes MG, Romani N, Hirmand H, Cameron PU, Hoffman L, Gezelter S, Schuler G, Steinman RM. 1994. Conjugates of dendritic cells and memory T lymphocytes from skin facilitate productive infection with HIV-1. *Cell* 78: 389-98.
663. Geijtenbeek TB, Kwon DS, Torensma R, van Vliet SJ, van Duijnhoven GC, Middel J, Cornelissen IL, Nottet HS, KewalRamani VN, Littman DR, Figdor CG, van Kooyk Y. 2000. DC-SIGN, a dendritic cell-specific HIV-1-binding protein that enhances trans-infection of T cells. *Cell* 100: 587-97.
664. Trumpfheller C, Park CG, Finke J, Steinman RM, Granelli-Piperno A. 2003. Cell type-dependent retention and transmission of HIV-1 by DC-SIGN. *Int Immunol* 15: 289-98
665. Manches O, Frleta D, Bhardwaj N. 2014. Dendritic cells in progression and pathology of HIV infection. *Trends Immunol* 35: 114-22
666. Granelli-Piperno A, Moser B, Pope M, Chen D, Wei Y, Isdell F, O'Doherty U, Paxton W, Koup R, Mojsov S, Bhardwaj N, Clark-Lewis I, Baggiolini M, Steinman RM. 1996. Efficient interaction of HIV-1 with purified dendritic cells via multiple chemokine coreceptors. *J Exp Med* 184: 2433-8.
667. Geijtenbeek TB, Torensma R, van Vliet SJ, van Duijnhoven GC, Adema GJ, van Kooyk Y, Figdor CG. 2000. Identification of DC-SIGN, a novel dendritic cell-specific ICAM-3 receptor that supports primary immune responses. *Cell* 100: 575-85.
668. Geijtenbeek TB, van Vliet SJ, Engering A, t Hart BA, van Kooyk Y. 2004. Self- and nonself-recognition by C-type lectins on dendritic cells. *Annu Rev Immunol* 22: 33-54.
669. Steinman RM. 2000. DC-SIGN: a guide to some mysteries of dendritic cells. *Cell* 100: 491-4.

670. Turville SG, Cameron PU, Handley A, Lin G, Pohlmann S, Doms RW, Cunningham AL. 2002. Diversity of receptors binding HIV on dendritic cell subsets. *Nat Immunol* 3: 975-83
671. Manel N, Littman DR. 2011. Hiding in plain sight: how HIV evades innate immune responses. *Cell* 147: 271-4
672. Kwon DS, Gregorio G, Bitton N, Hendrickson WA, Littman DR. 2002. DC-SIGN-mediated internalization of HIV is required for trans-enhancement of T cell infection. *Immunity* 16: 135-44.
673. Boggiano C, Manel N, Littman DR. 2007. Dendritic cell-mediated trans-enhancement of human immunodeficiency virus type 1 infectivity is independent of DC-SIGN. *J Virol* 81: 2519-23
674. Lambert AA, Gilbert C, Richard M, Beaulieu AD, Tremblay MJ. 2008. The C-type lectin surface receptor DCIR acts as a new attachment factor for HIV-1 in dendritic cells and contributes to trans- and cis-infection pathways. *Blood* 112: 1299-307
675. de Witte L, Bobardt M, Chatterji U, Degeest G, David G, Geijtenbeek TB, Gallay P. 2007. Syndecan-3 is a dendritic cell-specific attachment receptor for HIV-1. *Proc Natl Acad Sci U S A* 104: 19464-9
676. Piguet V, Caucheteux SM, Iannetta M, Hosmalin A. 2014. Altered antigen-presenting cells during HIV-1 infection. *Curr Opin HIV AIDS* 9: 478-84
677. Izquierdo-Useros N, Naranjo-Gomez M, Archer J, Hatch SC, Erkizia I, Blanco J, Borras FE, Puertas MC, Connor JH, Fernandez-Figueras MT, Moore L, Clotet B, Gummuluru S, Martinez-Picado J. 2009. Capture and transfer of HIV-1 particles by mature dendritic cells converges with the exosome-dissemination pathway. *Blood* 113: 2732-41
678. Hatch SC, Archer J, Gummuluru S. 2009. Glycosphingolipid composition of human immunodeficiency virus type 1 (HIV-1) particles is a crucial determinant for dendritic cell-mediated HIV-1 trans-infection. *J Virol* 83: 3496-506
679. Gummuluru S, Rogel M, Stamatatos L, Emerman M. 2003. Binding of human immunodeficiency virus type 1 to immature dendritic cells can occur independently of DC-SIGN and mannose binding C-type lectin receptors via a cholesterol-dependent pathway. *J Virol* 77: 12865-74.
680. Hanley TM, Blay Puryear W, Gummuluru S, Viglianti GA. 2010. PPARgamma and LXR signaling inhibit dendritic cell-mediated HIV-1 capture and trans-infection. *PLoS Pathog* 6: e1000981
681. Izquierdo-Useros N, Lorizate M, McLaren PJ, Telenti A, Krausslich HG, Martinez-Picado J. 2014. HIV-1 capture and transmission by dendritic cells: the role of viral glycolipids and the cellular receptor Siglec-1. *PLoS Pathog* 10: e1004146
682. Ganesh L, Leung K, Lore K, Levin R, Panet A, Schwartz O, Koup RA, Nabel GJ. 2004. Infection of specific dendritic cells by CCR5-tropic human immunodeficiency virus type 1 promotes cell-mediated transmission of virus resistant to broadly neutralizing antibodies. *J Virol* 78: 11980-7
683. McDonald D, Wu L, Bohks SM, KewalRamani VN, Unutmaz D, Hope TJ. 2003. Recruitment of HIV and its receptors to dendritic cell-T cell junctions. *Science* 300: 1295-7. Epub 2003 May 1.
684. Piguet V, Sattentau Q. 2004. Dangerous liaisons at the virological synapse. *J Clin Invest* 114: 605-10

685. Sol-Foulon N, Sourisseau M, Porrot F, Thoulouze MI, Trouillet C, Nobile C, Blanchet F, di Bartolo V, Noraz N, Taylor N, Alcover A, Hivroz C, Schwartz O. 2007. ZAP-70 kinase regulates HIV cell-to-cell spread and virological synapse formation. *Embo J* 26: 516-26
686. Feldmann J, Schwartz O. 2010. HIV-1 Virological Synapse: Live Imaging of Transmission. *Viruses* 2: 1666-80
687. Jolly C, Sattentau QJ. 2005. Human immunodeficiency virus type 1 virological synapse formation in T cells requires lipid raft integrity. *J Virol* 79: 12088-94
688. Nikolic DS, Lehmann M, Felts R, Garcia E, Blanchet FP, Subramaniam S, Piguet V. 2011. HIV-1 activates Cdc42 and induces membrane extensions in immature dendritic cells to facilitate cell-to-cell virus propagation. *Blood* 118: 4841-52
689. Felts RL, Narayan K, Estes JD, Shi D, Trubey CM, Fu J, Hartnell LM, Ruthel GT, Schneider DK, Nagashima K, Bess JW, Jr., Bavari S, Lowekamp BC, Bliss D, Lifson JD, Subramaniam S. 2010. 3D visualization of HIV transfer at the virological synapse between dendritic cells and T cells. *Proc Natl Acad Sci U S A* 107: 13336-41
690. Engering A, Van Vliet SJ, Geijtenbeek TB, Van Kooyk Y. 2002. Subset of DC-SIGN(+) dendritic cells in human blood transmits HIV-1 to T lymphocytes. *Blood* 100: 1780-6.
691. Sigal A, Kim JT, Balazs AB, Dekel E, Mayo A, Milo R, Baltimore D. 2011. Cell-to-cell spread of HIV permits ongoing replication despite antiretroviral therapy. *Nature* 477: 95-8
692. Murooka TT, Deruaz M, Marangoni F, Vrbanac VD, Seung E, von Andrian UH, Tager AM, Luster AD, Mempel TR. 2012. HIV-infected T cells are migratory vehicles for viral dissemination. *Nature* 490: 283-7
693. Kramer B, Pelchen-Matthews A, Deneka M, Garcia E, Piguet V, Marsh M. 2005. HIV interaction with endosomes in macrophages and dendritic cells. *Blood Cells Mol Dis* 35: 136-42
694. O'Brien M, Manches O, Sabado RL, Baranda SJ, Wang Y, Marie I, Rolnitzky L, Markowitz M, Margolis DM, Levy D, Bhardwaj N. 2011. Spatiotemporal trafficking of HIV in human plasmacytoid dendritic cells defines a persistently IFN-alpha-producing and partially matured phenotype. *J Clin Invest* 121: 1088-101
695. Fonteneau JF, Larsson M, Beignon AS, McKenna K, Dasilva I, Amara A, Liu YJ, Lifson JD, Littman DR, Bhardwaj N. 2004. Human immunodeficiency virus type 1 activates plasmacytoid dendritic cells and concomitantly induces the bystander maturation of myeloid dendritic cells. *J Virol* 78: 5223-32.
696. Fantuzzi L, Purificato C, Donato K, Belardelli F, Gessani S. 2004. Human immunodeficiency virus type 1 gp120 induces abnormal maturation and functional alterations of dendritic cells: a novel mechanism for AIDS pathogenesis. *J Virol* 78: 9763-72.
697. Silvin A, Manel N. 2015. Innate immune sensing of HIV infection. *Curr Opin Immunol* 32: 54-60
698. Alter G, Kavanagh D, Rihn S, Luteijn R, Brooks D, Oldstone M, van Lunzen J, Altfeld M. 2010. IL-10 induces aberrant deletion of dendritic cells by natural killer cells in the context of HIV infection. *J Clin Invest* 120: 1905-13
699. Lahaye X, Satoh T, Gentili M, Cerboni S, Conrad C, Hurbain I, El Marjou A, Lacabaratz C, Lelievre JD, Manel N. 2013. The capsids of HIV-1 and HIV-2 determine immune detection of the viral cDNA by the innate sensor cGAS in dendritic cells. *Immunity* 39: 1132-42

700. Manel N, Hogstad B, Wang Y, Levy DE, Unutmaz D, Littman DR. 2010. A cryptic sensor for HIV-1 activates antiviral innate immunity in dendritic cells. *Nature* 467: 214-7
701. Blanchet FP, Moris A, Nikolic DS, Lehmann M, Cardinaud S, Stalder R, Garcia E, Dinkins C, Leuba F, Wu L, Schwartz O, Deretic V, Piguet V. 2010. Human immunodeficiency virus-1 inhibition of immunoamphisomes in dendritic cells impairs early innate and adaptive immune responses. *Immunity* 32: 654-69
702. Trapp S, Derby NR, Singer R, Shaw A, Williams VG, Turville SG, Bess JW, Jr., Lifson JD, Robbiani M. 2009. Double-stranded RNA analog poly(I:C) inhibits human immunodeficiency virus amplification in dendritic cells via type I interferon-mediated activation of APOBEC3G. *J Virol* 83: 884-95
703. Bloch N, O'Brien M, Norton TD, Polsky SB, Bhardwaj N, Landau NR. 2014. HIV type 1 infection of plasmacytoid and myeloid dendritic cells is restricted by high levels of SAMHD1 and cannot be counteracted by Vpx. *AIDS Res Hum Retroviruses* 30: 195-203
704. Sunseri N, O'Brien M, Bhardwaj N, Landau NR. 2011. Human immunodeficiency virus type 1 modified to package Simian immunodeficiency virus Vpx efficiently infects macrophages and dendritic cells. *J Virol* 85: 6263-74
705. Gao D, Wu J, Wu YT, Du F, Aroh C, Yan N, Sun L, Chen ZJ. 2013. Cyclic GMP-AMP synthase is an innate immune sensor of HIV and other retroviruses. *Science* 341: 903-6
706. Yoh SM, Schneider M, Seifried J, Soonthornvacharin S, Akleh RE, Olivieri KC, De Jesus PD, Ruan C, de Castro E, Ruiz PA, Germanaud D, des Portes V, Garcia-Sastre A, Konig R, Chanda SK. 2015. PQBP1 Is a Proximal Sensor of the cGAS-Dependent Innate Response to HIV-1. *Cell* 161: 1293-305
707. Cavaleiro R, Tendeiro R, Foxall RB, Soares RS, Baptista AP, Gomes P, Valadas E, Victorino RM, Sousa AE. 2013. Monocyte and myeloid dendritic cell activation occurs throughout HIV type 2 infection, an attenuated form of HIV disease. *J Infect Dis* 207: 1730-42
708. Meylan PR, Guatelli JC, Munis JR, Richman DD, Kornbluth RS. 1993. Mechanisms for the inhibition of HIV replication by interferons-alpha, -beta, and -gamma in primary human macrophages. *Virology* 193: 138-48
709. Yan N, Regalado-Magdos AD, Stiggelbout B, Lee-Kirsch MA, Lieberman J. 2010. The cytosolic exonuclease TREX1 inhibits the innate immune response to human immunodeficiency virus type 1. *Nat Immunol* 11: 1005-13
710. Sabado RL, O'Brien M, Subedi A, Qin L, Hu N, Taylor E, Dibben O, Stacey A, Fellay J, Shianna KV, Siegal F, Shodell M, Shah K, Larsson M, Lifson J, Nadas A, Marmor M, Hutt R, Margolis D, Garmon D, Markowitz M, Valentine F, Borrow P, Bhardwaj N. 2010. Evidence of dysregulation of dendritic cells in primary HIV infection. *Blood* 116: 3839-52
711. Donaghy H, Gazzard B, Gotch F, Patterson S. 2003. Dysfunction and infection of freshly isolated blood myeloid and plasmacytoid dendritic cells in patients infected with HIV-1. *Blood* 101: 4505-11
712. Maniecki MB, Moller HJ, Moestrup SK, Moller BK. 2006. CD163 positive subsets of blood dendritic cells: the scavenging macrophage receptors CD163 and CD91 are coexpressed on human dendritic cells and monocytes. *Immunobiology* 211: 407-17
713. Brown KN, Wijewardana V, Liu X, Barratt-Boyes SM. 2009. Rapid influx and death of plasmacytoid dendritic cells in lymph nodes mediate depletion in acute simian immunodeficiency virus infection. *PLoS Pathog* 5: e1000413

714. Kaufmann DE, Kavanagh DG, Pereyra F, Zaunders JJ, Mackey EW, Miura T, Palmer S, Brockman M, Rathod A, Piechocka-Trocha A, Baker B, Zhu B, Le Gall S, Waring MT, Ahern R, Moss K, Kelleher AD, Coffin JM, Freeman GJ, Rosenberg ES, Walker BD. 2007. Upregulation of CTLA-4 by HIV-specific CD4+ T cells correlates with disease progression and defines a reversible immune dysfunction. *Nat Immunol* 8: 1246-54
715. Trautmann L, Janbazian L, Chomont N, Said EA, Gimmig S, Bessette B, Boulassel MR, Delwart E, Sepulveda H, Balderas RS, Routy JP, Haddad EK, Sekaly RP. 2006. Upregulation of PD-1 expression on HIV-specific CD8+ T cells leads to reversible immune dysfunction. *Nat Med* 12: 1198-202
716. Day CL, Kaufmann DE, Kiepiela P, Brown JA, Moodley ES, Reddy S, Mackey EW, Miller JD, Leslie AJ, DePierres C, Mncube Z, Duraiswamy J, Zhu B, Eichbaum Q, Altfeld M, Wherry EJ, Coovadia HM, Goulder PJ, Klenerman P, Ahmed R, Freeman GJ, Walker BD. 2006. PD-1 expression on HIV-specific T cells is associated with T-cell exhaustion and disease progression. *Nature* 443: 350-4
717. Sandler NG, Bosinger SE, Estes JD, Zhu RT, Tharp GK, Boritz E, Levin D, Wijeyesinghe S, Makamdop KN, del Prete GQ, Hill BJ, Timmer JK, Reiss E, Yarden G, Darko S, Contijoch E, Todd JP, Silvestri G, Nason M, Norgren RB, Jr., Keele BF, Rao S, Langer JA, Lifson JD, Schreiber G, Douek DC. 2014. Type I interferon responses in rhesus macaques prevent SIV infection and slow disease progression. *Nature* 511: 601-5
718. Jacquelin B, Mayau V, Targat B, Liovat AS, Kunkel D, Petitjean G, Dillies MA, Roques P, Butor C, Silvestri G, Giavedoni LD, Lebon P, Barre-Sinoussi F, Benecke A, Muller-Trutwin MC. 2009. Nonpathogenic SIV infection of African green monkeys induces a strong but rapidly controlled type I IFN response. *J Clin Invest* 119: 3544-55
719. Bosinger SE, Li Q, Gordon SN, Klatt NR, Duan L, Xu L, Francella N, Sidahmed A, Smith AJ, Cramer EM, Zeng M, Masopust D, Carlis JV, Ran L, Vanderford TH, Paiardini M, Isett RB, Baldwin DA, Else JG, Staprans SI, Silvestri G, Haase AT, Kelvin DJ. 2009. Global genomic analysis reveals rapid control of a robust innate response in SIV-infected sooty mangabeys. *J Clin Invest* 119: 3556-72
720. Bosinger SE, Johnson ZP, Folkner KA, Patel N, Hashempour T, Jochems SP, Del Rio Estrada PM, Paiardini M, Lin R, Vanderford TH, Hiscott J, Silvestri G. 2013. Intact type I Interferon production and IRF7 function in sooty mangabeys. *PLoS Pathog* 9: e1003597
721. Reitano KN, Kottilil S, Gille CM, Zhang X, Yan M, O'Shea MA, Roby G, Hallahan CW, Yang J, Lempicki RA, Arthos J, Fauci AS. 2009. Defective plasmacytoid dendritic cell-NK cell cross-talk in HIV infection. *AIDS Res Hum Retroviruses* 25: 1029-37
722. Tilton JC, Manion MM, Luskin MR, Johnson AJ, Patamawenu AA, Hallahan CW, Cogliano-Shutta NA, Mican JM, Davey RT, Jr., Kottilil S, Lifson JD, Metcalf JA, Lempicki RA, Connors M. 2008. Human immunodeficiency virus viremia induces plasmacytoid dendritic cell activation in vivo and diminished alpha interferon production in vitro. *J Virol* 82: 3997-4006
723. Kamga I, Kahi S, Develioglu L, Lichtner M, Maranon C, Deveau C, Meyer L, Goujard C, Lebon P, Sinet M, Hosmalin A. 2005. Type I interferon production is profoundly and transiently impaired in primary HIV-1 infection. *J Infect Dis* 192: 303-10
724. Bego MG, Cote E, Aschman N, Mercier J, Weissenhorn W, Cohen EA. 2015. Vpu Exploits the Cross-Talk between BST2 and the ILT7 Receptor to Suppress Anti-HIV-1 Responses by Plasmacytoid Dendritic Cells. *PLoS Pathog* 11: e1005024
725. Herbeuval JP, Grivel JC, Boasso A, Hardy AW, Chougnet C, Dolan MJ, Yagita H, Lifson JD, Shearer GM. 2005. CD4+ T-cell death induced by infectious and noninfectious HIV-

1: role of type 1 interferon-dependent, TRAIL/DR5-mediated apoptosis. *Blood* 106: 3524-31
726. Wilson EB, Yamada DH, Elsaesser H, Herskovitz J, Deng J, Cheng G, Aronow BJ, Karp CL, Brooks DG. 2013. Blockade of chronic type I interferon signaling to control persistent LCMV infection. *Science* 340: 202-7
727. Teijaro JR, Ng C, Lee AM, Sullivan BM, Sheehan KC, Welch M, Schreiber RD, de la Torre JC, Oldstone MB. 2013. Persistent LCMV infection is controlled by blockade of type I interferon signaling. *Science* 340: 207-11
728. Ueyama A, Yamamoto M, Tsujii K, Furue Y, Imura C, Shichijo M, Yasui K. 2014. Mechanism of pathogenesis of imiquimod-induced skin inflammation in the mouse: a role for interferon-alpha in dendritic cell activation by imiquimod. *J Dermatol* 41: 135-43
729. Guo B, Chang EY, Cheng G. 2008. The type I IFN induction pathway constrains Th17-mediated autoimmune inflammation in mice. *J Clin Invest* 118: 1680-90
730. Manches O, Munn D, Fallahi A, Lifson J, Chaperot L, Plumas J, Bhardwaj N. 2008. HIV-activated human plasmacytoid DCs induce Tregs through an indoleamine 2,3-dioxygenase-dependent mechanism. *J Clin Invest* 118: 3431-9
731. Manches O, Fernandez MV, Plumas J, Chaperot L, Bhardwaj N. 2012. Activation of the noncanonical NF-kappaB pathway by HIV controls a dendritic cell immunoregulatory phenotype. *Proc Natl Acad Sci U S A* 109: 14122-7
732. Frleta D, Ochoa CE, Kramer HB, Khan SA, Stacey AR, Borrow P, Kessler BM, Haynes BF, Bhardwaj N. 2012. HIV-1 infection-induced apoptotic microparticles inhibit human DCs via CD44. *J Clin Invest* 122: 4685-97
733. Buisson S, Benlahrech A, Gazzard B, Gotch F, Kelleher P, Patterson S. 2009. Monocyte-derived dendritic cells from HIV type 1-infected individuals show reduced ability to stimulate T cells and have altered production of interleukin (IL)-12 and IL-10. *J Infect Dis* 199: 1862-71
734. Miller EA, Spadaccia MR, O'Brien MP, Rolnitzky L, Sabado R, Manches O, Frleta D, Bhardwaj N. 2012. Plasma factors during chronic HIV-1 infection impair IL-12 secretion by myeloid dendritic cells via a virus-independent pathway. *J Acquir Immune Defic Syndr* 61: 535-44
735. Brenchley JM, Knox KS, Asher AI, Price DA, Kohli LM, Gostick E, Hill BJ, Hage CA, Brahmi Z, Khoruts A, Twigg HL, 3rd, Schacker TW, Douek DC. 2008. High frequencies of polyfunctional HIV-specific T cells are associated with preservation of mucosal CD4 T cells in bronchoalveolar lavage. *Mucosal Immunol* 1: 49-58
736. Jambo KC, Banda DH, Kankwatira AM, Sukumar N, Allain TJ, Heyderman RS, Russell DG, Mwandumba HC. 2014. Small alveolar macrophages are infected preferentially by HIV and exhibit impaired phagocytic function. *Mucosal Immunol* 7: 1116-26
737. Honeycutt JB, Wahl A, Baker C, Spagnuolo RA, Foster J, Zakharova O, Wietgrefe S, Caro-Vegas C, Madden V, Sharpe G, Haase AT, Eron JJ, Garcia JV. 2016. Macrophages sustain HIV replication in vivo independently of T cells. *J Clin Invest* 126: 1353-66
738. Costiniuk CT, Jenabian MA. 2014. The lungs as anatomical reservoirs of HIV infection. *Rev Med Virol* 24: 35-54
739. Fackler OT, Alcover A, Schwartz O. 2007. Modulation of the immunological synapse: a key to HIV-1 pathogenesis? *Nat Rev Immunol* 7: 310-7
740. Pion M, Granelli-Piperno A, Mangeat B, Stalder R, Correa R, Steinman RM, Piguet V. 2006. APOBEC3G/3F mediates intrinsic resistance of monocyte-derived dendritic cells to HIV-1 infection. *J Exp Med* 203: 2887-93

741. Muehlhoefer A, Saubermann LJ, Gu X, Luedtke-Heckenkamp K, Xavier R, Blumberg RS, Podolsky DK, MacDermott RP, Reinecker HC. 2000. Fractalkine is an epithelial and endothelial cell-derived chemoattractant for intraepithelial lymphocytes in the small intestinal mucosa. *J Immunol* 164: 3368-76.
742. Mahnke YD, Brodie TM, Sallusto F, Roederer M, Lugli E. 2013. The who's who of T-cell differentiation: human memory T-cell subsets. *Eur J Immunol* 43: 2797-809
743. Kleinsteuber K, Heesch K, Schattling S, Sander-Juelch C, Mock U, Riecken K, Fehse B, Fleischer B, Jacobsen M. 2012. SOCS3 promotes interleukin-17 expression of human T cells. *Blood* 120: 4374-82
744. Hastings WD, Anderson DE, Kassam N, Koguchi K, Greenfield EA, Kent SC, Zheng XX, Strom TB, Hafler DA, Kuchroo VK. 2009. TIM-3 is expressed on activated human CD4+ T cells and regulates Th1 and Th17 cytokines. *Eur J Immunol* 39: 2492-501
745. Eastman Q, Grosschedl R. 1999. Regulation of LEF-1/TCF transcription factors by Wnt and other signals. *Curr Opin Cell Biol* 11: 233-40
746. Zhang S, Li Y, Wu Y, Shi K, Bing L, Hao J. 2012. Wnt/beta-catenin signaling pathway upregulates c-Myc expression to promote cell proliferation of P19 teratocarcinoma cells. *Anat Rec (Hoboken)* 295: 2104-13
747. Hiyama E, Hiyama K. 2007. Telomere and telomerase in stem cells. *Br J Cancer* 96: 1020-4
748. Chambers I, Colby D, Robertson M, Nichols J, Lee S, Tweedie S, Smith A. 2003. Functional expression cloning of Nanog, a pluripotency sustaining factor in embryonic stem cells. *Cell* 113: 643-55
749. Brown MP, Nosaka T, Tripp RA, Brooks J, van Deursen JM, Brenner MK, Doherty PC, Ihle JN. 1999. Reconstitution of early lymphoid proliferation and immune function in Jak3-deficient mice by interleukin-3. *Blood* 94: 1906-14
750. Bonello-Palot N, Simoncini S, Robert S, Bourgeois P, Sabatier F, Levy N, Dignat-George F, Badens C. 2014. Prelamin A accumulation in endothelial cells induces premature senescence and functional impairment. *Atherosclerosis* 237: 45-52
751. Cui W, Kaech SM. 2010. Generation of effector CD8+ T cells and their conversion to memory T cells. *Immunol Rev* 236: 151-66
752. Liu X, Chen X, Zhong B, Wang A, Wang X, Chu F, Nurieva RI, Yan X, Chen P, van der Flier LG, Nakatsukasa H, Neelapu SS, Chen W, Clevers H, Tian Q, Qi H, Wei L, Dong C. 2014. Transcription factor achaete-scute homologue 2 initiates follicular T-helper-cell development. *Nature* 507: 513-8
753. Schmitt N, Liu Y, Bentebibel SE, Munagala I, Bourdery L, Venuprasad K, Banchereau J, Ueno H. 2014. The cytokine TGF-beta co-opts signaling via STAT3-STAT4 to promote the differentiation of human TFH cells. *Nat Immunol* 15: 856-65
754. Choi YS, Gullicksrud JA, Xing S, Zeng Z, Shan Q, Li F, Love PE, Peng W, Xue HH, Crotty S. 2015. LEF-1 and TCF-1 orchestrate T(FH) differentiation by regulating differentiation circuits upstream of the transcriptional repressor Bcl6. *Nat Immunol* 16: 980-90
755. Hermann-Kleiter N, Baier G. 2010. NFAT pulls the strings during CD4+ T helper cell effector functions. *Blood* 115: 2989-97
756. Ray JP, Staron MM, Shyer JA, Ho PC, Marshall HD, Gray SM, Laidlaw BJ, Araki K, Ahmed R, Kaech SM, Craft J. 2015. The Interleukin-2-mTORc1 Kinase Axis Defines the Signaling, Differentiation, and Metabolism of T Helper 1 and Follicular B Helper T Cells. *Immunity* 43: 690-702

757. Wichner K, Stauss D, Kampfrath B, Kruger K, Muller G, Rehm A, Lipp M, Hopken UE. 2015. Dysregulated development of IL-17-and IL-21-expressing follicular helper T cells and increased germinal center formation in the absence of RORgammat. *FASEB J*
758. Morita R, Schmitt N, Bentebibel SE, Ranganathan R, Bourdery L, Zurawski G, Foucat E, Dullaers M, Oh S, Sabzghabaei N, Lavecchio EM, Punaro M, Pascual V, Banchereau J, Ueno H. 2011. Human blood CXCR5(+)CD4(+) T cells are counterparts of T follicular cells and contain specific subsets that differentially support antibody secretion. *Immunity* 34: 108-21
759. Kawaguchi M, Onuchic LF, Li XD, Essayan DM, Schroeder J, Xiao HQ, Liu MC, Krishnaswamy G, Germino G, Huang SK. 2001. Identification of a novel cytokine, ML-1, and its expression in subjects with asthma. *J Immunol* 167: 4430-5
760. McAllister F, Henry A, Kreindler JL, Dubin PJ, Ulrich L, Steele C, Finder JD, Pilewski JM, Carreno BM, Goldman SJ, Pirhonen J, Kolls JK. 2005. Role of IL-17A, IL-17F, and the IL-17 receptor in regulating growth-related oncogene-alpha and granulocyte colony-stimulating factor in bronchial epithelium: implications for airway inflammation in cystic fibrosis. *J Immunol* 175: 404-12
761. Zrioual S, Ecochard R, Tournadre A, Lenief V, Cazalis MA, Miossec P. 2009. Genome-wide comparison between IL-17A- and IL-17F-induced effects in human rheumatoid arthritis synoviocytes. *J Immunol* 182: 3112-20
762. Yang XO, Chang SH, Park H, Nurieva R, Shah B, Acero L, Wang YH, Schluns KS, Broaddus RR, Zhu Z, Dong C. 2008. Regulation of inflammatory responses by IL-17F. *J Exp Med* 205: 1063-75
763. Lukacs NW, Prosser DM, Wiekowski M, Lira SA, Cook DN. 2001. Requirement for the chemokine receptor CCR6 in allergic pulmonary inflammation. *J Exp Med* 194: 551-5
764. Ito T, Carson WFt, Cavassani KA, Connett JM, Kunkel SL. 2011. CCR6 as a mediator of immunity in the lung and gut. *Exp Cell Res* 317: 613-9
765. Lafferty MK, Sun L, DeMasi L, Lu W, Garzino-Demo A. 2010. CCR6 ligands inhibit HIV by inducing APOBEC3G. *Blood* 115: 1564-71
766. Spolski R, Leonard WJ. 2014. Interleukin-21: a double-edged sword with therapeutic potential. *Nat Rev Drug Discov* 13: 379-95
767. Cosmi L, Cimaz R, Maggi L, Santarlasci V, Capone M, Borriello F, Frosali F, Querci V, Simonini G, Barra G, Piccinni MP, Liotta F, De Palma R, Maggi E, Romagnani S, Annunziato F. 2011. Evidence of the transient nature of the Th17 phenotype of CD4+CD161+ T cells in the synovial fluid of patients with juvenile idiopathic arthritis. *Arthritis Rheum* 63: 2504-15
768. Nistala K, Adams S, Cambrook H, Ursu S, Olivito B, de Jager W, Evans JG, Cimaz R, Bajaj-Elliott M, Wedderburn LR. 2010. Th17 plasticity in human autoimmune arthritis is driven by the inflammatory environment. *Proc Natl Acad Sci U S A* 107: 14751-6
769. Lee AW, Sharp ER, O'Mahony A, Rosenberg MG, Israelski DM, Nolan GP, Nixon DF. 2008. Single-cell, phosphoepitope-specific analysis demonstrates cell type- and pathway-specific dysregulation of Jak/STAT and MAPK signaling associated with in vivo human immunodeficiency virus type 1 infection. *J Virol* 82: 3702-12
770. Bailey JR, Bland PW, Tarlton JF, Peters I, Moorghen M, Sylvester PA, Probert CS, Whiting CV. 2012. IL-13 promotes collagen accumulation in Crohn's disease fibrosis by down-regulation of fibroblast MMP synthesis: a role for innate lymphoid cells? *PLoS One* 7: e52332

771. O'Reilly S. 2013. Role of interleukin-13 in fibrosis, particularly systemic sclerosis. *Biofactors* 39: 593-6
772. Gallo E, Katzman S, Villarino AV. 2012. IL-13-producing Th1 and Th17 cells characterize adaptive responses to both self and foreign antigens. *Eur J Immunol* 42: 2322-8
773. Beriou G, Costantino CM, Ashley CW, Yang L, Kuchroo VK, Baecher-Allan C, Hafler DA. 2009. IL-17-producing human peripheral regulatory T cells retain suppressive function. *Blood* 113: 4240-9
774. Ahmed R, Bevan MJ, Reiner SL, Fearon DT. 2009. The precursors of memory: models and controversies. *Nat Rev Immunol* 9: 662-8
775. Ponnappan S, Ponnappan U. 2011. Aging and immune function: molecular mechanisms to interventions. *Antioxid Redox Signal* 14: 1551-85
776. Sun H, Kim D, Li X, Kiselinova M, Ouyang Z, Vandekerckhove L, Shang H, Rosenberg ES, Yu XG, Lichterfeld M. 2015. Th1/17 Polarization of CD4 T Cells Supports HIV-1 Persistence during Antiretroviral Therapy. *J Virol* 89: 11284-93
777. Ancuta P, Monteiro P, RSekaly RP. 2010. Th17 lineage commitment and HIV-1 pathogenesis. *Current Opinion in HIV and AIDS* in press
778. Lecureuil C, Combadiere B, Mazoyer E, Bonduelle O, Samri A, Autran B, Debre P, Combadiere C. 2007. Trapping and apoptosis of novel subsets of memory T lymphocytes expressing CCR6 in the spleen of HIV-infected patients. *Blood* 109: 3649-57
779. Geldmacher C, Schuetz A, Ngwenyama N, Casazza JP, Sanga E, Saathoff E, Boehme C, Geis S, Maboko L, Singh M, Minja F, Meyerhans A, Koup RA, Hoelscher M. 2008. Early depletion of Mycobacterium tuberculosis-specific T helper 1 cell responses after HIV-1 infection. *J Infect Dis* 198: 1590-8
780. de Repentigny L, Lewandowski D, Jolicoeur P. 2004. Immunopathogenesis of oropharyngeal candidiasis in human immunodeficiency virus infection. *Clin Microbiol Rev* 17: 729-59, table of contents
781. Geginat J, Lanzavecchia A, Sallusto F. 2003. Proliferation and differentiation potential of human CD8+ memory T-cell subsets in response to antigen or homeostatic cytokines. *Blood* 101: 4260-6
782. Havenith SH, Remmerswaal EB, Idu MM, van Donselaar-van der Pant KA, van der Bom N, Bemelman FJ, van Leeuwen EM, ten Berge IJ, van Lier RA. 2014. CXCR5+CD4+ follicular helper T cells accumulate in resting human lymph nodes and have superior B cell helper activity. *Int Immunol* 26: 183-92
783. Xu Y, Weatherall C, Bailey M, Alcantara S, De Rose R, Estaquier J, Wilson K, Suzuki K, Corbeil J, Cooper DA, Kent SJ, Kelleher AD, Zaunders J. 2013. Simian immunodeficiency virus infects follicular helper CD4 T cells in lymphoid tissues during pathogenic infection of pigtail macaques. *J Virol* 87: 3760-73
784. Weber JP, Fuhrmann F, Hutloff A. 2012. T-follicular helper cells survive as long-term memory cells. *Eur J Immunol* 42: 1981-8
785. Boswell KL, Paris R, Boritz E, Ambrozak D, Yamamoto T, Darko S, Wloka K, Wheatley A, Narpala S, McDermott A, Roederer M, Haubrich R, Connors M, Ake J, Douek DC, Kim J, Petrovas C, Koup RA. 2014. Loss of circulating CD4 T cells with B cell helper function during chronic HIV infection. *PLoS Pathog* 10: e1003853
786. Buzon MJ, Sun H, Li C, Shaw A, Seiss K, Ouyang Z, Martin-Gayo E, Leng J, Henrich TJ, Li JZ, Pereyra F, Zurakowski R, Walker BD, Rosenberg ES, Yu XG, Lichterfeld M.

2014. HIV-1 persistence in CD4+ T cells with stem cell-like properties. *Nat Med* 20: 139-42
787. Cui G, Staron MM, Gray SM, Ho PC, Amezquita RA, Wu J, Kaech SM. 2015. IL-7-Induced Glycerol Transport and TAG Synthesis Promotes Memory CD8+ T Cell Longevity. *Cell* 161: 750-61
788. Housley WJ, O'Conor CA, Nichols F, Puddington L, Lingenheld EG, Zhu L, Clark RB. 2009. PPARgamma regulates retinoic acid-mediated DC induction of Tregs. *J Leukoc Biol* 86: 293-301
789. Szatmari I, Pap A, Ruhl R, Ma JX, Illarionov PA, Besra GS, Rajnavolgyi E, Dezso B, Nagy L. 2006. PPARgamma controls CD1d expression by turning on retinoic acid synthesis in developing human dendritic cells. *J Exp Med* 203: 2351-62
790. Iwata M, Yokota A. 2011. Retinoic acid production by intestinal dendritic cells. *Vitam Horm* 86: 127-52
791. Iwata M, Hirakiyama A, Eshima Y, Kagechika H, Kato C, Song SY. 2004. Retinoic acid imprints gut-homing specificity on T cells. *Immunity* 21: 527-38
792. Nickoloff BJ. 1991. The human progenitor cell antigen (CD34) is localized on endothelial cells, dermal dendritic cells, and perifollicular cells in formalin-fixed normal skin, and on proliferating endothelial cells and stromal spindle-shaped cells in Kaposi's sarcoma. *Arch Dermatol* 127: 523-9
793. Hotamisligil GS, Erbay E. 2008. Nutrient sensing and inflammation in metabolic diseases. *Nat Rev Immunol* 8: 923-34
794. Ocadlikova D, Trabanelli S, Salvestrini V, Ciciarello M, Evangelisti C, Lecciso M, Sabattini E, Righi S, Piccioli M, Pileri SA, Lemoli RM, Curti A. 2015. CD103 marks a subset of human CD34+-derived langerin+ dendritic cells that induce T-regulatory cells via indoleamine 2,3-dioxygenase-1. *Exp Hematol* 43: 268-76 e5
795. Bajana S, Herrera-Gonzalez N, Narvaez J, Torres-Aguilar H, Rivas-Carvalho A, Aguilar SR, Sanchez-Torres C. 2007. Differential CD4(+) T-cell memory responses induced by two subsets of human monocyte-derived dendritic cells. *Immunology* 122: 381-93
796. Segura E, Amigorena S. 2015. Cross-Presentation in Mouse and Human Dendritic Cells. *Adv Immunol* 127: 1-31
797. Verbrugghe P, Kujala P, Waelput W, Peters PJ, Cuvelier CA. 2008. Clusterin in human gut-associated lymphoid tissue, tonsils, and adenoids: localization to M cells and follicular dendritic cells. *Histochem Cell Biol* 129: 311-20
798. Muppidi JR, Lu E, Cyster JG. 2015. The G protein-coupled receptor P2RY8 and follicular dendritic cells promote germinal center confinement of B cells, whereas S1PR3 can contribute to their dissemination. *J Exp Med*
799. Heesters BA, Myers RC, Carroll MC. 2014. Follicular dendritic cells: dynamic antigen libraries. *Nat Rev Immunol* 14: 495-504
800. Wang Y, Wang J, Sun Y, Wu Q, Fu YX. 2001. Complementary effects of TNF and lymphotoxin on the formation of germinal center and follicular dendritic cells. *J Immunol* 166: 330-7
801. Cambi A, Gijzen K, de Vries l J, Torensma R, Joosten B, Adema GJ, Netea MG, Kullberg BJ, Romani L, Figdor CG. 2003. The C-type lectin DC-SIGN (CD209) is an antigen-uptake receptor for Candida albicans on dendritic cells. *Eur J Immunol* 33: 532-8
802. Soderlund J, Nilsson C, Lore K, Castanos-Velez E, Ekman M, Heiden T, Biberfeld G, Andersson J, Biberfeld P. 2004. Dichotomy between CD1a+ and CD83+ dendritic cells in lymph nodes during SIV infection of macaques. *J Med Primatol* 33: 16-24

803. Kawamura T, Gatanaga H, Borris DL, Connors M, Mitsuya H, Blauvelt A. 2003. Decreased stimulation of CD4+ T cell proliferation and IL-2 production by highly enriched populations of HIV-infected dendritic cells. *J Immunol* 170: 4260-6
804. Che KF, Sabado RL, Shankar EM, Tjomsland V, Messmer D, Bhardwaj N, Lifson JD, Larsson M. 2010. HIV-1 impairs in vitro priming of naive T cells and gives rise to contact-dependent suppressor T cells. *Eur J Immunol* 40: 2248-58
805. Schindler M, Wildum S, Casartelli N, Doria M, Kirchhoff F. 2007. Nef alleles from children with non-progressive HIV-1 infection modulate MHC-II expression more efficiently than those from rapid progressors. *AIDS* 21: 1103-7
806. Mintern JD, Macri C, Chin WJ, Panozza SE, Segura E, Patterson NL, Zeller P, Bourges D, Bedoui S, McMillan PJ, Idris A, Nowell CJ, Brown A, Radford KJ, Johnston AP, Villadangos JA. 2015. Differential use of autophagy by primary dendritic cells specialized in cross-presentation. *Autophagy* 11: 906-17
807. Fantuzzi L, Purificato C, Donato K, Belardelli F, Gessani S. 2004. Human immunodeficiency virus type 1 gp120 induces abnormal maturation and functional alterations of dendritic cells: a novel mechanism for AIDS pathogenesis. *J Virol* 78: 9763-72
808. Chougnet C, Gessani S. 2006. Role of gp120 in dendritic cell dysfunction in HIV infection. *J Leukoc Biol* 80: 994-1000
809. Diamond DC, Sleckman BP, Gregory T, Lasky LA, Greenstein JL, Burakoff SJ. 1988. Inhibition of CD4+ T cell function by the HIV envelope protein, gp120. *J Immunol* 141: 3715-7
810. Chirmule N, Kalyanaraman VS, Oyaizu N, Slade HB, Pahwa S. 1990. Inhibition of functional properties of tetanus antigen-specific T-cell clones by envelope glycoprotein GP120 of human immunodeficiency virus. *Blood* 75: 152-9
811. Oyaizu N, Chirmule N, Kalyanaraman VS, Hall WW, Pahwa R, Shuster M, Pahwa S. 1990. Human immunodeficiency virus type 1 envelope glycoprotein gp120 produces immune defects in CD4+ T lymphocytes by inhibiting interleukin 2 mRNA. *Proc Natl Acad Sci U S A* 87: 2379-83
812. Molon B, Gri G, Bettella M, Gomez-Mouton C, Lanzavecchia A, Martinez AC, Manes S, Viola A. 2005. T cell costimulation by chemokine receptors. *Nat Immunol* 6: 465-71. Epub 2005 Apr 10.
813. Trautmann A. 2005. Chemokines as immunotransmitters? *Nat Immunol* 6: 427-8.
814. Cavert W, Notermans DW, Staskus K, Wietgrefe SW, Zupancic M, Gebhard K, Henry K, Zhang ZQ, Mills R, McDade H, Schuwirth CM, Goudsmit J, Danner SA, Haase AT. 1997. Kinetics of response in lymphoid tissues to antiretroviral therapy of HIV-1 infection. *Science* 276: 960-4
815. Ohba K, Ryo A, Dewan MZ, Nishi M, Naito T, Qi X, Inagaki Y, Nagashima Y, Tanaka Y, Okamoto T, Terashima K, Yamamoto N. 2009. Follicular dendritic cells activate HIV-1 replication in monocytes/macrophages through a juxtacrine mechanism mediated by P-selectin glycoprotein ligand 1. *J Immunol* 183: 524-32
816. Acchioni C, Marsili G, Perrotti E, Remoli AL, Sgarbanti M, Battistini A. 2015. Type I IFN--a blunt spear in fighting HIV-1 infection. *Cytokine Growth Factor Rev* 26: 143-58
817. Wang Y, Xu L, Jiang L. 2015. miR-1271 promotes non-small-cell lung cancer cell proliferation and invasion via targeting HOXA5. *Biochem Biophys Res Commun* 458: 714-9

818. Arderiu G, Cuevas I, Chen A, Carrio M, East L, Boudreau NJ. 2007. HoxA5 stabilizes adherens junctions via increased Akt1. *Cell Adh Migr* 1: 185-95
819. Kim N, Kukkonen S, Gupta S, Aldovini A. 2010. Association of Tat with promoters of PTEN and PP2A subunits is key to transcriptional activation of apoptotic pathways in HIV-infected CD4+ T cells. *PLoS Pathog* 6: e1001103
820. Annunziato F, Cosmi L, Liotta F, Maggi E, Romagnani S. 2013. Main features of human T helper 17 cells. *Ann N Y Acad Sci* 1284: 66-70
821. Segura E, Amigorena S. 2013. Inflammatory dendritic cells in mice and humans. *Trends Immunol* 34: 440-5
822. Pepper M, Pagan AJ, Igyarto BZ, Taylor JJ, Jenkins MK. 2011. Opposing signals from the Bcl6 transcription factor and the interleukin-2 receptor generate T helper 1 central and effector memory cells. *Immunity* 35: 583-95
823. Cubas RA, Mudd JC, Savoye AL, Perreau M, van Grevenynghe J, Metcalf T, Connick E, Meditz A, Freeman GJ, Abesada-Terk G, Jr., Jacobson JM, Brooks AD, Crotty S, Estes JD, Pantaleo G, Lederman MM, Haddad EK. 2013. Inadequate T follicular cell help impairs B cell immunity during HIV infection. *Nat Med* 19: 494-9
824. Grimbacher B, Holland SM, Puck JM. 2005. Hyper-IgE syndromes. *Immunol Rev* 203: 244-50
825. Gaublomme JT, Yosef N, Lee Y, Gertner RS, Yang LV, Wu C, Pandolfi PP, Mak T, Satija R, Shalek AK, Kuchroo VK, Park H, Regev A. 2015. Single-Cell Genomics Unveils Critical Regulators of Th17 Cell Pathogenicity. *Cell*
826. Wang C, Yosef N, Gaublomme J, Wu C, Lee Y, Clish CB, Kaminski J, Xiao S, Zu Horste GM, Pawlak M, Kishi Y, Joller N, Karwacz K, Zhu C, Ordovas-Montanes M, Madi A, Wortman I, Miyazaki T, Sobel RA, Park H, Regev A, Kuchroo VK. 2015. CD5L/AIM Regulates Lipid Biosynthesis and Restrains Th17 Cell Pathogenicity. *Cell*
827. Chetoui N, Boisvert M, Gendron S, Aoudjit F. 2010. Interleukin-7 promotes the survival of human CD4+ effector/memory T cells by up-regulating Bcl-2 proteins and activating the JAK/STAT signalling pathway. *Immunology* 130: 418-26
828. Kondrack RM, Harbertson J, Tan JT, McBreen ME, Surh CD, Bradley LM. 2003. Interleukin 7 regulates the survival and generation of memory CD4 cells. *J Exp Med* 198: 1797-806
829. Li C, Ma H, Wang Y, Cao Z, Graves-Deal R, Powell AE, Starchenko A, Ayers GD, Washington MK, Kamath V, Desai K, Gerdes MJ, Solnica-Krezel L, Coffey RJ. 2014. Excess PLAC8 promotes an unconventional ERK2-dependent EMT in colon cancer. *J Clin Invest* 124: 2172-87
830. Costanzo A, Pediconi N, Narcisi A, Guerrieri F, Belloni L, Fausti F, Botti E, Levrero M. 2014. TP63 and TP73 in cancer, an unresolved "family" puzzle of complexity, redundancy and hierarchy. *FEBS Lett* 588: 2590-9
831. Goidts V, Bageritz J, Puccio L, Nakata S, Zapatka M, Barbus S, Toedt G, Campos B, Korshunov A, Momma S, Van Schaftingen E, Reifenberger G, Herold-Mende C, Lichter P, Radlwimmer B. 2012. RNAi screening in glioma stem-like cells identifies PFKFB4 as a key molecule important for cancer cell survival. *Oncogene* 31: 3235-43
832. Eriksson S, Graf EH, Dahl V, Strain MC, Yukl SA, Lysenko ES, Bosch RJ, Lai J, Chioma S, Emad F, Abdel-Mohsen M, Hoh R, Hecht F, Hunt P, Somsouk M, Wong J, Johnston R, Siliciano RF, Richman DD, O'Doherty U, Palmer S, Deeks SG, Siliciano JD. 2013. Comparative analysis of measures of viral reservoirs in HIV-1 eradication studies. *PLoS Pathog* 9: e1003174

833. Bruner KM, Hosmane NN, Siliciano RF. 2015. Towards an HIV-1 cure: measuring the latent reservoir. *Trends Microbiol* 23: 192-203
834. Allen CD, Cyster JG. 2008. Follicular dendritic cell networks of primary follicles and germinal centers: phenotype and function. *Semin Immunol* 20: 14-25
835. Rudnicka D, Feldmann J, Porrot F, Wietgrefe S, Guadagnini S, Prevost MC, Estaquier J, Haase AT, Sol-Foulon N, Schwartz O. 2009. Simultaneous cell-to-cell transmission of human immunodeficiency virus to multiple targets through polysynapses. *J Virol* 83: 6234-46
836. Mayer MJ, Klotz LH, Venkateswaran V. 2015. Metformin and prostate cancer stem cells: a novel therapeutic target. *Prostate Cancer Prostatic Dis* 18: 303-9